A Genomics Approach to Investigate the Molecular Control of Meiosis in *Triticum aestivum*

by

Timothy J. Sutton B. Ag. Sc. (Hons.)

This thesis is submitted in partial fulfilment of the requirements for the degree of

Doctor of Philosophy

In

The School of Agriculture and Wine
Waite Agricultural Research Institute
The University of Adelaide
Australia

May 2003

TABLE OF CONTENTS

LIST OF FIGURES

LIST OF TABLES

ABSTRACT

Meiosis is a cell division process central to the life cycle of all sexual eukaryotic organisms. Chromosome pairing, genetic recombination and subsequent nuclear division during meiosis produces four genetically distinct haploid gametes from a single diploid cell. Allohexaploid wheat (*Triticum aestivum*) behaves meiotically as a diploid, despite the existence in the genome of three closely related (homoeologous) genomes, A, B and D. Chromosome pairing during prophase I of meiosis in wheat is restricted to true homologous chromosomes, the result being the formation of 21 bivalents at meiotic metaphase I. The genetic control of chromosome pairing in wheat is under the control of several pairing homoeologous (*Ph*) genes, located predominantly on chromosome groups 3 and 5. The major suppressors of homoeologous pairing are *Ph1* and *Ph2*. Their cytogenetic effect has been intensively studied but at the molecular level little is known about their function. The isolation and characterisation of *Ph* genes from wheat would lead to greater understanding of chromosome pairing mechanisms in complex allopolyploids, and may enable development of effective strategies for alien gene introgression from related species to modern wheat cultivars.

In this study, several genomics-based approaches were adopted to explore the expressed portion of the wheat genome in order to identify and characterise genes that could function in the molecular processes regulating meiosis.

The first approach used comparative genetics to characterise the region deleted in the *ph2a* mutant (a deletion mutant at *Ph2*). The rice genomic region syntenous to that deleted in the *ph2a* mutant was identified through comparative mapping and used in searches of wheat databases to identify ESTs with significant similarity. Southern analysis confirmed a syntenous relationship in the wheat and rice genomic regions and defined precisely the position of the breakpoint in *ph2a*. What seems to be a terminal deletion on 3DS is estimated to be approximately 80 Mb in length. We can tentatively predict the identification of approximately 220 genes from the region deleted in *ph2a*. The putative role of identified candidate *Ph2* genes is discussed.

The second approach explored the validity of recent proposals suggesting the presence of a meiotic gene cluster in the region of *Ph2*. The transcriptional characteristics of genes linked to *Ph2* were investigated using data from wheat EST databases in combination with recently developed analysis software. The tissue-distribution of mRNAs derived from genes linked to *Ph2* is shown to resemble that of other large chromosomal regions in the wheat genome. It is concluded that the apparently high number of genes from the *Ph2* region expressed in wheat meiotic tissue is not indicative of a meiotic gene cluster in this region, but rather highlights the transcriptional complexity of meiotic anther tissue.

Finally, the meiotic expression pattern of approximately 1800 wheat genes was examined using cDNA microarrays. Two approaches were taken. Firstly, the applicability of microarrays to identify differentially expressed genes between wild-type anthers and anthers of three *Ph* mutant genotypes was investigated. These experiments failed to reveal significant down-regulation of genes in *Ph* mutant anthers compared to wild-type. Possible explanations are discussed. Secondly, the expression of all microarray clones was examined from pre-meiotic interphase through to the tetrad stage of meiosis. A number of candidate wheat genes involved in meiotic and anther developmental processes have been identified and are discussed.

Prior to this study, the methods available to identify wheat meiotic genes, in particular as candidates for *Ph2*, were limited. The recent development of genomics in plant biology provided an opportunity for a new approach towards gene discovery and genome structural analysis in relation to meiosis. This research illustrates the need for, and the effectiveness of a new approach to study meiosis, contributing to our knowledge of the structural and functional characteristics of genes linked to *Ph2*, and establishing a strong basis for further wheat meiotic gene characterisation.

DECLARATION

This work contains no material which has been accepted for the award of any other degree or diploma in any university or other tertiary institution and, to the best of my knowledge and belief, contains no material previously published or written by another person, except where due reference has been made in the text.

I give consent to this copy of my thesis, when deposited in the University Library, being available for loan and photocopying.

T. J. Sutton
May 2003

ACKNOWLEDGEMENTS

A number of people and institutions have provided support and assistance throughout the course of this study. I wish to express my appreciation to the following people for their contribution.

My supervisors Professor Peter Langridge and Dr Andreas Houben for their patient supervision, guidance throughout the course of this study and critical reading of this thesis. I particularly thank Professor Peter Langridge for his support of my research ideas and goals and I am extremely grateful for the exciting opportunities available to me throughout the course of this research.

Research fellow Dr Ute Baumann, for the countless times that I have sought opinion and advice over the past years, and for valuable suggestion and solution to the bioinformatic challenges of my research.

All members of the Langridge laboratory and the Department of Plant Science who have helped me during the course of this research. In particular I thank the help of Dr Ryan Whitford as both a colleague and good friend, and Dr Jason Able for his critical reading of this thesis. From DuPont Ag Biotech I thank Nathan Uhlmann, Dr Antoni Rafalski, Dr Scott Tingey and Dr Petra Wolters for excellent assistance with microarrays and the practical aspects of my research visits to the US. From the US Department of Agriculture I thank Dr Gerard Lazo and Dr Olin Anderson for supplying cDNA clones, extensive sequencing of my cDNA libraries and associated bioinformatic analysis.

Finally, I extend my profound gratitude to my wife Kristen, and family John, Elaine and Craig for their understanding, support and encouragement.

This research was financially supported through an Australian Postgraduate Award provided through the University of Adelaide, a scholarship provided by the Cooperative Research Centre for Molecular Plant Breeding, and assistance from DuPont Ag Biotech.

ABBREVIATIONS

aa	amino acid
aRNA	antisense ribonucleic acid
ATP	adenosine 5'-triphosphate
BAC	bacterial artificial chromosome
bp	base pair/s
BLAST	Basic Logical Alignment Search Tool
BSA	bovine serum albumin
$^{\circ}$C	degrees Celsius
CCV	Contig Constellation Viewer
cDNA	complementary deoxyribonucleic acid
cm	centimetre/s
cv	cultivar
Cy3	cyanine 3 dUTP
Cy5	cyanine 5 dUTP
dATP	2'-deoxyadenosine 5'-triphosphate
dCTP	2'-deoxycytidine 5'-triphosphate
dGTP	2'-deoxyguanosine 5'-triphosphate
dTTP	2'-deoxythymidine 5'-triphosphate
dUTP	2'-deoxyuridine 5'-triphosphate
DMSO	dimethyl sulfoxide
DNA	deoxyribonucleic acid
dNTP	deoxynucleoside triphosphate
DTT	diothiothreitol
EDTA	ethylenediaminetetraacetic acid
EMS	ethyl methane sulphonate
EST	expressed sequence tag
FISH	fluorescent *in situ* hybridisation
g	gram/s
x g	9.81 m/s^2
h	hour/s
IPTG	isopropyl-1-thio-b-D-galactosidase

IQR	interquartile range
ITEC	International Triticeae EST Cooperative
Kb	kilobase/s
kDa	kilodalton/s
L	litre/s
LB	Luria-Bertaini
M	molar
mA	milliampere
Mb	megabase/s
min	minute/s
mg	milligram/s
mL	millilitre/s
mM	millimolar
ng	nanogram/s
nm	nanometre/s
MOPS	3-(N-morpholino)propane-sulfonic acid
mRNA	messenger ribonucleic acid
OD_{260}	optical density at 260 nm
PAC	P1 artificial chromosome
PCR	polymerase chain reaction
poly(A)	polyadenylated
PVP	polyvinyl pyrollidone
RFLP	restriction-fragment length polymorphism
RNA	ribonucleic acid
RNase	ribonuclease
rpm	revolutions per minute
RT	room temperature
RT-PCR	reverse transcription-polymerase chain reaction
sarkosyl	N-lauroylsarcosine
SDS	sodium dodecyl sulphate
SSC	sodium chloride/sodium citrate
TAE	Tris/acetate/EDTA
Taq	*Thermus aquaticus*

TE	Tris/EDTA
Tris-HCl	Tris(hydroxymethyl)aminomethane hydrochloride
U	units
μFD	microfarad/s
μg	microgram/s
μL	microlitre/s
UV	ultraviolet
V	volt/s
v/v	volume/volume
W	watt/s
w/v	weight/volume
x-gal	5-bromo-4-chloro-3-indolyl-b-D-galactosidase

CHAPTER 1

LITERATURE REVIEW

1.1 Introduction

Meiosis (from the Greek meaning diminution) is a cell division process that is central to the life cycle of all sexual eukaryotic organisms. Meiosis consists of a single round of DNA replication followed by two rounds of chromosome segregation, which leads to the production of four haploid gametes from a single diploid cell.

In a mitotic division, following DNA replication (during the S phase), sister chromatids, which are joined at their centromeres, line up on the spindle with their kinetochore fibers pointing towards opposite poles. Contraction of spindle fibers then proceeds to separate sister chromatids, and they move to opposite poles of the cell to become individual chromosomes. A nuclear membrane forms around both groups of chromosomes and each new cell thus inherits one copy of each paternal chromosome and one copy of each maternal chromosome. The two diploid products from a mitotic division are identical.

In contrast to mitosis, meiosis produces four gametes that are genetically distinct, and contain the haploid complement of chromosomes. The cellular machinery that accomplishes this additional sorting during meiosis requires that homologous chromosomes recognise each other and pair subsequent to their alignment on the spindle apparatus. Homologous chromosome pairing is a fundamental component of meiotic division that has been the subject of much interest and debate since the early twentieth century.

A considerable amount of information is available on the events associated with meiosis in a number of eukaryotes including yeast (Roeder, 1995), *Drosophila melanogaster* (Orr-Weaver, 1995), *Caenorhabditis elegans* (Zetka and Rose, 1995), and plants (Dawe, 1998). Plant genes homologous to those of other organisms have been isolated from a

number of species, including *Arabidopsis thaliana* (Klimyuk and Jones, 1997; Sato *et al.*, 1995), lily (Kobayashi *et al.*, 1994) and wheat (Dong *et al.*, 2002; Ji and Langridge, 1994). Furthermore, a number of meiotic mutants have been identified in plant species such as *Arabidopsis* (Chaudhury *et al.*, 1994; Dawson *et al.*, 1993; Glover *et al.*, 1998; He *et al.*, 1996; Peirson *et al.*, 1996; Ross *et al.*, 1997; Spielman *et al.*, 1997), tomato (Moens, 1969), maize (Golubovskaya *et al.*, 1993; Golubovskaya *et al.*, 1997; Maguire *et al.*, 1993; Staiger and Cande, 1993), rice (Kitada and Omura, 1983; Kitada and Omura, 1984) and wheat (Roberts *et al.*, 1999; Sears, 1977; Wall *et al.*, 1971).

1.2 The anther and the stages of meiosis

The cereals provide an excellent model for studying chromosome behaviour. Numerous deletion and substitution lines are available, and they provide meiotic material at predictable and determinable stages. In wheat, each spike consists of twenty or more spikelets that have a defined sequence of maturity (Schwarzacher, 1997). Within each of the two major florets of each spikelet there are three synchronously developing anthers. The anther generally contains four distinct sacs, or loculi, in which the archesporial tissue is housed, and it is the cells of each archesporium that differentiate into a central core of meiocytes (Dickinson, 1987). Surrounding an estimated 200 to 300 meiocytes per anther (Bennett *et al.*, 1973) lies a single layer of cells known as the tapetal cells. Several layers of anther wall cells surround the tapetum, which is enclosed finally by an epidermis. Securing the anther and providing essential nutrients and water is a narrow filament.

Hexaploid wheat has one of the shortest meiotic divisions amongst higher plants. When the anther is approximately 1 millimetre in length, meiosis begins and continues for 24 hours at 20 °C (Bennett *et al.*, 1973). Bennett (1971) reported a 42 hour meiotic cycle in diploid *T. monococcum* and a 30 hour cycle in tetraploid *T. dicoccum*. This indicates that the duration of meiosis decreases as the ploidy level increases and has found to be the case for related allopolyploid and autopolyploid forms.

Premeiotic interphase precedes the beginning of meiosis and lasts approximately 48 hours in wheat grown at 20 °C (Bennett and Smith, 1972). During this time, meiocytes

and tapetal cells undergo synchronous DNA synthesis (S phase), which increases the DNA content in the nucleus from 2C to 4C. Concomitantly to this synthesis, binucleated cells are formed from a synchronous mitotic division of the tapetal nuclei and meiosis begins.

Meiosis comprises two meiotic divisions, each consisting of four stages: prophase I, metaphase I, anaphase I and telophase I, followed by prophase II, metaphase II, anaphase II and telophase II (**Figure 1.1**). Of all these stages, prophase I is the most complex and time consuming, and is divided into five sub-stages: leptotene, zygotene, pachytene, diplotene and diakinesis. Leptotene is the longest stage during prophase I, lasting approximately 10 hours in wheat (Bennett *et al.*, 1973), and it is at this time that the chromosomes become visible, identifiable as long threads with the sister chromatids pressed together. Sister chromatids of each leptotene chromosome are bound to a common protein core, known as an axial element. Leptotene also marks the fusion of the three cell nucleoli into one (Bennett *et al.*, 1973).

Zygotene follows leptotene and continues for approximately three to four hours (Bennett *et al.*, 1973). Chromosomes continue to condense and begin to pair at one or more points along their length. Chromosome telomeres orient in a polarised organisation at a specific site on the nuclear membrane, giving rise to the so-called "bouquet" arrangement (Dernburg *et al.*, 1995). Homologous chromosomes synapse along their length during zygotene. Using an electron microscope at the zygotene sub-stage has shown that pairing involves an association of the two axial cores of each pair of homologues (Moses, 1968). These paired axial cores form the lateral components of a ribbon-like structure known as the synaptonemal complex. Homoeologous multivalents are frequently observed during pairing in zygotene, however the resolution of strict bivalents is complete by the commencement of the next meiotic prophase I stage, pachytene.

Chromosomes continue to condense during pachytene, with this stage characterised by thick, fully synapsed threads. The chromosome complement is represented by the haploid number of bivalents. The genetically important phenomenon of crossing over between non-sister chromatids occurs at this stage of meiosis. According to Bennett *et al*. (1973), pachytene lasts for approximately 2 hours in wheat.

Figure 1.1: Meiosis.

Photographs are of *Lilium regale*. Modified from McLeish and Snoad (1958).

Leptotene

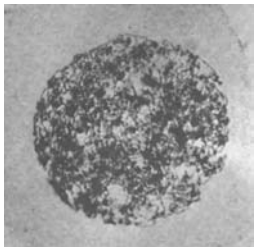

Zygotene

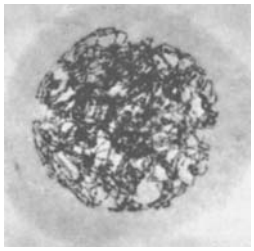

Pachytene

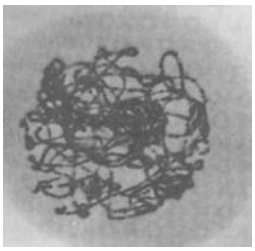

Diplotene

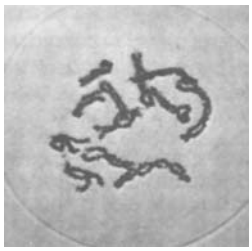

Diakinesis

Metaphase I

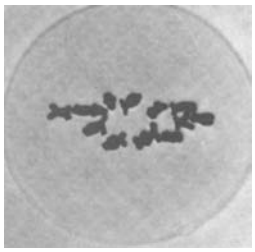

Early Anaphase I

Later Anaphase I

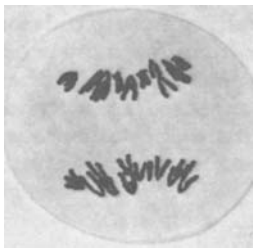

Telophase I

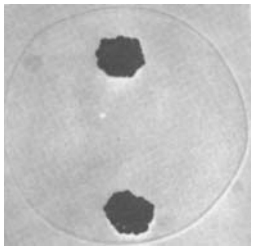

Interphase

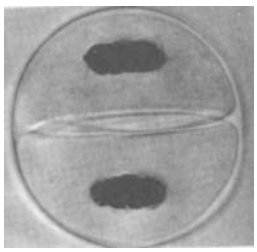

Prophase II

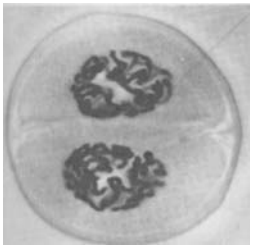

Metaphase II

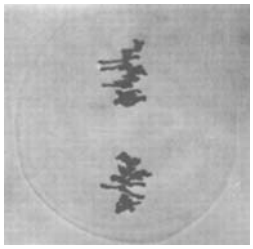

Anaphase II

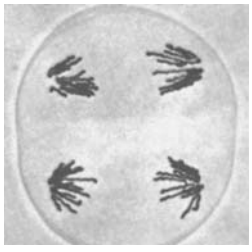

Telophase II

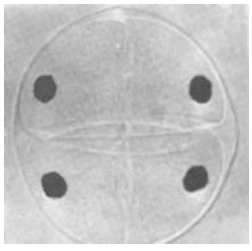

Tetrads

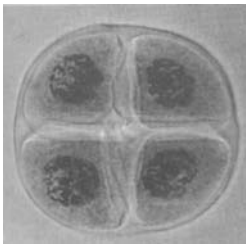

Immature pollen

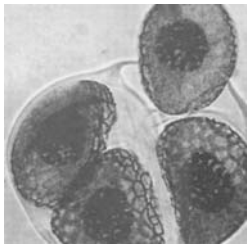

At the onset of diplotene, synapsed chromosomes begin to separate, however they retain an association at one or more sites along their length. Two of the four chromatids from each bivalent remain attached via chiasmata, which represent the points of physical exchange between chromatids of homologous chromosomes. The cytology of meiotic cells suggests that the role of chiasmata is to hold homologous chromosomes together to provide tension needed for proper orientation. Much of the synaptonemal complex separates from each bivalent as the homologues move apart.

During the final stage of prophase I, diakinesis, chromosomes reach their maximum condensation. Chiasmata that appeared during diplotene now progress to the ends of each chromosome, in a process known as terminalisation. Towards the end of diakinesis, spindle formation is initiated and the nuclear envelope breaks down. Diplotene and diakinesis collectively last for 1 hour in wheat (Bennett *et al.*, 1973).

The stages subsequent to prophase I comprise two successive nuclear divisions. These stages closely resemble their mitotic counterparts. However, the products of a single meiotic division are four cells with the haploid complement of chromosomes that have been subjected to genetic recombination.

1.3 The synaptonemal complex

Discovered by Moses (1956) and Fawcett (1956), the synaptonemal complex is strictly a meiotic structure that forms between homologous chromosomes during prophase I. A number of special cytological techniques have been employed to determine the sub-structure of the synaptonemal complex. These have been reviewed by Schmekel and Daneholt (1995). The structure and dimensions of the synaptonemal complex are highly conserved across species (von Wettstein *et al.*, 1984).

In the majority of organisms studied, homologous chromosome synapsis results in the formation of full length synaptonemal complexes, a crucial meiotic process that has been implicated in the development and regulation of crossover events, and is essential for the normal progression of homologue disjunction and chromosome reduction. During the

early stages of prophase I, sister chromatids of each chromosome develop a common proteinaceous core approximately 50 nm in diameter, called the axial element. As prophase I progresses, the proteinaceous components of the central element of the synaptonemal complex assemble between homologous axial elements, and bring about the complete synapsis of homologous chromosomes. Within the mature synaptonemal complex, axial elements are referred to as lateral elements, while the intervening space is called the synaptonemal complex central region, having an overall width of approximately 100 nm (Zickler and Kleckner, 1999). A structural component of the synaptonemal complex central regions are transverse filaments, many of which span its entire width, whilst others terminate at the central element (Schmekel and Daneholt, 1995). Surrounding the synaptonemal complex are the loops of chromatin that are anchored via the lateral elements (**Figure 1.2**).

In addition to the above-mentioned structures, small (50 nm to 200 nm diameter), transient, multi-component proteinaceous ovoid structures termed recombination nodules are observed on meiotic chromosomes. Meiotic nodules were first described by Gillies (1972), and subsequently Carpenter (1975) named them recombination nodules following recognition of correlations between nodules and crossovers in *Drosophila melanogaster* oocytes. Recombination nodules are associated with both developing and mature synaptonemal complexes from leptotene through to pachytene, of almost all investigated organisms. Two classes of recombination nodules have been observed, and are characterised in reference to their temporal appearance on meiotic chromosomes, size, shape and relative number (Albini and Jones, 1987; Carpenter, 1987; Carpenter, 1988; Stack and Anderson, 1986a; Zickler and Kleckner, 1999). Nodules appearing from leptotene/early zygotene to early-mid pachytene are known as early recombination nodules, and are generally observed on the axial elements of the synaptonemal complex (Zickler and Kleckner, 1999). Early recombination nodules have been observed on unpaired chromosomes (Albini and Jones, 1987; Stack and Anderson, 1986a), as well as on zygotene chromosomes in regions of non-homologous synapsis (Holboth, 1981; Stack *et al.*, 1993), observations that seem to support a possible role in homology searching. The association of early recombination nodules with axial elements also seems to indicate they may be involved with homologue recognition and synapsis (Anderson *et al.*, 2001). In addition, evidence indicates early recombination nodules have a role in the

Figure 1.2: The synaptonemal complex.

A: Generalised illustration. Modified from Dawe (1998).

B: Silver stained electron microscope view of synaptonemal complexes from the moth, *Hyalophora Columbia*. Two parallel lateral elements surrounded by chromatin loops are evident for each chromosome. Bar 1 μm. Modified from Roeder (1997).

A

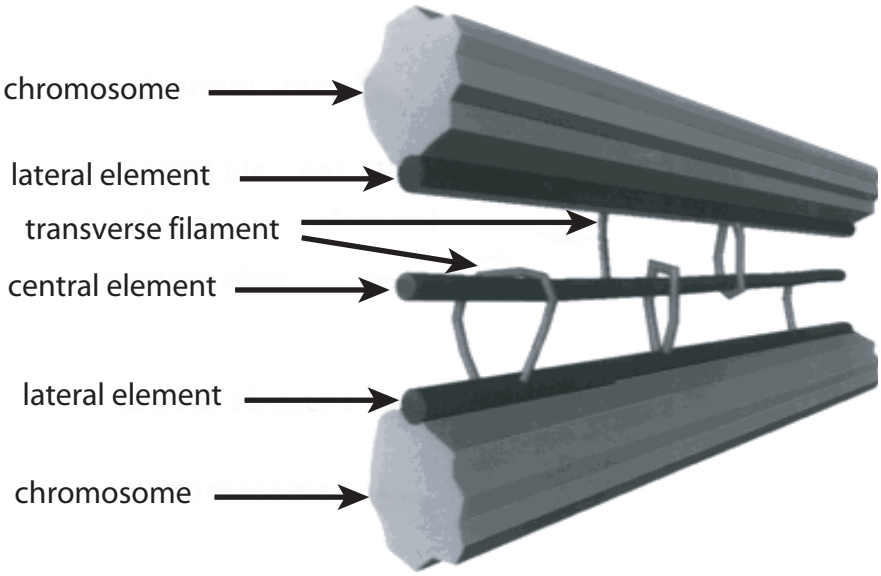
chromosome
lateral element
transverse filament
central element
lateral element
chromosome

B

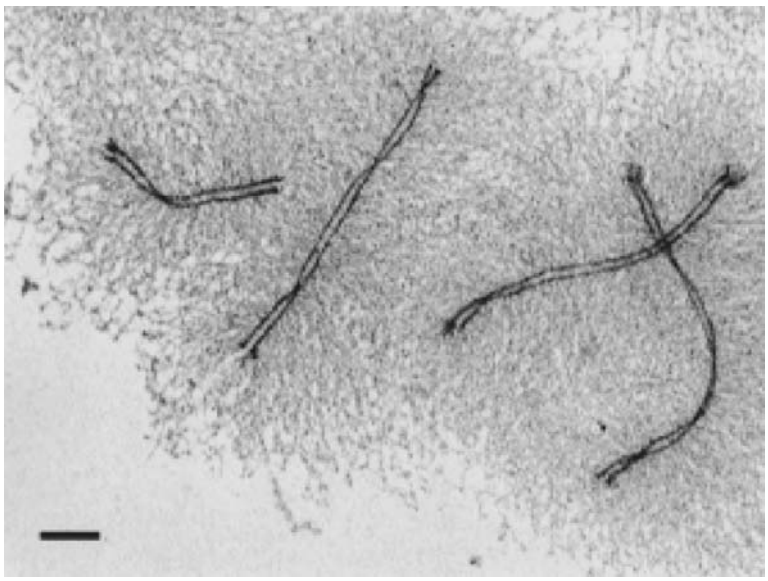

early events of recombination. The Rec-A related proteins, Rad51 and Dmc1, required for DNA homology searching in preparation for crossing over, have been localised to at least some early nodules (Anderson *et al.*, 1997; Moens *et al.*, 1997; Tarsounas *et al.*, 1999; Zickler and Kleckner, 1999). Early recombination nodules are common in regions of euchromatin, and relatively rare in heterochromatic regions (Anderson *et al.*, 2001).

Recently, the frequency and distribution of early recombination nodules in zygotene spreads has been examined across a range of monocot, dicot and lower vascular plant species (Anderson *et al.*, 2001). This study has indicated that the number of early nodules per unit length is higher for synaptonemal complex segments than for asynapsed axial elements, and that early nodule number is strongly correlated with synaptonemal complex length. In addition, different frequencies of early nodules were detected on the synaptonemal complexes from different species, an observation not correlated with genome size, chromosome number or phylogenetic class (Anderson *et al.*, 2001). Furthermore, the distribution of early recombination nodule spacing along synaptonemal complexes in euchromatin was random for each species (Anderson *et al.*, 2001).

During early pachytene, early recombination nodules either dissociate from the synaptonemal complex or are degraded, and the nodules present at pachytene are known as late recombination nodules. This temporal transformation leaves only a few late recombination nodules per meiotic bivalent (Stack and Anderson, 1986b; Stack and Anderson, 1986a), and it seems apparent that a subset of early nodules become late nodules, an assumption however, yet to be proven (Anderson *et al.*, 2001). Late recombination nodules occur associated with the central region of the synaptonemal complex, positioned either against the central elements or on top of the central region (Zickler and Kleckner, 1999). Early recombination nodules are more variable in size and shape than late nodules and are 2 to 20 times more abundant per unit length of synaptonemal complex (Albini and Jones, 1987; Carpenter, 1987; Carpenter, 1988; Stack and Anderson, 1986b; Stack and Anderson, 1986a; Zickler and Kleckner, 1999).

The presence and distribution of late nodules on pachytene chromosomes correlates with crossover recombination events (reviewed in Albini and Jones, 1988; Carpenter, 1979a; Carpenter, 1979b; Sherman and Stack, 1995; Stack *et al.,* 1993 and von Wettstein *et al.,*

1984), suggesting that late recombination nodules may represent architectural factors associated with recombination events. A number of studies have investigated this relationship and provided evidence that correlates the presence of late recombination nodules with chiasmata, or correlated changes in chiasmata frequency or localisation with changes in recombination nodule frequency (see Albini and Jones, 1988; Stack *et al.,* 1989 as examples). It seems that late recombination nodules may represent the molecular apparatus required for meiotic crossing over.

1.3.1 Molecular composition of the synaptonemal complex

Synaptonemal complexes were first purified as morphologically distinct structures by Heyting *et al.* (1985). Since this time, a number of protein components of the synaptonemal complex have been isolated and characterised. In yeast, the approach has involved screening meiotic mutants but in plants and animals it has generally involved isolating specific components of purified synaptonemal complexes, or the identification of genetic loci based on mutant phenotypes.

Genes encoding specific components of the central region include the *ZIP1* gene of *S. cerevisiae* (Sym *et al.*, 1993), *SCP1* from rat (Meuwissen *et al.*, 1992), and its homologue from hamster, *SYN1* (Dobson *et al.*, 1994). The protein products of these genes range from 875 to 997 amino acids and contain central regions of extended coiled-coil motifs. SCP1/Syn1 and Zip1 do not share significant sequence similarities, except in regions corresponding to α-helical coiled-coils (Meuwissen *et al.*, 1992). Expression of the genes *ZIP1* and *SCP1* has been shown to be specific to meiotic prophase I cells (Meuwissen *et al.*, 1992; Sym *et al.*, 1993). Specifically Zip1 and SCP1/Syn1 are components of the transverse filaments, as evidenced from the following observations: First, localisation of the proteins is observed to synapsed chromosomes, but not to unsynapsed axial elements (Dobson *et al.*, 1994; Meuwissen *et al.*, 1992; Sym *et al.*, 1993). Second, paired, but not intimately synapsed axial elements, are observed in a *zip1* null mutant (Nag *et al.*, 1995; Sym *et al.*, 1993). Third, when the length of the coiled-coil loop domain is increased, the distance between the axial elements increases (Sym and Roeder, 1995). Fourth, epitope mapping has physically positioned the proteins perpendicular to the length of the synaptonemal complex central region, with carboxyl

termini located in the region of lateral elements, and amino termini located near the middle of the central region (Dobson *et al.*, 1994; Liu *et al.*, 1996; Schmekel *et al.*, 1996). A number of other less extensively studied putative central region components have also been described from other species. For example, the maize mutant, *dy*, which exhibits an increased central region width may also indicate a further central region component (Maguire *et al.*, 1991).

Proteins specific to the lateral elements of the synaptonemal complex have also been identified. A major component of rodent lateral elements is the hamster Cor1 protein (Dobson *et al.*, 1994) and its rat homologue SCP3 (Lammers *et al.*, 1994). Cor1/SCP3 is a meiosis specific protein approximately 250 amino acids in length, with a putative C-terminal coiled-coil motif (Roeder, 1997). In addition to the rodent Cor1/SCP3 proteins, SCP2 from rat has been proposed as a component of the lateral elements in this organism (Offenberg *et al.*, 1998). Both SCP2 and Cor1/SCP3 have been localised to unsynapsed axial elements within the mature synaptonemal complex (Dobson *et al.*, 1994; Lammers *et al.*, 1994; Liu *et al.*, 1996). Interestingly, Cor1 remains associated with the chromosomes as the synaptonemal complex disassociates, and remains associated with the cores of chromosomes until metaphase I (Dobson *et al.*, 1994; Moens and Spyropoulos, 1995). From diplotene to metaphase I the protein accumulates at the centromeres, where it remains until rapid dissociation at metaphase II (Roeder, 1997). Similar findings have been reported for SCP2 and SCP3. However, SCP2 was not clearly retained after metaphase I. In addition to the mammalian axial element components, a number of yeast proteins have been investigated. The *S. cerevisiae* proteins Hop1 and Red1 (Hollingsworth *et al.*, 1990; Rockmill and Roeder, 1991) and Mek1/Mre4 (Rockmill and Roeder, 1991) appear to be associated with axial elements of the synaptonemal complex. Both Hop1 and Red1 are known to be present along the chromosome axes. Red1 is required for formation of axial/lateral elements (Rockmill and Roeder, 1991; Smith and Roeder, 1997), while Hop1 is required for synapsis but does not seem to be involved in the formation of axial/lateral elements (Hollingsworth and Byers, 1989). The Mek1/Mre4 protein localises to foci along the chromosomes and has been shown to be dependent on Red1 and Hop1, and furthermore, partial, discontinuous synaptonemal complex formation has been observed in a *mek1* mutant (Rockmill and Roeder, 1991). A *red1* mutant fails to assemble any observable axial

element or synaptonemal complex structure, and in a *hop1* mutant, axial elements are formed but the mature synaptonemal complex is absent (Hollingsworth and Byers, 1989; Klein *et al.*, 1999; Loidl *et al.*, 1994; Weiner and Kleckner, 1994). In addition, mutations in the *RED1*, *HOP1* and *MEK1*/*MRE4* genes have been shown to elicit effects on recombination. Rockmill and Roeder (1991) reported ten-fold reductions in meiotic recombination in *red1* and *mek1/mre4* mutants, as well as a 100-fold reduction in recombination for a *hop1* mutant. Phenotype analysis of *hop1, red1 and mek1/mre4* strains is suggested to imply that these three axis associated chromosomal proteins play important roles in organising chromosomes during prophase I (Zickler and Kleckner, 1999).

Homologues of the *S. cerevisiae HOP1* gene have been recently identified from two members of the Cruciferae family, *Arabidopsis thaliana* and *Brassica oleracea*. The *ASY1* gene from *Arabidopsis* encodes a Hop1-like protein, and was identified from a T-DNA tagged population (Ross *et al.*, 1997). The mutant, *asy1* was initially identified exhibiting 10 % fertility compared to that of wild-type *Arabidopsis* plants (Ross *et al.*, 1997). Male and female meiosis are affected in this mutant, the essential feature being that synapsis of homologous chromosomes is almost completely lacking, leading to a high proportion of unbalanced microspores and reduced fertility (Ross *et al.*, 1997). *ASY1* is composed of 22 exons and 21 introns, encoding a protein of 596 amino acids that exhibits 28 % identity and 51 % similarity to yeast Hop1 over the N-terminal region representing the HORMA domain (Armstrong *et al.*, 2002), a sequence found in a number of proteins that interact with chromatin (Aravind and Koonin, 1998). An orthologue to *ASY1*, *BoASY1*, from the closely related plant species *Brassica oleracea* has also been isolated (Armstrong *et al.*, 2002). The *BoASY1* gene is of similar structure to *ASY1*, and the translated proteins are of almost identical length, exhibiting 83 % identity and 90 % similarity (Armstrong *et al.*, 2002). In *Arabidopsis* and *Brassica*, Armstrong *et al*. (2002) have shown that Asy1 localises to the regions of chromosomes that associate with the axial/lateral elements of meiotic chromosomes, rather than representing a structural component of the synaptonemal complex itself. It has been proposed that Asy1 may possibly act by defining regions of chromatin that associate with the developing synaptonemal complex structure (Armstrong *et al.*, 2002). Southern analysis and database searching of the *Arabidopsis* genome sequence has indicated the

presence of a second *HOP1* related sequence in this plant species, *ASY2* (Armstrong *et al.*, 2002). *ASY2* is predicted to encode a larger protein than *ASY1* of 1552 amino acids, and the two sequences overlap for the first 300 amino acids with 57 % identity and 66 % similarity (Armstrong *et al.*, 2002). RT-PCR experiments have shown that *ASY2* is expressed (Armstrong *et al.*, 2002), and detailed characterisation of this gene is presumably in progress. Southern blot analysis has suggested that that a second *HOP1* related sequence is also present in the *Brassica oleracea* genome (Armstrong *et al.*, 2002).

In addition, the protein Him-3 has been identified from *C. elegans*. Him-3, a homologue of yeast Hop1, is a component of the meiotic chromosome core, and like the *Arabidopsis* homologue contains a HORMA domain (Hodgkin *et al.*, 1979; Zetka *et al.*, 1999). Several candidates for synaptonemal complex components have also been identified in preparations of isolated synaptonemal complexes of *Lilium* (Anderson *et al.*, 1994; Ohyama *et al.*, 1992). A unique heat shock protein Hsp70-2 has been localised along the synaptonemal complexes of mouse and hamster spermatocytes (Allen *et al.*, 1996). A component of the mitotic chromosome scaffold, Topoisomerase II has also been shown to localise along the lengths of yeast synaptonemal complexes (Klein *et al.*, 1992; Moens and Earnshaw, 1989).

1.4 Genetic recombination at meiosis

Recombination is the term used to describe the process of genetic exchange between sister chromatids during meiosis. It provides a potent source of genetic variation and also plays a mechanical role to ensure physical connections between homologous chromosomes, that allows them to orient properly on the spindle and thus segregate accurately to opposite poles during the first meiotic division. Genetic recombination has been most intensively studied in the fungi, largely due to the ability to recover and analyse all the products of a single meiosis. This applies both to the ordered eight-spored asci of *Ascobolus*, *Sordoria* and *Neurospora*, and the sectored clones of four spored *Saccharomyces* and *Schizosaccharomyces*. Reciprocal exchanges, or crossovers are the most common form of recombination and generally results in a 4:4 segregation ratio. Occasionally a heterozygous marker will not segregate 4:4 and will show an

aberrant pattern of segregation such as 6:2, 5:3, and aberrant 4:4 ratios. Aberrant segregation arises through the process of non-reciprocal exchange of information between DNA duplexes, called gene conversion, and also through post-meiotic segregation.

A number of molecular models have been developed to explain the results accumulated from the analysis of recombination events in these fungi. They include the Holliday model, the Meselson-Radding model and the double strand break repair model. These have been reviewed comprehensively by Szostak *et al.* (1983) and are briefly described below.

1.4.1 The Holliday and Meselson-Radding models of recombination

For a number of years the Holliday model (Holliday, 1964; Holliday, 1968) was widely accepted as the explanation for the relationship between aberrant segregation and crossing over. Following homologous chromosome pairing, single strand nicks form in strands of the same polarity, and at homologous sites in the molecules. The strands unwind in the region of the nicks, switch pairing partners and ligate to generate a region of symmetrical heteroduplex DNA on each of the two interacting non-sister strands, giving rise to a crossed strand known as a Holliday junction. Further unwinding may increase the length of the heteroduplex region, known as branch migration. A mismatch of base pairs may arise if the region of heteroduplex spans a heterozygous marker. Mismatch repair of these regions can result in gene conversion, such that if the mismatches on both duplexes are corrected in the same direction the 6:2 or 2:6 ratio will result. If mismatch in one duplex is corrected a 5:3 ratio will result, and a 4:4 segregation ratio will result if neither mismatch is repaired. Resolution of the Holliday junction may either occur via breakage and rejoining of either the originally crossed strands, or the non-crossed strands, implying that gene conversion will frequently be accompanied by recombination of flanking markers.

The Holliday model explained many aspects of recombination, including the various types of aberrant segregation, and the association of these segregation ratios with crossover events. One of the assumptions of the Holliday model however, was that

heteroduplex DNA occurred equally in both chromatids. The accuracy of this assumption became questionable following studies in *Ascobolus*. Stadler and Towe (1971) found that for this system heteroduplex DNA only occurs on one chromatid. These observations led to the proposal of a further model to explain recombination that made allowances for this data from *Ascobolus*. Meselson and Radding (1975) proposed a model for the formation of asymmetric heteroduplex DNA. Recombination is initiated by the transfer of a single stranded segment from one chromatid to its homologue, displacing the corresponding segment and forming a region of asymmetric heteroduplex DNA. The 3' end of the nicked strand acts as a primer for DNA synthesis from the complementary strand and displaces the strand ahead of it. In this manner, the recipient chromatid will have a region of heteroduplex DNA, whilst the donor duplex remains as a homoduplex. Resolution of the structure parallels that of the Holliday model.

The Meselson-Radding model enabled the explanation of the data from crosses in *Ascobolus* and yeast, however specific constraints resulting from further studies were placed on the model that led to the subsequent proposal of the double strand break repair model.

1.4.2 The double strand break repair model of recombination

At present, the most widely accepted models for meiotic recombination are based on the double strand break repair model (Szostak *et al.*, 1983). The model is based on data from fungi, bacteria and phage, and is initiated after chromosomes have aligned by the introduction of a double strand break into the recipient chromatid by a double strand endonuclease. Broken molecules are processed by resection of their 5’ ends from a 5’ to 3’ exonuclease to create 3’ single stranded overhangs. One of the free 3' single stranded ends then invades a homologous region of the donor duplex, displaces one of the strands and base pairs with the complementary single stranded sequence. As DNA synthesis proceeds, using the invading strands as templates, branch migration displaces the two newly synthesised strands. The ultimate result of these reactions following branch migration is the formation of two Holliday junctions, one defining the initiation point of the recombination event, and the other the point of resolution. Depending on the manner in which DNA strands in these junctions are resolved through separate cutting and re-

ligation, reciprocal crossovers and gene conversion events can result. The double strand break repair model adequately accounts for the observed properties of meiotic recombination in terms of aberrant segregation ratios, as described by Szostak *et al.* (1983).

To date meiotic recombination has been studied in a number of organisms, and the accumulating molecular evidence suggests that the most likely path of recombination follows the double strand break repair model proposed by Szostak *et al.* (1983). Briefly, this evidence includes: Firstly, the observation of meiotically induced double strand breaks at a number of recombination hotspots (Bullard *et al.*, 1996; Cao *et al.*, 1990; Goldway *et al.*, 1993; Sun *et al.*, 1989), their frequency and distribution being generally consistent with that of meiotic recombination events (Baudat and Nicolas, 1997; Klein *et al.*, 1996; Wu and Lichten, 1994): Secondly, the isolation of intermediates as predicted by the double strand break model, such as joint molecules that contain two Holliday junctions via 2D gel electrophoresis (Schwacha and Kleckner, 1994): Thirdly, the isolation of genes such as *SPO11*, purified from the covalently attached ends of double strand breaks (Keeney *et al.*, 1997), shown to be required for the initiation of meiotic recombination (Klapholz *et al.*, 1985).

1.4.3 Genes involved in recombination

In light of the various models that have been proposed to explain recombination processes, it follows that the sequential steps should involve predictable biochemical processes that would include breakage of DNA, the generation of regions of heteroduplex DNA, the coordinated and localised synthesis and degradation of DNA, and the subsequent rejoining of the free ends. Despite the anticipated sterility resulting from defects in chromosomal recombination, a number of genes have been cloned in recent years that are associated with various aspects of meiosis.

The *Escherichia coli* protein RecA (Roberts *et al.*, 1978) has been extensively studied and well characterised. RecA is a strand exchange enzyme that is known to polymerise on the 3' end of single stranded DNA and form a nucleoprotein filament following the formation of double strand breaks and the resection of the 5' end. RecA promotes

synapsis and strand transfer between homologous DNA molecules in an ATP dependant manner. A number of yeast homologues of *RECA* have been identified. They include *RAD51*, *DMC1*, *RAD55* and *RAD57*, mutations in which can lead to defects in the repair of resected double strand breaks (Bishop *et al.*, 1992; Schwacha and Kleckner, 1997; Shinohara *et al.*, 1992). Plant homologues of yeast *DMC1* and *RAD51* have been identified in *Arabidopsis* and tomato (Doutriaux *et al.*, 1998; Klimyuk and Jones, 1997; Stassen *et al.*, 1997), and moreover, sequences homologous to *RECA* have been identified in mammals. Dmc1 and Rad51 localise to discrete spots on meiotic chromosomes, and are postulated to be components of early recombination nodules in yeast (Bishop, 1994).

In addition to the genes described, there are other genes from yeast with predicted roles in the processing of double strand breaks during meiosis. These include *SPO11* (Klapholz *et al.*, 1985), *RAD50* (Alani *et al.*, 1990), *MRE11* (Ajimura *et al.*, 1993), *XRS2* (Ivanov *et al.*, 1992; Ivanov *et al.*, 1994), *MEI4* (Menees *et al.*, 1992), *MER2* (Rockmill *et al.*, 1995), and *REC102*, *REC104* and *REC114* (Bullard *et al.*, 1996). *RAD50*, *MRE11*, and *XRS2* also function in the repair of double strand breaks in non-meiotic cells.

Studies of mismatch repair has implicated a number of genes that are thought to be involved in the processing of recombination intermediates, and furthermore a great deal is known about proteins that are involved in the process of mismatch repair (reviewed in Kolodoner, 1996; Modrich and Lahue, 1996). In eukaryotes, homologues of the *E. coli* proteins MutS and MutL are involved in multiple pathways of recombination and repair. In yeast a number of genes have been shown to be required for mismatch repair, including three homologues of the bacterial MutS protein (Msh2, Msh3 and Msh6) and two homologues of the MutL protein (Pms1 and Mlh1) (Kolodoner and Marsischky, 1999). Analysis of the eukaryotic homologues of MutS and MutL indicate that they form heterodimers, which are thought to be specific for different forms of mismatch repair (Wang *et al.*, 1999b). Msh2-Msh6 functions in the repair of single base pair mismatches and small insertion/deletion loops, whereas the proposed role of Msh2-Msh3 is in the repair of specifically sized insertion/deletion loops (Johnson *et al.*, 1996; Marsischky *et al.*, 1996; Prolla *et al.*, 1994), reviewed in Kolodoner and Marsischky, (1999). Mlh1-Pms1 (the MutL related complex) has a major role in the Msh2-Msh6 and

Msh2-Msh3 pathways, and interacts with these two complexes. In addition to these findings, MutS and MutL homologues are also required for recombination in yeast, independent of their involvement in mismatch repair (Wang *et al.*, 1999b). Several mismatch repair homologues have been localised as discrete foci that correspond to late recombination nodules. These include Msh4, another MutS homologue from yeast. A reduction in crossing over is seen in the *msh4* null mutation, however no effect is seen in relation to gene conversion or mismatch repair (Ross-Macdonald and Roeder, 1994). The protein localises to discrete foci on pachytene chromosomes. Other components of late recombination nodules include the Mlh1 and Msh5 proteins. Null mutations in both of these genes confer decreases in crossing over. The mouse homologue of Mlh1 has similarly been shown to be a component of late recombination nodules, localising to foci on meiotic chromosomes during pachytene. The number of foci correlates with the number of crossovers. Recently, *TaMSH7*, a wheat cDNA homologue of the bacterial *MutS* gene and its homologues in yeast and human has been isolated by RT-PCR (Dong *et al.*, 2002). *TaMSH7* encodes a protein that exhibits conserved domains characteristic of other *MSH6* genes, and shows highest similarity to maize *MSH7* and *Arabidopsis MSH7* (Dong *et al.*, 2002). Interestingly, *TaMSH7* has been located to the region deleted on wheat chromosome 3DS in the chromosome pairing mutant *ph2a* (Dong *et al.*, 2002), which exhibits altered recombination frequency in interspecific hybrids.

Figure 1.3 illustrates the role of a number of characterised components of the double strand break repair recombination pathway.

1.5 Chromosome pairing

A critical event in meiosis occurs when homologous chromosomes recognise and pair with each other. The conceptual pairing of homologous chromosomes requires solutions to three fundamental problems: Firstly, how do chromosomes recognise their homologues and initiate the pairing process? Secondly, how do homologous chromosomes recognise one another across the distances of the nucleus, and thirdly, how are homologous chromosomes present in different locations brought together in space? Loidl (1990) identified three possible mechanisms that attempted to account for the mechanics of chromosome pairing during meiosis. These hypotheses are; somatic

Figure 1.3: The double strand break repair model of meiotic recombination.

The proposed point of action of a number of gene products is indicated. Shown are two double stranded DNA molecules, one in red and the other in blue. Gene products are indicated only where corresponding mutants have been shown to be defective at a specific step by genetic and/or physical assays. Modified from Roeder (1997).

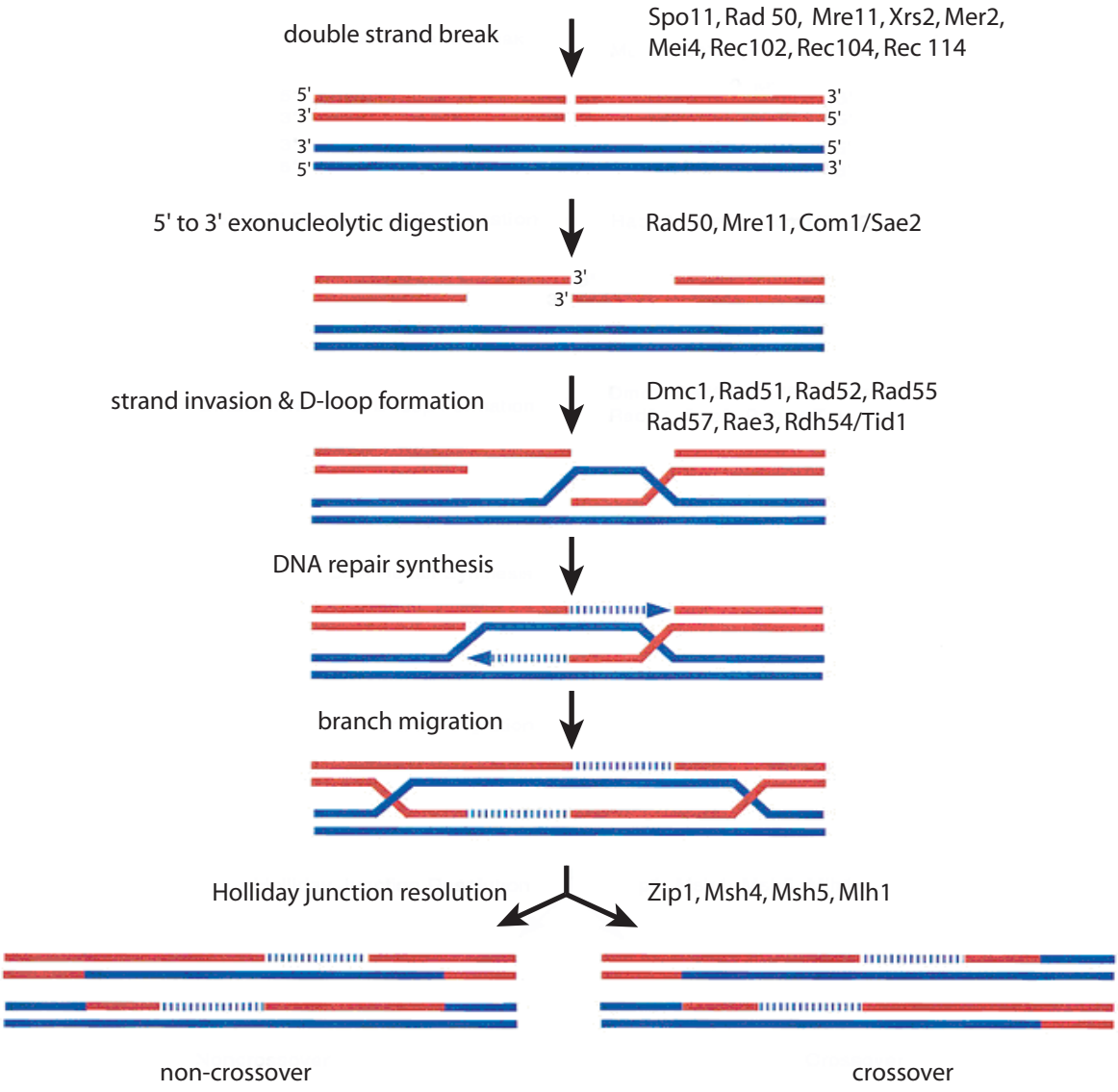
double strand break
Spo11, Rad 50, Mre11, Xrs2, Mer2,
Mei4, Rec102, Rec104, Rec 114
5'
3'
3'
5'
3'
5'
5'
3'
5' to 3' exonucleolytic digestion
Rad50, Mre11, Com1/Sae2
3'
3'
strand invasion & D-loop formation
Dmc1, Rad51, Rad52, Rad55
Rad57, Rae3, Rdh54/Tid1
DNA repair synthesis
branch migration
Holliday junction resolution
Zip1, Msh4, Msh5, Mlh1
non-crossover
crossover

chromosome disposition, specific interactions at prophase and random contacts at prophase.

The first of these hypotheses requires the non-random distribution of chromosomes within somatic or vegetative cells. A number of studies have provided evidence for homologous chromosome associations prior to early meiotic events. During the early stages of embryogenesis in *Drosophila*, homologous chromosomes are associated in somatic cells, and remain associated during subsequent cell cycles (Hiraoka *et al.*, 1993; von Wettstein *et al.*, 1984), a process that seems to begin at the centromere and migrate along the chromosome arm (Loidl *et al.*, 1994). The transition to meiosis in *Drosophila* involves a steady transformation from somatic association to chromosome synapsis. A number of other studies have provided evidence that seems to suggest a closer than random association of homologous chromosomes in somatic cells. Feldman (1966), examining root tip metaphases of allohexaploid wheat found that homologous chromosomes were situated closer, on average than non-homologous or indeed homoeologous chromosomes. Furthermore, during wheat anther development homologue associations are known to initiate at a pre-meiotic stage, with homologue association, seemingly involving the centromeres, apparent in both meiocytes and the surrounding tapetal cells (Aragon-Alcaide *et al.*, 1997b; Aragon-Alcaide *et al.*, 1997a). The presence of subsequent telomere clustering/bouquet formation in meiocytes, and apparent absence in tapetal cells seems to offer evidence against the requirement of such clustering in the homologue association process (Shaw and Moore, 1998). Evidence for non-meiotic homologue associations in yeast has been obtained using fluorescence *in situ* hybridisation (FISH), demonstrating the occupation of certain regions of the nucleus by homologues (Scherthan *et al.*, 1994). However, Shaw and Moore (1998) report that although a significant level of pre-meiotic association is observed, the level and indeed significance are still under debate. A number of reports contrast the results of studies such as the ones above that indicate a role of pre-meiotic associations in the chromosome pairing process. In many organisms such as maize, mice and humans, chromosomes are not paired pre-meiotically. FISH studies have shown that homologous chromosomes are not paired or associated, at least not in the last mitotic division preceding meiosis that was examined in these species. (Bass *et al.*, 1997; Scherthan *et al.*, 1996). Moreover, questions have been raised concerning claims of associations based merely on statistical

observations (Loidl, 1990). It is also possible that the association of homologous chromosomes fulfils other cellular requirements of the somatic cell in some species, rather than being a necessary prerequisite preceding homologous chromosome synapsis at meiosis.

The second of the hypotheses put forward by Loidl (1990), describes the situation where long range chromosome interactions are responsible for drawing chromosomes into alignment. In plants, Dawe (1998) comments that these interactions have largely been debated with reference to unsubstantiated elastic connectors (Maguire, 1977), and in context to an observed fibrillar material in cereal meiocytes (Bennett and Smith, 1979; Bennett *et al.*, 1979). During the homologue pairing process, which is distinct from chromosome synapsis in many organisms, chromosomes are aligned at physical distances much greater than the width of the synaptonemal complex. If chromosomes are not aligned at a pre-meiotic stage as discussed above, then perhaps the synaptonemal complex has some role to play in the aligning of chromosomes prior to synapsis. Studies examining the relationship between chromosome alignment and synaptonemal complex formation indicate that the former is not dependant on the formation of the latter. This prediction has been based on a number of observations from different organisms, that includes the clear aligning of homologues prior to formation of central region components of the synaptonemal complex, and the observation of homologue association in several mutants defective of synaptonemal complex formation (reviewed in Zickler and Kleckner, 1999). It seems clear that the role of the synaptonemal complex is independent to the initial aligning of homologous chromosomes prior to synapsis. Whether the alignment of chromosomes reflects long range connections between initially randomly located chromosomes or reflects connections that have evolved following homology recognition remains to be determined (Loidl, 1990).

The third of the hypotheses proposed by Loidl (1990) describes random contacts at prophase as a mechanism for pairing of homologues. If homology is identified at some stage during prophase I by a trial and error system, then it follows that there must exist some system that increases the efficiency of random contacts. Dawe (1998) mentions that the formation of the so-called ‘bouquet’ structure during prophase, whereby chromosome telomeres cluster to a small region of the nuclear envelope, may provide a

possible mechanism to enhance the chance of homologous contacts. Perhaps the clustering of telomeres on the nuclear envelope generates a general stirring process that increases the chances of homologous contacts occurring. There is however considerable evidence that seems to cast doubt on the idea that the clustering of telomeres during formation of the bouquet provides a mechanism to increase chance contacts between homologous chromosomes. In maize for example, it has been shown that ring chromosomes lacking telomeres pair normally with homologous ring or rod chromosomes, and in addition, a normal meiotic pairing phenotype is observed for newly broken maize chromosomes that are deficient for their telomeres (McClintock, 1941; McClintock, 1951; Schwartz, 1953). Furthermore, cytological evidence with respect to the temporal positioning of telomeres on the nuclear membrane in relation to pairing processes has not supported a role of the bouquet in chromosome pairing (reviewed by Loidl, 1990).

1.5.1 Molecular mechanisms for homology recognition

It is logical to suggest that accompanying any cytological model of chromosome pairing exists a series of molecular recognition events that allow conformation of the homology at the DNA level.

In early biochemical analyses of meiosis in lily (Hotta and Stern, 1971), it was noted that segments of DNA constituting approximately 0.3 % of the genome are replicated at zygotene. These DNAs were subsequently called ‘zygDNA’, and it has been proposed that this DNA may functions in the recognition of homology at different sites along homologous chromosomes via the formation of DNA duplexes (Stern and Hotta, 1987). The replication of zygDNA is semi-conservative in character and occurs in the vicinity of the synaptonemal complex. It is widely distributed in all chromosomes and consists of 2.5 Kb to 10 Kb segments (Stern and Hotta, 1985) that are of low copy number. Disruption of DNA synthesis by the application of inhibitors during the leptotene to zygotene interval has been shown to prevent chromosome pairing and the formation of the synaptonemal complex (Roth and Ito, 1967). ZygDNA has only been convincingly demonstrated in *Lilium*, although it is also thought to exist in mouse (Loidl, 1990). ZygDNA is replicated by the separation of strands, followed by nicking whereby single-

stranded tails are formed. These become involved in the formation of duplexes from complementary zygDNA strands furnished by pairs of homologous chromosomes (Loidl, 1990). The results from studies of zygDNA indicate a potential role in the control of pairing processes during meiosis. Further studies investigating this role will need to investigate the presence of similar molecular events in other species.

Smithies and Powers (1986) proposed a modification of the model of biparental duplex formation above, and used it to explain the frequent occurrence of gene conversions. They suggested that gene conversions may be the result of a recognition process whereby single-stranded 'feelers' invade and scan any DNA duplexes that they encounter, and form a biparental duplex with homologous sequences that they encounter. According to these researchers, multiple adjacent duplexes would provide stable connections, allow formation of the synaptonemal complex, and gene conversions would result from resolution of the biparental duplexes. Carpenter (1987) also provided an idea based on the above models. Rather than preceding synapsis, this model proposed that the homology check followed synapsis. If homology between the biparental duplexes was sufficient, then the synaptonemal complex would extend along the synapsed chromosomes, whereas if homology between the duplexes was inadequate, the synaptonemal complex would immediately disassociate from the complex. Comings and Riggs (1971) suggested a model that involved pairing proteins that are capable of binding to specific base sequences. Allosteric changes in these proteins following pairing would allow them to bind to proteins that interacted with homologous sequences of DNA. Pairing proteins situated along the length of the chromosomes would provide stable interactions between homologous chromosomes.

1.6 Chromosome pairing in *Triticum aestivum*

1.6.1 Genetic control of chromosome pairing

The common bread wheat, *Triticum aestivum* is an allohexaploid consisting of three genomes, A, B and D, each having seven chromosomes. *T. aestivum* is a model example of an allopolyploid and is thought to have arisen from two successive hybridisation events and chromosome doublings, involving three different species; A genome from *Triticum urartu* (2x=14); B genome from *Aegilops speltoides* (2x=14) (Blake *et al.*,

1998); and the D genome from *Aegilops tauschii* (2x=14). In hybrids between these diploid ancestors, regular chromosome pairing is observed (Sears, 1941), which has indicated that the homoeologous chromosomes of these diploid species are very closely related. Studies in hexaploid wheat by Sears (1952) similarly indicated that the corresponding chromosomes of the three related genomes A, B and D are very closely related. He observed the ability of an extra dose (tetrasomy) of one chromosome to compensate for the absence (nullisomy) of either of the two homoeologues.

Chromosome pairing during meiosis in *T. aestivum* is confined to strict homologues, despite the co-existence in the genome of homoeologous chromosomes that share considerable homology. This control maintains the integrity of the three genomes, and the cytological outcome of this is the presence of bivalents at metaphase I (Riley and Chapman, 1958; Sears, 1976), regular segregation and disomic inheritance.

The genetic control of chromosome pairing in hexaploid wheat resides with a series of genes that suppress and promote pairing. The strongest effect on pairing is associated with a gene (or genes) at the *Ph1* locus (pairing homoeologous), on the long arm of chromosome 5B that suppresses homoeologous chromosome pairing within the polyploid wheat genome (Riley and Chapman, 1958; Sears and Okamoto, 1958). In the absence of *Ph1*, homoeologous recombination can occur between wheat chromosomes and those from related species or genera (Koebner and Shepherd, 1985; Riley *et al.*, 1966). Dosage effects of *Ph1* (from 0 to 6 copies) have been demonstrated to effect chromosome synapsis and associations (Holm, 1988a; Holm, 1988b; Holm and Wang, 1988). Two copies of *Ph* generates the highest level of synapsis with the lowest multiple chromosome associations.

In addition to the *Ph1* gene on chromosome 5BL, another suppressor of homoeologous chromosome pairing has been identified on the short arm of chromosome 3D (Driscoll, 1972; Mello-Sampayo, 1971; Mello-Sampayo and Canas, 1973; Mello-Sampayo and Lorente, 1968; Riley *et al.*, 1960; Uphadya and Swaminathan, 1967), and another on the short arm of chromosome 3A (Driscoll, 1972; Mello-Sampayo and Canas, 1973). The 3DS gene (named *Ph2*) is more effective than the gene residing on 3A, but only about half as effective as *Ph1* (Sears, 1976). Driscoll (1973), has identified a third, minor

suppressor of homoeologous chromosome pairing and the magnitude of its effect is smaller than the genes on 5BL, 3DS and 3AS. Evidence from hybrids with rye indicates that deficiency for both 3AS and 3DS (*Ph2*) results in a level of pairing almost as high as that presumed maximum in plants nullisomic for 5BL (*Ph1*) (Mello-Sampayo and Canas, 1973). Furthermore, pairing levels in plants nullisomic for 3AS and 3DS is beyond the individual additive effects of these two suppressors, indicating a combined effect of these two deficiencies.

In addition to the suppressors, a number of genes have been identified that promote homoeologous chromosome pairing in *T. aestivum*. Chromosome 5BS harbours a gene known to promote pairing, called *Ph3* (Feldman and Mello-Sampayo, 1967; Riley *et al.*, 1966). The effect of *Ph3* is substantially less than that of *Ph1*, as evidenced by increased levels of pairing in plants nullisomic for 5B (Sears, 1976). Other promoters of pairing are located on 5DL (Feldman, 1966; Feldman, 1968; Mello-Sampayo, 1972; Riley *et al.*, 1966), 5AL (Feldman, 1966; Feldman, 1968; Riley *et al.*, 1966), 3AL (Mello-Sampayo and Canas, 1973) and 3DL (Driscoll, 1972).

A number of mutations at *Ph* loci have been obtained. These mutants are of particular value to molecular studies of chromosome pairing in meiosis. Using X-ray irradiation, Sears (1977) induced an interstitial deletion at the *Ph* locus. The mutant, *ph1b* phenotypically resembles nullisomic and ditelosomic 5B plants. The deleted segment of chromosome 5B in the *ph1b* line has been estimated at approximately 70 Mb in size (Gill *et al.*, 1996; Gill *et al.*, 1993). In addition, Sears (1977) induced a large terminal deletion, encompassing the *Ph2* gene on part of the short arm of chromosome 3D. The resulting mutant is known as *ph2a*. Furthermore, a point mutation at the *Ph2* locus was induced using EMS (Wall *et al.*, 1971), and the resulting mutant called *ph2b*. Both *ph2a* and *ph2b* reveal higher levels of homoeologous chromosome pairing in wheat hybrids, but do not affect chromosome pairing in wheat itself (Sears, 1977).

1.6.2 Models that account for the action of *Ph*

A number of attempts have been made to provide models that account for chromosome behaviour in allopolyploid wheat, in particular in relation to how the *Ph1* gene could

operate. Perhaps the earliest of these was proposed by Ansley (1958), who noted that the ratio of DNA to histones was lower in cells undergoing synapsis. It was subsequently proposed that the action of *Ph1* could be to alter this ratio, and through an unknown mechanism somehow affect chromosome behaviour in relation to pairing. Some ten years later, Riley (1968) proposed a further hypothesis that attempted to explain the action of *Ph1*. The basis of this model was that homologous and homoeologous pairing were at least partially separated during prophase I. After imprecise association of homologous and homoeologous chromosomes during the first stage of this process, controls were implemented and pairing was then restricted to homologous chromosomes. Riley proposed that *Ph1* abolished the first stage of pairing and restricted the process to the pairing of homologues, and subsequently the strict formation of bivalents during the second stage. The removal of the *Ph1* product, as in nullisomic 5B plants or *Ph1* mutants, would result in a long attraction phase and permit the association of homologues as well as homoeologous chromosomes. In contrast, additional doses of *Ph1* would terminate the attraction phase early enough such that homologous and homoeologous chromosomes would fail to associate completely. In support for the model of Riley (1968), Bennett and Kaltsikes (1973) reported differences in prophase I duration for diploid rye, tetraploid and hexaploid wheat, and hexaploid triticale. This model was however rejected when it was found that the duration of meiosis did not correlate with the presence/absence of *Ph1* (Bennett *et al.*, 1974). Meiosis in *Ph1* and *ph1* plants was found to be similar in length.

A further model of *Ph1* gene action was provided by Feldman and colleagues (Avivi and Feldman, 1980; Avivi *et al.*, 1982; Feldman, 1968; Feldman and Avivi, 1984; Yacobi *et al.*, 1985a; Yacobi *et al.*, 1985b) that was based on premeiotic, or somatic associations of chromosomes prior to pairing. *Ph1* was proposed to mediate the premeiotic spatial distribution of chromosomes, such that homologues are more intimately associated than non-homologous and homoeologous chromosomes. Because of their close proximity, pairing is largely between homologues and bivalents are formed. In plants nullisomic for 5B, or in *Ph1* mutants, the absence of the *Ph* gene product would allow for more random distribution of chromosomes in the nucleus, such that meiotic pairing could include both homologous and homoeologous chromosomes. Six copies of the *Ph1* gene would further suppress somatic chromosome associations and result in a random distribution of

chromosomes in the premeiotic nucleus. Feldman (1966) conceived that meiotic attraction forces are not strong enough to cause pairing of the distantly separated chromosomes, resulting in partial asynapsis. Homoeologous pairing would take place when homoeologous chromosomes by chance lie in closer proximity to each other than homologues.

Evidence indicates that the influence of *Ph* may be via an effect on the spindle that determines chromosome positioning. Spindles in mitotic cells of *ph1* plants are more sensitive to the effects of colchicine than those of *Ph1* plants, and indeed increased dosage of *Ph1* reduces the effects of this drug on microtubules (Avivi and Feldman, 1973; Avivi *et al.*, 1970; Ceoloni *et al.*, 1984). Recently it has been shown that the *Ph1* locus affects the association of homologues via centromere interactions during premeiotic floral development, and the association of sub-telomeric regions via telomeric clustering at the onset of meiotic prophase (Martinez-Perez *et al.*, 1999). *Ph1* has also been shown to affect centromere structure (Aragon-Alcaide *et al.*, 1997a) and also recombination between homoeologous chromosomes or segments (Dubcovsky *et al.*, 1995; Luo *et al.*, 1996). Premeiotic or somatic association of homologous chromosomes has been observed in other organisms that include yeast (Loidl *et al.*, 1994; Weiner and Kleckner, 1994), *Drosophila* (Hiraoka *et al.*, 1993) and maize (Maguire, 1983).

The molecular basis for chromosomal recognition and pairing during early meiosis in hexaploid wheat remains a subject of debate. Studies using FISH on mutant lines of *Ph1* have helped our understanding of the mode of action of the *Ph1* gene(s). Mutants at *Ph1* have altered chromosome/chromatin organisation and compaction, not only in meiotic cells but also in somatic cells (Aragon-Alcaide *et al.*, 1997a; Mikhailova *et al.*, 1998; Vega and Feldman, 1998). Premature separation of sister chromatids and extension of the centromeric chromatin in univalents at anaphase I is apparent. Observations also show that there is breakage of centromeres such that the two arms of a chromatid (or chromatid pair) are estranged from one another (Aragon-Alcaide *et al.*, 1997a; Vega and Feldman, 1998). *Ph1* mutants also seem to have alterations in the relative arrangement of homologous chromosomes both in meiotic and somatic cells (tapetal cells) (Mikhailova *et al.*, 1998). It seems that *Ph1* specifies or affects some basic component of chromosome structure. The pairing promotion effect of the *ph1b* mutation appears to

be greater on distant homoeologous partner metaphase I associations, whereas that of *ph2b* seems to be evenly distributed among all types of homoeologous associations. It is also suggested that the resolution of wheat x rye metaphase I associations into wheat x rye recombination events in *ph2b* is lower than that for *ph1b* (Benavente *et al.*, 1998). This finding suggests that distinct mechanisms are involved in the control on homoeologous synapsis and/or chiasma formation by the two *Ph* genes. Further support for different modes of diploidisation by *Ph1* and *Ph2* has been provided by detailed ultrastructural analysis. Martinez *et al.* (2001) have shown that only a few nuclei accomplish synapsis (synaptonemal complex formation) in the *ph2b* genotype, whereas most nuclei complete synapsis in the wild-type and *ph1b* genotypes, suggesting that neither *Ph1* nor *Ph2* affect synaptic restriction to bivalents at early prophase but have different effects on later synaptic behavior. *Ph2* seems to affect synaptic progression, probably in a similar way to a diploid species. It has been suggested that *Ph2* itself may not represent a pairing homoeologous locus, as is the case for *Ph1*, but one affecting synaptic progression (Martinez *et al.*, 2001). It seems apparent that deletion of the *Ph1* locus may affect several premeiotic and meiotic processes (Feldman, 1993; Luo *et al.*, 1996; Shaw and Moore, 1998), and that both the *Ph1* and the *Ph2* loci are unlikely to be controlled by single genes (Roberts *et al.*, 1999).

Recently, reports on studies involving *Ph1* (reviewed in Moore, 2002) are beginning to shed light on the possible function of genes at this locus. *Ph1* has been delimited to a region on chromosome 5BL containing fewer than seven genes, however it is still not known wether the phenotype controlled by *Ph1* is the result of more than one gene in this region, or a heterochromatin region with epigenetic effect (Moore, 2002). Moore (2002) has proposed a functional model for the action of *Ph1* that results in chromosome 'stickyness' in its absence. The presence of *Ph1* may provide chromosomes with a coating, envisaged to resemble 'teflon'. This may increase specificity in the pairing process and facilitate enzymatic interaction involved in the correction of non-homologous chromosome associations, with the overall effect being to promote homologous pairing (Moore, 2002). Although evidence from studies investigating the comparative effects of *Ph1* and *Ph2* indicate distinct mechanisms of control over pairing and/or chiasmata formation (Benavente *et al.*, 1998; Martinez *et al.*, 2001), studies of *Ph1* are providing valuable clues about the behaviour of meiotic chromosomes in

hexaploid wheat and the effects exerted by *Ph* genes. This information will be of unquestionable benefit to studies involving other *Ph* loci, such as *Ph2*.

Our studies on chromosome pairing in wheat have focussed on cloning genes from the region deleted in the *ph2a* mutant. Different approaches have resulted in the isolation of a number of genes from this region. These include; *Ta*MSH7 (Dong *et al.*, 2002), *WM5* (Thomas, 1997), a novel Glycine-Serine-Proline-Alanine rich protein; the *WM1* gene family (Ji, 1992; Whitford, 2002), a novel family of leucine rich repeat proteins comprising approximately 21 members, eleven being located within the region of the *ph2a* deletion; and *WM3* (Letarte, 1996), a gene with weak similarity to lipid transfer proteins. Given the complexity of meiotic processes and evidence suggesting a multigenic control of pairing, we have pursued research towards a more thorough identification of the genes located in this region.

1.7 Conclusion

The global economic significance of wheat as a commodity and essential food source has ensured that attempts to provide a supply of genetic variability continue. Throughout the world there are approximately 25000 wild relatives of wheat that represent a vast and potentially important source of new variation. The chromosomes that carry these genes are homoeologous to those of modern wheat and subsequently will not ordinarily pair and hence recombine at meiosis. This is mainly due to the action of various *Ph* genes. The *ph1b* mutant has enabled suppression of this activity and has been utilised in breeding programs to allow the introgression of alien chromatin from related species into modern wheats (Gale and Miller, 1987). Its use has however been limited, and achieving the levels of pairing and recombination required can be laborious. Accumulating molecular evidence is suggesting that the major effect of *Ph1* is to bring about homologous chromosome recognition and alignment prior to meiosis, and not to affect recombination *per se*, such that its absence will not necessarily produce homologous chromosome recombination. An understanding of the molecular mechanisms that regulate events such as chromosome pairing and recombination during meiosis will set the stage for efficient manipulation of alien gene introgression towards agronomic and economic improvement.

1.8 Research aims

The aim of this research is primarily to explore the expressed portion of the wheat genome for genes involved in meiosis. Our current knowledge of the molecular basis for meiosis in wheat is limited, and most fundamental questions remain unanswered.

In relation to meiotic chromosome pairing, the cytogenetic effects of *Ph* genes have been intensively studied and well documented but the molecular aspects of their dynamic control remain unknown. What is the molecular basis for homology recognition and pairing during the early stages of meiosis in complex allopolyploids like wheat? What are these genes and how could they function during early meiosis? Do *Ph1* and *Ph2* represent single genes, or do these loci each represent several genes affecting this process? Furthermore, from a broader perspective of meiotic control, a number of questions remain to be answered. What genes are required for meiosis in wheat? Does the core meiotic transcriptome of wheat resemble that of other, more characterised species, and to what degree?

In an attempt to explore these important questions and contribute to our understanding of the molecular basis for meiosis in wheat, several genomics-based approaches for gene identification and analysis are adopted.

CHAPTER 2

GENERAL MATERIALS AND METHODS

Methods were carried out according to standard procedures (Sambrook *et al.*, 1989) or using manufacturers specifications (except where cited in text). Materials and methods used routinely, and for the purpose of generating general resources for use throughout this study are described below. Specific methods that were used in particular parts of this study are described in the individual Chapters.

2.1 Plant genetic stocks

Plant stocks of *Triticum aestivum* (cv Chinese Spring) were obtained from Dr Ken Shepherd, Department of Plant Science, University of Adelaide, Australia. The mutant lines, *ph2a*, *ph2b* and *ph1b* were obtained from Prof. Moshe Feldman, Plant Genetics Institute, Israel. Wheat nullisomic-tetrasomic lines were obtained from A. Lukaszewski, University of California, Riverside, CA, USA. All plants were grown in soil prepared by the plant growth facility at the Waite Institute (University of Adelaide), in 13 to 25 cm pots under glasshouse conditions at 18 °C to 25 °C.

2.2 Collection and meiotic staging of wheat anthers

Microscopic staging of wheat anthers was performed as follows. Whole spikes were collected from wheat plants grown in the glasshouse. Single spikelets were dissected from the rachis, and all three anthers removed from the primary floret. Two anthers were immediately frozen in liquid nitrogen and stored at –80 °C for later use. The remaining anther was fixed in a solution of ethanol:acetic acid (3:1) for several minutes and crushed in a drop of aceto-orcein on a microscope slide. A coverslip was placed on the slide and excess stain was blotted away gently under Whatmann 3MM paper. Meiocytes were viewed under a light microscope to determine developmental stage. For consistency, anther collection was performed where possible before mid-morning on the day of harvest.

2.3 Bacterial strains, cloning vectors and electrophoretic size markers

The *E. coli* strain DH5α (Stratagene, USA) was used for general manipulation of recombinant plasmids.

-*E. coli* DH5α genotype: F^-, lac ZΔm15, end A1, recA1, hsR17, (rk^-, mk^-), sup44, thi-1, 1^-, gyrA96, Δ(lacZYA-argF).

The plasmid vectors pBluescript (Stratagene, USA) and pGEMT (Promega, USA) were used for cloning restriction fragments and PCR products respectively. The plasmid vector pSPORT1 (Invitrogen, Australia) was used for cDNA library construction.

Size markers for electrophoresis were as follows;

DNA gels	λ DNA cut with *Hin*d III
	λ DNA cut with *Bst*E II/*Sal* I.
	pUC19 plasmid DNA cut with *Dra* I/*Rsa* I
RNA gels	0.28 Kb to 6.58 Kb RNA Marker (Promega, USA)

2.4 Bacterial preparations and plasmid transformation

Liquid bacterial cultures were inoculated and grown overnight on an orbital shaker at 37 °C in LB media (1 % (w/v) bacto-tryptone, 0.5 % (w/v) bacto-yeast extract, 1 % (w/v) NaCl, pH 7.5) containing 100 μg/mL ampicillin. Solid cultures were grown on LB agar (LB media plus 15 g/L bacto-agar) containing 100 μg/mL ampicillin overnight in a 37 °C incubator.

2.4.1 *E. coli* transformation via heat shock

Competent cells were prepared and used for plasmid transformation according to the Inoue Method (Inoue *et al.*, 1990). Briefly, a frozen stock of *E. coli* strain DH5α was streaked onto an agar plate and cultured overnight at 37 °C. Ten to twelve colonies were selected and inoculated to 250 mL of SOB medium (2 % (w/v) Bacto-tryptone, 0.5 % (w/v) Bacto-yeast extract, 10 mM NaCl, 2.5 mM KCl) and grown at 23 °C to an optical

density of 0.6 (OD_{600}) with vigorous shaking. The culture was cooled on ice and transferred to 200 mL centrifuge bottles and pelleted at 4000 rpm in a GSA rotor at 4 °C for 10 min. The pelleted cells were resuspended in 80 mL ice cold Transformation Buffer (TB) (10 mM Pipes, 55 mM $MnCl_2$, 15 mM $CaCl_2$, 250 mM KCl), incubated on ice for 10 min, and centrifuged as above. The cell pellet was resuspended in 20 mL TB and DMSO was added with gentle swirling to a final concentration of 7 %. Following incubation on ice for 10 min, the cell suspension was dispensed into 1.5 mL Eppendorf tubes, snap frozen in liquid nitrogen and stored at –80 °C. For transformation, an aliquot of frozen cells were thawed on ice and gently mixed. 100 μL cells were added to the plasmid DNA being transformed (1 μL to 5 μL). Cells/plasmid mix was incubated on ice for 30 min. Cells were heat shocked at 42 °C for 30 sec, and immediately placed on ice for 5 min. 400 μL SOC medium (SOB with 10 mM $MgSO_4$, 10 mM $MgCl_2$, 0.35 % (w/v) glucose) was added to the cell suspension followed by incubation at 37 °C for 60 min with gentle shaking. 100 μL to 200 μL of transformed cells were plated onto LB agar containing 100 μg/μL ampicillin, 0.004 % (w/v) X-gal and 0.1 mM IPTG, and grown at 37 °C overnight.

2.4.2 *E. coli* transformation via electroporation

Transformation using electroporation was used in preference to the heat shock method when higher transformation efficiencies were required. Electrocompetent cells were prepared and used for plasmid transformation according to the methods supplied with the Gene-Pulser (Bio-Rad, USA). Briefly, 1 L of LB medium was inoculated with 10 mL of an overnight culture of *E.coli* strain DH5α, and grown to an optical density of 0.9 (OD_{600}). The culture was chilled on ice, transferred to 200 mL centrifuge tubes and the cells pelleted in a GSA rotor at 3000 rpm for 15 min at 4 °C. Pelleted cells were gently resuspended in 500 mL of ice-cold 10 % glycerol (v/v) solution. The cells were pelleted as above, and resuspended in 20 mL of ice-cold 10 % glycerol solution. Cells were transferred to 30 mL tubes, pelleted in a HB4 rotor at 4000 rpm for 15 min at 4 °C, and resuspended in 2.0 mL of ice-cold, 10 % glycerol solution. The electrocompetent cells were transferred to 1.5 mL Eppendorf tubes in aliquots of 80 μL, snap frozen in liquid nitrogen, and stored at –80 °C. Transformation of electrocompetent cells with plasmids

was performed according to the recommendations supplied with the Gene-Pulser (Bio-Rad, USA). Electrocompetent cells (40 μL) were combined with 1.0 μL MilliQ H_2O containing 5.0 ng of plasmid DNA or 60 ng of DNA from a ligation reaction. The mixture was transferred to an ice-cold, disposable electroporation cell (0.1 cm electrode gap, supplied with the Gene-Pulser), and subject to electroporation using the following conditions; 1.8 kV, 125 μFD and 200 Ω. Immediately following electroporation, the cells were mixed with 1.0 mL LB broth and incubated at 37 °C on an orbital shaker. 100 μL to 200 μL of transformed cells were plated onto LB agar containing 100 μg/μL ampicillin, 0.004 % (w/v) X-gal and 0.1 mM IPTG, and grown at 37 °C overnight.

2.5 Electrophoretic separation of DNA samples

Electrophoresis was carried out using standard procedures. Gels were cast from 0.8 % to 2.5 % (w/v) agarose in 1x TAE buffer (0.04 M Tris-acetate, 1.0 mM Na_2EDTA, pH 8.0), depending on the degree of resolution required. DNA samples were mixed with 0.2 volumes of 6x Ficoll loading buffer (15 % (w/v) Ficoll 400, 0.25 % (w/v) bromophenol blue, 0.25 % (w/v) xylene cyanol). Gels were electrophoresed in 1x TAE buffer at 40 V to 100 V from 30 min to 16 h. DNA was visualised by ethidium bromide staining (5 μg/μL) and photographed under UV light at either 302 nm (preparative gels) or 260 nm (gels for Southern analysis).

2.5.1 Isolation of fractionated DNA fragments from agarose gel

The isolation of DNA fragments from agarose gel was performed following either the Geneclean method (Bio101, from Bresatec, Australia), or using the QIAquick Gel Extraction Kit (Qiagen, Australia). Following fractionation of DNA and ethidium bromide staining, desired bands were excised from the gel whilst viewing on a long wave ultraviolet transilluminator (340 nm) and purified according to the manufacturers instructions. DNA was either eluted or resuspended in an appropriate volume of either 1x TE buffer (10 mM Tris-HCl, 0.1 mM Na_2EDTA, pH 8.0) or nanopure water, depending on whether the DNA was to be used for labelling or ligation purposes respectively.

2.6 Phenol:chloroform extraction and ethanol precipitation of DNA

DNA solutions were mixed with one volume of phenol/chloroform/iso-amyl alcohol (25:24:1), briefly vortexed and centrifuged for 10 min at 13000 rpm in a benchtop centrifuge. The aqueous phase was recovered and the extraction repeated as necessary. DNA was routinely precipitated from solutions with ethanol. Briefly, $1/10^{th}$ volume of 3 M NaAc (pH 4.8) was added followed by 2.5 volumes of ice-cold ethanol. The solutions were incubated on ice for 15 min, followed by centrifugation as above. Pellets were washed in 70 % ethanol prior to drying in a speedyvac or on the bench at RT.

2.7 Nucleic acid preparations

2.7.1 Plasmid DNA extraction

The alkaline lysis method of Sambrook *et al*. (1989) was used for the mini-scale preparation of plasmid DNA. A sterile culture tube containing 5 mL LB medium with 100 μg/mL ampicillin was inoculated with a single transformed bacterial colony and grown overnight on an orbital shaker at 37 °C. Cells were pelleted by centrifugation at 6000 rpm for 4 min in a benchtop centrifuge and the supernatant discarded. Cells were resuspended in 200 μL plasmid I solution (50 mM glucose, 25 mM Tris-HCl pH 8.0, 10 mM Na_2EDTA) and placed on ice for approximately 10 min. Lysis of bacterial cells was by the addition of 300 μL freshly made plasmid II solution (0.2 N NaOH, 1 % SDS), followed by placement on ice for a further 10 min. Chromosomal DNA and cell debris were precipitated by the addition of 300 μL 3 M NaAc pH 4.8, followed by gentle inversion of the tube, and placement on ice for several minutes. Following centrifugation at 12000 rpm for 5 min, the supernatant was transferred into a fresh 2 mL centrifuge tube and plasmid DNA was precipitated by the addition of 1 mL isopropanol and incubation at –80 °C for 30 min. DNA was recovered by centrifugation at 12000 rpm for 15 min at 4 °C, the pellet washed once in 1 mL 70 % ethanol and dried under vacuum. The DNA was resuspended in 50 μL R40 (40 μg/mL RNase A in TE buffer) and extracted with an equal volume of phenol/chloroform/iso-amyl alcohol (25:24:1). Plasmid DNA was precipitated with $1/10^{th}$ volume of 3 M NaAc (pH 4.8) and 2 volumes of 99 % ethanol and incubated at –80 °C for 30 min to 1 h. DNA was recovered by

centrifugation at 12000 rpm for 15 min at 4 °C, washed twice with 70 % ethanol, dried under vacuum and resuspended in 25 µL 1x TE buffer.

2.7.2 Cereal genomic DNA extraction

2.7.2.1 Small scale genomic DNA extraction

The method used for the small-scale extraction of DNA from leaves was modified from Pallotta *et al*. (2000). A 10 cm long piece of healthy leaf was placed in a 2 mL Eppendorf tube and frozen in liquid nitrogen. The sample was then crushed with a small pestle to a fine powder after which 600 µL DNA extraction buffer (1 % sarkosyl, 100 mM Tris-HCl, 100 mM NaCl, 10 mM EDTA, pH 8.5) was added and homogenised with the leaf powder to form a slurry. Extraction was performed by adding 600 µL of cold phenol/chloroform/iso-amyl alcohol (25:24:1) followed by mixing on an orbital rotor for 10 min. The sample was centrifuged for 10 min at 20160x g and the supernatant transferred to a fresh tube to repeat the phenol extraction step. After the supernatant was collected, 60 µL of 3 M NaAc (pH 4.8) and 600 µL isopropanol were added followed by gentle mixing at RT to allow the DNA to precipitate. The DNA was then pelleted by centrifugation for 5 min at 13000 rpm in a benchtop centrifuge, and the supernatant discarded. After washing the pellet with 1 mL 70 % ethanol, the DNA was air-dried and resuspended overnight at 4 °C in 50 µL R40.

2.7.2.2 Medium scale genomic DNA extraction

Following the methods of Pallotta *et al*. (2000), 2 g of fresh leaf material was frozen in liquid nitrogen and ground into a fine powder using a mortar and pestle. Once thawed, 4 mL DNA extraction buffer (1 % sarkosyl, 100 mM NaCl, 100 mM Tris-HCl, 10 mM EDTA, pH 8.5) was added and the mixture homogenised into a slurry. The slurry was transferred to a 10 mL tube and 4 mL phenol/chloroform/iso-amyl alcohol (25:24:1) was added. After gentle mixing on a rotor for 15 min the sample was centrifuged in a swing out rotor for 10 min at 3200x g. The aqueous phase was carefully poured into a silica matrix tube (Vacutainer) and re-extracted with 4 mL phenol/chloroform/iso-amyl alcohol (25:24:1) for 10 min. After a further centrifugation the aqueous phase was transferred to a clean 30 mL corex tube and DNA was precipitated by the addition of 400 µL 3 M

NaAc (pH 4.8) and 8 mL 99 % ethanol. DNA was spooled onto a glass rod and transferred to a fresh 2 mL centrifuge tube containing 1 mL 70 % ethanol. After a brief centrifugation (10000 rpm, 2 min to 3 min) the ethanol was removed and the pellet was air dried. DNA was resuspended in 100 μL to 200 μL R40 overnight at 4 °C.

2.7.3 RNA extraction

Prior to RNA extractions, plasticware and solutions were autoclaved 2 to 3 times. Glassware and ball bearings were rinsed in RNase-free water and subsequently baked at 180 °C for 16 h.

2.7.3.1 Total RNA extraction

Total RNA was extracted from wheat tissues using Trizol Reagent (Invitrogen, Australia). A maximum of 100 mg tissue was placed into a 2 mL Eppendorf tube, and 3 small ball bearings were added to the tube. The sample was frozen in liquid nitrogen, and tissue was ground by vigorous vortexing for 20 seconds. The tube was refrozen in liquid nitrogen and vortexed for an additional 20 seconds. This procedure was repeated 6 to 10 times until a fine powder was produced. 1.5 mL of Trizol reagent was then added to the tube containing tissue powder and ball bearings and the extraction procedure carried out according to the manufacturer's recommendations. The method of grinding followed by extraction in the same tube enabled complete recovery of RNA from small quantities of tissue and was important for wheat anther extractions where very small amounts of tissue were available. RNA pellets were resuspended in 1x TE buffer and quantified spectrophotometrically (Section 2.9).

2.7.3.2 Poly(A) RNA purification

For small quantities of RNA, poly(A) RNA was purified using the Dynabeads mRNA DIRECT Micro Kit (Dynal, Norway) according to the manufacturer's directions. For larger preparations, the Poly(A)Purist mRNA Purification Kit (Ambion, USA) was used following included protocols. Where possible, poly(A) RNA was quantified spectrophotometrically (Section 2.9).

2.8 Subcloning of DNA sequences

2.8.1 Dephosphorylation of vectors

Twenty micrograms of the plasmid vector pBluescript (Stratagene, USA) was digested with an appropriate restriction enzyme for 2 h at 37 °C. The reaction was extracted once with phenol/chloroform/iso-amyl alcohol (25:24:1), the DNA precipitated and resuspended in 20 μL of TE buffer. An aliquot of 10 μg of the digested plasmid was taken for the de-phosphorylation reaction. To the aliquot of DNA was added, 2 μL of 10x reaction buffer (supplied by the manufacturer), 1 U of calf intestinal phosphatase (Boehringer Mannheim, Germany) and water to a total reaction volume of 20 μL. The reaction was incubated at 37 °C for 1 h, the phosphatase heat denatured at 65 °C for 10 min and a further 0.5 U was added followed with an incubation of 30 min at 37 °C to ensure complete de-phosphorylation. The reaction was extracted twice with phenol/chloroform/iso-amyl alcohol (25:24:1). The DNA was precipitated with two volumes of 99 % ethanol and recovered by centrifugation for 15 min at 12000 rpm at 4 °C. Resuspension of the digested, de-phosphorylated plasmid DNA was in TE to a final concentration of 25 ng/μL.

2.8.2 Ligation of DNA sequences into plasmid vectors

The efficient ligation of DNA sequences into plasmid vectors requires the concentration of foreign DNA termini to be approximately twice the concentration of termini of the plasmid DNA (Sambrook *et al.*, 1989). This is to maximise the formation of monomeric plasmid:foreign DNA chimeras, rather than favouring the ligation of vector to vector, or the re-ligation of digested vectors. Selected PCR products and restriction fragments for cloning were purified from agarose gel (Section 2.5.1). PCR generated fragments were ligated into the plasmid vector pGEMT in a reaction volume of 10 μL, containing approximately 10 ng isolated PCR fragment, 25 ng vector, 1x ligase buffer (supplied by the manufacturer) and 1 μL T4 DNA ligase (1 Weiss unit, Boehringer Mannheim, Germany). Restriction fragments were ligated into the plasmid vector pBluescript (Stratagene, USA), in a similar reaction volume of 10 μL, containing approximately 20 ng of isolated DNA fragment, approximately 25 ng of digested, de-phosphorylated vector, 1x ligase buffer (supplied by the manufacturer), 0.5 μL of 10 mM ATP (pH 7.0)

and 1 μL of T4 DNA ligase (1 Weiss unit, Boehringer Mannheim, Germany). Ligation reactions were incubated at 15 °C overnight, after which they were directly used for transformation of *E. coli* (Section 2.4.2).

2.9 Spectrophotometric quantification of DNA and RNA

Following the resuspension of DNA and RNA samples, concentrations were determined spectrophotometrically. Two microlitres of the nucleic acid solution was diluted in 998 μL water and absorbance at 200 nm to 280 nm was measured using a Shimadzu UV-160A spectrophotometer. Nucleic acid concentration was estimated from the following equation:

[DNA/RNA] (μg/μL) =A_{260} x conversion factor (0.05 for DNA, 0.04 for RNA) x dilution factor (500)

2.10 PCR conditions and amplification of cloned inserts

Cloned insert DNA in plasmid vectors was amplified using PCR. The oligonucleotide primers M13 -40P (5' CAG GGT TTT CCC AGT CAC GAC 3') and M13 RSP (5' ACA GGA AAC AGC TAT GAC CAT G 3') were used for clones in the plasmid vectors pBluescript (Stratagene, USA) and pSPORT1 (Invitrogen, Australia), and the primers SP6 (5' GAT TTA GGT GAC ACT ATA G 3') and T7 (5' TAA TAC GAC TCA CTA TAG GG 3') for clones in pGEMT (Promega, USA). Primers were synthesised using an Applied Biosystems 392 oligonucleotide synthesiser according to the manufacturer's instructions. PCR products were synthesised using the following reaction components in 50 μL total volume: 1x Taq DNA polymerase buffer, 0.2 mM each dNTP, 1.5 mM $MgCl_2$, 50 pmol each primer, 0.05 to 0.5 μg plasmid DNA (or 1 μL bacterial culture), and 1 U Taq DNA polymerase (Invitrogen, Australia). Reactions were performed in a PTC-150 Mini Cycler (MJ Research, USA) using the following thermocycling conditions; 94 °C for 8 min, followed by 30 cycles of 94 °C for 1 minute, 55 °C or 58 °C for 1 min, 72 °C for 2 min with a final step of 72 °C for 8 min. PCR products were fractionated on 1 % to 2 % agarose gels. Where amplification failed under these reaction and cycling conditions, $MgCl_2$ concentration and cycling conditions were optimised.

Gene specific PCR primers were designed using VectorNTI Suite Version 6.0 software (Informax Inc., USA).

2.11 Preparation and ^{32}P labelling of DNA probes

The random oligo-priming method (Feinberg and Vogelstein, 1983) was used to radioactively label purified DNA sequences. Approximately 50 ng (2 μL to 5 μL) of purified DNA insert was mixed with 3 μL (0.3 μg/μL) of random labelling primers and TE to 8.5 μL, and the solution was denatured in boiling water for 8 min. Immediately following denaturation the mix was placed directly onto wet ice for 5 min to allow primer annealing. Added to this was 12.5 μL of 2x random oligolabelling buffer [40 μM d(ATP, GTP, TTP), 100 mM Tris pH 7.6, 100 mM NaCl, 20 mM $MgCl_2$, 200 μg/mL acetylated DNase free BSA (Fraction V, Sigma)], 4 μL [α-^{32}P]-dCTP (Amersham Biosciences, Australia), and 1 μL (2 U, Boehringer Mannheim, Germany) of DNA polymerase (Klenow fragment). The reaction was incubated at 37 °C for 45 min to 60 min and subsequently run through a G-100 Sephadex column for separation of unincorporated nucleotides from labelled DNA fragments (Sambrook *et al*. 1989), or purified using a QIAquick PCR Purification Kit (Qiagen, Australia) according to the manufacturer's instructions. Probes were denatured in a boiling water bath for 8 min and rapidly chilled on ice prior to use.

2.12 Southern blot analysis

2.12.1 DNA digestion and fractionation

Approximately 20 μg of genomic DNA was digested for 5 h at 37 °C with 20 U to 30 U of restriction enzyme in 20 μL reaction volume containing 1x restriction buffer (supplied by the manufacturer), 4 mM spermidine and 100 μg/mL DNase free BSA. Enzymes used for generation of Southern blots included *Bam*H I, *Eco*R I, *Hin*d III, *Eco*R V, *Xba* I and *Dra* I. Complete digestion was desirable for the preparation of Southern blots, hence 1 μL of the reaction was fractionated on a 1 % mini-gel after the 5 h digestion period to observe the extent of digestion. If genomic DNA was partially digested after this time, a further 10 U of enzyme was added and reaction was further incubated at 37 °C for 1 h to

2 h. Digested DNA was mixed with 3 μL 6x Ficoll dye and fractionated on a 1 % agarose gel in 1x TAE buffer at 30V for 16 h. Following electrophoresis the gel was stained in ethidium bromide for 15 min and photographed under UV light using Polaroid 667 black and white film.

2.12.2 Transfer of DNA to nylon membranes

After staining with ethidium bromide, gels were soaked in denaturing solution (1.5 M NaCl, 0.5 M NaOH) for 20 min to break the H-bonds between complementary strands of DNA, and rinsed in 10x SSC (1x, 0.15 M NaCl, 15 mM trisodium citrate pH 7.0) for 2 min. The gel was inverted and placed on a pad of three Whatmann 3MM papers, layered on a sponge soaked in 20x SSC. Air bubbles were rolled out from in between the papers and the gel using a Pasteur pipette, to ensure an even transfer. A sheet of Hybond-N^+ nylon membrane (Amersham Biosciences, Australia), previously soaked in boiling water for several minutes was laid on top of the gel. Air bubbles were again removed from the transfer path. Above the membrane was placed three Whatmann 3MM papers soaked in 20x SSC, followed by a stack of paper towels 5 cm thick. A glass plate was placed on top of this apparatus to act as a weight. Transfer was allowed to proceed for 8 h to 10 h by capillary blotting (Southern, 1975), periodically re-soaking the sponge with 20x SSC. After transfer the blot was disassembled in reverse order, and the position of the wells marked on the membrane with a soft pencil. The membrane was rinsed in 5x SSC for 2 min and blotted dry on Whatmann 3MM paper. A pad of Whatmann 3MM paper soaked with 0.4 M NaOH was prepared on a glass plate and the membrane was laid onto this, DNA side up. Following fixing of the DNA for 20 min, the membrane was soaked in neutralising solution (1.5 M NaCl, 0.05 M Tris-HCl, 0.001 M Na_2EDTA, pH 7.2) for 5 min and further rinsed in 2x SSC for 5 min. The membrane was then blotted dry, sealed in a plastic bag and stored in the dark at 4 °C until required.

2.12.3 Hybridisation and autoradiography

Membranes were pre-hybridised in 10 mL of a solution containing 500 μL sterile nanopure water, 3 mL 5x HSB (3 M NaCl, 100 mM PIPES, 25 mM Na_2EDTA pH 6.8), 3 mL Denhardt's III (2 % (w/v) gelatine, 2 % (w/v) ficoll, 2 % (w/v) PVP, 10 % (w/v)

SDS, 5 % (w/v) tetra sodium pyrophosphate, filtered through 1MM Whatmann paper), 3 mL 25 % (w/v) dextran sulphate and 500 μL denatured salmon sperm DNA (5 μg/mL). Membranes were placed in hybridisation bottles (Hybaid, USA), and pre-hybridisation solution pre-warmed to 60 °C was added. Pre-hybridisation was at 65 °C from 4 h to overnight. Pre-hybridisation solution was replaced with hybridisation solution (same as pre-hybridisation solution), and the probe added directly to the bottle containing the membrane. Hybridisation was allowed to proceed overnight at 65 °C. Residual, unbound DNA was removed from membranes by washing under increasingly stringent conditions at 65 °C for 30 min. Washes were as follows: 2x SSC, 0.1 % SDS; 1x SSC, 0.1 % SDS; 0.5x SSC, 0.1 % SDS; and 0.1x SSC, 0.1 % SDS. Membranes were blotted dry, sealed in plastic bags and exposed to X-ray film at –80 °C for 6 h to 14 days, depending on the intensity of the signal. X-ray film was developed using a Curix60 X-ray developer. In cases of low signal intensity, or where quantification of signal intensities was required, membranes were exposed to a phosphor screen for 1 h to 48 h, and scanned using a phosphorimager.

2.13 Northern blot analysis

2.13.1 Formaldehyde gel electrophoresis

Fractionation of RNA was carried out in the presence of denaturing agents, to prevent the formation of secondary structures. Approximately 10 μg of total RNA per lane was fractionated on a 1 % agarose gel containing 2.2 M formaldehyde, 0.02 M MOPS pH 7.0, 5 mM sodium acetate and 1 mM Na_2EDTA. Prior to loading, RNA samples were dried under vacuum and mixed with 2 μL 10x MOPS/EDTA buffer (0.5 M MOPS, 0.01 M EDTA, pH 7.0), and 13.5 μL of a solution of formamide/formaldehyde/water (3.5:10:3.5). RNA was gently dissolved, heated to 70 °C for 10 min and chilled on ice for several minutes. One microlitre of RNA loading buffer (322 μL 10x MOPS/EDTA buffer, 5 mg xylene cyanol, 5 mg bromocresol green, 178 μL 37 % formaldehyde, 500 μL formamide, and 400 mg sucrose) was added to the RNA solution, and the sample loaded onto the gel. Electrophoresis buffer used was 0.02 M MOPS pH 7.0, 5 mM NaAc and 1 mM Na_2EDTA. Following electrophoresis the gel was stained in ethidium

bromide for 15 min, destained in nanopure water for several hours and photographed under UV light using Polaroid 667 black and white film.

2.13.2 Transfer of RNA to nylon membranes

RNA gels were soaked in 10x SSC for 20 min and RNA was transferred to a nylon membrane (Hybond-N^+, Amersham Biosciences, Australia) using the capillary transfer method described in Section 2.12.2. Upon completion of the transfer, the filter was rinsed in 4x SSC for 1 min, blotted dry on Whatmann 3MM paper and dried under vacuum at 70 °C for 30 min. The RNA was then crosslinked to the membrane by irradiation under shortwave UV light (15 W, 254 nm, 24 cm above filter) for 7 min. Membranes were sealed in plastic bags and stored in the dark at 4 °C until required.

2.13.3 Hybridisation and autoradiography

Membranes were pre-hybridised in hybridisation bottles (Hybaid, USA) containing hybridisation solution (3 mL 50x Denhardt's reagent (Sambrook *et al.*, 1989), 50 % (v/v) formamide, 5x SSPE (for 1 L 20x; 175.3 g NaCl, 27.6 g NaH_2PO_4, 7.4 g EDTA. pH 7.4), 10 % SDS and 100 μg/mL yeast RNA) overnight at 42 °C. Hybridisation solution was replaced prior to adding the probe and membranes were incubated for 12 h to 24 h at 42 °C. Following hybridisation, membranes were washed sequentially at higher stringencies for 30 min at 65 °C. Washes were as follows: 2x SSC, 0.1 % SDS; 1x SSC, 0.1 % SDS; 0.5x SSC, 0.1 % SDS; and 0.1x SSC, 0.1 % SDS. Membranes were blotted dry after washing, sealed in plastic bags and exposed to X-ray film at –80 °C for an appropriate time, depending on the signal intensity. X-ray film was developed using a Curix60 X-ray developer.

2.14 Removal of radioactive probe from membranes

Bound probe was removed from membranes by incubating them for 30 min in 500 mL of boiling stripping solution (0.1 % SDS, 2 mM Na_2EDTA, pH 8.0) for 30 min, or until solution had reached RT. Membranes were sealed in plastic bags and re-exposed to X-

ray film for 2 days to ensure efficient removal of probe. Membranes were stored in the dark at 4 °C.

2.15 cDNA library construction

Total RNA for cDNA library construction was prepared according to the method described in Section 2.7.3.1, and spectrophotometrically quantified according to the method in Section 2.9. Poly(A) RNA was prepared using the Poly(A)Purist mRNA Purification Kit (Ambion, USA) according to the manufacturer's instructions. cDNA synthesis and directional cloning was performed using the SuperScript Plasmid System for cDNA Synthesis and Plasmid Cloning (Invitrogen, Australia) according to the manufacturer's instructions. Recombinant plasmids were transformed into ElectroMAX DH10B electrocompetent cells (Invitrogen, Australia) using the Gene-Pulser (Bio-Rad, USA) with settings supplied by the manufacturer of the cells. Library size was estimated by counting the number of colonies resulting from plating serial dilutions of transformed cells. Average insert size of cDNA libraries was determined by randomly selecting 50 colonies, purifying plasmid DNA, releasing cDNA inserts by restriction enzyme digestion and analysing insert size by agarose gel electrophoresis.

2.16 Sequencing

Sequencing reactions were performed using the ABI PRISM Dye Terminator Cycle Sequencing Core Kit (Perkin Elmer, USA) according to the manufacturer's directions. M13 forward and reverse sequencing primers were used when sequencing from plasmid templates, and gene specific primers when using PCR products as the template. Sequencing reactions were run on a ABI 3700 DNA sequencer (PE Applied Biosystems, USA) at the Institute of Medical and Veterinary Science (IMVS), Adelaide, Australia. Sequence editing was performed using VectorNTI Suite Version 6.0 software (Informax Inc., USA).

CHAPTER 3

A COMPARATIVE GENETIC STUDY OF THE WHEAT *PH2* REGION[1]

Abstract

Colinearity in gene content and order between rice and closely related grass species has emerged as a powerful tool for gene identification. Using a comparative genetics approach, we have identified the rice genomic region syntenous to the region deleted in the wheat chromosome pairing mutant *ph2a*, with a view to identifying genes at the *Ph2* locus that control meiotic processes. Utilising markers known to reside within the region deleted in *ph2a*, and data from wheat, barley and rice genetic maps, markers delimiting the region deleted on wheat chromosome 3DS in the *ph2a* mutant were used to locate the syntenous region on the short arm of rice chromosome 1. A contig of rice genomic sequence was identified from publicly available sequence information and used in BLAST searches to identify wheat ESTs exhibiting significant similarity. Southern analysis using a subset of identified wheat ESTs confirmed a syntenous relationship between the rice and wheat genomic regions and defined precisely the extent of the deleted segment in the *ph2a* mutant. A 6.58 Mb rice contig, generated from 60 overlapping rice chromosome 1 PAC clones spanning the syntenous rice region has enabled identification of 218 wheat ESTs putatively located in the region deleted in *ph2a*. What seems to be a terminal deletion on chromosome 3DS is estimated to be 80 Mb in length. Putative candidate genes that may contribute to the altered meiotic phenotype of *ph2a* are discussed.

[1] The contents of this Chapter have recently been prepared in manuscript format for publication. The manuscript submitted for publication is presented here with nominal changes. As such, sections of the introduction to this Chapter are repeated from Chapter 1.

3.1 Introduction

Bread wheat (*Triticum aestivum*) contains three closely related genomes: A, B, and D. Chromosome pairing during meiosis in this allohexaploid is confined to strict homologues, despite the co-existence in the genome of homoeologous chromosomes. This control maintains the integrity of the three genomes, and the cytological outcome of this diploid-like behaviour is the presence of 21 bivalents at metaphase I. The genetic control of chromosome pairing in wheat is dependent on a series of suppressing and promoting *Ph* (pairing homoeologous) genes (for review, see Sears, 1976). The strongest effect on pairing is associated with a gene (or genes) at the *Ph1* locus on the long arm of chromosome 5B, that suppresses homoeologous chromosome pairing within the polyploid wheat genome (Riley and Chapman, 1958; Sears and Okamoto, 1958). In the absence of *Ph1*, homoeologous recombination can occur between wheat chromosomes and those from related species or genera (Koebner and Shepherd, 1985; Riley *et al.*, 1966). In addition to *Ph1*, two further suppressors of homoeologous chromosome pairing have been identified. These include *Ph2*, located on the short arm of chromosome 3D (Mello-Sampayo, 1971; Mello-Sampayo and Lorente, 1968; Uphadya and Swaminathan, 1967) and another suppressor of smaller magnitude located on the short arm of chromosome 3A (Driscoll, 1972; Mello-Sampayo and Canas, 1973). The *Ph2* gene is more effective than the gene residing on 3AS but only about half as effective as *Ph1* (Sears, 1976). Evidence from hybrids with rye indicates that deficiency for both 3AS and 3DS (*Ph2*) results in a level of homoeologous pairing almost as high as that presumed maximum in plants nullisomic for 5BL (*Ph1*) (Mello-Sampayo and Canas, 1973). An X-ray induced deletion at the *Ph2* locus, *ph2a* (Sears, 1982), and a chemically induced mutant, *ph2b* (Wall *et al.*, 1971), have demonstrated that removal of the *Ph2* gene induces an intermediate level of homoeologous chromosome pairing in wheat hybrids with alien species but does not affect chromosome pairing in wheat itself (Sears, 1977; Sears, 1982). These observations suggest *Ph2* will be a valuable resource for the introgression of alien genes from related species into bread wheat, with minimum disruption of endogenous homologous chromosome pairing.

The molecular basis for chromosomal recognition and pairing during early meiosis in hexaploid wheat remains a subject of debate. Studies using fluorescent *in situ* hybridisation on mutant lines at *Ph1* have helped our understanding of the mode of

action of the *Ph1* gene(s). Mutants at *Ph1* have altered chromosome/chromatin organisation and compaction, not only in meiotic cells but also in somatic cells (Aragon-Alcaide *et al.*, 1997a; Mikhailova *et al.*, 1998; Vega and Feldman, 1998). Premature separation of sister chromatids and extension of the centromeric chromatin in univalents at anaphase I is apparent. Observations also show that there is breakage of centromeres such that the two arms of a chromatid (or chromatid pair) are estranged from one another (Aragon-Alcaide *et al.*, 1997a; Vega and Feldman, 1998). *Ph1* mutants also seem to have alterations in the relative arrangement of homologous chromosomes both in meiotic and somatic cells (tapetal cells) (Mikhailova *et al.*, 1998). It seems that *Ph1* specifies or affects some basic component of chromosome structure. The greater pairing promotion effect of the *ph1b* mutation (an X-ray induced deletion) appears to be relatively more on distant homoeologous partner metaphase I associations, whereas the lower promoting effect of *ph2b* is evenly distributed among all types of homoeologous associations. It is also suggested that the resolution of wheat x rye metaphase I associations into wheat x rye recombination events in *ph2b* is lower than that for *ph1b* (Benavente *et al.*, 1998). This finding suggests that distinct mechanisms are involved in the control of homoeologous synapsis and/or chiasma formation by the two *Ph* genes. Further support for different modes of diploidisation by *Ph1* and *Ph2* has been provided by detailed ultrastructural analysis. Martinez *et al*. (2001) have shown that only a few nuclei accomplish synapsis (synaptonemal complex formation) in the *ph2b* genotype, whereas most nuclei complete synapsis in the wild-type and *ph1b* genotype, suggesting that neither *Ph1* or *Ph2* affect synaptic restriction to bivalents at early prophase but have different effects on later synaptic behavior. It has been suggested that *Ph2* itself may not represent a pairing homoeologous locus, as is the case for *Ph1* but one affecting synaptic progression (Martinez *et al.*, 2001). It seems apparent that deletion of the *Ph1* locus may affect several premeiotic and meiotic processes (Feldman, 1993; Luo *et al.*, 1996; Shaw and Moore, 1998) and that both the *Ph1* and the *Ph2* loci are unlikely to be controlled by single genes (Roberts *et al.*, 1999).

Our studies on chromosome pairing in wheat have focussed on cloning genes from the region deleted in the *ph2a* mutant. Different approaches have resulted in the isolation of a number of genes from this region. These include; *TaMSH7* (Dong *et al.*, 2002), a wheat homologue of the yeast DNA mismatch repair gene *MSH6*; *WM5* (Thomas, 1997),

a novel Glycine-Serine-Proline-Alanine rich protein; the *WM1* gene family (Ji, 1992; Whitford, 2002), a novel family of leucine rich repeat proteins comprising approximately 21 members, eleven being located within the region deleted in *ph2a*; and *WM3* (Letarte, 1996), a gene with weak similarity to lipid transfer proteins. Given the complexity of meiotic processes and evidence suggesting a multigenic control of pairing, we have pursued research towards a more thorough identification of the genes located in this region using comparative genetics. A number of recent comparative genetic studies involving species within the grass family have revealed conservation of both gene content and order at the map and megabase level (for review, see Gale and Devos, 1998). Genetic maps of the Triticeae (including wheat, barley, rye and wild relatives) have been compared to maps of rice, maize and oat (Ahn *et al.*, 1993; Smilde *et al.*, 2001; Vandeynze *et al.*, 1995) and have shown that molecular markers on the linkage maps for these species detected with the same probes, are essentially homosequential. The *Gramineae* share extensive synteny across their genomes, allowing for one species to serve as the base for comparative genomics within the family (Moore *et al.*, 1995). Indeed the genomes of nine different grass species can be described in terms of 25 rice linkage blocks (Gale and Devos, 1998).

Here we describe a cross-species approach for gene identification based on comparative genetics between rice chromosome 1 and wheat group 3 chromosomes that reveals synteny at the gene level in the genomic regions analysed, and the size and predicted genetic content of the region deleted in the wheat *ph2a* mutant.

3.2 Materials and Methods

3.2.1 Plant Materials

Wild-type, nullisomic-tetrasomic derivatives (kindly provided by A. Lukaszewski, University of California, Riverside, CA, USA), and mutants *ph2a*, *ph2b*, and *ph1b* of wheat (*Triticum aestivum* cv. Chinese Spring) were grown under glasshouse conditions at 15 °C (night) to 23 °C (day) with a 14 h photoperiod.

3.2.2 DNA isolation and Southern analysis

Plant genomic DNA extraction and Southern analysis was performed according to Pallotta *et al*. (2000). Wheat EST (expressed sequence tag) clones used as probes for Southern analysis were either obtained from the International Triticeae EST cooperative (ITEC, http://wheat.pw.usda.gov/genome/) as plasmid clones, or were PCR amplified from cDNA. Plasmid vectors were isolated and manipulated according to standard procedures (Sambrook *et al.*, 1989) and PCR amplification of insert DNA was performed according to standard thermal cycling conditions using M13 forward and reverse primers. PCR amplification from cDNA was performed using sequence specific primers designed from EST sequences using VectorNTI Suite Version 6.0 software (Informax Inc., USA). Gene specific primer sequences are shown in **Table 3.1**. Thermal cycling conditions were performed according to individual primer-set annealing temperatures. Fragments were electrophoresed on 1 % agarose gels and purified using a QIAquick gel extraction kit (Qiagen, Australia) according to the manufacturer's instructions. All DNA fragments used for Southern analysis were sequenced using the ABI PRISM dye terminator cycle sequencing core kit (Perkin Elmer, USA) to confirm identity. Probes for Southern hybridisation were prepared by labelling PCR products with [α-^{32}P]dCTP using 9-mer random primers in the presence of dATP, dTTP, dGTP, 1x reaction buffer and 1 U Klenow Polymerase (Invitrogen, Australia). Unincorporated nucleotides were removed using a QIAquick PCR purification kit (Qiagen, Australia) according to the manufacturer's instructions. Membranes were washed to 0.2x or 0.1x SSC, 0.1 % SDS at 65 °C and exposed to X-ray film (Fuji) at –80 °C for 2 days to 14 days.

3.2.3 Comparative mapping between wheat, barley and rice

WM5 (Thomas, 1997), *MSH7* (Dong *et al.*, 2002), *WM3* (Letarte, 1996) and several members of the *WM1* gene family (Ji and Langridge, 1994; Whitford, 2002) have been localised to the region deleted in the *ph2a* mutant. Using these markers in combination with RFLP probes (Australian Triticeae Mapping Initiative) localised both inside and outside the *ph2a* deletion, the GrainGenes database (http://grain.jouy.inra.fr/ggpages/) was screened for comparative genetic maps between the grasses. Utilising comparative anchor probes (Vandeynze *et al.*, 1995) bordering the *ph2a* deletion region in wheat, the

Table 3.1: Oligonucleotide primer sequences designed for amplification of selected wheat ESTs for Southern analysis. EST number refers to numbering in **Table 3.2** and **Figure 3.1**

EST number	EST name	Forward primer (5'→3')	Reverse primer (5'→3')	Product length (bp)
1	whoh19k18	ACAACAGGAACAATGACAGCATCAA	TGGAGACGACGAACTGCCTATATTC	470
2	WHE1141_D09_G17	CCAGCCTCAATTTCAGGAATCCA	CACATCGGTCACGGTAATATCACCA	399
6	WHE2623_G11_N21	CGCTTCATCCAGGTGCAGGA	CCTGGAACCCACTCAAATTGTGAC	452
8	whh22j01	AGTTGGGCCAAGTACATGTCCATTT	AAAGGGTACACAGCTTCAGGAGCA	550
10	G05_q343_plate_11	GCCGAGCTTTTGGCTAAGATGCGT	TGCGCCCATGAACTACAGCAGC	386
13	whsl14h10	AAGTTCAGTGTGTCTTGGTTGCAGC	CACATACTCATCGAGGGGCCCTT	498
19	TaLr1103F09	TGCAGTGATGGTGGGCTTCTTC	TTGCTGGATGCAAGTGAGATTGAG	360
25	WHE4122_C11_E22	TCGGCACGAGGCAAACTTCC	CCAGATTTTGCAAGTTGGCGGT	528
26	WHE0973_H03_P05	CTGGCCTGGCCGAGCTGTCATAGAA	TGCGCAAGGGGAAGCACGAA	468
30	WHE0952_D09_G18	TCAGTTCCTGGGTTCGATCGC	CCACCATTGCTTCCACCTTCAA	395
42	WHE1118_A07_A14	CCATCATAAGCGTATCCGGGGC	TGAGCTCCAGAAGACCGGGGAT	429
45	whdl25l15	TCTGGCAAGTCAACACTCTCTGGG	CCAAGTCGTACCTTGATGAACTCCA	482
46	WHE2869_D07_H13	CGCCACGGTGATCACGCTCTACAA	TCGGGATCTTGGCTCCTCGTCTTC	567
47	WHE3565_F09_L17	GATGGTGACCGCGAAGCTCA	GCCACTTTGCGAAGCGTGCA	521
48	whfl18d17	TCACAGCACTGCACAATGAGTATCG	CTCTTCAGGTCGACCGTGGAGTT	441
50	WHE1128_G11_N22	TGGTGATCCAGGTGGTGCCGTA	CCATAGAATGCCCCGAAACTGTACC	361
54	PSR6173	AGGTTCGACTTCCTCGTCAAGCG	GGCATACCATCAGCAACAAGAGCTC	485
55	whyd20c23	GTCGCACTCCTCCTCTCCTATCCT	ATCCAAGGACAGAGAGCGGCTC	850
56	whe9f22	AAGCCCGAGAACGCGCTCAA	CGAGCACTGTCCTGTATGTCTCCCA	472
60	whoh2e03	TTCTCCTTGGGTCATTCTAAACCGG	CATGTATCTGCGGAACTTCTCGGC	464
189	WHE2301-2304_H06_H06	ACCGGCACGAATCTTGGTCA	GCGAGTCTTTCTCATTAGCACCAGT	448

rice region syntenous to that deleted in the wheat *ph2a* mutant was identified from the Japanese Rice Genome Research Program (RGP, http://rgp.dna.affrc.go.jp/), as described in the PhD thesis of Whitford (2002).

3.2.4 Rice PAC contig assembly and consensus sequence generation

Rice P1 artificial chromosome (PAC) clones (65 in total) were selected from RGP to construct a contig spanning the region predicted to be syntenous to that deleted in the *ph2a* mutant of Chinese Spring wheat. All clones were derived from the japonica cultivar-group. Sequence data for each of the 65 identified PAC clones was publicly available through GenBank and RGP. VectorNTI Suite Version 6.0 software (Informax Inc., USA) was used to generate a consensus sequence from overlapping PAC clones, eliminating redundant sequence from subsequent database searches. RiceGAAS software (http://ricegaas.dna.affrc.go.jp/) was used for visualisation of predicted coding sequences.

3.2.5 Identification of wheat ESTs with similarity to rice contig

To identify wheat ESTs exhibiting similarity to the rice contig, the sequence was spliced into subcontigs of approximately 100 Kb, which were used in a BLAST 2.0 blastn (Altschul *et al.*, 1997) search of the GenBank *Triticum aestivum* EST database (29th Oct. 2002, 257022 entries) for wheat ESTs exhibiting significant similarity (i.e. E-value significance $\leq 1e^{-25}$). ESTs were selected as representatives for predicted coding sequences within the rice contig by assessing the significance and position of similarity, and EST length. Selected wheat ESTs were used in blastn searches of GenBank non redundant databases, and blastx searches of GenBank non redundant and SwissProt databases to investigate putative function. Putative functions were assigned after examining all results of database searches.

3.2.6 Electronic expression analysis

To investigate the expression of identified wheat ESTs in meiotic tissue of wheat, an electronic expression analysis was performed using sequence data from a wheat meiotic anther cDNA library. This library was constructed in our laboratory as part of related

research on wheat meiosis, from wheat anthers at meiotic stages pre-meiosis to metaphase I inclusive. At the time of analysis, 9139 ESTs were available from this library, publicly available through GenBank (library name; wheat meiotic anther cDNA library, accession numbers CA483770-CA487130, CA496948-CA502725). Each of the selected wheat ESTs from database searches was used in a blastn search of this library to identify identical, representative sequences. To ensure that only identical, and not related sequences were identified from this analysis, an E-value cut-off significance level of $\leq 1e^{-80}$ was used.

3.3 Results

3.3.1 Identification of the rice region syntenous to the *ph2a* deletion in wheat

Comparative maps of wheat, barley and rice were analysed for molecular markers surrounding the postulated breakpoints of the *ph2a* deletion on 3DS of wheat. Previous studies (Thomas, 1997) had loosely localised the wheat region onto a barley consensus map (Langridge *et al.*, 1995), utilised because of a lack of suitably dense maps for wheat. This information and analysis enabled the identification of RFLP markers putatively located in the region flanking the wheat *ph2a* deletion that could be physically placed across comparative maps, in particular that of rice. These markers were used in BLAST searches of rice genomic sequence to identify rice PAC clones representing the regions syntenous to the predicted *ph2a* deleted segment on 3DS. We also used the gene markers *WM1.1*, *MSH7*, *WM5* and *WM3*, known to be located in the *ph2a* deleted region, to confirm identification of the rice region of interest. Homologues of these genes are present on the rice chromosome 1 sequence identified. Markers are ordered on rice chromosome 1 as follows; *WM1.1*, *MSH7*, *WM5* and *WM3* with the *WM1.1* gene located distal and *WM3* located proximal to the centromere.

3.3.2 Rice PAC physical map and consensus sequence construction

Comparative mapping highlighted 65 rice PAC clones located in the rice chromosome 1 short arm region (http://rgp.dna.affrc.go.jp/) predicted to be analogous to the region deleted in *ph2a* on wheat chromosome 3DS, representing a single contig spanning this rice region. To reduce double handling of redundant sequence from overlapping regions

of PACs, we generated a consensus sequence using Vector NTI Suite Version 6.0 software (Informax Inc., USA) that eliminated approximately 2.65 Mb of redundant sequence from overlapping PAC regions. RiceGAAS gene prediction software (http://ricegaas.DNA.affrc.go.jp/) indicated the presence of approximately 1500 coding sequences from this region. **Figure 3.1** illustrates the physical alignment of identified rice PAC clones and the resulting consensus sequence.

3.3.3 Identification of wheat ESTs from rice consensus

Although the rice region identified highlights potential coding sequences through automated gene prediction, there was no evidence that orthologous genes were present or even expressed in wheat. To address this problem the rice consensus sequence was used in blastn searches to identify wheat ESTs exhibiting significant similarity. We chose a significance level (E-value cut-off) of $1e^{-25}$ in blastn searches, for several reasons. Firstly, to ensure maximum likelihood of identifying potential wheat ESTs similar to the region given the expected differences between wheat and rice coding sequences at the DNA level. Secondly, although initial mapping with probes selected at a lower stringency of $1e^{-22}$ (for example, clone WHE1111_G08_N15, #174 in **Figure 3.1** and **Table 3.2**) resulted in positive assignment to the wheat *ph2a* deletion region, database searches at higher stringency would reduce the numbers of false ESTs identified. Clones previously identified using less stringent cut-off levels that have been positively assigned to the wheat *ph2a* deletion region by Southern analysis, have been included in this analysis. The results of BLAST searches using the rice consensus sequence against the wheat EST database were initially sorted according to regions of alignment. As expected, many regions from the rice sequence that code for highly expressed genes, identified large numbers of wheat ESTs in BLAST searches. In regions producing greater than one wheat EST hit, a representative was selected. The criteria for representative selection was based on the degree of similarity and EST length. In total, 306 wheat ESTs with similarity to the rice PAC consensus were selected. Of these, 99 % corresponded to predicted rice genes using RiceGAAS (http://ricegaas.dna.affrc.go.jp/). Where appropriate, ESTs originating from ITEC were selected due to accessibility of cDNA clones from this repository. To assess potential function of the ESTs identified, blastx searches were carried out against GenBank non-redundant and SwissProt

Figure 3.1: Wheat ESTs identified from the rice chromosome 1 region syntenous to the *ph2a* deletion in wheat.

Rice chromosome 1 PAC clones are represented by horizontal red bars with names and sizes in Kb written below. Grey sections at the ends of rows indicate continuation of the contig. Horizontal black lines represent the rice consensus sequence from overlapping rice PAC clones. Vertical lines represent wheat ESTs with significant similarity to the rice consensus. Black triangles represent wheat ESTs located by Southern analysis proximal to the predicted breakpoint (indicated by double headed arrow) in the wheat *ph2a* mutant. Green and red vertical bars and triangles represent wheat ESTs located by Southern analysis to be IN or OUT, respectively, of the *ph2a* deleted segment on wheat chromosome 3DS. Blue shaded boxes indicate the number of predicted genes from the corresponding rice consensus sequence. Each box corresponds to ~100 Kb rice sequence and is colour coded according to the scale below the figure, with a darker colouring reflecting a higher gene density. ESTs are numbered 1 to 306 (refer to **Table 3.2** for details) directly below the rice consensus. Rice genetic positions of the outermost rice PAC clones are beneath the name and size information. Orientation of the consensus with respect to the telomere and centromere is indicated. The positions of genes *WM1.1*, *MSH7*, *WM5* and *WM3* are indicated by text above appropriate vertical bars and triangles.

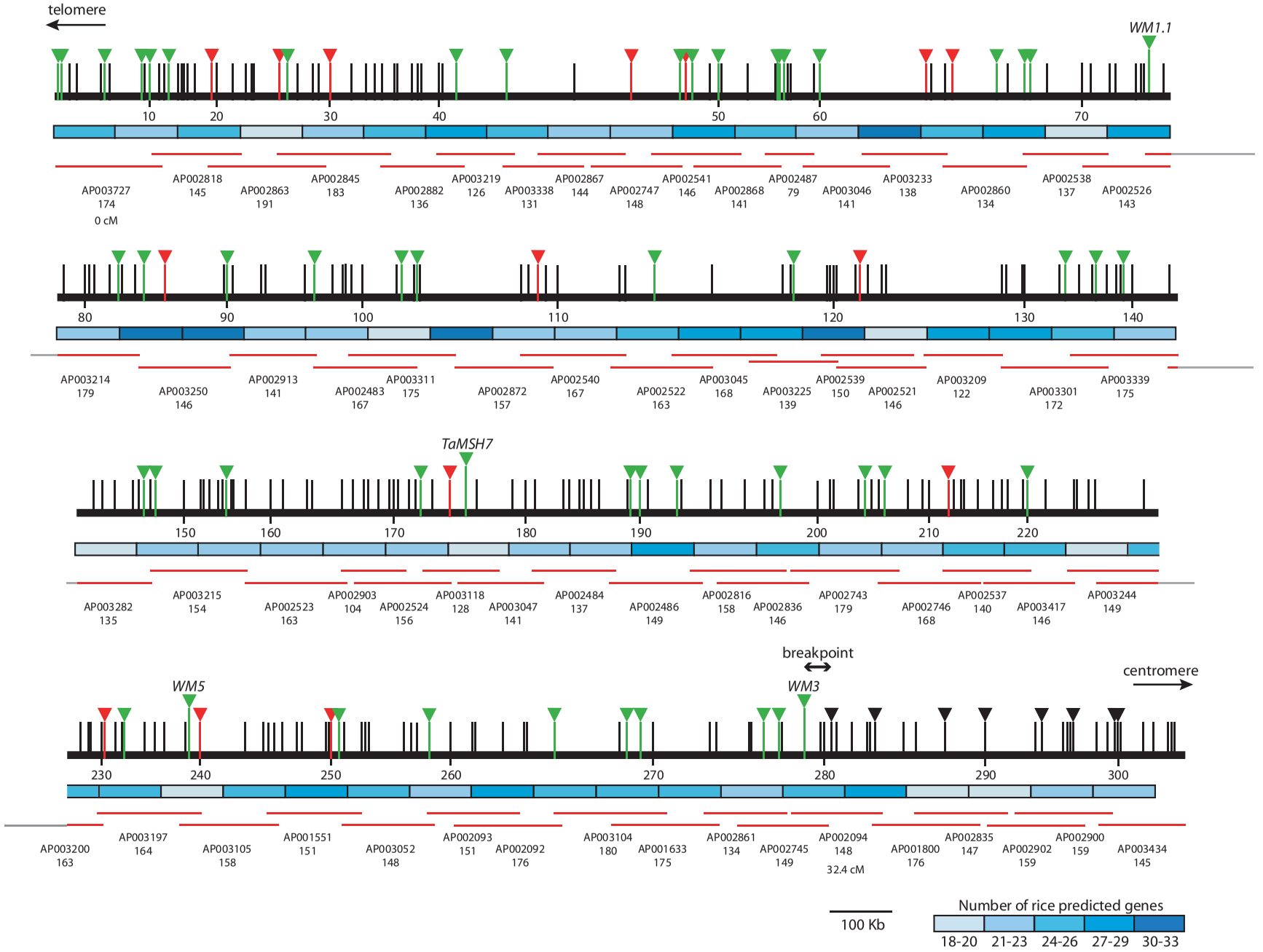
telomere
WM1.1
10
20
30
40
50
60
70
AP003727
174
0 cM
AP002818
145
AP002863
191
AP002845
183
AP002882
136
AP003219
126
AP003338
131
AP002867
144
AP002747
148
AP002541
146
AP002868
141
AP002487
79
AP003046
141
AP003233
138
AP002860
134
AP002538
137
AP002526
143
80
90
100
110
120
130
140
AP003214
179
AP003250
146
AP002913
141
AP002483
167
AP003311
175
AP002872
157
AP002540
167
AP002522
163
AP003045
168
AP003225
139
AP002539
150
AP002521
146
AP003209
122
AP003301
172
AP003339
175
TaMSH7
150
160
170
180
190
200
210
220
AP003282
135
AP003215
154
AP002523
163
AP002903
104
AP002524
156
AP003118
128
AP003047
141
AP002484
137
AP002486
149
AP002816
158
AP002836
146
AP002743
179
AP002746
168
AP002537
140
AP003417
146
AP003244
149
breakpoint
centromere
WM5
WM3
230
240
250
260
270
280
290
300
AP003200
163
AP003197
164
AP003105
158
AP001551
151
AP003052
148
AP002093
151
AP002092
176
AP003104
180
AP001633
175
AP002861
134
AP002745
149
AP002094
148
32.4 cM
AP001800
176
AP002835
147
AP002902
159
AP002900
159
AP003434
145
100 Kb
Number of rice predicted genes
18-20
21-23
24-26
27-29
30-33

Table 3.2: Details of wheat ESTs identified from the rice chromosome 1 region syntenous to the *ph2a* deletion in wheat.

[a] Clone numbers refer to numbering of wheat ESTs in **Figure 3.1**.
[b] Shading indicates clones that are present in the GenBank wheat meiotic anther cDNA library (Section 3.2.6).
[c] Data from Southern analysis is shown. Clones located within the region deleted in the *ph2a* mutant are indicated with IN, clones located outside the region deleted in the *ph2a* mutant are indicated with OUT. Clones not yet examined have been left blank.
[d] Species abbreviations: *Arabidopsis thaliana*, *At*; *Actinidia chinensis*, *Ac*; *Brassica rapa*, *Br*; *Cicer arietinum*, *Cc*; *Citrus limon*, *Cl*; *Dactylis glomerate*, *Dg*; *Deinococcus radiodurans*, *Dd*; *Gossypium hirsutum*, *Gh*; *Homo sapiens*, *Hs*; *Hordeum vulgare*, *Hv*; *Lupinus luteus*, *Ll*; *Lycopersicon esculentum*, *Le*; *Medicago sativa*, *Ms*; *Musa acuminata*, *Ma*; *Nicotiana tabacum*, *Nt*; *Nostoc* sp, *N*; *Oryza sativa*, *Os*; *Pisum sativum*, *Ps*; *Triticum aestivum*, *Ta*; *Zea mays*, *Zm*.
[e] The similarity of *WM1.1* to the homologous rice gene is low. Its position in the rice contig (**Figure 3.1**) was determined from structural analysis of genes residing in close proximity to *WM1.1*.
[f] This clone is representative of *WM5*.
[g] This clone is representative of *WM3*.
* Indicates a representative wheat EST identified from regions of repetitive rice sequence.

Wheat EST Identified					Predicted Function	
Fig 1[a]	Clone name[b]	GB Accn.	Similarity to rice Contig (E-value)	Southern analysis[c]	Best BLAST match[d]	E-value
1	whoh19k18*	BJ273901	7e-44	IN	putative protein [At]	2e-16
2	WHE1141_D09_G17	BE446088	1e-110	IN	pectinesterase (pectin methylesterase) [At]	3e-60
3	whyf10m08	BJ318267	2e-90		40S ribosomal protein S5 [Cc]	6e-90
4	WHE2602_H08_O16	BM136115	6e-63		putative sphingosine-1-phosphate lyase [Os]	2e-70
5	whdl13g10	BJ227358	8e-56		hypothetical protein [At]	7e-19
6	WHE2623_G11_N21	BM135760	1e-54	IN	DnaJ-like protein [At]	8e-28
7	whh2k22	BJ255857	2e-25		putative phospholipase [Os]	1e-96
8	whh22j01	BJ259861	1e-60	IN	hypothetical protein [Os]	6e-80
9	BRY_1230	BQ605703	2e-31		unknown protein [Os]	4e-62
10	G05_q343_plate_11	AL830011	6e-35	IN	putative DNA repair and recombination protein [Os]	1e-43
11	WHE4163_A08_A15	BQ839160	3e-34		hypothetical protein [Os]	1e-106
12	WHE0488_A10_A20	BM134279	1e-51		peptide transporter-like protein [Os]	2e-58
13	whsl14h10	BJ296750	4e-39	IN	3-beta-hydroxysteroid-delta(8),delta(7)-isomerase [Os]	6e-98
14	whdl8d20	BJ228793	4e-27		unknown protein [Os]	1e-32
15	D10_q343_plate_3	AL830295	1e-100		putative receptor ser/thr protein kinase [Os]	4e-68
16	wh27k14	BJ210385	6e-35		RING finger-like protein [At]	4e-67
17	WHE1755-1758_L19_L19	BE637768	6e-35		putative jasmonic acid regulatory protein [At]	3e-56
18	WHE1121_E09_I17	BE443677	7e-44		r40c1 protein [Os]	6e-65
19	TaLr1103F09*	BG909449	2e-62	OUT	tDET1 protein [Le]	2e-44
20	whf8i13	BJ248902	1e-36		unknown protein [Os]	1e-65
21	whr19k01	BJ280905	4e-27		cellulose synthase-9 [Zm]	1e-89
22	WHE0976_D06_G12	BE499944	8e-56		putative ribokinase [At]	3e-63
23	TaE05017D10R	BQ240436	7e-44		AtRer1B [At]	3e-19
24	whh7j02	BJ258409	2e-84		isoflavone reductase homolog IRL [Zm]	5e-83
25	WHE4122_C11_E22	BQ753044	5e-48	OUT	ataxia-telangiectasia mutated protein (Atm) [At]	6e-69
26	WHE0973_H03_P05	BE499313	1e-54	IN	1-deoxy-d-xylulose-5-phosphate reductoisomerase [Os]	1e-100
27	WHE4117_A10_A19*	BQ752609	3e-89		putative protein kinase [Os]	4e-83
28	WHE2065_B05_D09	BG313951	3e-95		unknown protein [Os]	4e-84
29	WHE0606_C01_E02	BE515833	2e-28		hypothetical protein [Os]	4e-41
30	WHE0952_D09_G18	BE498369	1e-113	OUT	Prolyl endopeptidase [Hs]	1e-62
31	whyf27l17	BJ322896	1e-30		hypothetical protein [Os]	1e-36
32	TaLr1174E09	BG909152	6e-26		putative protein [At]	2e-35
33	WHE4114_E12_I24	BQ744350	2e-62		putative co-repressor protein [Os]	e-116
34	whf23m12	BJ255444	1e-94		hypothetical protein [Dd]	4e-12
35	WHE0975_G10_M19	BE499733	7e-38		acetoacetyl-CoA thiolase [At]	1e-50
36	whoh3m20	BJ267114	3e-40		putative protein kinase [Os]	6e-81
37	WHE0367_B04_C07	BE490559	3e-37		leucine rich repeat protein family [At]	5e-16
38	SCL074.G11	BE418762	1e-76		hypothetical protein [Os]	6e-65
39	whyf12e05	BJ312833	2e-50		unknown protein [Os]	8e-47
40	TaE15020G05R	BQ245742	1e-26		hypothetical protein [Os]	6e-31
41	WHE0987-0990_J21_J21	BE500624	6e-26		no homologies found	
42	WHE1118_A07_A14	BE444341	1e-54	IN	unknown protein [Os]	1e-86
43	WHE1651-1654_C21_C21	BE591959	6e-29	IN	putative receptor serine/threonine kinase [Os]	8e-56
44	whoh15l02*	BJ273126	1e-57		TAK33 [Ta]	4e-75
45	whdl25l15	BJ226257	1e-121	OUT	putative eukaryotic release factor [Os]	1e-83
46	WHE2869_D07_H13	BQ295387	6e-35	IN	putative nodulin [Os]	2e-94
47	WHE3565_F09_L17	BQ805336	7e-81	OUT	fructose-bisphosphate aldolase 1, chloroplast precursor [Ps]	7e-92
48	whf18d17*	BJ251015	3e-46	IN	putative ATP-dependent RNA helicase A [Os]	9e-84
49	whdl16i14	BJ222861	5e-54		hypothetical protein [Os]	1e-74
50	WHE1128_G11_N22	BE444237	2e-65	IN	unknown protein [Os]	6e-38
51	JA1_4A_F02_T3	BE213544	4e-30		hypothetical protein [Dd]	2e-24
52	WHE3005_A05_A09	BQ280798	1e-42		no homologies found	
53	TaLr1147F05	BG906227	7e-41		hypothetical protein [Os]	7e-29
54	PSR6173	BE427255	2e-53	IN	fruit protein PKIWI502 [Ac]	1e-39
55	whyd20c23	BJ303565	1e-67	IN	unknown protein [Os]	2e-05
56	whe9f22*	BJ234265	1e-140	IN	Eukaryotic translation initiation factor 3 subunit 10 [Zm]	2e-91
57	WHE3455_C03_E05	BI479572	1e-29		SLL2-S9-protein [Br]	1e-48
58	WHE2321_C04_E07	BF484268	4e-27		putative nucleoside triphosphatase [At]	7e-18
59	WHE2868_A09_A18	BQ295265	1e-54		ABC transporter family protein [At]	1e-107
60	whoh2e03	BJ266828	2e-93	IN	N-acetylglucosaminyltransferase family protein [At]	1e-50
61	whoh15f01*	BJ273051	6e-29	OUT	hypothetical protein [Os]	1e-37
62	WHE0981_H10_P19	BE500242	1e-163		putative WD40-repeat protein [Os]	1e-39
63	JA1_5A_A06_T3*	BE216983	1e-142		putative spore coat protein [At]	5e-63
64	WHE1768_B02_C04	BF202992	2e-43	OUT	putative transcription factor [Os]	6e-35
65	WHE1107_H10_P19	BE442823	9e-56	IN	putative receptor-like protein kinase [Os]	2e-95
66	whh13d18	BJ257729	2e-50		putative mannose-6-phosphate isomerase [Os]	3e-89
67	WHE0765_E03_J05	BE497202	3e-40	IN	putative bifunctional nuclease [Os]	2e-81
68	WHE2321_A08_A15	BF484250	2e-28	IN	unknown protein [Os]	6e-52
69	WHE2506_F07_K14	BG604370	6e-60		unknown protein [At]	3e-54
70	whoh8m24	BJ270637	5e-47		unknown protein [Os]	8e-65
71	wh14i21	BJ216968	1e-121		unknown protein [Os]	4e-71
72	TaE05008B12R	BQ241187	8e-62		alpha-glucosidase precursor (maltase) [Hv]	3e-48
73	MUG021.B08	BE417453	8e-28		hypothetical protein [Os]	2e-23

Wheat EST Identified					Predicted Function	
Fig 1[a]	Clone name[b]	GB Accn.	Similarity to rice Contig (E-value)	Southern analysis[c]	Best BLAST match[d]	E-value
74	WHE0873_H10_P19	BG262284	7e-32		putative AP2 domain protein [Os]	5e-37
75	whyf21e19	BJ321529	2e-27		probable microsomal signal peptidase 22 kDa subunit [Os]	8e-67
76	WHE3027_E07_J13	BQ281977	1e-47		wound induced protein homolog [Os]	1e-47
77	*WM1.1*	X81369	note[e]	IN	putative Cf2/Cf5 disease resistance protein [Os]	6e-94
78	P39-4H	AW448346	4e-43		putative protein similar to *Mus musculus* SURF-5 gene [Os]	2e-53
79	WHE3026_A10_A20	BQ281843	5e-36		CRS2 [Zm]	8e-38
80	WHE3087_F04_K07	BQ283218	6e-41		hexose transporter [Zm]	3e-78
81	wh15p06	BJ217292	1e-27		unknown protein [At]	2e-30
82	WHE0427_A05_B09	BE403480	4e-26		hypothetical protein [Os]	1e-41
83	WHE1204_F07_L14	BE404301	1e-73		sterol-C5(6)-desaturase [Nt]	1e-86
84	WHE1451_A05_A09	BE445620	2e-38	IN	putative calmodulin-binding protein [Os]	2e-80
85	WHE2151_F07_K13	BF293281	1e-102		(1,4)-beta-xylan endohydrolase [Ta]	1e-116
86	WHE1659-1662_O23_O23	BE591405	5e-84		unknown protein [Os]	2e-42
87	WHE0765_C03_F05*	BE497181	1e-115	IN	heat shock protein 16.9B [Ta]	0
88	WHE2301-2304_B17_B17*	BF482732	2e-46	OUT	putative protein kinase [At]	3e-35
89	whsl22n20	BJ297977	2e-58		unknown protein [Os]	2e-40
90	WHE0973_C12_F23	BE499361	1e-104	IN	muconate cycloisomerase-like protein [Os]	7e-77
91	WHE0491_A12_A23	BM138310	6e-31		unknown protein [Os]	2e-48
92	MWL025.G03	BE415226	7e-34		unknown protein [Os]	2e-48
93	SCU004.D05	BE413918	1e-124		ribosomal protein L26 [Zm]	1e-126
94	WHE1788_A09_A18	BF484074	4e-42		putative DNA binding protein RAV2 [Os]	6e-34
95	WHE1121_F09_K17	BE443665	8e-52	IN	putative ATPase [At]	3e-94
96	WHE0435_C04_F07	BE403664	4e-26		hypothetical protein [Os]	9e-59
97	whh25k02	BJ260558	1e-90		CL50999_-1 mRNA sequence [Zm]	5e-33
98	whf8e23	BJ248853	5e-44		unknown protein [Os]	8e-97
99	TaLr1168A07	BG908437	2e-34		putative SqdX protein [Os]	2e-67
100	JA1_5C_H06_T3	BE217067	1e-78		peptide transporter [Hv]	1e-113
101	whr12j10	BJ282876	3e-48		putative peroxisomal Ca-dependent solute carrier protein [Os]	3e-65
102	WHE2117_H04_O07	BG275108	3e-33	IN	unknown protein [Os]	2e-45
103	whyd5g04	BJ306791	1e-41		unknown protein [Os]	3e-57
104	WHE1071-1074_F14_F14	BE489765	2e-64	IN	unknown protein [Os]	7e-53
105	whf19f19	BJ251268	3e-36		hypothetical protein [Os]	3e-45
106	WHE2342_C01_E02	BG263455	3e-33		putative UDP-glucuronyltransferase-like protein [Os]	3e-81
107	JJL005.C07	BE412338	4e-57		unknown protein [Os]	8e-37
108	WHE0973_G06_N11	BE499321	1e-81	OUT	unknown protein [Os]	3e-31
109	SCL074.D04*	BE418733	1e-32		triose-phosphate isomerase [Ta]	1e-104
110	whyf5i12	BJ319207	2e-40		putative CER3 [Os]	2e-71
111	WHE0331_B09_D17	BE426723	1e-140		putative glycoprotein [Os]	3e-98
112	WHE0443_C01_F01	BE404513	4e-29		putative protein phosphatase [At]	4e-81
113	WHE1126_G04_M08	BE444620	1e-141	IN	SLT1 protein [At]	1e-66
114	MUG002.E04*	BE415927	1e-122		histone H2B.2 [Ta]	5e-57
115	whh5n18	BJ263713	2e-31		unknown protein [Os]	2e-54
116	PSR123	AJ440545	6e-62		putative receptor-like protein kinase [Os]	3e-42
117	WHE0984_F02_K04	BF202262	6e-28	IN	splicing factor-like protein [At]	2e-31
118	WHE2456_G04_M08	BG312678	3e-33		DNAJ protein-like [At]	1e-31
119	whf3b01	BJ247635	2e-64		unknown protein [Os]	3e-93
120	whdl20e13	BJ229817	5e-29		SRP1 protein homolog [Os]	5e-94
121	whr13l13	BJ285984	5e-50		serine carboxypeptidase II-1 precursor (CP-MII.1) [Hv]	3e-70
122	TaLr1146G07	BG906160	1e-124		hypothetical protein [Os]	3e-91
123	WHE0811_D06_H11	BE518128	1e-103	OUT	arabinogalactan-like protein [Os]	1e-59
124	whoh20o07	BJ274150	3e-39		acyl-coA dehydrogenase [At]	2e-59
125	SUN002.B06	BE430373	4e-26		hypothetical protein [Os]	3e-32
126	whe23j15	BJ236898	1e-70		pyruvate decarboxylase (pdc2) [Zm]	1e-108
127	whyf2p17	BJ317895	5e-50		RNA/ssDNA-binding protein-like [At]	2e-46
128	whf20g09	BJ245838	1e-59		putative RNA helicase [Os]	5e-98
129	whsl21f08	BJ291030	6e-28		putative AP2-domain DNA-binding protein [Os]	1e-36
130	WHE3026_H02_O04	BQ281915	4e-94		hypothetical protein [Os]	7e-68
131	WHE0476_E01_I02	BM136718	5e-44		unknown protein [Os]	4e-25
132	WHE0965_H07_P13	BE498698	6e-28	IN	unknown protein [Os]	6e-59
133	AWB008.H12	BE400910	4e-38		glucose-6-phosphate/phosphate-translocator [Os]	1e-82
134	whf10c24	BJ243231	3e-73		hypothetical protein [Os]	1e-112
135	WHE0966_H05_P10	BE498786	4e-29	IN	hypothetical protein [Os]	4e-44
136	Ta01_01g10	BI750946	4e-35		hypothetical protein [Os]	4e-07
137	JJL005.C01	BE412332	2e-65		hypothetical protein [Os]	2e-57
138	WHE3074_E03_J06	BQ282608	2e-34		putative growth regulator protein [At]	7e-30
139	WHE0953_D10_H19	BQ169546	2e-37	IN	unknown protein [Os]	2e-24
140	WHE1071-1074_O10_O10	BQ161029	6e-31		Myb-related protein Hv33 [Hv]	3e-59
141	WHE1114_A05_A10	BE443067	5e-41		unknown protein [Os]	4e-32
142	whdl1f04	BJ224797	9e-58		putative carboxyl-terminal proteinase [Gh]	1e-86
143	whr6n23	BJ280174	3e-42		hypothetical protein [Os]	2e-70
144	whh2e17	BJ255760	1e-100		putative receptor-like kinase [Os]	1e-114
145	WHE0401_A06_A06	BE405863	2e-28		hypothetical protein [Os]	3e-18
146	WHE1205_B09_C17	BE404823	7e-40		Not56-like protein [At]	6e-60

Wheat EST Identified					Predicted Function	
Fig 1[a]	Clone name[b]	GB Accn.	Similarity to rice Contig (E-value)	Southern analysis[c]	Best BLAST match[d]	E-value
147	WHE1208_E07_J14	BE405004	2e-99	IN	putative RNA helicase, DRH1 [Os]	7e-97
148	AWB001.D06	BE400256	1e-126		phospholipase D alpha 1 (PLD alpha 1) [Zm]	5e-83
149	WHE2051_B11_C21	BQ172292	4e-32	IN	putative peroxidase [Os]	2e-17
150	WHE0615_D11_H21	BE517204	5e-50		hypothetical protein [Os]	1e-65
151	whe1o16	BJ232770	1e-62		putative MRP-like ABC transporter [Os]	1e-103
152	WHE2162_A01_B02	BQ169196	2e-58		putative THY5 protein [Os]	1e-20
153	WHE2602_E12_I24	BM136093	2e-27		putative cytochrome b5 reductase [Os]	3e-26
154	WHE0765_F10_L19	BE497220	1e-32		putative protein kinase [Os]	6e-72
155	whf8b15	BJ248806	1e-26		unknown protein [Os]	4e-57
156	WHE1201_H11_O21	BE404164	3e-36	IN	unknown protein [Os]	2e-70
157	WHE0626_C03_E06	BE517444	2e-34		expressed protein [At]	1e-09
158	whf27i23	BJ253147	2e-31		hypothetical protein [Os]	2e-45
159	whoh13d02	BJ267758	1e-29		anion exchange protein [At]	2e-80
160	whsl2a06*	BJ295169	1e-137		putative glucosyl transferase [Os]	1e-93
161	WHE0494_E07_J14	BQ162059	2e-31		hypothetical protein [At]	1e-13
162	whyd15h13	BJ302481	1e-32		LEUNIG [At]	3e-44
163	whdl9m24	BJ224274	1e-72		ubiquitin-specific protease 14 [At]	1e-87
164	whf26c07	BJ246877	9e-61		putative ABC transporter [At]	6e-30
165	whr1j12	BJ284228	4e-57		putative aspartate transaminase [Os]	3e-63
166	wh32n15	BJ211727	1e-125		protein phosphatase 2A B' regulatory subunit [At]	6e-82
167	WHE0982_B03_D06	BE500405	2e-40		unknown protein [Os]	3e-40
168	whyf5a06	BJ319114	7e-34		putative RING zinc finger protein [At]	2e-50
169	WHE0426_D01_G02	BE403178	3e-70		0-deacetylbaccatin III-10-O-acetyl transferase [Os]	3e-59
170	WHE0906_H04_O08	BE606786	2e-68		putative t-SNARE SED5 [Os]	3e-50
171	whdl19b19	BJ224517	2e-31		unknown protein [Os]	6e-08
172	TaE05032H06R	BQ239286	1e-29		hypothetical protein [Os]	8e-44
173	WHE2011_E08_J15	BF478695	5e-53		putative anthocyanin 5-O-glucosyltransferase [Os]	6e-27
174	WHE1111_G08_N15	BE444455	4e-22	IN	GTP-binding protein [Zm]	1e-77
175	WHE0904_G11_N22	BE606424	1e-132		putative extensin-like protein [Os]	3e-86
176	WHE1076_G08_M16	BE489272	6e-28	OUT	putative MAR-binding protein MFP1 [Os]	1e-37
177	*TaMSH7*	AF354709	1e-114	IN	mismatch repair protein MSH7 [Ta]	0
178	whf3g02	BJ247705	5e-47		putative heat-shock protein [Os]	6e-82
179	WHE1457_C03_F05*	BE446453	1e-38		small basic membrane integral protein ZmSIP1-2 [Zm]	3e-40
180	WHE0602_G01_M02	BE515673	1e-133		gigantea-like protein [Hv]	1e-117
181	wh12f14	BJ216454	7e-37		hypothetical protein [Os]	1e-06
182	WHE3021_A03_A05	BQ281411	2e-80		hypothetical protein [At]	2e-27
183	whsl1j20	BJ295096	1e-87		hypothetical protein [Os]	6e-77
184	whh4m22	BJ256308	1e-103		putative cytochrome P450 [Os]	3e-85
185	whyf9f02	BJ319592	6e-28		putative protein [At]	4e-18
186	wh8d20	BJ208428	1e-50		unknown protein [Os]	2e-22
187	WHE0615_H01_P01	BE517172	1e-53		small heat shock protein HSP17.8 [Ta]	6e-57
188	whsl19f08	BJ297152	1e-41		putative protein [Os]	1e-69
189	WHE2301-2304_H06_H06	BF482836	1e-47	IN	SSRP1 protein [Zm]	3e-79
190	WHE0839_B01_D01	BF473843	2e-28	IN	tRNA-glutamine synthetase [Ll]	7e-91
191	WHE0975_G01_M01	BE499742	1e-179		putative acetyl transferase [Os]	2e-39
192	WHE0801_B08_C15	BE517681	6e-28	IN	Similar to Ipomoea batatas SPF1 protein (S51529) [Os]	8e-17
193	whyd15j18	BJ308351	1e-44		twin LOV protein 1 [At]	1e-45
194	whyd5h19	BJ300999	1e-87		Similar to Spinacia oleracea protein kinase [Os]	1e-111
195	whyf3l10	BJ313119	4e-38		putative protein [At]	3e-77
196	whf9h05	BJ244367	3e-79		unknown protein [Os]	6e-39
197	whh1g13	BJ255579	3e-39		Myb-related transcription activator (MybSt1) [Os]	3e-49
198	WHE2301-2304_J12_J12	BF482847	1e-59		putative hyoscyamine 6-dioxygenase hydroxylase [At]	5e-71
199	WHE1134_F04_K08	BE445298	4e-32	IN	NADP-dependent malic enzyme, chloroplast precursor [Os]	1e-96
200	WHE1144_F05_L10	BE446241	8e-52		hypothetical protein [Os]	2e-77
201	whf28e13	BJ247248	8e-49		putative chloroplast outer envelope hexokinase 1 [Os]	1e-103
202	WHE0977_D04_H07	BE500038	1e-26		hypothetical protein [Os]	6e-41
203	whsl5j20	BJ295824	4e-26		profilin [Ma]	8e-62
204	WHE1142_H06_O12	BE446135	6e-28	IN	hypothetical protein [Os]	1e-32
205	whf13c20	BJ243861	6e-62		mitochondrial processing peptidase alpha-chain precursor [Dg]	9e-88
206	whsl21p04	BJ297752	9e-58		putative pyrophosphate-dependent phosphofructo-1-kinase [Os]	2e-69
207	whyf13m17	BJ314674	1e-26	IN	putative protein kinase [Os]	1e-90
208	WWS04.E7	BE420258	1e-137		putative zinc finger transcription factor [Os]	2e-72
209	WHE3002_C08_E16	BQ280553	1e-151		putative Myb-related transcription factor [Os]	3e-30
210	whdl9n15	BJ229111	1e-53		putative pollen specific protein SF21 [Os]	6e-66
211	WHE0980_F06_K12	BE500188	1e-41	OUT	Dof zinc finger protein [Os]	2e-34
212	whdl23e15	BJ225670	5e-45		putative RNA methyltransferase [Os]	1e-64
213	TaE05016G01R	BQ240493	1e-59		hypothetical protein [Os]	2e-68
214	WHE2051_D02_G03	BG313225	2e-27		unknown protein [Os]	3e-34
215	WHE0570_C11_F22	BE493178	1e-107		putative regulatory protein NPR1 [Os]	2e-69
216	WHE1105_C06_E11	BE442717	3e-45		unknown protein [Os]	3e-34
217	WHE0495_B10_C19	BM135204	1e-103		putative zinc finger protein [Os]	2e-68

Wheat EST Identified					Predicted Function	
Fig 1[a]	Clone name[b]	GB Accn.	Similarity to rice Contig (E-value)	Southern analysis[c]	Best BLAST match[d]	E-value
218	whyd21d18	BJ309698	1e-132		putative protein kinase APK1A At [Os]	2e-97
219	TaLr1166B04	BG908172	1e-129		hypothetical protein [Os]	1e-31
220	WHE2309_F04_K07	BF484211	6e-59	IN	hypothetical protein [Os]	2e-63
221	WHE3092_A07_A14	BQ283510	6e-28		hypothetical protein [Os]	1e-5
222	WHE1794_G10_N20	BF483431	8e-49		hypothetical protein [Os]	7e-26
223	TaE05019B09R	BQ240323	1e-102		nucleotide pyrophosphatase homolog [Os]	7e-61
224	TaLr1124E11	BG910018	2e-46		cytochrome P450-like protein [Os]	3e-41
225	WHE1783_D02_G03	BF202635	9e-55		putative ethylene-responsive RNA helicase [Os]	1e-125
226	whyf15n21	BJ320600	2e-40		casein kinase-like protein [Os]	8e-69
227	WHE2454_A05_B10	BG606850	2e-40		hypothetical protein [Os]	2e-41
228	PSR6217	BE427295	2e-40		putative transport protein homolog [Os]	8e-59
229	MUG011.D05	BE416498	5e-87		lysophospholipase-like protein [Os]	4e-82
230	whyd8d21	BJ310659	7e-37		phosphoribosylaminoimidazole carboxylase [N]	4e-38
231	WHE0970_H12_P24	BE499128	1e-32	OUT	autophagocytosis protein-like [At]	4e-40
232	whh5d05	BJ257946	3e-45		putative homeodomain-leucine zipper protein [Os]	2e-69
233	TaE05016C06R	BQ240533	7e-43		unknown protein [Os]	1e-75
234	WHE1774_F06_L12	BF201705	6e-28	IN	hypothetical protein [Os]	2e-61
235	WHE3074_H04_P08	BQ282639	1e-179		metallothionein-like protein [Os]	1e-19
236	WHE0838_D10_G20	BF474130	1e-137		putative CRK1 protein [Os]	4e-80
237	wh15e22	BJ217142	6e-31		putative protein kinase [Os]	4e-85
238	WHE0497_H08_P15	BM138453	2e-27		hypothetical protein [Os]	9e-40
239	TaE05006G10F (*WM5*)[g]	BQ238228	1e-28	IN	unknown protein [Os]	3e-32
240	WHE2301-2304_A17_A17	BF482642	2e-64	OUT	AGAMOUS protein [At]	8e-35
241	WHE612_B10_D20	BE516111	7e-40		putative zinc-finger protein [Os]	5e-50
242	WHE2630_C06_E12	BM137168	1e-26		unknown protein [Os]	5e-67
243	whr18h14	BJ283997	2e-31		unknown protein [Os]	9e-58
244	WHE3092_A07_A14	BQ283510	2e-31		hypothetical protein [Os]	1e-5
245	whyf20j18	BJ321363	1e-129		hypothetical protein [Os]	6e-67
246	WHE1071-1074_P19_P19	BE489800	3e-30		similar to Homo sapiens mRNA for KIAA0039 [Os]	4e-53
247	CNW01PL0329	BE401329	1e-62		no homologies found	-
248	AWB008.B10	BE400872	9e-55		60S ribosomal protein L11 (L5) [Ms]	3e-68
249	SUN000.D05	BE430212	4e-69		carnitine racemase-like protein [Os]	1e-26
250	WHE0959_B02_C03	BE499717	1e-50	OUT	Shaggy-related protein kinase delta (ASK-delta) [At]	5e-66
251	WHE2341_E12_I23	BG263402	3e-91	IN	putative peroxidase FLXPER4 [Os]	2e-64
252	WHE0369_G03_N05*	BE490678	3e-33		wpk4 protein kinase [Ta]	2e-97
253	WHE0765_E12_J23	BE497210	1e-120		hypothetical protein [Os]	5e-71
254	WHE1782_E07_I13	BF202860	1e-167		s-adenosylmethionine synthetase [Hv]	1e-102
255	TaE05018E09R	BQ240361	8e-89		hypothetical protein [Os]	2e-83
256	WHE1767_G07_M13	BF202364	3e-70		no homologies found	-
257	TaLr1155B01*	BG906898	1e-112		phosphoenolpyruvate carboxylase [Os]	2e-93
258	whr8n20*	BJ280549	2e-40		putative Ser/Thr protein kinase [At]	4e-54
259	WHE2476_C09_E18	BG314345	6e-31	IN	RNA-binding protein [Os]	3e-49
260	WHE0904_H06_P12	BE606431	5e-87		putative dioxygenase [Os]	3e-31
261	WHE3026_G02_M04	BQ281904	3e-67		putative heme-binding protein [Os]	6e-37
262	WHE0065_C09_F17	BE423366	1e-122		expressed protein [At]	4e-34
263	MWL006.D03*	BE414843	3e-88		putative cytochrome P450 [Os]	8e-47
264	WHE3092_A07_A14	BQ283510	4e-35		hypothetical protein [Os]	1e-5
265	WHE2851_A11_A21	BQ294574	2e-46		putative bZIP transcriptional activator RF2a [Os]	4e-44
266	AWB011.C09	BE400118	1e-53	IN	unknown protein [Os]	2e-30
267	WHE1137_F09_K17	BE444678	1e-38		putative isoamyl acetate-hydrolyzing esterase [At]	4e-47
268	WHE1114_G04_M08	BE443000	8e-49	IN	no homologies found	-
269	WHE1071-1074_G13_G13*	BE489760	3e-79	IN	putative lipase [Os]	7e-93
270	PSR6113	BE427202	2e-43		carboxypeptidase precursor-like protein [Os]	6e-47
271	WHE2857_H03_P05	BQ295064	4e-38		hypothetical protein [Os]	1e-22
272	whr9c22	BJ280602	3e-51		putative bromelain-like thiol protaease [Os]	1e-72
273	WHE0035.D05F990516	BQ168131	7e-77		unknown protein [Os]	6e-38
274	WHE3017_E09_I17	BQ281200	1e-29		unknown protein [Os]	1e-96
275	WHE1075_G05_M09	BE489185	1e-62	IN	hypothetical protein [Os]	3e-93
276	WHE0922_A12_A24	BF473137	5e-78	IN	putative phosphatidylethanolamine binding protein [Os]	3e-37
277	TaLr1158G02	BG907286	1e-69		putative ABC transporter ATP-binding protein [Os]	4e-87
278	WHE1798_H06_P12 (*WM3*)[g]	BF482281	3e-39	IN	putative nonspecific lipid-transfer protein precursor [Os]	6e-32
279	SCU004.H02*	BE413963	2e-77		putative endo-beta-1,4-glucanase [Os]	2e-56
280	WHE2327_H04_P07	BG605144	1e-62		unknown protein [Os]	2e-88
281	WHE0606_G01_M02	BE515856	3e-45	OUT	hypothetical protein [Os]	2e-55
282	whdl21j04	BJ225334	5e-41		hypothetical protein [Os]	5e-43
283	SUN005.A07	BE430626	4e-26		thaumatin-like protein [Ta]	4e-75
284	whsl9h04	BJ296557	6e-31		unknown protein [At]	7e-36
285	PSR7001	BE427421	4e-26		tonoplast membrane integral protein ZmTIP3-1 [Zm]	3e-44
286	WHE1778_B11_C21	BF202144	3e-76	OUT	unknown protein [Os]	1e-63
287	whe18n24	BJ235913	5e-47		vacuolar ATP synthase subunit E (CLVE-1) [Cl]	3e-45
288	whf4j06	BJ248017	2e-43		putative lipase [Os]	6e-76
289	WHE0902_B03_C06	BE606875	3e-54	OUT	putative receptor kinase [Os]	2e-49

Wheat EST Identified					Predicted Function	
Fig 1[a]	Clone name[b]	GB Accn.	Similarity to rice Contig (E-value)	Southern analysis[c]	Best BLAST match[d]	E-value
290	WHE1771_F06_K11	BF201528	1e-44	OUT	hypothetical protein [Os]	5e-34
291	WHE2117_H02_O03	BG275106	3e-76		3-methyl-2-oxobutanoate hydroxy-methyl-transferase like protein [Os]	3e-56
292	WHE0966_B06_D12	BE498855	7e-74	OUT	late embryogenesis abundant protein LEA14-A [Gh]	4e-45
293	WHE2957_G05_N09	BG606548	2e-37		hypothetical protein [Os]	1e-09
294	WHE3092_A07_A14	BQ283510	1e-26		hypothetical protein [Os]	1e-5
295	WHE0975_G11_M21	BE499732	3e-48		unknown protein [Os]	6e-43
296	WHE0616_E02_J04	BE517275	1e-135	OUT	similar to homeobox protein [At]	3e-91
297	whyf17a19	BJ314286	2e-46		unknown protein [Os]	3e-07
298	WHE1128_D05_H10	BE444200	1e-59		unknown protein [Os]	8e-21
299	WHE1759-1762_B24_B24	BF201900	2e-55	OUT	putative receptor protein kinase PERK1 [Os]	1e-78
300	WHE0960_A04_A08	BE499124	8e-49	OUT	RAS-related GTP-binding protein Rab7 family [Os]	2e-95
301	WHE0751_E02_I03	BE497369	1e-44		putative cytochrome P-450LXXIA1 (cyp71A1) family [Os]	8e-33
302	TaLr1175G09	BG909292	7e-74		hypothetical protein [Os]	3e-89
303	whr25n22	BJ282272	1e-122		putative D-isomer specific 2-hydroxyacid dehydrogenases protein [Os]	5e-76
304	whh14k05	BJ259035	8e-80		putative alcohol dehydrogenase/ribitol dehydrogenase [Os]	1e-102
305	WHE1134_G04_M08	BE445286	7e-31		hypothetical protein [Os]	6e-97
306	WHE2955_D07_G13	BG606387	8e-43		hypothetical protein [Os]	4e-69

databases. **Table 3.2** summarises the details of clones identified and their putative functions based on the GenBank annotations.

3.3.4 Synteny between the wheat 3DS and rice 1S genomic regions

To assess the degree of synteny between the region identified on rice chromosome 1 and the region deleted in the *ph2a* mutant, Southern analysis using a subset of the wheat clones was conducted. 76 wheat ESTs were selected for Southern analysis to physically cover the entire *ph2a* region and to extend past the deletion breakpoint. Two Southern hybridisations were performed for each wheat EST, one against digested genomic DNA of wheat nullisomic-tetrasomic aneuploid stocks for chromosomal assignment and one against digested wild-type, *ph2a*, *ph2b* and *ph1b* wheat genomic DNA for assignment either inside or outside the deleted segment of the *ph2a* mutant (**Figure 3.2**). Note that *ph2b* and *ph1b* genotypes were included for potential correlation to mutated regions in these genomes. Following the location of the physical position of the breakpoint in *ph2a*, we were able to make inferences regarding synteny in the analysed wheat and rice regions from Southern data of 68 clones distal to this position. Of these, 53 (78 %) were physically positioned within the *ph2a* deleted segment, and 15 (22 %) positioned out. Results are shown in **Figure 3.1** and **Table 3.2**. This analysis confirmed a high degree of synteny between the investigated wheat and rice regions. Significantly, no blocks of synteny breakdown were observed across the region. Southern analysis also indicated that the extent of the wheat *ph2a* deletion extends at least as far as the end of the genomic sequence for the short arm of rice chromosome 1, a point in close proximity to the telomere (Sasaki *et al.*, 2002). Our results suggest that the deleted region in *ph2a* involves a terminal segment on the short arm of chromosome 3D, confirming initial hypotheses by Sears (1982), who first suggested that *ph2a* encompassed a deficiency for a terminal segment of the short arm of 3D that includes the locus of *Ph2*.

3.3.5 Estimating the size of the *ph2a* deletion

Southern analysis allowed the position of the chromosomal breakpoint of *ph2a* to be determined. This has been physically resolved to be between wheat clones WHE1798_H06_P12 #278 (WM3) and WHE0606_G01_M02 #281 on 3DS. This corresponds to a physical distance in the syntenous rice region of 6.58 Mb and a genetic

Figure 3.2: Southern analysis locating clones to the region deleted in the wheat *ph2a* mutant.

Genomic DNA from *Triticum aestivum* cv. Chinese Spring (CS), *ph2a*, *ph2b*, *ph1b* and nullisomic-tetrasomic lines (shown as N3A-T3B, N3B-T3D and N3D-T3A) were digested with a range of restriction endonucleases and probed with [^{32}P]-labelled wheat clones to determine chromosomal location and physical position with respect to the region deleted in the *ph2a* mutant. Data shown is for clone WHE1142_H06_O12, #204 in **Figure 3.1** and **Table 3.2**, *Hin*d III restriction endonuclease digest.

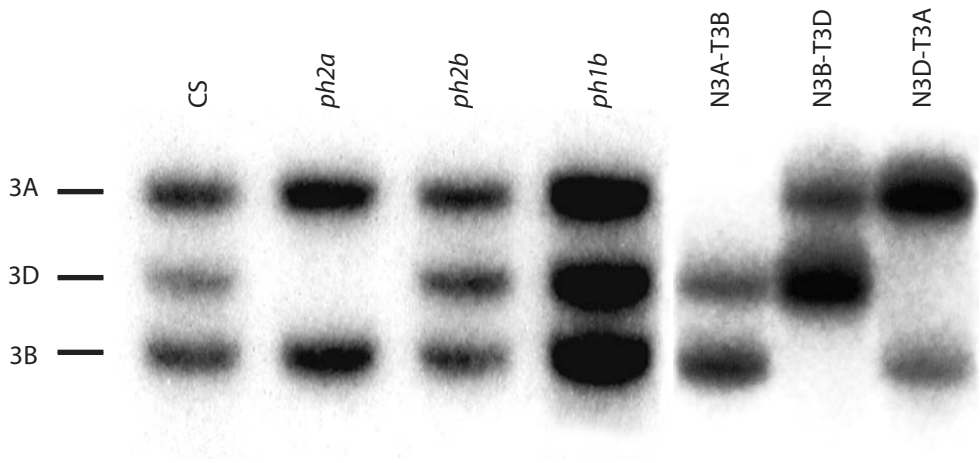
CS
ph2a
ph2b
ph1b
N3A-T3B
N3B-T3D
N3D-T3A
3A
3D
3B

distance of approximately 32 cM. All clones mapped proximal of the predicted breakpoint have been assigned by Southern analysis to chromosome 3D (with the exception of clone WHE1759-1762_B24_B24 #299 that maps to chromosome group 1). Based on the difference between the genome size and chromosome complement of hexaploid wheat (15,966 Mb per 1C nucleus, 2n = 42) and rice (431 Mb per 1C nucleus, 2n = 22) (Arumuganathan and Earle, 1991) the *ph2a* deletion is estimated to be approximately 80 Mb in length.

3.3.6 Analysis of rice and barley meiosis related phenotypic traits

Both the RiceGenes (superceded by Gramene, http://www.gramene.org/) and GrainGenes (http://grain.jouy.inra.fr/ggpages/) databases were screened for quantitative trait loci (QTL) in the syntenous rice region that could be associated with a meiotic gene effect. Only one such significant QTL (LOD>2.5, p-value=0.0001) was found localised to the syntenous region of the *ph2a* deletion on rice chromosome 1. The QTL is for spikelet fertility. No other mapped phenotypic traits related to meiosis were found localised to the short arm of rice chromosome 1. However, a gene termed *msg5* (male sterile 5) (Franckowiak, 1997) is located on the short arm of barley chromosome 3. It is not known if this gene resides in the region deleted in *ph2a*.

3.3.7 Genic content of the *Ph2* region and electronic expression analysis

Tentatively, we can predict the identification of approximately 218 genes located in the region of the *ph2a* deleted segment. This is based on the identification of 306 genes as a result of the BLAST searches with the rice genome sequence and the mapping result showing that 78 % of the 280 ESTs located distal to the predicted breakpoint are derived from genes within the deleted region. To gain an understanding of the function of genes identified as candidates at the *Ph2* locus, the results of BLAST searches were classified according to the Gene Ontology Consortium (http://www.geneontology.org/) and assigned by homology to categorised rice and *Arabidopsis* genes. Only genes located distal to the predicted breakpoint and not determined by Southern analysis to be located out of the *ph2a* region were included in the analysis. Of the 265 ESTs classified, 117 (44 %) could not be assigned to a functional class due to the absence of significant database hits, or hits to either hypothetical or unknown proteins. Genes encoding metabolic

enzymes, proteins involved in nucleic acid binding, those involved in ligand binding and carrier functions, signal transduction pathways, transcriptional regulation and transport processes are well represented (**Table 3.3**) and accounted for the majority of annotated functions.

To gain further insight into the putative function of the identified wheat ESTs and their relatedness to meiotic development in the anther, we performed an electronic expression analysis against the GenBank wheat meiotic anther cDNA library. Each of the wheat EST sequences identified from the assembled rice contig was used in stringent BLAST searches against the available 9139 ESTs from this library to identify the presence of homologous sequences. Of the 306 wheat ESTs analysed, 52 (17 %) were confirmed to be expressed in wheat anthers undergoing meiosis and are distributed evenly across the chromosomal region analysed. Wheat ESTs determined from this analysis to be expressed in meiotic anthers of wheat are highlighted in **Table 3.2**.

3.4 Discussion

This study has used colinearity of molecular markers in the grasses, in combination with the rice genome sequence to provide an analysis of genes in the *ph2a* region and identify *Ph2* candidates. Through searches of public wheat EST databases, 218 genes putatively located in this region were identified. Of these, 53 have been positively assigned to the region deleted in the *ph2a* mutant through Southern analysis.

Extensive synteny in gene order and content between rice and wheat has been well documented. Fine mapping indicates that DNA markers separated by ≤1.6 cM in rice have the same order on barley chromosomes (Dunford *et al.*, 1995), suggesting maintenance of colinearity between rice and members of the Triticeae at this level. In particular, recent studies investigating the relationship between rice chromosome 1 and barley chromosome 3H have demonstrated synteny on a mesoscale (1 to 10 cM) through comparative mapping, identifying conserved collinear positions for all single copy markers mapped (Smilde *et al.*, 2001). For the purposes of this study, it was imperative to confirm synteny in the wheat and rice genomic regions investigated. This was established by selecting a subset of wheat clones spanning the rice region and mapping

Table 3.3: Classification of identified wheat ESTs based on molecular function.

[a] Genes whose functions may be grouped into several classes are given multiple entries. Clones determined to be outside the region deleted in the *ph2a* mutant by Southern analysis have been excluded from analysis.

Molecular Function	Number of ESTs[a]
nucleic acid binding	
DNA binding	23 (4.5%)
RNA binding	14 (5.3%)
nuclease	1 (0.4%)
enzyme	
transferase	30 (11.3%)
hydrolase	28 (10.6%)
kinase	21 (7.9%)
oxidoreductase	8 (3.0%)
isomerase	7 (2.6%)
phosphatase	5 (1.9%)
helicase	5 (1.9%)
monooxygenase	4 (1.5%)
lyase	4 (1.5%)
ligase	1 (0.4%)
ligand binding or carrier	
nucleotide binding	17 (6.4%)
heavy metal binding	8 (3.0%)
protein binding	2 (0.8%)
lipid binding	2 (0.8%)
calcium binding	2 (0.8%)
electron transporter	1 (0.4%)
oxygen binding	1 (0.4%)
signal transducer	20 (7.5%)
transporter	19 (7.2%)
transcription regulator	15 (5.7%)
chaperone	5 (1.9%)
structural protein	4 (1.5%)
translation regulator	1 (0.4%)
enzyme regulator	1 (0.4%)
molecular function unknown	117 (44.2%)

them in wheat with respect to the *ph2a* deletion. Mapping data confirms a syntenic relationship in these regions of rice chromosome 1 and wheat 3DS at the macro-level but indicates differences at the micro-level. Micro-level differences cannot be solely attributed to low sequence similarity between the rice genomic sequence and the wheat ESTs. Many of the ESTs inside the predicted breakpoints that are chromosomally positioned out of the wheat *ph2a* deletion region by Southern analysis show expectation values $\leq 1e^{-50}$. Differences at the micro-level between these regions is most likely attributed to restructuring events (eg. gene duplication and deletion) after wheat and rice diverged from a common ancestor approximately 60 million years ago (Martin *et al.*, 1989; Wolfe *et al.*, 1989).

Several interesting observations were made concerning the genetic content of the rice region analysed. Analysis of database searches and automated gene predictions of the rice consensus sequence confirmed that a number of genes are duplicated or arrayed in tandem in this rice region. The presence of abundant gene families, pseudogenes, clustered tandem repeats of predicted coding sequence and duplicated genes has been previously described in detail for rice chromosome 1 (Sasaki *et al.*, 2002). A representative wheat EST with similarity to each of these repetitive rice sequences (marked in **Table 3.2**) was selected for inclusion in the clone list. This eliminated multiple representations of identical ESTs, a situation that would not necessarily reflect the genic content of the syntenous region in wheat for these particular genes. Southern data of four wheat ESTs corresponding to repetitive rice regions (clones #48, 56, 87 and 269) were obtained and allowed a comparison of banding patterns over five restriction enzyme digests of wild-type and *ph2a* genomic DNA. Southern hybridisations for three of these clones (#48, 56 and 269) are characterised by relatively simple banding patterns (three to five bands) and indicate that a maximum of two hybridising bands are absent from *ph2a* when compared to wild-type. This indicates the likely presence of one copy of each of these genes in the deleted region, an observation that contrasts the apparent duplications of the orthologous genes in the rice chromosome 1 region. The Southern hybridisation pattern for clone #87 is more complex (10 to 14 bands) with a maximum of three bands absent from *ph2a*. This is likely due to the presence in the wheat *Ph2* region of three genes, including clone #87, that exhibit similarity to heat shock proteins (**Table 3.2**). These results indicate that duplications seen in the rice chromosome 1 region do

not necessarily indicate a corresponding duplication in the wheat *Ph2* region. Database searches for wheat ESTs with similarity to the rice consensus sequence also identified regions of highly repetitive sequence. Wheat ESTs identified by similarity to highly repetitive rice sequence were eliminated from analysis due to the likelihood that they represented uncharacterised transposable elements. For example, clone CNW02EL006 (Accession #BE401694) was identified exhibiting significant similarity at approximately 25 positions in the rice consensus sequence and appears to be highly represented across the rice genome.

Automated gene predictions (RiceGAAS) from the 6.58 Mb rice contig indicate the presence of approximately 1500 coding sequences from this genomic region in rice. Due to inherent false predictions by such software, this is likely to be an over-estimation of the number of transcribed genes, and the presence of wheat orthologues for all of the predicted genes in this rice region seems unlikely. Our results do however indicate RiceGAAS to be a valuable tool for comparative genetic studies of this type in the grasses. We observed that 99 % of the wheat ESTs identified correspond to regions of rice predicted genes. Therefore, individual rice predicted gene sequences could have been used instead of large rice genomic sequences as the basis for wheat EST identification. This would simplify sequence handling and interpretation of BLAST results. Furthermore in relation to rice gene prediction, we examined the correlation between rice predicted gene density and wheat EST hits. As **Figure 3.1** illustrates, no relationship is apparent. Indeed, several areas of relatively high predicted gene density in rice produced either none or relatively few wheat EST hits at the E-value cut-off level of $\leq 1e^{-25}$ that we used. A number of possibilities could account for this observation. Perhaps these rice regions are characterised by highly variable sequence, such that wheat orthologues were not identified from BLAST searches using relatively stringent E-value cut-off levels. Perhaps the wheat transcriptome lacks orthologous sequences for these regions of predicted rice genes, or if present are too lowly expressed to be represented in wheat EST databases. The former explanation seems most likely. However, with at least one of these relatively gene-dense rice regions we found that a reduction of E-value cut-off to $\leq 1e^{-13}$ had no effect on the number of wheat EST hits. A further reduction to $\leq 1e^{-10}$ produced two wheat EST hits but this level of similarity may not be significant and Southern analysis would be needed to physically map these ESTs in wheat.

An important question arising from the results of this study relates to the genes identified in the *Ph2* region, and their relationship to the *Ph2* phenotype. Classification based on predicted molecular function indicates a spectrum of functions that would be expected from sampling a large chromosomal segment. The major groups of genes are represented. Distinguishing candidates for *Ph2* amongst the genes identified from this region is a challenging task. What is the function of *Ph2* and how do genes at this locus contribute to the intriguing ability of chromosomes to recognise and pair with homologous partners during meiosis? The precise mechanisms remain elusive despite extensive research to elucidate the function of *Ph* genes, in particular *Ph1* and *Ph2*. It is interesting that *Ph1* was originally defined by a deletion of approximately 70 Mb containing over 200 genes (Moore, 2002). This is similar to both the predicted size (80 Mb) and the estimated gene content (218) based on database EST hits, of the *ph2a* deletion region revealed in this study. The number of wheat ESTs putatively identified from the wheat *Ph2* region using the methods described in this paper may increase as efforts in wheat EST sequencing continue and more sequences representing lowly expressed genes are represented in databases. More information will be gathered as wheat EST databases expand.

Our analysis of the 280 wheat ESTs distal to the physical position of the breakpoint has initially involved the assessment of database searches to classify function. ESTs that could conceivably have a function in the broad spectrum of molecular events associated with meiotic control were selected for Southern analysis for positive assignment either in or out of the *ph2a* deletion. Two clones resulting from this process have been highlighted as potential candidates for genes at the *Ph2* locus. The EST G05_q343_plate_11 (#10 in **Table 3.2**), derived from a wheat pre-fertilisation ovule (cv. Florida) cDNA library exhibits 75 % identity at the amino acid level to a putative DNA repair and recombination protein from rice (**Figure 3.3 A**), and weaker identity (44 %) to a putative SNF2/RAD54 family DNA repair and recombination protein from *Arabidopsis*. Identity of 27 % is also seen to a human homologue of the yeast protein Rad26. Similarity to the wheat EST G05_q343_plate_11 in all cases is at the C-terminal region of these peptides. The interesting feature of the above three proteins is that they contain a SNF2-related N-terminal domain, found in proteins that are known to function

Figure 3.3: Predicted polypeptide sequence and similarity alignment of two wheat ESTs identified as candidates for *Ph2*.

A: Similarity at the amino acid level over the sequenced region of clone G05_q343_plate_11 to a putative DNA repair and recombination protein from rice. The position of the putative SNF2 family N-terminal domain is shown in the rice peptide sequence.

B: Similarity at the amino acid level over the sequenced region of clone WHE2301-2304_H06_H06 to the SSRP1 protein from maize. The position of the HMG_Box domain is shown in the maize peptide sequence.

A


```
Identities = 92/122 (75%)
Positives = 100/122 (81%)
Frame = +2

   G05_q343_plate_11:    2 ALSSAELLAKMRGTREGAASDALEHQLSLGSTSNQRPXXXXXXXXXXXXXXXNMIVQPEV 181
                           ALSSAELLA++RGTREGAASDALEHQL+LGS SN                +MIVQPEV
putative R&R protein: 1066 ALSSAELLARIRGTREGAASDALEHQLNLGSASNHT-SSSSGNGRASSSSTRSMIVQPEV 1124

   G05_q343_plate_11:  182 LIRQLCTFIQQNGGSASSTSLTEHFKNRIQPKDMLVFKNLLKEIATLQRGAGGATWVLKP 361
                           LIRQLCTFIQQ+GGSASSTS+TEHFKNRI  KDML+FKNLLKEIATLQRGA GATWVLKP
putative R&R protein: 1125 LIRQLCTFIQQHGGSASSTSITEHFKNRILSKDMLLFKNLLKEIATLQRGANGATWVLKP 1184

   G05_q343_plate_11:  362 EY 367
                           +Y
putative R&R protein: 1185 DY 1186
```

B


```
Identities = 146/185 (78%)
Positives = 160/185 (86%)
Frame = +3

WHE2301-2304_H06_H06: 84  MADGHLFNNILLGGRTGTNLGQFKVHSGGLAWKRQGGGKTIEIDKADLTSLTWMKVPRAY 263
                          M DGH FNNILLGGR GTN GQFKVHSGGLAWKRQGGGKTIEIDKAD+T++TWMKVPRAY
               SSRP1:  1  MTDGHHFNNILLGGRGGTNPGQFKVHSGGLAWKRQGGGKTIEIDKADVTAVTWMKVPRAY 60

WHE2301-2304_H06_H06: 264 QLGVRIKDGLSYTFIGFREQDVSSLINFMQKNLGISPDEKQLSXXXXXXXXXXXXXSMLT 443
                          QLGVRIK GL Y FIGFREQDVS+L NF+QKN+G++PDEKQLS             +MLT
               SSRP1: 61  QLGVRIKAGLFYRFIGFREQDVSNLTNFIQKNMGVTPDEKQLSVSGQNWGGIDIDGNMLT 120

WHE2301-2304_H06_H06: 444 FMVESKQAFEVSLADVSQTQIQGKTDVLLEFHVDDTTGANEKDSLMDMSFHVPTSNTQFP 623
                          FMV SKQAFEVSL DV+QTQ+QGKTDVLLE HVDDTTGANEKDSLMD+SFHVPTSNTQF
               SSRP1: 121 FMVGSKQAFEVSLPDVAQTQMQGKTDVLLELHVDDTTGANEKDSLMDLSFHVPTSNTQFV 180

WHE2301-2304_H06_H06: 624 GNENR 638
                          G+E+R
               SSRP1: 181 GDESR 185
```

in a number of processes that includes transcriptional regulation, DNA repair, DNA recombination and chromatin unwinding. The available sequence of clone G05_q343_plate_11 does not extend far enough in a 5' direction to reach the relative position of the SNF2 related domain in these proteins. However, significant similarity to these proteins over the sequenced region seems to warrant further analysis of the 5' region of this clone. We have previously reported the characterisation of *TaMSH7* (Dong *et al.*, 2002), a wheat cDNA homologue of the bacterial *MutS* gene that has been localised to the region deleted in the *ph2a* mutant. In eukaryotes, homologues of *E. coli* MutS and MutL are involved in multiple pathways of recombination and repair. The wheat EST clone G05_q343_plate_11 may represent a second gene in the *Ph2* region with a putative role in repair and recombination processes.

Secondly, the EST WHE2301-2304_H06_H06 (#189 in **Table 3.2**) has been identified as a *Ph2* candidate gene involved in chromatin structure. This EST exhibits 78 % identity at the amino acid level to the characterised SSRP1 protein from maize (**Figure 3.3 B**) (Rottgers *et al.*, 2000) and comparable levels of similarity to other characterised and putative homologues from other species. The structure-specific recognition protein 1 (SSRP1) is a member of the family of proteins that contain a high mobility group (HMG) domain DNA binding motif, so named because it specifically recognises structurally modified DNA (Bruhn *et al.*, 1992). HMG domain proteins are relatively abundant non-histone chromosomal associated proteins considered to represent architectural factors facilitating the assembly of specific nucleoprotein structures and have been implicated in the cellular processes of replication, recombination, repair and transcriptional regulation (Bustin, 1999; Bustin *et al.*, 1990; Crothers, 1993; Grasser, 1998; Grosschedl, 1995; Grosschedl *et al.*, 1994; Thomas and Travers, 2001). The SSRP1 proteins form a separate subgroup within the HMG domain protein family (Baxevanis and Landsman, 1995) but functionally their precise role remains elusive. The proteins are conserved across plants and mammals, implying a role in critical cellular functions. Southern analysis using the clones G05_q343_plate_11 and WHE2301-2304_H06_H06 as probes has indicated that both of these genes are represented by three copies in the wheat genome, each representative of the three genomes in this hexaploid species. Sequencing and further analysis of these genes will be a priority for our continued research. In particular, the comparison of these gene sequences from wild-type wheat and the *ph2b*

mutant will be of interest. *ph2b* is thought to represent a point mutant at the *Ph2* locus (Sears, 1982; Wall *et al.*, 1971).

Reports on studies involving *Ph1* (reviewed in Moore, 2002) are beginning to shed light on the possible function of genes at this locus. *Ph1* has been delimited to a region on chromosome 5BL containing less than seven genes, however it is still not known wether the phenotype controlled by *Ph1* is the result of more than one gene in this region, or a heterochromatin region with an epigenetic effect (Moore, 2002). Moore (2002) has proposed a functional model for the action of *Ph1* that results in chromosome 'stickyness' in its absence. The presence of *Ph1* may provide chromosomes with a coating, envisaged to resemble 'teflon'. This may increase specificity in the pairing process and facilitate enzymatic interaction involved in the correction of non-homologous chromosome associations, with the overall effect being to promote homologous pairing (Moore, 2002). The identification of a putative wheat homologue of SSRP1 located in the deleted segment of *ph2a* is interesting in the context of this functional model for the action of the *Ph1*. Removal of a copy of the SSRP1 homologue (as in *ph2a*) could be conceived to result in a physical change to the proteinaceous structure of the chromosomes, an effect that may alter the dynamics of homology recognition or the pairing process. Although evidence from studies investigating the comparative effects of *Ph1* and *Ph2* indicate distinct mechanisms of control over pairing and/or chiasmata formation (Benavente *et al.*, 1998; Martinez *et al.*, 2001), studies of *Ph1* are providing valuable clues about the behaviour of meiotic chromosomes in hexaploid wheat and the effects exerted by *Ph* genes. This information will be of unquestionable benefit to studies involving other *Ph* loci, such as *Ph2*.

In order to expand the information associated with each of the wheat ESTs and their predicted function in relation to *Ph2*, we performed an electronic expression analysis that aimed to highlight genes expressed in meiotic tissue. Genes contributing to the molecular control of homologous chromosome pairing would be expected to exhibit expression in pre-meiotic and/or meiotic wheat anthers. To perform this analysis we used the GenBank wheat meiotic anther cDNA library. At the time of analysis, 9139 ESTs were publicly available from this library, sequenced by the group of Dr. Olin Anderson, USDA, Albany CA, USA. Using high significance cut-off levels, 52 of the

306 identified wheat ESTs were found to be represented by homologous sequences in this library, indicating the expression of these genes in this tissue and developmental stage. Considering the large number of ESTs putatively identified from this wheat region, this analysis aimed to provide some indication of meiotic expression in order to emphasise genes with possible roles in anther development and meiotic processes. Expression of the identified wheat ESTs in cDNA libraries from non-meiotic tissues such as leaves and roots were not analysed in this study. There is no evidence indicating that genes from the *Ph2* locus would be exclusively expressed in meiotic tissue. Expression analysis of this type does however have limitations. For two reasons the absence of representative BLAST matches from this library does not necessarily rule out expression in this tissue. First, an intrinsic disadvantage of this type of analysis is that BLAST searches are limited to the sequenced regions of cDNA clones (ESTs). Often, for a particular gene, EST sequences will be derived from different length messenger RNAs and may result in non-overlapping sequence information. Such a situation would falsely exclude expression in this library. Second, clustering analysis (BLASTCLUST, NCBI, http://www.ncbi.nlm.nih.gov/) of the 9139 meiotic anther cDNA library ESTs indicates that approximately 65 % are singletons. In addition, a large proportion (75 %) of the 52 *ph2a*-region ESTs represented in this library appeared only once. This indicates that further sequencing of this library would yield substantial numbers of novel sequences derived from lowly expressed genes, and may permit further annotation of expression in this tissue for the wheat clones identified. The gene *TaMSH7* (#177 in **Table 3.2**) provides an example. Our analysis of electronic expression did not find this sequence amongst ESTs of the wheat meiotic anther cDNA library. This gene was however isolated using an RT-PCR strategy from total RNA of early meiotic anthers, and Northern data indicates expression of this gene in early meiotic tissues of wheat (Dong *et al.*, 2002). It seems likely that an EST derived from the lowly expressed mRNA of *TaMSH7* would appear with further sequencing of this library. Electronic expression studies in combination with BLAST information relating to putative function does however provide valuable insight into the roles of genes identified and may aid in selection of genes for further analysis.

Important research currently being conducted includes the continued mapping of candidates identified to definitively place genes in the region deleted in the *ph2a* mutant.

In addition, further sequencing of clones of interest and clones with unidentified function, to permit additional annotation of putative function is being continued. Furthermore, our continued research aims to address the following central questions. Firstly, what are the temporal expression patterns of each wheat candidate gene as meiosis in the anther progresses and secondly, do any of the genes identified exhibit differential expression between wild-type Chinese Spring wheat and *ph2a* mutant anthers? These questions are being addressed through the use of microarrays.

CHAPTER 4

IS *PH2* A MEIOTIC GENE CLUSTER?

4.1 Introduction

A number of studies in our laboratory have aimed to identify genes that could represent *Ph2*. Until the public release of the genomic sequence of rice chromosome 1, the approach was largely based on either identifying mRNAs showing a degree of meiotic specific expression based on differential or subtractive hybridisation strategies or via sequence similarity to characterised genes from other species. For four of these genes isolated in this manner, the finding that they are chromosomally positioned in the 3DS region deleted in the wheat mutant *ph2a* was fortuitous and led to investigations of putative function in relation to *Ph2*. These genes are *TaMSH7*, *WM5*, *WM3* and the *WM1* gene family, of which eleven members have been localised to the region deleted in *ph2a* and are genetically linked within 5 centimorgans (Whitford, 2002). Seven members of the *WM1* gene family (*WM1.1-1.3*, *WM1.7* and *WM1.10-1.12*) are clustered in a region of approximately 220 Kb (Whitford, 2002). Furthermore, mRNAs derived from *TaMSH7*, *WM5*, *WM3* and several members of the *WM1* gene family are expressed during meiosis in the wheat anther. From the Southern results presented in Chapter 3, showing that 78 % of the 280 wheat ESTs located distal to the predicted *ph2a* breakpoint are derived from genes within the *ph2a* deleted region, we are now able to extend the estimate of the number of genes identified in the region deleted in *ph2a* to greater than 200. Electronic expression analysis also described in Chapter 3 indicates that of all genes putatively identified from the region deleted in *ph2a*, almost 20 % are expressed in wheat anthers undergoing meiosis.

Collectively, the information described above has raised a number of interesting questions in relation to the possible function of genes in the chromosomal region linked to *Ph2*. Are 20 % of all wheat genes expressed in the anther during early meiosis, or does the chromosomal region in the vicinity of *Ph2* on the short arm of chromosome 3D

contain a cluster of functionally diverse genes that as a whole have an unusually high prevalence for expression in meiotic anthers? Are the *Ph2*-region genes expressed in other tissues of the wheat plant such as non-dividing leaf tissues or actively dividing root tips, to what degree, and how does this correlate with the expression patterns of genes from other large chromosomal regions in the wheat genome? The finding of a cluster of meiotically expressed genes in this region would be of great significance for research into meiosis in relation to *Ph2*. It may indicate a structurally important role for this chromosomal region in terms of providing transcriptional accessibility to important meiotic genes during meiosis when chromosomes are condensed and euchromatic regions largely inaccessible. This proposal has been tentatively suggested recently (Whitford, 2002) but evidence to support this idea has not yet been shown. This Chapter describes an approach that attempts to address this important question.

In recent years the number of ESTs in the public domain for many plant and animal species has increased dramatically. At present there are over 500000 ESTs available from members of the Triticeae, predominantly from *Triticum* and *Hordeum* species. All of these sequences and the details of the cDNA libraries are either accessible through the NCBI GenBank resource (dbEST) or through wEST (http://wheat.pw.usda.gov/wEST/), a USDA-ARS sponsored server of nucleic acid sequence data for Triticeae-associated research projects located at the USDA-ARS Western Regional Research Center, Albany, CA. The ESTs represented in these collections are derived from cDNA libraries of diverse plant tissues at developmentally defined stages and conditional treatments, and thus represent a valuable public resource available to explore the expressed portions of Triticeae genomes. In parallel with efforts by laboratories around the world to contribute to EST databases, there are also efforts to develop analytical tools to mine this information and address biological questions of interest. Several efforts are currently in progress to generate species- and tribe-specific consensus assemblies from all sequences derived from EST databases using various sequence assembly programs such as phrap, CAP3, CAP4, and d2_cluster. The results of these assemblies are contigs of overlapping ESTs, theoretically derived from the same gene. A contig of overlapping ESTs can be used to derive a consensus sequence for that particular mRNA, which in many cases is more informative in BLAST searches investigating function. Also, information regarding the expression of that particular gene may be derived from an analysis of the

tissue origin (cDNA library source) of all ESTs contributing to the assembly of the contig. For example, a contig formed from the assembly of ESTs predominantly from root cDNA library indicates that this particular gene (or predicted consensus sequence) is likely to be predominantly expressed in root tissue.

This has formed the basis for the development of a program called Contig Constellation Viewer (CCV) by G. Lazo and colleagues (Lazo, 2003) at the USDA-ARS, Albany CA. CCV, which is still under development, presents a means to query large collections of contig assemblies for information relating to the EST contribution of contigs, tissue sources of ESTs contributing to contigs, physically mapped chromosomal locations of ESTs contributing to contigs, or indeed any query associated with the annotation of sequences or libraries used for initial contig assembly. CCV graphically displays contig assembly information in the form of a circle, which contains at defined positions around its circumference a number of selected cDNA libraries, or pools of cDNA libraries from desired tissue sources or conditional treatments. Within the circle, any contigs from a database of previously performed assemblies that contain ESTs derived from any of the libraries selected to display will be shown and their relative position determined by a weighting algorithm (see Section 4.2.1). CCV is thus useful for investigating and displaying the relationship between cDNA libraries of different sources in terms of the number, type and expression pattern of specific sequences they contain.

In this Chapter, CCV was used to examine the tissue specificity and overall expression patterns in a range of selected tissues of the 306 wheat ESTs identified in Chapter 3 that show similarity to the rice chromosome 1 region syntenous to the region deleted in the wheat *ph2a* mutant. Furthermore, a brief analysis of the 9139 ESTs from the wheat meiotic anther cDNA library (wheat anthers at pre-meiosis to metaphase I inclusive) was performed to briefly investigate the diversity and tissue representation of sequences from this library.

4.2 Materials and methods

4.2.1 Contig assembly and display in CCV

The contig assembly framework on which the analysis for this Chapter was built was performed by G. Lazo (USDA-ARS, Albany CA). Briefly, the details of the procedure for contig assembly and display in the CCV program are described below.

All Triticeae ESTs sequenced at the USDA-ARS which are publicly available either through wEST, the Triticeae resource page of the USDA (wheat.pw.usda.gov/wEST) or through GenBank (dbEST) at NCBI (www.ncbi.nlm.nih.gov/dbEST/index.html), were partitioned out based on the cDNA library derivation. This collection of 117510 ESTs from the available libraries was assembled into 18876 contigs using the program phrap (penalty –5; minmatch 50; minscore 100) and stored in a local database accessible by CCV. In the program CCV, a number of selected cDNA libraries from the total collection used for initial contig assembly are chosen for analysis. CCV subsequently displays those contigs that are either wholly or in part formed from the assembly of one or more ESTs from at least one of the libraries selected for analysis. The position of contigs within the display is determined by a weighting algorithm that spatially distributes a contig based on numbers of ESTs derived from a library, the number of times an EST from a given library is represented in the contig and also the library size (Lazo, *pers.commun*.).

4.2.2 Analysis of the meiotic anther cDNA library and *Ph2*-region ESTs

4.2.2.1 Selection of libraries for display

Twenty eight cDNA libraries (**Table 4.1**) were selected for analysis in CCV to compare with the expression of ESTs from the wheat meiotic anther cDNA library and the 306 *Ph2*-region ESTs identified from comparative genetics studies in Chapter 3. Collectively these 28 cDNA libraries contain a total of 69532 sequences. Phrap assembled 44961 of these ESTs into 10533 contigs. All libraries were non-normalised and primarily derived from *Triticum aestivum*. The 28 libraries were selected such that the major plant tissue types were represented in CCV displays.

Table 4.1: Details of Triticeae cDNA libraries selected for CCV analysis.

Lib. name	Species	Tissue	Stage	# ESTs
TA054XXX	*T. aestivum*	anther	pre-meiosis-metaphase I	9139
TA016E1X	*T. aestivum*	crown	seedling	2997
TA038E1X	*T. aestivum*	crown	seedling	1231
TA012XXX	*T. aestivum*	embryo	mature, dormant seeds	2276
TA049E1X	*T. aestivum*	embryo	mature, dormant seeds	3111
TA001E1X	*T. aestivum*	endosperm	5-30 DPA	6116
TA0000FG	*T. aestivum*	spike	mature plant	727
TA009XXX	*T. aestivum*	spike	mature plant	11364
TA017E1X	*T. aestivum*	spike	post-anthesis	1277
TA018E1X	*T. aestivum*	spike	post-anthesis	3584
TA019E1X	*T. aestivum*	spike	pre-anthesis	14304
TA032E1X	*T. aestivum*	spike	post-anthesis	1325
TA027E1X	*T. aestivum*	leaf	full tillering	1055
TA031E1X	*T. aestivum*	leaf	full tillering	1320
TA036E1X	*T. aestivum*	leaf	full tillering	823
TA037E1X	*T. aestivum*	sheath	seedling	1154
TA005E1X	*T. aestivum*	whole plant	5-day old	897
TA007E1X	*T. aestivum*	whole plant	5-day old	1264
TA015E1X	*T. aestivum*	whole plant	14-day old	1123
TT039E1X	*T. turgidum*	whole plant	mature plant	1479
TA006E1X	*T. aestivum*	shoot	seedling	2590
TM011XXX	*T. monococcum*	shoot apex (vegetative)	5-week old plants	3031
TM043E1X	*T. monococcum*	shoot apex (early reproductive)	7-week old plants	3580
SC010XXX	*S. cereale*	root tip	seedling	1199
SC013XXX	*S. cereale*	root tip	seedling	778
TA047E1X	*T. aestivum*	root tip	seedling	1036
TA048E1X	*T. aestivum*	root tip	4-day old plants	1046
TA008E1X	*T. aestivum*	root	seedling	1842
			Total	**69532**

4.2.2.2 Contig contributions from ESTs of the meiotic anther cDNA library.

The wheat meiotic anther cDNA library (labelled TA054XXX in Figures of this Chapter) was included in the total Triticeae library collection used for initial contig assembly (Section 4.2.1). It was also selected as one of the 28 libraries to display in CCV. The expression patterns of ESTs represented in this library were displayed by identifying contigs formed wholly or in part by contributions from ESTs derived from this library. These contigs were selected and highlighted in relevant displays.

4.2.2.3 Contigs with similarity to ESTs derived from genes of the *Ph2* region

The 306 wheat ESTs identified in Chapter 3 that show similarity to the rice chromosome 1 region syntenous to the *ph2a* deleted region on 3DS do not represent a library as such and therefore a different method was used to display the expression patterns of these ESTs in CCV. Each of the 306 ESTs was used in BLAST searches of the complete contig database (Section 4.2.1) to identify contigs showing similarity. If contigs showing similarity were amongst the 10533 generated by contributions from ESTs of the 28 libraries selected for analysis in CCV, then these contigs are highlighted in relevant displays.

4.3 Results and discussion

4.3.1 CCV analysis of the *Ph2*-region ESTs

The primary question of interest in this Chapter was the following: Does *Ph2* represent a cluster of predominantly meiotically expressed genes? As discussed in the Introduction (Section 4.1), this has been tentatively suggested recently but evidence to support this idea is missing. To address this question, we analysed the expression distribution in major plant tissues of the wheat ESTs putatively identified from the region deleted in *ph2a* using CCV. Each of the 306 wheat ESTs were used in BLAST searches of assembled contigs from all available Triticeae libraries. When no E-value similarity cut-off was placed on these searches, 238 *Ph2*-region ESTs showed a degree of similarity to one of 10533 contigs generated by contribution from ESTs of the 28 Triticeae libraries selected for analysis. These contigs are highlighted in the CCV display of **Figure 4.1 A.**

When an E-value similarity cut-off level of ≤ 1e-^{10} was placed on these BLAST searches, 116 *Ph2*-region ESTs showed a degree of similarity to one of 10533 contigs generated by contribution from ESTs of the 28 Triticeae libraries selected for analysis. These contigs are highlighted in the CCV display of **Figure 4.1 B**.

From **Figure 4.1 A** and **B** we can make several observations and conclusions in relation to the expression and tissue specificity of ESTs derived from genes in the region deleted in *ph2a.* The highlighted contigs that show similarity to ESTs of the *ph2a* deletion region in BLAST searches are evenly distributed throughout the circle of both CCV displays. Therefore, the apparent expression and tissue specificity pattern of ESTs derived from the chromosomal region on 3DS linked to *Ph2* is not suggestive of the presence of a cluster of predominantly meiotically expressed genes in this region. There is no clustering of highlighted contigs around the wheat meiotic anther cDNA library (TA054XXX), or indeed in the vicinity of any libraries derived from mitotically active tissues such as root tips and the shoot apex. The even spatial distribution of highlighted contigs indicates that genes in the vicinity of *Ph2* are likely to be present in diverse tissues of the wheat plant. Furthermore, this pattern of broad tissue distribution is apparent with and without cut-off levels applied to the results of BLAST searches against assembled Triticeae contigs.

4.3.1.1 The distribution of contigs contributed by ESTs of other large chromosomal regions

Does the pattern of expression of ESTs derived from the region deleted in *ph2a* represent what could be described as the normal or expected tissue distribution of mRNAs transcribed from genes of a large chromosomal region? How does the expression of the *Ph2*-region ESTs, as determined by the CCV analysis of Section 4.3.1, compare to mRNAs derived from other large chromosomal regions of the wheat genome? To answer these questions we used data from an NSF-sponsored project (see http://wheat.pw.usda.gov/wEST/), that in a collaborative effort has chromosomally mapped a large number of selected wheat ESTs into bins along the 21 wheat chromosomes as defined by a set of characterised wheat deletion lines and other cytogenetic stocks. Currently in this project over 6000 probes have been tentatively

Figure 4.1: Weighted distribution of contig membership showing contigs with similarity to ESTs derived from the region deleted in the *ph2a* mutant.

In an assembly using 117510 Triticeae ESTs as a source, 18876 contigs were assembled using phrap. Shown here, as green spots are 10533 contigs which are represented by 44961 ESTs from the 28 cDNA libraries selected for display.

A: Circled spots indicate all contigs represented by ESTs of the 28 cDNA libraries displayed that show similarity in BLAST searches to wheat ESTs identified from the *ph2a* deletion region.

B: Circled spots indicate all contigs represented by ESTs of the 28 cDNA libraries displayed that show similarity at $\leq$ 1e-^{10} in BLAST searches to wheat ESTs identified from the *ph2a* deletion region. A single contig is highlighted in red, and its connection to libraries in the display shown as red lines.

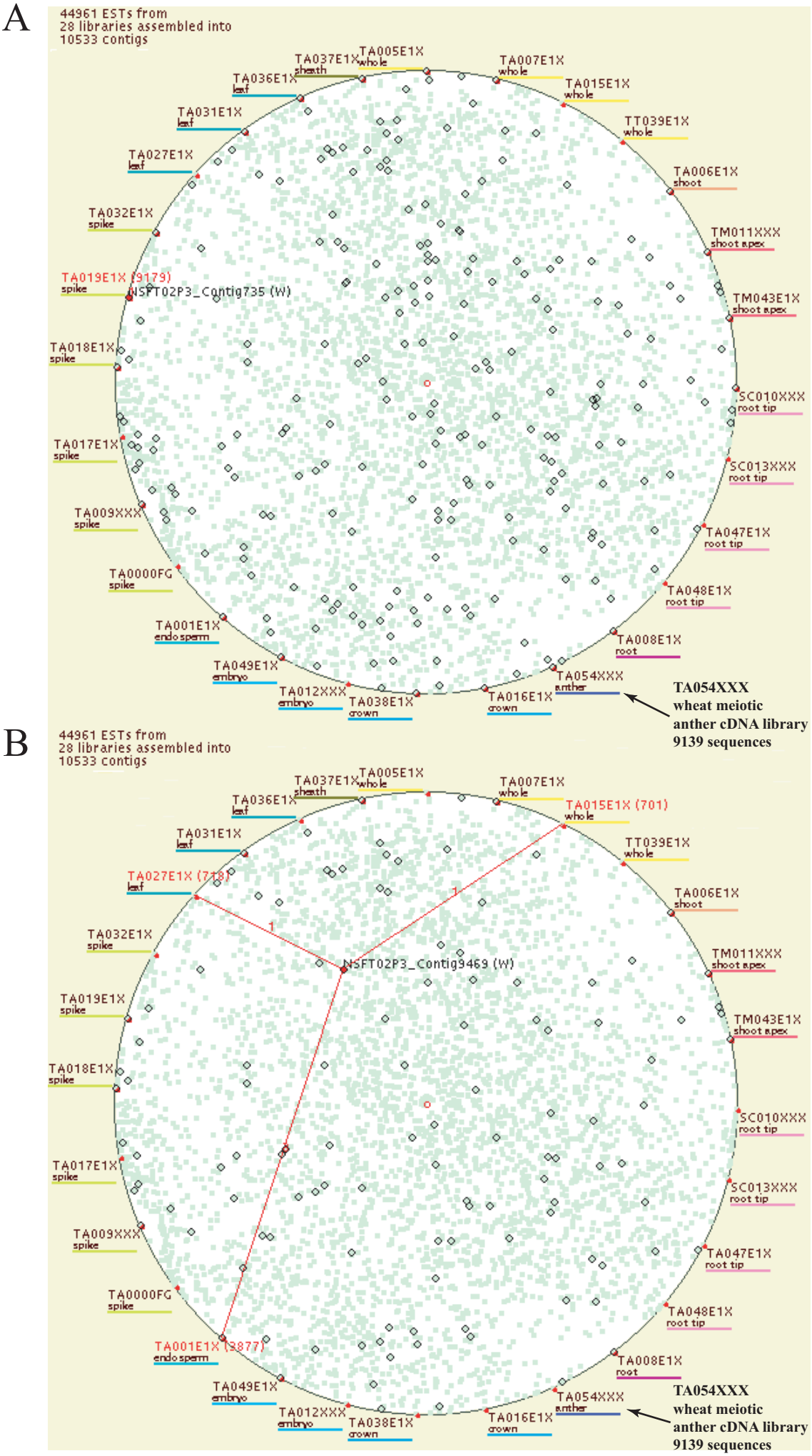
A
44961 ESTs from
28 libraries assembled into
10533 contigs
TA037E1X sheath
TA005E1X whole
TA007E1X whole
TA036E1X leaf
TA015E1X whole
TA031E1X leaf
TT039E1X whole
TA027E1X leaf
TA006E1X shoot
TA032E1X spike
TM011XXX shoot apex
TA019E1X (9179)
spike
NSFT02P3_Contig735 (W)
TM043E1X shoot apex
TA018E1X spike
SC010XXX root tip
TA017E1X spike
SC013XXX root tip
TA009XXX spike
TA047E1X root tip
TA0000FG spike
TA048E1X root tip
TA001E1X endosperm
TA008E1X root
TA049E1X embryo
TA054XXX anther
TA012XXX embryo
TA038E1X crown
TA016E1X crown
TA054XXX
wheat meiotic
anther cDNA library
9139 sequences
B
44961 ESTs from
28 libraries assembled into
10533 contigs
TA037E1X sheath
TA005E1X whole
TA007E1X whole
TA036E1X leaf
TA015E1X (701)
whole
TA031E1X leaf
TT039E1X whole
TA027E1X (718)
leaf
TA006E1X shoot
1
1
TA032E1X spike
TM011XXX shoot apex
NSFT02P3_Contig9469 (W)
TA019E1X spike
TM043E1X shoot apex
TA018E1X spike
SC010XXX root tip
TA017E1X spike
SC013XXX root tip
TA009XXX spike
TA047E1X root tip
TA0000FG spike
TA048E1X root tip
TA001E1X (3877)
endosperm
TA008E1X root
TA049E1X embryo
TA054XXX anther
TA012XXX embryo
TA038E1X crown
TA016E1X crown
TA054XXX
wheat meiotic
anther cDNA library
9139 sequences

mapped (Lazo, *pers*. *commun*.) using a set of 101 deletion lines that provide an average of thirteen deletions per chromosome resulting in bins averaging 10 cM. The chromosomal position of each EST bin determined from this deletion series is named according to its chromosome arm location (eg. 4BL), and its position in terms of chromosome arm fraction length determined from hybridisation and cytogenetic data (eg. 0.76-1.00).

Two of these deletion bins were selected for analysis in CCV to represent collections of genes from other large chromosomal regions in the wheat genome for comparison. These are; bin 4BL 0.86-1.00 from the long arm of chromosome 4B containing at present 183 tentatively mapped ESTs and, bin 5DL 0.76-1.00 from the long arm of chromosome 5D which contains at present 220 tentatively mapped ESTs. All contigs with contributions from ESTs of these mapped bins are shown in the 28-library CCV displays of **Figure 4.2**. It can be seen from the displays in **Figure 4.2** that highlighted contigs contributed by ESTs of these two chromosomal bins are distributed evenly throughout the circle. This pattern of distribution is similar to that observed from the analysis of contigs with similarity to ESTs derived from the region deleted in the *ph2a* mutant. This result confirms the conclusion from Section 4.3.1 that the chromosomal region in the vicinity of *Ph2* does not seem to be characterised by a cluster of genes predominantly expressed in meiotic or mitotically dividing tissues. Messenger RNAs derived from genes of the *Ph2* region appear to be normally distributed amongst various tissues of the wheat plant.

Furthermore, these results provide an insight into the transcriptional diversity of immature anther tissues. It was observed from Chapter 3 that almost 20 % of the 306 wheat ESTs identified from comparative genetics studies were represented in the wheat meiotic anther cDNA library. The similarities in the spatial distribution of contigs showing similarity to *Ph2*-region ESTs and contigs derived from contributions of ESTs from the two bins mapped to chromosomes 4BL and 5DL suggest that the finding of 20 % of all transcribed wheat genes in this tissue may represent the normal and diverse transcriptional composition of immature anther tissue.

Figure 4.2: Weighted distribution of contig membership contributed by ESTs derived from two chromosomally mapped EST bins.

In an assembly using 117510 Triticeae ESTs as a source, 18876 contigs were assembled using phrap. Shown here, as green spots are 10533 contigs which are represented by 44961 ESTs from the 28 cDNA libraries selected for display.

A: Circled spots indicate all contigs represented by ESTs of the 28 cDNA libraries displayed that have been chromosomally mapped using an aneuploid series of wheat deletion lines to bin 4BL 0.86-1.00.

B: Circled spots indicate all contigs represented by ESTs of the 28 cDNA libraries displayed that have been chromosomally mapped using an aneuploid series of wheat deletion lines to bin 5DL 0.76-1.00.

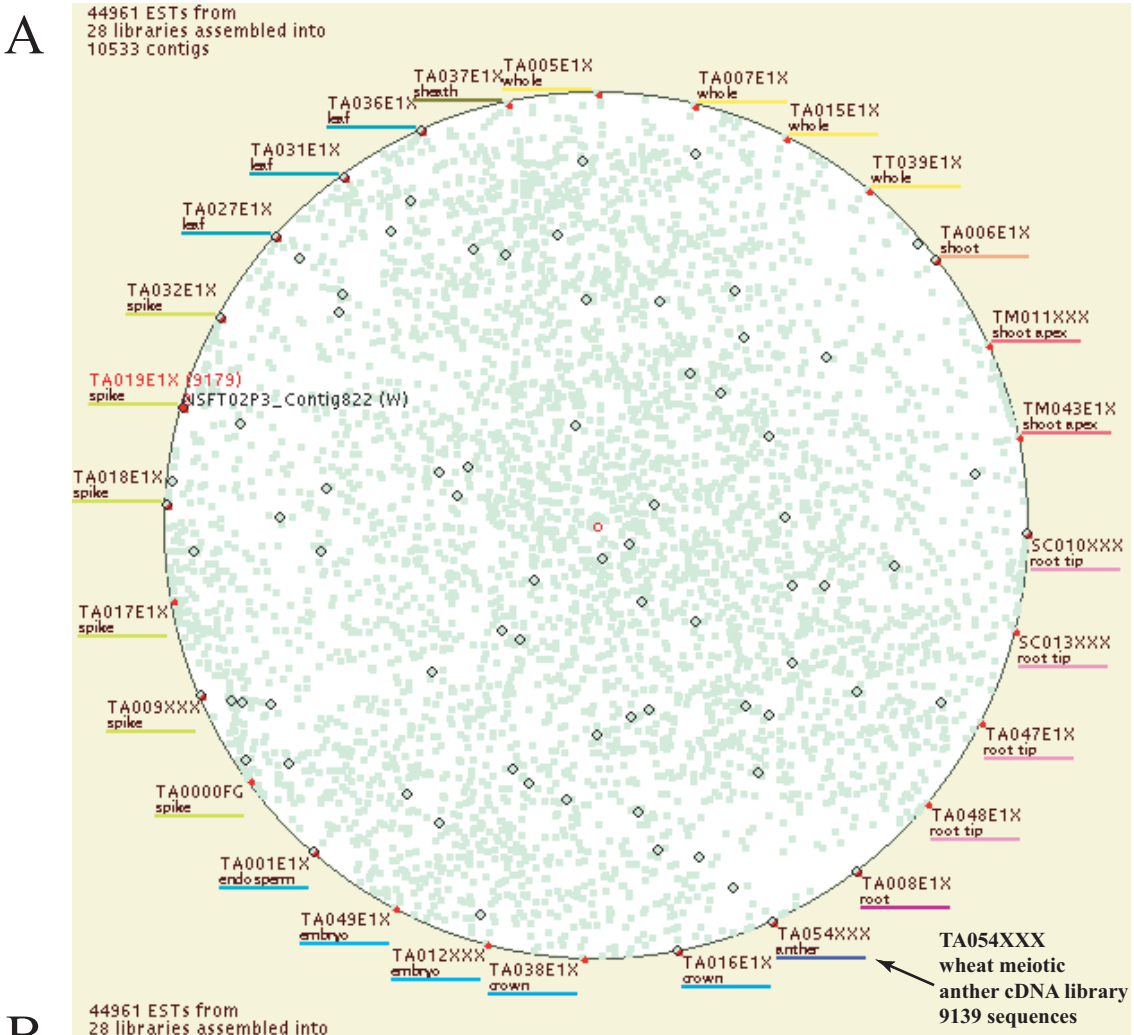
A
44961 ESTs from
28 libraries assembled into
10533 contigs
TA037E1X sheath
TA005E1X whole
TA007E1X whole
TA036E1X leaf
TA015E1X whole
TA031E1X leaf
TT039E1X whole
TA027E1X leaf
TA006E1X shoot
TA032E1X spike
TM011XXX shoot apex
TA019E1X (9179) spike
NSFT02P3_Contig822 (W)
TM043E1X shoot apex
TA018E1X spike
SC010XXX root tip
TA017E1X spike
SC013XXX root tip
TA009XXX spike
TA047E1X root tip
TA0000FG spike
TA048E1X root tip
TA001E1X endosperm
TA008E1X root
TA049E1X embryo
TA054XXX anther
TA012XXX embryo
TA038E1X grown
TA016E1X grown
TA054XXX
wheat meiotic
anther cDNA library
9139 sequences

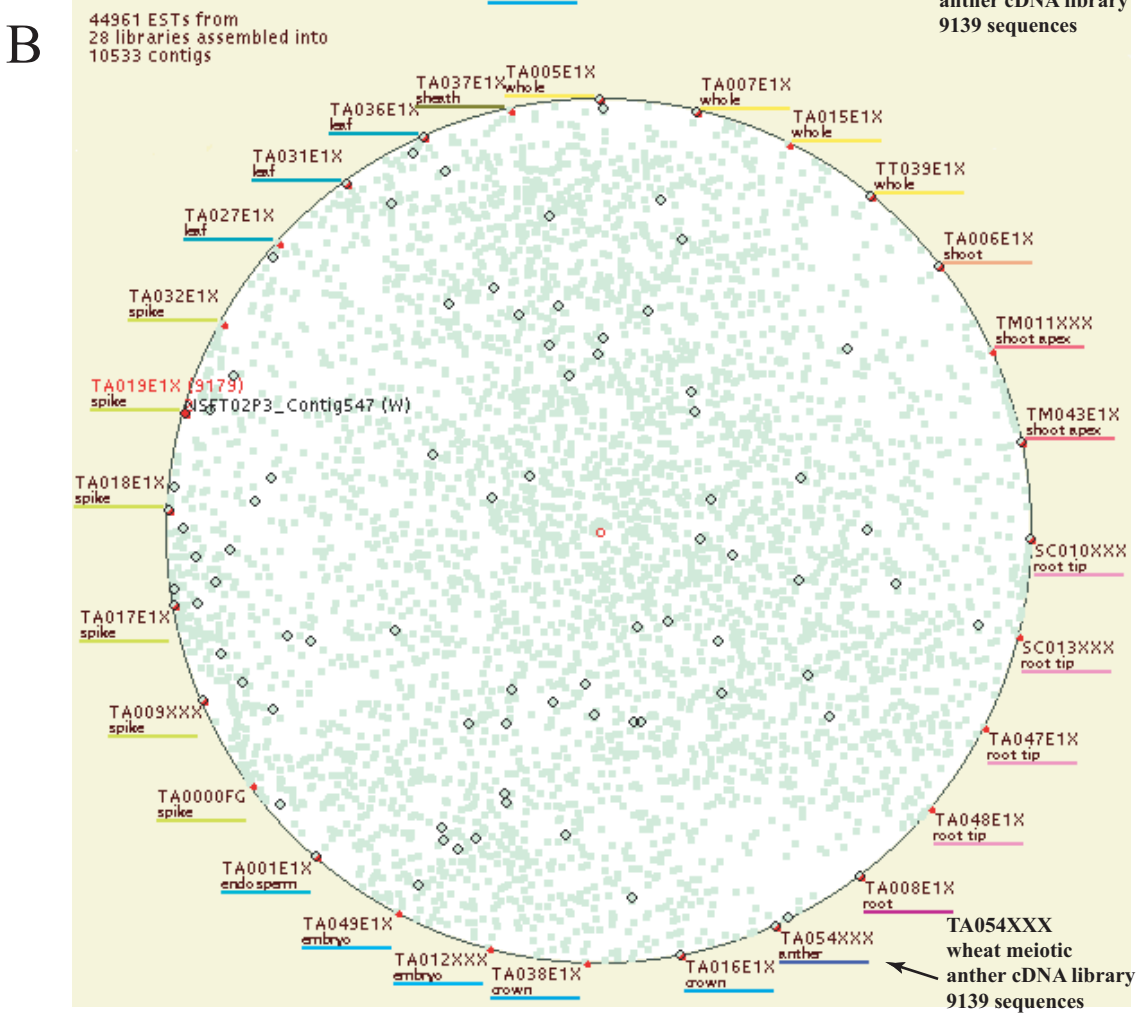
B
44961 ESTs from
28 libraries assembled into
10533 contigs
TA037E1X sheath
TA005E1X whole
TA007E1X whole
TA036E1X leaf
TA015E1X whole
TA031E1X leaf
TT039E1X whole
TA027E1X leaf
TA006E1X shoot
TA032E1X spike
TM011XXX shoot apex
TA019E1X (9179) spike
NSFT02P3_Contig547 (W)
TM043E1X shoot apex
TA018E1X spike
SC010XXX root tip
TA017E1X spike
SC013XXX root tip
TA009XXX spike
TA047E1X root tip
TA0000FG spike
TA048E1X root tip
TA001E1X endosperm
TA008E1X root
TA049E1X embryo
TA054XXX anther
TA012XXX embryo
TA038E1X grown
TA016E1X grown
TA054XXX
wheat meiotic
anther cDNA library
9139 sequences

4.3.2 CCV analysis of the wheat meiotic anther cDNA library

CCV was also used in this study to examine the tissue distribution of assembled contigs that were completely or in part formed by the contribution of ESTs from the wheat meiotic anther cDNA library. These are shown in **Figure 4.3**.

As previously mentioned, CCV is still under development and as such the purpose of this analysis was primarily to briefly investigate the effectiveness of CCV as a tool to broadly query the mRNA composition of diverse cDNA libraries with respect to the types of unique and common sequences they contain. Methods to enable queries of this nature would be valuable for researchers interested in investigating the transcriptional diversity of specific or unique tissues. These questions are difficult to answer with conventional one-on-one BLAST searches when large numbers of ESTs are available for the libraries under investigation. The CCV analysis of the wheat meiotic anther cDNA library is also presented here as a useful comparison to the displays of Section 4.3.1 above. It illustrates the types of distribution expected in CCV for EST collections that show a degree of tissue specificity or prevalence. This is seen for sequences derived from this tissue as the clustering of highlighted contigs towards the point on the circumference of the circle representing the wheat meiotic anther cDNA library TA054XXX in **Figure 4.3**.

It is interesting to observe a distortion in the clustering pattern of those highlighted contigs in close proximity to the circumference of the circle near TA054XXX. The majority of highlighted contigs in this region appear to be radiating towards the crown library TA016E1X rather than towards TA054XXX. This distribution can be explained in consideration of the other libraries used in the CCV displays of this analysis. The wheat meiotic anther library TA054XXX is not the only library selected containing anther tissues. Also included for CCV analysis were six whole spike libraries (**Table 4.1**) that were selected to predominantly represent floral tissues other than anthers in the wheat plant. The annotations for these libraries indicate that they were all prepared from spike tissues at the mature or post-anthesis stage, the exception however being the library TA019E1X which is annotated as being prepared from pre-anthesis spikes 2 cm in length to the yellow anther stage. The assumed presence of sequences derived from anther

Figure 4.3: Weighted distribution of contig membership contributed by ESTs from the wheat meiotic anther cDNA library.

In an assembly using 117510 Triticeae ESTs as a source, 18876 contigs were assembled using phrap. Shown here, as green spots are 10533 contigs which are represented by 44961 ESTs from the 28 cDNA libraries selected for display. Dark spots indicate contigs that are completely or in part derived from contributions of ESTs of the wheat meiotic anther cDNA library TA054XXX.

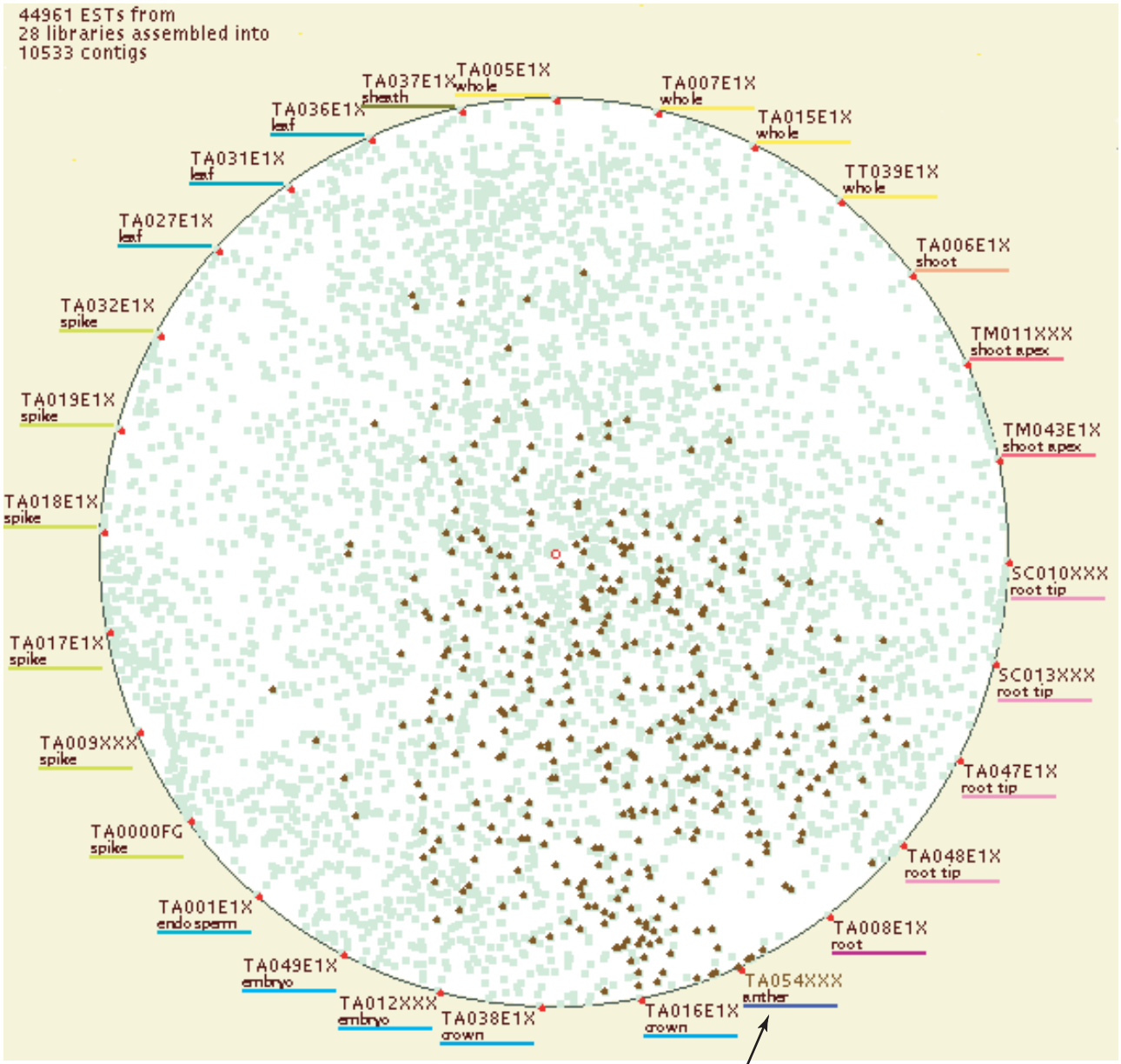

TA054XXX
wheat meiotic anther cDNA library
9139 sequences

tissues in these spike libraries provides an explanation for the observed trend of highlighted contigs near the circumference of the circle to radiate away from TA054XXX in the direction of the spike libraries to the left of the display in **Figure 4.3**. The effect of having spike libraries included in these displays is evident but appears to be relatively minor and indicates that their presence does not significantly affect the spatial distribution of contigs that appear to be derived from the assembly of ESTs showing a degree of specificity or prevalence in anther tissues.

4.4 Conclusions

From the results of the analysis performed in this Chapter, we can make a number of conclusions regarding both the transcriptional activity of sequences derived from the region deleted in the *ph2a* mutant and the effectiveness of programs such as CCV to investigate the complexity of sequence information represented in EST databases of important plant species.

Firstly, the chromosomal region linked to *Ph2* does not seem to be characterised by a cluster of genes with expression predominantly in actively dividing meiotic or mitotic tissue. Based on these results, it is difficult to favour the proposal that the chromosomal region in the vicinity of *Ph2* is structurally important for processes of meiotic and indeed mitotic transcription, although we cannot completely exclude this possibility. Rather, it seems that the pattern of expression of genes from this region resembles closely that observed for other large chromosomal regions of the genome. Secondly, it is apparent that wheat anther tissues are extremely diverse in terms of the transcriptional complexity of sequences they contain. CCV analysis suggests that finding 20 % of all transcribed wheat genes in anthers could approximate what may be considered normal for this tissue at this developmental stage, and highlights the challenges at hand for studies aiming to dissect out meiotic-related genes in the anther. Thirdly, the availability of software such as CCV in combination with contig assembly data from Triticeae crops will be central to exploit the vast array of EST information from publicly accessible databases. Here we used CCV to address some difficult but important questions of our research on meiosis in relation to *Ph2*. We found CCV to be an effective tool to explore the sequence diversity and commonality of cDNA libraries and other collections of EST sequences such as

those derived from the region deleted in the *ph2a* mutant. Communicating the advantages and disadvantages of such analysis programs to software developers will promote adaption to provide the flexibility required by researchers to effectively address biological questions from the wealth of EST resources available at present.

CHAPTER 5

TRANSCRIPT PROFILING DURING MEIOTIC DEVELOPMENT

5.1 Introduction

5.1.1 Microarray background

The emergence of molecular biology into the post-genomic era has been initiated by several high-throughput technologies, one of which is microarrays. Microarrays were first conceived in the early 1990's as a tool for gene screening and target identification. Since this time there has been an explosion in the number of research groups around the world implementing this technology. Out of necessity, developments in hardware, methodologies and data analysis have occurred concomitantly. Microarrays are now being applied to diverse research applications that includes gene discovery, disease characterisation, developmental biology, genotyping and polymorphism screening, mutation detection and toxicology.

Over the course of the last two decades, a number of molecular techniques have been developed for the detection and quantification of gene expression levels in biological samples. These include Northern blots (Alwine *et al.*, 1977), S1 nuclease protection (Berk and Sharp, 1977), subtractive hybridisation (Sargent and Dawid, 1983), semi-quantitative and quantitative RT-PCR (Powell *et al.*, 1987), the sequencing of cDNA libraries (Adams *et al.*, 1991; Okubo *et al.*, 1992), differential display (Liang and Pardee, 1992), serial analysis of gene expression (SAGE) (Velculescu *et al.*, 1995), and more recently, hybridisation to microarrays (Schena *et al.*, 1995). Microarrays represent a technological extension of existing hybridisation-based methods and in many ways, parallel RNA gel-blotting techniques.

Currently, two general types of DNA microarrays have been developed: fragment-based microarrays (Schena *et al.*, 1995), and oligonucleotide-based microarrays (Lipshutz *et al.*, 1995). Most commonly, DNA fragment-based microarrays are created by spotting

amplified cDNA fragments in a high density pattern onto a solid substrate such as a glass slide (cDNA microarrays). DNA fragment-based microarrays however, may also be constructed from genomic clones or DNA amplified from open reading frames identified in sequenced genomes. Oligonucleotide microarrays are either constructed by spotting pre-synthesised oligonucleotides onto a glass surface or by chemically synthesising approximately 25-mer oligonucleotides directly onto a glass or silicon surface using photolithograpy technology. Glass substrates currently remain the favored solid support for the manufacture of microarrays. The non-porous nature of glass enables the high density gridding of large numbers of individual DNA sequences and ensures that fluorescently labeled samples hybridised to microarrays have direct access to target sequences without the limitations of diffusion. Glass slides are also readily available, have low inherent fluorescence, and a variety of different surface chemistries are available to enable the stable attachment of nucleic acids. The use of glass surfaces in combination with fluorescent labeling and detection distinguishes microarrays from similar 'macroarray' hybridisation assays developed in the 1970's that utilise flexible membranes such as nitrocellulose and nylon, radioactivity and autoradiographic detection of signal intensities.

Figure 5.1 illustrates diagrammatically a generalised scheme for the construction and screening of a cDNA microarray, such as the one used in this study. Throughout this Chapter, DNA elements tethered to the microarray surface will be referred to as probes, and the free, fluorescently labeled nucleic acid samples applied to the microarray surface during hybridisation referred to as the targets. This is in concordance with accepted nomenclature for microarray hybridisation partners (*Nature Genetics* Supplement, Vol. 21(1), January 1999). Once a microarray has been fabricated by the robotic printing of PCR amplified cDNA clones at indexed locations onto a glass slide, hybridisations may be performed. Microarrays are ideally suited to making pair-wise comparisons, and expression analysis is generally carried out through the competitive hybridisation of two fluorescently labeled target RNA populations (commonly referred to as the test and reference). The fluorescent labels Cyanine 3 dUTP (Cy3) and Cyanine 5 dUTP (Cy5) are frequently paired for this purpose due to their widely separated excitation and emission spectra, high incorporation efficiencies with reverse trancriptases and good photostability. After a series of washing steps to remove unbound target and

Figure 5.1: A generalised scheme for the construction and screening of a cDNA microarray.

Clones selected for microarray printing are PCR amplified, purified, resuspended in an appropriate buffer and robotically printed at indexed locations onto a glass slide. Microarray targets (commonly referred to as the test and reference) are prepared via either direct or indirect fluorescent labeling, combined together and hybridised to the microarray. Non-specific hybridisation is removed through a series of increasingly stringent washing steps, and slides are scanned using a confocal laser scanner. Microarray images are captured as 16-bit TIFF files, and are the starting point for signal intensity quantification and generation of expression profiles.

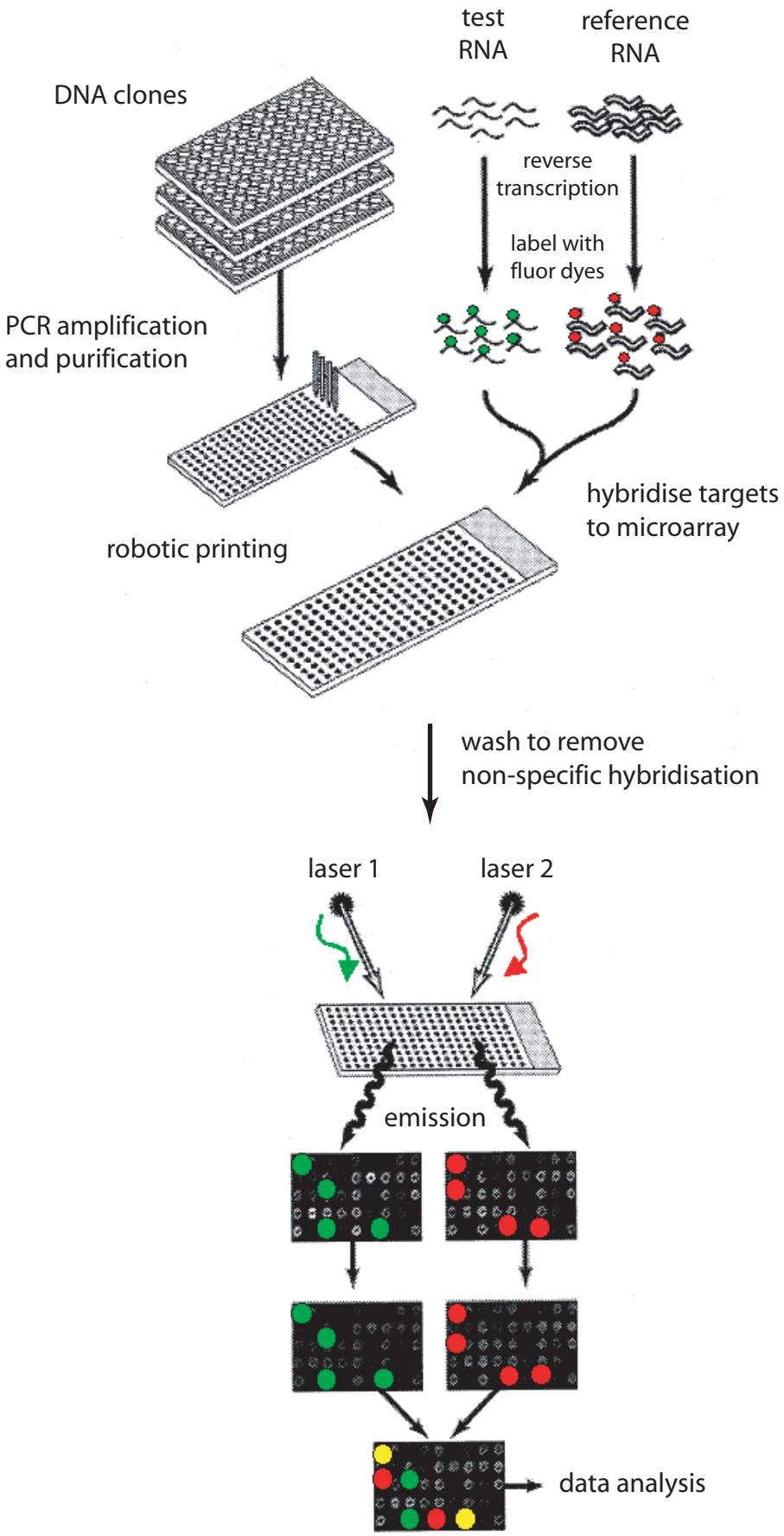
test
RNA
reference
RNA
DNA clones
reverse
transcription
label with
fluor dyes
PCR amplification
and purification
hybridise targets
to microarray
robotic printing
wash to remove
non-specific hybridisation
laser 1
laser 2
emission
data analysis

non-specific hybridisation, the fluorescent target that has hybridised to complementary probes on the microarray surface is excited by light using a specialised confocal laser scanner. The fluorescent intensity emitted by each spot at excitation spectra specific for Cy3 and Cy5 is indicative of the abundance of that particular mRNA species in the original test and reference target populations. Raw intensity values are subsequently subjected to a series of important statistical procedures, such as normalisation, and the resulting expression information is commonly represented as a ratio that compares the expression of each probe on the microarray in the test and reference tissue types.

5.1.2 Prospects for plant meiotic gene discovery

The majority of meiotic genes identified have been from the budding yeast *Saccharomyces cereviseae*, with recent estimates indicating that approximately 300 core genes may be specific for meiosis, and approximately 600 may be required for sporulation and gametogenesis in this organism (Schwarzacher, 2003). Many homologues to yeast genes of meiotic function have been identified in other lower eukaryotes such as *Schizosaccharomyces pombe*, *Caenorhabditis elegans* and *Drosophila melanogaster*, from mammals such as mouse and human, and higher plants such as *Arabidopsis thaliana*. The approach for gene identification has largely involved the use of forward genetics through insertional mutagenesis, and the availability of whole genome sequences. Our knowledge of meiotic gene function in higher plants has largely been led by studies in *Arabidopsis* using insertion tagging strategies. Indeed, the majority of meiotic genes cloned from higher plant species to date are from *Arabidopsis*.

In contrast to the advancements made in meiotic gene discovery in plants such as *Arabidopsis*, the progress of gene discovery in agriculturally important cereal crops such as wheat, barley, rice and maize has been difficult. Progress has been principally hampered by the large and complex nature of the genomes of these species. These species are not as amenable to forward genetic approaches such as insertional mutagenesis, and recent evidence also indicates that reverse genetic approaches to meiotic gene discovery in higher plants will be limited in their impact. For example, Mercier *et al*. (2001) recently demonstrated that even at low stringency search levels, approximately 30 % of non-plant meiosis related sequences showed similarity with one

or several *Arabidopsis* putative genes. Interesting patterns of meiotic gene conservation between distantly related species such as plants and yeast are emerging from the accumulating collection of *Arabidopsis* meiotic homologues. Overall, recombination genes appear to be highly conserved, compared to proteins of the synaptonemal complex and cohesion machinery (Schwarzacher, 2003), providing further evidence that reverse genetic approaches will be of value to some areas of meiotic gene discovery in higher plants but will be limited in effectiveness for others.

A number of studies have characterised the expression profiles of all genes from *Saccharomyces cereviseae* during mitosis (Cho *et al.*, 1998; Spellman *et al.*, 1998) and meiosis (Chu *et al.*, 1998; Mata *et al.*, 2002; Primig *et al.*, 2000), and have revealed striking gene expression regulation for large numbers of genes associated with landmark developmental events. Mata *et al*. (2002) for example, used microarrays to study the developmental expression of all yeast genes during meiosis and sporulation, and report regulation of more than 50 % of the genome. Until recently, studies based on whole genome analysis had not been possible for higher plant species, due to the unavailability of a completely sequenced model genome from which to base microarray construction. Indeed, in the literature at present there are no reports of studies of plant meiotic development based on microarray construction from the expressed portions of genomes (EST collections).

5.1.3 Experimental design

A microarray approach was used in this study as a means to investigate the meiotic expression of a collection of specifically selected wheat ESTs. The experiments described in this Chapter were designed to address two main biological questions in the context of our current knowledge of wheat meiosis. Firstly, to identify genes exhibiting differential expression during meiosis between three wheat mutants, *ph2a*, *ph2b*, *ph1b* and wild-type Chinese Spring wheat. These experiments aimed to identify genes from mutated regions in these genomes as candidates for *Ph* loci. Secondly, the microarray experiments aimed to investigate the temporal patterns of expression for all target genes on the microarray during meiotic development in the anther. These experiments aimed

to correlate gene expression with meiotic events in the wheat anther as a means to identify candidates for molecular control of these processes.

5.1.4 General considerations

The broad application of microarray technology to all areas of biological research has been limited by the requirement of large amounts of sample tissue. Typically 50 µg to 200 µg of total RNA, or 1 µg to 4 µg poly(A) RNA is required for microarray hybridisation using direct fluorescent labeling protocols. This amount is required of each test and reference sample, for each microarray hybridisation. This may equate to a requirement for several hundred milligrams of starting tissue and thus constrains the use of microarrays for transcript profiling in specific cell types and small tissue samples.

One approach to address the application of small tissue samples in microarray experiments has been the development of indirect labeling methods that increase fluorescent signal intensity. A recent report for example (Xiang *et al.*, 2002), primed first strand cDNA synthesis with modified amino C6dT-random hexamers (containing free amino groups on the 5' ends), and incorporated aminoallyl-dUTP into the products. Amine-modified primers are incorporated into cDNA along with aminoallyl nucleotides, and fluorescent dyes are then chemically added to the free amines, increasing intensity such that as little as 1 µg of total RNA from cell lines generated sufficient signal for microarray hybridisation. A general concern however with various indirect labeling methods has been reliability when compared to conventional direct labeling techniques, and their application to plant microarray research has not been extensively reviewed.

Currently, the most favored method to broaden the use of microarray studies for small tissue samples and cell types is based on linear T7 RNA amplification. The T7 based linear amplification method was first described as a tool for analysing gene expression in cerebellar tissues (Van Gelder *et al.*, 1990) and later in single, live rat hippocampus neurons (Eberwine *et al.*, 1992). Using either purified poly(A) RNA or total RNA as the starting material, first strand cDNA synthesis by reverse transcription is primed with a synthetic oligo(dT) primer containing the phage T7 RNA polymerase promoter sequence. Second strand cDNA is synthesised by conventional methods, involving

degradation of the poly(A) RNA strand with RNase H, and strand extension with *E. coli* DNA polymerase. Amplified antisense RNA (aRNA) is obtained from *in vitro* transcription of the double-stranded cDNA (ds cDNA) template using T7 RNA polymerase. Depending on initial quantities of starting RNA, a second round of amplification may be performed if required. Transcribed aRNA molecules lack the T7 RNA polymerase promoter sequence, and are not available as substrates for further RNA polymerase activity. Importantly, this results in linear amplification. For application to microarray experiments, aRNA is used as the template for reverse transcription incorporating fluorescent labels by conventional direct labeling methods. A number of protocols based on linear amplification mechanisms have been developed and systematically verified for use in microarray analyses. These have recently been reviewed and evaluated by Zhao *et al*. (2002), concluding that T7 amplification reproducibly generates amplified RNA that closely approximates original sample individual mRNA abundance for gene expression profiling using cDNA microarrays.

The practical considerations of performing the microarray experiments described in this study without amplification based techniques are overwhelming. Consider the alternative briefly, assuming the following: A minimum requirement of 2 µg poly(A) RNA for each test and reference tissue sample (including the dye-swap experiment), and, an average yield of less than 1 µg total RNA per meiotic anther, approximately 1 % of which is represented by recoverable poly(A) RNA. Approximately 3500 microscopically staged meiotic anthers would be required. This estimation also ignores the need to often repeat hybridisations, and the fact that not all meiotic stages are acquired from anther sampling with equal frequency, further increasing time devoted to microscopy. Large sampling of this kind would also affect the temporal distinction of individual meiotic stage collections. The above example illustrates the importance of effective amplification techniques to broaden the application of microarray technology in both plant and animal biology. An amplification protocol was adapted from that published by Salunga *et al*. (1999) for use in this study. A single round of amplification was performed for preparation of meiotic targets.

5.2 Materials and methods

5.2.1 Preparation of amplified meiotic targets for microarray hybridisation

An amplification procedure based on T7 RNA polymerase *in vitro* transcription was adopted in this study for production of targets for microarray hybridisation. The procedure is described below and illustrated diagrammatically in **Figure 5.2**.

5.2.1.1 Meiotic anther collection

Tissue collection for synthesis of microarray targets for hybridisation was carried out according to the method in Section 2.2. For microarray experiments investigating temporal expression during meiosis, six anther collections were prepared. For each meiotic stage (anthers at; pre-meiosis, leptotene to pachytene, diplotene to late anaphase I, telophase I to telophase II, tetrads) and for the reference tissue (anthers at immature pollen), approximately 20 staged anthers were pooled for subsequent RNA isolation, cDNA synthesis, amplification and Cy3/Cy5 labeling prior to microarray hybridisation (**Figure 5.3 A**). For microarray experiments investigating differential expression between *Ph* mutant and wild-type Chinese Spring wheat anthers, four anther collections were prepared. For each *Ph* mutant genotype (*ph2a*, *ph2b*, *ph1b*) and for wild-type Chinese Spring wheat (reference tissue), anthers were collected from a whole spike whose largest central floret contained anther pollen mother cells at metaphase I. Anthers from all primary and secondary florets were harvested and pooled for each genotype for subsequent RNA isolation, cDNA synthesis, amplification and Cy3/Cy5 labeling prior to microarray hybridisation (**Figure 5.3 B**). For the microarray experiment used to verify the T7-based amplification protocol for generation of hybridisation targets, poly(A) RNA was derived from a collection of wheat anthers at meiotic stages pre-meiosis to metaphase I inclusive.

5.2.1.2 Total RNA and poly(A) RNA isolation

For each collection of meiotic anthers, total RNA was isolated using Trizol reagent according to the protocol outlined in Section 2.7.3.1. Following drying, total RNA pellets were resuspended in 100 µL 10 mM Tris-HCl pH 7.5 on ice. Poly(A) RNA purification was performed using a modified protocol from the Dynabeads mRNA

Figure 5.2: Procedure for linear T7 RNA amplification of microarray targets.

An oligo dT primer containing the T7 RNA polymerase promoter sequence (oligo dT-T7 primer) is annealed to the polyadenylated tail of purified poly(A) RNA. First and second strand cDNA synthesis produces a double stranded cDNA transcription template. *In vitro* transcription by T7 RNA polymerase generates a pool of antisense RNA (aRNA) molecules that are the template for subsequent reverse transcription incorporating fluorescent dyes.

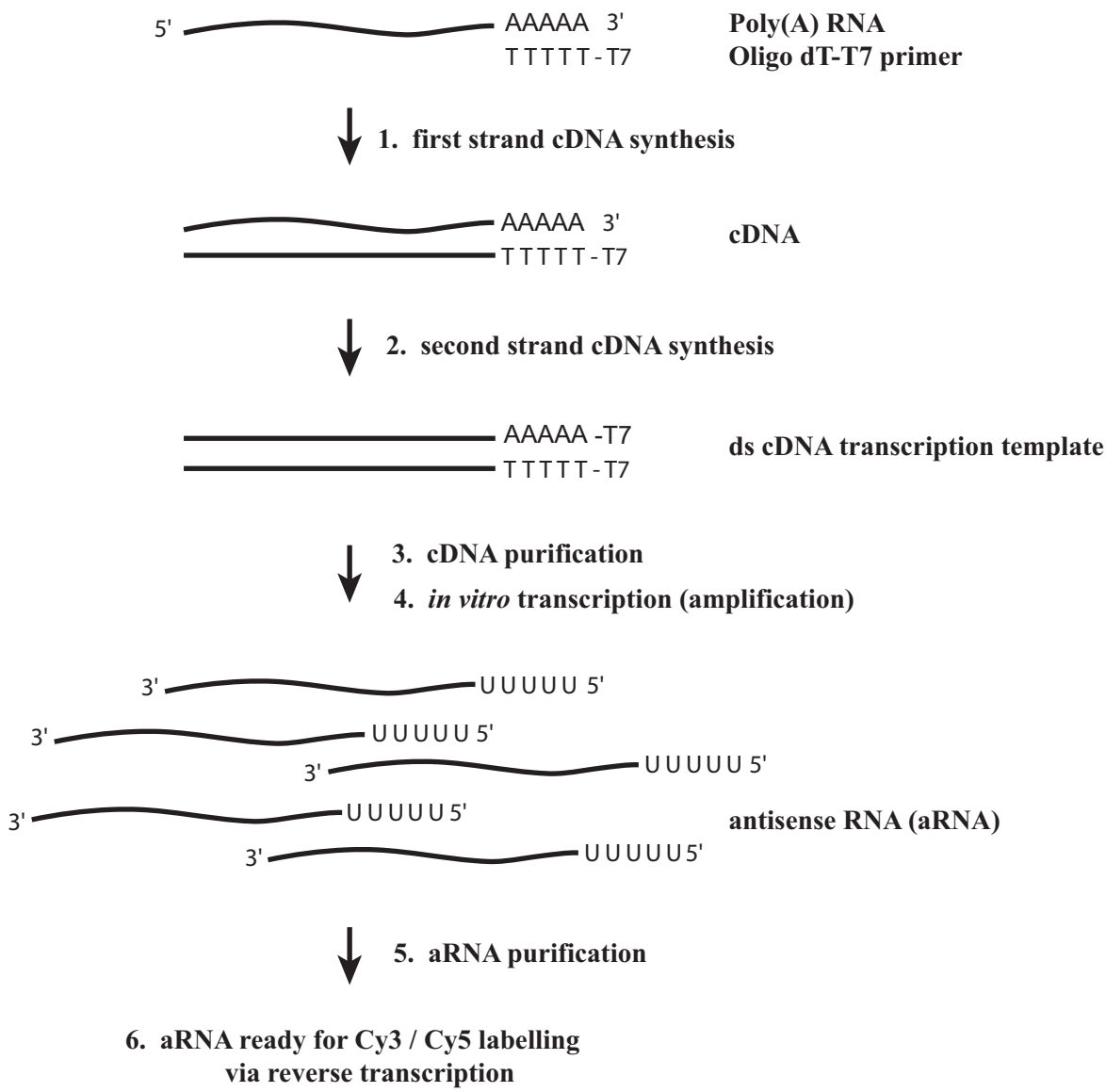
5'
AAAAA 3'
T T T T T - T7
Poly(A) RNA
Oligo dT-T7 primer
1. first strand cDNA synthesis
AAAAA 3'
T T T T T - T7
cDNA
2. second strand cDNA synthesis
AAAAA -T7
T T T T T - T7
ds cDNA transcription template
3. cDNA purification
4. in vitro transcription (amplification)
3' U U U U U 5'
3' U U U U U 5'
3' U U U U U 5'
3' U U U U U 5'
3' U U U U U 5'
antisense RNA (aRNA)
5. aRNA purification
6. aRNA ready for Cy3 / Cy5 labelling
via reverse transcription

Figure 5.3: The design of temporal series and *Ph* mutant vs. wild-type microarray experiments.

A: Targets for temporal series microarray experiments were prepared from microscopically staged meiotic anthers pooled into five developmental groups; pre-meiosis (pre-meiotic interphase), leptotene to pachytene, diplotene to late anaphase I, telophase I to telophase II and tetrads. Each meiotic stage target was hybridised in combination with a reference target derived from anthers containing pollen mother cells at the immature pollen stage of development. A common reference target was used in all meiotic stage hybridisations.

B: Targets for microarray experiments investigating differential expression between wild-type and three mutant genotypes *ph2a*, *ph2b* and *ph1b* were prepared from pooled anthers at the meiotic stages pre-meiosis to metaphase I. All anthers from primary and secondary florets were collected from a whole spike of each genotype whose largest central floret contained anther pollen mother cells at metaphase I. A common wild-type reference target was used in all hybridisations.

A

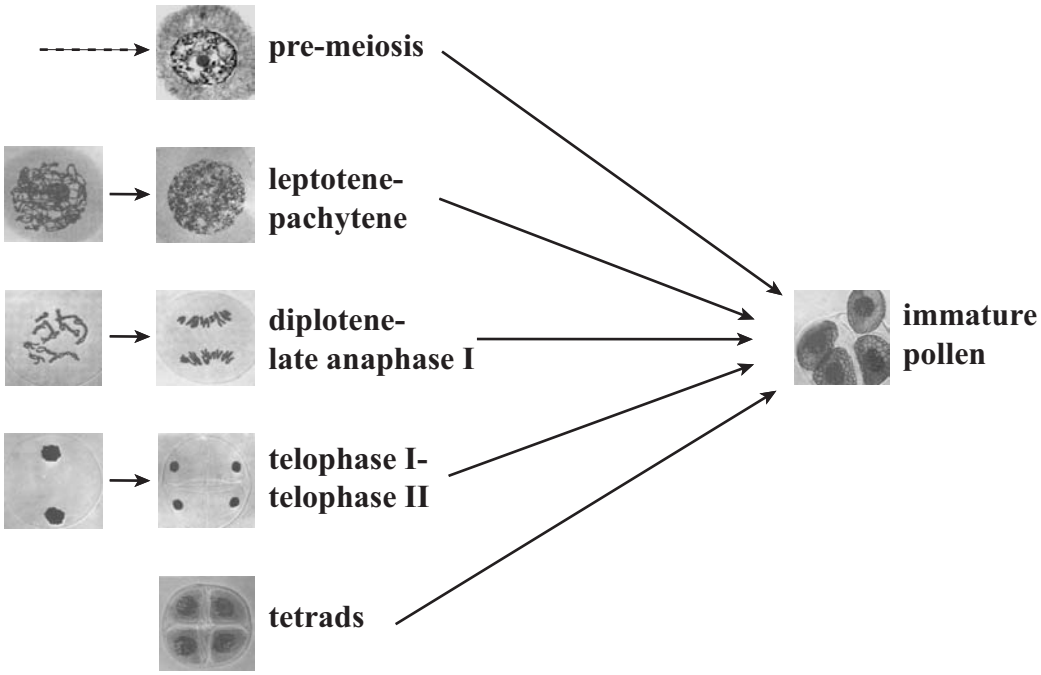
pre-meiosis
leptotene-
pachytene
diplotene-
late anaphase I
telophase I-
telophase II
tetrads
immature
pollen

B

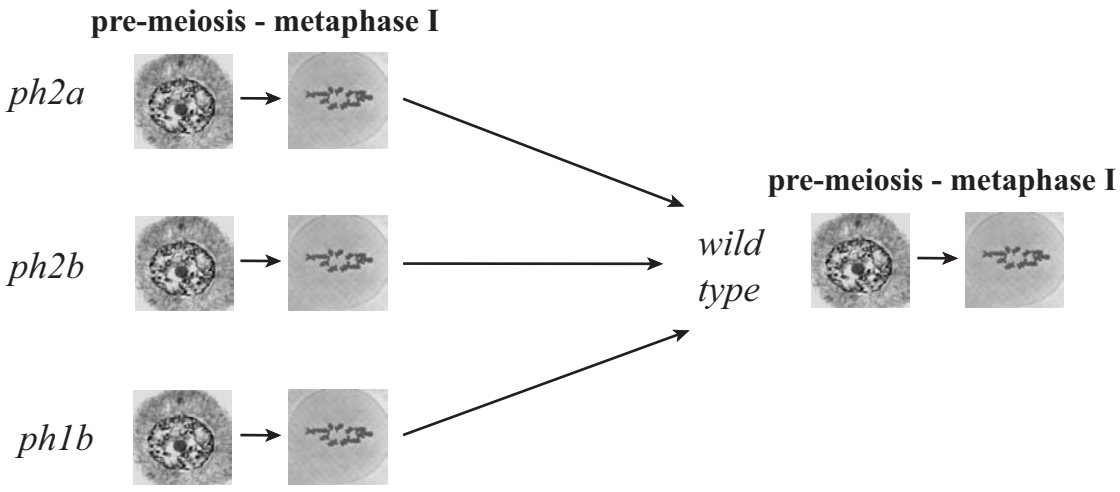
pre-meiosis - metaphase I
ph2a
ph2b
ph1b
wild
type
pre-meiosis - metaphase I

DIRECT Micro Kit (Dynal, Norway). 50 μL stock Dynabeads oligo $(dT)_{25}$ were prepared for poly(A) RNA purification by the removal of storage buffer on a Magnetic Particle Concentrator (Dynal, Norway), followed by a single wash and removal of 100 μL Binding Buffer (10 mM Tris-HCl pH 7.5, 500 mM LiCl, 1 mM EDTA). Dynabeads were resuspended in a further 100 μL Binding Buffer and kept on ice until use. Immediately prior to poly(A) RNA purification, the total RNA solution was heated at 65 °C for 2 min to disrupt secondary structures, and once cooled to RT added to 100 μL Dynabeads suspension prepared above. Hybridisation was carried out for 3 min to 5 min at RT on a rotating wheel. Total RNA/Dynabeads suspension was placed on a Magnetic Particle Concentrator, and the supernatant was removed and kept for later analysis if required. Dynabeads/poly(A) RNA hybrids were washed twice in Washing Buffer B (10 mM Tris-HCl, pH 7.5, 0.15 M LiCl, 1 mM EDTA). To elute bound poly(A) RNA, washed Dynabeads/poly(A) RNA hybrids were resuspended in 10 μL 10 mM Tris-HCl, incubated at 65 °C for 2 min and immediately placed onto a Magnetic Particle Concentrator. The supernatant containing purified poly(A) RNA was removed and stored on ice for immediate use or frozen at –80 °C until required.

5.2.1.3 First and second strand cDNA synthesis

The following oligo $(dT)_{21}$ primer containing the T7 RNA polymerase promoter sequence (Oligo dT-T7 primer) was used to prime cDNA synthesis from poly(A) RNA templates;

5' TCTAGTCGACGGCCAGTGAATTGTAATACGACTCACTATAGGGCG$(T)_{21}$ 3'

Primer binding prior to cDNA synthesis was carried out with the addition of 1 μL Oligo dT-T7 primer (0.5 mg/mL) to the poly(A) RNA sample prepared from Section 5.2.1.2, followed by heating at 70 °C for 10 min and immediate chilling on ice. The sample was collected at the bottom of the Eppendorf tube by a brief centrifugation step. First strand cDNA synthesis was carried out in a final reaction volume of 20 μL containing 11 μL poly(A) RNA/Oligo dT-T7 primer and 50 mM Tris-HCl pH 8.3, 75 mM KCl, 3 mM $MgCl_2$, 10 mM DTT, 500 μM each dATP, dCTP, dGTP, dTTP and 200 U SuperScript II reverse transcriptase (Invitrogen, Australia). Reverse transcription was carried out at 42

°C for 60 min. One microlitre was subsequently removed for a PCR control reaction (described in Section 5.3.3.2). Components of the second strand cDNA synthesis reaction were immediately added. Second strand cDNA synthesis was carried out in a final reaction volume of 150 µL containing 19 µL first strand cDNA and 25 mM Tris-HCl pH 7.5, 100 mM KCl, 5 mM $MgCl_2$, 10 mM $(NH_4)_2SO_4$, 0.15 mM ß-NAD^+, 250 µM each dATP, dCTP, dGTP, dTTP, 1.2 mM DTT, 10 U *E. coli* DNA ligase, 40 U *E. coli* DNA polymerase I and 2 U *E. coli* RNase H. The reaction was mixed by gentle pipetting and incubated at 16 °C for 2 h. 10 U T4 DNA polymerase were subsequently added followed by a further incubation at 16 °C for 10 min. The reaction was extracted once with 150 µL phenol/chloroform/iso-amyl alcohol (25:24:1), and the double stranded cDNA was purified using a QIAquick PCR purification kit (Qiagen, Australia) according to the manufacturer's directions. Following elution, the sample volume was reduced to 8 µL by vacuum centrifugation.

5.2.1.4 *In vitro* transcription (amplification)

The AmpliScribe T7 High Yield Transcription Kit (Epicentre, USA) components were used for *in vitro* transcription (amplification) from double stranded cDNA templates. To the 8 µL cDNA from Section 5.2.1.3, reaction components were added at room temperature, in the following order; 2 µL 10x Ampliscribe T7 buffer, 1.5 µL dATP, dCTP, dGTP and dUTP, 2 µL 0.1 M DTT, 2 µL T7 RNA polymerase. *In vitro* transcription was allowed to proceed for 3 h at 42 °C. Following incubation, 1 µL RNase-free DNase was added, and the reaction was incubated at 37 °C for 15 min. Antisense RNA (aRNA) was purified using an RNeasy mini kit (Qiagen, Australia) according to the manufacturers instructions. aRNA was eluted in 30 µL RNase-free water, spectrophotometrically quantified (as described in Section 2.9) and stored at –80 °C until required.

5.2.1.5 Target labelling

Target labeling was performed as follows: 1 µg aRNA, and 1µg random hexamers (Invitrogen, Australia) were mixed and heated at 70^{o}C for 10 min and immediately placed on ice. The first strand cDNA synthesis reaction consisted of 4 µL 5x

SuperScript II reaction buffer (Invitrogen, Australia), 2 μL 0.1 M DTT, 1 μL dNTP mix (1 mM each dATP, dGTP, dTTP, and 0.5 mM dCTP), 1 μL 1 mM fluorescent Cy3-dCTP or 1.5 μL 1mM fluorescent Cy5-dCTP (Amersham Biosciences, Australia) and an appropriate amount of RNase-free water to bring the final volume to 19 μL. The reaction was mixed well and incubated at RT for 10 min. SuperScript II reverse transcriptase (1 μL, 200 U/μL, Invitrogen, Australia) was added and the reaction was incubated at 42 ^{o}C for 1 h. Heating in boiling water for 3 min terminated the reaction. The RNA strand of the denatured cDNA-RNA hybrid was hydrolysed by adding 2 μL of 2.5 M NaOH and incubating at 37 ^{o}C for 15 min. The reaction was neutralised by adding 10 μL of 2 M HEPES pH 6.8. To remove free nucleotides and oligonucleotides, the cDNA strand was purified using a QIAquick PCR purification kit (Qiagen, Australia) according to the manufacturer's instructions. The fluorescent dye-labeled cDNA target was vacuum dried and stored at –20 ^{o}C until required.

5.2.2 Preparation of microarray slides

5.2.2.1 Amplification of probe sequences

PCR amplification of microarray probes was performed using 2 μL of an overnight bacterial culture as the template and primers directed to M13 reverse and forward sequences flanking the insert of the plasmid vector. The reaction was carried out in a total volume of 100 μL containing 1x reaction buffer, 2 mM $MgCl_2$, 0.2 mM each dNTP, 0.2 μM each M13 forward/reverse primer, 5 % DMSO, 2 μL bacterial culture and 2.5 U AmpliTaq Gold DNA polymerase (Applied Biosystems, Australia). Thermal cycling conditions were; 95 °C 10 min, 30 cycles of 94 °C 1 min, 55 °C 1 min, 72 °C 2 min, followed by 72 °C for 7 min. Amplified PCR products were purified using a Qiagen 96-well PCR purification kit (Qiagen, Australia) according to the manufacturer's instructions. The quality and quantity of purified PCR products was analysed by 1 % agarose gel electrophoresis, and PCR amplification repeated if required. PCR products were dried under vacuum and resuspended in 6 M sodium thiocyanate (NaSCN) solution, at the DNA concentration of 0.1 μg/μL or higher.

5.2.2.2 Robotic printing and slide blocking.

Glass slides (25 mm x 76 mm) utilising superamine coupling chemistry (TeleChem International Inc., CA USA) were used as the microarray substrate. Superamine substrates contain primary amine groups (NH_3^+) attached covalently to the glass surface. The amines carry a positive charge at neutral pH, allowing attachment of DNA through ionic interactions with a negatively charged phosphate backbone. Electrostatic attachment is supplemented by treatment with ultraviolet light or heat, which induces covalent attachment of the DNA to the surface. The combination of electrostatic binding and covalent attachment couples the DNA to the glass surface in a highly stable manner.

DNA solutions were spotted on slides using a Molecular Dynamics GenII Arrayer under >40 % humidity. Each slide contained 1830 different PCR products spotted in quadruplicate. Spot diameter was approximately 210 nm. Spotted slides were baked at 80 ^{o}C for 1 h to 2 h, and stored in a desiccation chamber under vacuum until use.

Prior to hybridisation, slides were treated with a blocking solution followed by a series of washing steps. Slides were immersed in isopropanol for 10 min and then transferred to a boiling water bath for 5 min. Slides were transferred to a preheated blocking solution containing 1 % (w/v) BSA fraction V (Sigma), 0.2 % (w/v) SDS, 3.5x SSC and incubated at 60 °C for 20 min. Slides were removed from blocking solution, immediately immersed in distilled water and dipped 50 times (minimising time in air). Washing was repeated an additional 4 times in fresh distilled water. Slides were transferred to an isopropanol bath and dipped in a similar manner 10 times. Slides were removed from isopropanol and dried immediately using compressed ultrapure nitrogen gas. This procedure minimised smearing on the glass surface and removed dust particles. Coverslips used in subsequent hybridisation steps were also blown down with ultrapure nitrogen gas to remove dust particles.

5.2.3 Hybridisation, washing and scanning

For each microarray experiment (e.g. test vs. reference), two hybridisations were performed. These so-called ‘dye swap’ hybridisations aim to minimise Cy3 or Cy5 fluorescent intensity bias due to factors such as unequal incorporation during labeling or

differing scanning properties of the two dyes. An example is represented by the following microarray experiment:

Slide 1; hybridised with test-Cy3, reference-Cy5
Slide 2; hybridised with test-Cy5, reference-Cy3

Purified targets were dissolved in 30 μL hybridisation solution (5x SSC, 100 mg/mL sheared salmon sperm DNA (Invitrogen, Australia), 0.1 % SDS, 100 mg/mL oligo$(dA)_{80}$ (Operon), 50 % deionised formamide (Sigma)) and denatured at 95 °C for 3 min. The contents of the tubes were gently mixed and centrifuged in a benchtop centrifuge at 14000 rpm for 2 min. Cy3 and Cy5 labeled target pairs were combined together, mixed and placed on the microarray surface. A coverslip was placed on the slide and hybridisation was performed overnight in the dark at 42 ^{o}C in a custom designed low-volume humidity chamber. After hybridisation each slide was washed in the dark in 50 mL of 2x SSC, 0.1 % SDS at 42 ^{o}C for 10 min, 1x SSC, 0.1 % SDS at 35 °C for 10 min, 0.1x SSC, 0.1 % SDS at 30 °C for 10 min and finally in two washes of 0.1 % SSC at RT for 5 min each. Slides were immediately rinsed in distilled water and dried with compressed nitrogen gas.

Slides were scanned with a Molecular Dynamics confocal laser scanner at 532 nm with a photomultiplier voltage of 700 V for Cy3 and 633 nm with a photomultiplier voltage of 800 V for Cy5.

5.2.4 Data analysis and quality control

5.2.4.1 Signal intensity acquisition and pseudocolour inspection

All aspects of primary microarray data analysis were performed with the software packages Spot (Buckley, 2000) and SMA (www.stat.berkeley.edu/users/terry/zarray /Software/smacode.html). Details of these packages and their functions can be found in Smyth *et al*. (2002) and Dudoit *et al*. (2002a). For each microarray hybridisation, Cy3 and Cy5 images (16-bit TIFF) were loaded into Spot for analysis, which initially involved the processes of spot-finding, raw signal intensity extraction and background correction. Array quality was also inspected at this stage through the generation of

pseudocolour images for each Cy3/Cy5 hybridisation. This diagnostic graphic is generated through the false-colouring and subsequent overlay of Cy3 (coloured green) and Cy5 (coloured red) output images. In this false-colour view of each microarray experiment, yellow indicates an equal balance of red and green signal intensities. An example of a pseudocolour image is presented in **Figure 5.4**. Pseudocolour images of each microarray hybridisation were visually inspected for quality characteristics that included: overall colour balance; spot morphology and uniformity; background artifacts such as dust and scratches; and overall uniformity of hybridisation. Where appropriate, bad spots or array sectors were flagged if of poor quality. Visual inspection also allowed for a preliminary assessment of array and hybridisation features that was useful for downstream statistical analysis such as normalisation in the software package SMA.

5.2.4.2 Data transformation and presentation

Throughout this Chapter the following notation is used to refer to microarray signal intensities. Foreground red and green signal intensities are given by *Rf* and *Gf* for each spot respectively, and background red and green signal intensities given by *Rb* and *Gb* for each spot respectively. Background corrected red (*R*) and green (*G*) signal intensities for each spot are thus given by $R = Rf - Rb$, and $G = Gf - Gb$ respectively. The signal intensity for each microarray spot is presented as the log-differential expression ratio (*M*), where $M = \log_2 R/G$. A number of analytical plots in addition require a measure of the log-intensity of spots (*A*), given by $A = ½ \log_2 RG$. *A* is a measure of the overall intensity of a spot.

Microarray expression ratios are best presented when log-transformed. Not doing so has the disadvantage of treating up- and down-regulated genes differently. For example, genes unchanged between a test and reference sample will have a ratio of 1, those up-regulated by a factor of 2 will have a ratio of 2, and genes down-regulated by a factor of 2 will have a ratio of 0.5. A suitable transformation of the expression ratio is the logarithm base 2, such as indicated above for *M* and *A*. The effect of $\log_2$ transformation is to treat up- and down-regulated genes in a similar fashion. Genes unchanged in an experiment have a $\log_2$ expression ratio (*M*) of 0, those up-regulated by a factor of 2 have $M = 1$, and those down-regulated by a factor of 2 have $M = -1$. Genes up-regulated by a

Figure 5.4: Pseudocolour image of Cy3/Cy5 signal intensities from microarray hybridisation.

Image obtained by overlaying Cy3 (coloured green) and Cy5 (coloured red) TIFF images.

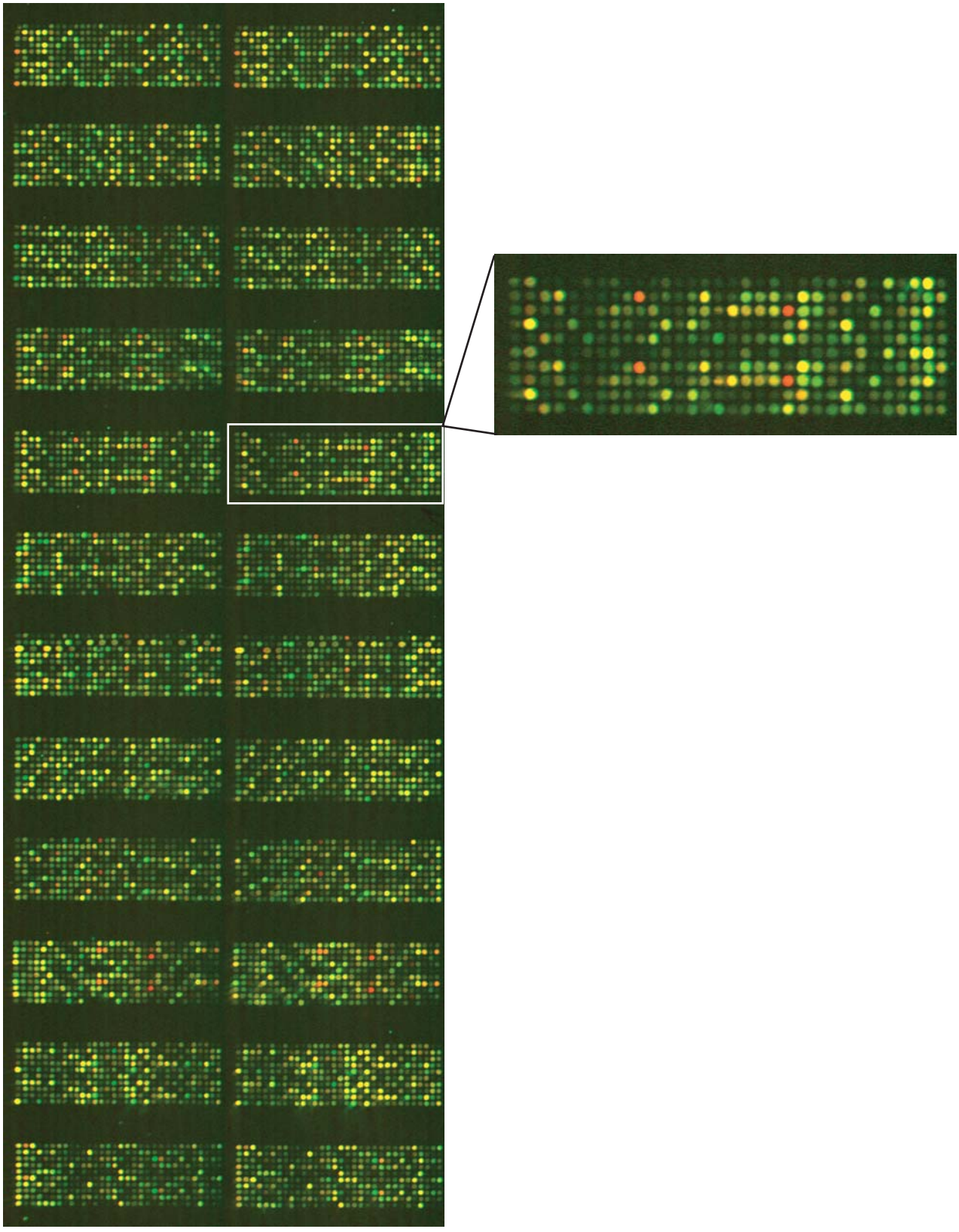

factor of 4 have $M = 2$, and those down-regulated by a factor of 4 have $M = -2$, and so on. Furthermore, the majority of raw signal intensity values from microarray experiments often fall within the lower limit (i.e. less than 1000) of the full 16-bit range from 0 to 65535 (Smyth *et al.*, 2002). Log transformation spreads expression data more evenly across this range and enables clearer graphical visualisation.

5.2.4.3 Hierarchical clustering

Hierarchical clustering (Eisen *et al.*, 1998) of microarray data was performed using the program GeneSpring (Silicon Genetics, Redwood City CA) with similarity measured using standard correlation and minimum distance set at 0.001.

5.3 Results and discussion

5.3.1 Microarray design

One of the most important aspects of microarray experimental design is the selection of gene fragments, or probes, to be printed onto the microarray surface. The probes used need to be selected such that results generated from subsequent hybridisations have maximum relevance to the biological questions under investigation. The cDNA microarray constructed in this study was designed specifically to address questions relating to the overall transcriptional control of meiotic development in wheat, and those relating to the genetic control of meiotic processes by genes at the *Ph* loci. In total, 1830 wheat sequences were selected for microarray construction. These originated from a number of sources, which are detailed below and listed in **Table 5.1**. Each group of probes selected for microarray printing has been given an identifying code, for identification and descriptive purposes. This is indicated in **Table 5.1**.

For the purpose of microarray probe selection, a large collection of genes expressed during meiotic development in wheat was desirable. These sequences were derived from a cDNA library constructed for this purpose. Approximately 500 mg of wheat anthers at stages pre-meiosis to metaphase I inclusive were microscopically staged, isolated (as described in Section 2.2) and used as the tissue source for cDNA library construction. The library consisted of approximately 1.3×10^6 independent clones, with an average

Table 5.1: Wheat sequences selected for microarray printing.

Clone source	Number of sequences	Identifying code
Wheat meiotic anther cDNA library clones	1569	WAW
ITEC clones from *ph2a* region	128	ITEC
BAC contig subclones	77	BAC
DuPont database putative meiosis homologues	49	DUP
controls	7	CON
total	1830	

insert size of 1.55 Kb. 1569 randomly picked clones were sequenced by DuPont Ag Biotech for microarray printing, and comprised the majority (86 %) of the probes on the microarray. These sequences are available through GenBank (library name, waw1c; accession numbers CA600774-CA599300; dbEST Library ID.12147). Assessment of these sequences by in-house analysis methods at DuPont indicated that the library was of high quality, containing low levels of redundancy (Rafalski, *pers.commun*.). Sequence clustering using the program BLASTCLUST (http://www.ncbi.nlm.nih.gov/) also indicates this, with approximately 65 % of the library representing singleton sequences. This library has subsequently been sequenced further by the group of Dr. Olin Anderson, USDA, Albany CA, USA, and 9139 ESTs are available under a different library entry from GenBank (library name, wheat meiotic anther cDNA library; accession numbers CA483770-CA487130, CA496948-CA502725; dbEST Library ID.12127).

In addition, 128 wheat EST clones were obtained from ITEC for microarray printing. These clones represent a subset of the wheat ESTs identified from comparative genetics studies carried out to investigate the genetic content of the *ph2a* deletion region (Chapter 3). Comparative genetics studies using the rice chromosome 1 region syntenous to the region deleted in the wheat chromosome pairing mutant *ph2a* identified 280 wheat ESTs putatively located in the deleted segment of *ph2a*. Of these 280 wheat ESTs, 128 corresponded to clones held in the repository at ITEC and were obtained for inclusion on the microarray. It is important to note that not all of the 128 ITEC ESTs selected for microarray printing are shown in **Table 3.2** of Chapter 3. Those wheat ESTs that are not indicated are however represented by similar wheat ESTs that match to the same rice genomic sequence that either have higher levels of similarity or have longer associated sequences. Database searches using the rice chromosome 1 genomic sequence against wheat EST databases were repeated after the selection of clones for microarray printing was completed. The purpose of repeating this analysis was to update this information for publication considering the recent increases in sequences in wheat EST databases.

As part of related research into meiosis in our laboratory, a 220 Kb BAC contig was identified and shotgun-sequenced from the region corresponding to the *ph2a* deletion in the D-genome progenitor of hexaploid wheat, *Triticum tauschii* (Whitford, 2002). Contained in the sequence of this BAC contig are seven members of the *WM1* gene

family (*WM1.1-1.3*, *WM1.7* and *WM1.10-1.12*). In addition to the seven *WM1* gene family members, a number of additional coding sequences were predicted from this 220 Kb genomic sequence using RiceGAAS gene prediction software (http://ricegaas.dna.affrc.go.jp/). It is thus possible that these predicted genes represent coding sequence from the region deleted in the *ph2a* mutant. BAC subclones generated in the initial phase of sequencing that correspond to assembled regions of putative coding sequence were identified and 77 of these were included on the microarray.

Collaboration established during the course of this study with DuPont Ag. Biotech, Delaware USA, enabled access to extensive EST databases of wheat. To maximise the relatedness of this microarray to wheat meiotic development, a search of these databases was performed to identify putative wheat homologues of characterised meiotic genes from other organisms. GenBank databases were screened to compile a collection of characterised genes involved in all aspects of meiosis, from a range of species. In cases where plant functional homologues of lower eukaryote meiotic genes have been characterised, the plant sequences were selected in preference. These sequences were used in BLAST searches of the DuPont wheat ESTs database to identify an EST showing the highest similarity. As the number of total clones printed on the array was not limiting, no similarity criterion was placed on these searches. The best BLAST match of all characterised meiotic genes was selected for microarray printing. This process resulted in the selection of 49 wheat ESTs.

In addition to the above groups of DNA probes, seven control sequences were printed onto the microarray. Several genes of interest in related projects of our laboratory were included, such as; two *WM1* gene family members, *WM1.1* and *WM1.7* (Whitford, 2002); the gene *WM5* (Thomas, 1997); and *TaMSH7* (Dong *et al.*, 2002). All of these clones have been localised by previous studies to the region deleted in the *ph2a* mutant. Wheat glyceraldehyde-3-phosphate dehydrogenase (GAPDH), ubiquitin and thioredoxin-H were also included in the control set of sequences printed on the microarray.

5.3.2 Data normalisation

Before biological comparisons can be made from microarray experiments, expression data must be normalised. Normalisation refers to the application of statistical methods to adjust and account for systematic sources of variation in a microarray experiment. Normalisation is essential to address biases observed in expression data that are derived from variation in the technology, rather than from biological variation between samples used for hybridisation. A number of common biases are frequently observed in microarray data. Red (Cy5)-green (Cy3) bias can result from either using unequal quantities of starting RNA, or from unequal label incorporation-efficiencies and scanning properties of the two dyes. The magnitude of the difference between red and green intensity may also be dependant on overall intensity *A* (as illustrated in Section 5.3.2.1). Unequal hybridisation intensity across the surface of a microarray is also frequently observed and may be attributed to factors such as a non-uniform distribution of hybridisation solution across the surface of the microarray, or related to uneven spotting volumes delivered from certain print-tips during the microarray manufacture process. Normalisation is also important in experiments where a number of arrays are directly compared, such as in a temporal series. Bias may arise from independent labeling reactions, or through different ambient conditions when experiments were performed. It is crucial that these factors are investigated and systematic sources of variation removed.

Graphical representation of microarray datasets indicated several predominant sources of variation. Three appropriate normalisation steps were implemented, as described below.

5.3.2.1 Within slide lowess normalisation

An $M = \log_2 R/G$ vs. $A = ½ \log_2 RG$ plot (*MA*-plot) was used to diagnose systematic within-slide variation and bias of intensity values from each microarray hybridisation. **Figure 5.5 A** illustrates an un-normalised *MA*-plot from one microarray hybridisation, and shows two prominent artifacts common to all microarray datasets obtained in this study.

Figure 5.5: *MA*-plots showing systematic sources of variation in microarray expression data and the effects of normalisation.

Data are from one meiotic stage vs. reference temporal microarray experiment.

A: Un-normalised *MA* plot showing the dependence of the log ratio *M* on overall spot intensity *A*, and the presence of spatial variation as shown by different coloured lines each fitted to spots derived from individual print-tip groups.

B: Normalised *MA*-plot showing the result of intensity, or *A* dependant normalisation and sub-array normalisation based on print-tip groups.

A

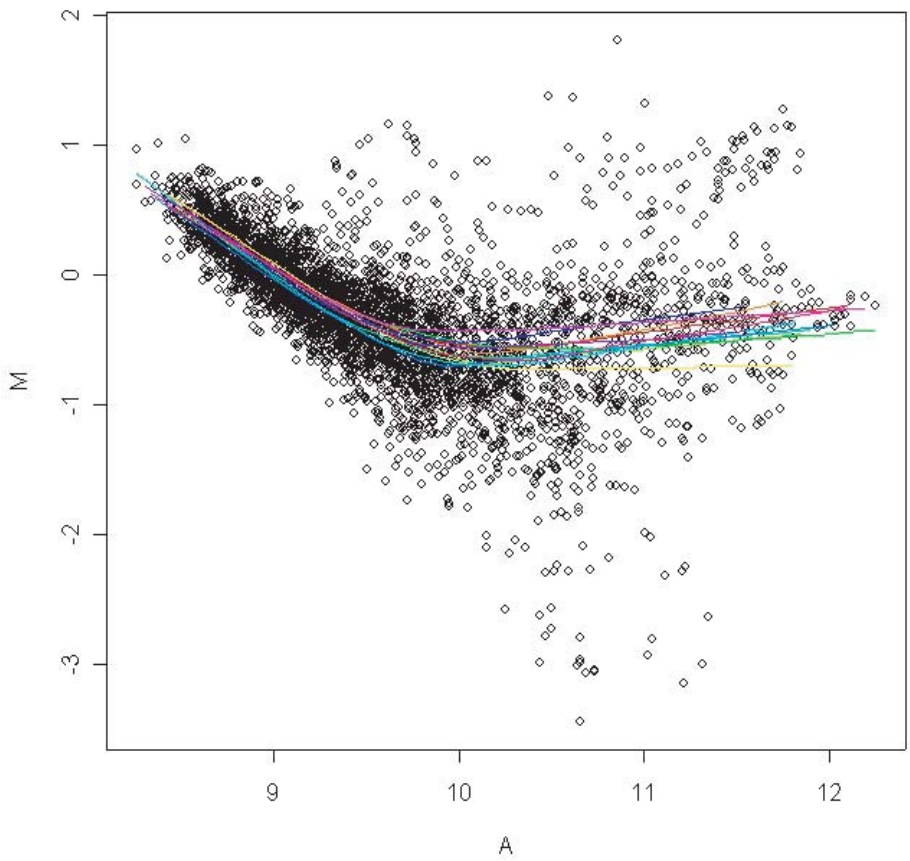

B

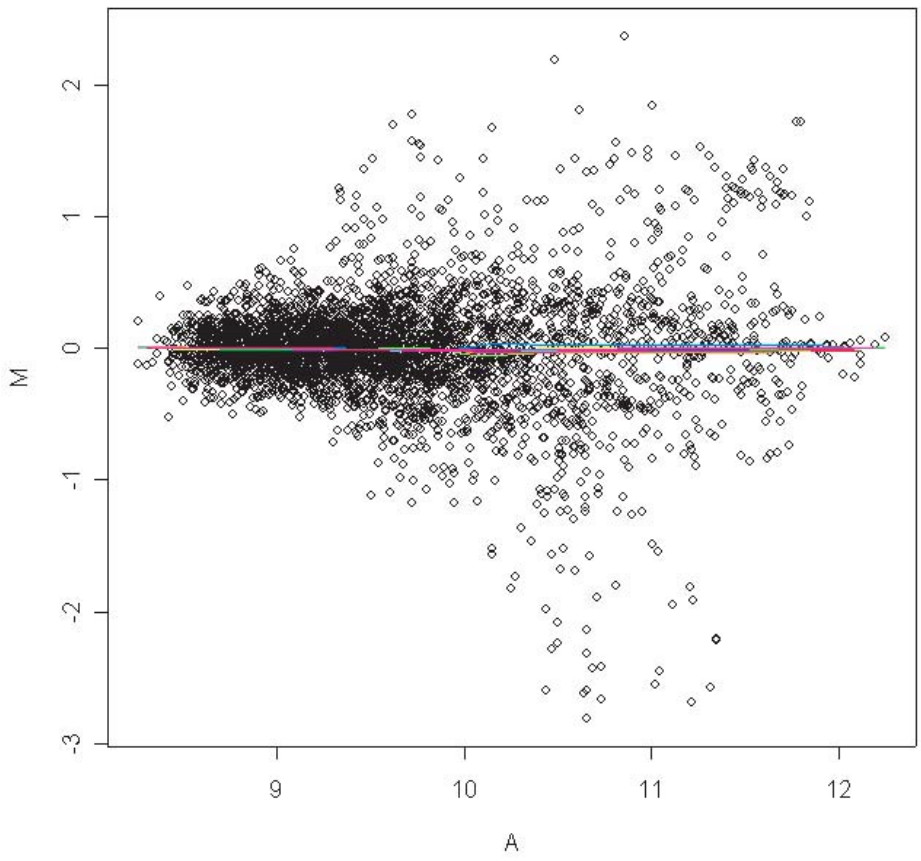

Firstly, **Figure 5.5 A** shows the dependence of the log ratio *M* on overall spot intensity *A*. The majority of points lie on a curve, and indicates that the Cy3-Cy5 dye bias depends upon the intensity of the spot. Since *M* is derived from calculating $\log_2 R/G$, we can infer that at low overall spot intensities (e.g. $A<9$), Cy5 signal intensities dominate over Cy3 such that *M* tends to be greater than 0. Likewise, at higher overall signal intensities (e.g. $A>9$), Cy3 signal intensities dominate over Cy5 such that *M* tends to be less than 0.

Secondly, **Figure 5.5 A** illustrates the effects of spatial variation on fluorescent intensity. This is visualised by fitting curves that correspond to spots from different regions of the microarray. Each grid (10 x 32 spots, shown in **Figure 5.4**) on the microarray can be correlated with a print-tip of the microarrayer print head cluster. This acts as a convenient means to identify sources of spatial variation across the slide. Curves were fitted to the *MA*-plot in **Figure 5.5 A** that correspond to spots from individual print-tip groups (shown as coloured lines), and suggests the existence of spatial or print-tip effects on overall fluorescent intensity. This effect is more pronounced at higher signal intensities (e.g. $A>10$), with the print-tip group curve in yellow separated slightly from the remaining 11 curves. This suggests print-tip effects on fluorescent intensity. The effect is however relatively minor. Although the above spatial variation is described as being attributed to print-tip groups, it should be noted that spatial effects can also be a consequence of factors such as unequal distribution of hybridisation solution beneath the coverslip, or non-uniform washing over the surface of the slide. However, in the example shown in **Figure 5.5 A** the effect of spatial variation on fluorescent intensity is predominantly limited to one print-tip group, suggesting an effect associated with deposition of DNA samples by a particular print-tip during the microarray manufacture process.

Intensity, or *A* dependant normalisation and sub-array normalisation based on print-tip groups was performed by fitting curves respectively to the complete dataset (not shown in **Figure 5.5**) and to spots derived from individual print tip groups, estimated using locally weighted linear regression (lowess) (Cleveland, 1979; Yang *et al.*, 2002a; Yang *et al.*, 2002b). Lowess is a robust scatterplot smoother, which uses local-linear fits (Dudoit *et al.*, 2002b). Writing the height of the curve for each value of *A* as $c(A)$, *M*-

values are normalised by subtracting this curve such that $M = M - c(A)$. Lowess normalisation is implemented in the SMA software (www.stat.berkeley.edu/users/terry /zarray/Software/smacode.html). Normalised data are shown in the *MA*-plot in **Figure 5.5 B**.

5.3.2.2 Between slide normalisation

Both the *Ph* mutant differential expression and temporal expression microarray experiments performed in this study required the use of multiple slides. It is beneficial in this circumstance to scale normalise *M*-values between arrays to make them more comparable. A side-by-side boxplot is useful for comparing *M*-values between arrays of a microarray experiment, by displaying graphically a number of features of the distribution of *M*-values. The boxplots in **Figure 5.6** show the effects of scale-normalisation between arrays to make slides of the same experiment more comparable. The coloured central box for each plot indicates the boundary of the lower and upper quartiles, corresponding to the 25th and 75th percentiles respectively and represents the inter-quartile range (IQR). The central horizontal line within each box represents the median, or the 50th percentile. The IQR for each plot represents the range covered by the middle 50 % of *M*-values for each slide. The two dashed lines (whiskers) outside the box extend to the smallest and largest *M*-values less than or equal to 1.5x IQR. Extreme values greater than 1.5x IQR above the 75th percentile and less than 1.5x IQR below the 25th percentile are plotted individually as small circles.

The un-normalised box plot of **Figure 5.6 A** illustrates variation in the distribution of *M*-values from slides of the *Ph* mutant vs wild-type microarray experiments. This is seen as a difference in the size of the IQR, and the extent of whiskers for each plot of *M*-values in this experiment series. Between slide normalisation was performed using the software SMA such that all slides in each experiment series exhibited the same median absolute deviation, as illustrated in the normalised boxplot of **Figure 5.6 B**.

Figure 5.6: Side-by-side box plots showing the effect of between slide scale normalisation.

Data are from *Ph* mutant vs. wild type microarray experiments. All slides from this experiment are shown. For each *Ph* mutant vs. wild-type hybridisation, slide II represents the dye swap experiment of slide I. The central coloured boxes represent the inter-quartile range (IQR), within the boundaries of the 25th and 75th percentiles and represents the middle 50 % of *M*-values from each microarray hybridisation. Dashed lines extend to the smallest and largest *M*-values less than or equal to 1.5x IQR. Extreme values greater than 1.5x IQR above the 75th percentile and less than 1.5x IQR below the 25th percentile are plotted individually as small circles.

A: Un-normalised *M*-values. Between slide variation is seen as differences in the IQR and the extent of whiskers for each microarray slide.

B: Normalised *M*-values, showing the effect of between slide normalisation to make slides of the same experiment series more comparable.

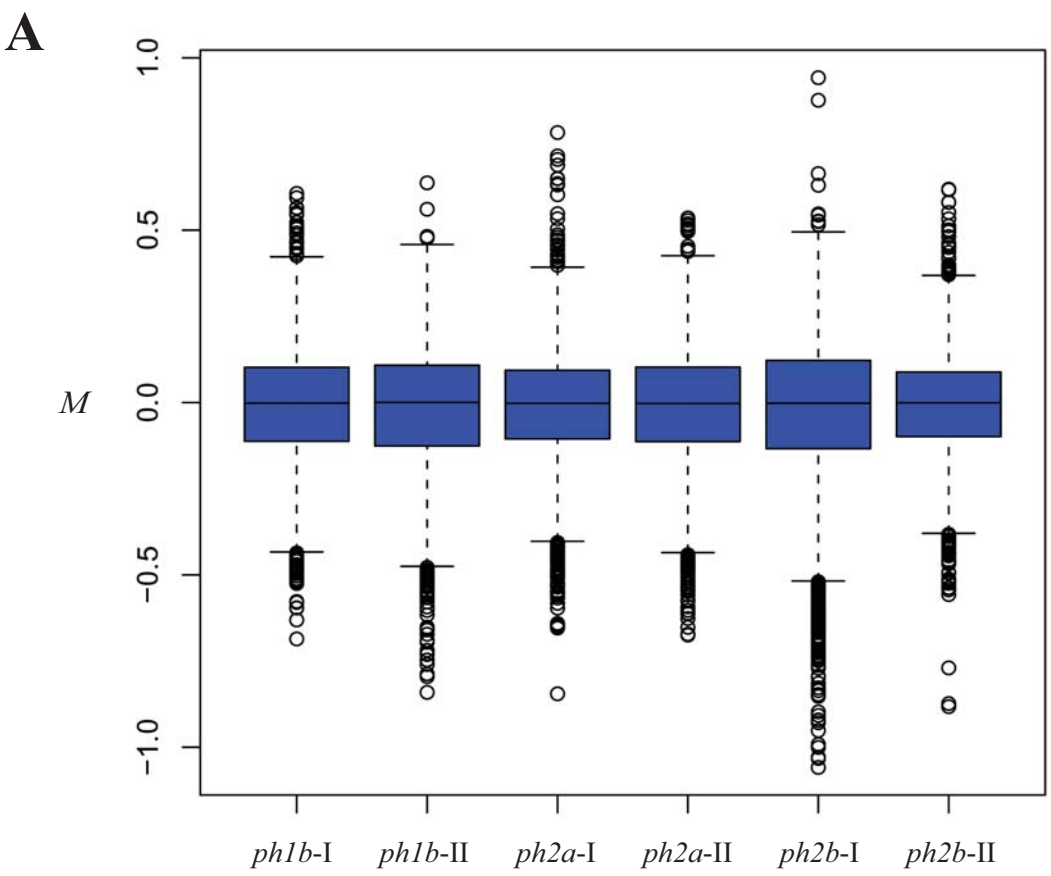
A
M
1.0
0.5
0.0
−0.5
−1.0
ph1b-I
ph1b-II
ph2a-I
ph2a-II
ph2b-I
ph2b-II

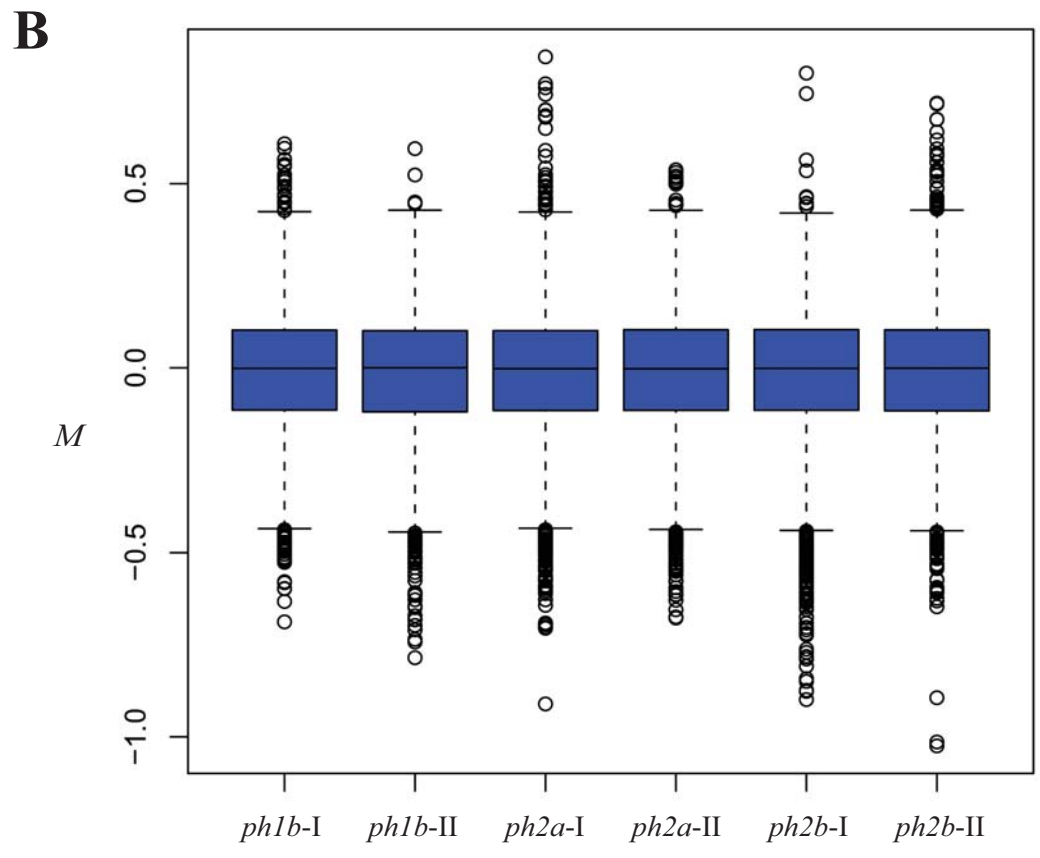
B
M
0.5
0.0
−0.5
−1.0
ph1b-I
ph1b-II
ph2a-I
ph2a-II
ph2b-I
ph2b-II

5.3.3 Verification and quality control of T7 amplification

5.3.3.1 A verification experiment

Microarray targets for hybridisation were prepared according to the T7 RNA amplification protocol described in Section 5.2.1. RNA amplification was necessary for the microarray experiments described in this Chapter due to the difficulty associated with obtaining sufficient poly(A) RNA from meiotically staged anthers. RNA amplification protocols for microarray hybridisation have been recently reviewed and evaluated (Zhao *et al.*, 2002), and shown to produce representative RNA samples for microarray hybridisation. However, T7 amplification protocols are relatively complex enzymatic reactions using small quantities of RNA as starting materials. Numerous enzymatic and reagent inputs are required, in addition to several clean up procedures. It was important in this context to evaluate the effectiveness of the amplification procedures and methodology used in this study. This was accomplished by designing a microarray experiment specifically to verify and evaluate targets produced using T7 amplification for gene expression studies, as generated using our laboratory equipment, reagents and enzymes.

The amplification verification microarray experiment designed is illustrated diagrammatically in **Figure 5.7**. The aim of this experiment was to investigate the expression ratio of all 1830 genes on the microarray when hybridised with the following two targets: One microarray target derived from fluorescently labeling 2 µg of purified meiotic anther poly(A) RNA, and another target derived from fluorescently labeling 2 µg of amplified antisense RNA (aRNA), amplified from a small quantity (100 ng) of the same meiotic anther poly(A) RNA. The basis for this experiment was as follows: If the amplification protocol used for target generation did not significantly distort the abundance of individual messenger RNAs as compared to the original starting poly(A) RNA, then each gene on the microarray will result with an *M*-value not significantly deviating from 0. Alternatively, if abundance was not preserved during amplification, then significant deviations from 0 would be expected for *M*.

Figure 5.7: Experimental design to evaluate T7 RNA amplification.

Purified poly(A) RNA from a collection of wheat anthers at pre-meiosis to metaphase I was used as the starting material to prepare two microarray targets for hybridisation. One fluorescently labeled microarray target (left of figure) was prepared using 2 µg poly(A) RNA as the template in reverse transcription. The other (right of figure) was prepared using 2 µg amplified RNA (aRNA) as the template in reverse transcription. This aRNA was amplified from 100 ng of the same poly(A) RNA used for synthesis of the target to the left. Dye swap hybridisations were also performed.

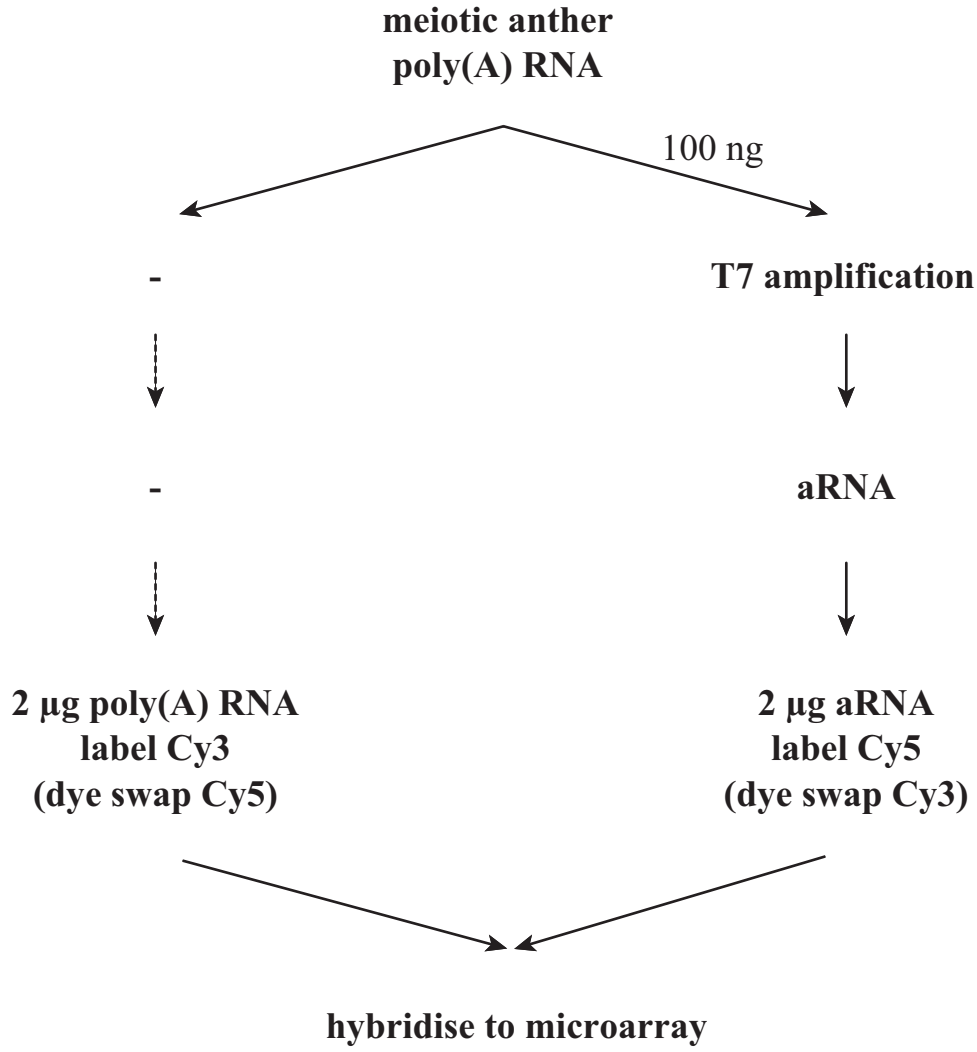
meiotic anther
poly(A) RNA
100 ng
-
T7 amplification
-
aRNA
2 µg poly(A) RNA
label Cy3
(dye swap Cy5)
2 µg aRNA
label Cy5
(dye swap Cy3)
hybridise to microarray

The boxplot in **Figure 5.8** shows the normalised *M*-values for all probe sequences on the microarray generated in this amplification verification experiment. It can be seen from the boxplot that the IQR (comprising 50 % of the *M*-values) extends from $M = -0.1$ to $M = 0.1$, and the vast majority of *M*-values fall in the range of the whiskers of this plot, i.e. $-0.3<M<0.3$. Using logarithm base 2 transformations of expression ratios, $M = 0.3$ corresponds to an approximate fold change of 1.2. A small percentage of total *M*-values (approximately 20, or 1.0 %) show $-0.5>M>0.5$, with maximum and minimum *M* values of approximately 0.8 and -0.7 respectively.

From the results obtained in this amplification verification experiment, we can conclude that aRNA provides a close approximation of the abundance profile of mRNAs in the original poly(A) RNA sample and that any bias introduced into gene expression profiling by amplification is minor. This result supports the findings of other researchers evaluating T7 amplification for gene expression studies. Zhao *et al*. (2002) for example, in a comprehensive evaluation of T7 amplification methodologies, found that less than 4 % of genes in their microarray experiments on average showed changes greater than two-fold using a common amplification procedure. The amplification procedure used in this study provided better representation of poly(A) RNA abundance. No genes in this experiment show changes greater than two-fold. Importantly, Zhao *et al*. (2002) have also demonstrated that reproducibility between different samples amplified by this technique is high. Of the genes that did change by greater than two-fold in their experiments after amplification, many did so in independent amplification reactions. This suggests that any changes that may result from T7 amplification should be reproducible between samples prepared using the same method, and in two-channel microarray experiments comparing amplified test vs. amplified reference targets, these changes should not significantly distort the resulting expression ratios.

5.3.3.2 Keeping track of amplification

During the synthesis of amplified targets, aliquots were removed for quality control purposes. Aliquots (1 μL) were removed immediately following the completion of first strand cDNA synthesis reactions for each amplified aRNA target generated. PCR was performed on these single stranded cDNA populations using two sets of gene specific

Figure 5.8: Box-plot of normalised *M*-values obtained in the microarray experiment to evaluate T7 RNA amplification.

The central coloured box represents the inter-quartile range (IQR), within the boundaries of the 25th and 75th percentiles and represents the middle 50 % of *M*-values from each microarray hybridisation. Dashed lines extend to the smallest and largest *M*-values less than or equal to 1.5x IQR. Extreme values greater than 1.5x IQR above the 75th percentile and less than 1.5x IQR below the 25th percentile are plotted individually as small circles.

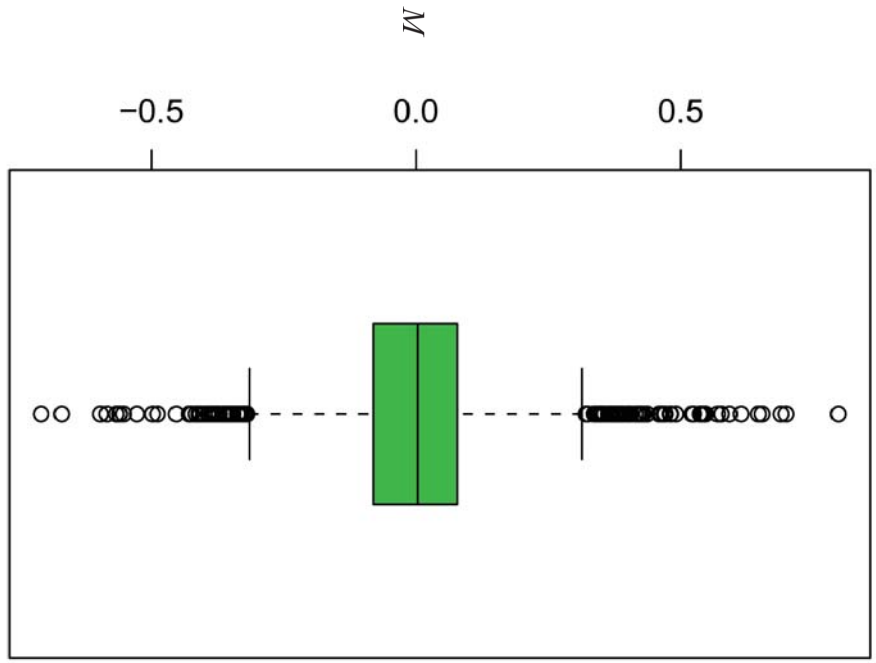
M
−0.5
0.0
0.5

primers to confirm successful isolation of total RNA, subsequent poly(A) RNA purification and first strand cDNA synthesis. Specific oligonucleotide primers were used to amplify small fragments of the genes *TaMSH7* and *WM5*. These genes were previously isolated in our laboratory and determined to be located on chromosome group 3. The 3D copies are located in the region deleted in the *ph2a* mutant (Dong *et al.*, 2002; Thomas, 1997). Both genes show relatively low expression in meiotic tissues of wheat. **Figure 5.9 A** shows the results of a quality control PCR reaction using primers specific to *TaMSH7* and *WM5*. The deletion of both of these genes in the *ph2a* mutant is evident from this gel photograph. The band intensity of the *TaMSH7* amplicon from *ph2a* is slightly weaker than for wild-type Chinese Spring, *ph1b* and *ph2b*. For *WM5*, two bands of slightly different size are expected using these specific primers designed for this gene. These are seen in wild-type Chinese Spring, *ph1b* and *ph2b*. For *ph2a*, the weaker upper band is absent. This band corresponds to the larger amplicon generated from amplification of the copy of *WM5* on chromosome 3DS, within the region deleted in the *ph2a* mutant.

5.3.3.3 Expected yields from amplification, and aRNA size spread

In general, the amplification reactions performed in this study yielded approximately 10 µg aRNA from 20 meiotic anthers. However, for unknown reasons yields of between 5 µg and 15 µg aRNA were sometimes observed from similar amounts of starting tissue. This effect is likely to be associated with sample recovery during early RNA isolation procedures. Where possible, amplified targets were only used where *in vitro* transcription yielded greater than 10 µg aRNA.

The quantity and size spread of targets reverse transcribed from aRNA templates was compared to those generated in a standard labeling reaction, i.e. reverse transcription from a poly(A) RNA template. Fluorescently labeled Cy3/Cy5-dCTP was substituted in this reaction for un-labeled dCTP, and approximately equal quantities of transcribed cDNA electrophoresed to examine molecule size spread. The result is shown in **Figure 5.9 B**. Targets generated from aRNA have similar properties to those generated from poly(A) RNA templates. It is apparent however that cDNA transcribed from a poly(A) RNA template contains a higher concentration of molecules larger than 2 Kb than cDNA

Figure 5.9: Quality control during T7 RNA amplification and a comparison of cDNA size distribution synthesised from poly(A) RNA and aRNA templates.

A: PCR using gene specific primers for *TaMSH7* and *WM5* was used as a diagnostic tool to confirm successful isolation of RNA and synthesis of first strand cDNA in preparation for T7 RNA amplification. Shown are amplicons from first strand cDNA synthesis for four anther preparations, Chinese Spring wild-type (CS), *ph1b*, *ph2a* and *ph2b*. Markers (M) are in Kb and C indicates the no template control reaction for each primer set.

B: The size distribution of cDNA reverse transcribed from poly(A) RNA templates primed with Oligo dT, and that reverse transcribed from aRNA templates primed with random 9-mer hexamers. Markers (M) are in Kb.

A

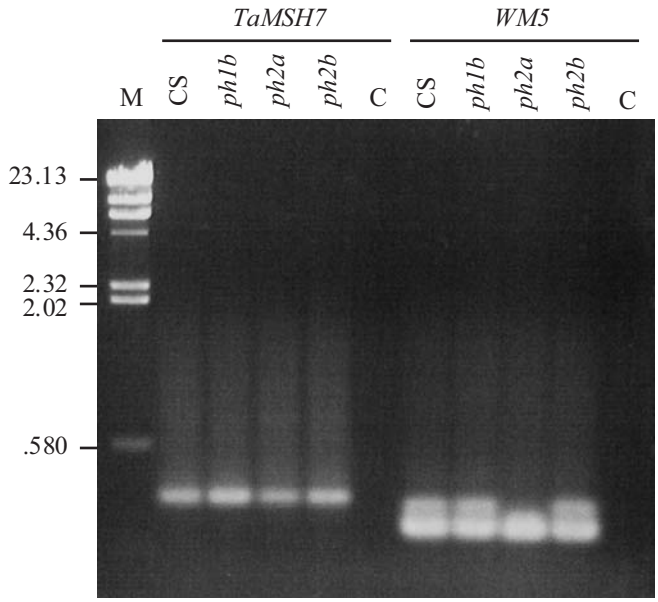
TaMSH7
WM5
M
CS
ph1b
ph2a
ph2b
C
CS
ph1b
ph2a
ph2b
C
23.13
4.36
2.32
2.02
.580

B

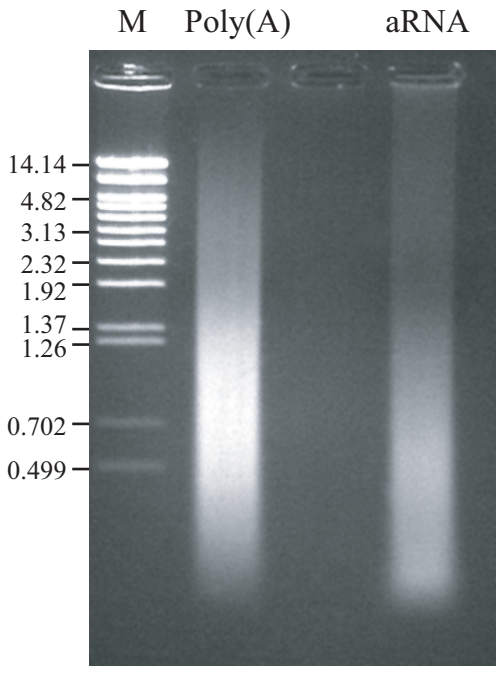
M
Poly(A)
aRNA
14.14
4.82
3.13
2.32
1.92
1.37
1.26
0.702
0.499

transcribed from an aRNA template. This may be explained through consideration of the numerous enzymatic steps required to produce aRNA, such as cDNA synthesis and *in vitro* transcription that tend to reduce overall molecule size through incomplete strand extension. In addition, reverse transcription from aRNA is primed with random hexamers, compared with oligo-dT priming for poly(A) RNA templates, again resulting in an overall reduction in molecule size. Molecule size is not however an important consideration for efficient microarray hybridisation.

5.3.4 Wild-type vs. *Ph* mutant differential expression

An experiment was carried out to investigate the expression level of each microarray probe between wild-type Chinese Spring anthers and anthers of each *Ph* mutant genotype, *ph1b*, *ph2a* and *ph2b*. The aim of this experiment was to identify genes exhibiting reduced expression in *Ph* mutant anthers that may be considered as candidates for genes at respective *Ph* loci. The microarray targets used for hybridisation were prepared as described in Section 5.2.1.1 and are illustrated in **Figure 5.3 B**.

The boxplot in **Figure 5.10** shows the normalised *M*-values for all microarray probes in each of the three differential expression experiments, *ph1b* vs. wild-type Chinese Spring, *ph2a* vs. wild-type and *ph2b* vs. wild-type. Negative *M*-values indicate lower expression in *Ph* mutant genotype anthers compared to wild-type anthers, while positive *M*-values indicate the reciprocal expression pattern. For each experiment, no genes exhibit *M*-values greater than 0.44, or less than -0.54, representing a maximum fold up-regulation in mutant compared to wild-type of 1.36, and maximum fold down-regulation in mutant compared to wild-type of 1.45. *M*-values for 50 % of microarray probes fall within the IQR that extends from approximately –0.05 to 0.05. The minimum and maximum *M*-values for each *Ph* mutant vs. wild-type experiment are as follows, with an indication of fold change written in brackets; *ph1b* vs. wild-type, -0.28 (1.22), 0.23 (1.18); *ph2a* vs. wild-type, -0.4 (1.32), 0.31 (1.24); *ph2b* vs. wild-type, -0.54 (1.45), 0.44 (1.36).

When considering significance criteria for differential expression, a number of alternatives are possible. Several statistical models have been proposed recently to identify cutoff levels for assigning significance to differential expression (for examples

Figure 5.10: Side-by-side box plot showing the range of normalised *M*-values from *Ph* mutant genotypes *ph1b*, *ph2a*, and *ph2b* compared to wild-type Chinese Spring wheat.

The central coloured box represents the inter-quartile range (IQR), within the boundaries of the 25th and 75th percentiles and represents the middle 50 % of *M*-values from each microarray hybridisation. Dashed lines extend to the smallest and largest *M*-values less than or equal to 1.5x IQR. Extreme values greater than 1.5x IQR above the 75th percentile and less than 1.5x IQR below the 25th percentile are plotted individually as small circles.

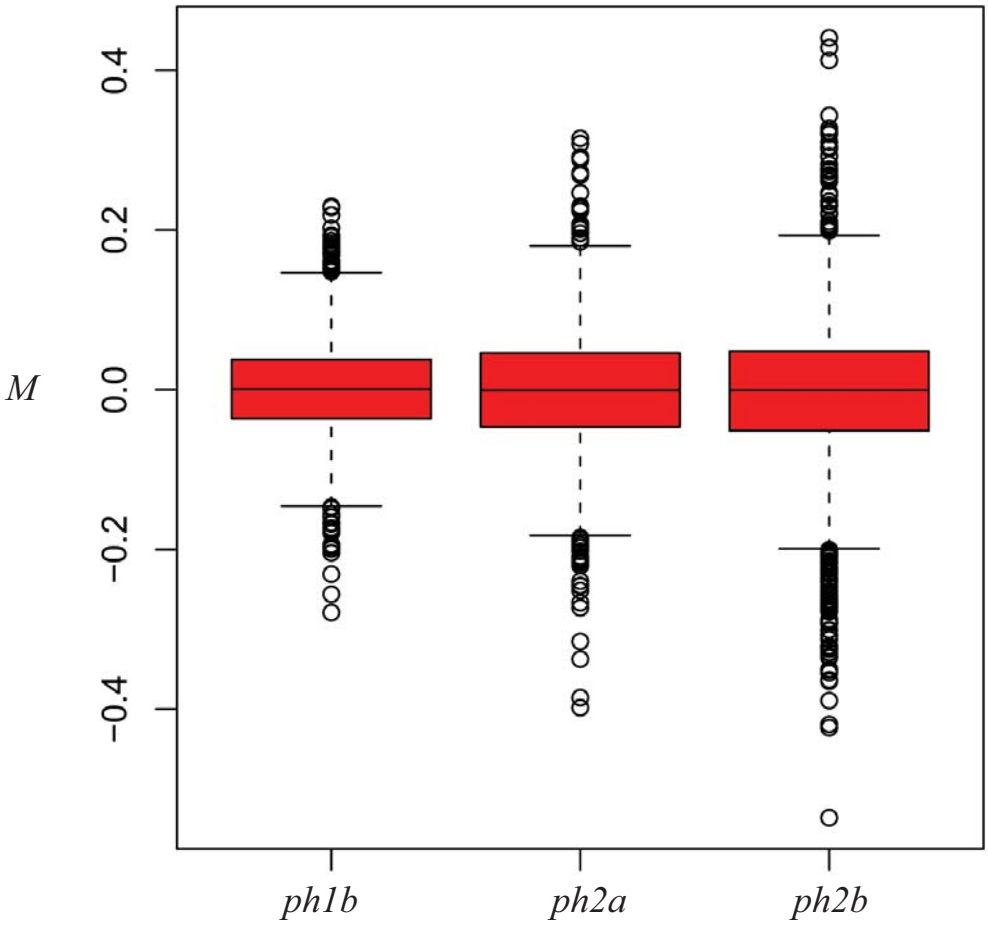
M
0.4
0.2
0.0
−0.2
−0.4
ph1b
ph2a
ph2b

see Dudoit *et al*., 2002b; Lonnstedt and Speed, 2002). This is currently a rapidly developing area of microarray analysis and researchers are yet to agree on the application and significance of a single statistical model that best defines differential expression. The empirical Bayes method and derivations thereof for analysing replicated microarray data are becoming accepted by many researchers (Lonnstedt and Speed, 2002). Currently we are investigating the application of these and other methods in our ongoing analysis of the microarray data generated in this study. One method that has been used in microarray research is that of a two-fold change cutoff level, such that a fold change of less than two cannot confidently define differential expression. In this context, the results from the *Ph* mutant vs. wild-type experiments suggest that no significant differential expression is observed for any of the 1830 microarray probe sequences. Significantly, this includes the 128 wheat ESTs selected for microarray printing that were identified showing similarity to the rice chromosome 1 region syntenous to the wheat 3DS region deleted in the *ph2a* mutant (Section 5.3.1 and Chapter 3).

It is interesting however to find correlation between the apparent up- and down-regulated genes in the three mutant experiments performed, even though *M*-values do not deviate to less or greater than –1.0 or 1.0 respectively. **Appendix 1** shows all *M*-values obtained for differential and temporal expression experiments. Highlighted in **Appendix 1** are the twenty-most down-regulated genes in mutant compared to wild-type in red, and the twenty-most up-regulated genes in mutant compared to wild-type in green for each of the three *Ph* mutant genotypes investigated. The overlap of these genes between *ph1b*, *ph2a* and *ph2b* is illustrated in the Venn diagrams of **Figure 5.11**. When comparing the top twenty down-regulated genes between *Ph* mutants, three genes are common to all genotypes, five are common to *ph1b* and *ph2a*, one common to *ph1b* and *ph2b*, and none to *ph2a* and *ph2b*. When comparing the top twenty up-regulated genes between *Ph* mutants, none are common to all genotypes, 11 are common to *ph1b* and *ph2a*, none common to *ph1b* and *ph2b*, and one to *ph2a* and *ph2b*.

Furthermore, examining the putative function of each of the twenty most down-regulated genes for each *Ph* mutant reveals the prevalence of microarray probes with identical predicted function within and between *Ph* mutant experiments. For example, microarray

Figure 5.11: The overlap in gene expression from *Ph* mutant vs. wild-type microarray experiments.

A: The top twenty down-regulated genes for *ph1b*, *ph2a* and *ph2b* compared to wild-type Chinese Spring.

B: The top twenty up-regulated genes for *ph1b*, *ph2a* and *ph2b* compared to wild-type Chinese Spring.

A

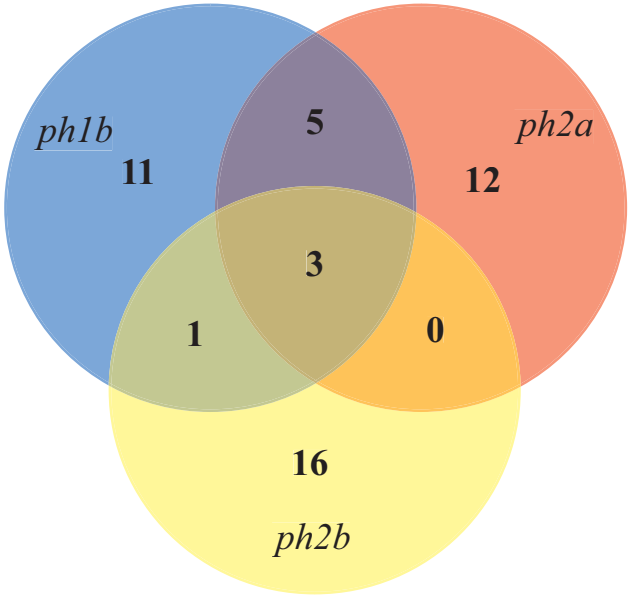

B

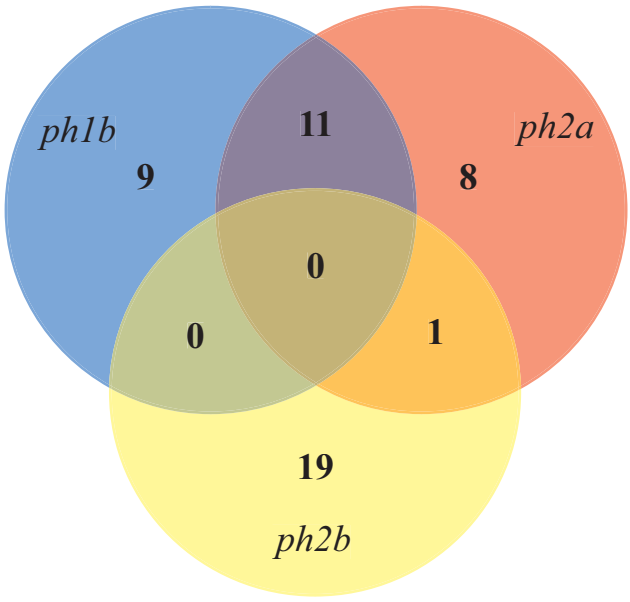

probes showing significant similarity to histone proteins are common to the list of the top twenty most down-regulated genes for *ph1*b (1 probe), *ph2a* (2 probes) and *ph2b* (2 probes). Two microarray probes showing similarity to dehydrin COR410 (cold-induced COR410 protein) are common to *ph1b* and *ph2a*. In *ph2b*, the top twenty most down-regulated genes are characterised by five microarray probes with similarity to enolase (2-phosphoglycerate dehydratase) and three microarray probes with similarity to 4-coumarate:coenzyme A ligase. Similar functional prevalence in the list of *ph1b* is observed with three microarray probes showing significant similarity to elongation factor 2 (EF-2).

Similar patterns are observed when examining the putative function of each of the twenty most up-regulated genes for each *Ph* mutant. Microarray probes showing significant similarity to 4-coumarate:coenzyme A ligase are observed in the lists of both *ph1b* (3 probes) and *ph2a* (3 probes). Furthermore, microarray probes showing significant similarity to CTP synthase are observed in the lists of both *ph1b* (3 probes) and *ph2a* (1 probe). In addition, microarray probes showing significant similarity to dihydroflavonol reductase are observed in the lists of both *ph1b* (1 probe) and *ph2a* (2 probes). In *ph2b*, the top twenty most up-regulated genes are characterised by three microarray probes with similarity to an S-adenosylmethionine decarboxylase precursor.

In light of *M*-values that are considered non-significant using a fold-change cutoff of two ($-1<M<1$), the significance of the above observations is difficult to interpret. The apparent correlation between genes in the top twenty most up- and down-regulated between each *Ph* mutant is interesting and seems to warrant further investigation. A detailed analysis of these correlations has not however been pursued in this study.

5.3.5 Temporal analysis of gene expression during meiosis

A temporal series of microarray experiments were performed to investigate the transcriptional regulation of each microarray probe during meiotic development in the wheat anther. Five microarray targets were prepared that represent temporally distinct phases of the meiotic cell cycle. Anthers were harvested, microscopically staged according to the method in Section 5.2.1.1, and pooled into temporal groups

corresponding to the following pollen mother cell meiotic cell division stages; pre-meiosis (pre-meiotic interphase), leptotene to pachytene, diplotene to late anaphase I, telophase I to telophase II and tetrads. Each temporal stage microarray target was hybridised against a common reference target, derived from anthers containing pollen mother cells at the immature pollen stage of development (**Figure 5.3 A**). The immature pollen reference tissue, against which temporal meiotic stage targets were compared, was chosen because it represented an identical but developmentally distinct tissue type to that of the meiotic stage targets. The defining difference being that meiosis was complete in pollen mother cells at the immature pollen stage of development. Given the relatively short time frame of approximately 24 hours for a meiotic cell division in hexaploid wheat (Bennett *et al.*, 1973), the transcriptional difference between the immature pollen reference tissue and the temporal meiotic stage targets should therefore be largely restricted to genes temporally expressed for specific meiotic requirements. In this way, genes required for developmental processes other than meiosis in the anther would be expected to show little transcriptional difference between test and reference targets, unless developmentally regulated in wheat anther tissue over the time frame of meiotic cell division.

Ten microarray slides were used for hybridisation to generate a transcriptional profile for each microarray probe from pre-meiosis to the tetrad stage of meiotic division. The expression profiles for all microarray probe sequences during meiosis are shown in **Figure 5.12**.

Several points are helpful to interpret the expression profiles from the line graph and box plot of **Figure 5.12**. Firstly, expression information (represented as *M*-values) indicates the relative presence or relative absence of a particular microarray probe in a meiotic stage target compared to that of the immature pollen reference target. For example, consider a positive *M*-value of 2, for a particular gene at leptotene to pachytene. This indicates that at leptotene to pachytene this gene is approximately four-fold up-regulated relative to its expression in anthers at the immature pollen stage of development. A negative value of 2 would indicate this gene is approximately four-fold down-regulated at leptotene to pachytene relative to its expression in anthers at the immature pollen stage of development. Thus, an *M*-value of 0 at leptotene to pachytene can indicate two

Figure 5.12: Expression profiles of all microarray probes from pre-meiosis to the tetrad stage of meiosis.

PM, pre-meiosis; LP, leptotene to pachytene; DA, diplotene to late anaphase I; TT, telophase I to telophase II; T, tetrads.

A: Line graph plotting normalised *M*-values for each microarray probe.

B: Side-by-side box plots plotting normalised *M*-values for each microarray probe.

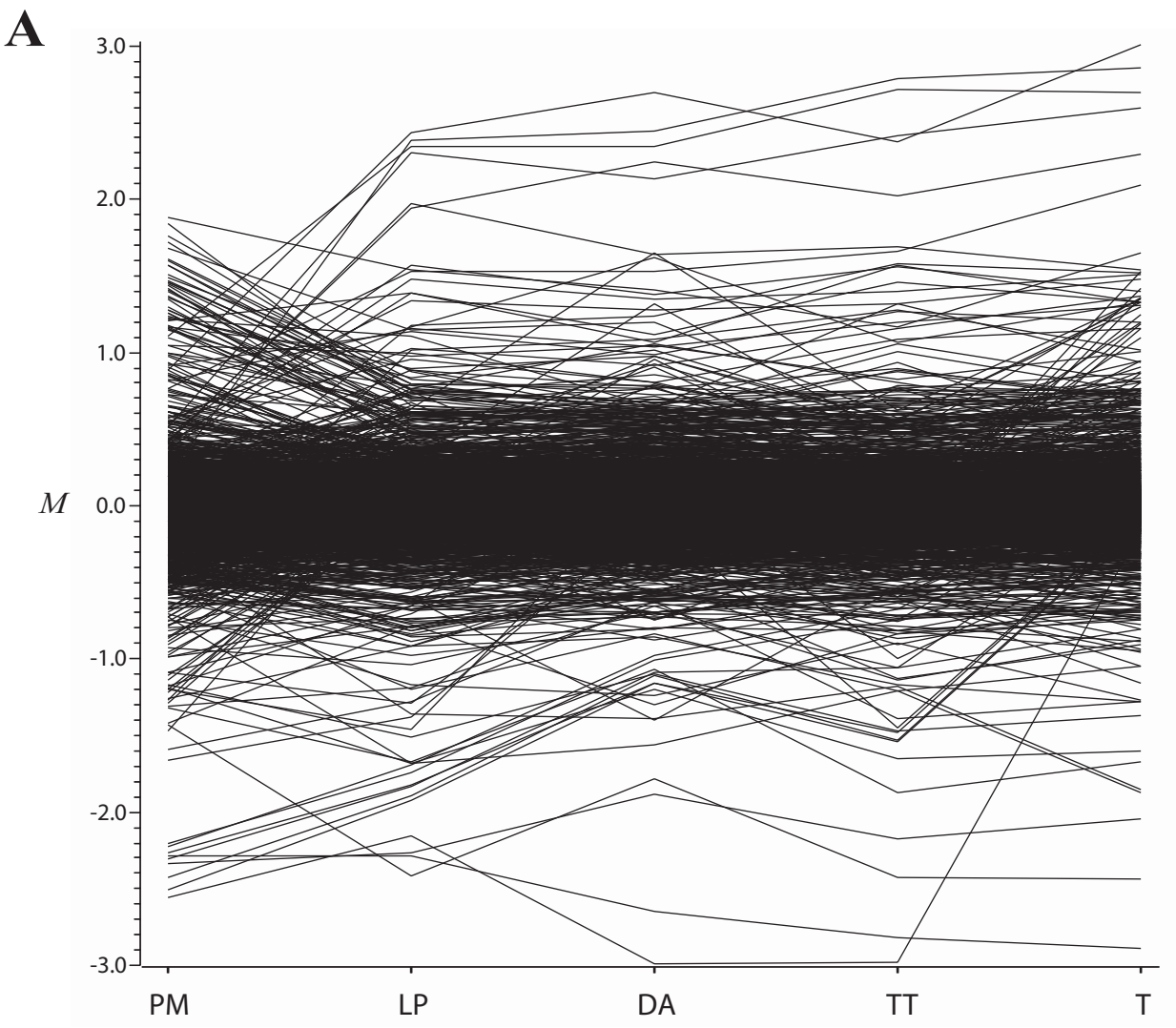
A
3.0
2.0
1.0
M
0.0
-1.0
-2.0
-3.0
PM
LP
DA
TT
T

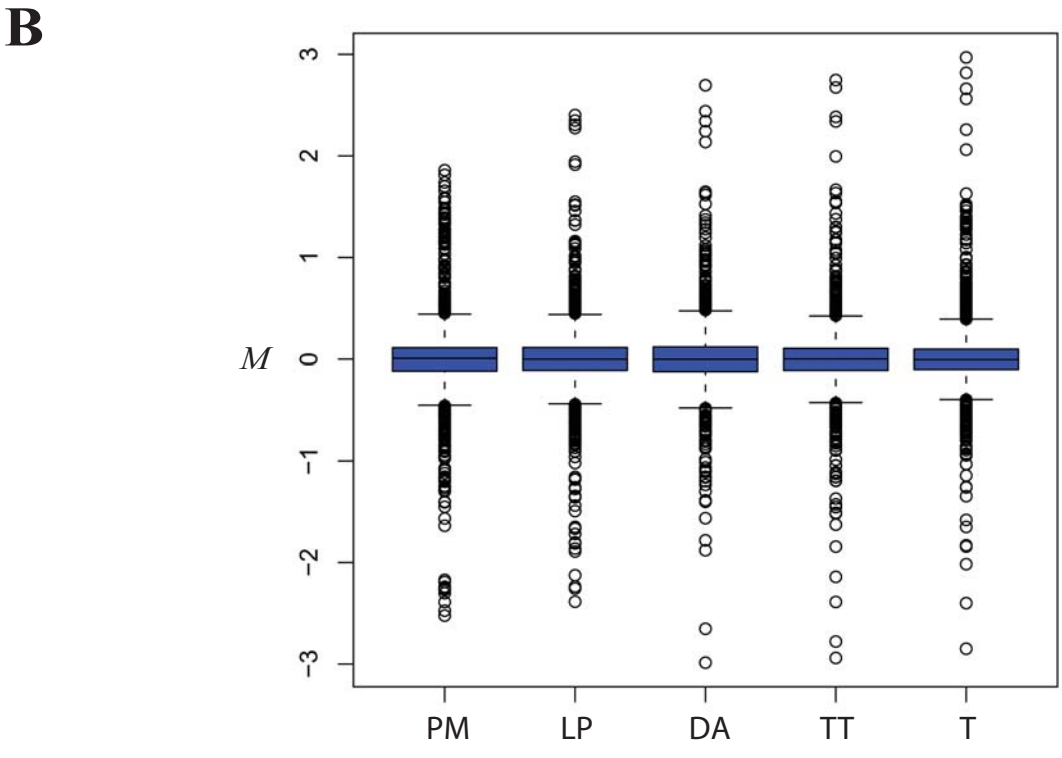
B
3
2
1
M
0
−1
−2
−3
PM
LP
DA
TT
T

possibilities. Either this gene is expressed at the same level at leptotene to pachytene and immature pollen stages, or equally, that the gene is not expressed at detectable levels in either microarray target. An *M*-value of 0 does not therefore suggest that a particular gene is not functionally required for meiotic development, rather that it is expressed at the same level in the non-meiotic reference tissue. In summary, the information from these microarray experiments indicates two points about a gene's transcriptional control. Firstly, whether it is temporally regulated from pre-meiosis to the tetrad stage of meiotic cell division, and secondly, its relative expression at each meiotic stage compared to that in non-meiotic anthers of the immature pollen reference target.

5.3.5.1 Consistency and verification of expression profiles

To assess the significance of the expression profiles obtained from temporal series microarray experiments, two analyses were performed. Firstly, it was important to examine the consistency of expression profiles from independent microarray probes that are predicted to have identical molecular function based on the results of BLAST searches. A number of groups of microarray probes of identical function were selected for investigation and the corresponding expression profiles graphically plotted. The profiles for eight such groupings are shown in **Figure 5.13 A-H**. The individual plots in **Figure 5.13** indicate that expression data is consistent for independent microarray probes of predicted identical function.

Secondly, to validate the expression profiles from microarray experiments in a biological sense, Northern hybridisation was performed for several selected microarray probes. A Northern blot was prepared that contained 5 μg total RNA isolated from independent collections of meiotic anthers at the same meiotic stages as those for microarray targets. Total RNA isolated from anthers containing pollen mother cells at the immature pollen stage of development was also included. Selected microarray probes were hybridised to Northern blots and radioactive hybridisation signal intensities quantified using a phosphorimager. To compare Northern hybridisation signal intensities to those obtained in microarray experiments, the $\log_2$ differential expression ratio was calculated from Northern hybridisation, given by $M = \log_2$ meiotic stage/immature pollen. The *M*-values from Northern hybridisation for three microarray probes were plotted against *M*-values

Figure 5.13: Consistency in expression profiles of microarray probes of predicted identical function.

A: protein disulfide isomerase
B: enoyl-[acyl-carrier-protein] reductase (NADH2)
C: CTP synthase
D: mitochondrial aldehyde dehydrogenase
E: dihydroflavonol reductase
F: histone group
G: transcription factor X1
H: dnaK-type molecular chaperone

PM, pre-meiosis; LP, leptotene to pachytene; DA, diplotene to late anaphase I; TT, telophase I to telophase II; T, tetrads.

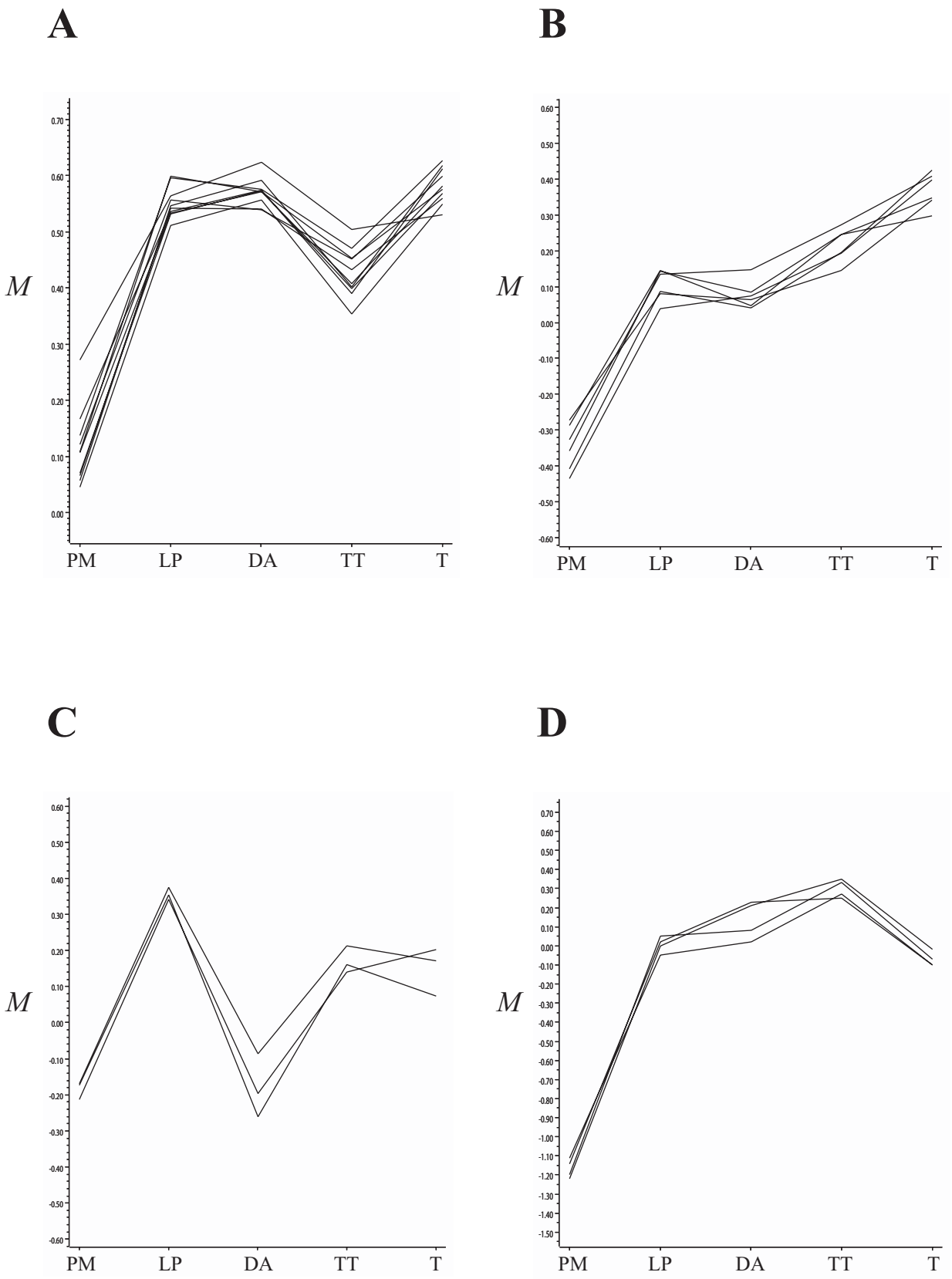
A
B
C
D
M
PM
LP
DA
TT
T

E

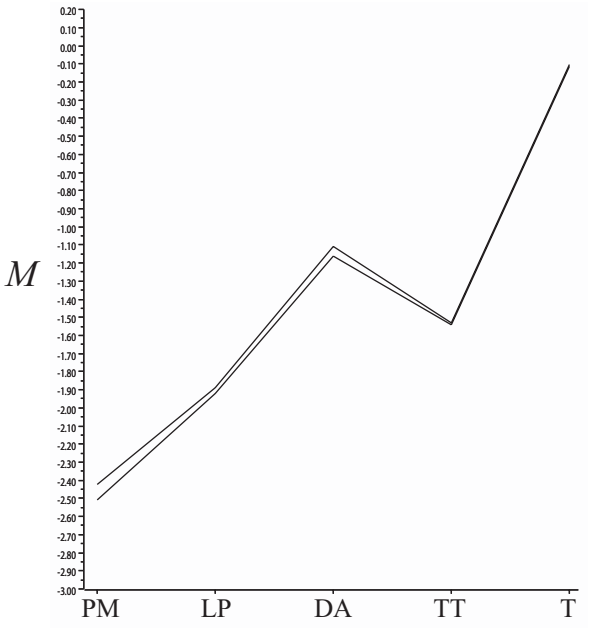

F

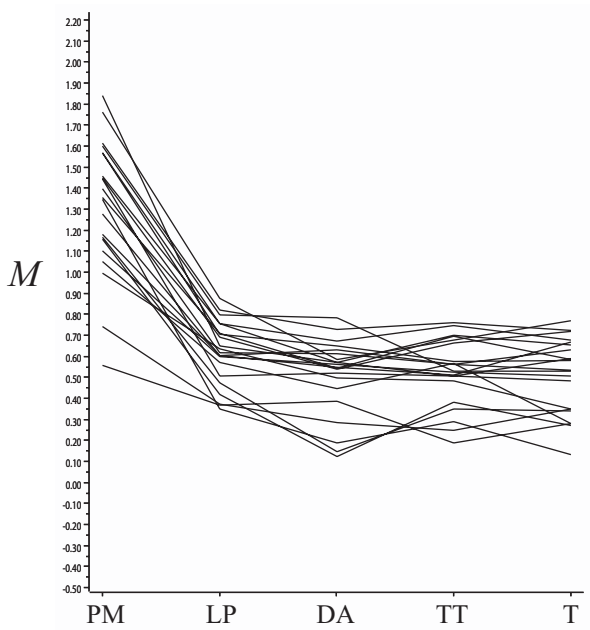

G

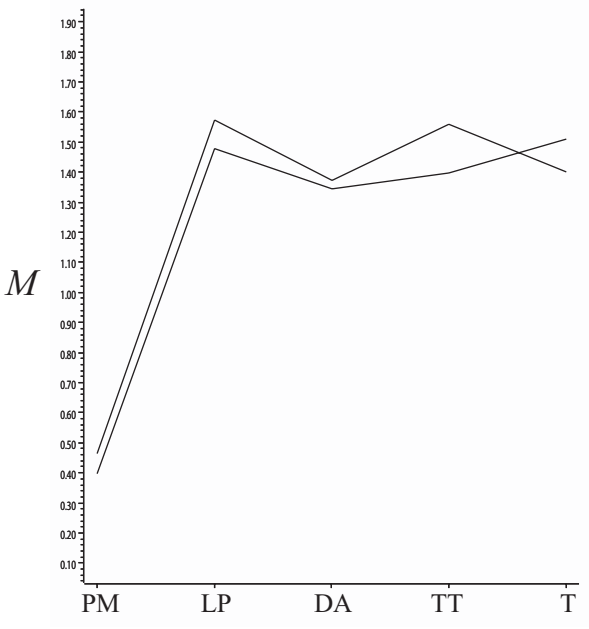

H

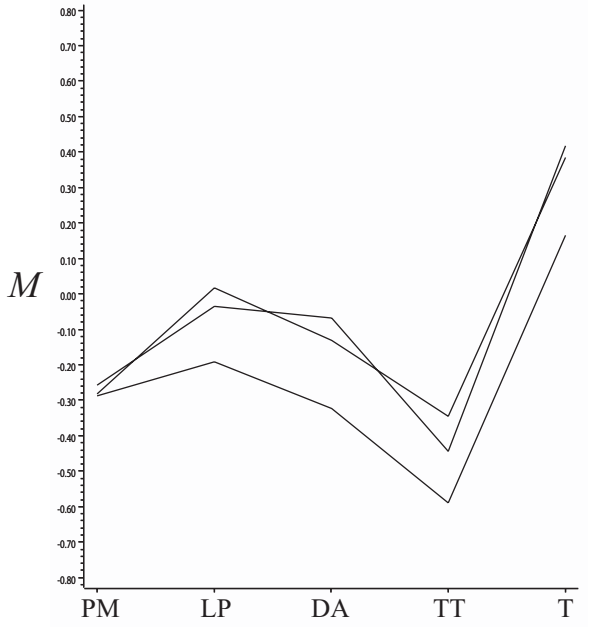

obtained from microarray hybridisation, and are shown in **Figure 5.14**. For the three microarray probes shown, it is apparent that overall patterns and trends in gene expression are comparable between microarray and Northern techniques. It is evident that temporal changes in expression indicated from microarray hybridisation are more subtle than those derived from Northern hybridisation, which may relate to the relative sensitivity of each gene expression analysis method.

5.3.5.2 Analysis of the differentially expressed genes during meiosis

A change of greater than two-fold was applied to *M*-values of all microarray probes to identify a subset of genes for further investigation showing differential expression in meiotic stages compared to immature pollen reference tissue. Genes were selected whose *M*-values were either greater than 0.90, or less than –0.90 in at least one of the five meiotic cell division stages from pre-meiosis through to tetrads. A cut-off level of *M* = +/-0.90 was chosen to allow for inclusion of genes showing differential expression closely approximating but slightly less than a two-fold change. One hundred and twenty eight microarray probes were identified based on these selection criteria. The majority of these genes (119, or 93 %) were derived from the wheat meiotic anther cDNA library (WAW identifying code). In addition, four BAC, three ITEC and two DUP clones were identified as showing significant differential expression for at least one meiotic timepoint.

5.3.5.2.1 Hierarchical clustering

Genes showing greater than an approximate two-fold change in at least one meiotic stage were subjected to hierarchical clustering (Eisen *et al.*, 1998), to identify groups showing similar expression profiles over the time course of meiosis. The results of expression profile clustering are shown in **Figure 5.15**. A number of expression profile groups are evident from **Figure 5.15**, and may be classified into several categories based on patterns of transcriptional control, such as; genes expressed predominantly during the premeiotic interphase immediately preceding the beginning of chromosome condensation during early meiosis; genes whose expression increases during leptotene to pachytene and remains relatively constant throughout subsequent stages; genes whose expression peaks during the later stages of meiosis; and various intermediate profiles that includes mRNAs

Figure 5.14: A comparison of expression profiles derived from microarray and Northern hybridisation.

Expression profiles for three microarray probes, #1778 (**A**), #1480 (**B**) and #267 (**C**) were determined by Northern hybridisation to total RNA isolated from anthers at pre-meiosis (PM), leptotene to pachytene (LP), diplotene to late anaphase I (DA), telophase I to telophase II (TT) and tetrads (T). Photographs of ethidium bromide stained RNA gels are shown for each Northern blot below hybridisation signals.

A

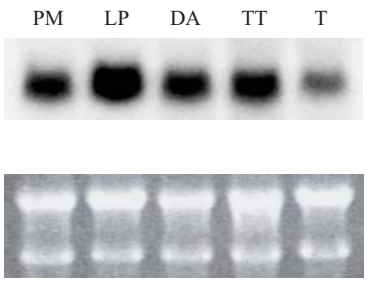
PM
LP
DA
TT
T

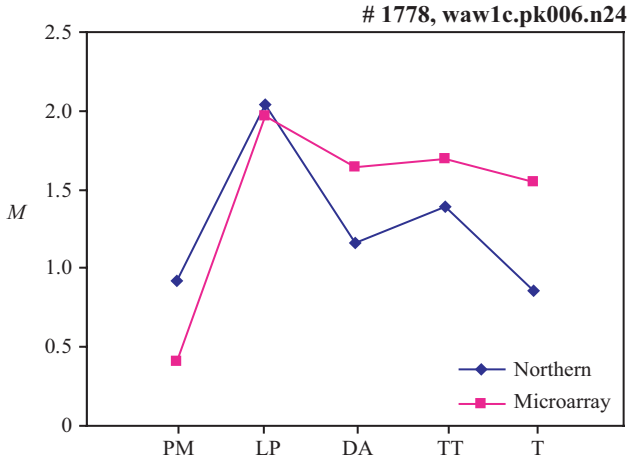
1778, waw1c.pk006.n24
2.5
2.0
1.5
1.0
0.5
0
M
Northern
Microarray
PM
LP
DA
TT
T

B

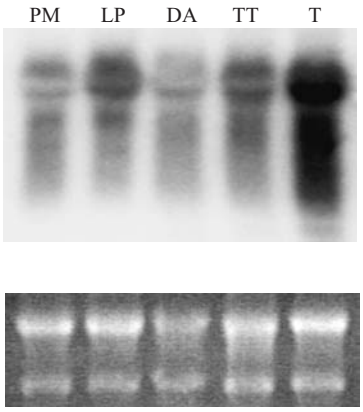
PM
LP
DA
TT
T

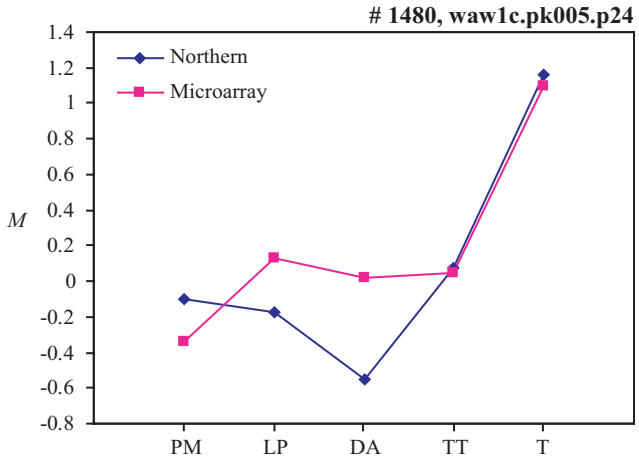
1480, waw1c.pk005.p24
1.4
1.2
1
0.8
0.6
0.4
0.2
0
-0.2
-0.4
-0.6
-0.8
M
Northern
Microarray
PM
LP
DA
TT
T

C

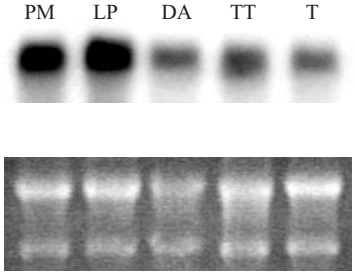
PM
LP
DA
TT
T

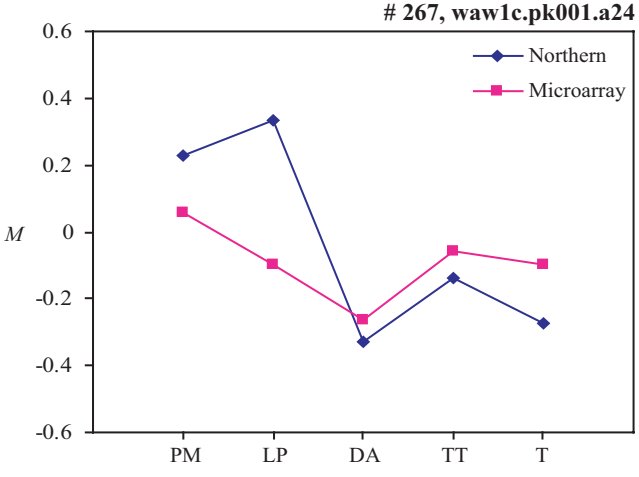
267, waw1c.pk001.a24
0.6
0.4
0.2
0
-0.2
-0.4
-0.6
M
Northern
Microarray
PM
LP
DA
TT
T

Figure 5.15: Hierarchical cluster analysis of 128 microarray probes showing greater than a two-fold change in at least one meiotic stage compared to the immature pollen reference tissue.

Each row represents a single microarray probe and each column a meiotic stage: PM, pre-meiosis; LP, leptotene to pachytene; DA, diplotene to late anaphase I; TT, telophase I to telophase II; T, tetrads. Colouring indicates *M*-values associated with each probe at each meiotic stage. Shades of red and green indicate relative induction or repression respectively compared to expression in the immature pollen reference tissue. Microarray probe numbers and BLAST results (**Appendix 1)** are indicated in the text. Species abbreviations e.g. [*At*] correspond to those indicated in **Appendix 1**. Six distinct cluster groups are shown (I-VI).

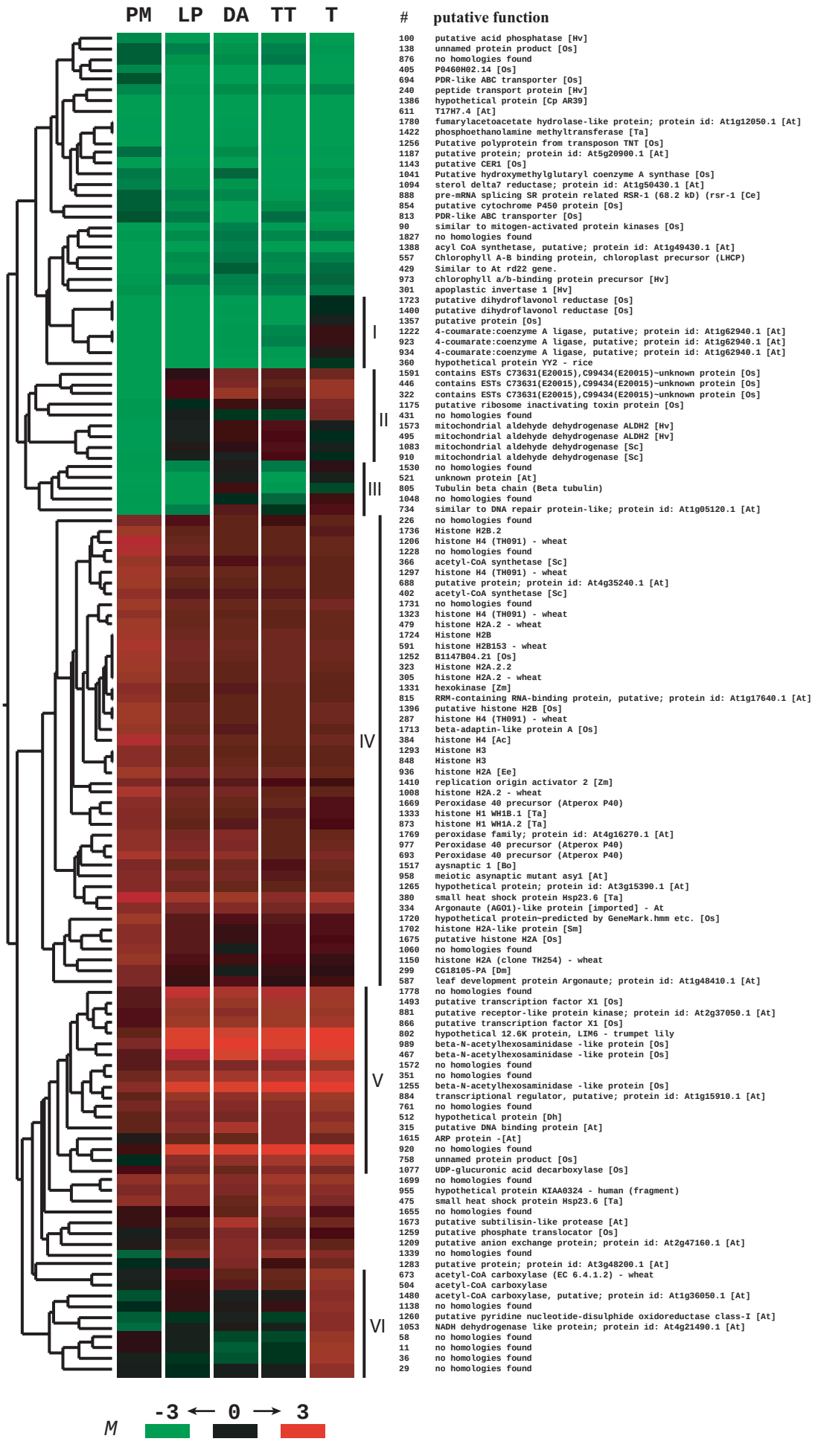
PM
LP
DA
TT
T
putative function
100 putative acid phosphatase [Hv]
138 unnamed protein product [Os]
876 no homologies found
405 P0460H02.14 [Os]
694 PDR-like ABC transporter [Os]
240 peptide transport protein [Hv]
1386 hypothetical protein [Cp AR39]
611 T17H7.4 [At]
1780 fumarylacetoacetate hydrolase-like protein; protein id: At1g12050.1 [At]
1422 phosphoethanolamine methyltransferase [Ta]
1256 Putative polyprotein from transposon TNT [Os]
1187 putative protein; protein id: At5g20900.1 [At]
1143 putative CER1 [Os]
1041 Putative hydroxymethylglutaryl coenzyme A synthase [Os]
1094 sterol delta7 reductase; protein id: At1g50430.1 [At]
888 pre-mRNA splicing SR protein related RSR-1 (68.2 kD) (rsr-1 [Ce]
854 putative cytochrome P450 protein [Os]
813 PDR-like ABC transporter [Os]
90 similar to mitogen-activated protein kinases [Os]
1827 no homologies found
1388 acyl CoA synthetase, putative; protein id: At1g49430.1 [At]
557 Chlorophyll A-B binding protein, chloroplast precursor (LHCP)
429 Similar to At rd22 gene.
973 chlorophyll a/b-binding protein precursor [Hv]
301 apoplastic invertase 1 [Hv]
1723 putative dihydroflavonol reductase [Os]
1400 putative dihydroflavonol reductase [Os]
1357 putative protein [Os]
1222 4-coumarate:coenzyme A ligase, putative; protein id: At1g62940.1 [At]
923 4-coumarate:coenzyme A ligase, putative; protein id: At1g62940.1 [At]
934 4-coumarate:coenzyme A ligase, putative; protein id: At1g62940.1 [At]
360 hypothetical protein YY2 - rice
1591 contains ESTs C73631(E20015),C99434(E20015)~unknown protein [Os]
446 contains ESTs C73631(E20015),C99434(E20015)~unknown protein [Os]
322 contains ESTs C73631(E20015),C99434(E20015)~unknown protein [Os]
1175 putative ribosome inactivating toxin protein [Os]
431 no homologies found
1573 mitochondrial aldehyde dehydrogenase ALDH2 [Hv]
495 mitochondrial aldehyde dehydrogenase ALDH2 [Hv]
1083 mitochondrial aldehyde dehydrogenase [Sc]
910 mitochondrial aldehyde dehydrogenase [Sc]
1530 no homologies found
521 unknown protein [At]
805 Tubulin beta chain (Beta tubulin)
1048 no homologies found
734 similar to DNA repair protein-like; protein id: At1g05120.1 [At]
226 no homologies found
1736 Histone H2B.2
1206 histone H4 (TH091) - wheat
1228 no homologies found
366 acetyl-CoA synthetase [Sc]
1297 histone H4 (TH091) - wheat
688 putative protein; protein id: At4g35240.1 [At]
402 acetyl-CoA synthetase [Sc]
1731 no homologies found
1323 histone H4 (TH091) - wheat
479 histone H2A.2 - wheat
1724 Histone H2B
591 histone H2B153 - wheat
1252 B1147B04.21 [Os]
323 Histone H2A.2.2
305 histone H2A.2 - wheat
1331 hexokinase [Zm]
815 RRM-containing RNA-binding protein, putative; protein id: At1g17640.1 [At]
1396 putative histone H2B [Os]
287 histone H4 (TH091) - wheat
1713 beta-adaptin-like protein A [Os]
384 histone H4 [Ac]
1293 Histone H3
848 Histone H3
936 histone H2A [Ee]
1410 replication origin activator 2 [Zm]
1008 histone H2A.2 - wheat
1669 Peroxidase 40 precursor (Atperox P40)
1333 histone H1 WH1B.1 [Ta]
873 histone H1 WH1A.2 [Ta]
1769 peroxidase family; protein id: At4g16270.1 [At]
977 Peroxidase 40 precursor (Atperox P40)
693 Peroxidase 40 precursor (Atperox P40)
1517 aysnaptic 1 [Bo]
958 meiotic asynaptic mutant asy1 [At]
1265 hypothetical protein; protein id: At3g15390.1 [At]
380 small heat shock protein Hsp23.6 [Ta]
334 Argonaute (AGO1)-like protein [imported] - At
1720 hypothetical protein~predicted by GeneMark.hmm etc. [Os]
1702 histone H2A-like protein [Sm]
1675 putative histone H2A [Os]
1060 no homologies found
1150 histone H2A (clone TH254) - wheat
299 CG18105-PA [Dm]
587 leaf development protein Argonaute; protein id: At1g48410.1 [At]
1778 no homologies found
1493 putative transcription factor X1 [Os]
881 putative receptor-like protein kinase; protein id: At2g37050.1 [At]
866 putative transcription factor X1 [Os]
802 hypothetical 12.6K protein, LIM6 - trumpet lily
989 beta-N-acetylhexosaminidase -like protein [Os]
467 beta-N-acetylhexosaminidase -like protein [Os]
1572 no homologies found
351 no homologies found
1255 beta-N-acetylhexosaminidase -like protein [Os]
884 transcriptional regulator, putative; protein id: At1g15910.1 [At]
761 no homologies found
512 hypothetical protein [Dh]
315 putative DNA binding protein [At]
1615 ARP protein -[At]
920 no homologies found
758 unnamed protein product [Os]
1077 UDP-glucuronic acid decarboxylase [Os]
1699 no homologies found
955 hypothetical protein KIAA0324 - human (fragment)
475 small heat shock protein Hsp23.6 [Ta]
1655 no homologies found
1673 putative subtilisin-like protease [At]
1259 putative phosphate translocator [Os]
1209 putative anion exchange protein; protein id: At2g47160.1 [At]
1339 no homologies found
1283 putative protein; protein id: At3g48200.1 [At]
673 acetyl-CoA carboxylase (EC 6.4.1.2) - wheat
504 acetyl-CoA carboxylase
1480 acetyl-CoA carboxylase, putative; protein id: At1g36050.1 [At]
1138 no homologies found
1260 putative pyridine nucleotide-disulphide oxidoreductase class-I [At]
1053 NADH dehydrogenase like protein; protein id: At4g21490.1 [At]
58 no homologies found
11 no homologies found
36 no homologies found
29 no homologies found
I
II
III
IV
V
VI
M
-3 ← 0 → 3

of relatively constant expression. Six distinct expression profile groups are shown in **Figure 5.15** (I-VI). To discuss the putative function of the genes identified as showing interesting temporal regulation throughout meiosis, the results of extensive BLAST searches using blastn, blastx and tblastx search algorithms have been studied. Genes are discussed in detail where the results of database searches may indicate a function in meiosis. Genes showing either no similarity in database searches, or similarity to hypothetical or putative proteins are not discussed in detail. Since all of the sequences on the microarray are ESTs (with the exception of BAC clones), the first and logical step for genes of interesting expression that lack significant database similarity would be to sequence more of the corresponding cDNA clones in an attempt to gain insight into putative function.

5.3.5.2.2 A comment on genes involved in cellular metabolism

The primary aim of the microarray experiments performed in this study was to correlate gene expression with events related to meiotic cell division, and to identify candidate wheat genes that may be involved in various aspects of these processes for future research. The results of these experiments has concomitantly revealed a number of distinct expression profiles corresponding to genes involved in pathways of cellular metabolism over the period from pre-meiotic interphase to the tetrad stage of pollen mother cell development. For several reasons, the significance of, and correlation between these expression patterns has not been thoroughly investigated: Firstly, it is considered unlikely that the observed temporal regulation of genes encoding metabolic enzymes is significantly related to the underlying genetic factors controlling meiosis. The microarray targets prepared for hybridisation were synthesised from RNA isolated from whole anthers. In addition to pollen mother cells, a significant component of total anther mass is derived from the non-meiotic cell types of the tapetal and epidermal layers. These cells are metabolically active during early anther development, and most likely play an important role in the synthesis of metabolites required for normal anther development and pollen maturation. Secondly, the design of microarray experiments in this study is not suited to examining the expression of genes involved in metabolism. This is mainly due to the use of the immature pollen reference tissue in microarray

hybridisations. It is not intuitive or logical to compare the expression of genes unrelated to meiotic development under such experimental conditions.

There should be no doubt however concerning the importance of transcriptional regulation of metabolic gene expression during anther and pollen development. It is known for example that cell cycle progression is dependent on conditions that maintain cellular metabolism and cell growth (reviewed in Muller *et al*. 1993). In this context, a few examples are briefly considered below. Acetyl coenzyme A (acetyl-CoA) and malonyl-CoA are the two precursors of *de novo* fatty acid biosynthesis. The broadly distributed acetate activating enzyme acetyl-CoA synthetase generates acetyl-CoA for entry into these pathways. Malonyl-CoA is formed as an additional precursor for fatty acid biosynthesis through the carboxylation of acetyl-CoA by acetyl-CoA carboxylase. The expression of the acetyl-CoA synthetase gene has been shown to be associated with the cell cycle. For example, using differential display to look for transcriptionally regulated mediators of the cell cycle in the protozoan *Tetrahymena pyriformis*, Wang *et al*. (1999a) found that acteyl-CoA synthetase was developmentally regulated during the cell cycle. A number of other studies have also investigated the expression of another enzyme involved in this pathway, aldehyde dehydrogenase, in relation to the prominence of ethanolic fermentation in developing pollen (Mellema *et al.*, 2002; op den Camp and Kuhlemeier, 1997; Tsuji *et al.*, 2003).

Another example is the regulation of hexokinase gene expression. The phosphorylation of glucose, a crucial step in cellular metabolism, is catalysed by hexokinases. A number of reports have investigated the expression of hexokinases in cellular division. For example, Netzker *et al*. (1994) examined the expression of glycolytic isozymes in rat thymocytes during cell cycle progression, and reported a peak in hexokinase activity and mRNA levels coinciding with the S-phase of the cell cycle. Similarly, Burger *et al*. (1994) investigated the induction of a number of metabolic genes during the cell cycle in synchronised human fibroblast lines and found that hexokinase mRNA expression was highest in the G1 phase. In plants, Menu *et al*. (2001) have characterised a cDNA encoding hexokinase from tomato, and examined the expression of this gene in a number of tissues and organs and during all stages of fruit development. They found hexokinase expression to be highest in floral tissue. During the stolon-tuber transition in potato,

Appeldoorn *et al*. (2002) have shown at the transcriptional level that hexokinase activities are restricted to the mitotically active (sub)apical region, which could suggest a role for these enzymes in cell division. In addition to these findings, there are a number of other reports investigating hexokinase expression during mitotic and meiotic division (see Downs *et al*., 1996; Mori *et al*., 1993 and Alekseev *et al*., 1986 for further examples).

The expression profiles of all genes encoding metabolic enzymes identified after a two-fold change criteria are shown in **Figure 5.16**. A number of microarray probes corresponding to metabolic enzymes display interesting expression changes over the time course experiments, and supports a requirement in the anther for higher turnover rates of glycolytic pathways and other metabolic activities during anther development. The changes of many metabolic genes during meiosis suggests that the regulation of their gene expression is an important process in the developing anther, and may relate to characteristic processes that could be investigated further in relation to current literature on these topics. For the reasons discussed above this has not been investigated further within the scope of this thesis.

5.3.5.2.3 Early expressed genes

5.3.5.2.3.1 Cluster group IV

Cluster group IV in **Figure 5.15** identifies 45 microarray probes showing highest expression at the premeiotic interphase preceding meiosis (pre-meiosis). Homology to histone proteins dominates the list of functional annotation for these 45 probes. Amongst the 45 probes in expression cluster IV, 21 have similarity to various proteins of the histone group, including histones H1, H2A, H2B, H3 and H4, four have similarity to peroxidase, two have similarity to acetyl-CoA synthetase, two have similarity to the meiotic asynaptic 1 protein (Asy1), two have similarity to the leaf development protein Argonaute, and nine probes either have no database match or exhibit similarity to uncharacterised proteins. Removing the above functional redundancy for those genes showing significant similarity to characterised proteins reveals 19 genes up-regulated during pre-meiosis compared to the non-meiotic immature pollen reference tissue. The expression profiles of these genes are shown in **Figure 5.17**. Pre-meiotic interphase

Figure 5.16: Temporal expression profiles of genes encoding metabolic enzymes.

PM, pre-meiosis; LP, leptotene to pachytene; DA, diplotene to late anaphase I; TT, telophase I to telophase II; T, tetrads.

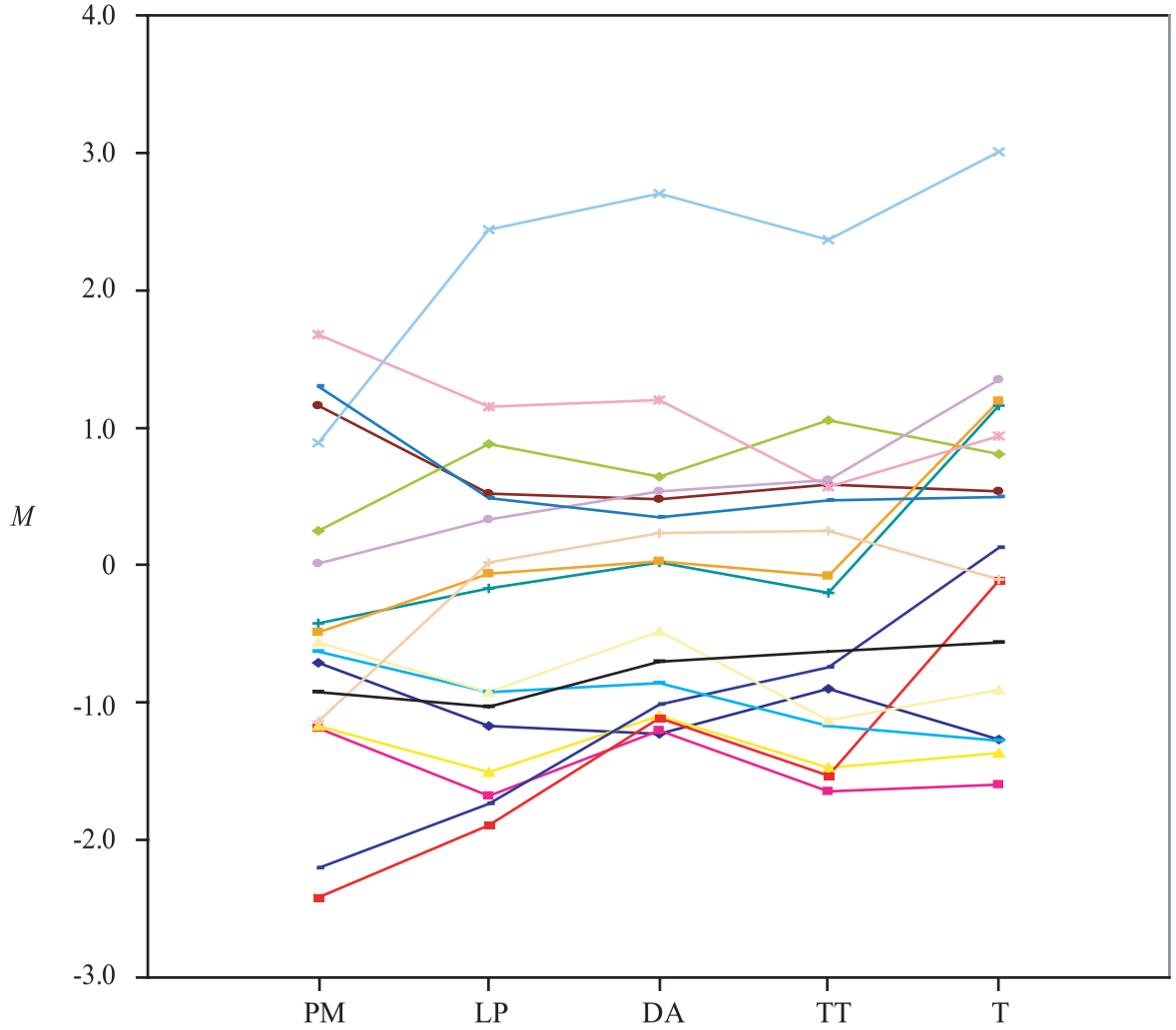

#	Function
100	putative acid phosphatase
1780	fumarylacetoacetate hydrolase-like protein
1422	phosphoethanolamine methyltransferase
1400	putative dihydroflavonol reductase
1331	hexokinase
1260	putative pyridine nucleotide-disulphide oxidoreductase class-I
1222	4-coumarate:coenzyme A ligase
1094	sterol delta7 reductase
1077	UDP-glucuronic acid decarboxylase
1053	NADH dehydrogenase like protein
1041	Putative hydroxymethylglutaryl coenzyme A synthase
989	beta-N-acetylhexosaminidase -like protein
693	Peroxidase 40 precursor (Atperox P40)
673	acetyl-CoA carboxylase
495	mitochondrial aldehyde dehydrogenase ALDH2
366	acetyl-CoA synthetase
301	apoplastic invertase 1

Figure 5.17: Temporal expression profiles of genes from cluster group IV.

PM, pre-meiosis; LP, leptotene to pachytene; DA, diplotene to late anaphase I; TT, telophase I to telophase II; T, tetrads.

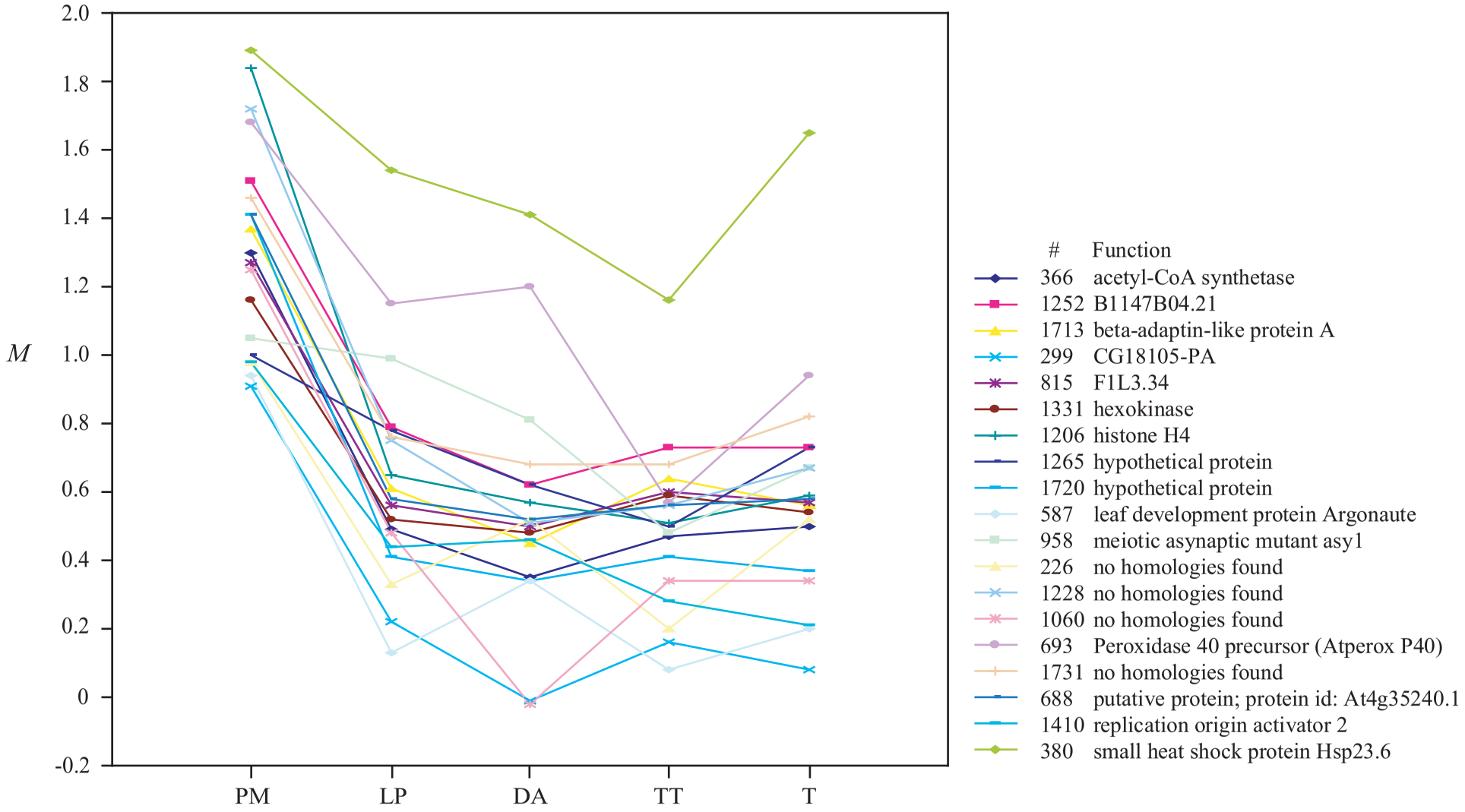
2.0
1.8
1.6
1.4
1.2
1.0
0.8
0.6
0.4
0.2
0
-0.2
M
PM
LP
DA
TT
T
Function
366 acetyl-CoA synthetase
1252 B1147B04.21
1713 beta-adaptin-like protein A
299 CG18105-PA
815 F1L3.34
1331 hexokinase
1206 histone H4
1265 hypothetical protein
1720 hypothetical protein
587 leaf development protein Argonaute
958 meiotic asynaptic mutant asy1
226 no homologies found
1228 no homologies found
1060 no homologies found
693 Peroxidase 40 precursor (Atperox P40)
1731 no homologies found
688 putative protein; protein id: At4g35240.1
1410 replication origin activator 2
380 small heat shock protein Hsp23.6

(pre-meiosis) in pollen mother cells is characterised predominantly by DNA synthesis in preparation for meiosis I. Although pre-meiosis is not technically a meiotic stage in itself, the apparent up-regulation of a number of genes required for early meiotic events is evidence for meiosis-related transcriptional activity at this stage, as discussed below.

Histone proteins

The packaging of newly replicated DNA during DNA synthesis requires the synthesis of a complete set of histone proteins. In eukaryotic cells the DNA double helix wraps around histone octamers to form the nucleosome, comprising the basic structural unit of a chromosome. A histone octamer contains two copies of each core histone protein (H2A, H2B, H3 and H4). The transcription of genes corresponding to each core histone protein, and histone H1, is up-regulated during pre-meiosis, correlating with the synthesis of DNA in preparation for meiotic division.

Replication origin activator protein

Expression of the gene corresponding to the microarray probe #1410 is up-regulated during pre-meiosis, and is interesting based on high levels of similarity of this EST (90 % at the amino acid level) to the replication origin activator proteins 2 and 3, ZmROA2/ZmROA3, from maize (Sabelli *et al.*, 1999). The replication origin activator proteins ZmROA1-3 share a high degree of homology with the MCM3 subfamily of yeast minichromosome maintenance (MCM) proteins (Gibson *et al.*, 1990; Hennessy *et al.*, 1990), essential factors in origin activation for the initiation of DNA replication, and as components of pre-replication complexes that limit DNA replication to once per cycle. In yeast, during mitotic G1 and early S phase, a complex formed by MCM proteins interacts with chromatin and other factors associated with replication origins, and allows replication to proceed. Following the initiation of replication, MCM complexes dissociate from chromatin and prevent further origin-initiated replication during the same cell cycle. The expression pattern of probe #1410 during meiosis is consistent with a role of initiation or regulation of DNA synthesis. The maize proteins ZmROA1-3 represent the only characterised homologues of the yeast MCM3 subfamily from higher plants. The transcription of mRNA from *ZmROA1-3* has been shown to be developmentally regulated, being particularly high in actively dividing tissues such as root apex, the developing cob and the coleoptile, and shown to be strongly correlated

with that of the histone H4 transcript in maize (Sabelli *et al.*, 1996). Furthermore, Sabelli *et al*. (1996) have isolated almost identical fragments using PCR from barley and *Arabidopsis*, that indicates high levels of conservation for MCM-related genes from higher plants. The maize proteins have been shown to be localised to the nucleus, where they overlap with chromatin during interphase, become distinct from chromatin during prophase, and appear completely dissociated from chromatin during chromosome segregation at mitosis (Sabelli *et al.*, 1999). These observations support a biological role of these proteins in controlling the frequency of DNA replication during the cell cycle. Given the distinct expression profile and a high level of similarity to the maize proteins ZmROA2 and ZmROA3, it seems likely that the microarray probe #1410 represents an uncharacterised homologue in the wheat genome.

Asynaptic 1 (*ASY1*)

Cluster group IV contains two microarray probes (#958 and #1517) with similarity to the *ASY1* gene from *Arabidopsis* (Ross *et al.*, 1997), and its functional homologue *BoASY1* from the closely related plant species *Brassica oleracea* (Armstrong *et al.*, 2002). A detailed description of these genes and their putative function can be found in Chapter 1, Section 1.3.1. In *Arabidopsis* and *Brassica*, Asy1 localises to the regions of chromosomes that associate with the axial/lateral elements of meiotic chromosomes. Rather than representing a structural component of the synaptonemal complex, it has been proposed that Asy1 may possibly act by defining regions of chromatin that associate with the developing synaptonemal complex structure (Armstrong *et al.*, 2002). The expression patterns of *ASY1* and *BoASY1* have been analysed in *Arabidopsis* and *Brassica* respectively (Armstrong *et al.*, 2002), and correlate with that observed for the microarray probes #958 and #1517. In meiotic anthers of *Brassica*, western blots indicate that the BoAsy1 protein accumulates during meiotic interphase, peaking at leptotene, before gradually decreasing in expression towards later meiotic stages (Armstrong *et al.*, 2002). Similarly, Armstrong *et al*. (2002) show a similar pattern of expression for the *ASY1* gene in *Arabidopsis* buds. However, a slight increase in expression was observed in extracts prepared from buds at the tetrad stage. Armstrong *et al*. (2002) suggest that this could be attributed to asynchrony between male and female meiosis in *Arabidopsis* buds, such that by the time pollen mother cells have reached the tetrad stage of meiosis, the embryo sac mother cells are undergoing prophase I. The

expression profiles of microarray probes showing similarity to *ASY1* (e.g. #958 in **Figure 5.17**) indicates up-regulation of this transcript at the tetrad stage of meiosis, providing evidence, in wheat at least, for increased transcription during male meiosis at this stage.

The presence of an *ASY1*-like gene in the wheat genome has been investigated in this study. Considering the role of Asy1/BoAsy1 during synaptonemal complex formation in members of the Cruciferae, and the proposal that the role of the *Ph2* locus in wheat may be to affect synaptic progression during early meiosis (Martinez *et al.*, 2001), we have pursued research to characterise this gene in wheat. Southern analysis against wheat nullisomic-tetrasomic addition lines indicates that an *ASY1*-like sequence is present in the wheat genome, and is represented by a single copy on chromosome 5D. Although not located in the region deleted in the *ph2a* mutant on chromosome 3DS or *ph1b* on 5BL, results from microarray experiments and Northern analysis (data not shown) indicate that transcription of this gene in wheat meiotic tissues correlates with an anticipated function in synaptonemal complex assembly during early prophase I. The wheat homologue of *ASY1* may represent part of the molecular machinery required during early meiotic development, and warrants further characterisation in this respect. It should also be noted that minor regulators of chromosome pairing have been identified on chromosome 5D (Section 1.6.1).

Beta-adaptin-like protein A

The microarray probe #1713 shows marked up-regulation during pre-meiosis, and like all genes in cluster group IV is expressed at a higher level in all meiotic stages compared to expression in the non-meiotic immature pollen reference tissue. The sequenced portion of probe #1713 shows 80 % identity at the amino acid level to a beta-adaptin-like protein A from rice. Weaker but significant similarity is seen to the same protein from *Arabidopisis*, and to other adaptor-related proteins from different species. Adaptins are subunits of adaptor protein complexes with a role in the formation of intracellular transport vesicles and the selection of cargo molecules for vesicle incorporation (Boehm and Bonifacino, 2001). Adaptins, and other related proteins, have critical roles in intracellular protein trafficking. Taken alone, such a function seems removed from the direct molecular events controlling meiosis. However, a number of studies have shown that various adaptor proteins interact with proteins that have been associated with cell

cycle control. For example, in humans, the mitotic checkpoint kinase BubR1 has been identified as a novel binding partner of beta2-adaptin, and subcellular immunolocalisation studies suggest that the interaction between BubR1 and beta2-adaptin could take place in the cytosol at any time during the cell cycle (Cayrol *et al.*, 2002). It has also been found that both BubR1 and its related kinase, Bub1, bind to beta-adaptins of other adaptor protein complexes (Cayrol *et al.*, 2002). Furthermore, it has been shown using the yeast two-hybrid system that the gene *ATM* (ataxia-telangiectasia mutated) interacts with beta-adaptin. The *ATM* gene is mutated in the human recessive autosomal chromosome instability disorder ataxia telangiectasia, and homologues have been identified from *Drosophila*, *Xenopus*, mouse and more recently *Arabidopsis* (Garcia *et al.*, 2000; Shiloh, 1997). The Atm protein is a member of a family of proteins sharing the PI 3-kinase domain, and has been implicated in a number of molecular pathways that includes the regulation of cell cycle progression. The Atm protein is induced by double strand breaks and some of the phosphorylation targets of Atm include proteins involved in apoptosis, cell cycle control and DNA repair. Recently, the *Arabidopsis* homologue of *ATM*, *AtATM* has been shown to be essential for meiosis (Garcia *et al.*, 2003). Garcia *et al*. (2003) have shown that upon irradiation, *atm* mutants do not transcribe genes required for the detection and repair of DNA breaks and that partial sterility observed in *atm* plants is the result of abundant fragmentation of chromosomes during meiosis.

A wheat EST with similarity to *AtATM* was identified in Chapter 3 of this study, showing similarity to the rice chromosome 1 region syntenous to that deleted in the wheat *ph2a* mutant, indicating that a putative homologue of *ATM* is present and transcribed in the wheat genome. Southern analysis has indicated that this gene is not located in the *ph2a* deletion region on 3DS. However, given the interesting meiotic expression of the microarray probe #1713, and evidence indicating the interaction of the beta-adaptin protein with components of the cell cycle control machinery, this gene represents an interesting candidate for further investigation in relation to wheat meiotic development.

Leaf development protein Argonaute 1

The microarray probes #334 and #587 fall into cluster group IV. The sequenced regions of these probes show similarity to the leaf development protein Argonaute 1 (ago1) from *Arabidopsis*. Argonaute has been characterised in *Arabidopsis* and shown to be essential for normal development of leaves and floral tissue, and the formation of auxillary meristems in this species (Bohmert *et al.*, 1998). *Arabidopsis* plants homozygous for *ago1* are described as being greatly disturbed in general body architecture, one of numerous developmental defects being that the inflorescence of *ago1* plants lack anthers, causing male sterility of the homozygous mutant plant (Bohmert *et al.*, 1998). Probe #587, which shows 60 % identity at the amino acid level over the sequenced region to the ago1 protein, exhibits an expression profile characteristic of other genes in cluster group IV, being up-regulated at pre-meiosis and falling to a relatively constant level of expression at leptotene to pachytene through to the tetrads stage of meiotic development. A slight peak in expression is observed for this microarray probe at the diplotene to late anaphase I stage. The expression profile however of probe #334 is somewhat different. Although exhibiting the same expression trend throughout meiosis, the reduction in expression from pre-meiosis to the leptotene to pachytene stage is not as dramatic. Probe #334 exhibits 51 % identity at the amino acid level over the sequenced region to the ago1 protein. Furthermore, in addition to these two microarray probes, four other sequences with significant similarity (75 %-92 % identity at the amino acid level) to ago1 and ago1-like proteins from *Arabidopsis* and rice are present on the microarray (#705, #772, #349, and #461). These four microarray probes are not represented in cluster group IV, or indeed in the list of 128 sequences identified as being differentially expressed greater than two-fold in at least one meiotic stage compared to the immature pollen reference tissue. Although showing slight up-regulation at pre-meiosis with an observed increase in expression at diplotene to late anaphase I, similar to probes #334 and #587, the expression profiles of these microarray probes does not correlate well with either *AGO1*-like sequences in cluster group IV. The expression of the *AGO1*-like sequence in wheat should be examined by Northern analysis to confirm developmental regulation of this gene during both anther development and meiosis. Given the developmental defects associated with inflorescence morphology in *ago1* mutants of *Arabidopsis*, it is possible that a homologue of this gene in wheat may define a critical component of normal anther development.

Small heat shock protein Hsp23.6

The heat shock proteins encompass a ubiquitous class of molecular chaperones present in eukaryotic and prokaryotic cells. The synthesis of heat shock proteins has been observed during normal cellular functions such as seed maturation and embryogenesis, and also in response to abiotic factors such as heat, cold, freezing, drought, heavy metal and oxidative stress. Approximately 20-40 different types of heat shock proteins are synthesised in plants under heat stress (Vierling, 1991). The small heat shock proteins comprise a diverse class of heat shock proteins that have low molecular masses of between 15-42 kDa. Based on sequence information and cellular localisation, five classes of small heat shock proteins have been classified in higher plants. Cytosolic I and cytosolic II small heat shock proteins are found in the cytosol, while the other three classes are found in the chloroplast, mitochondria and endoplasmic reticulum.

The precise function of heat shock proteins remains unclear. However, it is apparent that they can act as chaperones *in vitro* and *in vivo*, preventing either complete denaturation of proteins, or by supporting proper folding of proteins under or after protein denaturing conditions. It is also apparent that they have a role contributing to the tolerance of plants under environmental stress. The expression of genes encoding heat shock proteins has been reported during eukaryote cellular division, and furthermore, in mouse and hamster spermatocytes the heat shock protein HSP70-2 has been localised along the synaptonemal complex (Allen *et al.*, 1996). The expression pattern of the microarray probe #380 is interesting in this context. Another microarray probe with similarity to the small heat shock protein Hsp23.6 from wheat was identified as showing significant differential expression in at least one meiotic stage compared to the immature pollen reference tissue. This clone, #475, is shown in **Figure 5.15**. Hierarchical clustering separated these two clones based on slightly different expression profiles. It is apparent however, that both are characterised by increased expression in meiotic tissue compared to the non-meiotic reference. This is interesting when considering similarity of other microarray probes to heat shock proteins from other classes and their expression profiles. In addition to the probes #380 and #475, thirteen other microarray probes exhibit similarity to heat shock proteins; eleven with similarity to either the high molecular weight class HSP70, HSP80 or HSP82, and two with similarity to the low molecular

weight class HSP16.9. None of these classes of heat shock protein exhibit significant expression changes during the meiotic time series examined, and appear in general to be expressed at the same level in meiotic anthers as in non-meiotic immature pollen anthers. This suggests a distinct role for heat shock proteins of the small class Hsp23.6 during either meiosis or early anther development. It is known that small heat shock proteins are expressed during meiotic prophase in lily microsporocytes. Several cDNA clones specific to meiotic prophase in lily have been isolated using subtractive hybridisation that show similarity to the small heat protein HSP17.5 from *Glycine max* (Kobayashi *et al.*, 1994).

These findings are interesting when considering the results of comparative genetics studies in Chapter 3. Three wheat ESTs with similarity to heat shock proteins were identified as showing significant similarity to the rice chromosome 1 region syntenous to that deleted in the *ph2a* mutant. These three ESTs (#87, #178 and #187 in **Table 3.2** of Chapter 3) respectively show similarity to the small heat shock protein 16.9B from wheat, a putative heat shock protein from rice that appears to belong to the HSP70 class, and the small heat shock protein HSP17.8 from wheat. Southern analysis using wheat EST #87 as a probe indicated the presence of sequences belonging to the small heat shock protein class in the region deleted in the *ph2a* mutant (Section 3.4).

The above data suggests a possible role for small heat shock proteins in either meiosis or other developmental events in the wheat anther at the time of meiosis. This role may be associated with the maintenance of protein conformation, or the targeting of proteins to organelle structures in either pollen mother cells or the surrounding tapetal cells. Perhaps the expression of heat shock proteins in reproductive tissues provides a protective mechanism to ensure correct protein tertiary structure during meiotic cell division under conditions of environmental stress. It is also possible that heat shock proteins have a function related to the interaction of proteins at the site of synapsing chromosomes within the developing synaptonemal complex, as data from mice and hamsters may suggest. A number of these possibilities could be explored further in relation to the function of small heat shock proteins in wheat anthers at meiosis, and that of the phenotype conferred by the deletion of the *Ph2* locus.

In addition to the genes discussed above, a number of microarray probes from cluster group IV exhibit interesting expression patterns during the early stages of meiosis in wheat anthers. It is difficult to speculate about the function of these genes during anther development, considering they either show no similarity, or similarity to uncharacterised proteins in either blastn or blastx database searches. These genes are nonetheless important candidates for meiotic control in wheat, and may represent important genes controlling early molecular events during meiosis. The cDNA clones from which these microarray probes were derived should be sequenced to a greater extent and examined by Northern analysis to confirm expression profiles. This may provide interesting research avenues to investigate.

5.3.5.2.3.2 Cluster group V

In addition to the genes of cluster group IV, hierarchical clustering reveals another expression profile group that contains genes up-regulated during the early stages of meiosis. Cluster group V (**Figure 5.18**) identifies genes with distinct up-regulation at the leptotene to pachytene stages of early meiosis. In general, after an initial peak in expression during leptotene to pachytene, the expression of these genes remains more or less constant throughout subsequent stages. The leptotene to pachytene sub-stages of meiotic prophase I are characterised by a number of significant cytological and molecular events. Chromosomes condense and first become visible during leptotene, visible as long threads and with the sister chromatids of each chromosome bound to the common proteinaceous core of the axial element. Zygotene chromosomes continue to condense and it is at this stage that the first signs of pairing are observed, involving the association of the axial cores of each pair of homologous chromosomes. Complete synapsis along the length of homologous chromosomes during zygotene results in the formation of the strictly meiotic structure, the synaptonemal complex. Chromosomes continue to condense throughout pachytene, and it is also at this stage that crossing over between non-sister chromatids is observed. The identification of genes that display marked expression changes at the leptotene to pachytene stage of meiosis are therefore of interest as candidates that may be involved in important meiotic processes such as pairing, synaptonemal complex formation and recombination.

Figure 5.18: Temporal expression profiles of genes from cluster group V.

PM, pre-meiosis; LP, leptotene to pachytene; DA, diplotene to late anaphase I; TT, telophase I to telophase II; T, tetrads.

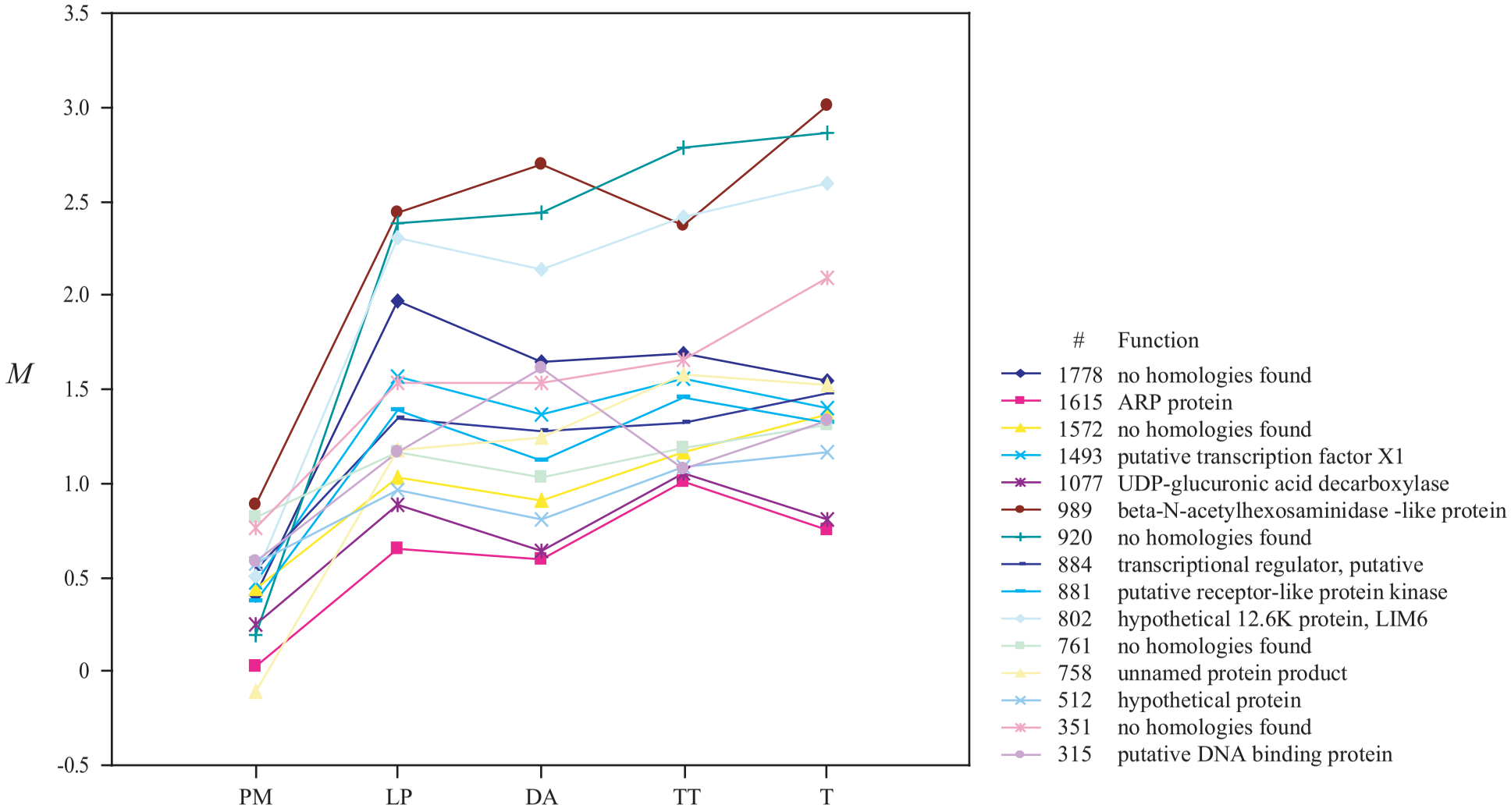
3.5
3.0
2.5
2.0
1.5
1.0
0.5
0
-0.5
M
PM
LP
DA
TT
T
Function
1778 no homologies found
1615 ARP protein
1572 no homologies found
1493 putative transcription factor X1
1077 UDP-glucuronic acid decarboxylase
989 beta-N-acetylhexosaminidase -like protein
920 no homologies found
884 transcriptional regulator, putative
881 putative receptor-like protein kinase
802 hypothetical 12.6K protein, LIM6
761 no homologies found
758 unnamed protein product
512 hypothetical protein
351 no homologies found
315 putative DNA binding protein

A non-redundant set of 15 microarray probes are given by cluster group V. Of these, the only sequence showing similarity to genes of putative meiotic function was that of probe #802, which shows low levels of similarity at the amino acid level to a cDNA induced in meiotic prophase from Lily microspores, *LIM6* (Kobayashi *et al.*, 1994). This represents the only database match for the sequence of probe #802. The sequence of the clone *LIM6* similarly has no significant database matches. On Northern blots of various lily tissues, *LIM6* displays a meiotic specific expression that begins at zygotene and continues to be expressed through to the tetrad stage of meiosis. However, the sequence similarity of these two sequences is low (42 % identity over a stretch of approximately 50 amino acids), and further sequencing is required to clarify a relationship between probe #802 and *LIM6* from lily.

Seven microarray probes that either display similarity to uncharacterised proteins, or lack similarity to any sequences in database searches fall into cluster group V. Two probes in particular (#1778 and #920) show significant up-regulation in expression from pre-meiosis to the leptotene to pachytene stage of meiosis. Probe #920 for example is characterised by an increase in expression from pre-meiosis to the leptotene to pachytene stage of approximately five-fold, and increases to almost seven-fold at the tetrad stage compared to the non-meiotic immature pollen reference tissue. The distinct temporal up-regulation of several of these genes warrants further analysis and characterisation in respect to important molecular processes occurring in the meiotic anther at this stage. The presence in cluster group V of three microarray probes showing similarity to transcription factors may also be of importance at this stage of meiotic cell division. It is possible that the increased expression of these genes initiates the synthesis of specific proteins that are required for downstream meiotic events such as chromosome segregation or cytokinesis. These possibilities could be investigated using protein interaction studies. It is important to note here that the microarray probe #1615 (ARP protein) most likely functions as an apurinic endonuclease and redox factor (Babiychuk *et al.*, 1995), as opposed to that of the group of well characterised actin-related proteins (ARP proteins). This is not immediately apparent upon database searches due to discrepancies in nomenclature for these and other so-called ARP proteins.

5.3.5.2.3.3 Cluster group II

Cluster group II (**Figure 5.19**) identifies four microarray probes that display a marked up-regulation during the leptotene to pachytene stage of meiosis. The defining feature of these profiles relates to the *M*-values for the relative expression of these genes. In contrast to cluster group V, the increase in expression of genes in cluster group II from pre-meiosis to the leptotene to pachytene stage results in an expression at the leptotene to pachytene stage that equates that in the immature pollen reference tissue, hence the arrival at $M = 0$ during the leptotene to pachytene stage for all four expression profiles. This indicates that these genes are expressed predominantly in anthers at the immature pollen stage, and that the expression of these genes continues after the tetrad stage of development. Aside from the apparent expression of these genes in anthers at immature pollen, a sharp increase in transcription is observed over the temporal series from pre-meiosis to the tetrad stage of meiosis. This trend continues through to the diplotene to late anaphase I stage for probe #446.

5.3.5.2.4 Mid-late expressed genes

5.3.5.2.4.1 Cluster group III

A cluster of five genes was identified through hierarchical clustering that exhibit an interesting pattern of expression that is characterised by two distinct peaks, the first corresponding to the diplotene to anaphase I meiotic stage, and the second corresponding to the tetrad stage (**Figure 5.20**). The microarray probe #805 shows 91 % identity at the amino acid level to the tubulin beta chain (beta tubulin) from barley. Tubulin is a hetereodimer consisting of two closely related polypeptides, alpha and beta tubulin. Tubulin polymerises into long chains to form a major constituent of microtubules, a major class of filaments of the cytoskeleton. In most organisms tubulin genes constitute multigene families and have been extensively characterised in relation to their function as components of essential cytoskeletal filaments.

A major function of microtubules during cell division is the mitotic and meiotic spindle apparatus that is used to position chromosomes within the dividing cell. The expression of beta tubulin in wheat meiotic anthers correlates with a temporal requirement of tubulin for microtubule formation during meiosis. The expression of the beta tubulin gene is

Figure 5.19: Temporal expression profiles of genes from cluster group II.

PM, pre-meiosis; LP, leptotene to pachytene; DA, diplotene to late anaphase I; TT, telophase I to telophase II; T, tetrads.

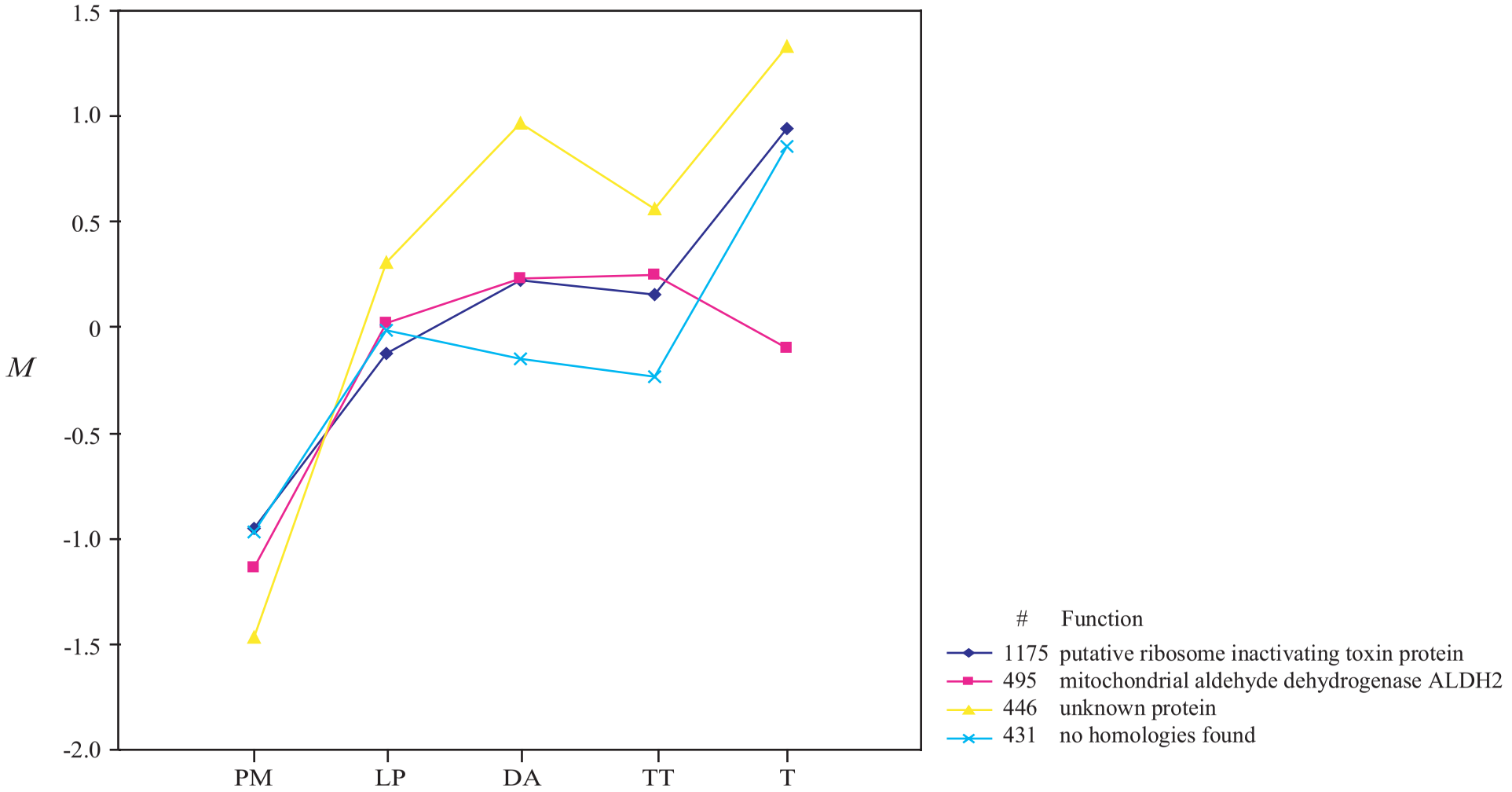
1.5
1.0
0.5
0
-0.5
-1.0
-1.5
-2.0
M
PM
LP
DA
TT
T
Function
1175 putative ribosome inactivating toxin protein
495 mitochondrial aldehyde dehydrogenase ALDH2
446 unknown protein
431 no homologies found

Figure 5.20: Temporal expression profiles of genes from cluster group III.

PM, pre-meiosis; LP, leptotene to pachytene; DA, diplotene to late anaphase I; TT, telophase I to telophase II; T, tetrads.

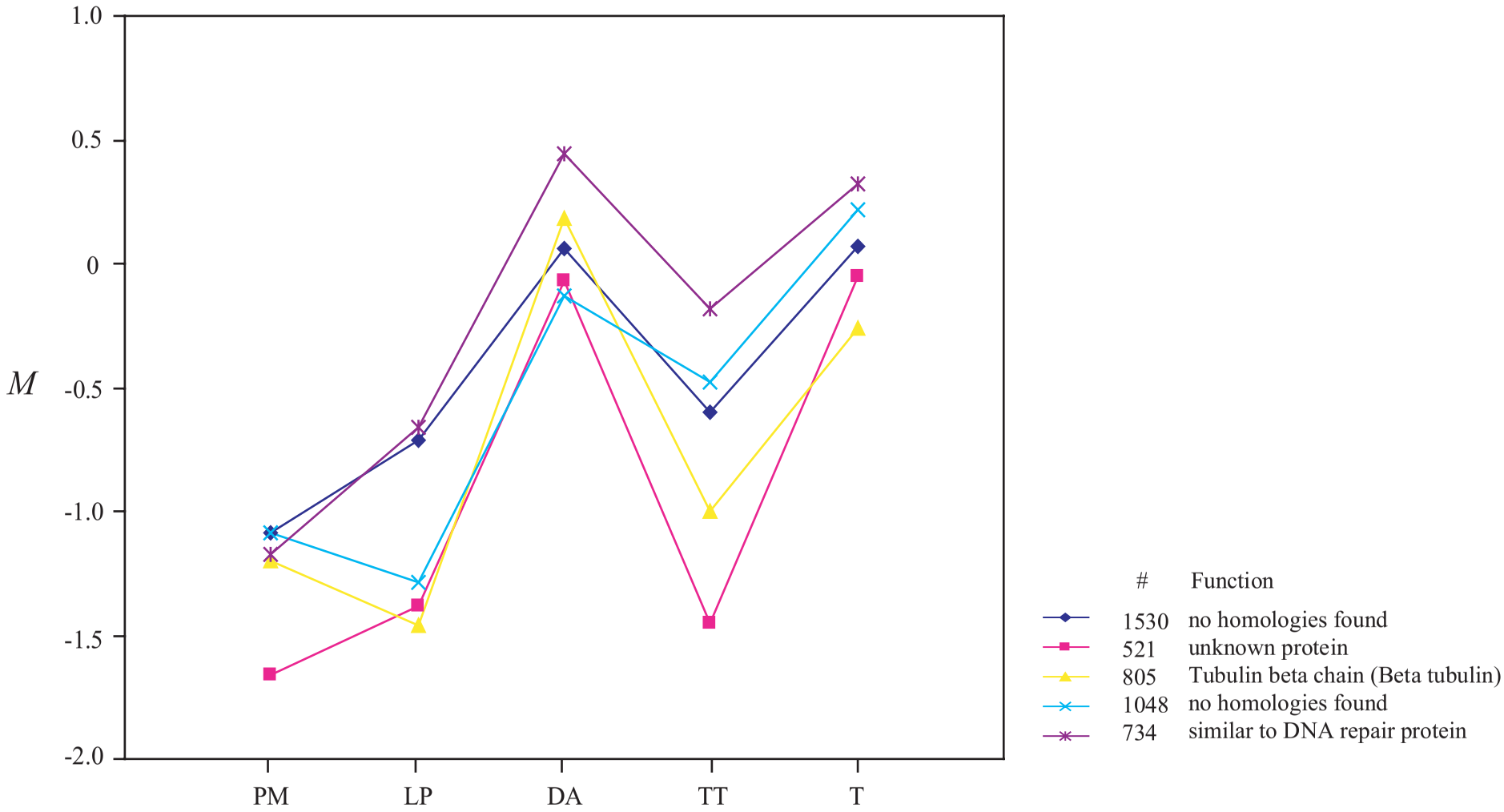
1.0
0.5
0
-0.5
-1.0
-1.5
-2.0
M
PM
LP
DA
TT
T
Function
1530 no homologies found
521 unknown protein
805 Tubulin beta chain (Beta tubulin)
1048 no homologies found
734 similar to DNA repair protein

seen to peak at some point between the meiotic stages of pachytene and late anaphase I, such that the expression of this gene at diplotene to late anaphase I equals that in the immature pollen reference. Given the critical function of tubulin in the meiotic spindle, it is likely that the expression increase derives from stages closer to pachytene, the point that the cell cytoskeletal structure becomes important for chromosome motility during the nuclear division of meiosis I. It is interesting that overall expression decreases between late anaphase I and telophase II, stages that encompass the second meiotic nuclear division during meiosis. It seems that expression of beta tubulin preceding late anaphase I sustains both the first and second nuclear divisions, or that an alternative tubulin gene is expressed during the second meiotic division. An increase in expression at the tetrad stage of meiosis seems to suggest a role for this tubulin in the development of immature pollen in the maturing anther. A number of studies have shown that specific members of tubulin gene families, of both the alpha and beta classes are expressed predominantly in pollen, elongating pollen tubes and ovules, and are important proteins for pollen development and pollen tube growth upon germination (see Evrard *et al*., 2002; Villemur *et al*., 1994 and Rogers *et al*., 1993 as examples).

Microarray probe #805 is the only sequence present on the microarray with similarity to beta tubulin. However, it is interesting to find that eight probes on the microarray show similarity to the tubulin alpha chain protein from various plant species. Considering that all of these sequences (alpha tubulin and #805, beta tubulin) are derived from randomly picked clones of the WAW wheat meiotic anther cDNA library, the relative prevalence of each tubulin type in anthers at pre-meiosis to metaphase I becomes apparent. Furthermore, the expression profiles for all alpha tubulin genes remains constant around $M = 0$ for all meiotic stages. This information suggests that alpha tubulin is also expressed in meiotic anthers of wheat, and at a similar level in anthers containing pollen mother cells at the immature pollen stage of development. The expression of alpha tubulin genes does not appear to be developmentally regulated throughout meiosis, unlike that of beta tubulin transcripts.

Also falling into expression cluster III is the microarray probe #734 that shows significant similarity to a number of interesting proteins. Firstly, blastx searches indicate that that at the amino acid level probe #734 is most similar to a putative protein from rice

(86 % identity) and to a RING finger-like protein from *Arabidopsis* (55 % identity). However, weaker similarity is also seen to a number of putative DNA repair proteins, such as; a DNA repair protein-like sequence from *Arabidopsis* (33 % identity), an *Arabidopsis* protein with similarity to nucleotide excision repair proteins (37 % identity), a SNF2 family DNA repair protein from yeast (36 % identity) and the DNA repair protein rad8 from yeast (34 % identity). In all of the above cases, the similarity of the microarray probe #734 is close to the C-terminal end of these peptide sequences. All of the above protein sequences contain a putative conserved SNF2 family N-terminal domain, a structural motif found in a variety of proteins known to function in processes that include DNA repair and recombination, chromatin unwinding and transcriptional regulation.

For several reasons, these findings are of particular significance to studies of meiosis in wheat. Firstly, the expression profile of microarray probe #734 indicates strong temporal regulation throughout meiosis, that increases sharply following pre-meiosis and peaks during the diplotene to late anaphase I meiotic stages. Given the similarity observed in blastx searches, this could be suggestive of a function for the gene corresponding to probe #734 in molecular events such as recombination and repair during the stages of meiosis I. Secondly, comparative genetic studies investigating the genic content of the region deleted in *ph2a* on chromosome 3DS (Chapter 3) identified the wheat EST G05_q343_plate_11 (#10 in **Table 3.2**, Chapter 3). This EST was shown to be located in the region deleted in the *ph2a* mutant by Southern analysis, and was identified as a candidate for the *Ph2* gene. This assessment was based on observed similarity in the predicted polypeptide sequence of G05_q343_plate_11 to several proteins containing a putative conserved SNF2 family N-terminal domain. These include a putative DNA repair and recombination protein from rice (75 % identity at the amino acid level), a putative SNF2/RAD54 family DNA repair and recombination protein from *Arabidopsis* (44 % identity), and a human homologue of the yeast protein Rad26 (27 % identity). Similar to the microarray probe waw1c.pk003.h17 (#734), the similarity of the EST G05_q343_plate_11 to these proteins is near the C-terminal end of these peptide sequences.

The ESTs G05_q343_plate_11 and waw1c.pk003.h17 (#734) do not overlap in sequence, and show different hits in searches of protein databases. However, a common feature of the respective database hits for each sequence is similarity to proteins containing an SNF2 family N-terminal domain. Furthermore, the EST waw1c.pk003.h17 (#734) does not show any similarity to the rice chromosome 1 genomic sequence that identified the EST G05_q343_plate_11 in Chapter 3. Based on an analysis restricted to the sequenced portions of the ESTs described above, it is difficult to hypothesise about the genic origin of these sequences. It is not known whether these two ESTs are derived from the same gene in the wheat genome, or from different genes that may be functionally related. Database searches of the *Triticum aestivum* EST database however provide some clues. Both sequences have significant matches to very few wheat ESTs in the public databases, indicating that both genes are lowly expressed. The EST G05_q343_plate_11, derived from a wheat pre-fertilisation ovule library identifies another EST from this library, in addition to two ESTs from a seven day-old seedling cDNA library. The EST waw1c.pk003.h17, derived from the wheat meiotic anther cDNA library (WAW) identifies another sequence from this library, in addition to two ESTs from a spikelet at late flowering cDNA library, and one EST from a seedling cDNA library. Collectively the above information suggests that these two ESTs may be derived from different genes of similar function, but this cannot be definitively shown without further sequencing and associated molecular analysis. Furthermore, nothing at present is known about the prevalence or function of proteins containing SNF2-like structural motifs in wheat. Research to characterise the function of the genes corresponding to the wheat ESTs G05_q343_plate_11 and waw1c.pk003.h17 should be of high priority for investigation of meiosis in wheat, especially in relation to the phenotype resulting from the deletion of the *Ph2* locus. This may be a productive research area for studies of *Ph2*.

5.3.5.2.5 Late expressed genes

5.3.5.2.5.1 Cluster group VI

Cluster group VI (**Figure 5.21**) identifies eight microarray probes whose expression profiles are characterised by an approximate 2.5-fold up-regulation at the tetrad stage of meiosis compared to expression during earlier meiotic stages. Perhaps with the

Figure 5.21: Temporal expression profiles of genes from cluster group VI.

PM, pre-meiosis; LP, leptotene to pachytene; DA, diplotene to late anaphase I; TT, telophase I to telophase II; T, tetrads.

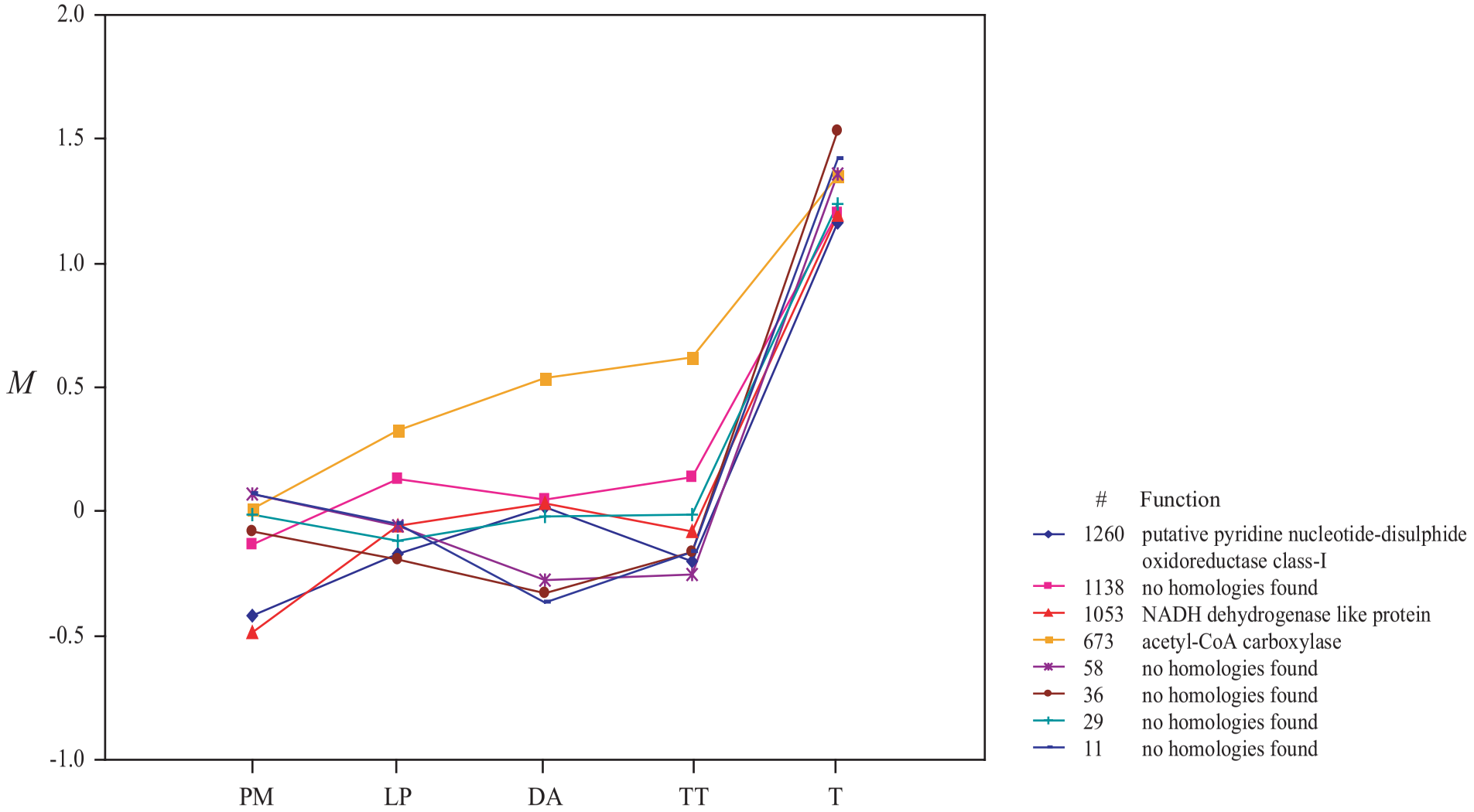
2.0
1.5
1.0
0.5
0
-0.5
-1.0
M
PM
LP
DA
TT
T
Function
1260 putative pyridine nucleotide-disulphide oxidoreductase class-I
1138 no homologies found
1053 NADH dehydrogenase like protein
673 acetyl-CoA carboxylase
58 no homologies found
36 no homologies found
29 no homologies found
11 no homologies found

exception of microarray probe #673, the expression patterns of genes in cluster group VI suggests a more or less equal level of transcription from pre-meiosis to the end of telophase II as that in anthers containing pollen mother cells at the immature pollen stage of meiosis (i.e. $M = \sim 0$). This pattern of transcriptional regulation suggests a function for these genes during the formation of the tetrad structure or during the early stages of uninucleate immature pollen development immediately following meiosis II.

Of the eight microarray probes in cluster group VI, three show significant similarity to genes encoding metabolic enzymes, and five have no significant database hits. It is interesting that four of the sequences with no significant homologies are derived from the BAC subgroup of probes selected for microarray printing (#58, #36, #29, and #11). These BAC sequences were derived from subclones prepared for the shotgun cloning approach used to sequence a 220 Kb BAC contig derived from the region corresponding to the *ph2a* deletion in the D-genome progenitor of hexaploid wheat, *Triticum tauschii* (Whitford, 2002). An analysis of the sequence of the 220 Kb BAC sequence assembled (Whitford, *pers*. *commun*.) reveals that these four microarray probes correspond to independent regions annotated as *Angela*-type copia-like retrotransposable elements (Wicker *et al.*, 2001). BLAST searches of TREP, the Triticeae Repeat Sequence Database (Wicker *et al.*, 2002) also indicate such a function for these four BAC microarray probes. Evidence from the sequence and detailed characterisation of a 211 Kb genomic sequence of *Triticum monococcum* genomic DNA indicates that *Angela* retrotransposable elements contributed to more than 24 % of this sequence (Wicker *et al.*, 2001). The observed consistency in expression profiles for each of these four independent *Angela* retrotransposable elements indicates a significant increase in the transcriptional activity of these repetitive sequences in the wheat genome during the later stages of meiosis II. The functional significance of such a pattern of expression for these ubiquitous repetitive DNA elements may become clearer as efforts to understand the basis of genome organisation and evolution in members of the Triticeae continue.

5.3.5.2.5.2 Cluster group I

The four microarray probes identified in cluster group I (**Figure 5.22**) are characterised by three distinct expression profiles during meiosis. The defining feature of the profiles are *M*-values less than 0 for each meiotic stage up to the tetrads stage of meiosis, where

Figure 5.22: Temporal expression profiles of genes from cluster group I.

PM, pre-meiosis; LP, leptotene to pachytene; DA, diplotene to late anaphase I; TT, telophase I to telophase II; T, tetrads.

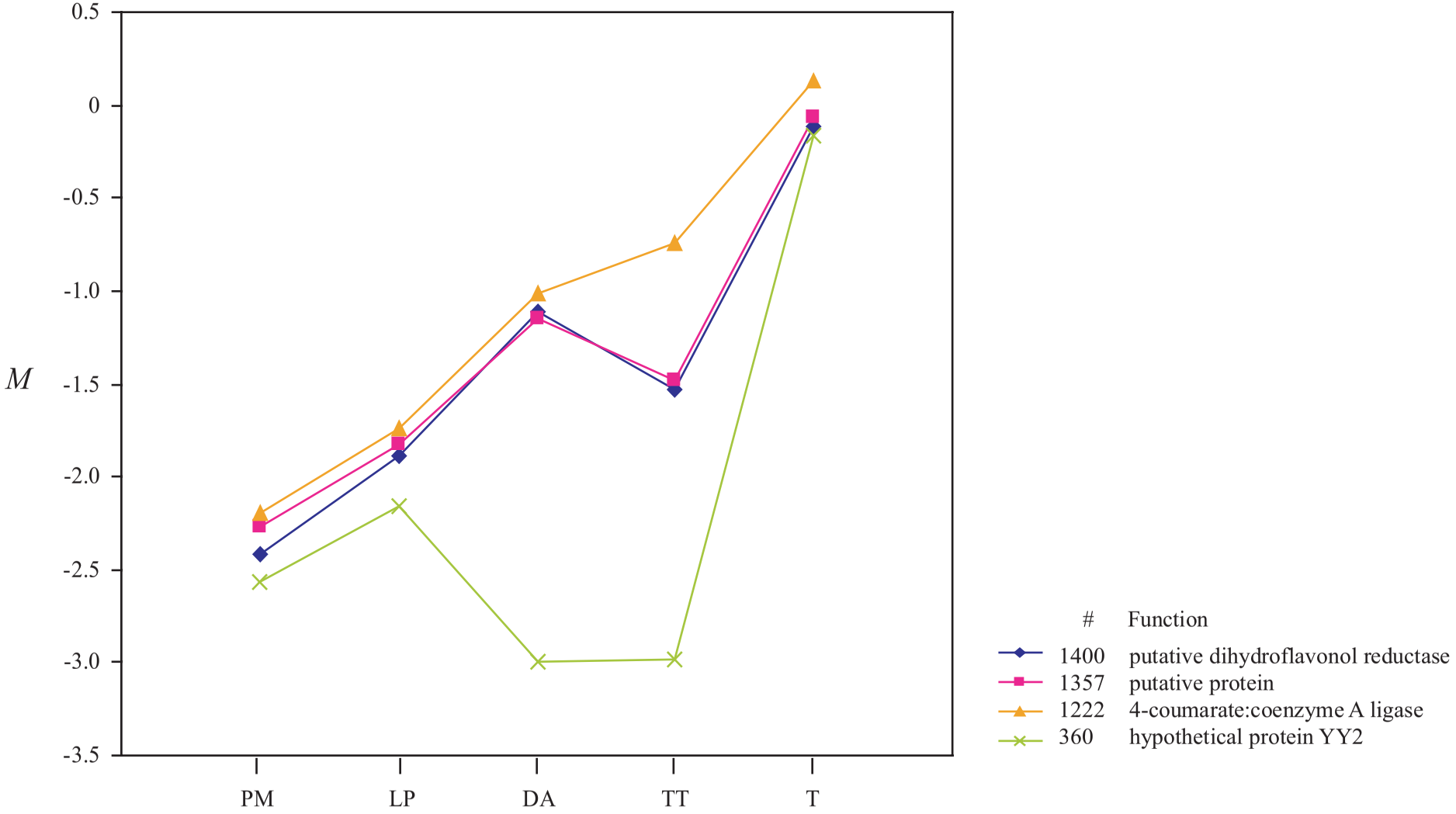
0.5
0
-0.5
-1.0
-1.5
-2.0
-2.5
-3.0
-3.5
M
PM
LP
DA
TT
T
Function
1400 putative dihydroflavonol reductase
1357 putative protein
1222 4-coumarate:coenzyme A ligase
360 hypothetical protein YY2

expression equals that of the immature pollen reference tissue. This expression profile is suggestive of an important role in early pollen development. In this context microarray probe #360 is particularly interesting considering its similarity over the sequenced region to the rice hypothetical protein YY2 and distinct expression profile. The rice YY2 protein shows similarity to chalcone synthase (Hihara *et al.*, 1996) and is one of several anther specific proteins that have been isolated from rice. The promoter elements of these tissue specific proteins have been of particular interest in the generation of male-sterility. YY2 is encoded by a single gene in the rice genome and is expressed specifically in tapetal cells of anthers at the uninucleate microspore stage (Hihara *et al.*, 1996). The expression of YY2 is reduced in mature anthers (Hihara *et al.*, 1996). Several other rice proteins have been identified with similar tissue specific characteristics to YY2. The protein YY1 (Hihara *et al.*, 1996) and proteins Osc4 and Osc6 (Tsuchiya *et al.*, 1994) have been isolated from rice anthers. The mRNAs encoding these proteins are prevalent soon after meiosis and their levels become reduced in mature anthers. The function of these proteins is unknown due to the absence of similarity to characterised molecules.

Several observations suggest that microarray probe #360 is derived from the wheat gene homologous to anther specific *YY2* in rice. The expression profile of probe #360 is indicative of a gene expressed specifically during early anther development, soon after the completion of meiosis II. The tissue specificity of this wheat gene is also supported through database searches of the *Triticum aestivum* EST database. Of six significant database hits to the sequence of probe #360, three are derived from the wheat meiotic anther cDNA library (WAW), and three from pre-anthesis spike cDNA libraries. Furthermore, like YY2, the sequenced region of probe #360 displays similarity to chalcone synthase. The isolation and characterisation of the promoter sequence of this gene may be useful for transgenically directing expression specifically to tapetal tissues during early pollen development in the wheat anther.

5.4 General discussion and conclusions

5.4.1 *Ph* mutant vs. wild-type microarray experiments

The identification of genes derived from regions deleted in *Ph* mutants has been the focus of much research. In this study the applicability of microarrays to identify differentially expressed genes between wild-type anthers and anthers of the *Ph* genotypes *ph1b*, *ph2a* and *ph2b* was investigated. These experiments failed to reveal significant down-regulation of genes in *Ph* mutant anthers compared to wild-type. This result is important for the *Ph2* experiments. For *ph1b* it could logically be argued that this result may be due to the absence on the microarray of sequences derived from the region deleted in this mutant. Since the genic content of this region is not publicly known at present, no priority for sequences deleted in this mutant could be made. For *ph2b*, a point mutant at the *Ph2* locus, it could be argued that differential expression would only be observed if point mutations altered significantly the transcriptional activity of genes or affected the ability of mutant mRNA to hybridise to the wild-type probe, and if these genes were indeed present on the microarray. It is more likely that the effect of point mutations in *ph2b* is to alter protein function. In this case, mRNA expressed from mutated genes is expected to be expressed at similar levels in mutant and wild-type plants. The experiments comparing expression in *ph2a* relative to wild-type however provide more conclusive evidence as to the effectiveness of this approach in wheat. A subset of microarray probes was selected for printing that were identified as showing significant similarity to the rice chromosome 1 region syntenous to that deleted in the *ph2a* mutant. Comparative genetic studies described in Chapter 3 have shown that approximately 78 % of the wheat ESTs identified using this approach are located in the region deleted in *ph2a*. Thus, it is expected that a significant number of the 128 ITEC ESTs selected for microarray analysis are derived from genes within the chromosomal region deleted in *ph2a*. None of these sequences have *M*-values that indicate down-regulation in mutant anthers compared to wild-type. Indeed, no ITEC microarray probes are present in the list of the top twenty down-regulated genes in *ph2a*. This result indicates the limitations of microarrays for studies of this type in wheat.

A major factor contributing to this result is likely to be the polyploid nature of the wheat genome. Most genes in the wheat genome are represented at least six times; in the

simplest case each copy is represented by the three homoeologous genomes A, B and D. Although this is not exclusively the case for all genes, it is known to be the situation for many investigated wheat genes. Deletions such as *ph1b* and *ph2a* will therefore, for many genes, not result in the complete absence of transcribed mRNA. Thus in microarray experiments, mRNAs derived from genes in homoeologous genomes may be present and participate in hybridisation. The reduced levels of these particular mRNAs may also be compensated to some degree by increased transcription of genes from the homoeologous genomes. These factors may result in slight changes in overall mRNA levels for a particular gene deleted in *ph1b* or *ph2a*, and these differences are likely to be outside the range of detection of cDNA microarray technology. In light of the above complexity for studies of this type in wheat, a number of possibilities could be considered. One of these may be to investigate the effects of increasing the stringency of hybridisation and washing conditions. The aim of such an approach would be to reduce cross hybridisation to microarray spots from homoeologous genes. Such sequence-based hybridisation discrimination between genes of homoeologous genomes may aid in the visualisation of slight differential expression in mutant genotypes compared to wild-type. However, such experiments are technically demanding and subject to large error rates.

In an attempt to investigate further the significance of the results from *Ph* mutant differential expression experiments, the top twenty up- and down-regulated genes for each *Ph* mutant were investigated. Several microarray probes were found to be common to the up- and down-regulated gene lists of mutant genotypes. Furthermore, a similar correlation was seen for different microarray probes of identical function. Although these correlations are potentially very interesting in relation to *Ph* loci, the overlap in gene function does not necessarily agree with the cytological and phenotypic data accumulated from studies of *Ph* gene function. It is therefore proposed that these observations are related to factors other than differential expression brought about by mutated regions in these genomes. A major factor contributing to these observations may relate to temporal differences in meiotic development between the independent collections of anthers from each *Ph* mutant genotype and wild-type Chinese Spring. Anther collections for each genotype were derived from a whole spike whose largest central floret was determined to be at metaphase I. This method of collection makes the assumption that the spread of meiotic stages in anthers up and down the remaining spike

will be consistent between different genotypes. If, for example, the spread of meiotic stages in anthers isolated from wild-type Chinese Spring were significantly different to those of *Ph* mutants, then by virtue of this inconsistency, genes that show strong temporal regulation during meiosis may appear to be differentially expressed in *Ph* mutant vs. wild-type microarray experiments. This explanation for the observed correlations in the top twenty up- and down-regulated genes for each *Ph* mutant genotype is supported to some degree in the results obtained. Consider the list of twenty down-regulated genes in *ph2a*. In the analysis of temporal expression during meiosis, four of the microarray probes in this list were classified during hierarchical clustering into cluster group I (**Figure 5.22**). Three of these probes have similarity to 4-coumarate:coenzyme A ligase, and one has similarity to the hypothetical protein YY2 from rice. Each of these genes displays significant temporal regulation during meiosis, and supports the proposal that differences in the temporal distribution of anthers from each *Ph* mutant and wild-type may be a factor contributing to the observed correlations between gene lists of each mutant genotype. With this in mind however, it should be noted that the microarray experiments performed in this study are very much still a work in progress, and part of continuing analysis will involve further investigation of these results and their significance in relation to deletions at each *Ph* locus, particularly in *ph2a*.

5.4.2 Temporal microarray experiments

In contrast to the effectiveness of experiments investigating differential expression in *Ph* mutant anthers, microarray experiments to investigate temporal gene expression during meiosis produced valuable results, and have provided a strong basis for further gene characterisation. The analysis of microarray expression profiles in combination with extensive database searching provided a means to identify a number of candidate wheat genes putatively involved in meiotic and anther developmental processes. Several of these show significant similarity to characterised proteins from other organisms, and in many cases it is evident from published studies that, at the level of transcription, putative wheat orthologues show similar patterns of regulation over the meiotic anther time course examined. These findings are particularly important as they indicate the relative

success of these experiments in predicting an expression trend throughout meiosis for all of the genes investigated.

A number of wheat genes with distinct expression profiles were also identified in this study that show no significant similarity at either the DNA or protein level to characterised sequences from other species. Further sequencing of the cDNA clones corresponding to these genes should be a priority in an attempt to assign putative function. Given the differences in codon usage and gene sequence divergence between the Triticeae and organisms such as fungi and mammals, from which the majority of characterised meiosis genes have been isolated, obtaining the predicted primary polypeptide sequence derived from these wheat genes would be important. The presence of conserved functional domains in these sequences may provide clues about meiotic function in relation to characterised genes from diverged species. A relationship between database homology and landmark developmental events in meiosis may then be evident and an assessment made concerning the importance of these genes for continued research. Genes of unknown function after this process remain interesting. These sequences may represent genes required for meiosis or early anther development in wheat that are either present and uncharacterised in other organisms, or are unique to wheat and other members of the Triticeae. This could be determined through searches of non-redundant EST databases and databases of complete genome sequences such as that from *Arabidopsis*. Genes in this category that are preferentially expressed during pre-meiotic interphase or prophase I could be further considered in relation to their roles in important early meiotic events such as homologous chromosome pairing, under the control of genes at *Ph* loci.

5.4.3 Experimental design

A number of factors can be considered with respect to the design of the microarray experiments presented in this Chapter. Since the inception of microarrays as tools to investigate gene expression in developing tissues, significant progress has been made in both the application of downstream analytical tools and the concepts behind experimental design to best address specific biological questions.

Protocols based on T7 RNA amplification are becoming generally accepted by many researchers as tools to broaden the application of microarray research to small, often difficult to obtain tissue samples and biopsy specimens. This study utilised a modified T7 RNA amplification protocol to investigate gene expression in wheat anthers, and the results generated have confirmed their potential for application to studies of gene regulation in genetically complex plant species such as wheat. Furthermore, over the last two to three years microarray researchers have been witness to a growing contribution from statisticians in all aspects of microarray analysis. These collaborations have been fundamental to the development of scientifically sound approaches to microarray experimentation and data analysis. Many early models of global normalisation, for example, were based largely on relatively simple assumptions, the major one being that dye bias is constant on the log-scale across the entire range of the data. Normalisation methods based on housekeeping or reference genes also have limitations. Housekeeping genes often show sample specific bias, and by nature tend to be relatively highly expressed such that commonly observed intensity dependant dye bias does not become apparent for lowly expressed genes. With good reason, many of these approaches are being developed into more sophisticated statistical correction methods that address the underlying variance of microarray data. These advances have been of great benefit to the microarray community, and to researchers exploiting the wealth of data emerging from microarray laboratories around the world. The normalisation sections of this Chapter describe the implementation of current statistical models to address and correct for sources of variation and bias observed in the data extracted from microarray experiments.

In relation to the design of test and reference target populations used in these experiments, a number of considerations can be made for future experimental design. A number of limitations were placed on the interpretation of results from temporal expression microarray experiments. This was largely due to the use of the immature pollen reference sample. A consequence of this experimental design was that the expression of each microarray probe at each meiotic stage had to be interpreted in terms of its expression in anthers containing pollen mother cells at the immature pollen stage of development. This initially seemed logical, considering both the non-meiotic nature of this tissue, and its similarity to the five meiotic stage targets in terms of common anther

cell types. In hindsight however, and in the context of recent descriptions of appropriate experimental design in the literature (Smyth *et al.*, 2002), a number of possibilities for superior experimental setup could be considered. The removal of the immature pollen tissue type would be appropriate, since the levels of gene expression in this tissue were not of primary interest to the aims of these experiments. With the five meiotic stage targets of interest, several experimental designs could be considered to address gene expression during meiosis in these time course experiments. Firstly, a reference sample could be prepared from combining equal quantities of each meiotic stage target. Each stage could thus be compared to this common reference source. Secondly, a saturated design could be implemented such that each meiotic stage target would be compared to all other stages in the experiment series. Thirdly, the time course experiment could be set up in such a way to compare each stage to the following stage in the temporal series. For example, time 0 compared to time 1, time 1 compared to time 2, time 2 compared to time 3 and so on. Time 0 would also then be compared to the final time point in the temporal series. All of the above possible experimental designs should include the dye swap experiments. Either of these approaches would ensure that maximum relevance to primary biological questions was derived from microarray expression data, and would aid in the interpretation of results from such experiments.

The experimental design of *Ph* mutant vs. wild-type differential expression microarray experiments was satisfactory. Wild-type tissues make appropriate reference targets for comparative hybridisation.

As a result of the microarray experiments described in this Chapter, a number of wheat genes of interest to meiotic and anther developmental processes have been identified and can be considered for further investigation. From 1830 microarray probes, 128 were selected for hierarchical clustering based on a two-fold change level of expression. Cluster groups I-VI represent the major expression clusters and comprise a non-redundant collection of more than 50 genes of potential interest to future research. Many are unknown in function and the cDNA clones derived from these genes should be sequenced further. In addition, approximately 40 other genes that have not been discussed in detail here could be considered for future research. These genes represent those microarray probes selected for hierarchical clustering that are not part of the major

expression clusters I-VI. Collectively the result of this work provides a strong basis for further gene characterisation and study of meiosis in wheat.

CHAPTER 6

GENERAL DISCUSSION

Broadening our current knowledge of the molecular basis of meiosis in agriculturally important plant species such as wheat would not only enable further understanding of this fundamentally important biological process, but could present opportunities for wheat breeding programs to more effectively exploit the genetic diversity of distantly related species for cultivar improvement. Wheat *Ph* genes have been studied in this regard for many years. A great deal is known about the cytogenetic effect of *Ph1* and *Ph2* on chromosome pairing behavior during early meiotic prophase I but to date the molecular basis for their control remains unknown. This is not only the case for *Ph* genes. From a cytogenetic perspective meiotic division in wheat has been well studied. Wheat chromosomes are large, easily visible and the sampling of anthers, although laborious, provides sufficient and predictable meiotic material for microscopy. However, factors such as the large genome size of wheat and the added complexity of polyploidy have been challenges for wheat researchers investigating the molecular basis of meiosis. At the molecular level, much is yet to be discovered. Very few meiotic genes from wheat have been characterised.

When this research began, attempts to identify candidate *Ph2* genes from the region deleted in the *ph2a* mutant had been the focus of extensive research in our laboratory. The approach used was based on differential or subtractive hybridisation strategies to identify genes with a degree of meiotic specific expression, or using PCR strategies based on the sequence of characterised meiotic genes from other species. Genes identified by this approach were chromosomally mapped and in several cases found to be located in the region deleted in *ph2a*. These genes are *WM5* (Thomas, 1997), *WM3* (Letarte, 1996), *TaMSH7* (Dong *et al.*, 2002) and eleven members of the *WM1* gene family (Ji, 1992; Whitford, 2002). Structurally, we knew little about the deleted segment in *ph2a*, both in the context of breakpoint position and deletion size. Although several

genes had been located to the deleted segment of *ph2a* and studied in detail as candidates for *Ph2*, we had no means to estimate the likely number of genes located in the *ph2a* deleted segment on 3DS. Functional analysis of *WM5*, *WM3*, *TaMSH7* and *WM1* family members also suggested the presence of a cluster of meiotically expressed genes in the *Ph2* region. This idea was based on a degree of meiotic specific expression observed for these genes, and the physical clustering of approximately seven members of the *WM1* gene family in a region of approximately 220 Kb within the region deleted in *ph2a* (Whitford, 2002). At the time, the approaches available to identify meiotic genes, in particular as candidates for *Ph2*, were limited. Furthermore, the tools and resources needed to address questions of tissue specific gene clustering in the region of *Ph2* were not available. Microarrays had not been extensively applied in plant biology to address questions of gene expression in specific tissue types and cell samples, especially from polyploid species such as wheat. Synteny of gene order and content between members of the grass family was apparent from comparative mapping studies, but the comprehensive application of these findings to facilitate gene discovery in species like wheat awaited the complete sequence of chromosomes from a model species such as rice, where synteny was evident and likely to be of use.

During the course of this research, new approaches to investigate meiosis and the structure of the *Ph2* region became possible. It is evident now that a new approach was necessary and warranted.

The first public release of a rice chromosome sequence was for chromosome 1 (Sasaki *et al.*, 2002). This represented a significant milestone for cereal genome research. Being syntenous to wheat group 3 chromosomes it enabled a comprehensive comparative genetics approach to study the structure and genic content of the region deleted in *ph2a*. This research (Chapter 3) has contributed much to our knowledge of this region. We are now able to estimate the size of the deleted segment in *ph2a* to be approximately 80 Mb in length. This is larger than we had previously thought. Furthermore, it appears that the deletion is terminal on 3DS, which supports initial hypotheses by Sears (1982). As a result of this work we can extend the number of genes identified from the region deleted in *ph2a* from 14 to greater than 200, of which two are considered worthy to examine in detail as *Ph2* candidates. High levels of synteny are evident in the analysed wheat and

rice genomic regions, as shown by extensive Southern mapping, and this work has demonstrated a systematic and effective method to exploit grass genome synteny for sequence-based gene identification in wheat.

The recent expansion in wheat EST databases, and the developmet of software to query sequences from diverse cDNA libraries enabled us to address the question of whether there is a meiotic gene cluster in the region of *Ph2*. It is apparent from this analysis (Chapter 4) that the transcriptional characteristics of genes linked to *Ph2* resemble those of other large chromosomal regions in the wheat genome, and show no apparent prevalence for expression in meiotic tissues. This is an important finding, illustrating that approaches used prior to this research to identify *Ph2* based on expression specificity in meiotic tissues are likely to be insufficient. Furthermore, Chapter 4 highlighted the diversity of gene expression in wheat meiotic anthers, showing that as many as 20 % of all expressed wheat genes may be present in this tissue and developmental stage. This percentage was higher than expected, and again highlights the complexity associated with approaches to identify the *Ph2* gene(s) based on expression in meiotic anther tissue alone, and the need for a new approach. To complement the findings of comparative genetic studies in relation to *Ph2* and to conduct a broader investigation of gene expression during meiosis in the wheat anther, a microarray approach was used (Chapter 5). Importantly, these experiments illustrate the potential of microarrays to investigate gene regulation in large, polyploid genome species such as wheat. Microarrays should serve future attempts to explore the expressed portions of the wheat genome, the function of which is largely unknown at present.

Collectively, the result of this research provides a strong base from which a new series of opportunities can be considered, as discussed below.

The continued investigation of the genic content of the region deleted in the *ph2a* mutant should now focus on further sequencing of cDNA clones corresponding to genes identified in this region. The function of approximately 45 % of the wheat ESTs putatively identified from the region distal to the breakpoint in *ph2a* is unknown (**Table 3.3**), with no informative BLAST search results. The majority of the sequences from these cDNAs are derived from the 5' end of the corresponding clones and therefore, in

the first instance, the 3' end of these clones should be sequenced which may provide information on possible function. Genes of interest should be chromosomally mapped with respect to the deleted region of *ph2a* by Southern analysis.

We should also consider further the two *Ph2* candidate genes identified and discussed in Chapter 3. The ESTs G05_q343_plate_11 (#10 in **Table 3.2**) and WHE2301-2304_H06_H06 (#189 in **Table 3.2**) show sequence similarity to proteins implicated in processes that could affect the dynamics of chromosome pairing during early meiosis. These ESTs should be sequenced further using cDNA clones to derive the full mRNA sequence. Northern analysis would clarify the level of expression in the *ph2a* mutant, and in different tissues of the wheat plant, including meiotically staged anthers. If either of these genes are expressed in wheat anthers during pre-meiotic interphase or prophase I, further experiments such as protein immunolocalisation of the gene products in wheat floral tissues may reveal more about their function in relation to meiotic chromosome behaviour.

These experiments would contribute more to our understanding of the genic content and structural characteristics of genes linked to *Ph2* on chromosome 3D. We should however consider other experiments to complement these findings, which will ultimately aid in the cloning of the *Ph2* gene(s). These experiments would be to generate more deletion and point mutants at *Ph2*. It is anticipated that mutagenesis will be an important step to enable the cloning of the *Ph2* gene(s), for reasons discussed below.

Since the molecular function of the *Ph2* gene(s) is not known, it will be difficult to identify *Ph2* from the collection of candidates that further sequencing and Southern analysis will present. The function of *Ph1* for example remains unknown although the locus containing *Ph1* has recently been delimited to a region containing fewer than seven genes (Gill *et al.*, 1993; Roberts *et al.*, 1999). It is also unknown whether the phenotype controlled by *Ph1* is the result of more than one gene in this region (Moore, 2002). For *Ph2* candidates, a comparison of gene nucleotide sequences from wild-type Chinese Spring and *ph2b* genotypes could be performed to search for insertions or deletions that may reflect the altered meiotic phenotype of *ph2b*. The genomic sequence of each candidate *Ph2* gene from *ph2b* and wild-type Chinese Spring would be required. This

approach is however tedious for large numbers of candidates. Attempts at functional complementation through transformation of *ph2a* and *ph2b* genotypes with *Ph2* candidates could also be considered. However, at present this approach remains technically difficult for wheat and not practical for a large number of candidate genes. Chinese Spring, the parental line of the *ph2a* and *ph2b* mutants, has not yet been transformed.

Furthermore, we should not consider the list of wheat ESTs identified with similarity to the rice chromosome 1 region to represent the entire genic content of the region deleted in *ph2a*. It is possible that the *Ph2* gene(s) may be absent from the collection of genes identified (**Table 3.2**). The sequence-based approach to identify these genes was based on, and in some respects limited by, the genomic sequence of the rice chromosome region syntenous to the region deleted in *ph2a*. This raises the important question of whether a *Ph*-like sequence is present in this rice genomic region, or indeed anywhere in the rice genome. What could the function of *Ph*-related genes in a diploid species be? Did the *Ph* genes of hexaploid wheat evolve from ancestral sequences as a result of polyploidisation events in emerging species, and if so how similar are these genes today? Perhaps *Ph*-like genes exist in diploid species and function during meiosis, but in allopolyploids like hexaploid wheat, these genes evolved to perform additional functions related to the resolution of incorrect homoeologous associations during or preceding meiosis I. Some evidence does suggest the presence of *Ph1* alleles in other species. For example, chromosome 5G from the tetraploid wheat *Triticum timopheevi* can partially compensate for the absence of *Ph1* (Ozkan and Feldman, 2001). Furthermore, diploid rye chromosome 5R (homoeologous to 5B), when present in three copies in hexaploid wheat hybrids can compensate, albeit incompletely for the absence of *Ph1* (Bielig and Driscoll, 1970; Mikhailova *et al.*, 1998; Miller and Riley, 1972). Fewer than three copies of 5R has no observable effect on pairing. This evidence suggests the presence of *Ph1* alleles in related species and apparent variation in their effectiveness to compensate for the absence of *Ph1* in hexaploid wheat. Nothing however is known about the presence of *Ph*-like sequences in distantly related species like rice.

The *Ph2* gene(s) may also be absent from the list of genes identified from the region deleted in *ph2a* for other reasons. The mRNA(s) of *Ph2* may be expressed at very low

levels in wheat tissues. They may not be represented by ESTs in wheat databases and in this circumstance could not have been identified by the approach used here. If *Ph*-related sequences do exist in the rice genome, and we assume that ESTs derived from *Ph2* are present in wheat databases, then the approach used in this study may not have identified a wheat EST due to low sequence similarity. Recall that an E-value cutoff was applied to the results of wheat EST database BLAST searches using rice genomic sequence (Section 3.2.5). The comparative genetics approach used here also assumed that if sequences related to *Ph2* are present in the rice genome, that they are chromosomally located in a position syntenous to that in wheat.

In consideration of the possible limitations discussed above for comparative genetics approaches using *ph2a* to identify the *Ph2* gene(s), it becomes apparent that the availability of more deletion mutants at this locus would be an important and perhaps essential resource to productively continue this research and expedite the cloning of this gene. The characterisation of the genic content of the region deleted in the *ph2a* mutant provides a strong basis from which to characterise new deletion mutants at the *Ph2* locus. In effect, this work has identified many molecular markers in the region containing *Ph2* on chromosome 3D, at a density much higher than could be derived from current recombination maps of this wheat chromosome. From this information the opportunity to develop a broad coverage of 3DS-specific PCR assays to screen for, and characterise physically, any induced deletions along this chromosomal region is available. Once the extent of new physical deletions is characterised, cytogenetic analyses of chromosome pairing behavior could identify those plants likely to be deficient for the region containing *Ph2*. A similar approach was used to characterise fast-neutron induced deletion mutants at the *Ph1* locus (Gill *et al.*, 1993; Roberts *et al.*, 1999) to facilitate identification of the positional location and characterisation of *Ph1* on 5BL. The aim of mutagenesis would be to more accurately define the region containing the *Ph2* locus so that molecular approaches to identify *Ph2*, such as sequencing candidates from *ph2b* and complementation through transformation, can more feasibly be considered. Mutagenesis and the necessary subsequent analysis would be a complex and long term project, but one that should be considered.

The prospects for further research to characterise genes of potentially interesting function from temporal microarray experiments will depend largely on the function of the individual genes being investigated. Initially this should involve further sequencing and confirmation by Northern analysis of the pattern of transcriptional regulation predicted by microarray experiments. The expression of genes of interest could also be examined in other wheat tissues to provide further insight into putative function. Downstream experiments will be directed by the aims of the specific research being conducted.

Aside from investigating the applicability of microarrays to identify differential expression between the *Ph* mutant and wild-type wheat anthers, a major focus of the microarray approach used in this research was to identify genes that display interesting temporal regulation throughout meiosis. A number of genes, the majority of which are uncharacterised in wheat, have been identified in this regard and present new opportunities for continued research to advance our knowledge of meiosis in the reproductive tissues of important grass species such as wheat. The hierarchical cluster groups I-VI identified and discussed in Chapter 5 represent a dissection of the significant microarray expression profiles based on similarity in transcriptional regulation. This information should provide a sound starting point to focus on genes that may function at specific stages of the meiotic cell cycle or during early anther development.

In recent years, the plant research community has witnessed a fundamental shift in the approach to analyse large and complex genomes. Genomics is changing the magnitude and depth of biological questions that we can now hope to address effectively. This has largely been due to the development of high throughput technologies, advances in genome sequencing of model plant species such as rice and *Arabidopsis*, and the adoption by plant genomics researchers of many conceptual and technical advances fostered by initiatives such as the Human Genome Project.

Genomics is accelerating the acquisition of knowledge relating to many areas of plant research. It is expected that this trend will continue. Biologists are poised to better investigate the functional and structural characteristics of plant genomes and broaden our knowledge of complex cellular processes that have been traditionally difficult to understand. It is imperative to converge these developments with agriculturally relevant

breeding information and objectives. It is anticipated that such collaborations will aid crop improvement and assist plant breeders as they confront the agricultural challenges of the future.

APPENDIX 1

Table legend: Gene expression data obtained from temporal and *Ph* mutant microarray experiments. Each microarray probe is given a number (#) from 1-1830 and clone origin is indicated by an identification code (ID) (**Table 5.1**). The clone name is given (EST name) and is identical to that in GenBank, except for BAC and CON clones which are not ESTs. Expression data (*M*-values) for temporal expression microarray experiments, and *Ph* mutant differential expression experiments are given where: PM is pre-meiosis; LP is leptotene to pachytene; DA is diplotene to late anaphase I; TT is telophase I to telophase II; T is tetrads; *1b* is *ph1b*; *2a* is *ph2a*; *2b* is *ph2b*. The top blastx hit to each microarray probe from the GenBank non-redundant database is given and the degree of similarity (E-val). For *Ph* mutant experiments, the top twenty down-regulated genes for each mutant genotype compared to wild-type Chinese Spring are highlighted in red, and those up-regulated compared to wild-type in green (see Section 5.3.4 for details).

[Species Abbreviations]: *Alcelaphine herpesvirus 1 Ah; Arabidopsis thaliana At; Brassica napus Bn; Caenorhabditis briggsae Cb; Caenorhabditis elegans Ce; Capsicum annuum Ca; Cucumis melo Cm; Cucurbita maxima Cma; Deinococcus radiodurans Dr; Dictyostelium discoideum Dd; Drosophila melanogaster Dm; Glycine max Gm; Hevea brasiliensis Hb; Homo sapiens Hs; Hordeum vulgare Hv; Leishmania major Lm; Lilium longiflorum Ll; Lolium perenne Lp; Lotus japonicus Lj; Lycopersicon esculentum Le; Magnaporthe grisea Mg; Medicago sativa Ms; Mercurialis annua Ma; Mesembryanthemum crystallinum Mc; Mus musculus Mm; Mycobacterium tuberculosis Mt; Neurospora crassa Nc; Nicotiana plumbaginifolia Npl; Nicotiana tabacum Nt; Nostoc punctiforme Np; Oryza australiensis Oau; Oryza sativa Os; Oryzias latipes Ol; Pinus sylvestris Ps; Plasmodium falciparum Pf; Prunus armeniaca Par; Pseudomonas alcaligenes Pa; Schizosaccharomyces pombe Sp; Secale cereale Sc; Solanum melongena Sm; Solanum tuberosum St; Sorghum bicolor Sb; Staphylococcus epidermidis Se; Streptomyces coelicolor Sco; Triticum aestivum Ta; Triticum monococcum Tm; Xanthomonas campestris Xc; Zea mays Zm*.

#	ID	EST name	Temporal *M*					*Ph* mutant *M*			Top BLASTx hit	e-val
			PM	LP	DA	TT	T	*1b*	*2a*	*2b*		
1	BAC	bactt61g.pk001.a16	-0.13	0.30	-0.10	0.19	0.09	0.05	-0.08	-0.02	p53 [*Hs*]	1e-126
2	BAC	bactt61g.pk002.a15	-0.21	-0.04	0.01	0.21	0.02	0.07	0.03	-0.02	OSJNBa0066B06.11 [*Os*]	0.002
3	BAC	bactt61g.pk002.c4	-0.28	-0.18	-0.38	-0.29	-0.16	0.03	0.09	-0.04	similar to KIAA1856 protein [*Hs*]	0.25
4	BAC	bactt61g.pk002.c5	0.02	-0.07	-0.15	-0.10	-0.07	-0.01	-0.08	-0.03	no homologies found	-
5	BAC	bactt61g.pk002.d1	-0.06	-0.07	0.14	-0.07	-0.03	0.01	0.00	0.19	no homologies found	-
6	BAC	bactt61g.pk002.d12	0.02	0.08	-0.05	0.03	0.02	0.03	-0.04	-0.04	no homologies found	-
7	BAC	bactt61g.pk002.d13	-0.01	-0.11	0.00	-0.03	-0.05	-0.06	0.05	-0.08	TNP2-like protein [*Sb*]	1e-29
8	BAC	bactt61g.pk002.e13	-0.10	-0.13	0.02	0.02	0.00	-0.02	0.06	-0.04	HV711N16.8 [*Hv*]	2e-8
9	BAC	bactt61g.pk002.e23	0.04	-0.11	0.07	0.05	0.05	0.03	0.05	0.00	no homologies found	-
10	BAC	bactt61g.pk002.f19	0.28	0.11	0.16	0.11	0.10	0.08	0.15	0.09	no homologies found	-
11	BAC	bactt61g.pk002.g1	0.07	-0.05	-0.37	-0.16	1.42	-0.03	0.00	0.01	no homologies found	-
12	BAC	bactt61g.pk002.h17	0.01	-0.04	0.02	0.05	-0.09	-0.03	-0.03	0.02	putative Cf2/Cf5 disease resistance protein [*Os*]	2e-34
13	BAC	bactt61g.pk002.h9	0.07	0.02	0.15	0.06	0.15	0.00	-0.02	-0.01	no homologies found	-
14	BAC	bactt61g.pk002.i13	0.26	-0.02	-0.05	0.04	0.01	-0.02	-0.02	-0.04	B1033B05.10 [*Os*]	4e-10
15	BAC	bactt61g.pk002.i16	0.01	0.01	-0.07	0.02	-0.03	0.05	-0.06	-0.06	hypothetical protein [*Sb*]	5e-28
16	BAC	bactt61g.pk002.i17	0.01	-0.08	-0.08	-0.03	-0.02	0.03	0.00	0.08	HV711N16.8 [*Hv*]	1e-12
17	BAC	bactt61g.pk002.i22	-0.01	-0.05	0.06	-0.06	0.01	0.06	0.02	0.02	hypothetical protein [*Os*]	6e-22
18	BAC	bactt61g.pk002.j15	-0.02	-0.07	0.10	-0.03	-0.05	0.01	-0.11	0.01	no homologies found	-
19	BAC	bactt61g.pk002.j21	0.05	0.00	0.00	-0.12	-0.02	0.10	0.13	-0.07	hypothetical protein [*Os*]	6e-22
20	BAC	bactt61g.pk002.k2	-0.09	-0.19	0.06	-0.08	-0.02	0.02	0.01	0.09	putative hydroxyproline-rich glycoprotein [*Os*]	2e-26
21	BAC	bactt61g.pk002.k24	0.07	-0.06	0.12	0.04	0.10	0.02	0.00	0.08	no homologies found	-
22	BAC	bactt61g.pk002.l12	0.07	0.05	0.05	-0.09	-0.12	-0.09	0.02	-0.03	no homologies found	-
23	BAC	bactt61g.pk002.l20	-0.18	0.05	-0.11	-0.07	-0.01	0.06	0.09	-0.02	AWJL175 protein - wheat	4e-23
24	BAC	bactt61g.pk002.l6	-0.02	0.07	-0.01	-0.04	-0.04	0.02	-0.02	-0.10	hypothetical protein [*Np*]	0.19
25	BAC	bactt61g.pk002.m17	0.13	-0.12	-0.11	-0.11	-0.14	0.06	0.02	-0.09	HV711N16.8 [*Hv*]	3e-9
26	BAC	bactt61g.pk002.m18	0.09	0.08	0.05	-0.02	0.10	-0.02	0.12	0.03	AWJL218 protein - wheat	7e-64
27	BAC	bactt61g.pk002.m24	-0.14	-0.04	-0.08	-0.19	-0.22	0.17	0.05	-0.03	no homologies found	-
28	BAC	bactt61g.pk002.m4	-0.02	-0.13	-0.02	-0.15	-0.04	0.06	0.00	0.02	putative reverse transcriptase [*Sb*]	5e-5
29	BAC	bactt61g.pk002.n22	-0.01	-0.12	-0.02	-0.01	1.24	0.02	0.10	-0.02	putative protein; protein id: At5g07750.1 [*At*]	0.21
30	BAC	bactt61g.pk002.n4	0.08	-0.10	0.01	-0.17	0.02	0.01	-0.01	-0.03	Athila ORF 1, putative; protein id: At1g41795.1 [*At*]	3e-19
31	BAC	bactt61g.pk002.n6	0.02	0.01	0.00	-0.09	-0.13	-0.02	-0.09	-0.06	p6.9 [Heliocoverpa armigera nucleopolyhedrovirus G4]	0.35
32	BAC	bactt61g.pk002.n9	0.22	0.09	0.03	0.14	-0.02	0.05	0.09	0.03	AWJL218 protein - wheat	6e-58
33	BAC	bactt61g.pk002.o15	-0.04	-0.09	-0.14	-0.02	-0.08	-0.01	0.06	-0.04	hypothetical protein [*Os*]	8e-17
34	BAC	bactt61g.pk002.o6	-0.04	0.14	0.07	-0.03	0.00	-0.04	-0.08	0.01	no homologies found	-
35	BAC	bactt61g.pk002.p11	-0.04	-0.13	-0.19	-0.09	-0.08	-0.01	0.12	-0.02	no homologies found	-
36	BAC	bactt61g.pk002.p19	-0.08	-0.19	-0.33	-0.16	1.53	0.03	-0.06	0.08	no homologies found	-
37	BAC	bactt61g.pk002.p4	-0.08	-0.16	-0.04	-0.06	-0.13	-0.01	-0.02	-0.03	no homologies found	-
38	BAC	bactt61g.pk002.p7	-0.05	-0.09	-0.16	-0.04	-0.14	-0.03	0.05	0.00	no homologies found	-
39	BAC	bactt61g.pk003.a11	0.12	-0.11	-0.11	-0.06	0.01	-0.05	0.07	0.08	putative dehydrogenase [*Pa*]	0.026
40	BAC	bactt61g.pk003.a17	0.02	-0.01	-0.01	-0.01	-0.03	-0.02	0.05	-0.03	HV711N16.8 [*Hv*]	4e-9
41	BAC	bactt61g.pk003.a6	0.10	-0.03	0.04	-0.02	-0.05	-0.02	0.05	0.08	no homologies found	-
42	BAC	bactt61g.pk003.a8	0.15	0.06	0.01	0.03	-0.02	-0.04	0.05	0.13	putative Cf2/Cf5 disease resistance protein [*Os*]	2e-17
43	BAC	bactt61g.pk003.c16	0.07	0.03	0.03	-0.06	0.00	0.06	-0.06	0.03	no homologies found	-
44	BAC	bactt61g.pk003.c2	0.48	-0.08	-0.03	0.00	0.06	0.05	0.07	0.20	putative reverse transcriptase [*Sb*]	4e-4
45	BAC	bactt61g.pk003.c24	-0.05	0.03	0.05	-0.03	0.03	0.02	-0.09	0.02	no homologies found	-
46	BAC	bactt61g.pk003.c3	-0.04	-0.10	-0.05	-0.02	-0.05	0.05	0.03	-0.04	TNP2-like protein [*Sb*]	2e-91
47	BAC	bactt61g.pk003.c4	-0.03	-0.08	-0.09	-0.06	-0.09	0.00	-0.07	-0.06	no homologies found	-
48	BAC	bactt61g.pk003.c5	0.07	0.00	-0.06	-0.06	-0.12	0.00	0.04	-0.02	hypothetical protein [*Sb*]	9e-19
49	BAC	bactt61g.pk003.c8	-0.02	-0.07	-0.06	-0.02	-0.16	0.12	0.06	-0.02	putative Cf2/Cf5 disease resistance protein [*Os*]	5e-34
50	BAC	bactt61g.pk003.d3	-0.02	-0.08	0.18	-0.11	-0.06	0.00	0.04	0.06	Hypothetical protein, similarity to putative retroelement [*Os*]	3e-05
51	BAC	bactt61g.pk003.e23	0.10	-0.14	-0.03	-0.13	0.01	0.06	0.00	-0.09	no homologies found	-
52	BAC	bactt61g.pk003.e6	0.12	0.06	0.04	0.09	-0.13	-0.01	-0.15	0.01	DNA gyrase B subunit [marine CFB-group bacterium]	0.49
53	BAC	bactt61g.pk003.e8	0.41	-0.06	-0.01	0.01	0.16	0.02	-0.01	0.30	no homologies found	-
54	BAC	bactt61g.pk003.f15	0.01	-0.16	-0.03	-0.09	0.63	-0.01	0.02	-0.11	dna ligase [*Sp*]	0.58
55	BAC	bactt61g.pk003.f7	0.16	-0.09	0.00	0.20	-0.08	0.01	-0.07	-0.01	no homologies found	-
56	BAC	bactt61g.pk003.g15	-0.03	-0.08	-0.13	-0.04	-0.09	0.01	0.00	-0.01	no homologies found	-
57	BAC	bactt61g.pk003.h1	-0.16	0.04	0.10	-0.13	0.12	-0.06	0.00	-0.04	Sukkula-1b polyprotein [*Hv*]	2e-50
58	BAC	bactt61g.pk003.i11	0.07	-0.06	-0.28	-0.25	1.36	-0.04	0.02	0.05	no homologies found	-
59	BAC	bactt61g.pk003.i24	-0.01	-0.10	0.01	-0.07	-0.03	0.06	0.13	-0.03	no homologies found	-
60	BAC	bactt61g.pk003.i4	-0.04	-0.04	0.00	-0.05	-0.06	-0.01	0.17	-0.01	P0665D10.7 [*Os*]	0.16
61	BAC	bactt61g.pk003.i6	-0.05	-0.13	0.03	-0.05	-0.25	-0.03	0.04	-0.18	no homologies found	-
62	BAC	bactt61g.pk003.j11	-0.07	-0.02	0.03	-0.09	-0.02	-0.05	0.03	0.09	Unknown protein [*Os*]	1e-04
63	BAC	bactt61g.pk003.j15	0.09	-0.13	-0.11	0.00	-0.16	-0.04	0.03	-0.06	AWJL175 protein - wheat	3e-69
64	BAC	bactt61g.pk003.k1	0.09	-0.12	0.07	0.12	-0.02	0.07	0.14	0.03	no homologies found	-
65	BAC	bactt61g.pk003.k10	0.11	0.05	-0.12	-0.05	-0.11	0.02	0.04	0.06	no homologies found	-
66	BAC	bactt61g.pk003.k14	0.20	0.04	0.09	0.06	-0.06	0.02	0.03	0.02	no homologies found	-
67	BAC	bactt61g.pk003.k23	0.12	-0.06	0.03	0.09	-0.08	0.02	-0.05	-0.15	pigpen [*Mm*]	0.73
68	BAC	bactt61g.pk003.l1	0.18	0.07	0.11	-0.02	0.04	0.02	-0.09	0.02	putative Cf2/Cf5 disease resistance protein [*Os*]	4e-27
69	BAC	bactt61g.pk003.l11	-0.16	-0.14	0.08	-0.18	-0.04	0.06	0.01	-0.05	no homologies found	-
70	BAC	bactt61g.pk003.m15	0.06	0.03	0.07	0.09	0.04	0.07	0.10	0.11	unknown protein; protein id: At2g35110.1 [*At*]	0.17
71	BAC	bactt61g.pk003.m20	0.05	0.22	0.08	0.21	0.20	0.01	-0.03	-0.05	no homologies found	-
72	BAC	bactt61g.pk003.m22	-0.03	-0.09	0.06	0.03	0.10	0.05	0.14	0.30	no homologies found	-
73	BAC	bactt61g.pk003.m3	0.04	0.01	-0.17	-0.03	-0.10	-0.08	0.06	-0.05	hypothetical predicted protein L1508.06, unknown function [*Lm*]	0.081
74	BAC	bactt61g.pk003.n11	-0.20	-0.07	-0.10	-0.01	0.04	-0.02	0.00	0.07	ebiP7148 [Anopheles gambiae str. PEST]	1e-04
75	BAC	bactt61g.pk003.n15	-0.01	-0.08	-0.02	-0.08	0.02	-0.08	0.08	-0.08	HV711N16.8 [*Hv*]	0.43
76	BAC	bactt61g.pk003.n23	0.00	0.00	0.07	0.01	0.05	0.08	-0.07	-0.05	polyprotein [*Oau*]	8e-87
77	BAC	bactt61g.pk003.o12	0.02	0.23	0.18	0.44	0.09	0.10	0.00	0.03	putative retroelement [*Os*]	6e-28
78	CON	*GAPDH*	-0.24	-0.16	-0.17	-0.14	-0.09	0.01	-0.02	-0.01	GAPDH	0
79	CON	*TaMSH7*	0.10	-0.22	-0.49	-0.33	-0.19	0.05	-0.05	-0.02	mismatch repair protein MSH7 [*Ta*]	0
80	CON	thioredoxin	0.04	0.04	0.00	-0.05	0.06	0.08	-0.02	-0.02	thioredoxin	0
81	CON	ubiquitin	-0.53	-0.44	-0.17	-0.30	-0.37	-0.03	-0.13	-0.04	ubiquitin	0
82	CON	*WM1.1*	-0.01	0.08	-0.02	0.15	0.10	-0.02	0.03	0.06	putative Cf2/Cf5 disease resistance protein [*Os*]	6e-94
83	CON	*WM1.7*	0.00	0.09	0.07	-0.01	-0.03	-0.11	-0.05	-0.09	putative Cf2/Cf5 disease resistance protein [*Os*]	6e-94
84	CON	*WM5*	0.31	0.06	0.22	-0.09	0.20	0.01	-0.08	-0.01	unknown protein [*Os*]	3e-32
85	DUP	wdk1c.pk0001.h8	-0.12	-0.27	-0.27	-0.17	-0.06	0.02	0.00	-0.01	expressed protein; protein id: At1g15270.1	2e-04
86	DUP	wdk1c.pk013.p10	-0.49	-0.26	-0.27	-0.16	-0.18	-0.04	0.02	0.00	OSJNBa0088K19.3 [*Os*]	6e-35
87	DUP	wdk1c.pk023.c21	0.26	-0.02	0.05	-0.10	-0.08	-0.05	-0.04	0.03	putative MLH1 [*Os*]	1e-46
88	DUP	wdk2c.pk005.e3	-0.20	-0.32	-0.08	-0.19	-0.22	-0.06	-0.01	-0.02	protein T19E23.13 [imported] - *At*	2e-38
89	DUP	wdk3c.pk006.f24	-0.26	-0.04	-0.07	-0.44	0.42	-0.10	-0.08	0.16	dnaK-type molecular chaperone HSP70 - barley	2e-69
90	DUP	wdk9n.pk001.j19	-1.31	-1.19	-0.66	-1.14	-0.87	0.09	0.09	-0.22	similar to mitogen-activated protein kinases [*Os*]	2e-62
91	DUP	wdk9n1.pk001.a3	0.00	-0.06	-0.19	-0.24	-0.24	0.04	-0.01	-0.09	putative RAD50 DNA repair protein; protein id: At2g31970.1[*At*]	8e-36
92	DUP	wds3f.pk001.e2	-0.03	-0.13	-0.26	-0.21	-0.07	-0.02	0.03	-0.01	nonhistone chromosomal protein 6B	3e-25

#	ID	EST name	Temporal *M*					*Ph* mutant *M*			Top BLASTx hit	e-val
			PM	LP	DA	TT	T	*1b*	*2a*	*2b*		
93	DUP	wkm1c.pk0003.b8	0.21	0.58	0.60	0.33	0.55	0.04	0.07	0.04	Rad51 [*Os*]	2e-15
94	DUP	wkm1c.pk005.d13	0.73	0.27	0.35	0.18	0.17	-0.02	0.05	-0.18	Guanine nucleotide –binding protein beta subunit – like protein (GPB-LR) (RWD)	2e-79
95	DUP	wkm1c.pk006.b15	-0.19	-0.15	-0.06	-0.12	-0.05	-0.05	-0.09	-0.05	non-cell-autonomous heat shock cognate protein 70 [*Cma*]	4e-88
96	DUP	wkm1c.pk006.l12	-0.08	-0.21	-0.09	-0.20	-0.07	0.03	0.00	-0.03	heat shock protein 70, cytosolic [imported] - spinach	2e-70
97	DUP	wl1n.pk0146.e4	0.06	0.13	0.09	-0.07	0.05	0.04	-0.07	0.05	DNA repair protein-like; protein id: At5g50340.1 [*At*]	1e-36
98	DUP	wle1n.pk0023.a5	-0.01	-0.38	-0.30	-0.52	-0.24	0.00	0.09	-0.01	no homologies found	-
99	DUP	wle1n.pk0055.h9	-0.05	-0.17	-0.17	-0.19	-0.06	0.03	0.09	0.10	B1144G04.20 [*Os*]	6e-13
100	DUP	wle1n.pk0091.c3	-0.71	-1.17	-1.23	-0.90	-1.27	-0.11	0.09	-0.09	putative acid phosphatase [*Hv* subsp. vulgare]	9e-39
101	DUP	wlk1.pk0014.c7	-0.04	-0.11	0.03	-0.16	-0.07	-0.06	-0.09	0.03	TATA box binding protein (TBP) associated factor (TAF) -like protein; protein id: At3g54280.1 [*At*]	5e-31
102	DUP	wlk1.pk0014.h12	0.10	0.01	0.08	-0.02	0.20	-0.03	0.00	0.03	P0431G06.3 [*Os*]	4e-30
103	DUP	wlk1.pk0020.e12	-0.06	-0.19	-0.34	-0.27	-0.14	0.12	0.01	-0.06	MAP kinase kinase [*Ms* subsp. x varia]	1e-56
104	DUP	wlk1.pk0023.g2	-0.03	-0.19	-0.14	-0.16	0.05	0.03	0.00	0.05	homeobox gene [*Os*]	2e-63
105	DUP	wlk8.pk0002.a6	0.21	-0.09	0.05	-0.11	-0.11	0.02	0.09	-0.04	ribosomal protein L7, putative; protein id: At1g80750.1 [*At*]	2e-11
106	DUP	wlk8.pk0019.b7	0.31	0.11	0.30	0.00	-0.09	-0.03	0.00	-0.06	putative recA protein; protein id: At2g19490.1 [*At*]	7e-11
107	DUP	wlm0.pk0018.d5	0.05	0.01	-0.06	-0.06	-0.06	-0.04	-0.11	-0.08	expressed protein; protein id: At3g20810.1 [*At*]	1e-04
108	DUP	wlm0.pk0035.a10	0.27	0.01	0.05	0.01	-0.06	0.09	0.04	-0.02	putative mitogen activated protein kinase kinase; protein id: At3g04910.1 [*At]*	5e-30
109	DUP	wlm1.pk0002.f7	-0.47	-0.81	-0.56	-0.86	-0.73	0.02	0.06	-0.12	expressed protein; protein id: At2g21970.1[*At]*	2e-12
110	DUP	wlm1.pk0019.b9	0.03	-0.16	-0.08	-0.13	-0.04	0.07	0.00	0.08	no homologies found	-
111	DUP	wlm1.pk0020.e5	-0.03	-0.25	-0.13	-0.29	-0.43	-0.04	-0.08	-0.04	calcium/calmodulin-dependent protein kinase CaMK3 [*Nt*]	2e-42
112	DUP	wlm1.pk0023.b10	-0.06	-0.25	-0.20	-0.17	-0.02	0.06	0.10	0.03	putative glutathione S-transferase [*Os*]	6e-16
113	DUP	wlm12.pk0002.g6	0.14	-0.11	-0.16	-0.09	-0.18	0.10	0.12	0.06	Hypothetical protein [*Os*]	3e-29
114	DUP	wlm96.pk029.d3	0.04	-0.25	-0.25	-0.22	-0.13	-0.03	0.04	0.07	expressed protein; protein id: At1g55000.1 [*At*]	2e-22
115	DUP	wlm96.pk040.e3	-0.16	-0.16	-0.12	-0.08	-0.06	-0.08	-0.04	0.00	no homologies found	-
116	DUP	wlm96.pk061.c14	0.04	-0.15	-0.27	-0.25	-0.16	-0.01	0.02	0.04	recombinational repair protein [*Mg*]	5e-68
117	DUP	wlmk1.pk0021.c9	0.12	-0.15	-0.22	-0.26	-0.22	-0.01	0.14	-0.13	MADS-box protein AGL14	1e-17
118	DUP	wlmk4.pk0009.b2	0.05	-0.16	-0.29	-0.17	-0.13	-0.14	0.11	0.05	unknown protein; protein id: At1g10500.1 [*At*]	3e-17
119	DUP	wlmk8.pk0021.c6	0.02	-0.08	0.00	-0.13	-0.02	-0.02	-0.06	-0.06	no homologies found	-
120	DUP	wlmk8.pk0022.c11	0.01	0.07	0.12	-0.08	0.00	-0.03	-0.01	-0.05	NBS-LRR-like protein [*Os*]	1e-40
121	DUP	wlmk8.pk0026.e5	-0.03	0.07	0.00	0.03	0.02	-0.06	-0.10	0.07	MAP kinase kinase 1 [*Os*]	7e-55
122	DUP	wpa1c.pk002.k8	-0.06	-0.20	-0.25	-0.13	-0.04	0.02	0.06	0.01	putative peroxidase [*Os*]	6e-35
123	DUP	wpa1c.pk003.b17	-0.07	-0.07	-0.12	-0.12	-0.10	0.01	0.07	0.02	Anther-specific protein MZm3-3 precursor	2e-14
124	DUP	wr1.pk0065.h7	0.19	-0.06	-0.07	-0.28	-0.03	0.00	-0.10	0.06	putative RAD51B-like DNA repair protein; protein id: At2g28560.1 [*At*]	4e-18
125	DUP	wr1.pk0092.a3	-0.05	-0.04	0.09	0.04	0.12	0.03	0.01	0.08	similar to DNA repair protein-like;protein id: At1g05120.1 [*At*]	2e-40
126	DUP	wr1.pk0104.d7	0.06	0.19	0.38	0.07	0.46	0.06	0.03	0.04	Rad51 [*Os*]	1e-14
127	DUP	wre1.pk0001.e2	-0.10	-0.17	0.00	-0.23	-0.14	0.03	-0.13	-0.04	ubiquitin-specific protease 24 (UBP24), putative; protein id: At4g30890.1 [*At]*	9e-19
128	DUP	wre1n.pk0011.b10	-0.05	-0.16	-0.42	-0.17	-0.19	-0.01	-0.07	-0.02	probable topoisomerase VIA [imported] - *At*	2e-30
129	DUP	wre1n.pk0119.h9	0.03	-0.10	-0.31	-0.22	-0.22	0.02	0.04	0.04	RNA helicase RH13 [imported] - *At* (fragment)	4e-36
130	DUP	wre1n.pk0126.f7	0.03	-0.14	-0.04	-0.26	-0.11	-0.06	0.03	-0.03	AMP-binding protein; protein id: At5g16370.1 [*At*]	6e-33
131	DUP	wre1n.pk0130.c12	-0.06	-0.12	-0.13	-0.20	0.01	0.05	-0.04	-0.01	topoisomerase II; protein id: At3g23890.1*At*]	4e-45
132	DUP	wre1n.pk0139.a6	-0.50	-0.68	-0.55	-0.54	-0.47	-0.28	0.17	0.15	no homologies found	-
133	DUP	wre1n.pk189.d12	0.03	-0.07	-0.04	-0.28	-0.19	0.03	-0.02	-0.06	maize EST AI621709, similar to an *At* chromosome BAC genomic sequence (AC006193); unknown protein *[Os]*	3e-20
134	ITEC	AWB001.D06F000328	0.89	0.10	-0.08	0.01	-0.13	-0.04	-0.02	-0.04	Phospholipase D alpha 1(PLD alpha 1)(Choline phosphatase 1)	7e-83
135	ITEC	AWB007.D11F000328	-0.06	-0.11	-0.11	-0.21	-0.17	0.03	0.08	-0.07	hypothetical protein~similar to *At* chromosome 3,F28L1.7 [*Os*]	3e-04
136	ITEC	AWB008.B10F000328	0.09	0.14	-0.01	0.15	0.15	-0.01	-0.02	0.12	unnamed protein product [*Os*]	2e-68
137	ITEC	AWB008.H12F000328	0.13	0.22	-0.02	0.24	0.15	-0.07	-0.01	0.16	putative glucose-6-phosphate/phosphate-tranlocator [*Os*]	2e-82
138	ITEC	AWB011.C09F000328	-0.40	-0.62	-0.88	-0.64	-0.96	-0.03	0.02	-0.06	unnamed protein product [*Os*]	2e-30
139	ITEC	CSB005F08F990908	-0.14	-0.44	-0.41	-0.33	-0.33	-0.01	0.04	-0.05	OSJNBa0089K24.2 [*Os*]	3e-40
140	ITEC	CSB008D09F990908	0.06	-0.05	-0.15	-0.05	-0.02	-0.05	0.07	0.08	expressed protein; protein id: At1g29250.1	1e-42
141	ITEC	WHE0065_C09_F17ZS	0.51	-0.20	-0.75	-0.36	-0.42	-0.02	0.06	-0.06	unnamed protein product [*Os*]	3e-57
142	ITEC	WHE0602_G01_M02ZA	-0.01	-0.01	-0.09	0.08	0.08	0.00	0.02	0.03	gigantea-like protein [*Hv*]	1e-117
143	ITEC	WHE0605_E12_I23ZA	0.11	0.04	-0.03	0.09	0.03	0.02	-0.04	0.04	unnamed protein product [*Os*]	2e-39
144	ITEC	WHE0606_D12_G24ZA	-0.26	-0.17	-0.17	-0.17	-0.15	0.01	0.00	0.10	RNA-binding protein, putative; protein id: At3g14450.1 [*At*]	6e-25
145	ITEC	WHE0606_G01_M02ZA	-0.01	-0.09	-0.13	0.00	0.06	0.03	0.02	-0.03	unnamed protein product [*Os*]	3e-55
146	ITEC	WHE0615_D11_H21ZA	-0.39	-0.53	-0.07	-0.33	-0.32	0.05	-0.01	0.01	OSJNBa0089K24.9 [*Os*]	2e-65
147	ITEC	WHE0616_E02_J04ZA	0.11	0.00	-0.04	-0.09	0.03	-0.01	0.05	0.05	similar to homeobox protein [*At*]	4e-91
148	ITEC	WHE0626_C03_E06ZA	0.05	-0.03	-0.11	-0.03	-0.07	-0.03	0.07	0.09	expressed protein; protein id: At3g15630.1 [*At*]	2e-09
149	ITEC	WHE0627_B09_D17ZA	0.00	-0.02	-0.01	0.03	-0.03	-0.01	0.10	0.04	hypothetical protein XP_099468 [*Hs*]	0.077
150	ITEC	WHE0765_C03_F05ZS	0.01	-0.17	-0.24	-0.04	0.18	0.06	-0.04	0.05	16.9 KD class I heat shock protein (heat shock protein 17) (HSP 16.9)	1e-61
151	ITEC	WHE0765_E03_J05ZS	-0.01	-0.18	-0.37	-0.26	-0.14	-0.01	0.03	-0.07	unnamed protein product [*Os*]	2e-81
152	ITEC	WHE0765_E12_J23ZS	-0.48	-0.36	-0.34	-0.34	-0.27	0.02	0.07	-0.03	OSJNBa0016I09.7 [*Os*]	6e-71
153	ITEC	WHE0765_F10_L19ZS	-0.07	-0.24	-0.25	-0.24	-0.09	0.03	-0.01	-0.04	putative protein kinase [*Os*]	7e-72
154	ITEC	WHE0766_C02_F04ZS	0.26	-0.01	-0.40	0.05	0.15	0.02	0.08	0.09	16.9 KD class I heat shock protein (heat shock protein 17) (HSP 16.9)	3e-61
155	ITEC	WHE0801_B08_C15ZS	0.84	0.31	0.17	0.32	0.33	-0.02	-0.08	-0.19	unnamed protein product [*Os*]	1e-16
156	ITEC	WHE0802_D08_G16ZS	-0.27	-0.44	-0.48	-0.49	-0.46	-0.01	-0.02	-0.01	putative RNA helicase, DRH1 [*Os*]	9e-23
157	ITEC	WHE0808_B04_D08ZS	-0.17	-0.24	-0.18	-0.24	-0.11	0.05	0.09	-0.03	P0489A01.18 [*Os*]	1e-16
158	ITEC	WHE0811_D06_H11ZS	0.29	-0.09	-0.10	-0.03	-0.07	0.02	0.06	0.02	unnamed protein product [*Os*]	2e-59
159	ITEC	WHE0815_C11_F21ZS	0.76	0.36	0.34	0.29	0.33	0.01	0.01	-0.20	putative MAR-binding protein MFP1 [*Os*]	4e-58
160	ITEC	WHE0838_D10_G20ZS	-0.02	-0.02	0.04	-0.11	-0.13	0.02	0.03	0.05	putative CRK1 protein [*Os*]	5e-80
161	ITEC	WHE0839_B01_D01ZS	0.08	-0.15	-0.12	-0.22	-0.27	-0.01	-0.03	0.11	unnamed protein product [*Os*]	1e-104
162	ITEC	WHE0857_F07_L13ZS	0.09	-0.36	-0.35	-0.43	-0.17	-0.02	-0.06	-0.04	GA 3beta-hydroxylase [*Os*]	1e-37
163	ITEC	WHE0870_H07_P14ZS	0.09	-0.22	-0.34	-0.30	-0.06	0.05	-0.04	0.03	RAB7A [*Lj*]	5e-47
164	ITEC	WHE0873_H10_P19ZS	0.21	0.06	0.05	-0.03	-0.09	-0.06	0.05	-0.05	unnamed protein product [*Os*]	6e-37
165	ITEC	WHE0902_B03_C06ZS	0.00	-0.23	-0.20	-0.27	-0.18	-0.05	-0.05	-0.05	unnamed protein product [*Os*]	2e-49
166	ITEC	WHE0904_G11_N22ZS	0.07	-0.15	-0.29	-0.15	-0.03	0.00	0.04	0.02	putative extensin-like protein [*Os*]	4e-86
167	ITEC	WHE0904_H06_P12ZS	-0.02	-0.13	-0.22	-0.17	-0.07	-0.01	-0.07	0.07	unnamed protein product [*Os*]	3e-31
168	ITEC	WHE0906_H04_O08ZS	-0.30	-0.35	-0.11	-0.22	-0.19	0.14	0.09	0.07	putative t-SNARE SED5 [*Os*]	4e-50
169	ITEC	WHE0922_A12_A24ZS	0.03	-0.27	-0.34	-0.24	-0.21	-0.02	-0.07	0.06	putative phophatidylethanolamine binding protein [*Os*]	4e-37
170	ITEC	WHE0931_H04_P07ZS	0.24	0.03	0.14	-0.02	0.04	0.06	0.07	-0.01	protein F1N21.20 [imported] - *At*	2e-45
171	ITEC	WHE0953_D10_H19ZS	-0.03	-0.35	-0.36	-0.42	-0.15	-0.02	0.09	0.10	contains ESTs C73890(E20948),C99695(E21103)~unknown protein [*Os*]	2e-24
172	ITEC	WHE0959_B02_C03ZS	0.03	-0.11	-0.03	-0.12	0.01	-0.07	0.00	-0.01	unnamed protein product [*Os*]	2e-65
173	ITEC	WHE0960_A04_A08ZS	0.03	-0.28	-0.36	-0.35	0.13	-0.03	-0.02	0.00	RAS-related GTP-binding protein Rab7 family [*Os*]	2e-95
174	ITEC	WHE0962_H09_P18ZS	0.42	0.11	-0.02	0.07	0.08	0.00	-0.02	-0.03	Unknown protein [*Os*]	3e-29
175	ITEC	WHE0965_H07_P13ZS	0.32	0.15	0.27	0.00	0.11	-0.02	-0.03	-0.01	contains ESTs AU165886 (E60331), AU030841 (E60331)~similar to *At* chromosome 2, At2g40550~unknown	8e-64
176	ITEC	WHE0966_B06_D12ZS	0.05	-0.15	-0.44	-0.22	-0.12	-0.02	0.00	0.04	putative late embryogenesis abundant protein LEA14-A [*Os*]	1e-56
177	ITEC	WHE0966_H05_P10ZS	0.09	-0.10	-0.08	-0.11	-0.07	-0.02	0.01	-0.01	hypothetical protein,similar to *At* chromosome 5,MCK7.19[*Os*]	5e-44

			Temporal *M*					*Ph* mutant *M*				
#	ID	EST name	PM	LP	DA	TT	T	*1b*	*2a*	*2b*	Top BLASTx hit	e-val
178	ITEC	WHE0970_H12_P24ZS	0.22	0.01	-0.06	0.06	0.00	-0.01	-0.02	0.00	B1015E06.2 [*Os*]	5e-40
179	ITEC	WHE0972_A04_A08ZS	0.19	0.04	0.04	-0.04	0.01	0.08	0.08	-0.03	unnamed protein product [*Os*]	6e-39
180	ITEC	WHE0973_C12_F23ZS	0.65	0.11	-0.18	-0.10	0.01	-0.01	0.05	0.02	putative muconate cycloisomerase-like protein [*Os*]	8e-77
181	ITEC	WHE0973_G06_N11ZS	-0.02	-0.03	-0.19	-0.17	-0.04	0.03	0.06	0.01	P0416D03.30 [*Os*]	4e-31
182	ITEC	WHE0974_H05_P10ZS	0.13	-0.27	-0.38	-0.34	-0.19	-0.02	-0.03	0.06	unnamed protein product [*Os*]	6e-10
183	ITEC	WHE0975_G01_M01ZS	-0.16	-0.30	-0.27	-0.21	-0.25	-0.05	-0.04	-0.01	unnamed protein product [*Os*]	4e-98
184	ITEC	WHE0975_G11_M21ZS	-0.12	-0.16	-0.15	-0.18	-0.15	0.04	0.01	0.02	P0492F05.25 [*Os*]	8e-43
185	ITEC	WHE0977_D04_H07ZS	-0.32	-0.47	-0.32	-0.36	-0.09	0.02	0.04	-0.05	P0710E05.11 [*Os*]	8e-41
186	ITEC	WHE0980_F06_K12ZS	-0.07	-0.09	-0.14	-0.12	0.01	-0.04	0.01	-0.11	Dof zinc finger protein [*Os*]	2e-34
187	ITEC	WHE0981_H10_P19ZS	0.19	0.08	-0.02	-0.02	0.13	0.01	-0.01	-0.01	putative WD40-repeat protein [*Os*]	4e-92
188	ITEC	WHE0982_B03_D06ZS	-0.21	-0.42	-0.36	-0.47	0.11	0.04	0.14	0.09	P0406H10.4 [*Os*]	4e-40
189	ITEC	WHE0984_F02_K04ZS	0.21	0.17	0.07	0.11	0.13	0.01	-0.05	-0.03	splicing factor-like protein [*At*]	2e-31
190	ITEC	WHE0995-0998_P15_P15ZS	-0.19	-0.13	-0.13	-0.13	-0.05	0.07	0.09	0.03	no homologies found	-
191	ITEC	WHE1060_B10_C20ZS	-0.23	-0.32	-0.23	-0.30	-0.04	0.03	0.06	0.06	contains EST AU081362(R10239)~unknown protein [*Os*]	4e-11
192	ITEC	WHE1071-1074_F14_F14ZS	-0.05	-0.08	-0.20	-0.03	0.03	-0.05	0.02	0.02	P0024G09.19 [*Os*]	9e-53
193	ITEC	WHE1071-1074_G13_G13ZS	-0.28	-0.49	-0.48	-0.60	-0.51	0.00	0.01	-0.01	unnamed protein product [*Os*]	8e-93
194	ITEC	WHE1071-1074_O10_O10ZS	-0.06	-0.22	-0.33	-0.18	0.08	-0.02	-0.02	0.00	MybHv33 [*Hv* subsp. vulgare]	3e-58
195	ITEC	WHE1071-1074_P02_P02ZS	0.04	-0.22	-0.31	-0.22	-0.12	0.05	0.08	0.05	unnamed protein product [*Os*]	8e-17
196	ITEC	WHE1071-1074_P19_P19ZS	0.15	0.08	-0.18	0.09	0.20	0.01	0.08	0.05	unnamed protein product [*Os*]	5e-53
197	ITEC	WHE1075_G05_M09ZS	-0.01	-0.16	-0.21	-0.19	-0.05	0.02	-0.03	0.01	P0665D10.16 [*Os*]	4e-93
198	ITEC	WHE1076_G08_M16ZS	0.09	-0.13	-0.25	-0.17	-0.09	-0.06	-0.07	0.05	putative MAR-binding protein MFP1 [*Os*]	2e-37
199	ITEC	WHE1101_D11_G21ZS	0.06	-0.09	-0.14	-0.21	0.02	0.05	0.03	0.04	P0666G04.18 [*Os*]	2e-44
200	ITEC	WHE1105_C06_E11ZS	-0.01	-0.10	-0.31	-0.23	-0.16	0.08	0.06	-0.03	P0001B06.19 [*Os*]	3e-34
201	ITEC	WHE1107_B07_D13ZS	0.02	-0.31	-0.57	-0.37	-0.24	-0.02	0.01	0.02	P0701D05.10 [*Os*]	1e-38
202	ITEC	WHE1107_H10_P19ZS	0.24	0.00	-0.49	-0.07	-0.10	0.00	-0.04	0.01	putative receptor-like protein kinase [*Os*]	2e-95
203	ITEC	WHE1109_F08_K15ZS	0.16	0.16	0.30	0.39	0.46	-0.05	0.01	-0.08	putative protein kinase [*Os*]	2e-81
204	ITEC	WHE1111_G08_N15ZS	0.09	-0.10	-0.03	-0.09	-0.04	-0.08	-0.13	0.00	putative GTP-binding protein [*Os*]	9e-77
205	ITEC	WHE1114_A05_A10ZS	0.03	-0.21	-0.13	-0.25	-0.13	0.02	-0.15	-0.01	OJ1276_B06.30 [*Os*]	5e-32
206	ITEC	WHE1114_G04_M08ZS	-0.07	-0.38	-0.36	-0.46	-0.18	-0.06	-0.03	-0.03	no homologies found	-
207	ITEC	WHE1121_F09_K17ZS	0.05	-0.02	-0.15	-0.07	0.01	-0.04	-0.09	-0.02	AAA-ATPase-like protein [*Os*]	4e-99
208	ITEC	WHE1126_G04_M08ZS	-0.05	-0.07	-0.05	-0.18	0.08	-0.09	-0.11	-0.05	P0009G03.13 [*Os*]	3e-83
209	ITEC	WHE1128_D05_H10ZS	0.12	-0.05	-0.07	-0.03	0.00	-0.01	0.02	0.08	P0452F10.4 [*Os*]	1e-20
210	ITEC	WHE1134_F04_K08ZS	-0.36	-0.63	-0.59	-0.61	-0.56	0.02	-0.02	0.11	unnamed protein product [*Os*]	4e-96
211	ITEC	WHE1137_F09_K17ZS	0.20	-0.26	-0.28	-0.28	-0.15	-0.06	0.01	0.01	unnamed protein product [*Os*]	4e-72
212	ITEC	WHE1142_H06_O12ZS	0.05	-0.27	-0.38	-0.39	-0.12	0.01	-0.01	0.09	P0710E05.22 [*Os*]	1e-32
213	ITEC	WHE1144_F05_L10ZS	0.04	-0.21	-0.19	-0.19	-0.11	0.03	0.01	0.15	P0710E05.6 [*Os*]	2e-77
214	ITEC	WHE1147_E04_J07ZS	-0.17	-0.49	-0.70	-0.57	-0.61	-0.05	-0.12	-0.03	putative hexose transporter [*Os*]	4e-30
215	ITEC	WHE1201_H11_O21ZS	0.11	-0.11	-0.35	-0.18	-0.07	-0.03	0.04	0.13	OSJNBa0089K24.24 [*Os*]	2e-70
216	ITEC	WHE1205_B09_C17ZS	0.00	-0.08	-0.15	-0.14	-0.12	0.02	-0.03	0.17	At2g47760/F17A22.15 [*At*]	7e-60
217	ITEC	WHE1208_E07_J14ZS	0.29	0.26	0.09	0.13	0.16	-0.03	-0.09	-0.08	putative RNA helicase, DRH1 [*Os*]	9e-97
218	ITEC	WHE1211_A09_B17ZS	0.14	0.01	-0.02	-0.03	0.10	0.03	0.01	-0.03	cytochrome-b5 reductase - like protein; protein id: At5g20080.1 [*At*]	8e-80
219	ITEC	WHE1413-1416_K02_K02ZS	-0.49	-0.60	-0.58	-0.46	-0.41	0.01	-0.02	0.05	unnamed protein product [*Os*]	3e-33
220	ITEC	WHE1413-1416_M07_M07ZS	-0.10	-0.17	-0.10	-0.16	-0.02	0.05	0.13	0.18	no homologies found	-
221	ITEC	WHE1451_A05_A09ZS	0.07	-0.21	-0.32	-0.25	-0.12	-0.02	-0.02	0.03	putative calmodulin-binding protein [*Os*]	2e-80
222	ITEC	WHE1457_C03_F05ZS	-0.21	0.64	0.61	0.76	0.86	0.07	-0.07	0.07	P0666G04.16 [*Os*]	5e-42
223	ITEC	WHE1651-1654_C21_C21ZS	-0.08	-0.17	-0.26	-0.26	-0.11	0.02	-0.11	-0.02	putative receptor serine/threonine kinase [*Os*]	8e-56
224	ITEC	WHE1659-1662_O23_O23ZS	0.02	-0.08	-0.13	-0.06	-0.02	0.05	-0.06	-0.10	OSJNBa0083M16.33 [*Os*]	3e-42
225	ITEC	WHE1755-1758_G03_G03ZS	0.61	0.27	0.08	0.20	0.16	-0.05	-0.06	-0.01	OSJNBa0089K24.28 [*Os*]	1e-48
226	ITEC	WHE1755-1758_J14_J14ZS	0.98	0.33	0.52	0.20	0.52	0.01	-0.01	-0.26	no homologies found	-
227	ITEC	WHE1759-1762_B24_B24ZS	0.13	-0.27	-0.29	-0.34	-0.17	-0.09	-0.05	-0.07	putative receptor protein kinase PERK1 [*Os*]	2e-78
228	ITEC	WHE1759-1762_D08_D08ZS	0.03	-0.18	-0.22	-0.25	-0.23	0.02	0.14	0.10	P0701D05.6 [*Os*]	8e-38
229	ITEC	WHE1767_G07_M13ZS	-0.01	-0.01	0.04	0.00	0.06	0.05	-0.08	0.03	CG10713-PA [*Dm*]	0.15
230	ITEC	WHE1768_B02_C04ZS	0.01	-0.07	-0.02	0.06	-0.06	0.05	0.02	-0.04	putative transcription factor [*Os*]	7e-35
231	ITEC	WHE1768_H12_O24ZS	-0.07	-0.12	-0.28	-0.13	-0.03	0.03	0.00	0.07	P0019D06.11 [*Os*]	1e-61
232	ITEC	WHE1771_F06_K11ZS	0.09	0.05	-0.02	0.05	0.07	-0.02	0.06	0.05	P0417G05.19 [*Os*]	7e-34
233	ITEC	WHE1774_F06_L12ZS	0.01	-0.12	-0.18	-0.12	-0.09	-0.09	0.01	0.03	B1015E06.6 [*Os*]	3e-61
234	ITEC	WHE1778_B11_C21ZS	0.09	-0.06	-0.04	-0.03	0.05	-0.02	0.13	0.07	unnamed protein product [*Os*]	2e-63
235	ITEC	WHE1782_E07_I13ZS	-0.03	-0.06	-0.02	-0.07	-0.07	0.06	0.00	0.05	S-adenosylmethionine synthetase 1 (Methionine adenosyltransferase 1) (AdoMet synthetase 1)	1e-101
236	ITEC	WHE1783_D02_G03ZS	-0.21	-0.31	-0.26	-0.20	-0.13	-0.01	-0.08	0.00	putative ethylene-responsive RNA helicase [*Os*]	1e-125
237	ITEC	WHE1787_E11_I21ZS	0.03	0.05	0.06	-0.05	0.07	0.03	0.00	0.11	P0489A05.4 [*Os*]	3e-38
238	ITEC	WHE1788_A06_A12ZS	0.00	-0.28	-0.27	-0.29	-0.11	0.02	0.03	0.05	hypothetical protein~similar to *At* chromosome 3, T18N14.110 [*Os*]	4e-48
239	ITEC	WHE1788_A09_A18ZS	-0.12	-0.15	-0.20	-0.11	-0.07	0.01	0.06	0.13	putative DNA binding protein RAV2 [*Os*]	7e-34
240	ITEC	WHE1792_H10_O20ZS	-0.75	-0.97	-0.79	-0.82	-0.72	0.07	0.15	-0.02	peptide transport protein - barley	2e-54
241	ITEC	WHE1794_G10_N20ZS	-0.32	-0.21	0.10	-0.35	-0.09	-0.07	0.06	0.04	P0419B01.1 [*Os*]	1e-25
242	ITEC	WHE1798_D05_H10ZS	-0.01	-0.21	-0.36	-0.21	-0.17	0.05	0.01	0.01	P0443D08.1 [*Os*]	2e-20
243	ITEC	WHE2051_B11_C21ZS	-0.35	-0.42	-0.28	-0.47	-0.25	0.05	0.08	-0.07	putative peroxidase [*Os*]	4e-79
244	ITEC	WHE2051_D02_G03ZS	-0.21	-0.22	-0.18	-0.09	-0.09	0.06	0.00	-0.03	P0671B11.30 [*Os*]	3e-34
245	ITEC	WHE2112_H03_P06ZS	0.02	-0.09	-0.03	-0.07	-0.04	-0.01	-0.09	-0.04	P0489A05.26 [*Os*]	2e-44
246	ITEC	WHE2117_H04_O07ZS	0.01	-0.30	-0.25	-0.40	-0.42	0.03	-0.03	0.04	P0019D06.23 [*Os*]	2e-45
247	ITEC	WHE2301-2304_A17_A17ZS	-0.54	-0.83	-0.55	-0.84	-0.66	0.05	0.03	0.04	MADS box transcription factor [*Ta*]	4e-39
248	ITEC	WHE2301-2304_B17_B17ZS	0.10	-0.13	-0.56	-0.17	-0.25	-0.04	-0.02	-0.06	P0034C09.1 [*Os*]	8e-43
249	ITEC	WHE2301-2304_H06_H06ZS	0.06	-0.10	-0.26	-0.20	-0.05	0.00	0.05	0.05	unnamed protein product [*Os*]	2e-82
250	ITEC	WHE2301-2304_H09_H09ZS	-0.25	-0.35	0.19	-0.09	0.10	-0.04	0.04	-0.06	unnamed protein product [*Os*]	5e-86
251	ITEC	WHE2301-2304_J12_J12ZS	0.04	-0.19	-0.39	-0.33	-0.09	0.04	0.01	0.04	hyoscyamine 6-dioxygenase hydroxylase, putative; protein id: At1g35190.1	6e-71
252	ITEC	WHE2301-2304_O04_O04ZS	0.01	-0.32	-0.58	-0.34	-0.34	0.08	0.23	0.13	P0665D10.8 [*Os*]	2e-48
253	ITEC	WHE2301-2304_O19_O19ZS	0.36	0.19	0.13	0.18	0.23	0.02	-0.09	-0.01	OSJNBa0089K24.26 [*Os*]	7e-56
254	ITEC	WHE2309_F04_K07ZS	0.02	-0.10	-0.17	-0.10	-0.06	0.05	0.03	0.06	P0001B06.29 [*Os*]	3e-63
255	ITEC	WHE2314_H05_O10ZS	0.04	-0.18	-0.33	-0.08	-0.01	-0.06	0.08	0.01	high pI alpha-glucosidase [*Hv*]	5e-84
256	ITEC	WHE2321_A08_A15ZS	-0.34	0.11	0.11	0.05	0.63	-0.07	-0.06	-0.04	unnamed protein product [*Os*]	8e-52
257	ITEC	WHE2321_C08_E15ZS	-0.32	-0.54	-0.34	-0.56	-0.33	-0.05	0.00	0.06	MADS box transcription factor [*Ta*]	2e-87
258	ITEC	WHE2324_D11_H22ZS	-0.49	-0.77	-0.72	-0.78	-0.89	-0.02	0.04	0.06	unnamed protein product [*Os*]	1e-11
259	ITEC	WHE2334_E09_I18ZS	-0.15	-0.24	-0.31	-0.23	-0.23	0.01	-0.12	-0.12	putative protein kinase [*Os*]	4e-51
260	ITEC	WHE2337_F01_K01ZS	0.01	-0.31	-0.32	-0.42	-0.24	0.06	0.02	0.04	Probable microsomal signal peptidase 22 kDa subunit (SPase 22 kDa subunit) (SPC22)	3e-65
261	ITEC	WHE2341_E12_I23ZS	-0.01	-0.21	-0.36	-0.11	0.00	-0.01	0.07	0.08	unnamed protein product [*Os*]	3e-64
262	WAW	waw1c.pk001.a12	0.24	0.02	-0.09	0.11	0.05	0.07	0.02	-0.04	gene_id:K15E6.9~unknown protein [*At*]	8e-60
263	WAW	waw1c.pk001.a14	-0.04	-0.06	0.04	0.04	0.16	0.03	0.08	-0.07	YY1 protein precursor	3e-19
264	WAW	waw1c.pk001.a16	-0.17	-0.13	-0.33	-0.18	0.43	-0.03	0.00	0.04	Putative vacuolar sorting receptor protein homolog [*Os*]	5e-16
265	WAW	waw1c.pk001.a17	-0.03	-0.12	-0.07	-0.11	0.03	0.01	-0.03	0.00	subtilisin-like serine protease; protein id: At4g34980.1	4e-17
266	WAW	waw1c.pk001.a20	0.37	0.27	0.25	0.17	0.08	0.08	0.04	0.02	cytoplasmic ribosomal protein L18 [*Os*]	3e-90

			Temporal *M*					*Ph* mutant *M*				
#	ID	EST name	PM	LP	DA	TT	T	*1b*	*2a*	*2b*	Top BLASTx hit	e-val
267	WAW	waw1c.pk001.a24	0.06	-0.10	-0.26	-0.06	-0.10	0.03	-0.04	-0.06	putative synaptobrevin [*At*]	2e-54
268	WAW	waw1c.pk001.a4	-0.02	-0.34	-0.32	-0.37	-0.22	-0.08	-0.13	0.00	putative impotin alpha 1b [*Os*]	7e-65
269	WAW	waw1c.pk001.a6	0.01	0.09	0.06	0.16	0.04	0.05	0.02	-0.06	F14N23.20 [*At*]	1e-29
270	WAW	waw1c.pk001.a7	-0.03	0.19	0.01	0.09	0.18	0.00	-0.15	-0.03	no homologies found	-
271	WAW	waw1c.pk001.a8	-0.09	0.19	0.11	0.21	0.12	0.02	-0.04	0.19	no homologies found	-
272	WAW	waw1c.pk001.c1	-0.39	-0.09	0.09	0.09	0.06	-0.02	0.01	-0.03	hypothetical protein~similar to *Os* chromosome 10, OSJNBa0042H09.20 [*Os]*	7e-27
273	WAW	waw1c.pk001.c10	0.05	0.06	0.10	0.01	-0.03	-0.01	-0.03	-0.16	OCL3 protein [*Zm*]	2e-13
274	WAW	waw1c.pk001.c15	0.04	-0.13	-0.13	-0.15	0.05	-0.08	0.01	-0.01	bZip DNA binding protein; protein id: At2g40620.1	6e-06
275	WAW	waw1c.pk001.c19	0.04	0.07	0.05	0.02	-0.03	-0.08	-0.05	-0.02	Elongation factor 1-alpha (EF-1-ALPHA)	1e-099
276	WAW	waw1c.pk001.c2	0.07	0.03	0.01	-0.03	-0.13	0.01	0.00	0.02	expressed protein; protein id: At3g15000.1 [*At*]	5e-20
277	WAW	waw1c.pk001.c20	0.33	0.00	0.23	0.08	0.01	0.04	0.09	0.03	ribosomal protein L32 [*Ma*]	5e-60
278	WAW	waw1c.pk001.c4	0.09	0.04	0.19	0.14	-0.03	0.11	-0.04	0.03	RAD23 protein homolog - rice	1e-59
279	WAW	waw1c.pk001.e1	0.17	0.08	0.13	0.09	-0.03	0.03	-0.02	0.06	unnamed protein product [*Os*]	3e-70
280	WAW	waw1c.pk001.e10	0.00	-0.05	-0.05	-0.06	0.02	-0.07	-0.11	0.01	no homologies found	-
281	WAW	waw1c.pk001.e12	-0.18	0.04	-0.05	-0.04	0.18	0.02	-0.09	0.01	NTGP5 [*Nt*]	2e-37
282	WAW	waw1c.pk001.e14	0.03	0.11	-0.02	0.03	0.08	0.07	-0.01	0.08	Contains similarity to formin binding protein 11 from *Mm* gb|AF135439 and contains multiple FF PF|01846 and WW	0.004
283	WAW	waw1c.pk001.e17	-0.29	-0.15	-0.25	-0.07	-0.35	0.00	-0.04	0.13	cytosolic aldehyde dehydrogenase RF2D [*Zm*]	1e-44
284	WAW	waw1c.pk001.e4	0.08	0.07	0.27	0.03	0.13	-0.09	-0.01	0.03	unknown protein [*At*]	6e-26
285	WAW	waw1c.pk001.e6	0.00	-0.09	-0.11	-0.18	-0.08	-0.01	0.05	-0.06	no homologies found	-
286	WAW	waw1c.pk001.e9	-0.24	-0.35	-0.19	-0.31	-0.29	0.12	0.14	0.09	peroxiredoxin [*Os*]	6e-50
287	WAW	waw1c.pk001.g16	1.46	0.74	0.55	0.65	0.69	0.11	0.08	-0.11	histone H4 (TH091) - wheat	5e-41
288	WAW	waw1c.pk001.g3	0.08	-0.41	-0.61	-0.55	-0.86	-0.13	-0.10	-0.07	HISTIDINe-RICH GLYCOPROTEIN PRECURSOR	0.18
289	WAW	waw1c.pk001.i10	-0.08	-0.16	-0.13	-0.11	-0.01	-0.01	-0.07	0.06	heat shock protein 70, cytosolic [imported] - spinach	2e-81
290	WAW	waw1c.pk001.i12	-0.06	-0.03	0.04	-0.03	0.08	-0.02	-0.07	-0.04	no homologies found	-
291	WAW	waw1c.pk001.i13	-0.25	-0.05	0.02	-0.08	-0.05	-0.03	-0.03	0.06	expressed protein; protein id: At3g17300.1	7e-08
292	WAW	waw1c.pk001.i14	0.05	0.14	0.31	0.28	0.09	-0.02	-0.10	0.01	nuclear transcription factor SLN1 [*Hv*]	7e-25
293	WAW	waw1c.pk001.i16	0.10	0.16	0.23	0.17	0.15	0.03	0.03	0.06	unknown [*At*]	3e-64
294	WAW	waw1c.pk001.i17	0.15	0.19	0.25	0.26	0.08	0.00	-0.05	0.09	26S proteasome regulatory subunit; protein id: At2g39990.1:	4e-23
295	WAW	waw1c.pk001.i18	-0.02	0.09	0.08	0.06	-0.02	-0.06	-0.04	0.03	Elongation factor 1-alpha (EF-1-ALPHA)	3e-99
296	WAW	waw1c.pk001.i2	0.19	0.03	-0.01	0.03	-0.02	0.04	0.00	-0.01	putative cyclase associated protein CAP; protein id: At4g34490.1[*At*]	7e-41
297	WAW	waw1c.pk001.i3	-0.01	-0.10	-0.08	0.01	-0.05	-0.05	-0.04	0.01	unknown protein [*Os*]	1e-09
298	WAW	waw1c.pk001.i4	-0.03	-0.12	0.02	-0.05	-0.03	0.06	0.14	0.07	Putative Transcription initiation factor IIE, beta subunit [*Os*]	5e-35
299	WAW	waw1c.pk001.i6	0.91	0.22	-0.01	0.16	0.08	-0.01	0.04	0.00	CG18105-PA [*Dm*]	0.72
300	WAW	waw1c.pk001.i7	0.31	0.09	-0.07	0.04	-0.16	-0.06	-0.02	-0.04	Putative 40S Ribosomal protein [*Os*]	5e-07
301	WAW	waw1c.pk001.k10	-0.92	-1.03	-0.70	-0.63	-0.56	0.11	0.25	0.27	apoplastic invertase 1 [*Hv* subsp. vulgare]	6e-42
302	WAW	waw1c.pk001.k13	0.05	0.18	0.26	0.13	0.13	0.15	0.06	-0.07	hypothetical protein T24D18.12 - *At*	4e-49
303	WAW	waw1c.pk001.k14	0.68	0.32	0.30	0.28	0.18	0.00	0.19	-0.15	Unknown protein [Lactococcus lactis subsp. lactis]	8e-04
304	WAW	waw1c.pk001.k15	0.27	0.21	0.06	0.23	0.12	-0.01	0.06	0.00	dihydrolipoamide S-acetyltransferase [*Zm*]	2e-38
305	WAW	waw1c.pk001.k19	1.36	0.71	0.55	0.70	0.58	-0.02	-0.10	-0.29	histone H2A.2 - wheat	3e-35
306	WAW	waw1c.pk001.k21	0.18	0.39	0.77	0.25	0.40	0.04	-0.04	0.01	no homologies found	-
307	WAW	waw1c.pk001.k9	0.07	0.00	0.05	0.04	-0.05	-0.02	0.08	-0.09	no homologies found	-
308	WAW	waw1c.pk001.m1	-0.01	0.36	0.15	0.27	0.30	-0.01	-0.08	-0.05	unknown protein [*At*]	2e-31
309	WAW	waw1c.pk001.m10	0.06	0.06	0.08	0.07	0.03	-0.01	-0.03	-0.02	P0470A12.14 [*Os*]	7e-79
310	WAW	waw1c.pk001.m13	-0.01	-0.01	-0.18	-0.03	0.06	0.06	0.07	0.08	no homologies found	-
311	WAW	waw1c.pk001.m14	0.15	0.20	-0.04	0.10	0.06	-0.07	0.00	0.06	T27G7.17 [*At*]	5e-64
312	WAW	waw1c.pk001.m19	-0.02	0.06	-0.01	0.11	0.04	0.05	0.02	0.03	putative protein; protein id: At5g23550.1 [*At*]	5e-24
313	WAW	waw1c.pk001.m2	0.08	-0.01	0.15	-0.03	0.02	0.05	0.06	-0.05	G-protein beta-subunit (transducin) family; protein id: At2g43770.1 [*At]*	2e-31
314	WAW	waw1c.pk001.m20	0.02	0.14	0.12	0.15	0.06	0.08	-0.04	-0.04	SPP30 homolog [*Os*]	2e-26
315	WAW	waw1c.pk001.m3	0.58	1.17	1.61	1.07	1.33	-0.04	0.01	-0.02	putative DNA binding protein [*At*]	2e-10
316	WAW	waw1c.pk001.m6	-0.48	0.07	-0.13	0.21	0.06	0.03	-0.06	-0.02	unknown protein [*At*]	1e-13
317	WAW	waw1c.pk001.m8	-0.32	-0.48	-0.50	-0.76	-0.28	0.00	0.08	0.07	Ca2+/H+ antiporter [*Zm*]	1e-21
318	WAW	waw1c.pk001.m9	0.02	0.18	0.58	0.11	0.02	0.07	0.03	-0.07	AT5g66560/K1F13_23 [*At*]	6e-15
319	WAW	waw1c.pk001.o10	-0.28	-0.53	-0.38	-0.38	-0.60	0.03	0.07	-0.11	OJ000223_09.1 [*Os*]	1e-25
320	WAW	waw1c.pk001.o14	-0.04	-0.06	-0.28	-0.09	-0.14	0.03	0.14	0.09	Thioredoxin - like protein; protein id: At4g29670.1 [*At*]	4e-04
321	WAW	waw1c.pk001.o22	0.33	0.06	-0.34	0.04	-0.24	0.10	0.13	0.12	acidic ribosomal protein P2a-4 [*Zm*]	1e-13
322	WAW	waw1c.pk002.a10	-1.27	0.30	1.32	0.43	1.35	0.03	0.02	-0.27	contains ESTs C73631(E20015),C99434(E20015)~unknown protein [*Os*]	3e-18
323	WAW	waw1c.pk002.a11	1.46	0.75	0.57	0.70	0.65	-0.03	-0.02	-0.24	Histone H2A.2.2	4e-51
324	WAW	waw1c.pk002.a12	0.47	0.20	0.38	0.26	0.13	0.06	-0.11	-0.05	chromatin complex subunit A101 [*Zm*]	2e-54
325	WAW	waw1c.pk002.a13	0.11	-0.02	-0.07	0.02	-0.15	0.03	-0.03	0.02	putative Ruv DNA-helicase [Cicer arietinum]	1e-88
326	WAW	waw1c.pk002.a14	-0.11	-0.18	-0.08	-0.09	-0.17	0.02	0.03	0.08	acylaminoacyl-peptidase like protein; protein id: At4g14570.1 [*At*]	2e-16
327	WAW	waw1c.pk002.a16	-0.18	-0.13	0.09	-0.04	-0.05	0.01	-0.10	-0.05	putative DnaJ protein; protein id: At1g79940.1 [*At*]	2e-57
328	WAW	waw1c.pk002.a17	-0.04	-0.05	-0.05	0.01	0.07	0.09	-0.05	0.00	no homologies found	-
329	WAW	waw1c.pk002.a18	0.11	0.06	0.07	0.07	0.10	0.00	-0.07	0.03	cleavage and polyadenylation specificity factor; protein id: At5g23880.1[*At]*	3e-18
330	WAW	waw1c.pk002.a19	0.07	0.16	0.15	0.13	0.14	0.02	-0.03	0.00	RIKEN cDNA 2210416J16 [*Mm*]	0.11
331	WAW	waw1c.pk002.a20	0.06	0.15	0.08	0.13	0.08	0.00	-0.07	0.02	putative CCAAT displacement protein [*Os*]	9e-70
332	WAW	waw1c.pk002.a22	0.08	-0.03	0.04	-0.01	-0.06	-0.05	0.02	-0.05	isoleucyl-tRNA synthetase; protein id: At5g49030.1 [*At*]	1e-51
333	WAW	waw1c.pk002.a23	-0.15	0.11	-0.15	0.01	0.12	0.05	-0.10	0.03	hypothetical protein [*At*]	1e-40
334	WAW	waw1c.pk002.a24	1.17	0.98	1.04	0.83	1.00	-0.11	-0.18	-0.12	Argonaute (AGO1)-like protein [imported] - *At*	2e-53
335	WAW	waw1c.pk002.a4	0.15	0.03	-0.20	-0.04	0.26	-0.03	0.03	0.12	putative protein; protein id: At3g58170.1 [*At*]	2e-22
336	WAW	waw1c.pk002.a5	-0.04	0.13	0.19	0.04	0.04	0.13	-0.06	0.04	no homologies found	-
337	WAW	waw1c.pk002.a6	0.20	0.11	0.18	0.15	0.00	0.08	0.04	0.11	60S ribosomal protein L3	1e-10
338	WAW	waw1c.pk002.a7	0.31	0.05	-0.10	0.11	0.04	0.03	0.04	0.08	putative 40S ribosomal protein S12 [*Os*]	8e-43
339	WAW	waw1c.pk002.a8	0.20	0.11	0.10	0.03	-0.06	-0.05	0.05	0.02	putatative pyrophosphate--fructose-6-phosphate1 phosphotransferase [*Os*]	4e-76
340	WAW	waw1c.pk002.a9	0.07	-0.02	-0.06	0.05	-0.02	0.06	-0.06	-0.03	no homologies found	-
341	WAW	waw1c.pk002.b10	-0.30	-0.47	-0.42	-0.56	-0.51	0.04	0.10	-0.06	Triosephosphate isomerase, chloroplast precursor (TIM)	1e-106
342	WAW	waw1c.pk002.b11	-0.03	0.02	-0.02	0.01	-0.05	-0.01	-0.05	-0.07	OJ1484_G09.12 [*Os*]	3e-12
343	WAW	waw1c.pk002.b12	0.20	0.56	0.72	0.39	0.20	-0.05	-0.04	-0.09	pyruvate kinase; protein id: At5g08570.1 [*At*]	7e-74
344	WAW	waw1c.pk002.b13	-0.13	-0.04	-0.12	-0.02	0.06	-0.03	-0.06	0.07	GSH-dependent dehydroascorbate reductase 1 [*Os*]	2e-84
345	WAW	waw1c.pk002.b14	-0.08	-0.08	-0.10	-0.09	0.06	0.15	0.05	0.02	similar to NBS-LRR type resistance gene [*Os*]	1e-15
346	WAW	waw1c.pk002.b15	-0.02	-0.06	-0.06	0.02	0.03	0.03	-0.04	0.05	no homologies found	-
347	WAW	waw1c.pk002.b16	-0.10	0.03	0.15	0.07	-0.02	-0.02	-0.05	-0.09	DNA ligase IV [*At*]	1e-49
348	WAW	waw1c.pk002.b17	0.23	0.16	0.15	0.08	0.02	-0.04	-0.06	-0.18	translation initiation factor eIF-2 gamma subunit, putative; protein id: At1g04170.1,	8e-88
349	WAW	waw1c.pk002.b18	0.24	0.08	0.12	0.17	-0.05	-0.05	-0.07	-0.08	Argonaute (AGO1)-like protein [*At*]	2e-86
350	WAW	waw1c.pk002.b19	0.05	0.02	-0.02	0.00	-0.08	-0.01	-0.05	-0.01	hypothetical protein; protein id: At4g25330.1 [*At*]	9e-4
351	WAW	waw1c.pk002.b20	0.76	1.53	1.53	1.66	2.09	0.19	0.22	0.11	no homologies found	-
352	WAW	waw1c.pk002.b21	0.21	-0.01	0.04	0.00	-0.08	-0.10	-0.05	-0.09	Tubulin alpha chain	2e-92

			Temporal *M*					*Ph* mutant *M*				
#	ID	EST name	PM	LP	DA	TT	T	*1b*	*2a*	*2b*	Top BLASTx hit	e-val
353	WAW	waw1c.pk002.b22	0.24	-0.07	-0.23	0.04	0.00	0.06	-0.07	-0.15	hypothetical protein [*Os*]	3e-15
354	WAW	waw1c.pk002.b23	0.10	0.09	0.11	0.10	0.09	0.08	-0.12	-0.01	nicotianamine aminotransferase [*Hv* subsp. vulgare]	5e-96
355	WAW	waw1c.pk002.b24	-0.42	-0.63	-0.56	-0.36	-0.45	0.13	-0.05	0.17	no homologies found	-
356	WAW	waw1c.pk002.b3	0.01	0.25	0.36	0.40	0.25	-0.02	0.05	-0.03	hypothetical protein F15B8.20 - *At*	3e-25
357	WAW	waw1c.pk002.b4	-0.04	0.03	0.06	-0.04	0.11	0.01	-0.07	0.11	Dof zinc finger protein [*Os*]	3e-34
358	WAW	waw1c.pk002.b5	0.04	0.01	0.09	0.15	0.03	0.04	-0.06	0.02	expressed protein; protein id: At1g21200.1 [*At]*	3e-10
359	WAW	waw1c.pk002.b6	-0.11	-0.20	-0.26	-0.15	-0.01	-0.03	0.10	0.08	cold acclimation protein WCOR413-like protein beta form [*Ta*]	1e-84
360	WAW	waw1c.pk002.b8	-2.56	-2.16	-2.99	-2.98	-0.16	0.03	0.00	-0.37	hypothetical protein YY2 - rice	6e-11
361	WAW	waw1c.pk002.b9	0.12	0.02	-0.07	0.08	-0.01	0.03	-0.01	-0.02	14-3-3-like protein A (14-3-3A)	2e-74
362	WAW	waw1c.pk002.c1	-0.38	-0.42	-0.38	-0.33	-0.63	-0.09	-0.17	0.02	unknown protein [*Os*]	4e-52
363	WAW	waw1c.pk002.c10	0.01	0.03	0.08	0.01	-0.06	0.10	-0.03	-0.04	P0010B10.21 [*Os*]	6e-50
364	WAW	waw1c.pk002.c12	-0.02	-0.05	-0.19	-0.05	-0.11	-0.06	0.03	-0.07	no homologies found	-
365	WAW	waw1c.pk002.c14	0.16	0.02	-0.08	0.05	0.10	-0.05	0.04	0.02	Putative cyclin-dependent kinase regulatory subunit [*Os*]	3e-38
366	WAW	waw1c.pk002.c16	1.30	0.49	0.35	0.47	0.50	0.03	-0.02	-0.26	acetyl-CoA synthetase [*St*]	1e-109
367	WAW	waw1c.pk002.c17	-0.73	0.16	0.47	0.24	0.36	0.01	0.04	0.06	MtN3 [Medicago truncatula]	3e-26
368	WAW	waw1c.pk002.c18	-0.26	-0.39	-0.19	-0.37	-0.54	-0.02	-0.07	-0.09	putative protein; protein id: At4g10850.1 [*At*]	3e-36
369	WAW	waw1c.pk002.c2	-0.77	-0.43	-0.29	-0.31	-0.51	0.14	0.11	-0.01	sucrase-like protein; protein id: At4g26620.1 [*At]*	5e-36
370	WAW	waw1c.pk002.c20	0.06	0.03	-0.04	0.06	-0.08	-0.04	-0.17	-0.12	no homologies found	-
371	WAW	waw1c.pk002.c22	-0.11	0.03	-0.11	-0.01	-0.04	0.10	-0.07	0.16	Peroxidase 40 precursor (Atperox P40)	1e-36
372	WAW	waw1c.pk002.c24	-0.14	0.57	0.59	0.35	0.45	-0.06	0.01	0.09	sulfate adenylyltransferase (EC 2.7.7.4) - maize	1e-101
373	WAW	waw1c.pk002.c3	-0.13	-0.19	-0.17	-0.12	-0.19	0.04	-0.02	0.04	putative protein; protein id: At5g52560.1 [*At*]	5e-50
374	WAW	waw1c.pk002.c5	0.24	0.24	0.15	0.26	0.23	0.06	0.03	0.01	TaWIN1 [*Ta*]	5e-70
375	WAW	waw1c.pk002.c6	0.06	0.02	-0.22	-0.03	-0.14	-0.03	-0.04	0.07	no homologies found	-
376	WAW	waw1c.pk002.d1	0.14	0.20	-0.10	0.08	-0.08	0.08	-0.03	0.05	cysteine-rich hair keratin associated protein - rabbit	0.76
377	WAW	waw1c.pk002.d10	0.08	0.07	-0.02	0.11	0.06	0.01	0.01	0.05	no homologies found	-
378	WAW	waw1c.pk002.d12	-0.05	-0.20	-0.07	-0.04	-0.10	0.02	0.08	0.07	nitrate transporter NTL1, putative; protein id:At1g33440.1 [*At*]	5e-12
379	WAW	waw1c.pk002.d14	0.13	0.12	0.09	0.27	0.07	-0.03	0.06	0.10	no homologies found	-
380	WAW	waw1c.pk002.d15	1.89	1.54	1.41	1.16	1.65	-0.01	-0.07	0.01	small heat shock protein Hsp23.6 [*Ta*]	6e-55
381	WAW	waw1c.pk002.d16	0.35	0.29	0.24	0.18	0.37	-0.04	0.08	0.01	P0501G01.6 [*Os*]	1e-46
382	WAW	waw1c.pk002.d17	0.02	0.07	0.22	0.17	0.25	0.05	0.11	-0.02	putative purple acid phosphatase [*Os*]	1e-43
383	WAW	waw1c.pk002.d18	-0.05	-0.05	-0.05	0.05	0.05	0.03	-0.10	0.05	no homologies found	-
384	WAW	waw1c.pk002.d19	1.76	0.88	0.59	0.68	0.77	0.14	0.15	-0.06	histone H4 [Allium cepa]	1e-18
385	WAW	waw1c.pk002.d2	0.08	-0.01	0.22	-0.05	0.11	-0.01	0.05	0.03	P0005A05.26 [*Os*]	9e-95
386	WAW	waw1c.pk002.d20	0.01	-0.08	-0.25	0.00	0.01	-0.06	-0.07	0.00	nitrate transporter NTL1, putative; protein id:At1g33440.1 [*At*]	5e-12
387	WAW	waw1c.pk002.d21	0.11	0.00	-0.04	-0.03	-0.14	0.10	-0.07	-0.04	hypothetical protein; protein id: At1g49540.1 [*At*]	3e-40
388	WAW	waw1c.pk002.d22	0.00	-0.01	-0.05	0.00	-0.04	-0.01	0.03	0.03	mitotic checkpoint protein-like; protein id: At5g49880.1 [*At*]	1e-17
389	WAW	waw1c.pk002.d24	-0.07	0.25	0.30	0.23	0.26	0.06	-0.08	0.09	no homologies found	-
390	WAW	waw1c.pk002.d3	-0.10	-0.01	0.05	-0.02	-0.05	-0.06	0.05	-0.05	programmed cell death 7; apoptosis-related protein ES18 [*Hs*]	0.25
391	WAW	waw1c.pk002.d4	-0.08	-0.03	-0.05	0.16	-0.01	0.00	-0.04	0.03	contains ESTs D47783 (S13470), AU081374 (S13470)~unknown protein [*Os*]	5e-24
392	WAW	waw1c.pk002.d5	-0.46	0.02	0.03	0.31	0.16	0.09	-0.03	-0.06	putative tetrafunctional protein of glyoxysomal fatty acid beta-oxidation [*Os*]	4e-74
393	WAW	waw1c.pk002.d6	-0.12	0.00	0.00	0.04	-0.07	-0.10	-0.15	-0.06	H+-transporting two-sector ATPase (EC 3.6.3.14) beta chain, mitochondrial - wheat	3e-45
394	WAW	waw1c.pk002.d7	0.06	0.10	0.16	0.05	0.28	0.00	-0.08	-0.02	putative thiolase [*Os*]	1e-60
395	WAW	waw1c.pk002.d8	-0.14	-0.15	0.00	-0.07	0.09	0.03	-0.04	-0.01	putative casein kinase [*Os*]	3e-68
396	WAW	waw1c.pk002.d9	-0.20	-0.09	0.00	-0.02	-0.04	0.03	-0.02	0.03	putative cinnamyl-alcohol dehydrogenase [*Os*]	1e-89
397	WAW	waw1c.pk002.e1	0.00	-0.10	-0.08	-0.06	0.01	0.04	-0.05	0.01	SP8 binding protein homolog - cucumber	5e-32
398	WAW	waw1c.pk002.e10	-0.06	0.36	0.50	0.19	0.68	0.01	0.04	0.32	PAPS-reductase-like protein [Catharanthus roseus]	1e-24
399	WAW	waw1c.pk002.e11	-0.06	-0.04	0.30	-0.07	-0.08	0.07	0.00	-0.10	no homologies found	-
400	WAW	waw1c.pk002.e12	0.03	-0.04	0.04	-0.05	-0.06	-0.06	-0.14	-0.10	Putative calmodulin-binding protein similar to ER66 [*Os*]	2e-43
401	WAW	waw1c.pk002.e13	0.05	0.10	0.10	0.16	0.06	0.00	-0.07	-0.07	Hypothetical protein [*Os*]	3e-18
402	WAW	waw1c.pk002.e16	1.26	0.47	0.49	0.42	0.53	-0.01	-0.04	-0.22	acetyl-CoA synthetase [*St*]	1e-109
403	WAW	waw1c.pk002.e18	-0.04	-0.06	-0.08	0.08	0.01	0.05	0.05	-0.01	no homologies found	-
404	WAW	waw1c.pk002.e19	-0.09	0.01	0.18	-0.04	0.19	0.03	-0.07	0.01	glycoside hydrolase family 47 family; protein id: At1g27520.1 [*At*]	4e-76
405	WAW	waw1c.pk002.e2	-0.72	-1.68	-1.56	-1.21	-1.87	0.07	-0.06	-0.19	P0460H02.14 [*Os*]	8e-08
406	WAW	waw1c.pk002.e20	-0.04	-0.01	0.16	-0.02	-0.17	-0.12	0.01	-0.01	putative tubby protein [*Os*]	1e-24
407	WAW	waw1c.pk002.e21	-0.14	-0.08	-0.06	0.03	-0.11	-0.01	-0.01	0.10	contains similarity to RNA-binding protein~gene_id:MPL12.3 [*At*]	0.3
408	WAW	waw1c.pk002.e22	0.13	0.02	0.17	0.10	0.19	0.09	0.01	-0.01	succinyl-CoA ligase alpha subunit [*Le*]	1e-79
409	WAW	waw1c.pk002.e24	0.01	0.00	0.04	0.04	0.04	-0.04	0.16	0.00	g-RICH	0.13
410	WAW	waw1c.pk002.e3	-0.07	-0.36	0.01	-0.22	-0.31	-0.06	-0.03	-0.12	putative 5-3 exoribonuclease [*Os*]	3e-76
411	WAW	waw1c.pk002.e4	0.37	0.17	0.27	0.10	0.12	-0.02	0.09	-0.12	no homologies found	-
412	WAW	waw1c.pk002.e6	-0.08	-0.10	0.11	-0.08	-0.07	-0.01	-0.06	-0.04	Hypothetical protein [*Os*]	1e-11
413	WAW	waw1c.pk002.e7	-0.01	-0.04	0.17	-0.02	0.01	-0.03	0.08	-0.02	nucleic acid binding protein - rice	4e-55
414	WAW	waw1c.pk002.e8	0.09	-0.09	-0.05	-0.08	-0.14	-0.05	-0.09	-0.04	Putative RNA-binding protein [*Os*]	7e-22
415	WAW	waw1c.pk002.e9	0.08	-0.05	-0.29	-0.33	-0.35	0.00	0.11	-0.26	glycine-rich RNA-binding protein GRP1 - wheat	1e-41
416	WAW	waw1c.pk002.f1	-0.28	-0.07	-0.07	-0.05	0.07	0.01	0.04	0.11	truncated acetyl Co-A acetyltransferase-like protein [*Hb*]	3e-40
417	WAW	waw1c.pk002.f10	0.01	-0.07	0.05	-0.03	-0.03	0.03	0.04	0.04	transcription factor HBP-1b(c1) - wheat (fragment)	6e-22
418	WAW	waw1c.pk002.f11	-0.14	-0.13	0.04	0.01	-0.18	-0.06	-0.02	-0.09	cyclic nucleotide-regulated ion channel, putative; protein id: At4g30360.1 [*At*]	0.39
419	WAW	waw1c.pk002.f12	0.08	0.02	-0.01	-0.05	-0.14	0.10	0.15	-0.04	no homologies found	-
420	WAW	waw1c.pk002.f13	-0.04	-0.06	-0.01	-0.01	-0.14	0.02	-0.01	-0.03	p6.9 [Heliocoverpa armigera nucleopolyhedrovirus G4]	0.15
421	WAW	waw1c.pk002.f14	-0.16	-0.21	-0.12	-0.29	-0.21	0.01	-0.06	-0.16	P-type ATPase [*Hv*]	1e-112
422	WAW	waw1c.pk002.f15	-0.29	-0.17	-0.19	-0.12	-0.20	0.04	-0.13	-0.02	protein disulfide isomerase, putative; protein id: At1g35620.1 [*At*]	2e-61
423	WAW	waw1c.pk002.f16	-0.05	-0.13	-0.14	-0.11	-0.23	-0.04	-0.08	0.09	putative resistance protein [*Tm*]	4e-16
424	WAW	waw1c.pk002.f18	0.11	0.00	0.15	0.04	0.01	-0.03	-0.11	-0.03	no homologies found	-
425	WAW	waw1c.pk002.f19	-0.67	-0.52	-0.62	-0.44	-0.48	0.07	0.20	0.14	chlorophyll a/b-binding protein CP29 precursor - barley	3e-28
426	WAW	waw1c.pk002.f2	0.18	0.00	0.02	0.01	0.10	0.05	-0.05	-0.16	Proteasome subunit alpha type 5 (20S proteasome alpha subunit E) (20S proteasome subunit alpha-5)	4e-52
427	WAW	waw1c.pk002.f20	-0.34	-0.55	-0.18	-0.44	-0.62	0.03	-0.10	0.01	Lipoxygenase 1	1e-20
428	WAW	waw1c.pk002.f21	0.09	0.01	0.08	0.10	-0.03	0.10	-0.04	0.01	OJ1174_D05.12 [*Os*]	7e-33
429	WAW	waw1c.pk002.f22	-1.26	-0.92	-0.40	-0.81	-0.53	-0.02	0.00	-0.21	EST AU029260(E30024) corresponds to a region of the predicted gene.~Similar to *At* rd22 gene.	2e-17
430	WAW	waw1c.pk002.f23	-0.47	-0.01	0.11	0.29	0.19	0.04	-0.02	0.05	putative tetrafunctional protein of glyoxysomal fatty acid beta-oxidation [*Os*]	5e-71
431	WAW	waw1c.pk002.f24	-0.97	-0.01	-0.15	-0.23	0.86	0.07	0.05	0.25	no homologies found	-
432	WAW	waw1c.pk002.f3	0.27	0.20	0.19	0.23	0.06	-0.17	-0.12	-0.05	Eukaryotic translation initiation factor 3 subunit 8 (eIF3 p110) (eIF3c)	4e-35
433	WAW	waw1c.pk002.f7	-0.07	-0.15	-0.03	-0.15	-0.32	-0.04	-0.08	0.05	alternative oxidase [*Ta*]	8e-55
434	WAW	waw1c.pk002.f8	-0.13	-0.25	-0.16	-0.20	-0.16	0.00	-0.01	0.05	nonclathrin coat protein zeta2-COP [*Zm*]	2e-64
435	WAW	waw1c.pk002.f9	-0.07	0.02	0.03	0.01	0.18	-0.08	-0.11	0.16	HSP70 [*Ta*]	9e-85
436	WAW	waw1c.pk002.g1	-0.05	-0.14	-0.25	-0.14	0.27	-0.14	-0.12	-0.09	4-coumarate--CoA ligase 4CL3 [*Lp*]	6e-46

			Temporal *M*					*Ph* mutant *M*				
#	ID	EST name	PM	LP	DA	TT	T	*1b*	*2a*	*2b*	Top BLASTx hit	e-val
437	WAW	waw1c.pk002.g10	0.86	0.02	0.05	0.19	-0.03	-0.20	-0.39	-0.54	P0492F05.26 [*Os*]	2e-59
438	WAW	waw1c.pk002.g11	0.15	0.33	0.90	0.20	0.13	0.00	-0.04	-0.10	no homologies found	-
439	WAW	waw1c.pk002.g12	0.20	0.11	0.10	0.17	-0.09	0.05	0.02	0.10	60S ribosomal protein L3	1e-10
440	WAW	waw1c.pk002.g14	-0.02	-0.10	-0.03	-0.12	0.18	0.05	-0.09	-0.02	26S proteasome regulatory subunit (RPN6), putative; protein id: At1g29150.1	9e-46
441	WAW	waw1c.pk002.g15	0.10	0.01	0.05	-0.04	0.02	0.03	-0.02	-0.17	hypothetical protein FLJ14166 [*Hs*]	0.22
442	WAW	waw1c.pk002.g17	0.26	0.01	0.04	0.03	-0.12	0.03	-0.06	0.08	no homologies found	-
443	WAW	waw1c.pk002.g18	-0.35	-0.27	-0.21	-0.20	-0.17	0.09	0.05	0.06	Triosephosphate isomerase, cytosolic (TIM)	2e-44
444	WAW	waw1c.pk002.g19	0.15	-0.12	-0.10	-0.08	-0.21	0.03	0.07	-0.09	40S ribosomal protein S4	4e-80
445	WAW	waw1c.pk002.g2	0.05	0.00	0.25	0.05	-0.02	0.04	0.03	0.04	hypothetical protein; protein id: At4g31200.1 [*At*]	4e-45
446	WAW	waw1c.pk002.g20	-1.47	0.31	0.97	0.56	1.33	0.02	-0.03	-0.17	contains ESTs C73631(E20015),C99434(E20015)~unknown protein [*Os*]	3e-18
447	WAW	waw1c.pk002.g22	-0.07	0.46	0.70	0.56	0.61	-0.05	0.00	-0.13	dwarf protein, OSDIM - rice	5e-75
448	WAW	waw1c.pk002.g23	0.46	0.16	0.21	0.10	-0.05	0.01	-0.01	-0.03	guanine nucleotide-binding protein beta subunit-like protein (GPB-LR) (RWD)	3e-67
449	WAW	waw1c.pk002.g24	-0.39	-0.19	-0.28	-0.12	-0.05	-0.09	-0.07	0.41	S-adenosylmethionine decarboxylase precursor [*Ta*]	1e-102
450	WAW	waw1c.pk002.g3	-0.06	-0.33	-0.34	-0.36	-0.25	-0.02	-0.06	-0.04	synaptobrevin 7B, putative; protein id: At1g04750.1 [*At*]	8e-25
451	WAW	waw1c.pk002.g4	0.04	0.05	0.15	0.13	0.05	-0.06	-0.06	-0.02	streptococcal hemagglutinin protein [*Se* ATCC 12228]	0.032
452	WAW	waw1c.pk002.g6	0.14	0.07	-0.11	0.15	0.00	-0.06	-0.08	0.03	aldehyde dehydrogenase [*Os*]	1e-101
453	WAW	waw1c.pk002.h1	0.00	-0.04	-0.08	-0.05	-0.03	-0.01	-0.03	0.00	no homologies found	-
454	WAW	waw1c.pk002.h10	0.21	0.09	0.16	0.16	-0.04	-0.08	0.07	-0.01	putative alpha-glucosidase 1 [*Os*]	6e-57
455	WAW	waw1c.pk002.h12	0.24	0.29	0.35	0.30	0.30	0.05	0.00	0.02	hypothetical protein F6I7.10 - *At*	2e-29
456	WAW	waw1c.pk002.h13	0.38	0.27	0.29	0.37	0.18	-0.07	-0.09	0.04	aspartate-tRNA ligase homolog F6E21.100 - *At*	3e-64
457	WAW	waw1c.pk002.h14	-0.30	-0.10	0.08	-0.07	-0.10	0.04	0.02	-0.09	EST AU082557(R0845) corresponds to a region of the predicted gene.~Similar to *At* cystathionine	4e-56
458	WAW	waw1c.pk002.h15	-0.08	-0.01	0.05	0.06	0.07	-0.04	-0.04	0.01	no homologies found	-
459	WAW	waw1c.pk002.h16	-0.02	-0.15	-0.08	0.11	-0.03	0.00	-0.04	-0.05	putative protein; protein id: At5g23850.1 [*At*]	2e-50
460	WAW	waw1c.pk002.h17	-0.53	-0.42	-0.55	-0.39	-0.24	0.05	0.06	-0.13	cysteine proteinase (EC 3.4.22.-), glucose starvation-induced - maize (fragment)	1e-46
461	WAW	waw1c.pk002.h19	0.16	0.06	0.21	0.08	0.06	-0.09	-0.12	-0.09	Argonaute (AGO1)-like protein [*At*]	3e-25
462	WAW	waw1c.pk002.h2	0.07	0.13	-0.04	0.15	0.19	0.06	0.03	-0.03	Ubiquinol-cytochrome C reductase iron-sulfur subunit, mitochondrial precursor (Rieske iron-sulfur protein) (RISP)	6e-85
463	WAW	waw1c.pk002.h20	0.14	0.35	0.44	0.35	0.24	0.02	-0.06	-0.23	no homologies found	-
464	WAW	waw1c.pk002.h21	-0.08	0.33	0.16	0.32	0.23	-0.03	0.00	-0.08	Cysteine synthase (O-acetylserine sulfhydrylase) (O-acetylserine (Thiol)-lyase) (CSase A) (OAS-TL A)	2e-27
465	WAW	waw1c.pk002.h22	0.15	0.19	-0.05	0.04	-0.05	-0.03	-0.03	0.02	no homologies found	-
466	WAW	waw1c.pk002.h24	0.20	0.22	0.14	0.03	0.05	-0.03	-0.13	-0.08	putative serine protease [*Os*]	4e-14
467	WAW	waw1c.pk002.h3	0.43	1.94	2.24	2.02	2.29	0.02	0.02	0.10	beta-N-acetylhexosaminidase -like protein [*Os*]	0.57
468	WAW	waw1c.pk002.h4	-0.19	-0.19	-0.07	-0.20	-0.24	-0.02	-0.09	-0.08	cellulose synthase-1 [*Zm*]	1e-112
469	WAW	waw1c.pk002.h7	0.40	0.01	-0.29	-0.02	-0.13	0.00	0.06	0.17	putative 60S acidic ribosomal protein P2A [*Os*]	1e-29
470	WAW	waw1c.pk002.h8	-0.06	0.14	-0.06	-0.03	0.36	0.00	0.01	0.08	RNA-binding protein, putative; protein id: At1g32790.1	3e-25
471	WAW	waw1c.pk002.h9	-0.39	-0.04	0.37	-0.08	-0.13	0.00	-0.02	-0.14	bHLH protein; protein id: At2g16910.1 [*At*]	0.47
472	WAW	waw1c.pk002.i1	0.13	0.01	-0.22	-0.06	0.00	0.07	0.06	0.07	no homologies found	-
473	WAW	waw1c.pk002.i10	0.05	0.14	-0.01	0.01	0.11	-0.02	-0.02	0.04	hypothetical protein; protein id: At3g04740.1 [*At*]	5e-53
474	WAW	waw1c.pk002.i12	0.15	0.08	0.05	0.04	-0.01	-0.01	0.04	-0.05	SET domain protein 110 [*Zm*]	4e-26
475	WAW	waw1c.pk002.i13	1.22	1.10	0.65	1.31	0.94	0.01	-0.05	0.06	small heat shock protein Hsp23.6 [*Ta*]	2e-61
476	WAW	waw1c.pk002.i14	-0.34	-0.59	-0.59	-0.38	-0.35	-0.05	-0.06	-0.07	contains ESTs AU094020(E1880),AU094021(E1880)~similar to protein kinase SRPK2 (serine/arginine-rich protein-specific	6e-32
477	WAW	waw1c.pk002.i15	-0.59	-0.33	-0.27	-0.15	-0.26	0.08	-0.03	0.02	xanthine dehydrogenase 1 [*At*]	4e-82
478	WAW	waw1c.pk002.i16	-0.09	-0.05	-0.12	0.15	-0.08	0.12	0.04	0.18	putative ATP synthase; protein id: At2g21870.1	3e-26
479	WAW	waw1c.pk002.i18	1.40	0.62	0.61	0.56	0.63	0.01	-0.03	-0.33	histone H2A.2 - wheat	2e-45
480	WAW	waw1c.pk002.i22	0.06	0.01	0.10	0.06	0.06	-0.02	0.03	-0.02	putative protein; protein id: At5g49830.1 [*At*]	1e-53
481	WAW	waw1c.pk002.i24	0.23	0.12	0.19	0.19	0.17	-0.07	-0.12	-0.03	Putative cyclin-dependent kinase regulatory subunit [*Os*]	3e-38
482	WAW	waw1c.pk002.i3	-0.05	0.01	0.06	-0.04	-0.15	0.05	-0.22	0.06	OSJNBb0024F06.14 [*Os*]	2e-87
483	WAW	waw1c.pk002.i4	-0.02	0.07	-0.11	0.03	-0.02	-0.07	-0.02	0.08	NADP-dependant malate dehydrogenase [Sorghum verticilliflorum]	3e-40
484	WAW	waw1c.pk002.i6	-0.02	-0.02	-0.01	0.03	0.02	0.06	-0.02	0.01	unknown protein [*At*]	0.34
485	WAW	waw1c.pk002.i8	-0.18	-0.15	-0.16	-0.11	-0.04	-0.01	-0.03	0.11	putative protein; protein id: At4g25730.1 [*At*]	4e-09
486	WAW	waw1c.pk002.i9	0.19	0.11	0.12	0.15	-0.10	0.04	-0.04	-0.07	60S ribosomal protein L5	5e-68
487	WAW	waw1c.pk002.j1	-0.18	-0.08	-0.02	-0.02	-0.05	-0.02	-0.11	-0.02	CTV.22 [Poncirus trifoliata]	2e-46
488	WAW	waw1c.pk002.j10	0.08	-0.11	-0.27	-0.13	-0.09	0.04	0.09	-0.02	no homologies found	-
489	WAW	waw1c.pk002.j12	-0.02	-0.04	-0.04	0.02	-0.14	0.00	-0.01	-0.01	hypothetical protein [*Hv* subsp. vulgare]	2e-61
490	WAW	waw1c.pk002.j13	-0.08	-0.04	-0.09	-0.11	-0.13	-0.10	-0.03	-0.04	putative 1-aminocyclopropane-1-carboxylate deaminase [Betula pendula]	2e-71
491	WAW	waw1c.pk002.j14	0.55	0.24	0.11	0.17	0.01	0.02	-0.01	-0.05	guanine nucleotide-binding protein beta subunit-like protein (GPB-LR) (RWD)	2e-61
492	WAW	waw1c.pk002.j15	0.05	-0.02	-0.24	0.08	-0.05	0.00	-0.05	-0.01	hypothetical transmembrane protein L8032.05a [*Lm*]	0.97
493	WAW	waw1c.pk002.j16	0.24	-0.01	0.14	0.12	-0.10	0.05	-0.13	-0.17	hypothetical protein; protein id: At3g24780.1 [*At*]	3e-08
494	WAW	waw1c.pk002.j17	-0.07	-0.09	0.03	-0.01	-0.25	-0.01	-0.01	-0.09	protein phosphatase regulatory subunit-like [*Os*]	1e-44
495	WAW	waw1c.pk002.j18	-1.14	0.02	0.23	0.25	-0.10	0.01	0.02	-0.11	mitochondrial aldehyde dehydrogenase ALDH2 [*Hv* subsp. vulgare]	6e-48
496	WAW	waw1c.pk002.j19	-0.07	0.16	0.00	0.19	0.24	0.02	-0.06	0.15	no homologies found	-
497	WAW	waw1c.pk002.j2	-0.39	0.03	0.36	0.03	-0.17	0.00	-0.01	-0.13	bHLH protein; protein id: At2g16910.1 [*At*]	4e-17
498	WAW	waw1c.pk002.j21	-0.01	-0.10	0.21	0.05	-0.08	0.03	-0.05	0.08	Unknown protein [*Os*]	3e-76
499	WAW	waw1c.pk002.j22	0.04	0.04	0.18	0.08	-0.12	-0.03	-0.05	-0.14	hypothetical protein; protein id: At3g24780.1 [*At*]	3e-08
500	WAW	waw1c.pk002.j23	0.04	-0.05	-0.05	-0.10	-0.12	0.03	0.00	0.07	expressed protein; protein id: At2g32700.1 [*At*]	6e-26
501	WAW	waw1c.pk002.j24	0.15	0.02	-0.02	0.10	-0.05	-0.13	-0.03	-0.09	Tubulin alpha chain	2e-17
502	WAW	waw1c.pk002.j3	0.12	-0.08	0.30	-0.08	-0.04	0.05	0.12	-0.09	putative xyloglucan endotransglycosylase [*At*]	1e-19
503	WAW	waw1c.pk002.j4	0.08	-0.01	0.12	0.04	-0.06	-0.06	-0.06	-0.03	succinate dehydrogenase flavoprotein alpha subunit (emb|CAA05025.1); protein id: At5g66760.1	8e-69
504	WAW	waw1c.pk002.j5	-0.07	0.21	0.46	0.57	1.29	-0.02	-0.02	0.01	acetyl-CoA carboxylase	1e-102
505	WAW	waw1c.pk002.j6	0.00	-0.01	0.05	0.09	0.05	0.02	-0.11	-0.06	no homologies found	-
506	WAW	waw1c.pk002.j7	0.08	-0.02	-0.02	-0.08	-0.11	-0.08	-0.05	-0.12	OSJNBb0043H09.3 [*Os*]	3e-17
507	WAW	waw1c.pk002.j8	0.00	0.00	0.16	-0.02	-0.02	0.08	0.05	0.03	P0014E08.3 [*Os*]	6e-43
508	WAW	waw1c.pk002.j9	-0.06	0.09	0.03	0.01	0.07	0.02	0.11	0.09	isoflavone reductase homolog IRL	1e-49
509	WAW	waw1c.pk002.k1	0.61	0.08	-0.25	0.11	0.09	0.01	0.07	0.03	no homologies found	-
510	WAW	waw1c.pk002.k10	-0.07	0.00	0.02	-0.07	0.07	0.03	-0.15	0.01	no homologies found	-
511	WAW	waw1c.pk002.k11	0.16	0.02	0.11	0.01	-0.01	0.03	-0.04	-0.02	60S ribosomal protein L9	5e-32
512	WAW	waw1c.pk002.k12	0.57	0.96	0.81	1.09	1.16	0.11	0.06	0.19	hypothetical protein [Desulfitobacterium hafniense]	0.86
513	WAW	waw1c.pk002.k13	-0.15	-0.05	0.01	0.07	0.08	-0.01	0.14	0.00	hypoxanthine-guanine phosphoribosyltransferase 1 [*At*]	2e-32
514	WAW	waw1c.pk002.k14	0.08	-0.08	-0.18	0.00	-0.15	-0.04	-0.13	0.08	aldehyde dehydrogenase [*Os*]	7e-94
515	WAW	waw1c.pk002.k15	-0.44	-0.20	-0.22	-0.09	-0.07	-0.20	-0.12	0.29	OSJNBa0029H02.26 [*Os*]	8e-17
516	WAW	waw1c.pk002.k16	0.19	0.12	0.00	0.10	0.13	-0.03	-0.01	0.00	unknown protein; protein id: At2g34750.1 [*At*]	5e-06
517	WAW	waw1c.pk002.k17	0.08	0.06	0.00	0.04	0.05	0.05	-0.13	0.02	hypothetical protein [*At*]	6e-42
518	WAW	waw1c.pk002.k18	-0.05	-0.12	-0.11	-0.02	0.00	-0.01	0.05	0.04	no homologies found	-

#	ID	EST name	Temporal *M*					*Ph* mutant *M*			Top BLASTx hit	e-val
			PM	LP	DA	TT	T	*1b*	*2a*	*2b*		
519	WAW	waw1c.pk002.k2	-0.05	-0.10	0.12	-0.05	-0.03	0.16	0.00	-0.02	emb|CAB09999.1~gene_id:F4B12.6~similar to unknown protein [*At*]	1e-49
520	WAW	waw1c.pk002.k21	-0.06	-0.07	0.27	-0.08	-0.05	-0.01	0.06	-0.07	no homologies found	-
521	WAW	waw1c.pk002.k22	-1.66	-1.38	-0.07	-1.45	-0.05	-0.01	0.03	-0.01	unknown protein [*At*]	0.003
522	WAW	waw1c.pk002.k23	0.15	0.12	0.13	0.12	-0.01	0.13	-0.07	-0.03	very large virion protein (tegument) [Bovine herpesvirus 1]	0.098
523	WAW	waw1c.pk002.k4	0.30	0.14	0.03	0.10	0.08	-0.07	0.03	-0.05	no homologies found	-
524	WAW	waw1c.pk002.k6	0.03	-0.03	-0.10	-0.04	-0.07	0.02	0.10	0.01	no homologies found	-
525	WAW	waw1c.pk002.k7	-0.17	0.35	-0.26	0.16	0.07	0.17	0.19	0.02	putative CTP synthase [*Os*]	1e-11
526	WAW	waw1c.pk002.k8	-0.16	-0.35	-0.23	-0.43	-0.57	-0.04	-0.11	-0.07	putative protein; protein id: At4g10850.1 [*At*]	2e-28
527	WAW	waw1c.pk002.l1	0.03	-0.06	-0.13	0.01	-0.03	0.09	-0.02	0.14	putative ATP synthase; protein id: At2g21870.1	3e-26
528	WAW	waw1c.pk002.l10	0.10	-0.03	-0.09	-0.05	-0.02	-0.02	0.02	0.00	26S proteasome regulatory particle triple-A ATPase subunit1 [*Os*]	1e-93
529	WAW	waw1c.pk002.l11	-0.38	-0.79	-0.41	-0.68	-0.58	-0.06	-0.13	-0.13	H+-exporting ATPase (EC 3.6.3.6) - maize	1e-41
530	WAW	waw1c.pk002.l12	0.11	0.09	-0.10	0.08	0.02	0.00	0.04	-0.03	Dof zinc finger protein [*Os*]	3e-34
531	WAW	waw1c.pk002.l13	0.38	0.07	-0.01	0.00	-0.05	-0.06	-0.11	0.03	Eukaryotic peptide chain release factor subunit 1-3 (eRF1-3) (Eukaryotic release factor 1-3) (Omnipotent suppressor)	7e-83
532	WAW	waw1c.pk002.l14	0.16	-0.02	0.00	-0.01	-0.04	-0.01	0.06	0.00	B1008C01.10 [*Os*]	2e-13
533	WAW	waw1c.pk002.l16	-0.01	0.00	0.02	0.09	0.06	0.07	-0.14	0.02	hypothetical protein [*Os*]	2e-68
534	WAW	waw1c.pk002.l17	-0.24	-0.11	-0.09	0.02	-0.08	0.12	0.02	0.06	no homologies found	-
535	WAW	waw1c.pk002.l18	-0.21	-0.30	-0.29	-0.20	-0.15	-0.06	-0.11	0.00	putative DNA binding protein [*Os*]	4e-09
536	WAW	waw1c.pk002.l19	-0.23	-0.09	-0.07	-0.03	0.00	-0.01	-0.11	-0.02	non-cell-autonomous heat shock cognate protein 70 [*Cma*]	4e-97
537	WAW	waw1c.pk002.l20	0.03	-0.07	-0.06	0.03	0.02	-0.12	-0.09	0.03	putative protein; protein id: At4g38890.1 [*At*]	2e-32
538	WAW	waw1c.pk002.l21	-0.51	0.23	-0.33	0.19	0.01	-0.18	-0.24	-0.06	dehydrin COR410 (cold induced COR410 protein)	1e-44
539	WAW	waw1c.pk002.l22	0.25	0.06	-0.30	-0.02	-0.15	0.03	0.06	0.17	probable 12-oxophytodienoate reductase (EC 1.3.1.42) CPRD8, drought-inducible - cowpea	7e-86
540	WAW	waw1c.pk002.l23	-0.29	-0.19	-0.01	-0.10	0.01	0.02	-0.01	-0.09	no homologies found	-
541	WAW	waw1c.pk002.l24	0.16	0.22	0.14	0.21	0.13	0.00	0.04	-0.02	P0666G04.6 [*Os*]	5e-40
542	WAW	waw1c.pk002.l3	0.09	0.11	-0.05	0.08	0.10	0.04	-0.02	-0.03	OSJNBa0090K04.11 [*Os*]	0.11
543	WAW	waw1c.pk002.l4	0.07	-0.16	-0.19	-0.10	-0.07	-0.01	0.03	0.01	MAP kinase kinase [*Zm*]	0.02
544	WAW	waw1c.pk002.l5	0.02	0.10	0.22	0.02	0.09	-0.07	-0.03	-0.04	similar to 5-hydroxytryptamine receptor 3 subunit C [*Hs*]	0.2
545	WAW	waw1c.pk002.l6	-0.78	0.20	0.14	-0.09	0.15	0.04	-0.03	0.15	protein disulfide isomerase [Triticum turgidum subsp. durum]	2e-07
546	WAW	waw1c.pk002.l7	-0.03	0.13	0.20	0.21	0.12	-0.09	-0.03	-0.08	leucine-rich repeat protein; contains similarity to elicitor-inducible receptor EIR [*At*]	7e-64
547	WAW	waw1c.pk002.l8	0.04	-0.06	-0.10	0.07	-0.02	-0.14	-0.05	-0.05	hypothetical protein [*Os*]	6e-68
548	WAW	waw1c.pk002.l9	0.31	0.34	0.00	0.48	0.61	-0.06	-0.10	0.30	heat shock protein 70 homolog {clone CHEM 3} [*Zm*=maize, cv. INRA 258, mercuric chloride-treated, leaves, Peptide	0.073
549	WAW	waw1c.pk002.m1	-0.06	0.02	0.17	0.06	-0.02	0.00	0.01	0.09	no homologies found	-
550	WAW	waw1c.pk002.m10	0.17	-0.09	-0.04	-0.25	-0.31	0.12	0.07	-0.27	glycine-rich RNA-binding protein, low-temperature-responsive - barley	5e-39
551	WAW	waw1c.pk002.m11	-0.05	0.04	0.00	0.00	-0.04	0.09	0.00	0.03	no homologies found	-
552	WAW	waw1c.pk002.m12	-0.10	0.06	-0.02	0.09	-0.10	0.05	0.01	0.04	putative nuclear matrix protein [*Os*]	4e-5
553	WAW	waw1c.pk002.m13	-0.29	0.02	0.28	0.00	-0.15	0.07	0.01	-0.13	bHLH protein; protein id: At2g16910.1 [*At*]	6e-16
554	WAW	waw1c.pk002.m14	0.06	-0.02	-0.04	-0.09	0.00	-0.04	-0.02	0.13	no homologies found	-
555	WAW	waw1c.pk002.m15	-0.07	-0.15	-0.10	-0.18	-0.08	0.00	0.11	-0.09	cyclin [*Os*]	2e-12
556	WAW	waw1c.pk002.m16	0.13	0.04	0.01	0.02	0.03	0.00	0.01	0.02	Similar to *At* DNA chromosome 4, ESSA I contig fragment No. 6; calcium channel protein alpha-1 chain	2e-76
557	WAW	waw1c.pk002.m17	-1.42	-0.79	-0.56	-0.74	-0.69	0.23	0.11	-0.01	Chlorophyll A-B binding protein, chloroplast precursor (LHCII type I CAB) (LHCP)	5e-65
558	WAW	waw1c.pk002.m18	0.02	-0.04	-0.04	-0.01	-0.06	-0.03	0.07	0.01	putative protein; protein id: At4g25730.1 [*At*]	4e-10
559	WAW	waw1c.pk002.m2	0.72	0.22	0.02	0.11	0.07	-0.09	-0.02	0.27	contains similarity to O-linked GlcNAc transferase~gb|AAB84589.1~gene_id:K14A17.11 [*At]*	7e-72
560	WAW	waw1c.pk002.m20	0.20	-0.12	-0.10	-0.09	-0.16	0.08	-0.06	0.16	hypothetical protein; protein id: At1g05950.1 [*At*]	7e-08
561	WAW	waw1c.pk002.m21	-0.06	0.06	-0.14	0.10	-0.13	0.01	-0.07	0.14	unnamed protein product [*Os*]	1e-10
562	WAW	waw1c.pk002.m22	0.01	0.00	-0.20	0.01	-0.11	-0.03	-0.06	0.08	no homologies found	-
563	WAW	waw1c.pk002.m23	0.06	0.04	-0.04	0.14	-0.02	-0.02	0.02	0.00	Elongation factor 1-alpha (EF-1-APLHA)	4e-79
564	WAW	waw1c.pk002.m24	0.17	0.14	0.10	-0.01	-0.06	-0.04	0.01	-0.01	putative receptor-like protein [*Os*]	1e-96
565	WAW	waw1c.pk002.m3	0.27	-0.03	-0.22	-0.09	-0.19	-0.15	-0.07	-0.05	Elongation factor 2 (EF-2)	2e-98
566	WAW	waw1c.pk002.m4	-0.14	-0.09	-0.03	0.00	-0.07	0.03	0.04	0.05	cytoplasmic aconitate hydratase; protein id: At2g05710.1 [*At*]	2e-68
567	WAW	waw1c.pk002.m6	-0.06	-0.20	-0.05	-0.07	-0.16	0.19	-0.10	-0.03	no homologies found	-
568	WAW	waw1c.pk002.m7	-0.05	-0.12	0.03	-0.10	-0.02	-0.05	-0.10	0.02	Ubiquitin-activating enzyme E1 2	6e-49
569	WAW	waw1c.pk002.m8	0.08	-0.13	-0.24	-0.08	-0.31	-0.02	0.01	0.03	no homologies found	-
570	WAW	waw1c.pk002.n1	-0.51	-0.61	-0.34	-0.63	-0.41	0.06	-0.03	0.01	MADS box transcription factor [*Ta*]	1e-68
571	WAW	waw1c.pk002.n12	-0.29	-0.12	-0.02	-0.02	0.25	0.03	-0.01	0.08	Putative inositol 1,3,4-trisphosphate 5/6-kinase [*Os*]	1e-98
572	WAW	waw1c.pk002.n13	0.07	-0.04	-0.11	-0.03	-0.08	0.04	0.06	-0.07	unconventional myosin XI [Vallisneria gigantea]	0.36
573	WAW	waw1c.pk002.n15	0.08	-0.07	0.02	0.00	-0.03	0.09	-0.13	-0.01	no homologies found	-
574	WAW	waw1c.pk002.n16	-0.02	0.24	0.66	0.48	0.29	0.17	0.06	0.10	no homologies found	-
575	WAW	waw1c.pk002.n17	0.13	0.45	0.43	0.42	0.20	0.02	-0.04	0.00	expressed protein; protein id: At3g19460.1 [*At*]	3e-15
576	WAW	waw1c.pk002.n2	0.00	0.14	-0.14	0.03	0.03	-0.05	0.04	0.05	expressed protein; protein id: At1g02390.1 [*At]*	1e-29
577	WAW	waw1c.pk002.n20	0.20	-0.14	-0.17	-0.06	-0.20	0.13	-0.04	0.11	nascent polypeptide associated complex alpha chain, putative; protein id: At3g12390.1 [*At*]	4e-44
578	WAW	waw1c.pk002.n21	-0.32	-0.37	-0.47	-0.29	-0.49	-0.03	0.04	0.15	no homologies found	-
579	WAW	waw1c.pk002.n23	-0.05	-0.05	-0.04	-0.01	0.04	-0.01	0.01	0.04	protein F8K7.16 [imported] - *At*	2e-05
580	WAW	waw1c.pk002.n4	0.25	-0.08	-0.16	-0.13	-0.25	0.02	-0.03	-0.13	Importin beta-like protein [*Os* (indica cultivar-group)]	5e-93
581	WAW	waw1c.pk002.n5	0.04	-0.02	0.04	-0.10	-0.11	-0.01	-0.04	-0.04	Similar to putative SEC14 cytosolic factor. (Q10137) [*Os*]	4e-58
582	WAW	waw1c.pk002.n6	0.01	0.07	0.12	0.00	0.05	0.03	-0.09	0.01	EST AU082557(R0845) corresponds to a region of the predicted gene.~Similar to *At* cystathionine	1e-54
583	WAW	waw1c.pk002.n7	-0.06	0.01	-0.10	0.04	-0.11	-0.07	-0.01	0.04	no homologies found	-
584	WAW	waw1c.pk002.n8	-0.13	-0.36	-0.19	-0.33	-0.39	0.03	0.01	-0.02	adenosine kinase [*Zm*]	1e-103
585	WAW	waw1c.pk002.n9	0.04	0.03	-0.03	0.05	-0.05	-0.05	-0.03	-0.01	putative protein kinase [*Os*]	0.005
586	WAW	waw1c.pk002.o1	0.19	-0.04	-0.05	-0.04	-0.03	0.15	0.05	0.13	putative 60s Ribosomal protein L25 [*Os* (indica cultivar-group)]	7e-48
587	WAW	waw1c.pk002.o11	0.94	0.13	0.34	0.08	0.20	-0.10	-0.16	-0.27	leaf development protein Argonaute; protein id: At1g48410.1[*At*]	1e-23
588	WAW	waw1c.pk002.o12	-0.16	-0.22	-0.16	-0.15	-0.20	0.00	0.09	-0.04	Cysteine proteinase 1 precursor	3e-62
589	WAW	waw1c.pk002.o14	-0.44	-0.38	-0.11	-0.46	-0.39	-0.05	-0.08	-0.15	Adenosylhomocysteinase (S-adenosyl-L-homocysteine hydrolase) (AdoHcyase)	2e-87
590	WAW	waw1c.pk002.o16	-0.07	-0.13	0.05	-0.07	-0.05	-0.04	-0.14	-0.02	no homologies found	-
591	WAW	waw1c.pk002.o17	1.61	0.82	0.73	0.76	0.72	0.04	-0.01	-0.23	histone H2B153 - wheat	1e-53
592	WAW	waw1c.pk002.o18	0.35	0.17	0.37	-0.01	0.12	0.03	0.08	-0.09	xyloglucan endotransglycosylase, putative; protein id: At4g03210.1:	1e-42
593	WAW	waw1c.pk002.o19	0.09	0.13	-0.02	0.07	-0.05	-0.08	0.00	0.01	unknown protein; protein id: At3g48380.1 [*At*]	2e-23
594	WAW	waw1c.pk002.o2	0.31	0.05	0.10	-0.06	-0.10	0.00	0.02	-0.05	probable tyrosine-tRNA ligase (EC 6.1.1.1) - common tobacco	4e-43
595	WAW	waw1c.pk002.o20	-0.12	0.41	0.08	0.24	0.06	0.18	0.23	0.04	putative lipid transfer protein [*Os*]	7e-24
596	WAW	waw1c.pk002.o21	-0.29	-0.29	-0.24	-0.32	-0.27	-0.04	-0.01	0.14	no homologies found	-
597	WAW	waw1c.pk002.o22	0.28	-0.02	-0.38	-0.08	-0.24	0.06	0.07	0.16	putative 60S acidic ribosomal protein P2A [*Os*]	5e-25

#	ID	EST name	Temporal *M*					*Ph* mutant *M*			Top BLASTx hit	e-val
			PM	LP	DA	TT	T	*1b*	*2a*	*2b*		
598	WAW	waw1c.pk002.o23	0.01	0.12	0.03	0.16	0.07	-0.09	-0.04	0.32	contains similarity to O-linked GlcNAc transferase~gb|AAB84589.1~gene_id:K14A17.11 [*At*]	6e-68
599	WAW	waw1c.pk002.o3	0.10	0.07	-0.03	0.01	0.05	0.06	0.01	-0.02	spliceosome associated protein - like [*At*]	2e-08
600	WAW	waw1c.pk002.o4	-0.35	-0.35	-0.11	-0.14	-0.08	0.03	-0.02	0.02	Vacuolar ATP synthase subunit B isoform 1 (V-ATPase B subunit 1) (Vacuolar proton pump B subunit 1)	4e-89
601	WAW	waw1c.pk002.o5	-0.01	0.03	-0.04	0.05	-0.06	0.08	0.06	0.05	no homologies found	-
602	WAW	waw1c.pk002.o6	0.09	0.24	0.56	0.20	0.19	0.03	-0.06	-0.06	S-adenosyl-L-methionine: L-methionine S-methyltransferase [*Hv*]	3e-66
603	WAW	waw1c.pk002.o7	-0.20	0.18	-0.07	0.15	-0.17	-0.08	0.12	0.01	unknown protein; protein id: At3g48380.1 [*At*]	7e-22
604	WAW	waw1c.pk002.o8	-0.21	-0.52	-0.69	-0.56	-0.51	0.06	0.10	0.08	no homologies found	-
605	WAW	waw1c.pk002.p1	-0.04	0.04	-0.08	0.00	-0.11	-0.02	0.10	0.01	no homologies found	-
606	WAW	waw1c.pk002.p10	0.00	-0.09	0.12	-0.07	0.08	0.00	0.09	0.02	similar to hypothetical protein Y39B6B.gg [imported] - *Ce* [*Mm*]	1e-12
607	WAW	waw1c.pk002.p11	0.00	-0.01	-0.11	-0.05	0.03	0.00	0.01	-0.02	no homologies found	-
608	WAW	waw1c.pk002.p12	-0.09	-0.03	-0.13	-0.07	-0.02	-0.06	-0.04	0.01	KIAA0301 [*Hs*]	0.056
609	WAW	waw1c.pk002.p13	-0.24	-0.14	-0.26	-0.55	0.23	-0.08	-0.17	0.17	Luminal binding protein 2 precursor (BiP2) (Heat shock protein 70 homolog 2) (B70) (B-70)	2e-20
610	WAW	waw1c.pk002.p15	-0.33	-0.03	-0.75	-0.18	-0.48	0.06	0.07	0.06	hypothetical protein [Stx2 converting bacteriophage I]	0.81
611	WAW	waw1c.pk002.p16	-2.29	-2.29	-2.65	-2.82	-2.89	0.04	0.20	0.16	T17H7.4 [*At*]	0.6
612	WAW	waw1c.pk002.p17	-0.08	0.30	0.45	0.31	0.27	0.04	-0.08	-0.06	P0470A12.7 [*Os*]	2e-91
613	WAW	waw1c.pk002.p18	0.00	0.28	0.40	0.38	0.14	0.03	-0.01	0.04	no homologies found	-
614	WAW	waw1c.pk002.p19	0.17	-0.02	-0.08	0.01	-0.05	0.05	0.10	-0.04	kinesin-like protein K8 [*Dd*]	0.63
615	WAW	waw1c.pk002.p2	-0.33	-0.18	0.19	0.14	0.17	-0.03	0.06	0.14	P0665D10.11 [*Os*]	3e-45
616	WAW	waw1c.pk002.p20	-0.09	0.11	0.08	0.10	0.09	0.03	0.01	0.04	unknown protein; protein id: At1g25682.1 [*At*]	2e-64
617	WAW	waw1c.pk002.p21	0.26	0.16	0.15	0.18	-0.01	0.00	0.04	-0.06	60S ribosomal protein L7A	3e-24
618	WAW	waw1c.pk002.p22	0.02	0.09	-0.01	0.07	0.07	0.02	0.06	-0.05	putative cleavage and polyadenylation specificity factor; protein id: At1g61010.1	3e-24
619	WAW	waw1c.pk002.p23	0.29	0.06	-0.18	0.08	-0.08	-0.07	0.09	0.03	hypothetical protein XP_109742 [*Mm*]	0.24
620	WAW	waw1c.pk002.p24	0.17	-0.04	-0.16	0.02	-0.07	0.03	0.11	0.04	P0529E05.20 [*Os*]	1e-50
621	WAW	waw1c.pk002.p3	-0.20	0.00	0.09	0.02	0.05	-0.01	-0.07	-0.06	putative DnaJ protein; protein id: At1g79940.1 [*At*]	5e-49
622	WAW	waw1c.pk002.p4	0.01	-0.06	-0.02	0.06	0.03	0.04	0.06	0.00	hypothetical protein [*Dr*]	0.43
623	WAW	waw1c.pk002.p5	0.02	0.22	0.12	0.10	-0.04	-0.01	0.06	0.03	putative CCAAT displacement protein [*Os*]	2e-71
624	WAW	waw1c.pk002.p6	-0.04	-0.02	-0.01	0.01	0.02	0.04	-0.07	-0.06	no homologies found	-
625	WAW	waw1c.pk002.p7	-0.26	-0.22	-0.31	-0.10	-0.03	-0.01	0.09	0.06	Actin-depolymerizing factor 3 (ADF 3) (ZmABP3) (ZmADF3)	7e-45
626	WAW	waw1c.pk003.a10	0.62	0.12	-0.05	0.03	-0.05	-0.04	0.03	0.11	hypothetical protein; protein id: At4g17120.1 [*At*]	7e-37
627	WAW	waw1c.pk003.a11	-0.22	-0.25	0.06	-0.20	-0.18	-0.08	0.03	-0.15	no homologies found	-
628	WAW	waw1c.pk003.a12	-0.80	-0.74	-0.70	-0.56	-0.51	0.07	0.13	-0.14	Phosphoglycerate kinase, chloroplast precursor	9e-83
629	WAW	waw1c.pk003.a15	0.01	0.00	0.01	-0.07	0.00	0.00	0.05	-0.05	no homologies found	-
630	WAW	waw1c.pk003.a16	-0.02	0.03	0.04	0.10	0.23	0.01	0.12	0.10	ESTs C99033(E4350),C99032(E4350),D46006(S10372), D47177(S12347),C28582(C61678),C27203(C51329)	7e-97
631	WAW	waw1c.pk003.a22	0.05	-0.04	-0.14	-0.09	0.02	-0.01	0.04	0.05	no homologies found	-
632	WAW	waw1c.pk003.a24	0.06	0.06	0.07	0.02	-0.06	0.02	0.06	-0.08	LlFtsZ [*Ll*]	2e-18
633	WAW	waw1c.pk003.a5	0.23	0.26	0.09	0.12	-0.01	-0.01	0.00	-0.24	putative translation initiation factor eIF-2, gamma subunit [*At*]	5e-12
634	WAW	waw1c.pk003.a7	0.12	0.61	0.52	0.47	0.52	0.08	0.04	0.03	Pyruvate kinase, cytosolic isozyme	1e-24
635	WAW	waw1c.pk003.a8	-0.37	-0.32	-0.40	-0.18	-0.18	0.00	0.04	0.05	contains ESTs AU094020(E1880),AU094021(E1880)~similar to protein kinase SRPK2	4e-08
636	WAW	waw1c.pk003.a9	0.56	0.37	0.39	0.19	0.28	-0.20	-0.25	-0.27	histone H1 (clone TH32) - wheat	4e-27
637	WAW	waw1c.pk003.b11	0.16	0.26	0.28	0.21	0.09	-0.13	-0.21	-0.07	60S ribosomal protein L4-B (L1) [*At*]	1e-70
638	WAW	waw1c.pk003.b12	-0.07	-0.20	-0.19	-0.24	-0.08	-0.04	0.03	-0.02	U2 snRNP auxiliary factor, small subunit [*Os*]	1e-56
639	WAW	waw1c.pk003.b13	0.10	-0.21	-0.17	-0.21	-0.06	-0.02	-0.05	-0.05	unknown protein; protein id: At2g37520.1 [*At*]	1e-08
640	WAW	waw1c.pk003.b14	0.26	0.14	0.04	0.25	0.05	0.06	-0.02	0.06	Putative mitotic control protein dis3 [*Os*]	5e-26
641	WAW	waw1c.pk003.b15	-0.04	-0.42	-0.47	-0.19	-0.31	-0.10	-0.27	-0.20	putative beta-alanine-pyruvate aminotransferase; protein id: At2g38400.1	2e-45
642	WAW	waw1c.pk003.b16	-0.09	-0.06	-0.07	-0.07	-0.03	0.02	0.13	0.00	unnamed protein product [*Os*]	0.17
643	WAW	waw1c.pk003.b17	0.26	0.22	0.34	0.35	0.25	-0.01	0.07	0.05	no homologies found	-
644	WAW	waw1c.pk003.b18	0.65	0.39	0.44	0.43	0.45	-0.08	-0.01	-0.10	hypothetical protein; protein id: At4g09810.1 [*At*]	2e-51
645	WAW	waw1c.pk003.b19	-0.32	-0.27	0.00	-0.03	-0.06	-0.01	0.00	-0.04	no homologies found	-
646	WAW	waw1c.pk003.b21	0.08	0.13	0.03	0.29	0.26	-0.12	-0.22	0.13	HSP80-2 [*Ta*]	7e-83
647	WAW	waw1c.pk003.b22	-0.07	0.12	0.20	0.08	0.23	0.04	0.00	0.05	putative late embryogenesis abundant protein [*Os*]	3e-52
648	WAW	waw1c.pk003.b23	0.03	0.14	0.13	0.09	0.02	0.04	-0.02	-0.01	unknown protein [*At*]	7e-43
649	WAW	waw1c.pk003.b24	-0.10	-0.01	-0.06	0.04	0.12	0.14	-0.01	0.09	putative immediate early protein [*Ah*]	3e-06
650	WAW	waw1c.pk003.b4	0.15	0.17	0.28	0.10	0.04	0.03	-0.09	-0.04	unknown protein [*At*]	4e-52
651	WAW	waw1c.pk003.b8	0.03	0.01	0.04	0.00	0.00	0.02	0.05	0.03	putative protein; protein id: At4g34360.1 [*At*]	7e-23
652	WAW	waw1c.pk003.b9	0.11	0.17	0.33	0.21	0.10	0.10	0.04	-0.04	prohibitin [*Zm*]	3e-77
653	WAW	waw1c.pk003.c1	0.01	0.03	0.23	-0.02	0.10	-0.05	-0.02	-0.06	hypothetical protein [Azotobacter vinelandii]	0.33
654	WAW	waw1c.pk003.c10	-0.01	0.00	-0.06	-0.04	-0.08	-0.01	-0.09	-0.04	protein phosphatase 2C [*Mc*]	1e-40
655	WAW	waw1c.pk003.c11	-0.31	-0.22	-0.39	-0.20	-0.26	0.10	-0.02	-0.05	ESTs AU082454(S3638),D41267(S3638) correspond to a region of the predicted gene.~Similar to *At* DNA	4e-65
656	WAW	waw1c.pk003.c15	0.82	0.26	0.19	0.10	0.29	-0.14	0.03	0.00	delta-COP [*Zm*]	6e-49
657	WAW	waw1c.pk003.c16	-0.15	-0.30	-0.10	-0.30	-0.17	0.07	0.00	0.10	putative phi-1-like phosphate-induced protein [*At*]	2e-15
658	WAW	waw1c.pk003.c17	-0.46	-0.49	-0.13	-0.36	-0.35	-0.11	-0.21	-0.09	polyubiquitin - maize	6e-38
659	WAW	waw1c.pk003.c18	0.15	-0.05	-0.28	-0.20	-0.25	-0.07	0.02	-0.16	DEAD/DEAH box RNA helicase, putative; protein id: At2g42520.1 [*At*]	8e-45
660	WAW	waw1c.pk003.c2	-0.22	-0.55	-0.31	-0.30	-0.38	-0.05	-0.09	0.05	polyubiquitin - garden snapdragon (fragment)	7e-82
661	WAW	waw1c.pk003.c21	0.02	-0.14	-0.17	-0.22	-0.23	0.00	0.10	-0.06	no homologies found	-
662	WAW	waw1c.pk003.c3	-0.38	-0.32	-0.08	-0.18	-0.10	-0.04	-0.05	0.01	no homologies found	-
663	WAW	waw1c.pk003.c6	-0.10	0.00	0.06	0.03	0.02	-0.04	0.03	-0.02	pyruvate decarboxylase [*Zm*]	2e-35
664	WAW	waw1c.pk003.c8	0.04	0.06	0.02	0.03	0.00	-0.01	0.07	0.04	putative ribosomal RNA apurinic site specific lyase [*Os*]	4e-16
665	WAW	waw1c.pk003.c9	0.00	-0.07	-0.02	-0.04	-0.01	0.01	-0.04	0.10	putative heat-shock protein [*Os*]	2e-84
666	WAW	waw1c.pk003.d10	0.11	-0.12	-0.02	-0.07	-0.01	-0.02	-0.07	0.03	no homologies found	-
667	WAW	waw1c.pk003.d11	-0.50	-0.29	-0.32	-0.17	-0.30	-0.03	-0.04	-0.06	Phytepsin precursor (Aspartic proteinase)	1e-66
668	WAW	waw1c.pk003.d12	0.13	0.19	0.15	0.19	0.18	0.00	0.02	0.12	pyruvate dehydrogenase E1 beta subunit isoform 2 [*Zm*]	3e-97
669	WAW	waw1c.pk003.d14	0.00	0.37	0.60	0.44	0.41	-0.10	-0.04	-0.14	dwarf protein, OSDIM - rice	3e-71
670	WAW	waw1c.pk003.d15	-0.28	-0.17	-0.15	-0.09	-0.10	-0.16	-0.12	0.28	S-adenosylmethionine decarboxylase precursor [*Ta*]	6e-17
671	WAW	waw1c.pk003.d16	0.44	0.39	0.20	0.33	0.25	-0.10	-0.08	-0.39	ankyrin-like protein [*St*]	8e-19
672	WAW	waw1c.pk003.d18	-0.10	0.11	0.06	0.16	0.25	0.10	-0.05	0.11	YY1 protein precursor	4e-19
673	WAW	waw1c.pk003.d20	0.01	0.33	0.54	0.62	1.35	-0.03	-0.03	0.03	acetyl-CoA carboxylase (EC 6.4.1.2) - wheat	1e-115
674	WAW	waw1c.pk003.d21	0.07	0.24	-0.26	0.14	-0.16	0.05	-0.08	0.00	putative protein; protein id: At3g52870.1 [*At*]	9e-32
675	WAW	waw1c.pk003.d22	-0.19	0.22	0.07	0.33	0.09	0.09	0.12	0.17	no homologies found	-
676	WAW	waw1c.pk003.d23	-0.07	0.14	-0.01	0.17	0.05	0.03	0.04	0.22	ascorbate peroxidase [*Hv*]	4e-73
677	WAW	waw1c.pk003.d4	-0.04	0.35	0.46	0.27	0.45	0.06	-0.03	0.12	P0431G06.3 [*Os*]	6e-67
678	WAW	waw1c.pk003.d5	0.17	0.10	0.11	0.13	-0.03	-0.05	-0.03	-0.18	serine/threonine-protein kinase Mak (male germ cell-associated kinase)-like protein [*At*]	3e-67
679	WAW	waw1c.pk003.d6	-0.15	-0.34	-0.22	-0.16	-0.32	-0.01	-0.01	-0.02	putative Cdc2-related protein kinase CRK2 [Beta vulgaris]	8e-80
680	WAW	waw1c.pk003.d8	0.11	0.04	0.34	0.00	0.01	-0.02	-0.02	-0.03	contains EST D23238(C2469)~kinase-like protein [*Os*]	7e-05

#	ID	EST name	Temporal *M*					*Ph* mutant *M*			Top BLASTx hit	e-val
			PM	LP	DA	TT	T	*1b*	*2a*	*2b*		
681	WAW	waw1c.pk003.e11	0.00	-0.10	-0.02	-0.02	-0.04	0.00	-0.07	-0.12	hypothetical protein~similar to *At* chromosome 5, MCK7.19 [*Os*]	4e-61
682	WAW	waw1c.pk003.e13	-0.91	0.02	0.11	-0.29	0.10	-0.02	-0.04	0.11	protein disulfide isomerase 2 precursor [*Ta*]	1e-106
683	WAW	waw1c.pk003.e14	-0.15	0.03	0.15	0.11	0.30	0.04	0.04	0.00	putative acetyl transferase [*Os*]	3e-45
684	WAW	waw1c.pk003.e15	-0.06	0.14	0.26	0.03	-0.02	0.05	0.02	0.02	myb-related protein - barley	2e-31
685	WAW	waw1c.pk003.e16	-0.05	0.01	-0.12	0.11	-0.07	-0.08	-0.04	-0.05	polyadenylate-binding protein - wheat	3e-27
686	WAW	waw1c.pk003.e17	-0.07	-0.20	-0.28	-0.24	-0.31	0.01	-0.01	-0.04	mRNA cap methyltransferase-like protein [*At*]	3e-16
687	WAW	waw1c.pk003.e19	0.07	0.17	-0.07	0.17	0.27	0.03	-0.08	0.09	no homologies found	-
688	WAW	waw1c.pk003.e2	1.41	0.58	0.52	0.56	0.58	0.09	0.12	-0.09	putative protein; protein id: At4g35240.1 [*At*]	9e-26
689	WAW	waw1c.pk003.e20	0.00	0.34	0.42	0.18	0.23	0.03	0.05	0.02	putative pectin methylesterase [*Os*]	2e-67
690	WAW	waw1c.pk003.e22	-0.14	0.03	0.11	-0.02	0.06	-0.02	-0.07	0.00	pyruvate dehydrogenase E1 alpha subunit [*Zm*]	4e-63
691	WAW	waw1c.pk003.e3	0.28	0.17	0.30	0.26	0.15	-0.01	-0.13	-0.20	inorganic pyrophosphatase -like protein; protein id: At3g53620.1 [*At*]	6e-73
692	WAW	waw1c.pk003.e7	-0.29	0.14	0.05	0.25	0.35	0.07	0.00	0.02	enoyl-[acyl-carrier-protein] reductase (NADH2) (EC 1.3.1.9) precursor - common tobacco	3e-89
693	WAW	waw1c.pk003.e8	1.68	1.15	1.20	0.57	0.94	-0.03	-0.13	0.04	Peroxidase 40 precursor (Atperox P40)	3e-23
694	WAW	waw1c.pk003.e9	-0.32	-1.36	-1.39	-1.18	-1.86	-0.04	0.00	-0.01	PDR-like ABC transporter [*Os*]	2e-95
695	WAW	waw1c.pk003.f10	-0.10	0.00	0.08	-0.01	-0.08	0.03	-0.02	0.00	succinate dehydrogenase flavoprotein alpha subunit (emb|CAA05025.1); protein id: At5g66760.1	1e-100
696	WAW	waw1c.pk003.f11	-0.09	0.07	0.09	0.09	0.03	0.03	0.08	0.05	no homologies found	-
697	WAW	waw1c.pk003.f12	0.20	0.10	0.27	0.17	0.06	-0.01	-0.10	-0.01	cellulose synthase-1 [*Zm*]	2e-88
698	WAW	waw1c.pk003.f13	-0.12	-0.09	0.11	-0.05	-0.07	-0.02	0.05	-0.04	gene_id:MNF13.29~unknown protein [*At*]	3e-34
699	WAW	waw1c.pk003.f14	0.09	0.22	0.23	0.23	0.35	0.05	0.01	0.07	serine/threonine protein phosphatase; protein id: At5g55260.1 [*At*]	1e-103
700	WAW	waw1c.pk003.f15	0.01	-0.20	0.14	-0.08	-0.11	-0.05	-0.10	-0.02	26S proteasome regulatory subunit (RPN2), putative; protein id: At2g32730.1 [*At*]	1e-85
701	WAW	waw1c.pk003.f16	0.30	0.19	0.35	0.23	0.19	0.06	-0.04	-0.03	no homologies found	-
702	WAW	waw1c.pk003.f17	0.09	0.14	-0.02	0.01	-0.05	0.02	-0.12	-0.04	similar to 26S proteasome subunit4 [*Os*]	1e-41
703	WAW	waw1c.pk003.f19	0.39	0.59	0.57	0.67	0.73	-0.02	0.02	-0.08	putative cyclin Ia [*Os*]	6e-23
704	WAW	waw1c.pk003.f2	-0.06	0.07	0.13	0.14	-0.01	0.03	0.06	0.01	unknown protein; protein id: At1g05350.1 [*At*]	5e-08
705	WAW	waw1c.pk003.f20	0.37	0.09	0.23	0.09	-0.02	-0.09	-0.11	-0.17	Argonaute (AGO1)-like protein [*At*]	2e-54
706	WAW	waw1c.pk003.f24	0.13	0.10	0.26	0.24	0.07	0.01	-0.04	-0.02	mitochondrial processing peptidase beta subunit [*Cm*]	1e-79
707	WAW	waw1c.pk003.f6	0.10	0.18	-0.01	0.09	0.04	-0.06	0.00	-0.03	putative zinc-finger helicase [*Os*]	7e-38
708	WAW	waw1c.pk003.f7	-0.06	-0.17	-0.23	-0.17	-0.20	-0.02	0.07	0.06	unknown protein [*At*]	3e-11
709	WAW	waw1c.pk003.f8	-0.09	-0.11	-0.02	-0.02	-0.02	0.00	0.04	-0.10	ADP,ATP carrier protein, mitochondrial precursor (ADP/ATP translocase) (Adenine nucleotide translocator) (ANT)	8e-82
710	WAW	waw1c.pk003.g1	-0.03	-0.02	0.03	0.11	0.07	0.14	0.01	0.23	no homologies found	-
711	WAW	waw1c.pk003.g10	0.82	0.57	0.61	0.60	0.49	-0.08	-0.12	-0.05	DNA topoisomerase II (PsTopII)	1e-06
712	WAW	waw1c.pk003.g11	0.04	-0.17	0.04	-0.25	0.06	-0.07	0.00	-0.13	probable glucan 1,3-beta-glucosidase (EC 3.2.1.58) ExoII - barley	1e-101
713	WAW	waw1c.pk003.g12	0.05	-0.02	-0.04	0.00	-0.04	-0.07	0.06	0.04	NAD-dependent isocitrate dehydrogenase [*Nt*]	4e-54
714	WAW	waw1c.pk003.g13	0.13	0.14	0.23	0.10	0.23	0.01	-0.04	0.06	putative transcription initiation factor [*Os*]	9e-31
715	WAW	waw1c.pk003.g15	0.08	0.07	0.02	-0.06	0.12	0.07	0.01	-0.10	no homologies found	-
716	WAW	waw1c.pk003.g16	0.02	-0.12	0.05	-0.13	-0.21	0.03	0.01	-0.03	expressed protein; protein id: At2g01600.1 [*At*]	3e-71
717	WAW	waw1c.pk003.g19	0.34	0.05	0.15	0.07	0.00	0.04	-0.01	-0.02	26S proteasome regulatory particle non-ATPase subunit8 [*Os*]	3e-82
718	WAW	waw1c.pk003.g2	-0.04	0.00	0.14	0.01	0.11	0.00	0.04	0.04	putative protein; protein id: At4g35240.1 [*At*]	2e-23
719	WAW	waw1c.pk003.g20	0.02	0.13	0.06	0.12	-0.01	-0.02	0.00	0.03	unknown protein; protein id: At1g76850.1 [*At*]	1e-58
720	WAW	waw1c.pk003.g21	0.29	0.06	-0.06	0.10	0.00	0.07	0.03	0.04	putative 60S ribosomal protein L22; protein id: At3g05560.1	9e-26
721	WAW	waw1c.pk003.g24	-0.44	-0.30	-0.18	-0.12	-0.23	-0.06	-0.11	-0.03	polyubiquitin [*Ps*]	2e-86
722	WAW	waw1c.pk003.g3	0.05	-0.10	-0.01	0.03	-0.03	-0.10	-0.01	0.03	oj991113_30.20 [*Os*]	0.075
723	WAW	waw1c.pk003.g5	0.01	-0.04	0.03	0.02	0.03	-0.05	0.01	-0.02	OSJNBa0060B20.10 [*Os*]	7e-51
724	WAW	waw1c.pk003.g6	-0.10	-0.05	0.12	0.00	0.11	-0.01	0.01	-0.03	OSJNBa0064H22.15 [*Os*]	0.006
725	WAW	waw1c.pk003.g7	-0.36	0.14	0.08	0.25	0.30	0.01	-0.06	0.02	enoyl-[acyl-carrier-protein] reductase (NADH2) (EC 1.3.1.9) precursor - common tobacco	6e-90
726	WAW	waw1c.pk003.g8	-0.14	-0.12	0.03	-0.05	0.07	-0.04	-0.06	-0.02	similar to p23 {*Bn*}; protein id: At3g03773.1 [*At*]	1e-30
727	WAW	waw1c.pk003.h1	0.15	0.05	0.17	0.17	0.37	0.04	-0.01	-0.03	no homologies found	-
728	WAW	waw1c.pk003.h10	0.16	0.23	0.31	0.01	0.03	0.04	-0.03	-0.04	translocation protein in type III secretion [Pseudomonas aeruginosa PA01]	0.68
729	WAW	waw1c.pk003.h12	0.27	0.17	0.19	0.15	-0.01	-0.08	-0.03	-0.13	TUBULIN ALPHA CHAIN	2e-90
730	WAW	waw1c.pk003.h13	-0.02	-0.08	-0.11	-0.20	-0.23	0.04	0.05	-0.15	glycine-rich RNA-binding protein GRP1 - wheat	7e-44
731	WAW	waw1c.pk003.h14	-0.29	-0.11	-0.19	-0.12	-0.04	-0.03	-0.03	-0.06	S-adenosylmethionine synthetase 2 (Methionine adenosyltransferase 2) (AdoMet synthetase 2)	1e-104
732	WAW	waw1c.pk003.h15	0.23	0.10	-0.01	0.13	0.10	0.03	-0.03	0.11	cycloartenol synthase [Avena strigosa]	4e-09
733	WAW	waw1c.pk003.h16	-0.32	-0.09	-0.19	0.02	0.05	0.00	-0.11	0.34	S-adenosylmethionine decarboxylase precursor [*Ta*]	1e-100
734	WAW	waw1c.pk003.h17	-1.17	-0.66	0.44	-0.18	0.32	-0.05	-0.04	0.08	similar to DNA repair protein-like;protein id:At1g05120.1 [*At*]	2e-14
735	WAW	waw1c.pk003.h18	0.13	0.02	-0.29	0.02	-0.17	-0.11	-0.03	-0.01	putative eukaryoticrelease factor [*Os*]	2e-93
736	WAW	waw1c.pk003.h19	-0.68	0.37	0.23	0.79	0.74	0.10	0.15	0.13	no homologies found	-
737	WAW	waw1c.pk003.h20	-0.32	0.10	0.45	0.23	0.05	0.06	0.03	-0.10	putative elicitor response protein [*Os*]	3e-45
738	WAW	waw1c.pk003.h23	-0.09	-0.22	0.00	-0.15	-0.07	-0.03	-0.02	0.06	glutamate decarboxylase [*Os*]	3e-87
739	WAW	waw1c.pk003.h24	-0.13	0.01	-0.11	0.04	-0.09	0.04	-0.07	0.01	hypothetical protein T32E8.1 [imported] - *At*	9e-63
740	WAW	waw1c.pk003.h4	0.33	0.37	0.52	0.47	0.40	-0.12	-0.08	-0.09	UTP-glucose-1-phosphate uridyltltransferase (UDP-glucose pyrophosphorylase) (UDPGP) (UGPASE)	9e-54
741	WAW	waw1c.pk003.h6	-0.09	-0.22	-0.11	-0.23	-0.11	-0.03	0.02	-0.07	DNA Damage Inducible; binds to T- and V- snare complexes; Ddi1p [*Sc*]	0.28
742	WAW	waw1c.pk003.h8	0.08	0.08	-0.01	-0.04	0.09	-0.06	-0.02	-0.01	no homologies found	-
743	WAW	waw1c.pk003.h9	-0.81	-0.56	-0.03	-0.14	0.10	0.00	-0.01	-0.01	hypothetical protein; protein id: At3g11330.1 [*At*]	1e-08
744	WAW	waw1c.pk003.i12	0.45	0.52	0.45	0.35	0.30	0.04	-0.12	0.03	DNA topoisomerase II [*Nt*]	6e-37
745	WAW	waw1c.pk003.i13	0.25	0.10	-0.07	0.07	-0.18	0.00	0.10	0.14	ribosomal protein L15 [*Hs*]	1e-16
746	WAW	waw1c.pk003.i15	-0.06	-0.17	-0.13	-0.05	-0.10	0.04	0.02	-0.06	no homologies found	-
747	WAW	waw1c.pk003.i16	0.22	0.06	-0.19	0.01	0.23	0.00	0.02	0.08	putative acetoacyl-CoA-thiolase [*Os*]	9e-50
748	WAW	waw1c.pk003.i17	0.02	0.01	0.02	0.02	-0.02	-0.11	0.09	0.05	contains similarity to pherophorin~gene_id:T5M7.14 [*At*]	2e-67
749	WAW	waw1c.pk003.i18	-0.34	0.36	0.05	0.20	0.32	0.02	-0.14	0.19	calreticulin - barley (fragment)	6e-84
750	WAW	waw1c.pk003.i19	0.19	0.09	-0.15	0.12	0.05	0.07	0.05	-0.13	no homologies found	-
751	WAW	waw1c.pk003.i2	-0.03	0.15	0.10	0.15	0.08	-0.04	-0.03	0.01	no homologies found	-
752	WAW	waw1c.pk003.i20	0.01	0.08	0.29	0.14	0.20	0.07	-0.04	0.01	no homologies found	-
753	WAW	waw1c.pk003.i21	0.01	0.00	0.38	0.09	0.22	0.05	0.01	0.03	expressed protein; protein id: At1g21680.1 [*At*]	8e-22
754	WAW	waw1c.pk003.i23	-0.15	-0.06	-0.12	-0.10	-0.13	0.13	0.01	0.00	unnamed protein product [*Os*]	4e-36
755	WAW	waw1c.pk003.i24	-0.19	-0.19	-0.11	-0.18	0.01	-0.01	-0.09	0.04	heat shock cognate protein HSC70 [*Bn*]	1e-70
756	WAW	waw1c.pk003.i3	0.02	0.21	0.11	0.13	0.21	-0.04	-0.05	-0.01	putative protein phosphatase 2A regulatory subunit [*Os*]	0.25
757	WAW	waw1c.pk003.i4	-0.01	0.24	-0.06	0.17	0.37	0.06	0.04	0.03	Unknown protein [*At*]	3e-46
758	WAW	waw1c.pk003.i5	-0.11	1.18	1.24	1.58	1.52	0.18	0.01	0.09	unnamed protein product [*Os*]	2e-41
759	WAW	waw1c.pk003.i7	-0.06	-0.05	0.03	0.08	0.03	0.07	0.00	0.09	no homologies found	-
760	WAW	waw1c.pk003.i9	0.05	0.25	0.08	0.09	-0.15	-0.12	-0.20	-0.07	expressed protein; protein id: At2g32970.1 [*At*]	1e-54
761	WAW	waw1c.pk003.j1	0.82	1.16	1.03	1.19	1.31	0.10	0.13	0.15	no homologies found	-
762	WAW	waw1c.pk003.j10	0.20	0.01	-0.03	0.05	-0.15	-0.07	-0.01	0.04	Elongation factor 1-alpha (EF-1-ALPHA)	4e-32

			Temporal *M*					*Ph* mutant *M*				
#	ID	EST name	PM	LP	DA	TT	T	*1b*	*2a*	*2b*	Top BLASTx hit	e-val
763	WAW	waw1c.pk003.j11	0.03	0.03	-0.01	0.00	0.06	0.03	-0.01	0.00	expressed protein; protein id: At1g13380.1 [*At*]	3e-63
764	WAW	waw1c.pk003.j12	0.50	-0.08	-0.02	0.05	-0.05	0.11	-0.05	-0.02	no homologies found	-
765	WAW	waw1c.pk003.j13	-0.42	-0.54	-0.32	-0.54	-0.73	-0.05	-0.04	-0.17	Adenosylhomocysteinase (S-adenosyl-L-homocysteine hydrolase) (AdoHcyase)	1e-109
766	WAW	waw1c.pk003.j14	-0.14	-0.15	-0.01	-0.20	0.06	-0.01	0.06	0.07	transposon protein, putative; protein id: At1g27850.1 [*At*]	3e-30
767	WAW	waw1c.pk003.j15	0.26	0.24	0.13	0.17	0.00	-0.02	-0.02	0.08	hypothetical protein D430026C09 [*Mm*]	0.034
768	WAW	waw1c.pk003.j17	-0.08	0.11	0.28	0.08	-0.01	-0.02	0.00	-0.02	no homologies found	-
769	WAW	waw1c.pk003.j19	0.13	0.07	0.11	0.08	0.22	-0.04	0.02	-0.09	putative serine/threonine protein kinase [*Os*]	5e-55
770	WAW	waw1c.pk003.j20	-0.26	-0.30	-0.03	-0.24	-0.39	-0.02	-0.12	0.07	cytosolic aconitase [*Nt*]	2e-86
771	WAW	waw1c.pk003.j21	-0.13	0.05	-0.10	0.28	-0.01	0.05	0.11	0.04	no homologies found	-
772	WAW	waw1c.pk003.j22	0.23	0.11	0.07	0.09	0.10	-0.10	-0.08	-0.06	AGO1 homologous protein [*Os*]	1e-80
773	WAW	waw1c.pk003.j24	-0.45	0.25	0.02	0.09	0.33	-0.02	-0.15	0.12	calreticulin precursor - maize	1e-86
774	WAW	waw1c.pk003.j3	0.42	0.15	-0.05	0.12	0.00	0.00	-0.11	0.01	nucleosome assembly protein I - wheat (fragment)	1e-23
775	WAW	waw1c.pk003.j5	-0.49	-0.65	-0.48	-0.58	-0.47	0.09	0.08	-0.01	MADS box transcription factor [*Ta*]	1e-72
776	WAW	waw1c.pk003.j6	0.41	0.36	0.62	0.46	0.67	0.06	0.09	-0.06	putative cyclin Ia [*Os*]	6e-23
777	WAW	waw1c.pk003.j8	0.23	0.09	0.07	0.10	0.13	-0.06	-0.15	-0.03	Putative cytosolic tRNA-Ala synthetase [*Os*]	9e-08
778	WAW	waw1c.pk003.j9	0.03	-0.14	-0.19	-0.19	-0.26	-0.05	0.11	-0.10	U2 snRNP auxiliary factor, small subunit [*Os*]	1e-100
779	WAW	waw1c.pk003.k10	-0.05	-0.14	-0.13	-0.01	-0.11	0.01	-0.05	-0.07	no homologies found	-
780	WAW	waw1c.pk003.k11	0.02	-0.06	-0.01	-0.06	-0.15	-0.05	0.01	-0.02	Elongation factor 1-alpha (EF-1-ALPHA)	2e-97
781	WAW	waw1c.pk003.k15	-0.29	-0.19	-0.32	-0.59	0.16	-0.08	-0.09	0.14	dnaK-type molecular chaperone BiP - rice	4e-84
782	WAW	waw1c.pk003.k16	0.10	0.03	0.11	-0.06	-0.09	0.02	0.16	-0.06	unnamed protein product [*Os*]	2e-19
783	WAW	waw1c.pk003.k18	-0.03	-0.13	-0.21	-0.14	-0.20	-0.02	-0.12	0.01	putative Ran binding protein [*Os*]	1e-74
784	WAW	waw1c.pk003.k2	-0.21	0.40	-0.21	0.26	0.18	0.19	0.09	0.13	CTP-synthetase, putative; protein id: At3g12670.1 [*At*]	9e-19
785	WAW	waw1c.pk003.k21	-0.10	0.02	0.09	0.05	0.12	-0.15	-0.01	0.03	OSJNBa0050F15.12 [*Os*]	9e-05
786	WAW	waw1c.pk003.k22	-0.05	0.00	0.00	-0.02	-0.08	-0.04	0.06	-0.10	KH domain protein; protein id: At5g53060.1 [*At*]	3e-39
787	WAW	waw1c.pk003.k23	-0.02	0.23	0.01	0.22	-0.04	-0.03	-0.02	0.09	no homologies found	-
788	WAW	waw1c.pk003.k3	-0.11	0.15	0.21	0.09	-0.11	-0.01	-0.01	0.01	Fructose-bisphosphate aldolase, cytoplasmic isozyme	2e-88
789	WAW	waw1c.pk003.k4	0.24	0.25	0.50	0.01	0.31	0.03	-0.05	-0.01	kinesin-like protein [*At*]	2e-05
790	WAW	waw1c.pk003.k5	-0.12	-0.17	0.07	-0.13	0.02	0.03	0.00	0.12	no homologies found	-
791	WAW	waw1c.pk003.k6	0.02	-0.03	-0.09	-0.22	-0.04	0.00	0.12	-0.12	no homologies found	-
792	WAW	waw1c.pk003.k7	-0.47	-0.49	-0.19	-0.37	-0.31	-0.08	-0.11	-0.06	AT4g05320/C17L7_240 [*At*]	2e-83
793	WAW	waw1c.pk003.k9	0.01	0.03	-0.08	-0.04	0.00	-0.01	0.13	-0.04	no homologies found	-
794	WAW	waw1c.pk003.l10	0.23	0.27	0.24	0.22	0.10	-0.02	0.05	-0.07	set domain protein; transcriptional silencing [*Sp*]	1e-24
795	WAW	waw1c.pk003.l12	0.33	0.50	0.53	0.30	0.31	-0.02	-0.11	-0.15	putative diacylglycerol kinase [*Os*]	2e-61
796	WAW	waw1c.pk003.l13	0.09	0.11	0.21	0.15	0.10	-0.01	0.02	-0.01	expressed protein; protein id: At3g10940.1 [*At*]	4e-53
797	WAW	waw1c.pk003.l14	0.06	0.02	0.01	0.03	0.00	0.05	0.01	-0.05	no homologies found	-
798	WAW	waw1c.pk003.l16	0.01	-0.03	0.24	0.07	0.02	0.02	0.12	0.08	putative NADPH dependent mannose 6-phosphate reductase [*At*]	1e-68
799	WAW	waw1c.pk003.l17	-0.07	0.09	-0.05	0.08	0.42	0.01	-0.01	0.19	putative dihydrolipoamide S-acetyltransferase [*At*]	9e-29
800	WAW	waw1c.pk003.l18	-0.12	-0.16	-0.06	-0.13	-0.01	-0.01	-0.02	0.04	no homologies found	-
801	WAW	waw1c.pk003.l19	0.15	0.19	0.19	0.17	0.11	-0.06	-0.08	-0.04	actin [imported] - rape	1e-102
802	WAW	waw1c.pk003.l21	0.51	2.31	2.14	2.42	2.60	0.01	0.05	0.04	thypothetical 12.6K protein, LIM6 - trumpet lily (fragment)	0.17
803	WAW	waw1c.pk003.l23	-0.32	-0.12	-0.03	-0.03	-0.41	0.02	0.08	0.11	no homologies found	-
804	WAW	waw1c.pk003.l24	-0.18	-0.31	-0.14	-0.27	-0.32	0.00	-0.08	0.02	Eukaryotic translation initiation factor 5 (eIF-5)	1e-76
805	WAW	waw1c.pk003.l6	-1.20	-1.46	0.18	-1.00	-0.26	-0.07	-0.06	-0.12	Tubulin beta chain (Beta tubulin)	6e-32
806	WAW	waw1c.pk003.l7	-0.48	-0.15	-0.06	-0.07	-0.04	-0.02	-0.02	-0.02	Catalase isozyme 1	1e-93
807	WAW	waw1c.pk003.l8	0.07	0.01	0.09	0.00	-0.12	-0.02	-0.10	-0.06	putative AAA-metalloprotease [*Os*]	0.005
808	WAW	waw1c.pk003.m11	0.06	-0.25	0.13	-0.06	0.09	-0.05	0.08	0.03	no homologies found	-
809	WAW	waw1c.pk003.m13	0.08	-0.04	-0.03	0.04	0.10	0.13	-0.05	-0.12	putative gag-pol polyprotein [*Os*]	2e-56
810	WAW	waw1c.pk003.m14	0.06	-0.13	-0.13	-0.15	-0.12	0.12	0.03	0.27	B1033B05.2 [*Os*]	2e-06
811	WAW	waw1c.pk003.m16	0.28	-0.05	0.02	-0.05	-0.12	0.02	0.07	0.06	40S ribosomal protein S4	6e-93
812	WAW	waw1c.pk003.m17	0.08	0.01	0.00	-0.10	-0.06	0.07	0.00	0.00	putative peptide chain release factor subunit 1 (ERF1) [*Os*]	1e-79
813	WAW	waw1c.pk003.m19	-0.34	-0.60	-1.40	-0.54	-1.04	0.05	-0.04	-0.05	PDR-like ABC transporter [*Os*]	1e-27
814	WAW	waw1c.pk003.m23	0.32	0.18	0.05	0.13	0.02	-0.05	-0.01	-0.05	guanine nucleotide-binding protein beta subunit-like protein (GPB-LR) (RWD)	6e-63
815	WAW	waw1c.pk003.m24	1.27	0.56	0.50	0.60	0.57	0.00	-0.07	-0.18	RRM-containing RNA-binding protein, putative; protein id: At1g17640.1 [*At*]	4e-56
816	WAW	waw1c.pk003.m3	0.28	0.13	0.10	0.09	0.06	-0.06	-0.07	-0.11	putative UDP-glucose dehydrogenase [*Sb*]	9e-49
817	WAW	waw1c.pk003.m5	0.40	0.16	0.11	0.10	-0.10	-0.06	-0.01	-0.01	Putative 40S Ribosomal protein [*Os*]	1e-85
818	WAW	waw1c.pk003.m7	0.18	0.12	0.30	-0.13	-0.04	0.00	0.02	-0.14	auxin response factor 10 [*Os*]	5e-59
819	WAW	waw1c.pk003.m8	0.01	0.14	0.11	0.07	0.09	-0.08	-0.16	-0.13	unknown protein [*At*]	1e-19
820	WAW	waw1c.pk003.m9	0.54	0.09	0.01	0.19	0.08	-0.26	-0.34	-0.31	no homologies found	-
821	WAW	waw1c.pk003.n10	0.14	-0.06	-0.14	-0.08	-0.11	0.07	0.09	0.11	putative small nuclear ribonucleoprotein polypeptide G; protein id: At3g11500.1 [*At*]	6e-35
822	WAW	waw1c.pk003.n12	-0.03	-0.05	-0.07	-0.04	-0.02	-0.06	-0.04	0.04	dihydroxyacid dehydratase, putative; protein id: At3g23940.1	2e-73
823	WAW	waw1c.pk003.n14	0.10	0.55	0.36	0.27	0.45	0.00	0.01	0.05	putative protein; protein id: At3g57890.1 [*At*]	3e-20
824	WAW	waw1c.pk003.n16	-0.06	-0.22	-0.38	-0.12	-0.17	-0.02	0.03	0.04	no homologies found	-
825	WAW	waw1c.pk003.n17	0.03	0.25	0.17	0.22	0.21	0.05	0.00	0.03	unknown protein [*At*]	4e-54
826	WAW	waw1c.pk003.n18	0.00	-0.02	-0.02	-0.03	0.00	0.01	0.04	-0.02	no homologies found	-
827	WAW	waw1c.pk003.n2	-0.17	0.29	0.28	0.26	0.27	-0.05	0.04	0.06	diphosphonucleotide phosphatase 1 [*Zm*]	3e-14
828	WAW	waw1c.pk003.n20	-0.08	-0.05	0.22	-0.07	0.36	-0.02	-0.12	-0.14	Phenylalanine ammonia-lyase	2e-87
829	WAW	waw1c.pk003.n21	0.03	0.01	-0.02	-0.06	0.04	-0.04	-0.06	-0.11	polyprotein [*Os*]	5e-32
830	WAW	waw1c.pk003.n22	0.39	0.31	0.24	0.36	0.26	0.03	0.01	0.05	Elongation factor 1-gamma (EF-1-gamma) (eEF-1B gamma)	2e-43
831	WAW	waw1c.pk003.n23	-0.16	-0.02	-0.20	-0.04	-0.03	0.05	0.06	0.12	2-oxoglutarate/malate translocator; protein id: At5g64290.1 [*At*]	1e-57
832	WAW	waw1c.pk003.n4	0.07	-0.06	-0.12	-0.06	-0.21	-0.01	0.01	-0.04	unknown protein; protein id: At2g18900.1 [*At*]	1e-07
833	WAW	waw1c.pk003.n6	-0.09	-0.17	-0.15	-0.14	-0.03	0.06	0.04	0.02	putative zinc finger protein [*Os*]	8e-52
834	WAW	waw1c.pk003.n7	-0.14	-0.14	-0.01	-0.05	-0.06	-0.02	0.10	0.12	phospoenolpyruvate carboxylase [*Ta*]	1e-46
835	WAW	waw1c.pk003.n9	0.11	-0.03	0.04	-0.05	-0.08	0.02	0.02	-0.04	RNA-binding protein-like [*At*]	4e-39
836	WAW	waw1c.pk003.o1	-0.27	0.08	0.06	0.15	0.34	0.01	0.00	-0.03	enoyl-[acyl-carrier-protein] reductase (NADH2) (EC 1.3.1.9) precursor - common tobacco	3e-48
837	WAW	waw1c.pk003.o10	0.20	0.07	-0.02	-0.07	-0.06	-0.04	0.03	-0.08	hypothetical protein F8F16.240 - *At*	1e-35
838	WAW	waw1c.pk003.o12	-0.50	-0.60	-0.40	-0.72	-0.67	0.08	-0.04	-0.08	possible aldehyde decarbonylase [*At*]	8e-24
839	WAW	waw1c.pk003.o13	-0.07	0.09	-0.06	0.15	0.07	-0.14	0.00	-0.04	Expressed protein; protein id: At5g04930.1[*At*]	4e-38
840	WAW	waw1c.pk003.o14	-0.03	-0.13	0.04	-0.16	-0.20	0.06	-0.05	-0.02	putative nucleolar protein [*Sb*]	4e-73
841	WAW	waw1c.pk003.o15	0.07	0.30	0.21	0.22	0.29	0.01	-0.05	0.09	P-type ATPase [*Hv*]	2e-74
842	WAW	waw1c.pk003.o17	-0.02	0.00	-0.11	-0.08	-0.01	-0.02	0.01	-0.03	En/Spm-like transposon protein; protein id: At2g42840.1 [*At*]	0.7
843	WAW	waw1c.pk003.o18	-0.35	-0.23	-0.09	-0.23	-0.13	-0.08	-0.13	0.00	Putative heat shock 70 KD protein, mitochondrial precursor [*Os*]	1e-101
844	WAW	waw1c.pk003.o2	-0.18	0.01	-0.15	0.05	-0.05	-0.07	-0.06	-0.05	unknown [*At*]	2e-48
845	WAW	waw1c.pk003.o20	0.00	-0.14	-0.19	-0.32	-0.27	0.03	0.11	-0.19	hypothetical protein~similar to *Os* chromosome 10, OSJNBa0042H09.20 [*Os*]	4e-16
846	WAW	waw1c.pk003.o22	-0.24	0.31	0.15	0.16	0.25	0.02	-0.05	0.08	hypothetical protein XP_065062 [*Hs*]	0.59
847	WAW	waw1c.pk003.o23	-0.31	-0.46	-0.34	-0.40	-0.26	0.12	0.00	0.13	contains EST AU089749(S14720)~similar to Cicer arietinum ,CAA10129.1~unknown protein [*Os*]	0.01

			Temporal *M*					*Ph* mutant *M*				
#	ID	EST name	PM	LP	DA	TT	T	*1b*	*2a*	*2b*	Top BLASTx hit	e-val
848	WAW	waw1c.pk003.o24	1.18	0.60	0.63	0.56	0.53	0.03	-0.02	-0.24	Histone H3	7e-70
849	WAW	waw1c.pk003.o4	0.64	0.38	0.47	0.44	0.32	-0.02	-0.06	-0.02	DNA topoisomerase II [*Nt*]	3e-34
850	WAW	waw1c.pk003.o6	-0.85	-0.64	-0.51	-0.48	-0.42	0.02	0.14	-0.14	Phosphoglycerate kinase, chloroplast precursor	3e-83
851	WAW	waw1c.pk003.o7	0.02	0.03	0.14	0.00	0.04	-0.03	0.04	-0.07	no homologies found	-
852	WAW	waw1c.pk003.o8	-0.01	0.01	-0.12	0.04	0.12	0.12	0.00	0.07	no homologies found	-
853	WAW	waw1c.pk003.o9	0.11	0.15	0.03	0.08	0.12	-0.02	-0.02	-0.12	hypothetical protein [imported] - *At*	4e-05
854	WAW	waw1c.pk003.p1	-0.40	-0.78	-1.30	-0.84	-0.75	-0.07	-0.04	-0.12	putative cytochrome P450 protein [*Os*]	1e-76
855	WAW	waw1c.pk003.p10	-0.08	0.20	0.01	0.17	0.22	0.12	0.10	0.00	Hypothetical protein [*Os*]	0.002
856	WAW	waw1c.pk003.p12	0.03	0.13	0.13	0.20	-0.08	-0.01	-0.01	-0.03	no homologies found	-
857	WAW	waw1c.pk003.p14	0.00	0.13	-0.03	0.16	0.05	0.05	0.08	0.08	Ferredoxin, chloroplast precursor	2e-39
858	WAW	waw1c.pk003.p16	0.34	-0.05	-0.05	-0.08	-0.06	0.00	0.06	0.07	porphobilinogen deaminase [*Ta*]	2e-78
859	WAW	waw1c.pk003.p19	0.16	-0.07	-0.02	0.02	0.05	-0.11	-0.04	0.03	putative arm repeat containing protein [*Os*]	0.36
860	WAW	waw1c.pk003.p2	0.04	-0.06	0.11	-0.04	-0.08	-0.05	0.02	-0.07	ESTs AU082563(S20379),D15187(C0226), AU082476(C0226),AU082563(S20379)	1e-89
861	WAW	waw1c.pk003.p20	-0.34	-0.02	-0.10	0.01	0.14	0.07	0.14	-0.03	arginine/serine-rich protein, putative; protein id: At1g16610.1:	0.27
862	WAW	waw1c.pk003.p22	0.86	0.25	0.18	0.13	0.39	0.02	-0.01	0.03	putative protein; protein id: At4g03000.1 [*At*]	1e-05
863	WAW	waw1c.pk003.p4	-0.04	0.08	0.10	0.10	0.05	-0.03	-0.04	0.00	Elongation factor 1-alpha (EF-1-ALPHA)	1e-92
864	WAW	waw1c.pk003.p7	-0.20	-0.21	-0.17	-0.11	-0.05	-0.05	0.03	-0.02	oj000126_13.5 [*Os*]	3e-52
865	WAW	waw1c.pk004.a10	0.08	-0.01	0.10	-0.10	0.10	-0.09	-0.02	-0.04	ESTs C27722(C52692),AU058088(S0509) correspond to a region of the predicted gene.~Similar to *At*	0.001
866	WAW	waw1c.pk004.a12	0.40	1.48	1.34	1.40	1.51	0.04	-0.04	0.09	putative transcription factor X1 [*Os* subsp. japonica]	4e-52
867	WAW	waw1c.pk004.a13	-0.39	-0.21	-0.23	-0.07	-0.07	0.05	0.15	-0.13	hypothetical protein (repetitive element TCb1 No.5) - *Cb*	0.009
868	WAW	waw1c.pk004.a15	-0.12	-0.11	0.11	-0.13	0.01	-0.05	-0.07	-0.42	plasma membrane H+ ATPase [*Os*]	1e-106
869	WAW	waw1c.pk004.a16	-0.44	0.04	0.07	0.19	0.40	0.09	0.08	0.06	probable enoyl-[acyl-carrier-protein] reductase (NADH2) (EC 1.3.1.9) - rice	2e-82
870	WAW	waw1c.pk004.a17	-0.17	-0.35	0.22	-0.34	-0.23	-0.10	-0.03	-0.29	no homologies found	-
871	WAW	waw1c.pk004.a18	0.02	0.14	0.17	0.01	0.08	0.06	0.00	0.04	B1129G05.13 [*Os*]	1e-59
872	WAW	waw1c.pk004.a20	0.06	0.04	0.14	0.07	-0.01	-0.04	-0.01	0.01	gene_id:MKD15.6~unknown protein [*At*]	3e-59
873	WAW	waw1c.pk004.a21	1.05	0.57	0.45	0.57	0.28	-0.12	-0.16	-0.23	histone H1 WH1A.2 [*Ta*]	3e-16
874	WAW	waw1c.pk004.a22	-0.04	0.06	0.13	0.13	0.10	0.11	0.09	0.00	putative MAP3K epsilon protein kinase [*Os*]	1e-117
875	WAW	waw1c.pk004.a24	-0.30	-0.09	-0.05	-0.05	-0.01	0.09	0.01	0.15	unnamed protein product [*Os*]	2e-37
876	WAW	waw1c.pk004.a3	-0.37	-0.85	-0.81	-0.60	-1.16	-0.05	0.09	-0.09	no homologies found	-
877	WAW	waw1c.pk004.a4	0.01	-0.05	-0.03	-0.06	-0.05	0.03	0.03	0.03	no homologies found	-
878	WAW	waw1c.pk004.a5	-0.53	-0.15	-0.25	-0.27	-0.22	0.06	0.09	0.02	expressed protein; protein id: At2g20890.1	1e-39
879	WAW	waw1c.pk004.a9	-0.15	0.05	0.04	-0.31	0.48	-0.10	-0.19	0.10	Endoplasmin homolog precursor (GRP94 homolog)	2e-71
880	WAW	waw1c.pk004.b10	-0.15	-0.11	-0.06	-0.07	0.16	-0.10	-0.11	0.09	HSP70 [*Ta*]	1e-29
881	WAW	waw1c.pk004.b11	0.37	1.39	1.12	1.45	1.32	0.05	0.05	0.00	putative receptor-like protein kinase; protein id: At2g37050.1 [*At*]	1e-26
882	WAW	waw1c.pk004.b12	-0.03	-0.22	-0.03	-0.33	-0.30	0.00	-0.04	-0.14	myb-related protein - barley	1e-50
883	WAW	waw1c.pk004.b13	-0.15	-0.03	-0.07	-0.12	0.07	0.02	0.11	-0.02	receptor protein kinase PERK1 [*Bn*]	0.12
884	WAW	waw1c.pk004.b14	0.54	1.34	1.28	1.32	1.48	0.00	0.02	0.06	transcriptional regulator, putative; protein id: At1g15910.1 [*At*]	1e-41
885	WAW	waw1c.pk004.b17	0.03	-0.03	0.05	0.04	0.03	0.03	0.09	-0.01	no homologies found	-
886	WAW	waw1c.pk004.b18	-0.01	0.09	0.03	0.09	0.01	0.04	-0.05	0.11	unknown protein [*At*]	2e-58
887	WAW	waw1c.pk004.b19	-0.23	-0.02	-0.17	-0.16	-0.20	0.09	-0.15	0.03	Oslre1p [*Os*]	9e-84
888	WAW	waw1c.pk004.b20	-0.38	-0.68	-0.70	-1.06	-0.80	0.02	-0.05	-0.02	pre-mRNA splicing SR protein related RSR-1 (68.2 kD) (rsr-1) [*Ce*]	0.005
889	WAW	waw1c.pk004.b21	0.02	-0.11	0.11	-0.03	-0.06	-0.05	-0.06	0.44	cell cycle control crn (crooked neck) protein-like [*At*]	1e-56
890	WAW	waw1c.pk004.b22	-0.11	0.13	0.14	0.03	0.18	0.01	0.15	0.19	gamma-tocopherol methyltransferase [Perilla frutescens]	6e-78
891	WAW	waw1c.pk004.b23	-0.52	0.01	-0.04	0.32	-0.09	-0.06	-0.05	-0.10	phosphatase 2A regulatory A subunit [*Os*]	5e-82
892	WAW	waw1c.pk004.b24	0.26	0.04	-0.08	0.07	-0.11	-0.01	0.03	0.05	ribosomal protein L17.1, cytosolic - barley	2e-30
893	WAW	waw1c.pk004.b5	-0.14	-0.08	0.08	0.08	0.10	0.07	0.01	0.05	putative ATP synthase; protein id: At2g21870.1	4e-26
894	WAW	waw1c.pk004.b6	-0.02	-0.37	-0.10	-0.24	-0.34	0.04	-0.07	-0.07	unknown protein; protein id: At1g79150.1 [*At*]	1e-26
895	WAW	waw1c.pk004.b8	-0.08	-0.15	-0.23	-0.13	-0.08	-0.06	0.06	0.04	heparan sulfate 6-O-sulfotransferase 1 [*Mm*]	0.24
896	WAW	waw1c.pk004.b9	0.13	0.09	-0.13	0.01	0.06	-0.02	0.05	0.10	no homologies found	-
897	WAW	waw1c.pk004.c1	0.15	0.13	0.14	0.15	0.00	-0.12	-0.03	-0.01	no homologies found	-
898	WAW	waw1c.pk004.c10	-0.24	-0.16	-0.02	-0.07	0.02	-0.02	-0.06	-0.09	OSJNBb0091e11.1 [*Os*]	5e-22
899	WAW	waw1c.pk004.c11	0.28	0.16	0.22	0.18	0.25	0.07	0.01	-0.01	ebiP1363 [Anopheles gambiae str. PEST]	4e-08
900	WAW	waw1c.pk004.c12	0.19	-0.01	-0.10	-0.09	-0.16	0.00	0.14	-0.20	unknown protein; protein id: At2g04039.1	1e-15
901	WAW	waw1c.pk004.c13	-0.12	-0.09	-0.18	-0.01	0.10	-0.06	-0.01	0.01	no sequence information	
902	WAW	waw1c.pk004.c14	-0.30	-0.27	-0.44	-0.62	-0.64	-0.03	0.09	0.05	putative sterol 4-alpha-methyl-oxidase [*Zm*]	1e-77
903	WAW	waw1c.pk004.c15	0.13	0.14	0.26	0.10	0.13	-0.01	-0.05	0.03	At1g73430/T9L24_16 [*At*]	5e-67
904	WAW	waw1c.pk004.c16	0.01	-0.02	0.10	-0.01	-0.01	-0.02	0.02	-0.04	putative amino acid transport protein [*Os*]	2e-21
905	WAW	waw1c.pk004.c18	0.24	0.01	-0.26	-0.11	0.01	-0.01	-0.02	-0.01	similar to erine protease [*Os*]	3e-09
906	WAW	waw1c.pk004.c19	0.04	-0.29	-0.05	-0.25	0.81	-0.08	0.01	-0.09	unnamed protein product [*Os*]	6e-20
907	WAW	waw1c.pk004.c2	-0.40	-0.25	0.10	0.02	0.10	0.18	0.05	-0.01	glutathione transferase F5 [*Ta*]	2e-95
908	WAW	waw1c.pk004.c20	0.25	0.08	0.04	0.08	-0.21	0.02	0.05	-0.06	60S ribosomal protein L7A	4e-24
909	WAW	waw1c.pk004.c21	-0.04	0.03	0.05	0.06	-0.01	-0.06	0.00	0.01	protein T6D22.2 [imported] - *At*	9e-95
910	WAW	waw1c.pk004.c22	-1.11	-0.05	0.02	0.27	-0.10	0.01	0.04	-0.09	mitochondrial aldehyde dehydrogenase [*Sc*]	1e-120
911	WAW	waw1c.pk004.c24	-0.58	-0.26	-0.25	-0.05	-0.14	0.15	0.12	0.13	Acyl carrier protein III, chloroplast precursor (ACP III)	2e-66
912	WAW	waw1c.pk004.c3	-0.01	-0.03	-0.03	-0.10	0.00	-0.05	-0.07	0.00	no homologies found	-
913	WAW	waw1c.pk004.c4	0.12	-0.07	0.10	-0.10	-0.03	-0.05	-0.04	0.04	unknown protein; protein id: At1g73960.1 [*At*]	5e-72
914	WAW	waw1c.pk004.c5	-0.13	-0.13	0.25	-0.13	-0.06	-0.19	-0.40	-0.36	pathogenesis-related protein [*Os*]	3e-14
915	WAW	waw1c.pk004.c6	0.03	-0.09	0.26	-0.07	0.01	0.02	-0.05	-0.07	expressed protein; protein id: At1g76950.1 [*At]*	1e-79
916	WAW	waw1c.pk004.c7	0.10	0.13	-0.06	-0.01	-0.11	0.07	0.03	-0.07	glycosyl hydrolase family 85; protein id: At5g05460.1 [*At*]	3e-40
917	WAW	waw1c.pk004.c8	-0.09	-0.07	-0.12	0.01	-0.08	0.04	-0.01	-0.06	nitrate transporter [*Os*]	4e-89
918	WAW	waw1c.pk004.c9	0.29	0.60	0.62	0.54	0.81	-0.09	-0.06	0.00	OSJNBa0072K14.10 [*Os*]	2e-11
919	WAW	waw1c.pk004.d1	-0.20	-0.43	-0.31	-0.28	-0.10	0.04	0.03	0.04	unknown protein; protein id: At1g15860.1 [*At*]	3e-43
920	WAW	waw1c.pk004.d11	0.19	2.38	2.44	2.79	2.86	0.02	-0.07	-0.05	no homologies found	-
921	WAW	waw1c.pk004.d12	-0.03	-0.08	-0.03	-0.29	-0.11	-0.01	0.02	-0.01	maize EST AI621709, similar to an *At]* thialiana chromosome BAC genomic sequence (AC006193); unknown protein *[Os]*	8e-39
922	WAW	waw1c.pk004.d14	-0.47	-0.36	-0.09	-0.33	-0.58	0.00	-0.05	-0.23	methionine synthase protein [*Sb*]	1e-112
923	WAW	waw1c.pk004.d15	-2.22	-1.69	-0.98	-0.68	0.15	0.23	0.29	-0.32	4-coumarate:coenzyme A ligase, putative; protein id: At1g62940.1 [*At*]	8e-27
924	WAW	waw1c.pk004.d16	0.18	0.05	-0.01	0.00	-0.16	0.14	0.14	-0.03	oj000126_13.8 [*Os*]	2e-62
925	WAW	waw1c.pk004.d18	0.05	0.03	0.02	-0.03	0.05	0.05	0.06	-0.09	similar to Kinesin-like protein KIF1C [*Hs*]	2e-05
926	WAW	waw1c.pk004.d19	0.21	0.74	0.66	0.88	0.68	0.04	-0.01	0.01	d-TDP-glucose dehydratase [Phragmites australis]	3e-95
927	WAW	waw1c.pk004.d2	-0.17	-0.09	-0.10	0.17	0.19	0.01	-0.05	0.09	endomembrane protein 70, putative; protein id: At4g12650.1 [*At*]	6e-37
928	WAW	waw1c.pk004.d20	-0.11	-0.02	-0.03	0.02	-0.15	0.01	0.09	0.16	probable Na+/Ca2+ antiporter [imported] - *At*	3e-20
929	WAW	waw1c.pk004.d21	-0.19	-0.19	-0.24	-0.19	-0.13	0.11	-0.03	0.02	Peroxidase 40 precursor (Atperox P40)	6e-44
930	WAW	waw1c.pk004.d22	-0.02	-0.08	-0.12	-0.14	-0.21	-0.04	0.01	0.02	Alpha-1,4 glucan phosphorylase, L isozyme, chloroplast precursor (Starch phosphorylase L)	0.015
931	WAW	waw1c.pk004.d23	-0.43	-0.40	-0.32	-0.32	-0.40	0.05	0.09	0.05	r40g2 protein - rice (fragment)	1e-81
932	WAW	waw1c.pk004.d3	-0.04	0.10	-0.01	0.05	-0.03	-0.03	-0.03	-0.09	ppg3 [*Lm*]	0.004
933	WAW	waw1c.pk004.d4	0.05	0.47	0.50	0.51	0.30	0.01	0.00	0.00	expressed protein; protein id: At1g77610.1 [*At]*	8e-67

#	ID	EST name	Temporal *M*					*Ph* mutant *M*			Top BLASTx hit	e-val
			PM	LP	DA	TT	T	*1b*	*2a*	*2b*		
934	WAW	waw1c.pk004.d6	-2.30	-1.84	-1.09	-1.06	0.03	0.22	0.29	-0.33	4-coumarate:coenzyme A ligase, putative; protein id: At1g62940.1 [*At*]	4e-35
935	WAW	waw1c.pk004.d7	-0.09	-0.08	-0.13	-0.14	-0.13	0.02	-0.08	0.02	hypothetical protein [*Os*]	4e-69
936	WAW	waw1c.pk004.d8	1.49	0.89	0.78	0.70	0.63	0.00	0.02	-0.31	histone H2A [Euphorbia esula]	7e-37
937	WAW	waw1c.pk004.d9	-0.40	-0.54	-0.38	-0.30	-0.40	0.00	-0.09	0.03	poly-ubiquitin	1e-13
938	WAW	waw1c.pk004.e1	-0.06	-0.20	-0.29	-0.13	-0.07	0.00	0.02	0.14	unnamed protein product [*Os*]	6e-40
939	WAW	waw1c.pk004.e10	0.00	0.01	0.03	-0.01	0.04	0.04	-0.15	-0.03	no homologies found	-
940	WAW	waw1c.pk004.e12	0.02	-0.02	-0.01	-0.05	0.03	0.00	-0.11	-0.04	putative transporter [*Os*]	2e-91
941	WAW	waw1c.pk004.e15	-0.14	-0.21	-0.31	-0.24	-0.42	0.04	0.09	0.06	putative (1-4)-beta-mannan endohydrolase [*Os*]	3e-82
942	WAW	waw1c.pk004.e16	0.11	0.20	0.41	0.30	0.07	0.05	0.09	-0.01	alcohol dehydrogenase 2 [*Os*]	8e-96
943	WAW	waw1c.pk004.e17	-0.15	0.08	-0.03	0.06	0.00	-0.04	0.01	-0.02	putative protein; protein id: At4g30700.1 [*At*]	2e-42
944	WAW	waw1c.pk004.e18	0.01	0.12	0.10	0.11	0.16	0.04	-0.04	-0.01	Similar to SEC7 protein, *Sc*, PIR2:S49764; Contains Immunoglobulins and major histocompatibility	1e-101
945	WAW	waw1c.pk004.e19	-0.03	0.09	0.13	-0.02	0.01	0.00	0.07	0.00	phosphate transport protein, mitochondrial - maize	1e-36
946	WAW	waw1c.pk004.e2	0.06	-0.04	-0.04	0.04	0.08	0.06	0.01	0.04	P0002B05.11 [*Os*]	3e-46
947	WAW	waw1c.pk004.e20	-0.09	0.04	-0.01	0.07	0.02	0.00	0.08	-0.01	no homologies found	-
948	WAW	waw1c.pk004.e22	-0.44	0.28	0.02	0.19	0.37	0.04	-0.06	0.16	calreticulin - barley (fragment)	2e-43
949	WAW	waw1c.pk004.e24	-0.11	0.10	0.01	0.06	0.13	-0.02	-0.08	0.07	no homologies found	-
950	WAW	waw1c.pk004.e3	0.05	0.05	0.23	0.05	0.10	-0.12	0.03	-0.26	expressed protein; protein id: At1g70090.1 [*At*]	1e-55
951	WAW	waw1c.pk004.e4	0.55	0.19	0.04	0.13	0.01	0.01	-0.06	0.06	putative branched-chain amino acid aminotransferase; protein id: At3g05190.1	1e-62
952	WAW	waw1c.pk004.e5	0.56	0.29	0.12	0.12	0.08	0.03	-0.09	-0.04	P0701D05.9 [*Os*]	4e-38
953	WAW	waw1c.pk004.e6	0.16	-0.06	-0.09	0.12	-0.01	-0.03	-0.02	0.08	putative protein; protein id: At4g30700.1 [*At*]	1e-42
954	WAW	waw1c.pk004.e7	0.14	-0.02	-0.11	0.02	0.01	0.07	-0.06	-0.07	no homologies found	-
955	WAW	waw1c.pk004.e8	0.91	1.14	0.98	1.26	1.19	0.06	0.05	0.01	hypothetical protein KIAA0324 - human (fragment)	0.2
956	WAW	waw1c.pk004.f1	-0.13	-0.07	-0.01	-0.06	0.07	0.14	-0.03	0.03	contains ESTs D22419(C10991),AU100646(C10991)~similar to *At* chromosome 2, At2g16920~unknown	1e-11
957	WAW	waw1c.pk004.f10	-0.19	-0.20	0.02	-0.11	-0.10	0.00	0.00	-0.08	unnamed protein product [*Os*]	1e-105
958	WAW	waw1c.pk004.f11	1.05	0.99	0.81	0.48	0.67	0.00	-0.11	0.04	meiotic asynaptic mutant asy1, putative; protein id: At1g67370.1[*At*]	5e-08
959	WAW	waw1c.pk004.f12	0.25	0.03	0.02	0.26	0.23	0.01	-0.09	-0.23	succinyl-CoA ligase beta subunit [*At*]	7e-74
960	WAW	waw1c.pk004.f13	0.22	0.23	0.49	0.06	0.15	0.05	-0.03	-0.04	hypothetical protein~similar to *At* chromosome 1, F5I14.2 [*Os*]	1e-9
961	WAW	waw1c.pk004.f14	0.07	0.01	-0.30	-0.02	-0.10	-0.17	-0.05	0.05	putativeelongation factor 2 [*Os*]	4e-97
962	WAW	waw1c.pk004.f15	-0.49	-0.51	-0.24	-0.37	-0.34	-0.06	-0.13	-0.06	AT4g05320/C17L7_240 [*At*]	1e-79
963	WAW	waw1c.pk004.f16	0.19	-0.08	-0.02	0.12	0.01	0.00	-0.11	-0.03	hypothetical protein XP_174748 [*Hs*]	0.13
964	WAW	waw1c.pk004.f18	-0.01	-0.04	0.00	0.00	-0.17	0.01	-0.04	0.02	Putative hydrolase [*Os*]	8e-87
965	WAW	waw1c.pk004.f2	0.03	0.20	0.29	0.13	0.15	0.09	0.05	-0.06	hypothetical protein~similar to *At* chromosome 3, F17A17.29 [*Os*]	2e-86
966	WAW	waw1c.pk004.f20	0.15	0.48	0.49	0.57	0.40	0.07	0.07	0.00	alcohol dehydrogenase [*Hv*]	1e-86
967	WAW	waw1c.pk004.f21	0.13	0.03	-0.04	-0.05	0.05	0.04	0.04	0.05	no homologies found	-
968	WAW	waw1c.pk004.f22	0.33	0.06	0.37	0.06	-0.09	-0.02	-0.01	-0.09	unnamed protein product [*Os*]	1e-118
969	WAW	waw1c.pk004.f24	0.02	0.08	-0.06	-0.02	-0.11	-0.01	0.03	-0.02	Putative reverse transcriptase [*Os*]	1e-15
970	WAW	waw1c.pk004.f3	0.28	0.10	-0.25	0.14	0.02	0.03	0.02	0.10	no homologies found	-
971	WAW	waw1c.pk004.f6	-0.03	0.02	-0.05	0.06	0.07	-0.03	-0.03	0.08	contains similarity to unknown protein~gb|AAF35182.1~gene_id:MGF10.5 [*At*]	9e-5
972	WAW	waw1c.pk004.f7	0.04	0.12	0.10	0.15	0.07	0.08	-0.05	0.04	P0503E05.11 [*Os*]	7e-19
973	WAW	waw1c.pk004.f8	-0.99	-0.65	-0.66	-0.57	-0.47	0.02	0.07	0.04	chlorophyll a/b-binding protein precursor [*Hv*]	4e-89
974	WAW	waw1c.pk004.f9	0.08	0.18	0.35	0.22	0.12	-0.03	-0.04	0.06	unknown protein [*At*]	7e-49
975	WAW	waw1c.pk004.g10	0.56	0.25	0.26	0.16	0.08	0.00	-0.07	-0.01	t-complex polypeptide 1 [Bruguiera sexangula]	8e-93
976	WAW	waw1c.pk004.g11	0.28	0.24	-0.05	0.21	0.10	-0.10	-0.08	0.04	no homologies found	-
977	WAW	waw1c.pk004.g12	1.23	0.90	0.98	0.52	0.74	-0.03	-0.17	0.08	Peroxidase 40 precursor (Atperox P40)	5e-33
978	WAW	waw1c.pk004.g13	0.08	0.03	0.03	0.03	0.06	-0.02	0.02	-0.01	P0410E03.2 [*Os*]	2e-11
979	WAW	waw1c.pk004.g14	-0.10	0.03	-0.09	0.02	-0.06	0.03	0.14	-0.09	putative expressed protein [*Sb*]	1e-43
980	WAW	waw1c.pk004.g15	0.06	0.33	0.33	0.31	0.34	0.03	-0.05	-0.01	dolichyl-di-phosphooligosaccharide-protein glycotransferase (oligosaccharyltransferase)-like; protein id:	2e-40
981	WAW	waw1c.pk004.g16	-0.33	-0.28	-0.12	-0.11	0.14	-0.04	-0.10	0.01	putative GDSL-motif lipase/acylhydrolase; protein id: At3g04290.1 [*At*]	4e-35
982	WAW	waw1c.pk004.g17	0.03	0.05	-0.14	0.07	0.11	0.00	-0.03	0.03	no homologies found	-
983	WAW	waw1c.pk004.g18	-0.04	0.17	0.02	0.13	-0.06	0.04	0.02	0.13	putative WD-40 repeat protein [*Os*]	1e-99
984	WAW	waw1c.pk004.g19	-0.89	0.09	0.18	-0.20	0.23	0.01	-0.11	0.13	protein disulfide isomerase [Triticum turgidum subsp. durum]	2e-94
985	WAW	waw1c.pk004.g2	-0.36	-0.06	-0.14	-0.03	0.06	0.07	0.15	-0.15	hypothetical protein (repetitive element TCb1 No.5) - *Cb*	0.032
986	WAW	waw1c.pk004.g20	-0.02	0.01	-0.05	0.07	0.01	-0.01	-0.03	0.04	Unknown protein [*Os*]	2e-80
987	WAW	waw1c.pk004.g22	0.11	-0.05	-0.25	0.03	0.06	0.05	0.03	0.10	SGT1 [*Hv*]	1e-75
988	WAW	waw1c.pk004.g24	0.06	0.37	0.44	0.36	0.77	-0.09	0.00	0.00	Hypothetical protein [*Os*]	3e-27
989	WAW	waw1c.pk004.g4	0.89	2.44	2.70	2.37	3.01	0.06	0.02	-0.08	beta-N-acetylhexosaminidase -like protein [*Os*]	1e-47
990	WAW	waw1c.pk004.g5	-0.20	-0.19	0.03	-0.06	-0.07	0.07	0.07	-0.06	Cytochrome P450 98A1	2e-12
991	WAW	waw1c.pk004.g6	0.26	0.25	0.23	0.27	0.23	0.05	0.00	0.11	P0697C12.11 [*Os*]	5e-13
992	WAW	waw1c.pk004.g7	0.02	-0.17	-0.04	-0.06	-0.18	0.10	-0.02	0.01	ribosomal protein s6 RPS6-2 [*Zm*]	2e-58
993	WAW	waw1c.pk004.g8	-0.06	-0.16	-0.08	-0.04	0.02	0.01	-0.02	-0.02	no homologies found	-
994	WAW	waw1c.pk004.h1	-0.10	0.12	0.39	0.25	0.10	0.01	0.03	0.00	allene oxide synthase [*Hv* subsp. vulgare]	5e-93
995	WAW	waw1c.pk004.h11	-0.06	-0.09	-0.11	-0.05	-0.09	-0.07	0.07	0.07	expressed protein; protein id: At1g26270.1	3e-09
996	WAW	waw1c.pk004.h12	0.08	0.07	-0.06	0.02	0.06	0.06	-0.03	0.00	no homologies found	-
997	WAW	waw1c.pk004.h13	0.05	-0.06	-0.06	-0.11	0.26	-0.02	-0.07	0.06	no homologies found	-
998	WAW	waw1c.pk004.h15	-0.13	0.02	-0.02	0.09	0.01	-0.03	-0.07	-0.04	sister of P-glycoprotein [Fundulus heteroclitus]	0.67
999	WAW	waw1c.pk004.h16	0.09	0.18	0.01	0.10	-0.04	0.00	0.06	0.07	hypothetical protein; protein id: At3g06880.1 [*At*]	8e-04
1000	WAW	waw1c.pk004.h17	-0.02	0.07	-0.15	0.17	-0.02	0.08	0.07	-0.06	putative synaptobrevin [*At*]	5e-69
1001	WAW	waw1c.pk004.h18	0.06	-0.15	-0.04	-0.03	-0.15	0.00	0.08	0.01	peptide synthetase [Mycobacterium smegmatis]	0.99
1002	WAW	waw1c.pk004.h19	0.00	0.04	0.16	0.02	0.03	0.03	0.15	0.01	hypothetical protein~predicted by FGENESH etc. [*Os*]	4e-05
1003	WAW	waw1c.pk004.h20	-0.36	-0.16	-0.02	-0.22	-0.25	0.09	0.06	-0.02	subtilisin-like serine protease, putative; protein id: At3g14067.1 [*At*]	2e-77
1004	WAW	waw1c.pk004.h22	-0.35	-0.26	0.06	-0.22	-0.30	-0.05	0.01	-0.09	methionine synthase protein [*Sb*]	1e-60
1005	WAW	waw1c.pk004.h23	-0.01	0.09	0.12	0.14	-0.08	0.02	0.15	0.02	LRK1 protein [*Os*]	1e-103
1006	WAW	waw1c.pk004.h24	0.74	0.37	0.29	0.25	0.35	-0.01	-0.07	-0.15	Histone H2A.2.1	4e-16
1007	WAW	waw1c.pk004.h3	0.13	0.02	-0.17	0.03	0.03	0.00	0.07	0.09	no homologies found	-
1008	WAW	waw1c.pk004.h4	1.60	0.80	0.79	0.53	0.53	-0.08	-0.01	-0.25	histone H2A.2 - wheat	9e-52
1009	WAW	waw1c.pk004.h6	0.06	-0.21	-0.25	-0.23	-0.29	-0.02	0.02	0.03	peroxisomal copper-containing amine oxidase [*Gm*]	1e-14
1010	WAW	waw1c.pk004.h7	0.13	-0.02	0.05	0.07	0.07	-0.09	0.01	-0.04	P0046E05.21 [*Os*]	1e-22
1011	WAW	waw1c.pk004.h9	-0.08	-0.05	0.12	0.06	-0.07	0.01	0.01	-0.03	no homologies found	-
1012	WAW	waw1c.pk004.i1	0.10	0.08	-0.04	0.09	0.03	0.05	-0.04	-0.08	no homologies found	-
1013	WAW	waw1c.pk004.i10	0.04	0.13	0.19	0.03	0.00	0.00	0.02	-0.03	calmodulin-binding protein; protein id: At2g18750.1 [*At*]	1e-47
1014	WAW	waw1c.pk004.i11	-0.05	-0.21	-0.24	-0.19	-0.26	0.01	-0.01	0.05	hypothetical protein~similar to *Os* chromosome 1 P0460H02.9 [*Os*]	0.72
1015	WAW	waw1c.pk004.i12	0.02	0.35	0.24	0.26	0.25	0.01	0.04	0.03	transport protein; protein id: At4g14160.1 [*At*]	7e-74
1016	WAW	waw1c.pk004.i13	-0.46	0.08	-0.20	0.00	0.00	-0.05	-0.06	0.06	calreticulin precursor - maize	4e-97
1017	WAW	waw1c.pk004.i14	0.02	0.17	0.33	0.18	0.07	0.02	-0.08	-0.12	kinase-like protein [*At*]	1e-04

			Temporal *M*					*Ph* mutant *M*				
#	ID	EST name	PM	LP	DA	TT	T	*1b*	*2a*	*2b*	Top BLASTx hit	e-val
1018	WAW	waw1c.pk004.i15	-0.03	-0.05	-0.09	0.00	-0.31	-0.11	-0.04	0.06	putative protein; protein id: At3g53690.1 [*At*]	4e-11
1019	WAW	waw1c.pk004.i16	0.01	-0.07	0.09	-0.04	0.12	-0.05	-0.04	-0.09	putative transporter [*Os*]	1e-82
1020	WAW	waw1c.pk004.i18	-0.17	-0.05	-0.07	0.15	0.07	0.03	-0.02	0.07	putative ATP synthase; protein id: At2g21870.1	2e-29
1021	WAW	waw1c.pk004.i19	-0.54	-0.74	-0.59	-0.60	-0.69	-0.05	-0.14	-0.16	plasma membrane H+-ATPase [*Hv* subsp. vulgare]	1e-82
1022	WAW	waw1c.pk004.i2	-0.23	-0.10	0.06	0.00	0.22	0.04	-0.05	0.09	putative mitogen-activated protein kinase [*Os*]	2e-09
1023	WAW	waw1c.pk004.i20	-0.27	0.06	0.03	0.15	0.23	0.04	0.01	0.15	ESTs C99033(E4350),C99032(E4350),D46006(S10372), D47177(S12347),C28582(C61678),C27203(C51329)	2e-84
1024	WAW	waw1c.pk004.i21	-0.21	0.34	-0.20	0.14	0.20	0.20	0.09	0.05	putative CTP synthase [*Os*]	1e-81
1025	WAW	waw1c.pk004.i22	0.04	-0.22	-0.06	-0.21	-0.06	-0.04	-0.07	0.00	SIGNAL RECOGNITION PARTICLE 54 KD PROTEIN 1 (SRP54)	5e-96
1026	WAW	waw1c.pk004.i23	0.23	0.13	0.07	-0.01	0.07	-0.01	-0.08	0.01	expressed protein; protein id: At1g73030.1	6e-62
1027	WAW	waw1c.pk004.i24	0.19	0.09	0.20	0.08	-0.01	0.01	0.00	0.00	60S ribosomal protein L3	1e-117
1028	WAW	waw1c.pk004.i5	0.10	0.14	0.12	0.08	0.06	0.01	0.00	-0.02	hypothetical protein XP_150039 [*Mm*]	6e-04
1029	WAW	waw1c.pk004.i6	0.07	0.02	0.49	0.01	0.17	0.05	-0.02	-0.01	ubiquitin / ribosomal protein CEP52 - turnip	1e-39
1030	WAW	waw1c.pk004.i8	-0.02	0.31	0.28	0.31	0.34	-0.06	-0.20	-0.15	permease [*At*]	1e-24
1031	WAW	waw1c.pk004.i9	0.10	0.09	0.15	0.09	0.06	0.03	-0.02	-0.34	Putative enolase (2-phospho-D-glycerate hydroylase) [*Os*]	1e-57
1032	WAW	waw1c.pk004.j1	0.19	0.61	0.54	0.69	0.53	0.05	0.09	0.00	alcohol dehydrogenase [*Hv*]	3e-88
1033	WAW	waw1c.pk004.j13	-0.07	-0.19	-0.19	-0.18	-0.29	0.00	-0.10	0.02	Hypothetical protein [*At*]	5e-06
1034	WAW	waw1c.pk004.j14	-0.08	0.03	-0.12	-0.32	0.36	-0.07	-0.15	0.09	endoplasmin homolog precursor (GRP94 homolog)	2e-64
1035	WAW	waw1c.pk004.j15	-0.05	0.00	-0.04	0.10	0.02	0.02	-0.03	-0.04	gene_id:K9P8.8~pir||T09896~strong similarity to unknown protein [*At*]	3e-7
1036	WAW	waw1c.pk004.j16	-0.04	-0.18	-0.36	-0.16	-0.34	0.01	-0.04	0.06	small Ras-related GTP-binding protein [*Ta*]	3e-55
1037	WAW	waw1c.pk004.j17	0.33	0.32	0.02	0.27	0.07	-0.07	-0.01	0.04	no homologies found	-
1038	WAW	waw1c.pk004.j18	0.20	0.04	0.03	0.27	0.13	-0.05	-0.12	-0.20	succinyl-CoA ligase beta subunit [*At*]	4e-79
1039	WAW	waw1c.pk004.j19	0.08	0.16	0.32	0.16	0.14	0.02	0.04	0.05	At2g5740/F3N11.19 [*At*]	2e-30
1040	WAW	waw1c.pk004.j20	0.14	0.04	0.20	0.08	0.19	0.00	0.05	0.01	Putative pyrophosphate--fructose-6-phosphate 1-phosphotransferase [*Os*]	3e-87
1041	WAW	waw1c.pk004.j22	-0.56	-0.92	-0.48	-1.13	-0.91	0.09	0.09	0.04	Putative hydroxymethylglutaryl coenzyme A synthase [*Os*]	3e-40
1042	WAW	waw1c.pk004.j23	-0.05	0.08	0.10	0.11	0.13	-0.01	0.05	0.03	expressed protein; protein id: At4g31410.1	3e-41
1043	WAW	waw1c.pk004.j24	0.10	0.09	0.11	0.04	0.03	-0.02	0.01	-0.03	3-oxoacyl-[acyl-carrier-protein] synthase (EC 2.3.1.41) precursor [similarity] - barley	4e-36
1044	WAW	waw1c.pk004.j3	-0.11	0.04	0.01	0.09	0.08	-0.06	-0.05	0.11	no homologies found	-
1045	WAW	waw1c.pk004.j4	-0.06	0.02	-0.18	0.01	-0.02	0.00	0.03	0.20	no homologies found	-
1046	WAW	waw1c.pk004.j5	0.00	-0.17	-0.12	-0.23	-0.32	0.04	-0.01	0.01	putative ATP-dependent RNA helicase [*Os*]	1e-103
1047	WAW	waw1c.pk004.j6	0.05	0.27	-0.11	0.20	0.18	0.06	0.03	0.19	no homologies found	-
1048	WAW	waw1c.pk004.j9	-1.09	-1.29	-0.13	-0.48	0.22	-0.12	-0.06	-0.10	no homologies found	-
1049	WAW	waw1c.pk004.k1	-0.18	-0.32	-0.41	-0.26	-0.44	0.04	-0.08	0.00	no homologies found	-
1050	WAW	waw1c.pk004.k10	-0.46	0.13	0.25	0.01	0.06	-0.02	0.01	0.07	protein disulfide isomerase 2 precursor [*Ta*]	2e-64
1051	WAW	waw1c.pk004.k12	0.15	0.08	0.04	0.11	0.08	0.00	0.01	0.05	no homologies found	-
1052	WAW	waw1c.pk004.k13	0.02	-0.04	0.11	-0.04	0.00	0.04	-0.05	-0.01	contains ESTs C19491(E10494),C99236(E10494)~similar to vesicle soluble NSF attachment protein receptor [*Os*	4e-66
1053	WAW	waw1c.pk004.k14	-0.49	-0.06	0.03	-0.08	1.19	-0.01	-0.04	0.03	NADH dehydrogenase like protein; protein id:At4g21490.1[*At*]	1e-78
1054	WAW	waw1c.pk004.k15	0.07	0.08	-0.04	0.05	0.01	0.07	0.01	0.05	DNA-directed RNA polymerase II 13.6K chain; protein id: At3g52090.1*At]*	3e-47
1055	WAW	waw1c.pk004.k16	-0.08	-0.11	-0.20	-0.07	-0.24	0.10	0.05	0.03	putative RecA protein [*Os*]	6e-45
1056	WAW	waw1c.pk004.k18	0.21	0.04	-0.12	0.07	0.07	-0.02	0.04	-0.01	unknown protein; protein id: At1g05785.1 [*At*]	2e-26
1057	WAW	waw1c.pk004.k19	-0.11	0.23	0.31	0.23	0.04	-0.12	-0.12	0.01	unnamed protein product [*Os*]	4e-55
1058	WAW	waw1c.pk004.k20	0.15	0.46	0.52	0.55	0.30	-0.04	-0.04	-0.05	pyruvate kinase; protein id: At5g08570.1 [*At*]	1e-100
1059	WAW	waw1c.pk004.k22	0.10	0.01	-0.19	0.11	0.27	0.00	0.04	0.03	hypothetical protein; protein id: At2g22120.1 [*At*]	2e-25
1060	WAW	waw1c.pk004.k23	1.25	0.48	-0.02	0.34	0.34	0.00	-0.03	-0.10	no homologies found	-
1061	WAW	waw1c.pk004.k24	0.35	0.38	0.17	0.30	0.22	-0.05	0.00	0.01	protein synthesis initiation factor eIF2 alpha [*At*]	8e-04
1062	WAW	waw1c.pk004.k4	-0.09	-0.02	-0.03	-0.03	-0.04	0.05	0.08	0.04	Glyceraldehyde 3-phosphate dehydrogenase, cytosolic	2e-95
1063	WAW	waw1c.pk004.k5	-0.20	-0.09	0.00	-0.02	0.07	-0.04	0.03	-0.01	AT5g42350/MDH9_4 [*At*]	1e-07
1064	WAW	waw1c.pk004.k6	-0.26	-0.31	-0.14	-0.44	-0.30	-0.03	-0.08	0.01	polyadenylate-binding protein - wheat	1e-77
1065	WAW	waw1c.pk004.k7	-0.76	0.11	0.08	-0.10	0.20	-0.01	-0.04	0.15	protein disulfide isomerase 3 precursor [*Ta*]	9e-61
1066	WAW	waw1c.pk004.k8	0.15	0.00	-0.01	0.05	-0.08	0.01	0.01	-0.02	putative protein; protein id: At3g51460.1 [*At*]	2e-41
1067	WAW	waw1c.pk004.k9	0.06	0.11	-0.06	0.09	0.04	0.01	-0.04	-0.01	putative Sec24-like COPII protein [*At*]	1e-64
1068	WAW	waw1c.pk004.l1	-0.50	0.15	0.29	0.41	0.90	-0.02	-0.07	-0.04	ESTs AU082304(C61278),C93463(C50982) correspond to a region of the predicted gene.~Similar to *At* DNA	3e-75
1069	WAW	waw1c.pk004.l11	-0.12	-0.02	0.10	0.11	0.17	0.05	0.10	0.04	no homologies found	-
1070	WAW	waw1c.pk004.l12	-0.03	-0.08	-0.14	-0.34	-0.10	-0.02	-0.06	0.07	signal recognition particle receptor-like protein; protein id: At4g30600.1 [*At]*	3e-99
1071	WAW	waw1c.pk004.l13	-0.06	-0.05	-0.03	-0.11	0.09	-0.06	0.14	-0.01	unnamed protein product [*Os*]	0.27
1072	WAW	waw1c.pk004.l14	-0.02	0.39	0.37	0.42	0.39	0.00	0.03	0.21	HSP100/ClpB, putative; protein id: At5g15450.1 [*At*]	4e-97
1073	WAW	waw1c.pk004.l16	0.26	0.13	-0.10	0.12	0.23	-0.03	0.15	-0.02	heparan sulfate 6-O-sulfotransferase 1 [*Mm*]	0.29
1074	WAW	waw1c.pk004.l17	0.00	-0.06	0.11	-0.08	-0.03	-0.06	0.01	0.02	no homologies found	-
1075	WAW	waw1c.pk004.l19	-0.01	-0.04	-0.05	-0.05	-0.04	-0.09	-0.05	-0.09	expressed protein; protein id: At2g03120.1 [*At]*	2e-37
1076	WAW	waw1c.pk004.l20	-0.15	0.06	0.11	0.03	0.18	0.06	0.03	-0.01	unknown protein; protein id: At1g50030.1 [*At*]	1e-60
1077	WAW	waw1c.pk004.l21	0.25	0.88	0.64	1.05	0.81	0.06	0.03	0.08	UDP-glucuronic acid decarboxylase [*Os*]	3e-99
1078	WAW	waw1c.pk004.l22	-0.13	-0.23	-0.17	-0.19	-0.16	-0.01	0.00	-0.05	expressed protein; protein id: At2g03350.1 [*At*]	1e-46
1079	WAW	waw1c.pk004.l23	-0.37	-0.12	-0.14	-0.11	-0.01	-0.20	-0.10	0.26	OSJNBa0029H02.26 [*Os*]	2e-15
1080	WAW	waw1c.pk004.l24	-0.06	-0.03	-0.02	-0.04	-0.11	0.07	-0.05	0.04	putative mitochondrial inner membrane translocating protein; protein id: At2g20510.1 [*At*]	4e-58
1081	WAW	waw1c.pk004.l3	0.29	0.74	0.10	0.77	0.33	0.06	0.12	0.05	B1129G05.13 [*Os*]	3e-49
1082	WAW	waw1c.pk004.l5	0.08	0.11	0.02	0.10	0.04	-0.02	-0.02	0.00	histone acetyl transferase [*Zm*]	5e-07
1083	WAW	waw1c.pk004.l6	-1.20	0.05	0.08	0.33	-0.07	0.00	0.13	-0.12	mitochondrial aldehyde dehydrogenase [*Sc*]	1e-108
1084	WAW	waw1c.pk004.l7	0.26	0.18	0.09	0.16	0.03	-0.02	0.08	-0.05	unknown protein; protein id: At3g23530.1 [*At]*	6e-51
1085	WAW	waw1c.pk004.l9	-0.07	-0.13	-0.19	-0.01	-0.13	-0.05	-0.03	0.00	putative protein; protein id: At5g47780.1 [*At]*	1e-102
1086	WAW	waw1c.pk004.m1	0.21	0.20	0.08	0.10	0.14	-0.04	0.02	-0.10	Claustrin like family member [*Ce*]	0.67
1087	WAW	waw1c.pk004.m10	0.24	0.04	0.03	0.02	-0.10	-0.09	-0.07	0.01	eukaryotic release factor 1 homolog (gb|AAA91169.1); protein id: At5g47880.1 [*At]*	1e-105
1088	WAW	waw1c.pk004.m12	0.09	-0.10	0.09	-0.01	-0.09	-0.08	0.00	-0.13	gb protein [*Sb*]	9e-48
1089	WAW	waw1c.pk004.m13	-0.08	-0.02	-0.03	-0.05	-0.01	-0.05	0.02	0.00	no homologies found	-
1090	WAW	waw1c.pk004.m14	-0.09	0.05	0.14	-0.02	0.24	-0.05	0.08	0.05	RNA-binding protein, putative; protein id: At1g32790.1	2e-21
1091	WAW	waw1c.pk004.m16	0.07	-0.09	-0.25	-0.05	-0.08	0.04	0.04	0.03	no homologies found	-
1092	WAW	waw1c.pk004.m17	0.07	-0.06	0.02	-0.07	0.06	0.04	0.06	-0.04	DNA-directed RNA polymerase II, third largest subunit; protein id: At2g15430.1	2e-38
1093	WAW	waw1c.pk004.m18	0.07	-0.04	-0.05	-0.11	-0.14	-0.05	-0.05	-0.21	putative homeodomain-leucine zipper protein [*Os*]	4e-67
1094	WAW	waw1c.pk004.m19	-0.63	-0.92	-0.86	-1.17	-1.28	-0.03	0.02	-0.14	sterol delta7 reductase; protein id: At1g50430.1 supported by cDNA: gi_20466245	4e-55
1095	WAW	waw1c.pk004.m22	0.01	0.03	-0.04	0.16	-0.02	0.03	0.10	-0.09	no homologies found	-
1096	WAW	waw1c.pk004.m24	0.56	0.31	0.41	0.22	0.09	-0.03	-0.09	-0.18	putative receptor-like protein kinase [*Os*]	4e-89
1097	WAW	waw1c.pk004.m3	-0.14	-0.07	-0.02	0.03	-0.15	0.02	0.05	0.06	putative cinnamyl-alcohol dehydrogenase [*Os*]	2e-16
1098	WAW	waw1c.pk004.m4	0.25	-0.07	0.12	0.10	0.10	-0.06	-0.04	-0.12	hypothetical protein [*Os*]	2e-13
1099	WAW	waw1c.pk004.m6	0.02	-0.37	-0.36	-0.29	-0.11	-0.03	0.05	0.06	hypothetical protein p85RF [imported] - *Par*	4e-49

#	ID	EST name	Temporal *M*					*Ph* mutant *M*			Top BLASTx hit	e-val
			PM	LP	DA	TT	T	*1b*	*2a*	*2b*		
1100	WAW	waw1c.pk004.m7	0.26	0.18	0.11	0.06	0.02	-0.02	-0.09	-0.06	putative phenylalanyl-tRNA synthetase beta-subunit; PheHB; protein id: At1g72550.1	6e-15
1101	WAW	waw1c.pk004.m8	-0.03	0.00	0.01	-0.13	0.10	0.09	0.03	0.01	no homologies found	-
1102	WAW	waw1c.pk004.n1	0.16	0.02	0.15	-0.02	0.01	0.05	0.01	0.01	DNA mismatch repair protein MSH2 (MUS1)	1e-61
1103	WAW	waw1c.pk004.n13	-0.41	-0.27	-0.27	-0.13	-0.30	-0.06	-0.03	-0.06	Phytepsin precursor (Aspartic proteinase)	2e-91
1104	WAW	waw1c.pk004.n14	-0.21	0.09	0.42	0.29	0.08	0.06	0.03	-0.05	putative elicitor response protein [*Os*]	1e-45
1105	WAW	waw1c.pk004.n15	-0.05	0.09	0.08	0.23	0.14	0.03	0.04	-0.02	no homologies found	-
1106	WAW	waw1c.pk004.n16	0.61	0.18	0.21	0.06	0.09	-0.01	0.05	-0.12	no homologies found	-
1107	WAW	waw1c.pk004.n17	-0.24	-0.18	-0.16	-0.10	-0.20	0.03	0.03	0.11	Triosephosphate isomerase, cytosolic (TIM)	2e-26
1108	WAW	waw1c.pk004.n18	-0.11	-0.07	-0.06	0.00	-0.06	-0.01	0.05	0.04	E2, ubiquitin-conjugating enzyme, putative; protein id: At1g16890.1	2e-82
1109	WAW	waw1c.pk004.n19	0.21	0.00	0.08	-0.01	0.02	0.04	0.01	0.03	histone acetyl transferase [*Zm*]	6e-12
1110	WAW	waw1c.pk004.n2	0.53	0.50	0.65	0.23	0.52	0.01	0.02	0.05	no homologies found	-
1111	WAW	waw1c.pk004.n20	0.00	0.01	-0.14	0.01	-0.09	0.08	0.06	-0.04	disease resistance protein RPM1 homolog [*Sb*]	2e-07
1112	WAW	waw1c.pk004.n21	0.30	-0.01	0.02	-0.06	-0.01	0.01	0.04	-0.21	HMG1/2-like protein	3e-33
1113	WAW	waw1c.pk004.n22	-0.19	-0.01	-0.16	-0.14	0.17	0.07	-0.05	0.09	unknown protein [*At*]	2e-60
1114	WAW	waw1c.pk004.n23	-0.21	0.10	-0.18	0.06	0.03	0.05	0.12	0.25	gamma-type tonoplast intrinsic protein [*Ta*]	1e-70
1115	WAW	waw1c.pk004.n24	-0.01	0.12	0.13	0.11	-0.04	-0.04	-0.04	-0.06	no homologies found	-
1116	WAW	waw1c.pk004.n4	-0.11	-0.43	-0.14	-0.35	-0.24	-0.02	-0.10	0.03	no homologies found	-
1117	WAW	waw1c.pk004.n5	0.32	0.55	0.67	0.52	0.22	-0.06	-0.03	-0.13	pyruvate kinase; protein id: At5g08570.1 [*At*]	6e-99
1118	WAW	waw1c.pk004.n6	0.02	0.07	-0.01	0.03	0.07	0.00	0.05	0.10	no homologies found	-
1119	WAW	waw1c.pk004.n7	0.00	-0.27	-0.20	-0.12	-0.13	-0.06	-0.02	0.01	kinesin-related protein; protein id: At3g45850.1 [*At*]	8e-25
1120	WAW	waw1c.pk004.n8	-0.42	-0.06	0.13	0.07	0.11	0.06	-0.03	-0.03	bHLH protein; protein id: At2g16910.1 [*At*]	2e-18
1121	WAW	waw1c.pk004.n9	-0.02	-0.10	-0.08	-0.01	-0.10	-0.03	0.10	0.01	gene_id:MZE19.4~unknown protein [*At*]	4e-43
1122	WAW	waw1c.pk004.o1	0.53	0.30	0.34	0.07	0.05	-0.04	-0.11	0.04	putative DNA gyrase A subunit [*At*]	2e-67
1123	WAW	waw1c.pk004.o10	0.05	-0.26	-0.33	-0.18	-0.21	0.13	0.07	-0.01	unnamed protein product [*Os*]	1e-79
1124	WAW	waw1c.pk004.o12	0.02	-0.11	0.08	-0.03	-0.11	-0.03	-0.03	-0.05	lipase-like protein; protein id: At4g18550.1 [*At*]	1e-34
1125	WAW	waw1c.pk004.o14	-0.24	-0.12	-0.07	-0.16	-0.09	0.08	0.07	-0.07	KIAA1681 protein [*Hs*]	0.37
1126	WAW	waw1c.pk004.o15	0.26	0.01	0.07	0.04	-0.12	-0.01	-0.10	-0.04	P0686E09.16 [*Os*]	1e-100
1127	WAW	waw1c.pk004.o18	-0.10	0.34	0.64	0.29	0.20	0.11	0.01	0.04	putative protein; protein id: At5g26940.1 [*At*]	4e-06
1128	WAW	waw1c.pk004.o19	0.47	0.53	0.29	0.51	0.60	-0.03	-0.17	0.16	70 kDa peptidylprolyl isomerase (Peptidylprolyl cis-trans isomerase) (PPiase) (Rotamase)	2e-73
1129	WAW	waw1c.pk004.o2	-0.02	-0.13	-0.25	-0.11	0.00	0.07	-0.06	0.04	glyoxalase II [*Os*]	2e-20
1130	WAW	waw1c.pk004.o20	-0.10	0.02	-0.16	0.02	-0.13	-0.04	0.02	0.08	Elongation factor 1-alpha (EF-1-ALPHA)	1e-116
1131	WAW	waw1c.pk004.o22	-0.35	0.00	-0.03	-0.13	-0.19	-0.01	-0.02	-0.12	Putative RNA-binding protein [*Os*]	1e-31
1132	WAW	waw1c.pk004.o24	-0.05	-0.15	-0.03	-0.12	-0.16	-0.11	-0.02	-0.06	HSP associated protein like; protein id: At4g22670.1	3e-26
1133	WAW	waw1c.pk004.o4	-0.16	0.20	0.27	0.31	0.35	0.00	0.06	0.02	type 1 membrane protein, putative; protein id: At3g24160.1:	2e-18
1134	WAW	waw1c.pk004.o6	0.16	0.28	0.21	0.13	0.07	-0.06	-0.07	-0.02	probable protein kinase - maize (fragment)	2e-91
1135	WAW	waw1c.pk004.o8	-0.38	-0.88	-0.58	-0.72	-0.65	-0.04	-0.10	-0.08	plasma membrane H+-ATPase [*Hv* subsp. vulgare]	2e-82
1136	WAW	waw1c.pk004.o9	-0.13	-0.07	-0.15	0.01	0.06	0.01	-0.02	-0.01	no homologies found	-
1137	WAW	waw1c.pk004.p1	-0.03	0.00	-0.04	-0.08	0.04	-0.02	0.00	-0.02	no homologies found	-
1138	WAW	waw1c.pk004.p10	-0.13	0.13	0.05	0.14	1.20	-0.01	0.00	0.03	no homologies found	-
1139	WAW	waw1c.pk004.p12	0.27	0.09	0.06	0.20	0.17	0.00	-0.09	-0.05	GTP-binding protein [*Ca*]	9e-86
1140	WAW	waw1c.pk004.p13	0.06	0.37	-0.21	0.25	0.06	0.06	0.01	-0.02	receptor protein kinase -like; protein id: At3g46290.1 [*At*]	0.011
1141	WAW	waw1c.pk004.p14	-0.19	0.04	0.17	-0.04	-0.08	0.01	0.07	0.03	bHLH protein; protein id: At2g16910.1 [*At*]	1e-19
1142	WAW	waw1c.pk004.p15	-0.01	-0.07	-0.15	-0.12	0.26	0.02	0.08	0.07	no homologies found	-
1143	WAW	waw1c.pk004.p16	-1.43	-2.42	-1.78	-2.42	-2.43	-0.05	-0.16	-0.18	putative CER1 [*Os*]	6e-82
1144	WAW	waw1c.pk004.p17	0.17	0.18	0.25	0.04	0.07	0.04	0.03	-0.09	G-protein beta-subunit (transducin) family; protein id: At2g43770.1 [*At]*	7e-93
1145	WAW	waw1c.pk004.p18	0.14	0.10	0.03	0.07	-0.04	0.02	0.06	0.02	putative 40S ribosomal protein S3 [*Ta*]	1e-88
1146	WAW	waw1c.pk004.p19	-0.17	-0.10	-0.09	-0.01	-0.01	0.04	0.04	0.01	putative pyruvate kinase [*Os*]	1e-108
1147	WAW	waw1c.pk004.p2	0.19	-0.11	-0.12	-0.05	-0.01	0.01	-0.05	0.01	no homologies found	-
1148	WAW	waw1c.pk004.p21	0.00	0.01	0.12	0.05	0.00	-0.06	0.01	0.07	no homologies found	-
1149	WAW	waw1c.pk004.p22	-0.02	0.05	-0.06	0.09	-0.07	0.00	0.05	-0.04	At1g61040/T7P1_17 [*At*]	2e-10
1150	WAW	waw1c.pk004.p23	1.35	0.35	0.19	0.29	0.13	-0.10	-0.07	-0.29	histone H2A (clone TH254) - wheat	6e-40
1151	WAW	waw1c.pk004.p24	0.33	0.05	-0.02	0.06	-0.03	-0.05	-0.03	-0.07	replication factor C 36kDa subunit [*Os*]	1e-102
1152	WAW	waw1c.pk004.p3	-0.11	0.13	-0.03	0.04	0.36	0.00	-0.01	0.09	Sec61p [*Ta*]	6e-97
1153	WAW	waw1c.pk004.p4	0.19	0.51	0.52	0.37	0.49	0.07	-0.01	0.10	unknown [*At*]	2e-46
1154	WAW	waw1c.pk004.p7	-0.64	-0.60	-0.23	-0.48	-0.25	-0.13	-0.19	-0.08	putative protein; protein id: At5g18430.1 [*At*]	2e-15
1155	WAW	waw1c.pk004.p8	-0.30	-0.22	-0.19	-0.20	-0.08	-0.03	-0.05	0.01	Glyceraldehyde 3-phosphate dehydrogenase, cytosolic	3e-84
1156	WAW	waw1c.pk004.p9	-0.04	-0.02	-0.04	0.05	-0.04	0.00	0.00	0.00	unknown protein; protein id: At1g63050.1 [*At*]	1e-73
1157	WAW	waw1c.pk005.a10	-0.08	-0.04	0.03	0.02	0.32	0.00	-0.04	-0.05	unnamed protein product [*Os*]	1e-40
1158	WAW	waw1c.pk005.a11	0.17	0.14	0.22	0.12	0.04	0.00	0.01	0.10	putative protein; protein id: At5g14790.1 [*At]*	4e-29
1159	WAW	waw1c.pk005.a12	-0.35	-0.05	-0.10	-0.16	-0.15	-0.05	-0.04	0.04	putative DNA binding protein [*At*]	7e-33
1160	WAW	waw1c.pk005.a13	-0.40	-0.63	-0.39	-0.52	-0.47	-0.03	0.01	-0.05	MADS box transcription factor [*Ta*]	2e-80
1161	WAW	waw1c.pk005.a14	-0.07	0.01	0.06	0.12	0.01	0.06	-0.03	0.01	no homologies found	-
1162	WAW	waw1c.pk005.a15	0.19	0.06	0.19	0.12	-0.08	0.04	-0.01	-0.03	60S ribosomal protein L3	1e-108
1163	WAW	waw1c.pk005.a16	0.13	0.30	0.29	0.16	0.08	-0.05	0.00	0.16	DNA Helicase [*At*]	1e-13
1164	WAW	waw1c.pk005.a18	-0.08	-0.01	0.05	-0.02	-0.13	0.05	-0.05	-0.09	unknown protein [*At*]	3e-08
1165	WAW	waw1c.pk005.a20	-0.10	-0.12	0.08	-0.07	-0.11	0.08	0.00	-0.13	unknown protein; protein id: At2g47350.1 [*At*]	0.35
1166	WAW	waw1c.pk005.a21	0.25	0.15	0.10	0.10	0.02	-0.06	0.05	-0.10	no homologies found	-
1167	WAW	waw1c.pk005.a23	-0.05	-0.04	0.02	-0.04	0.01	-0.01	-0.08	0.10	no homologies found	-
1168	WAW	waw1c.pk005.a24	0.24	0.47	0.55	0.39	0.46	-0.06	-0.02	-0.08	protein disulfide-isomerase-like protein; protein id: At3g54960.1 [*At*]	1e-36
1169	WAW	waw1c.pk005.a3	0.23	0.18	-0.04	0.08	0.08	0.01	0.01	-0.06	no homologies found	-
1170	WAW	waw1c.pk005.a4	0.03	0.31	-0.07	0.29	0.28	-0.03	0.06	0.08	Putative endosomal protein [*Os*]	7e-05
1171	WAW	waw1c.pk005.a5	0.59	0.18	0.16	0.10	0.11	-0.02	0.03	-0.02	putative polypyrimidine tract-binding protein [*Os*]	9e-10
1172	WAW	waw1c.pk005.a6	0.01	0.13	0.25	0.27	0.11	0.02	0.00	-0.06	OSJNBa0016I09.22 [*Os*]	5e-45
1173	WAW	waw1c.pk005.a7	0.01	0.10	0.04	0.15	0.05	0.00	0.00	0.03	no homologies found	-
1174	WAW	waw1c.pk005.a8	-0.09	-0.03	-0.10	-0.08	-0.05	-0.01	0.07	-0.08	P0681F05.21 [*Os*]	2e-13
1175	WAW	waw1c.pk005.a9	-0.95	-0.12	0.22	0.16	0.94	0.17	0.23	0.13	putative ribosome inactivating toxin protein [*Os*]	7e-07
1176	WAW	waw1c.pk005.b12	-0.33	-0.24	-0.28	-0.26	-0.02	-0.07	-0.03	-0.04	no homologies found	-
1177	WAW	waw1c.pk005.b13	0.29	0.05	0.16	0.02	-0.09	0.03	-0.04	-0.30	60S ribosomal protein L2 (L8) (ribosomal protein TL2)	1e-100
1178	WAW	waw1c.pk005.b14	0.19	0.38	0.38	0.30	0.58	-0.04	-0.06	0.12	no homologies found	-
1179	WAW	waw1c.pk005.b15	-0.19	-0.02	0.07	-0.01	-0.03	0.08	-0.04	0.14	EST AU056133(S20320) corresponds to a region of the predicted gene.~Similar to *Ce* cosmid D1054;	2e-04
1180	WAW	waw1c.pk005.b16	-0.07	0.01	0.02	0.07	-0.05	-0.02	0.00	0.04	expressed protein; protein id: At3g26890.1 [*At*]	1e-15
1181	WAW	waw1c.pk005.b18	0.05	-0.06	-0.19	-0.03	0.11	-0.01	0.10	0.04	OSJNBb0011N17.17 [*Os*]	4e-14
1182	WAW	waw1c.pk005.b20	0.11	-0.08	-0.20	-0.02	-0.23	-0.05	0.00	-0.31	putative protein; protein id: At5g53850.1 [*At*]	4e-51
1183	WAW	waw1c.pk005.b24	-0.02	0.09	0.41	0.13	0.31	0.01	-0.06	-0.05	putative dynamin-like protein ADL2 [*Os*]	5e-60
1184	WAW	waw1c.pk005.b3	0.06	0.02	0.02	0.09	0.06	-0.02	0.00	0.09	putative dihydroorotate dehydrogenase [*Os*]	2e-70
1185	WAW	waw1c.pk005.b4	0.18	0.29	0.41	0.35	0.30	0.01	0.03	0.02	expressed protein; protein id: At3g15180.1 [*At*]	1e-31
1186	WAW	waw1c.pk005.b5	0.15	0.17	0.14	0.23	0.04	0.01	-0.05	0.03	hypothetical protein AT4g37210 [imported] - *At*	1e-22
1187	WAW	waw1c.pk005.b6	-0.54	-1.20	-0.83	-1.21	-1.05	0.00	-0.09	0.03	putative protein; protein id: At5g20900.1 [*At]*	2e-21

			Temporal *M*					*Ph* mutant *M*				
#	ID	EST name	PM	LP	DA	TT	T	*1b*	*2a*	*2b*	Top BLASTx hit	e-val
1188	WAW	waw1c.pk005.b7	0.18	0.16	0.24	0.07	-0.04	-0.05	0.01	-0.02	arginine/serine-rich protein, putative; protein id: At1g16610.1:	1e-36
1189	WAW	waw1c.pk005.b8	0.01	0.11	0.16	0.10	0.08	0.06	0.03	-0.03	OJ1612_A04.2 [*Os*]	2e-33
1190	WAW	waw1c.pk005.b9	0.13	-0.02	0.11	0.07	0.27	-0.06	0.01	0.02	hypothetical protein; protein id: At1g51130.1 [*At*]	1e-23
1191	WAW	waw1c.pk005.c10	-0.20	-0.08	0.02	-0.11	0.00	-0.07	-0.01	-0.01	unnamed protein product [*Mm*]	0.033
1192	WAW	waw1c.pk005.c11	0.02	-0.11	0.02	-0.16	0.00	-0.08	-0.07	-0.06	unknown protein [*Os*]	2e-65
1193	WAW	waw1c.pk005.c12	0.01	0.15	0.06	0.07	0.04	0.09	-0.01	0.01	Vrga1 [Aegilops ventricosa]	2e-26
1194	WAW	waw1c.pk005.c13	-0.03	0.25	0.06	0.09	0.10	0.02	0.09	-0.05	no homologies found	-
1195	WAW	waw1c.pk005.c14	0.07	0.05	0.25	-0.04	0.05	-0.03	-0.02	-0.06	actin bundling protein ABP135 [imported] - trumpet lily	2e-78
1196	WAW	waw1c.pk005.c15	-0.19	-0.18	-0.33	-0.26	-0.18	0.04	0.18	0.07	no homologies found	-
1197	WAW	waw1c.pk005.c16	-0.32	0.61	0.35	0.40	0.54	0.04	0.11	0.31	putative chloroplast-targeted beta-amylase [*Os*]	9e-19
1198	WAW	waw1c.pk005.c17	0.34	0.11	-0.20	0.06	-0.18	0.02	-0.05	0.14	OSJNBa0072F16.2 [*Os*]	5e-88
1199	WAW	waw1c.pk005.c18	-0.29	-0.16	-0.01	-0.01	-0.03	-0.03	-0.07	-0.03	polynucleotide adenylyltransferase homolog T16I18.60 - *At*	4e-66
1200	WAW	waw1c.pk005.c19	-0.15	-0.16	-0.12	-0.06	0.03	-0.05	-0.04	-0.06	unnamed protein product [*Os*]	2e-57
1201	WAW	waw1c.pk005.c20	-0.19	0.01	-0.16	0.00	-0.13	0.03	-0.04	0.02	peroxisomal multifunctional protein [*Os*]	5e-94
1202	WAW	waw1c.pk005.c21	-0.22	-0.04	0.25	0.03	-0.12	0.09	0.00	-0.03	saccharopin dehydrogenase-like protein [*Hv*]	6e-83
1203	WAW	waw1c.pk005.c22	-0.08	-0.05	-0.12	-0.10	-0.06	0.09	-0.02	0.00	putative protein; protein id: At3g54190.1 [*At*]	1e-11
1204	WAW	waw1c.pk005.c23	0.17	0.14	-0.02	0.07	0.14	0.00	0.00	0.06	expressed protein; protein id: At2g42070.1 [*At*]	9e-24
1205	WAW	waw1c.pk005.c4	-0.02	0.02	0.05	-0.03	-0.02	0.03	-0.09	0.08	OSJNBb0091e11.5 [*Os*]	2e-29
1206	WAW	waw1c.pk005.c5	1.84	0.65	0.57	0.51	0.59	-0.02	0.12	-0.06	histone H4 (TH091) - wheat	2e-39
1207	WAW	waw1c.pk005.c6	-0.02	0.06	0.07	0.01	0.05	0.01	-0.12	0.01	protein F14J16.20 [imported] - *At*	5e-80
1208	WAW	waw1c.pk005.c7	0.31	0.25	0.29	0.18	0.19	0.04	-0.14	-0.01	putative mRNA export protein [*Os*]	1e-64
1209	WAW	waw1c.pk005.c8	0.04	0.76	1.06	0.81	0.57	-0.05	-0.08	-0.25	putative anion exchange protein; protein id: At2g47160.1	2e-94
1210	WAW	waw1c.pk005.c9	0.14	0.13	-0.05	0.15	-0.01	-0.01	-0.14	-0.06	no homologies found	-
1211	WAW	waw1c.pk005.d1	0.23	0.15	0.17	0.01	0.07	0.01	0.08	-0.08	putative protein transport protein SEC13 [*At*]	3e-30
1212	WAW	waw1c.pk005.d10	-0.08	0.04	-0.02	-0.03	-0.14	0.05	0.02	0.03	ketol-acid reductoisomerase; protein id: At3g58610.1,	2e-12
1213	WAW	waw1c.pk005.d11	0.19	-0.13	-0.17	-0.15	-0.09	-0.04	0.08	0.03	putative protein kinase APK1B [*Os*]	9e-90
1214	WAW	waw1c.pk005.d12	0.05	0.61	0.55	0.89	0.71	-0.06	-0.21	-0.06	ARP protein - *At*	2e-48
1215	WAW	waw1c.pk005.d13	0.07	0.04	-0.01	-0.04	0.12	0.02	0.01	-0.02	hypothetical protein; protein id: At2g35140.1 [*At*]	4e-08
1216	WAW	waw1c.pk005.d14	0.25	-0.13	-0.20	-0.12	-0.31	-0.18	-0.05	-0.06	putativeelongation factor 2 [*Os*]	3e-83
1217	WAW	waw1c.pk005.d15	-0.24	-0.11	-0.12	0.01	0.15	-0.04	-0.07	0.01	14-3-3 protein - barley	8e-58
1218	WAW	waw1c.pk005.d16	-0.09	0.06	0.07	0.15	0.01	0.02	0.03	0.04	agCP11392 [Anopheles gambiae str. PEST]	0.096
1219	WAW	waw1c.pk005.d17	-0.06	0.05	0.11	-0.05	-0.04	0.07	0.08	0.01	expressed protein; protein id: At1g75340.1 [*At*]	0.048
1220	WAW	waw1c.pk005.d19	-0.09	-0.06	0.04	-0.02	0.07	-0.02	0.13	-0.04	putative Nramp1 protein [*Os*]	5e-82
1221	WAW	waw1c.pk005.d2	-0.02	0.01	-0.20	0.08	0.05	-0.14	-0.04	-0.09	hypothetical protein [*Pf* 3D7]	0.94
1222	WAW	waw1c.pk005.d20	-2.20	-1.74	-1.01	-0.74	0.13	0.19	0.31	-0.35	4-coumarate:coenzyme A ligase, putative; protein id: At1g62940.1 [*At*]	2e-63
1223	WAW	waw1c.pk005.d21	0.03	0.20	0.07	0.14	0.10	0.01	0.08	0.06	1-phosphatidylinositol-4-phosphate kinase-like~contains ESTs AU030318(E50902),AU030317(E50902) [*Os*]	6e-27
1224	WAW	waw1c.pk005.d22	0.10	-0.01	-0.04	-0.10	-0.05	-0.01	0.04	-0.07	Vng2439h [Halobacterium sp. NRC-1]	0.73
1225	WAW	waw1c.pk005.d3	-0.29	0.12	0.13	0.27	0.27	0.00	-0.03	0.09	type 1 membrane protein, putative; protein id: At3g24160.1:	1e-15
1226	WAW	waw1c.pk005.d4	0.10	0.11	0.20	0.14	0.09	-0.09	0.01	0.03	gene_id:MDC11.12~pir||I52882~similar to unknown protein [*At*]	6e-38
1227	WAW	waw1c.pk005.d5	-0.25	-0.17	-0.12	-0.20	-0.08	-0.05	0.13	-0.02	hypothetical protein Rv3494c [*Mt* H37Rv]	0.17
1228	WAW	waw1c.pk005.d6	1.72	0.75	0.51	0.56	0.67	0.05	0.15	-0.06	no homologies found	-
1229	WAW	waw1c.pk005.d7	-0.37	0.48	-0.04	0.33	0.35	0.09	0.06	0.03	Lon protease homolog 2, mitochondrial precursor	1e-102
1230	WAW	waw1c.pk005.d8	0.04	0.09	0.07	0.07	0.04	0.09	-0.10	-0.05	hypothetical protein; protein id: At1g64790.1 [*At*]	7e-95
1231	WAW	waw1c.pk005.d9	-0.05	0.09	0.17	0.03	-0.06	0.04	-0.01	0.06	putative glutamine-dependent NAD synthetase [*Os*]	1e-110
1232	WAW	waw1c.pk005.e1	0.11	0.00	-0.05	0.03	-0.02	0.04	0.00	0.00	COP8 (constitutive photomorphogenic) homolog [*At*]	6e-60
1233	WAW	waw1c.pk005.e10	0.08	0.00	0.00	0.00	0.07	0.03	0.15	-0.02	putative TATA binding protein-associated factor [*Os*]	9e-63
1234	WAW	waw1c.pk005.e11	0.07	-0.03	0.12	-0.02	0.05	-0.02	-0.03	-0.03	SDL-1 protein [*Npl*]	7e-55
1235	WAW	waw1c.pk005.e12	-0.09	-0.04	-0.08	0.00	0.14	0.07	0.09	0.00	kinase-like protein [*Os*]	1e-15
1236	WAW	waw1c.pk005.e13	0.12	-0.03	0.03	0.00	-0.02	-0.02	0.03	0.00	putative ARP2/3 protein complex subunit p41; protein id: At2g31300.1 [*At*]	2e-28
1237	WAW	waw1c.pk005.e15	-0.04	-0.02	0.01	-0.01	-0.03	0.01	0.10	-0.02	no homologies found	-
1238	WAW	waw1c.pk005.e16	0.06	0.11	0.10	0.10	0.11	0.00	0.09	0.08	putative membrane protein [*Sco* A3(2)]	0.11
1239	WAW	waw1c.pk005.e17	-0.15	-0.03	-0.04	-0.06	-0.32	-0.01	0.06	0.10	OJ1340_C08.26 [*Os*]	2e-84
1240	WAW	waw1c.pk005.e18	0.04	-0.03	-0.13	-0.03	-0.02	0.02	-0.10	0.03	no homologies found	-
1241	WAW	waw1c.pk005.e20	-0.07	-0.10	-0.17	-0.11	0.03	-0.01	0.04	-0.03	P0489A01.8 [*Os*]	3e-25
1242	WAW	waw1c.pk005.e21	0.16	0.16	0.08	0.23	0.18	-0.02	-0.08	-0.09	succinyl-CoA ligase beta subunit; protein id: At2g20420.1:	7e-51
1243	WAW	waw1c.pk005.e22	0.72	0.60	0.45	0.44	0.63	0.18	0.31	0.19	defensin [*Ta*]	1e-21
1244	WAW	waw1c.pk005.e23	-0.19	0.14	0.05	0.17	0.30	0.03	0.05	0.03	putative protein; protein id: At5g49830.1 [*At*]	4e-07
1245	WAW	waw1c.pk005.e24	0.14	-0.01	-0.05	-0.05	-0.16	-0.02	0.03	0.02	putative 40S ribosomal protein S3 [*Ta*]	1e-62
1246	WAW	waw1c.pk005.e4	-0.44	0.15	-0.07	-0.03	0.13	-0.11	0.04	-0.06	guanylate kinase [*Ll*]	2e-11
1247	WAW	waw1c.pk005.e6	0.14	0.25	0.05	0.23	0.00	-0.08	-0.03	0.02	Elongation factor 1-alpha (EF-1-ALPHA))	7e-33
1248	WAW	waw1c.pk005.e7	-0.36	-0.37	-0.02	-0.29	-0.54	-0.07	-0.03	-0.11	methionine synthase protein [*Sb*]	3e-44
1249	WAW	waw1c.pk005.e8	0.04	0.30	0.12	0.30	0.21	0.03	0.04	0.04	expressed protein; protein id: At5g14030.1 [*At*]	0.015
1250	WAW	waw1c.pk005.f1	0.24	0.13	-0.01	0.09	0.03	-0.01	0.00	0.15	no homologies found	-
1251	WAW	waw1c.pk005.f10	0.26	-0.12	-0.16	-0.14	-0.16	0.03	0.04	-0.20	P0415C01.20 [*Os*]	0.12
1252	WAW	waw1c.pk005.f11	1.51	0.79	0.62	0.73	0.73	-0.04	-0.04	-0.27	B1147B04.21 [*Os*]	2e-30
1253	WAW	waw1c.pk005.f12	0.08	-0.07	0.00	-0.03	0.27	-0.07	0.02	-0.07	ras-related GTP-binding protein, putative; protein id: At3g12160.1 [*At*]	8e-86
1254	WAW	waw1c.pk005.f13	0.02	0.22	0.28	0.17	0.32	-0.17	-0.20	0.00	AT3g57880/T10K17_90 [*At*]	6e-32
1255	WAW	waw1c.pk005.f14	1.11	2.34	2.34	2.71	2.70	0.07	-0.04	-0.06	beta-N-acetylhexosaminidase -like protein [*Os*]	3e-93
1256	WAW	waw1c.pk005.f15	-1.32	-1.67	-1.06	-1.87	-1.67	-0.04	0.02	-0.07	Putative polyprotein from transposon TNT [*Os*]	4e-26
1257	WAW	waw1c.pk005.f16	-0.15	-0.32	-0.43	-0.14	-0.40	0.03	0.00	0.01	putative RNA binding protein [*Os*]	4e-14
1258	WAW	waw1c.pk005.f17	0.10	0.22	0.17	0.18	0.09	-0.03	-0.01	-0.32	Enolase (2-phosphoglycerate dehydratase) (2-phospho-D-glycerate hydro-lyase) (OSE1)	1e-106
1259	WAW	waw1c.pk005.f18	-0.04	0.43	0.93	0.48	0.30	0.00	-0.01	-0.08	putative phosphate translocator [*Os*]	6e-54
1260	WAW	waw1c.pk005.f19	-0.42	-0.17	0.02	-0.20	1.16	0.00	-0.08	0.01	putative pyridine nucleotide-disulphide oxidoreductase class-I [*At*]	4e-60
1261	WAW	waw1c.pk005.f2	-0.30	-0.07	-0.07	0.06	-0.02	-0.01	0.05	-0.03	putative protein kinase APK1B [*Os*]	1e-81
1262	WAW	waw1c.pk005.f20	0.29	0.23	0.14	0.09	-0.09	-0.04	-0.07	-0.04	agCP1970 [Anopheles gambiae str. PEST]	0.17
1263	WAW	waw1c.pk005.f21	0.09	0.00	0.01	0.00	-0.01	0.00	-0.14	-0.09	putative protein kinase [*Sb*]	4e-36
1264	WAW	waw1c.pk005.f22	0.15	0.06	0.17	0.07	-0.05	0.00	-0.07	-0.01	unnamed protein product [*Os*]	1e-83
1265	WAW	waw1c.pk005.f24	1.00	0.78	0.62	0.50	0.73	-0.03	-0.07	0.01	hypothetical protein; protein id: At3g15390.1 [*At*]	3e-09
1266	WAW	waw1c.pk005.f4	0.03	-0.01	-0.01	0.00	0.04	0.03	0.00	-0.05	hypothetical protein [*Os*]	2e-14
1267	WAW	waw1c.pk005.f6	0.01	0.03	0.07	0.07	-0.11	0.03	0.03	0.04	expressed protein; protein id: At5g07900.1	3e-10
1268	WAW	waw1c.pk005.f7	0.01	-0.02	0.05	-0.03	-0.17	0.02	0.07	-0.03	P0501G01.5 [*Os*]	0.068
1269	WAW	waw1c.pk005.f8	-0.18	0.07	0.19	0.01	-0.03	-0.01	-0.04	0.08	vacuolar ATP synthase subunit C, putative; protein id: At1g12840.1:	5e-31
1270	WAW	waw1c.pk005.f9	0.15	0.11	-0.07	0.13	-0.06	0.03	0.04	-0.02	hypothetical protein; protein id: At3g04380.1 [*At*]	1e-77
1271	WAW	waw1c.pk005.g1	0.07	-0.01	0.05	-0.05	0.10	0.02	-0.09	0.01	molybdenum cofactor biosynthesis protein Cnx1 [*Hv*]	8e-73
1272	WAW	waw1c.pk005.g10	-0.13	0.00	0.09	-0.03	-0.04	0.01	0.00	-0.05	putative protein; protein id: At5g14530.1 [*At*]	3e-94
1273	WAW	waw1c.pk005.g11	-0.05	-0.03	-0.05	-0.06	-0.04	-0.04	0.09	-0.05	gp108R [Rabbit fibroma virus]	0.8

			Temporal *M*					*Ph* mutant *M*				
#	ID	EST name	PM	LP	DA	TT	T	*1b*	*2a*	*2b*	Top BLASTx hit	e-val
1274	WAW	waw1c.pk005.g12	-0.05	0.02	0.00	0.11	0.06	0.00	0.10	0.03	plastidic ATP sulfurylase [*Os* (indica cultivar-group)]	4e-55
1275	WAW	waw1c.pk005.g13	0.06	-0.07	0.07	-0.05	0.01	0.03	-0.08	0.01	putative aminopeptidase [*At*]	5e-77
1276	WAW	waw1c.pk005.g14	-0.28	0.02	-0.13	-0.35	0.38	-0.08	-0.16	0.12	dnaK-type molecular chaperone HSP70 - barley	2e-83
1277	WAW	waw1c.pk005.g15	0.27	0.00	-0.15	-0.02	-0.02	0.01	0.04	0.20	hypothetical protein [imported] - *At*	0.019
1278	WAW	waw1c.pk005.g16	0.01	-0.10	-0.37	-0.12	-0.11	-0.02	0.04	-0.03	putative protein; protein id: At5g20170.1 [*At*]	2e-32
1279	WAW	waw1c.pk005.g17	-0.19	-0.36	-0.62	-0.44	-0.38	-0.03	0.12	0.23	no homologies found	-
1280	WAW	waw1c.pk005.g18	-0.13	-0.08	0.19	-0.22	-0.18	-0.03	0.16	0.03	GDSL-motif lipase/hydrolase-like protein [*At*]	6e-35
1281	WAW	waw1c.pk005.g19	0.36	0.05	-0.01	-0.06	-0.06	0.04	0.08	-0.15	putative TATA binding protein-associated factor [*Os*]	2e-73
1282	WAW	waw1c.pk005.g2	0.12	-0.12	0.02	-0.11	0.76	0.00	0.02	-0.13	unnamed protein product [*Os*]	5e-26
1283	WAW	waw1c.pk005.g20	-0.14	-0.01	0.96	0.18	0.69	0.08	0.21	0.05	putative protein; protein id: At3g48200.1 [*At*]	5e-29
1284	WAW	waw1c.pk005.g21	-0.33	-0.11	0.16	0.04	-0.01	-0.12	-0.07	-0.10	unknown protein [*Os*]	2e-44
1285	WAW	waw1c.pk005.g22	-0.12	0.20	0.01	0.33	0.07	-0.03	0.08	-0.01	no homologies found	-
1286	WAW	waw1c.pk005.g23	0.04	-0.09	-0.15	-0.13	-0.26	0.02	-0.06	-0.09	hypothetical protein; protein id: At1g09060.1 [*At*]	2e-21
1287	WAW	waw1c.pk005.g3	-0.41	0.09	0.04	0.20	0.42	0.03	0.09	0.06	probable enoyl-[acyl-carrier-protein] reductase (NADH2) - rice	4e-69
1288	WAW	waw1c.pk005.g4	0.00	0.25	-0.04	0.25	0.00	0.06	0.04	0.00	no homologies found	-
1289	WAW	waw1c.pk005.g5	-0.02	0.10	0.04	-0.01	0.06	0.00	0.09	0.20	putative manganese transport protein [*Os*]	8e-54
1290	WAW	waw1c.pk005.g6	0.01	-0.08	-0.11	0.04	0.01	0.02	0.02	0.27	putative membrane protein [*Sco* A3(2)]	0.11
1291	WAW	waw1c.pk005.g8	-0.07	-0.07	-0.06	-0.03	-0.19	-0.05	0.03	0.02	KIAA1856 protein [*Hs*]	0.4
1292	WAW	waw1c.pk005.g9	0.39	0.26	0.12	0.20	0.05	-0.06	-0.04	-0.42	60S ACIDIC ribosomal protein P0	7e-13
1293	WAW	waw1c.pk005.h1	1.10	0.60	0.56	0.53	0.51	-0.09	-0.09	-0.25	Histone H3	9e-70
1294	WAW	waw1c.pk005.h10	0.18	0.02	-0.22	-0.14	-0.19	0.01	0.01	-0.02	unknown protein [*Sb*]	2e-55
1295	WAW	waw1c.pk005.h11	-0.30	-0.27	-0.23	-0.27	-0.32	0.02	-0.08	0.02	putative 2,3-bisphosphoglycerate-independent phosphoglycerate mutase [*Os*]	2e-95
1296	WAW	waw1c.pk005.h12	0.10	0.23	0.41	0.52	0.76	-0.01	0.01	-0.14	putative beta-fructofuranosidase [*Os*]	8e-68
1297	WAW	waw1c.pk005.h13	1.57	0.70	0.65	0.58	0.58	-0.03	0.02	-0.20	histone H4 (TH091) - wheat	3e-39
1298	WAW	waw1c.pk005.h14	-0.25	-0.09	0.13	-0.10	-0.12	0.00	0.04	0.06	expressed protein; protein id: At3g02420.1	7e-37
1299	WAW	waw1c.pk005.h15	0.02	-0.12	0.05	-0.04	-0.15	-0.02	-0.12	0.00	protein F7F22.4 [imported] - *At*	3e-43
1300	WAW	waw1c.pk005.h17	0.06	-0.08	0.05	-0.05	-0.01	0.03	-0.04	-0.06	kinesin-like protein [*Os*]	9e-29
1301	WAW	waw1c.pk005.h18	0.07	0.01	-0.01	-0.07	-0.01	-0.04	-0.02	-0.05	no homologies found	-
1302	WAW	waw1c.pk005.h19	-0.08	0.02	0.11	0.18	0.02	-0.06	0.10	0.10	alpha-N-acetylglucosaminidase; protein id: At5g13690.1 [*At*]	1e-100
1303	WAW	waw1c.pk005.h2	-0.02	-0.05	-0.04	-0.01	-0.12	-0.06	-0.08	-0.02	F26G16.7 protein - *At*	8e-27
1304	WAW	waw1c.pk005.h20	-0.87	0.08	0.08	-0.14	0.12	0.03	-0.04	0.17	protein disulfide isomerase 3 precursor [*Ta*]	1e-101
1305	WAW	waw1c.pk005.h21	0.08	0.00	-0.08	-0.11	-0.14	-0.03	0.03	-0.04	putative protein kinase [*Sb*]	4e-34
1306	WAW	waw1c.pk005.h22	0.02	-0.11	0.54	-0.13	0.15	0.03	0.06	0.02	similar to *At* chromosome 3, T5N23.140 [*Os*]	1e-40
1307	WAW	waw1c.pk005.h23	0.43	0.13	-0.08	0.21	0.12	-0.03	-0.05	-0.03	putative GTP-binding protein; protein id: At1g30580.1 [*At*]	4e-28
1308	WAW	waw1c.pk005.h24	0.13	-0.10	-0.56	-0.08	-0.19	0.07	-0.03	0.09	no homologies found	-
1309	WAW	waw1c.pk005.h3	-0.12	-0.09	-0.04	-0.02	-0.07	0.05	0.09	0.01	E2, ubiquitin-conjugating enzyme, putative; protein id: At1g16890.1	1e-82
1310	WAW	waw1c.pk005.h4	-0.60	-0.68	-0.46	-0.55	-0.51	-0.03	-0.07	0.10	unnamed protein product [*Os*]	7e-90
1311	WAW	waw1c.pk005.h5	0.00	0.00	-0.20	-0.08	-0.02	-0.01	0.07	-0.02	no homologies found	-
1312	WAW	waw1c.pk005.h6	-0.09	-0.08	-0.06	-0.17	-0.23	0.01	-0.04	-0.18	putative protein; protein id: At4g19670.1 [*At*]	1e-06
1313	WAW	waw1c.pk005.h7	0.18	0.07	0.10	0.12	0.10	0.04	-0.06	0.01	unnamed protein product [*Os*]	1e-106
1314	WAW	waw1c.pk005.h8	-0.47	-0.17	0.05	-0.03	0.38	0.03	0.05	-0.11	phosphogluconate dehydrogenase (decarboxylating) (EC 1.1.1.44), cytosolic - maize	1e-101
1315	WAW	waw1c.pk005.h9	0.00	-0.12	-0.18	-0.06	-0.18	-0.05	-0.03	0.01	hypothetical protein; protein id: At2g20650.1 [*At*]	2e-20
1316	WAW	waw1c.pk005.i10	0.19	0.13	0.16	0.10	0.03	0.03	0.07	-0.18	unknown protein; protein id: At1g31870.1 [*At*]	2e-18
1317	WAW	waw1c.pk005.i11	0.08	-0.03	-0.04	-0.17	0.01	-0.15	0.03	0.08	no homologies found	-
1318	WAW	waw1c.pk005.i12	0.18	0.01	-0.09	-0.13	-0.18	0.00	-0.11	-0.01	putative Ran binding protein [*Os*]	6e-55
1319	WAW	waw1c.pk005.i13	0.11	0.03	-0.15	0.00	-0.07	0.00	-0.01	0.07	barley stem rust resistance protein [*Hv* subsp. spontaneum]	5e-51
1320	WAW	waw1c.pk005.i14	-0.40	-0.76	-0.69	-0.58	-0.77	-0.03	-0.02	-0.05	unknown protein; protein id: At2g38110.1 [*At*]	2e-75
1321	WAW	waw1c.pk005.i15	0.24	0.43	0.34	0.19	0.48	-0.09	0.03	-0.07	permease; protein id: At5g49990.1 [*At*]	5e-13
1322	WAW	waw1c.pk005.i16	-0.03	0.05	0.08	0.00	-0.16	-0.10	-0.06	-0.07	phosphate transport protein, mitochondrial - maize	9e-53
1323	WAW	waw1c.pk005.i17	1.28	0.60	0.55	0.51	0.67	0.04	-0.01	-0.13	histone H4 (TH091) - wheat	2e-39
1324	WAW	waw1c.pk005.i18	0.13	0.23	0.14	0.23	0.08	0.01	-0.04	-0.03	unknown protein; protein id: At5g08630.1 [*At*]	6e-35
1325	WAW	waw1c.pk005.i19	0.01	-0.03	0.05	-0.07	-0.01	-0.03	0.07	0.02	P0682B08.20 [*Os*]	1e-60
1326	WAW	waw1c.pk005.i20	-0.08	0.04	0.13	0.13	-0.02	0.01	-0.01	0.05	succinate dehydrogenase flavoprotein alpha subunit (emb|CAA05025.1); protein id: At5g66760.1	1e-102
1327	WAW	waw1c.pk005.i21	0.16	-0.09	-0.17	0.06	-0.09	0.04	-0.01	-0.02	no homologies found	-
1328	WAW	waw1c.pk005.i22	0.07	0.02	-0.25	0.02	-0.12	0.03	-0.02	0.04	hypothetical protein [Magnetospirillum magnetotacticum]	0.019
1329	WAW	waw1c.pk005.i23	0.13	-0.05	0.14	-0.01	-0.01	0.08	-0.06	-0.06	hypothetical protein; protein id: At4g31010.1 [*At]*	2e-73
1330	WAW	waw1c.pk005.i24	0.04	0.26	0.25	0.19	0.06	0.04	0.09	0.01	unknown protein [*At*]	1e-96
1331	WAW	waw1c.pk005.i5	1.16	0.52	0.48	0.59	0.54	0.02	-0.01	-0.21	hexokinase [*Zm*]	1e-51
1332	WAW	waw1c.pk005.i6	0.24	0.07	0.04	0.04	-0.02	-0.02	0.02	0.00	ribosomal protein L21 [imported] - rice	1e-81
1333	WAW	waw1c.pk005.i7	1.00	0.63	0.50	0.48	0.35	-0.07	-0.21	-0.17	histone H1 WH1B.1 [*Ta*]	3e-33
1334	WAW	waw1c.pk005.i8	0.15	0.25	0.28	0.23	0.28	0.02	-0.08	0.01	Ca2+-dependent lipid-binding protein, putative [*At*]	3e-48
1335	WAW	waw1c.pk005.j1	-0.64	-0.68	-0.42	-0.48	-0.37	0.08	0.09	-0.32	no homologies found	-
1336	WAW	waw1c.pk005.j10	-0.21	0.00	0.24	-0.06	0.06	0.09	0.10	0.08	SAR DNA binding protein [*Os*]	0.023
1337	WAW	waw1c.pk005.j11	0.02	0.06	0.00	0.02	-0.27	0.00	-0.09	0.05	unnamed protein product [*Os*]	1e-109
1338	WAW	waw1c.pk005.j12	0.09	-0.02	-0.15	-0.10	-0.11	0.03	0.12	-0.04	putative small nuclear ribonucleoprotein U1A [*Os*]	5e-79
1339	WAW	waw1c.pk005.j13	-0.48	1.02	1.08	1.28	1.02	0.15	0.09	0.04	no homologies found	-
1340	WAW	waw1c.pk005.j14	0.08	0.07	0.08	0.08	-0.13	-0.05	-0.01	0.03	Elongation factor 1-alpha (EF-1-ALPHA)	3e-78
1341	WAW	waw1c.pk005.j15	-0.27	-0.22	-0.26	-0.03	-0.12	-0.02	0.07	0.00	putative thiolase [*Os*]	5e-43
1342	WAW	waw1c.pk005.j16	0.19	-0.04	-0.03	-0.11	-0.05	-0.03	0.04	-0.12	putative RNA binding protein [*Os*]	2e-25
1343	WAW	waw1c.pk005.j18	-0.48	0.18	0.08	0.02	0.23	-0.02	-0.08	0.09	calreticulin precursor - maize	3e-95
1344	WAW	waw1c.pk005.j19	0.01	0.04	0.09	-0.05	0.07	-0.02	0.15	0.01	P0407B12.8 [*Os*]	0.34
1345	WAW	waw1c.pk005.j2	-0.13	0.13	0.44	0.28	0.02	0.06	0.12	0.01	putative elicitor response protein [*Os*]	6e-21
1346	WAW	waw1c.pk005.j20	0.06	-0.12	-0.42	-0.22	-0.18	-0.01	-0.02	0.09	no homologies found	-
1347	WAW	waw1c.pk005.j21	0.03	0.03	-0.06	0.08	0.03	-0.02	0.03	-0.10	extensin - Volvox carteri (fragment)	0.76
1348	WAW	waw1c.pk005.j22	-0.17	-0.08	-0.19	-0.17	-0.23	0.02	0.05	0.06	putative EREBP-type transcription factor [*Os*]	4e-72
1349	WAW	waw1c.pk005.j23	0.01	-0.04	-0.22	0.10	-0.08	0.00	0.01	0.14	hemagglutinin [Skunkpox virus]	0.12
1350	WAW	waw1c.pk005.j24	0.14	0.07	0.12	0.16	0.04	-0.03	-0.06	-0.09	14-3-3-like protein A (14-3-3A)	3e-66
1351	WAW	waw1c.pk005.j4	0.06	-0.07	-0.11	-0.03	-0.05	0.00	0.03	0.05	hypothetical protein; protein id: At1g63810.1 [*At*]	2e-12
1352	WAW	waw1c.pk005.j5	-0.18	-0.14	-0.04	-0.11	-0.10	-0.03	-0.10	-0.04	putative poly(A) polymerase; protein id: At4g32850.1 [*At*]	7e-60
1353	WAW	waw1c.pk005.j6	0.06	0.22	0.11	0.21	0.10	-0.02	0.07	0.03	unknown protein [*At*]	6e-20
1354	WAW	waw1c.pk005.j7	-0.10	-0.05	-0.04	-0.04	-0.22	0.00	-0.04	0.10	Putative quinone oxidoreductase [*Os*]	1e-102
1355	WAW	waw1c.pk005.j8	0.11	-0.06	0.04	-0.15	-0.23	-0.02	0.00	0.06	no homologies found	-
1356	WAW	waw1c.pk005.j9	-0.05	0.17	0.16	-0.01	0.23	-0.03	-0.07	0.02	no homologies found	-
1357	WAW	waw1c.pk005.k1	-2.27	-1.83	-1.15	-1.48	-0.06	0.13	0.14	-0.01	Putative protein [*Os*]	9e-44
1358	WAW	waw1c.pk005.k10	-0.20	-0.41	-0.25	-0.20	-0.33	-0.01	0.05	0.05	putative carnitine/acylcarnitine translocase; tRNA-Gly; tRNA-Met [*Os*]	4e-60
1359	WAW	waw1c.pk005.k11	0.04	-0.10	-0.16	-0.14	0.01	0.09	0.01	-0.02	expressed protein; protein id: At2g01270.1 [*At]*	2e-54
1360	WAW	waw1c.pk005.k12	0.06	-0.06	-0.01	-0.06	-0.07	-0.02	-0.06	0.05	26S proteasome regulatory particle triple-A ATPase subunit2b [*Os*]	6e-65
1361	WAW	waw1c.pk005.k13	0.16	0.26	0.18	0.26	0.21	-0.15	-0.13	-0.33	unknown protein; protein id: At3g05700.1 [*At*]	9e-04

			Temporal *M*					*Ph* mutant *M*				
#	ID	EST name	PM	LP	DA	TT	T	*1b*	*2a*	*2b*	Top BLASTx hit	e-val
1362	WAW	waw1c.pk005.k14	-0.67	0.07	0.15	-0.22	0.22	0.00	-0.04	0.13	protein disulfide isomerase [Triticum turgidum subsp. durum]	3e-88
1363	WAW	waw1c.pk005.k15	0.04	0.00	0.00	0.09	-0.03	-0.03	-0.06	0.01	LRR19 [*Ta*]	5e-82
1364	WAW	waw1c.pk005.k16	0.40	0.38	0.37	0.20	0.21	-0.12	0.00	-0.04	contains similarity to RNA-binding protein~gene_id:MSL3.12 [*At*]	7e-31
1365	WAW	waw1c.pk005.k17	-0.13	-0.28	-0.28	-0.14	0.01	0.06	0.01	-0.06	no homologies found	-
1366	WAW	waw1c.pk005.k18	-0.41	-0.60	-0.74	-0.40	-0.81	-0.04	-0.01	0.00	cysteine protease component of protease-inhibitor complex [*Zm*]	3e-74
1367	WAW	waw1c.pk005.k19	-0.12	-0.01	0.01	0.10	-0.04	-0.08	-0.03	-0.03	dentin phosphoryn [*Hs*]	3e-04
1368	WAW	waw1c.pk005.k2	0.07	-0.06	0.00	0.00	-0.09	-0.06	0.13	0.07	no homologies found	-
1369	WAW	waw1c.pk005.k20	-0.07	0.15	0.51	0.35	0.02	0.07	-0.03	-0.07	OSJNBa0014K08.18 [*Os*]	1e-52
1370	WAW	waw1c.pk005.k23	-0.03	0.29	0.04	0.07	-0.02	-0.03	0.07	0.01	farnesyl-diphosphate farnesyltransferase (EC 2.5.1.21) - maize	4e-98
1371	WAW	waw1c.pk005.k24	0.52	0.13	0.10	0.14	0.25	0.02	0.04	0.08	methylenetetrahydrofolate reductase [*Zm*]	1e-64
1372	WAW	waw1c.pk005.k3	-0.36	-0.33	-0.15	-0.20	-0.05	-0.03	-0.12	0.03	putative GDSL-motif lipase/acylhydrolase; protein id: At3g04290.1 [*At*]	3e-35
1373	WAW	waw1c.pk005.k4	0.46	-0.01	-0.17	-0.04	-0.24	-0.08	-0.11	-0.03	putative T-complex protein 1, theta subunit (TCP-1-Theta) [*At*]	2e-84
1374	WAW	waw1c.pk005.k5	0.01	-0.19	-0.10	-0.04	-0.53	0.00	-0.03	0.02	P0681F05.35 [*Os*]	1e-56
1375	WAW	waw1c.pk005.k6	-0.08	0.13	-0.12	-0.02	0.15	-0.05	-0.04	0.05	Sec61p [*Ta*]	2e-26
1376	WAW	waw1c.pk005.k7	-0.02	-0.27	-0.35	-0.30	-0.37	0.05	0.09	-0.02	expressed protein; protein id: At1g29250.1	3e-42
1377	WAW	waw1c.pk005.k8	-0.05	-0.19	-0.01	-0.12	-0.13	0.05	0.11	-0.06	CG3218-PA [*Dm*]	0.3
1378	WAW	waw1c.pk005.k9	0.00	-0.06	0.23	-0.03	-0.09	-0.08	0.03	-0.18	CAA30379.1 protein [*Os*]	2e-12
1379	WAW	waw1c.pk005.l1	-0.26	-0.02	-0.32	-0.21	-0.31	0.01	0.11	0.16	cyclophilin A-2 [*Ta*]	6e-89
1380	WAW	waw1c.pk005.l10	-0.13	0.06	-0.08	0.09	-0.04	0.00	0.01	0.07	similar to *At* putative chloroplast outer envelope 86-like protein (AC002330) [*Os*]	8e-53
1381	WAW	waw1c.pk005.l11	0.30	0.50	0.01	0.30	0.07	0.04	0.06	-0.15	expressed protein; protein id: At5g35730.1 [*At*]	2e-64
1382	WAW	waw1c.pk005.l12	0.15	-0.02	0.11	-0.02	-0.01	-0.04	-0.05	-0.02	Elongation factor 1-alpha (EF-1-ALPHA)	1e-103
1383	WAW	waw1c.pk005.l13	0.06	0.16	0.18	0.34	0.41	0.02	0.03	0.08	ATP synthase gamma chain, mitochondrial precursor	1e-56
1384	WAW	waw1c.pk005.l14	0.06	0.02	-0.14	-0.03	-0.10	-0.06	-0.12	0.08	kinesin-like protein [*Os*]	3e-77
1385	WAW	waw1c.pk005.l15	0.66	0.19	0.39	0.06	0.11	-0.03	-0.03	-0.13	probable replication protein A1 - rice	4e-97
1386	WAW	waw1c.pk005.l16	-2.33	-2.27	-1.88	-2.17	-2.04	0.18	0.21	0.21	hypothetical protein [Chlamydophila pneumoniae AR39]	9e-22
1387	WAW	waw1c.pk005.l17	0.07	-0.08	-0.01	-0.16	-0.03	0.02	0.00	-0.07	putative putative sister-chromatide cohesion protein; protein id: At2g47980.1	5e-62
1388	WAW	waw1c.pk005.l18	-1.59	-1.28	-0.63	-1.39	-1.28	0.00	0.04	0.05	acyl CoA synthetase, putative; protein id: At1g49430.1,	6e-72
1389	WAW	waw1c.pk005.l19	-0.07	-0.05	-0.06	-0.11	-0.04	-0.04	-0.11	0.00	Putative DNA2-NAM7 helicase family protein [*Os*]	9e-93
1390	WAW	waw1c.pk005.l2	0.04	-0.06	-0.02	-0.08	-0.16	0.07	0.03	0.01	PolI-like DNA polymerase [*Os*]	5e-77
1391	WAW	waw1c.pk005.l20	-0.07	-0.09	-0.01	-0.07	-0.03	0.00	-0.01	-0.05	P0413G02.23 [*Os*]	4e-47
1392	WAW	waw1c.pk005.l21	0.14	0.21	0.19	0.09	-0.08	-0.02	0.00	0.02	perlecan (heparan sulfate proteoglycan 2) [*Mm*]	0.8
1393	WAW	waw1c.pk005.l22	-0.16	-0.42	-0.34	-0.29	-0.34	0.03	-0.08	-0.04	26S proteasome RPT6a subunit [Dactylis glomerata]	4e-63
1394	WAW	waw1c.pk005.l23	0.00	0.08	0.02	0.04	0.11	-0.07	0.12	0.05	no homologies found	-
1395	WAW	waw1c.pk005.l4	-0.03	-0.02	0.01	0.07	0.01	-0.07	-0.04	0.02	putative chloroplast inner envelope protein [*Os*]	7e-80
1396	WAW	waw1c.pk005.l5	1.45	0.69	0.54	0.66	0.72	0.02	-0.10	-0.24	putative histone H2B [*Os*]	2e-28
1397	WAW	waw1c.pk005.l6	-0.22	-0.03	0.09	0.06	0.12	0.09	0.03	0.09	putative S-receptor kinase [*Os*]	1e-36
1398	WAW	waw1c.pk005.l8	-0.05	-0.01	0.01	-0.07	0.14	-0.06	0.14	0.01	P0009G03.26 [*Os*]	2e-13
1399	WAW	waw1c.pk005.l9	0.13	0.13	0.10	0.10	0.13	-0.07	0.04	-0.06	hypothetical protein [*Os*]	2e-21
1400	WAW	waw1c.pk005.m1	-2.42	-1.89	-1.11	-1.53	-0.11	0.15	0.21	-0.04	putative dihydroflavonol reductase [*Os*]	3e-59
1401	WAW	waw1c.pk005.m10	-0.12	0.03	0.20	0.07	0.04	0.07	0.09	-0.07	saccharopin dehydrogenase-like protein [*Hv* subsp. spontaneum]	1e-80
1402	WAW	waw1c.pk005.m11	-0.11	-0.04	0.07	-0.13	-0.14	-0.14	-0.25	-0.21	Ser/Thr kinase	2e-96
1403	WAW	waw1c.pk005.m12	-0.09	-0.07	-0.06	-0.04	0.04	0.03	-0.08	0.02	no homologies found	-
1404	WAW	waw1c.pk005.m13	-0.11	-0.08	-0.20	-0.05	-0.10	0.03	0.04	0.05	molybdenum cofactor biosynthesis protein Cnx1 [*Hv*]	4e-89
1405	WAW	waw1c.pk005.m14	0.00	-0.02	-0.10	0.01	-0.08	-0.02	-0.03	-0.06	Unknown protein [*Os*]	1e-5
1406	WAW	waw1c.pk005.m15	0.12	0.43	0.22	0.28	0.09	-0.05	-0.03	-0.03	hypothetical protein [*Os*]	2e-60
1407	WAW	waw1c.pk005.m16	-0.17	-0.03	-0.01	0.02	0.14	0.07	0.00	-0.07	phosphoglucomutase-like protein [*Os*]	5e-75
1408	WAW	waw1c.pk005.m17	0.24	0.23	0.25	0.10	0.07	-0.02	-0.03	0.01	hypothetical protein [*Os*]	1e-37
1409	WAW	waw1c.pk005.m18	0.04	-0.02	-0.06	-0.03	0.04	-0.03	-0.04	0.12	expressed protein; protein id: At1g21200.1 [*At*]	2e-29
1410	WAW	waw1c.pk005.m19	0.98	0.44	0.46	0.28	0.21	-0.03	-0.09	-0.07	replication origin activator 2 [*Zm*]	3e-96
1411	WAW	waw1c.pk005.m2	-0.47	-0.62	-0.37	-0.55	-0.41	-0.04	0.04	0.01	no homologies found	-
1412	WAW	waw1c.pk005.m20	-0.36	-0.22	-0.06	-0.16	-0.05	-0.04	0.17	0.03	putative betanidin 6-O-glucosyltransferase [*Os*]	4e-50
1413	WAW	waw1c.pk005.m21	-0.19	-0.16	-0.09	-0.27	-0.15	-0.01	0.04	-0.02	plasma membrane intrinsic protein 2-1 [Pyrus communis]	3e-88
1414	WAW	waw1c.pk005.m22	0.26	0.68	0.01	0.56	0.67	-0.01	0.09	-0.01	ATPase [*St*]	1e-56
1415	WAW	waw1c.pk005.m23	-0.11	0.14	-0.05	-0.15	0.49	-0.08	-0.17	0.10	calnexin - maize (fragment)	9e-82
1416	WAW	waw1c.pk005.m24	-0.45	-0.30	0.25	-0.18	-0.04	0.02	0.06	0.00	unknown protein [*Os*]	5e-06
1417	WAW	waw1c.pk005.m3	0.11	0.07	-0.07	-0.28	0.54	-0.09	-0.16	0.14	OSJNBb0012E08.10 [*Os*]	8e-72
1418	WAW	waw1c.pk005.m4	-0.13	0.00	-0.01	0.02	0.06	0.02	0.05	0.07	hypothetical protein, 5'-partial [*Os*]	5e-90
1419	WAW	waw1c.pk005.m6	0.14	0.18	0.15	0.02	-0.10	-0.07	0.00	-0.11	putative arm repeat protein [*Os*]	2e-59
1420	WAW	waw1c.pk005.m7	0.00	-0.01	-0.06	0.07	-0.01	-0.01	-0.08	-0.03	no homologies found	-
1421	WAW	waw1c.pk005.m8	-0.30	-0.20	-0.13	-0.07	-0.09	0.02	0.12	0.02	putative protein; protein id: At3g43550.1 [*At*]	2e-34
1422	WAW	waw1c.pk005.m9	-1.17	-1.51	-1.10	-1.47	-1.37	0.05	0.09	0.05	phosphoethanolamine methyltransferase [*Ta*]	2e-80
1423	WAW	waw1c.pk005.n1	0.13	0.31	0.17	0.36	0.40	-0.17	-0.25	0.22	heat shock protein 80 [*Ta*]	4e-79
1424	WAW	waw1c.pk005.n11	-0.03	0.19	0.15	0.17	0.14	0.04	0.08	0.02	putative protein; protein id: At3g55070.1 [*At*]	4e-08
1425	WAW	waw1c.pk005.n12	-0.20	-0.39	-0.72	-0.48	-0.40	0.01	0.11	0.03	no homologies found	-
1426	WAW	waw1c.pk005.n13	0.01	-0.05	0.06	0.00	-0.02	-0.03	-0.11	0.05	ethylene receptor homologue [*Zm*]	2e-54
1427	WAW	waw1c.pk005.n14	0.10	0.12	0.24	0.04	0.28	-0.04	-0.09	-0.04	putative beta-D-galactosidase [*Os*]	1e-82
1428	WAW	waw1c.pk005.n15	-0.15	-0.22	-0.05	-0.25	-0.14	-0.03	0.00	-0.04	DRPLA protein [*Hs*]	0.47
1429	WAW	waw1c.pk005.n16	0.04	0.12	0.06	0.24	-0.04	-0.03	-0.01	0.03	unknown protein [*At*]	6e-20
1430	WAW	waw1c.pk005.n17	-0.16	-0.15	-0.03	-0.11	0.00	0.02	0.12	-0.01	putative arm repeat containing protein [*Os*]	3e-81
1431	WAW	waw1c.pk005.n19	0.00	-0.11	-0.19	-0.17	-0.19	-0.02	0.06	-0.04	Lon protease homolog 2, mitochondrial precursor	1e-101
1432	WAW	waw1c.pk005.n2	-0.55	0.16	0.00	0.32	0.34	0.05	0.07	0.04	putative disulfide-isomerase precursor [*Os*]	8e-94
1433	WAW	waw1c.pk005.n20	-0.19	-0.02	0.00	-0.11	0.09	0.03	-0.01	0.07	serine/threonine protein kinase; protein id: At5g08160.1,	2e-43
1434	WAW	waw1c.pk005.n21	0.01	-0.08	-0.01	-0.11	-0.10	0.02	0.13	0.05	no homologies found	-
1435	WAW	waw1c.pk005.n23	0.11	0.10	-0.18	0.20	-0.06	0.00	-0.01	0.01	P0507H06.12 [*Os*]	1e-20
1436	WAW	waw1c.pk005.n3	0.03	-0.08	0.02	-0.05	0.08	-0.06	-0.12	0.12	no homologies found	-
1437	WAW	waw1c.pk005.n4	0.05	-0.22	-0.18	-0.07	-0.17	0.04	-0.03	-0.03	OSJNBa0029H02.6 [*Os*]	1e-54
1438	WAW	waw1c.pk005.n5	-0.12	-0.23	-0.18	-0.19	-0.18	-0.01	-0.05	-0.04	translation initiation factor eIF-4 gamma homolog F27H5.30 [similarity] - *At*	2e-41
1439	WAW	waw1c.pk005.n6	-0.35	-0.18	-0.29	-0.21	-0.28	-0.05	0.03	0.01	unknown protein [*At*]	4e-24
1440	WAW	waw1c.pk005.n7	-0.18	-0.04	0.18	-0.06	0.09	-0.08	0.10	-0.02	bHLH protein; protein id: At2g16910.1 [*At*]	2e-08
1441	WAW	waw1c.pk005.n8	0.00	-0.12	0.08	-0.16	-0.05	0.12	0.05	0.07	P0407B12.8 [*Os*]	0.34
1442	WAW	waw1c.pk005.o1	0.07	0.32	0.38	0.53	0.27	-0.02	-0.11	-0.09	putative trehalose-6-phosphate synthase homolog [*Os*]	1e-94
1443	WAW	waw1c.pk005.o10	-0.01	0.06	0.03	-0.03	0.07	-0.07	0.08	0.06	Putative wall-associated kinase 2 [*Os*]	1e-47
1444	WAW	waw1c.pk005.o11	-0.29	0.25	0.37	0.35	0.30	-0.03	-0.05	0.01	B1065E10.22 [*Os*]	1e-43
1445	WAW	waw1c.pk005.o13	-0.08	-0.20	-0.07	-0.16	-0.30	0.03	0.00	0.04	GDP dissociation inhibitor protein - rice	4e-95
1446	WAW	waw1c.pk005.o14	0.09	-0.03	-0.05	-0.15	-0.11	-0.07	0.02	0.02	unknown protein [*At*]	2e-65
1447	WAW	waw1c.pk005.o15	-0.10	0.01	-0.03	0.02	-0.06	0.05	-0.02	0.02	no sequence information	
1448	WAW	waw1c.pk005.o16	-0.10	0.12	0.17	0.13	-0.03	-0.06	0.06	-0.05	putative leucine-rich repeat transmembrane protein kinase [*Os*]	7e-69

			Temporal *M*					*Ph* mutant *M*				
#	ID	EST name	PM	LP	DA	TT	T	*1b*	*2a*	*2b*	Top BLASTx hit	e-val
1449	WAW	waw1c.pk005.o17	0.04	0.19	0.28	0.26	-0.02	0.03	0.01	-0.03	Elongation factor 1-alpha (EF-1-ALPHA)	1e-109
1450	WAW	waw1c.pk005.o18	-0.53	0.13	0.29	-0.06	0.16	-0.05	-0.03	-0.09	protein kinase-like - *At*	1e-07
1451	WAW	waw1c.pk005.o19	0.03	0.17	0.12	0.05	0.03	-0.03	-0.09	0.03	similar to *At* transport inhibitor response 1 (TIR1) (T48087) [*Os*]	1e-104
1452	WAW	waw1c.pk005.o2	-0.05	0.22	0.21	0.15	0.02	0.01	0.01	-0.04	unnamed protein product [*Os*]	2e-85
1453	WAW	waw1c.pk005.o20	-0.38	-0.45	-0.12	-0.46	-0.22	0.01	0.14	0.10	putative alanine transaminase [*Os*]	1e-109
1454	WAW	waw1c.pk005.o21	0.07	-0.07	0.03	-0.03	0.12	0.03	-0.02	0.17	no homologies found	-
1455	WAW	waw1c.pk005.o22	-0.73	0.19	0.15	-0.06	0.25	0.02	0.03	0.16	protein disulfide isomerase [Triticum turgidum subsp. durum]	3e-07
1456	WAW	waw1c.pk005.o23	0.15	0.11	0.14	0.18	-0.01	-0.12	-0.04	-0.13	Tubulin alpha-2 chain	1e-85
1457	WAW	waw1c.pk005.o3	0.00	0.38	0.20	0.15	0.42	-0.08	-0.14	-0.15	permease; protein id: At5g49990.1 [*At*]	5e-13
1458	WAW	waw1c.pk005.o4	0.06	0.02	-0.04	0.05	0.05	0.04	0.00	0.17	Unknown protein [*Os*]	2e-5
1459	WAW	waw1c.pk005.o5	-0.15	0.05	-0.15	0.07	-0.07	-0.03	0.09	-0.02	similar to DNA repair protein-like; protein id: At1g05120.1[*At*]	3e-50
1460	WAW	waw1c.pk005.o6	-0.52	-0.31	-0.22	-0.22	-0.30	-0.11	-0.05	-0.08	Phytepsin precursor (Aspartic proteinase)	3e-79
1461	WAW	waw1c.pk005.o7	0.01	0.00	-0.12	-0.01	0.00	0.01	-0.02	0.00	no homologies found	-
1462	WAW	waw1c.pk005.o8	0.27	0.27	0.09	0.22	0.03	0.01	-0.02	-0.01	DNA Helicase [*At*]	7e-12
1463	WAW	waw1c.pk005.o9	0.01	-0.18	-0.33	-0.08	-0.12	-0.02	0.11	-0.02	hypothetical protein [*Os*]	2e-17
1464	WAW	waw1c.pk005.p1	-0.03	0.04	0.21	-0.02	0.00	0.04	-0.05	0.03	Conserved Unknown protein [*Os*]	4e-35
1465	WAW	waw1c.pk005.p10	-0.67	-0.22	-0.07	-0.13	0.72	0.10	0.06	-0.01	unknown protein; protein id: At1g09430.1 [*At*]	1e-65
1466	WAW	waw1c.pk005.p11	-0.33	0.02	-0.23	-0.06	0.01	-0.04	0.03	0.13	no homologies found	-
1467	WAW	waw1c.pk005.p12	0.08	0.13	-0.07	-0.08	0.09	0.00	0.01	0.08	hypothetical protein; protein id: At1g16290.1 [*At*]	1e-48
1468	WAW	waw1c.pk005.p13	-0.08	-0.21	-0.20	-0.10	-0.19	0.05	0.02	-0.05	putative ADP-ribosylation factor [*Os*]	7e-89
1469	WAW	waw1c.pk005.p14	0.11	0.00	-0.18	0.02	-0.01	0.03	0.05	0.10	no homologies found	-
1470	WAW	waw1c.pk005.p15	-0.02	0.03	-0.04	0.14	-0.11	0.04	-0.04	0.02	putative growth regulator protein [*At*]	1e-06
1471	WAW	waw1c.pk005.p16	0.59	0.22	-0.12	0.15	-0.05	-0.05	0.06	0.01	no homologies found	-
1472	WAW	waw1c.pk005.p17	0.24	0.06	0.11	0.05	-0.14	-0.04	0.05	-0.04	no homologies found	-
1473	WAW	waw1c.pk005.p18	0.24	0.07	0.11	0.07	-0.03	-0.01	0.07	-0.02	40S ribosomal protein S4	7e-89
1474	WAW	waw1c.pk005.p19	-0.07	0.00	0.07	0.05	0.09	0.11	0.13	-0.06	hypothetical protein Tnp2 - garden snapdragon transposable element Tam1	5e-25
1475	WAW	waw1c.pk005.p2	0.01	0.01	-0.02	0.01	-0.07	0.08	0.03	0.00	OSJNBa0094O15.2 [*Os*]	3e-51
1476	WAW	waw1c.pk005.p20	-0.50	-0.45	-0.45	-0.39	-0.34	0.03	0.09	-0.05	triose phosphate translocator [*Ta*]	5e-41
1477	WAW	waw1c.pk005.p21	-0.03	0.11	0.23	0.24	0.13	0.01	0.10	-0.02	putative hydroxymethyltransferase [*Os*]	3e-10
1478	WAW	waw1c.pk005.p22	0.22	0.12	0.24	0.19	0.26	0.02	0.04	-0.04	mitochondrial processing peptidase alpha-chain precursor [Dactylis glomerata]	6e-89
1479	WAW	waw1c.pk005.p23	-0.16	0.04	0.05	0.03	0.10	-0.01	0.02	-0.06	ethylene response element binding protein [*Ta*]	1e-59
1480	WAW	waw1c.pk005.p24	-0.34	0.13	0.02	0.04	1.10	-0.04	0.02	0.10	acetyl-CoA carboxylase, putative; protein id: At1g36050.1 [*At*]	2e-54
1481	WAW	waw1c.pk005.p4	-0.25	-0.19	-0.08	-0.08	0.07	0.10	0.01	-0.02	nucleoid DNA-binding - like protein; protein id: At3g54400.1	3e-24
1482	WAW	waw1c.pk005.p5	0.02	0.11	0.10	0.08	0.00	-0.05	0.01	-0.31	Enolase (2-phosphoglycerate dehydratase) (2-phospho-D-glycerate hydro-lyase) (OSE1)	8e-52
1483	WAW	waw1c.pk005.p6	0.11	0.11	0.07	0.03	0.09	-0.09	-0.03	0.03	hypothetical protein; protein id: At1g59077.1 [*At*]	5e-20
1484	WAW	waw1c.pk005.p7	0.19	0.10	0.26	0.06	0.02	-0.03	-0.06	-0.06	Unknown protein [*Os*]	1e-81
1485	WAW	waw1c.pk005.p8	0.76	0.34	0.04	0.23	0.34	-0.01	-0.02	0.09	contains EST C29177(C63963)~similar to zinc finger protein [*Os*]	4e-47
1486	WAW	waw1c.pk005.p9	-0.33	-0.33	-0.25	-0.27	-0.17	0.03	0.02	0.00	3-ketoacyl-CoA thiolase [*Os*]	2e-07
1487	WAW	waw1c.pk006.a10	-0.08	0.09	0.31	0.23	0.15	-0.02	0.11	0.04	hypothetical protein; protein id: At1g30910.1 [*At*]	4e-44
1488	WAW	waw1c.pk006.a11	0.25	0.28	0.19	0.28	0.23	0.07	0.05	0.15	hypothetical protein T8K14.14 [imported] - *At*	6e-76
1489	WAW	waw1c.pk006.a12	0.13	0.06	0.15	0.11	0.05	0.03	-0.03	0.07	Unknown protein [*At*]	2e-55
1490	WAW	waw1c.pk006.a14	-0.02	0.07	-0.06	0.11	0.17	0.04	0.02	0.00	expressed protein; protein id: At3g20920.1	1e-54
1491	WAW	waw1c.pk006.a15	0.10	-0.14	-0.20	-0.22	-0.14	0.03	0.00	0.00	putative purple acid phosphatase [*Os*]	1e-53
1492	WAW	waw1c.pk006.a16	-0.06	-0.19	-0.16	-0.17	0.17	0.06	0.00	0.02	ESTs AU082452(S2330),AU058131(S5384),D40386(S2330), D23841(R0349)	2e-09
1493	WAW	waw1c.pk006.a17	0.47	1.57	1.37	1.56	1.40	0.00	-0.10	0.03	putative transcription factor X1 [*Os* subsp. japonica]	7e-23
1494	WAW	waw1c.pk006.a18	-0.07	-0.26	-0.35	-0.17	-0.16	-0.04	-0.01	0.01	Rad50-interacting protein 1;hypothetical protein FLJ11785[*Hs*]	0.37
1495	WAW	waw1c.pk006.a19	-0.17	-0.10	-0.15	-0.02	-0.12	0.00	-0.03	0.01	expressed protein; protein id: At1g11240.1	4e-09
1496	WAW	waw1c.pk006.a20	-0.12	0.00	-0.06	-0.09	0.02	0.04	-0.02	0.06	no homologies found	-
1497	WAW	waw1c.pk006.a21	-0.02	0.09	0.22	0.19	0.54	0.03	0.10	-0.03	VIP2 protein [Avena fatua]	3e-37
1498	WAW	waw1c.pk006.a22	0.61	0.35	0.22	0.43	0.13	0.05	0.04	0.33	putative 3,4-dihydroxy-2-butanone kinase	6e-66
1499	WAW	waw1c.pk006.a23	0.03	0.11	0.05	0.08	0.25	0.05	-0.03	0.03	similar to putative [*Mm*]	0.59
1500	WAW	waw1c.pk006.a24	0.06	0.18	-0.01	0.06	0.02	0.00	0.00	0.01	chloroplast import-associated channel protein homolog; protein id: At3g46740.1 [*At*]	7e-92
1501	WAW	waw1c.pk006.a4	-0.11	-0.06	0.30	-0.04	0.03	-0.04	0.06	-0.03	starch synthase IIa-2 [*Ta*]	1e-100
1502	WAW	waw1c.pk006.a5	0.01	0.01	0.11	0.04	-0.15	-0.02	0.02	-0.01	elongation factor 1-alpha (EF-1-APLHA)	1e-100
1503	WAW	waw1c.pk006.a6	0.26	0.08	-0.01	0.17	0.02	-0.01	0.16	-0.01	no homologies found	-
1504	WAW	waw1c.pk006.a9	0.06	0.03	-0.06	-0.01	0.03	0.03	0.09	0.06	possible apospory-associated protein	1e-55
1505	WAW	waw1c.pk006.b10	0.09	-0.10	-0.03	0.06	-0.16	0.13	0.00	0.03	probable ribosomal protein S8 - barley (fragment)	8e-59
1506	WAW	waw1c.pk006.b11	-0.27	-0.17	-0.16	-0.12	0.03	0.13	0.09	0.03	N-hydroxycinnamoyl/benzoyltransferase [Ipomoea batatas]	8e-27
1507	WAW	waw1c.pk006.b12	0.02	-0.02	-0.11	-0.14	0.05	-0.01	-0.10	-0.06	no homologies found	-
1508	WAW	waw1c.pk006.b13	-0.03	0.05	0.04	-0.06	-0.09	0.03	-0.01	0.02	no homologies found	-
1509	WAW	waw1c.pk006.b14	0.03	0.09	-0.08	0.07	-0.07	-0.02	0.04	-0.01	no homologies found	-
1510	WAW	waw1c.pk006.b15	0.07	-0.02	-0.18	-0.06	-0.06	0.05	0.05	-0.10	AT3g61130/T20K12_30 [*At*]	6e-33
1511	WAW	waw1c.pk006.b16	0.00	-0.02	0.06	-0.04	-0.06	-0.02	-0.05	-0.08	elongation factor 1 alpha [Stevia rebaudiana]	6e-92
1512	WAW	waw1c.pk006.b17	-0.43	-0.63	-0.61	-0.66	-0.69	-0.02	0.02	0.01	argBPIB [*Hs*]	0.46
1513	WAW	waw1c.pk006.b18	0.13	0.15	0.00	0.17	0.10	0.04	0.20	-0.05	OSJNBb0043H09.7 [*Os*]	3e-60
1514	WAW	waw1c.pk006.b19	-0.13	-0.15	-0.16	-0.18	-0.11	0.01	0.04	-0.01	ethylene-forming-enzyme-like dioxygenase-like protein [*Os*]	4e-48
1515	WAW	waw1c.pk006.b20	-0.05	-0.03	-0.05	-0.10	0.07	0.00	0.16	0.01	putative protein; protein id: At5g51110.1 [*At*]	3e-44
1516	WAW	waw1c.pk006.b24	-0.69	0.16	-0.25	0.09	0.12	-0.23	-0.32	-0.05	dehydrin COR410 (cold induced COR410 protein)	2e-41
1517	WAW	waw1c.pk006.b3	0.93	0.68	0.76	0.36	0.70	-0.04	-0.08	0.04	aysnaptic 1 [Brassica oleracea var. alboglabra]	4e-31
1518	WAW	waw1c.pk006.b4	0.06	-0.02	0.07	-0.08	-0.12	-0.03	0.06	-0.09	unknown protein [*At*]	8e-21
1519	WAW	waw1c.pk006.b5	-0.33	-0.51	-0.63	-0.61	-0.71	-0.08	-0.12	-0.14	plasma membrane H+-ATPase [*Hv* subsp. vulgare]	2e-67
1520	WAW	waw1c.pk006.b6	-0.30	-0.81	-0.45	-0.91	-0.58	-0.07	-0.04	-0.15	plasma membrane H+-ATPase [*Hv* subsp. vulgare]	2e-58
1521	WAW	waw1c.pk006.b8	-0.01	0.16	0.11	0.05	0.08	-0.10	0.00	-0.11	LTP-like protein; anther specific protein [*Zm*]	7e-26
1522	WAW	waw1c.pk006.b9	0.18	0.08	0.14	0.11	0.19	0.05	0.10	-0.04	P0466H10.20 [*Os*]	4e-23
1523	WAW	waw1c.pk006.c1	0.12	0.00	0.10	0.06	0.17	0.02	0.01	-0.07	putative CAD ATPase [*Os*]	7e-85
1524	WAW	waw1c.pk006.c10	-0.09	0.15	0.02	0.30	0.44	-0.02	0.00	0.09	Putative ATP synthase gamma chain, mitochondrial precursor [*Os*]	2e-78
1525	WAW	waw1c.pk006.c11	0.03	-0.02	-0.21	0.05	0.00	-0.02	0.03	0.03	hypothetical protein AT4g30860 [imported] - *At*	1e-46
1526	WAW	waw1c.pk006.c12	-0.08	-0.12	0.02	-0.06	-0.02	-0.08	0.10	0.00	hypothetical protein; protein id: At1g74690.1 [*At*]	3e-08
1527	WAW	waw1c.pk006.c13	-0.20	-0.04	0.05	-0.10	-0.11	0.01	-0.02	-0.02	hypothetical protein~predicted by GlimmerM~similar to *At* chromosome3,At3g23330 [*Os]*	1e-12
1528	WAW	waw1c.pk006.c14	-0.16	0.00	0.10	0.02	0.14	0.08	0.05	0.02	no homologies found	-
1529	WAW	waw1c.pk006.c15	-0.21	0.01	0.20	0.05	0.22	0.08	0.08	0.13	Acyl carrier protein II, chloroplast precursor (ACP II)	4e-33
1530	WAW	waw1c.pk006.c16	-1.09	-0.71	0.06	-0.60	0.07	-0.04	-0.02	0.04	no homologies found	-
1531	WAW	waw1c.pk006.c17	-0.10	0.11	0.24	0.16	0.07	-0.07	0.01	-0.08	transport protein, putative; protein id: At1g05520.1 [*At*]	4e-38
1532	WAW	waw1c.pk006.c18	-0.16	0.00	0.09	0.13	-0.05	0.09	0.00	0.03	unknown protein [*Os*]	8e-67
1533	WAW	waw1c.pk006.c19	0.07	-0.05	-0.06	-0.03	-0.13	-0.04	-0.07	-0.09	hypothetical protein; protein id: At1g73390.1 [*At*]	5e-16
1534	WAW	waw1c.pk006.c2	-0.17	-0.20	-0.14	-0.19	0.01	-0.06	-0.12	0.11	HSP70 [*Ta*]	2e-97

			Temporal *M*					*Ph* mutant *M*				
#	ID	EST name	PM	LP	DA	TT	T	*1b*	*2a*	*2b*	Top BLASTx hit	e-val
1535	WAW	waw1c.pk006.c20	0.01	0.02	0.06	-0.07	-0.10	-0.03	0.06	-0.02	no homologies found	-
1536	WAW	waw1c.pk006.c21	-0.13	0.13	-0.04	0.01	0.05	0.03	-0.05	-0.02	no homologies found	-
1537	WAW	waw1c.pk006.c22	0.11	0.18	0.20	0.08	0.14	-0.13	-0.05	-0.12	endomembrane protein 70, putative;protein id:At3g13772.1[*At*]	3e-80
1538	WAW	waw1c.pk006.c23	0.10	-0.09	0.10	-0.07	-0.09	0.02	0.00	0.00	constitutive photomorphogenic 11 [*Os* subsp. indica]	5e-48
1539	WAW	waw1c.pk006.c3	0.11	-0.03	-0.10	-0.03	-0.14	-0.02	-0.01	-0.06	no homologies found	-
1540	WAW	waw1c.pk006.c4	-0.26	-0.20	-0.01	-0.16	-0.09	0.04	0.07	0.05	r40c1 protein - rice	9e-71
1541	WAW	waw1c.pk006.c5	0.06	-0.11	-0.03	-0.03	0.11	-0.07	-0.14	-0.06	unnamed protein product [*Os*]	1e-118
1542	WAW	waw1c.pk006.c6	-0.22	-0.17	0.08	-0.07	-0.06	-0.02	0.00	-0.17	unknown protein [*At*]	2e-58
1543	WAW	waw1c.pk006.c8	0.03	0.06	0.05	0.11	0.27	-0.04	-0.04	-0.02	putative ubiquitin carboxyl-terminal hydrolase [*At*]	1e-76
1544	WAW	waw1c.pk006.c9	0.00	-0.10	-0.17	-0.17	-0.17	0.04	-0.02	0.04	26S proteasome regulatory particle triple-A ATPase subunit4b [*Os*]	1e-107
1545	WAW	waw1c.pk006.d1	0.07	0.16	0.08	0.10	0.07	0.08	0.00	-0.05	no homologies found	-
1546	WAW	waw1c.pk006.d10	-0.01	-0.06	-0.22	0.01	-0.05	-0.08	-0.04	0.00	water-stress protein [*Zm*]	1e-36
1547	WAW	waw1c.pk006.d11	-0.12	-0.07	-0.11	-0.19	-0.15	0.07	0.11	-0.14	GATA transcription factor 3; protein id: At4g34680.1 [*At*]	0.12
1548	WAW	waw1c.pk006.d13	0.26	0.00	0.06	-0.03	-0.05	-0.06	-0.06	-0.14	no homologies found	-
1549	WAW	waw1c.pk006.d14	-0.24	-0.24	-0.12	-0.12	-0.20	-0.03	0.08	0.09	Triosephosphate isomerase, cytosolic (TIM)	1e-38
1550	WAW	waw1c.pk006.d15	-0.06	-0.02	0.18	0.02	-0.03	-0.02	-0.06	0.12	Snf2-related CBP activator protein, putative; protein id: At3g12810.1 [*At*]	1e-101
1551	WAW	waw1c.pk006.d16	-0.10	0.05	-0.19	0.00	-0.15	-0.08	0.03	0.14	no homologies found	-
1552	WAW	waw1c.pk006.d17	-0.61	-0.47	-0.35	-0.38	-0.45	0.10	0.17	-0.02	Photosystem I reaction center subunit VI, chloroplast precursor (PSI-H) (Light-harvesting complex I 11 kDa protein)	2e-49
1553	WAW	waw1c.pk006.d18	-0.49	0.05	0.41	0.25	0.13	0.03	0.07	0.03	putative elicitor response protein [*Os*]	2e-49
1554	WAW	waw1c.pk006.d19	0.30	0.02	-0.19	0.02	-0.02	0.13	0.07	-0.22	40S ribosomal protein S9-like; protein id: At5g39850.1 [*At*]	1e-87
1555	WAW	waw1c.pk006.d2	0.10	0.25	0.15	0.24	0.16	-0.03	0.00	0.04	no homologies found	-
1556	WAW	waw1c.pk006.d20	0.09	0.07	0.18	0.12	0.07	-0.07	-0.11	-0.06	putative actin [*Os*]	1e-108
1557	WAW	waw1c.pk006.d21	0.51	0.44	0.59	0.14	0.25	-0.02	0.01	-0.09	hypothetical protein; protein id: At1g75150.1 [*At*]	5e-16
1558	WAW	waw1c.pk006.d22	0.04	0.07	-0.04	0.04	0.05	0.09	0.00	-0.02	no homologies found	-
1559	WAW	waw1c.pk006.d23	0.28	0.35	0.37	0.32	0.16	-0.04	-0.06	-0.08	glycyl tRNA synthetase, putative [*At*]	2e-74
1560	WAW	waw1c.pk006.d24	0.00	0.15	0.01	0.11	-0.01	-0.04	0.03	-0.05	no homologies found	-
1561	WAW	waw1c.pk006.d3	0.24	0.33	0.35	0.40	0.33	0.02	-0.02	-0.03	Elongation factor 1-gamma (EF-1-gamma) (eEF-1B gamma)	3e-57
1562	WAW	waw1c.pk006.d4	0.00	0.21	0.18	0.18	-0.03	-0.02	0.10	0.01	myb-related protein - barley	2e-57
1563	WAW	waw1c.pk006.d5	-0.43	-0.27	-0.15	-0.17	-0.25	-0.06	-0.08	0.01	vacuolar proton-ATPase [*Hv* subsp. vulgare]	1e-103
1564	WAW	waw1c.pk006.d6	0.13	0.14	-0.10	0.01	-0.16	-0.06	0.04	0.07	no homologies found	-
1565	WAW	waw1c.pk006.d7	-0.04	-0.07	-0.02	0.07	-0.12	-0.11	0.02	0.03	unknown protein; protein id: At1g77460.1 [*At*]	2e-59
1566	WAW	waw1c.pk006.d8	0.37	0.13	0.26	0.14	-0.09	0.02	0.01	-0.01	60S ribosomal protein L3	5e-85
1567	WAW	waw1c.pk006.d9	0.33	0.24	0.20	0.22	0.08	0.03	0.03	-0.06	guanine nucleotide-binding protein beta subunit-like protein (GPB-LR) (RWD)	2e-50
1568	WAW	waw1c.pk006.e11	0.02	0.05	0.02	0.04	0.11	0.06	-0.06	0.00	putative protein kinase [*Os*]	5e-59
1569	WAW	waw1c.pk006.e12	-0.12	-0.29	-0.27	-0.18	-0.16	0.03	0.14	0.04	no homologies found	-
1570	WAW	waw1c.pk006.e13	0.16	0.00	-0.07	0.00	-0.06	-0.10	-0.04	-0.07	Tubulin alpha chain	6e-87
1571	WAW	waw1c.pk006.e15	-0.23	0.04	0.16	0.11	-0.09	-0.01	-0.04	0.00	putative fructose 1-,6-biphosphate aldolase [*Ta*]	1e-104
1572	WAW	waw1c.pk006.e16	0.44	1.03	0.91	1.16	1.37	0.10	0.10	0.18	no homologies found	-
1573	WAW	waw1c.pk006.e17	-1.22	0.00	0.21	0.35	-0.02	0.03	0.06	-0.07	mitochondrial aldehyde dehydrogenase ALDH2 [*Hv*]	8e-45
1574	WAW	waw1c.pk006.e18	-0.12	-0.09	-0.06	0.00	-0.02	0.01	0.06	0.08	expressed protein; protein id: At1g73470.1 [*At*]	7e-30
1575	WAW	waw1c.pk006.e19	-0.11	-0.14	0.07	-0.12	-0.07	-0.02	-0.03	0.14	phospoenolpyruvate carboxylase [*Ta*]	3e-77
1576	WAW	waw1c.pk006.e2	0.23	0.17	0.18	0.15	0.10	0.09	0.01	0.03	putative translation initiation factor; protein id: At1g10840.1:	1e-71
1577	WAW	waw1c.pk006.e20	-0.02	-0.26	-0.34	-0.22	-0.31	0.04	0.03	0.08	no homologies found	-
1578	WAW	waw1c.pk006.e21	0.15	-0.12	-0.18	-0.06	-0.32	-0.16	-0.03	-0.15	tubulin alpha-6 chain (TUA6); protein id: At4g14960.1,	1e-84
1579	WAW	waw1c.pk006.e22	-0.16	-0.12	-0.19	-0.13	-0.24	-0.01	0.04	0.09	P0415A04.11 [*Os*]	4e-86
1580	WAW	waw1c.pk006.e23	0.31	0.25	0.28	0.27	0.08	0.03	0.04	-0.06	unknown [*At*]	9e-32
1581	WAW	waw1c.pk006.e24	-0.22	-0.31	0.03	-0.11	-0.28	-0.02	0.08	-0.03	B1097D05.23 [*Os*]	6e-14
1582	WAW	waw1c.pk006.e3	0.00	0.07	0.13	0.09	-0.06	-0.08	0.00	0.05	Elongation factor 1-alpha (EF-1-ALPHA)	4e-93
1583	WAW	waw1c.pk006.e4	-0.05	0.00	-0.05	0.00	0.00	-0.08	-0.15	0.11	hypothetical protein 1 - Madagascar periwinkle	1e-11
1584	WAW	waw1c.pk006.e5	0.16	0.16	0.02	0.04	-0.17	-0.05	0.01	0.15	no homologies found	-
1585	WAW	waw1c.pk006.e6	-0.04	-0.37	0.14	-0.48	-0.38	-0.13	-0.21	-0.21	homeoprotein Sail - fruit fly (*Dm*)	0.51
1586	WAW	waw1c.pk006.e8	-0.16	0.13	0.27	0.30	0.31	0.02	0.04	-0.12	Cysteine synthase (O-acetylserine sulfhydrylase) (O-acetylserine (Thiol)-lyase) (CSase A) (OAS-TL A)	5e-97
1587	WAW	waw1c.pk006.e9	-0.26	-0.18	-0.15	-0.32	-0.12	0.02	0.02	-0.08	putative protein; protein id: At5g13260.1 [*At*]	2e-22
1588	WAW	waw1c.pk006.f1	-0.34	-0.69	-0.61	-0.62	-0.75	-0.05	-0.01	0.06	hypothetical protein [Oenococcus oeni MCW]	0.59
1589	WAW	waw1c.pk006.f10	0.01	0.01	-0.02	0.03	-0.12	-0.04	0.05	-0.04	no homologies found	-
1590	WAW	waw1c.pk006.f11	0.15	0.03	0.04	0.13	0.07	-0.03	-0.03	0.01	hypothetical protein [Haemophilus somnus 129PT]	0.33
1591	WAW	waw1c.pk006.f12	-1.29	0.09	0.79	0.48	0.71	0.05	-0.02	-0.20	contains ESTs C73631(E20015),C99434(E20015)~unknown protein [*Os*]	0.011
1592	WAW	waw1c.pk006.f14	0.35	0.41	0.42	0.35	0.18	-0.07	-0.15	-0.07	ankyrin-like protein [*Os*]	2e-96
1593	WAW	waw1c.pk006.f15	0.06	-0.17	-0.16	-0.02	-0.09	-0.04	0.05	0.04	ATP/ADP carrier protein [Triticum turgidum]	1e-114
1594	WAW	waw1c.pk006.f16	0.01	0.01	-0.05	0.12	-0.07	0.04	-0.03	0.00	no homologies found	-
1595	WAW	waw1c.pk006.f17	0.02	-0.02	-0.04	-0.03	0.07	0.10	-0.08	0.01	hypothetical protein [*Os*]	0.061
1596	WAW	waw1c.pk006.f18	0.08	0.06	-0.03	0.01	-0.05	0.15	0.01	-0.07	no homologies found	-
1597	WAW	waw1c.pk006.f19	0.13	0.19	0.12	0.05	0.08	-0.06	-0.03	-0.10	endomembrane protein 70, putative; protein id: At3g13772.1 [*At*]	3e-94
1598	WAW	waw1c.pk006.f2	0.05	-0.13	-0.02	-0.24	-0.15	0.03	0.05	-0.06	putative ribosomal protein S18 [*Ta*]	2e-74
1599	WAW	waw1c.pk006.f20	-0.17	0.37	-0.09	0.21	0.17	0.09	0.12	0.04	putative CTP synthase [*Os*]	3e-63
1600	WAW	waw1c.pk006.f21	0.04	-0.04	-0.11	-0.11	-0.11	0.07	0.01	-0.06	no homologies found	-
1601	WAW	waw1c.pk006.f22	-0.01	0.15	-0.14	0.08	0.04	-0.06	0.06	0.02	F-box protein ZTL/LKP1/ADO1, AtFBX2b; protein id: At5g57360.1:	0.006
1602	WAW	waw1c.pk006.f23	-0.11	-0.25	-0.40	-0.27	-0.41	0.00	0.01	0.12	no homologies found	-
1603	WAW	waw1c.pk006.f24	-0.14	-0.14	-0.09	-0.17	-0.38	0.04	0.10	0.09	putative auxin-responsive GH3 [*Os*]	1e-101
1604	WAW	waw1c.pk006.f3	-0.46	-0.62	-0.81	-0.56	-0.94	-0.05	-0.04	-0.09	unnamed protein product [*Os*]	7e-81
1605	WAW	waw1c.pk006.f4	0.49	0.30	0.42	0.21	0.30	0.02	-0.04	-0.11	SMC4 protein [*Os*]	1e-80
1606	WAW	waw1c.pk006.f6	-0.07	-0.10	-0.11	-0.16	-0.29	-0.06	-0.05	-0.08	ORF4 [TT virus]	0.003
1607	WAW	waw1c.pk006.f7	0.37	0.56	0.47	0.50	0.42	-0.05	-0.19	-0.03	amelogenin [Paleosuchus palpebrosus]	0.39
1608	WAW	waw1c.pk006.f8	0.01	0.14	-0.13	0.00	0.20	0.00	0.00	0.08	aggrecan 1; aggrecan, structural proteoglycan of cartilage [Rattus norvegicus]	0.62
1609	WAW	waw1c.pk006.f9	-0.37	-0.21	0.09	-0.18	-0.24	-0.01	0.02	-0.06	methionine synthase [*Zm*]	1e-72
1610	WAW	waw1c.pk006.g1	-0.15	-0.04	-0.13	-0.13	-0.01	-0.04	-0.03	0.06	unnamed protein product [*Os*]	5e-23
1611	WAW	waw1c.pk006.g11	-0.05	-0.10	-0.14	-0.04	-0.13	-0.04	-0.01	-0.03	Putative polyprotein from transposon TNT [*Os*]	1e-10
1612	WAW	waw1c.pk006.g12	-0.56	-0.44	-0.22	-0.41	-0.65	-0.04	0.05	-0.19	methionine synthase protein [*Sb*]	1e-114
1613	WAW	waw1c.pk006.g13	-0.58	-0.36	0.01	-0.19	0.30	0.02	0.00	-0.12	ESTs D24970(R2869),AU031961(R2869) correspond to a region of the predicted gene.~Similar to *Zm* putative cytosolic	2e-94
1614	WAW	waw1c.pk006.g14	-0.15	-0.24	0.02	-0.18	0.05	0.01	-0.02	-0.03	putative chalcone synthase [*Os*]	5e-82
1615	WAW	waw1c.pk006.g15	0.03	0.65	0.60	1.01	0.75	-0.12	-0.13	-0.15	ARP protein - *At*	1e-48
1616	WAW	waw1c.pk006.g16	0.02	0.19	0.32	0.18	0.22	-0.04	0.10	0.01	no homologies found	-
1617	WAW	waw1c.pk006.g17	0.12	0.10	-0.13	0.25	0.24	-0.01	-0.06	0.09	peptidylprolyl isomerase (ROF1); protein id: At3g25230.1 [*At*]	2e-54
1618	WAW	waw1c.pk006.g18	-0.18	0.10	0.41	0.11	0.13	-0.01	0.10	-0.03	cytochrome p450 (CYP78A9); protein id: At3g61880.1	6e-29
1619	WAW	waw1c.pk006.g19	0.25	0.08	-0.02	0.02	-0.20	-0.09	-0.03	-0.08	Putative 40S Ribosomal protein [*Os*]	2e-96

#	ID	EST name	Temporal *M*					*Ph* mutant *M*			Top BLASTx hit	e-val
			PM	LP	DA	TT	T	*1b*	*2a*	*2b*		
1620	WAW	waw1c.pk006.g2	-0.60	-0.44	-0.36	-0.50	-0.73	-0.11	-0.10	-0.21	Phospholipase D alpha 1 precursor (PLD alpha 1) (Choline phosphatase 1)	3e-86
1621	WAW	waw1c.pk006.g20	0.00	-0.12	-0.07	-0.17	0.00	0.06	0.15	-0.15	P0480C01.17 [*Os*]	2e-37
1622	WAW	waw1c.pk006.g21	0.01	-0.11	-0.11	-0.13	-0.15	-0.02	0.01	0.08	Putative quinone oxidoreductase [*Os*]	2e-40
1623	WAW	waw1c.pk006.g22	0.01	-0.03	0.10	0.05	0.02	0.11	-0.01	-0.08	RNA helicase [*At*]	1e-98
1624	WAW	waw1c.pk006.g23	-0.29	-0.23	-0.21	-0.22	-0.31	-0.02	-0.05	-0.05	vacuolar targeting receptor bp-80 [*Ta*]	3e-45
1625	WAW	waw1c.pk006.g24	0.13	-0.07	-0.05	-0.17	-0.13	0.02	0.17	-0.12	Putative aminotransferase [*Os*]	9e-56
1626	WAW	waw1c.pk006.g3	0.13	0.73	0.69	0.76	0.75	0.02	0.02	-0.04	alcohol dehydrogenase [*Hv*]	2e-90
1627	WAW	waw1c.pk006.g4	-0.08	0.63	0.56	0.78	0.52	0.06	0.02	0.08	aspartate aminotransferase, cytoplasmic (transaminase A)	8e-92
1628	WAW	waw1c.pk006.g5	-0.56	-0.25	-0.26	-0.09	0.59	0.09	0.00	0.03	unknown protein; protein id: At1g09430.1 [*At*]	1e-104
1629	WAW	waw1c.pk006.g6	0.10	-0.08	-0.11	-0.21	0.45	-0.02	-0.07	0.04	Glucan endo-1,3-beta-glucosidase GII precursor ((1->3)-beta-glucan endohydrolase GII)	9e-45
1630	WAW	waw1c.pk006.g7	0.10	-0.07	-0.11	-0.24	-0.18	-0.09	-0.03	-0.17	ATP-dependent RNA helicase-like protein - *At*	9e-13
1631	WAW	waw1c.pk006.g8	-0.02	-0.38	-0.34	-0.24	-0.34	-0.06	0.03	0.12	no homologies found	-
1632	WAW	waw1c.pk006.g9	-0.17	-0.04	0.10	-0.09	-0.16	0.08	-0.01	-0.02	no homologies found	-
1633	WAW	waw1c.pk006.h1	0.29	0.46	0.55	0.53	0.68	-0.04	-0.13	0.24	heat shock protein 82	1e-78
1634	WAW	waw1c.pk006.h10	0.37	0.43	0.64	0.18	0.33	-0.06	-0.10	-0.12	putative cdc21 protein [*Os*]	7e-23
1635	WAW	waw1c.pk006.h11	0.14	0.15	0.08	0.06	0.03	-0.03	-0.04	-0.05	putative thioredoxin reductase [*Os*]	1e-101
1636	WAW	waw1c.pk006.h12	-0.56	-0.03	0.15	0.31	0.18	0.00	-0.05	-0.03	putative tetrafunctional protein of glyoxysomal fatty acid beta-oxidation [*Os*]	1e-101
1637	WAW	waw1c.pk006.h13	-0.04	-0.04	-0.06	-0.01	-0.02	0.07	0.13	0.02	GTP cyclohydrolase I [*Le*]	6e-59
1638	WAW	waw1c.pk006.h14	0.30	0.28	0.17	0.22	0.07	0.04	0.02	-0.01	putative translation initiation factor; protein id: At1g10840.1:	1e-70
1639	WAW	waw1c.pk006.h15	0.12	0.27	0.03	0.20	0.13	0.04	0.02	-0.01	putative multispanning membrane protein [*At*]	1e-47
1640	WAW	waw1c.pk006.h16	-0.11	-0.22	-0.22	-0.07	-0.09	0.00	0.20	-0.02	At2g42220/T24P15.13 [*At*]	2e-53
1641	WAW	waw1c.pk006.h17	0.09	0.10	0.25	0.07	-0.08	0.01	0.00	0.05	no homologies found	-
1642	WAW	waw1c.pk006.h18	-0.86	0.06	0.15	-0.20	0.14	0.04	-0.05	0.11	protein disulfide isomerase 2 precursor [*Ta*]	1e-116
1643	WAW	waw1c.pk006.h19	-0.22	-0.08	-0.03	-0.12	-0.13	0.16	-0.11	0.06	P0703B11.24 [*Os*]	2e-22
1644	WAW	waw1c.pk006.h2	0.25	0.19	0.21	0.19	0.16	0.00	-0.07	0.08	putative peptide chain release factor subunit 1 (ERF1) [*Os*]	5e-14
1645	WAW	waw1c.pk006.h20	-0.12	0.09	0.05	0.08	0.20	0.04	-0.10	0.04	unknown protein [*At*]	2e-27
1646	WAW	waw1c.pk006.h21	0.07	-0.01	0.03	0.06	0.09	-0.02	0.02	0.08	P0666G04.6 [*Os*]	1e-49
1647	WAW	waw1c.pk006.h22	-0.12	-0.08	0.01	0.02	0.09	-0.06	-0.08	-0.01	protein kinase MK6 [*Mc*]	2e-98
1648	WAW	waw1c.pk006.h23	-0.16	-0.17	-0.01	-0.09	-0.08	-0.01	-0.05	0.10	ACCase [*Ta*]	1e-109
1649	WAW	waw1c.pk006.h24	0.00	-0.09	-0.04	0.01	0.12	0.09	0.10	0.22	no homologies found	-
1650	WAW	waw1c.pk006.h3	0.03	0.00	-0.03	0.05	-0.15	0.00	-0.06	0.05	putative seryl-tRNA synthetase [*Os*]	2e-71
1651	WAW	waw1c.pk006.h4	0.09	-0.02	0.03	-0.01	-0.11	-0.01	-0.04	-0.09	no homologies found	-
1652	WAW	waw1c.pk006.h5	0.16	0.20	0.22	0.18	0.18	-0.03	-0.04	0.03	putative glucose-6-phosphate dehydrogenase; protein id: At1g09420.1 [*At]*	2e-78
1653	WAW	waw1c.pk006.h6	-0.18	0.07	0.07	0.02	0.00	-0.02	-0.02	0.03	pyrophosphate-dependent phosphofructokinase beta subunit [Citrus x paradisi]	4e-72
1654	WAW	waw1c.pk006.h7	-0.49	-0.36	-0.19	-0.42	-0.27	0.12	0.10	0.03	Rieske Fe-S precursor protein [*Os*]	2e-10
1655	WAW	waw1c.pk006.h8	0.12	0.30	0.52	0.94	0.40	0.02	0.08	0.04	no homologies found	-
1656	WAW	waw1c.pk006.h9	0.03	0.10	0.15	0.10	0.04	-0.03	-0.03	-0.35	Enolase (2-phosphoglycerate dehydratase) (2-phospho-D-glycerate hydro-lyase) (OSE1)	1e-111
1657	WAW	waw1c.pk006.i10	-0.53	-0.02	0.16	0.32	0.18	-0.03	0.00	-0.04	putative tetrafunctional protein of glyoxysomal fatty acid beta-oxidation [*Os*]	1e-105
1658	WAW	waw1c.pk006.i11	0.30	0.12	0.08	0.03	0.10	0.02	0.01	0.01	ES43 protein - barley	1e-104
1659	WAW	waw1c.pk006.i13	0.00	-0.26	-0.44	-0.22	-0.51	0.03	-0.04	-0.04	hypothetical protein; protein id: At3g11964.1 [*At*]	2e-44
1660	WAW	waw1c.pk006.i15	0.12	-0.06	0.04	0.01	-0.03	0.08	0.02	0.01	Ribosomal protein L18a	1e-93
1661	WAW	waw1c.pk006.i16	0.02	-0.09	-0.16	-0.22	-0.23	-0.05	0.13	-0.22	putative aldolase; protein id: At4g10750.1 [*At*]	5e-46
1662	WAW	waw1c.pk006.i17	-0.04	0.13	-0.02	0.14	-0.03	-0.05	0.00	0.11	3'-5' exonuclease, putative; protein id: At1g56310.1 [*At*]	5e-29
1663	WAW	waw1c.pk006.i18	0.04	-0.11	-0.26	-0.17	-0.17	-0.04	0.14	-0.10	expressed protein; protein id: At1g63690.1 [*At]*	2e-50
1664	WAW	waw1c.pk006.i19	0.08	0.07	-0.16	0.07	-0.10	0.01	-0.12	0.07	no homologies found	-
1665	WAW	waw1c.pk006.i2	-0.14	-0.04	-0.18	0.06	-0.13	0.03	0.04	-0.01	no homologies found	-
1666	WAW	waw1c.pk006.i20	-0.19	-0.11	-0.09	-0.05	0.01	-0.07	-0.18	-0.11	no homologies found	-
1667	WAW	waw1c.pk006.i21	-0.05	-0.02	-0.04	0.00	-0.08	-0.09	-0.06	-0.12	no homologies found	-
1668	WAW	waw1c.pk006.i22	-0.01	-0.07	-0.05	-0.02	-0.07	0.10	0.05	-0.04	P0432C03.20 [*Os*]	1e-19
1669	WAW	waw1c.pk006.i23	1.14	0.71	0.63	0.64	0.36	-0.04	-0.10	0.07	Peroxidase 40 precursor (Atperox P40)	5e-32
1670	WAW	waw1c.pk006.i24	-0.22	-0.04	-0.13	-0.07	-0.04	-0.03	0.01	0.06	cytosolic glyceraldehyde-3-phosphate dehydrogenase GAPDH [*Ta*]	1e-100
1671	WAW	waw1c.pk006.i3	-0.06	-0.04	0.14	0.00	-0.12	0.00	0.07	-0.11	hypothetical protein [*Os*]	2e-15
1672	WAW	waw1c.pk006.i4	0.29	0.12	0.13	0.08	0.04	0.04	0.01	0.07	26S proteasome regulatory particle non-ATPase subunit8 [*Os*]	1e-51
1673	WAW	waw1c.pk006.i5	0.14	0.63	1.65	0.62	0.76	-0.06	0.07	-0.05	putative subtilisin-like protease [*At*]	6e-13
1674	WAW	waw1c.pk006.i6	0.01	-0.18	-0.17	-0.13	-0.33	-0.03	-0.05	-0.09	C2H2 type zinc finger containing protein (28.5 kD) [*Ce*]	0.13
1675	WAW	waw1c.pk006.i7	1.16	0.42	0.13	0.38	0.27	-0.01	0.02	-0.28	putative histone H2A [*Os*]	8e-39
1676	WAW	waw1c.pk006.i8	0.11	-0.01	0.00	-0.11	-0.07	0.00	0.09	-0.11	putative protein; protein id: At4g25730.1 [*At*]	6e-51
1677	WAW	waw1c.pk006.i9	0.02	-0.01	0.04	0.01	0.20	-0.01	0.03	0.05	P0413G02.23 [*Os*]	9e-05
1678	WAW	waw1c.pk006.j1	-0.08	-0.16	0.00	-0.05	0.03	-0.03	-0.02	-0.02	similar to choriogenin Hminor [*Ol*] [*Mm*]	5e-10
1679	WAW	waw1c.pk006.j10	0.13	0.04	0.35	0.03	0.03	0.01	-0.06	-0.04	putative protein; protein id: At5g42950.1 [*At*]	6e-14
1680	WAW	waw1c.pk006.j13	-0.27	-0.26	-0.12	-0.39	-0.17	0.07	-0.09	0.07	Distal-less [Ciona intestinalis]	9e-05
1681	WAW	waw1c.pk006.j14	0.34	0.36	0.43	0.48	0.51	-0.03	-0.02	-0.08	similar to ebiP4655 [*Hs*]	0.001
1682	WAW	waw1c.pk006.j15	0.20	0.11	0.21	0.10	0.17	0.00	-0.09	-0.04	Contains similarity to gb|CAB16841 trichohyalin like protein from *At*. [*Os*]	2e-17
1683	WAW	waw1c.pk006.j16	0.07	0.04	-0.10	0.05	0.12	0.07	0.02	0.02	OSJNBa0031O09.02 [*Os*]	1e-08
1684	WAW	waw1c.pk006.j17	-0.21	-0.13	-0.08	-0.04	-0.01	-0.05	-0.06	0.09	acetyl-CoA carboxylase (EC 6.4.1.2) - wheat	1e-114
1685	WAW	waw1c.pk006.j18	-0.79	0.07	0.14	-0.19	0.16	0.04	-0.04	0.10	protein disulfide isomerase 2 precursor [*Ta*]	1e-100
1686	WAW	waw1c.pk006.j19	0.05	0.01	-0.06	-0.06	0.06	-0.03	0.03	-0.01	putative protein; protein id: At4g30700.1 [*At*]	2e-42
1687	WAW	waw1c.pk006.j2	-0.11	-0.10	0.04	-0.05	-0.10	0.02	-0.07	0.07	unknown protein [*At*]	6e-33
1688	WAW	waw1c.pk006.j20	0.05	-0.07	0.01	-0.07	-0.18	-0.01	0.06	-0.17	pseudo-response regulator 1; protein id: At5g61380.1	3e-36
1689	WAW	waw1c.pk006.j21	-0.19	0.04	-0.10	-0.24	0.47	-0.07	-0.19	0.08	OSJNBb0012E08.10 [*Os*]	5e-96
1690	WAW	waw1c.pk006.j22	0.19	0.25	0.32	0.15	0.19	0.05	0.00	0.01	L-galactono-gamma-lactone dehydrogenase [*Nt*]	2e-56
1691	WAW	waw1c.pk006.j23	-0.16	-0.16	0.02	-0.23	-0.05	0.04	0.05	-0.12	lipase-like protein [*Os*]	3e-74
1692	WAW	waw1c.pk006.j24	-0.18	-0.37	-0.64	-0.31	-0.33	0.00	0.06	-0.02	wsv285 [shrimp white spot syndrome virus]	0.58
1693	WAW	waw1c.pk006.j4	0.09	0.03	0.12	0.02	-0.11	-0.06	0.04	-0.03	unknown protein; protein id: At1g04190.1 [*At]*	8e-68
1694	WAW	waw1c.pk006.j5	0.31	0.73	0.86	0.62	0.55	-0.05	0.05	0.02	unknown protein [*At*]	3e-41
1695	WAW	waw1c.pk006.j6	-0.06	-0.06	-0.10	0.00	0.00	0.06	0.02	0.06	no homologies found	-
1696	WAW	waw1c.pk006.j7	-0.02	0.11	0.26	0.12	0.04	0.01	0.09	-0.03	hypothetical protein XP_196822 [*Mm*]	0.029
1697	WAW	waw1c.pk006.j8	0.13	-0.03	0.11	-0.09	-0.21	-0.01	0.02	-0.07	putative ubiquitin carboxyl-terminal hydrolase [*Os*]	2e-44
1698	WAW	waw1c.pk006.j9	0.34	0.24	0.14	0.18	0.08	0.01	0.08	0.01	no homologies found	-
1699	WAW	waw1c.pk006.k10	1.21	1.38	1.06	1.57	1.33	0.15	0.17	0.09	no homologies found	-
1700	WAW	waw1c.pk006.k11	0.06	0.19	0.22	0.06	0.06	-0.04	-0.11	-0.06	expressed protein; protein id: At1g04080.1 [*At*]	4e-45
1701	WAW	waw1c.pk006.k12	0.11	-0.01	-0.01	-0.05	-0.10	0.12	-0.01	0.04	KIAA0807 protein [*Hs*]	0.008
1702	WAW	waw1c.pk006.k13	1.17	0.47	0.15	0.35	0.34	-0.01	0.00	-0.29	histone H2A-like protein [*Sm*]	4e-39
1703	WAW	waw1c.pk006.k14	-0.04	-0.08	-0.46	-0.09	-0.05	0.06	0.12	0.28	no homologies found	-
1704	WAW	waw1c.pk006.k15	-0.15	-0.03	-0.11	-0.12	0.02	0.02	0.04	0.08	Glyceraldehyde 3-phosphate dehydrogenase, cytosolic 3	8e-86
1705	WAW	waw1c.pk006.k16	0.11	-0.11	-0.12	-0.14	-0.19	0.05	0.07	-0.04	Collagen alpha 2(VI) chain precursor	0.041

			Temporal *M*					*Ph* mutant *M*				
#	ID	EST name	PM	LP	DA	TT	T	*1b*	*2a*	*2b*	Top BLASTx hit	e-val
1706	WAW	waw1c.pk006.k17	-0.15	-0.11	-0.14	-0.10	-0.03	-0.03	0.00	-0.08	heat shock protein, 70K, chloroplast - cucumber	8e-15
1707	WAW	waw1c.pk006.k19	-0.02	0.00	0.07	0.08	0.02	-0.06	-0.01	0.03	no homologies found	-
1708	WAW	waw1c.pk006.k2	-0.24	-0.08	-0.04	-0.14	-0.04	-0.01	0.00	0.02	Glyceraldehyde 3-phosphate dehydrogenase, cytosolic 3	5e-74
1709	WAW	waw1c.pk006.k20	-0.02	0.14	0.39	0.10	-0.02	0.01	-0.03	0.07	no homologies found	-
1710	WAW	waw1c.pk006.k21	0.02	0.01	-0.01	0.03	-0.03	0.02	-0.07	0.01	60S ribosomal protein L5	3e-79
1711	WAW	waw1c.pk006.k22	0.07	-0.01	0.00	-0.12	-0.03	0.12	0.00	-0.04	no homologies found	-
1712	WAW	waw1c.pk006.k23	0.01	0.26	0.44	0.46	0.42	0.03	-0.10	0.07	unknown protein [*At*]	6e-78
1713	WAW	waw1c.pk006.k3	1.37	0.61	0.45	0.64	0.56	0.05	-0.01	-0.27	beta-adaptin-like protein A [*Os*]	2e-69
1714	WAW	waw1c.pk006.k4	0.33	0.00	-0.05	0.02	-0.04	-0.01	-0.04	0.04	putative disease resistance protein (3' partial) [*Os*]	0.004
1715	WAW	waw1c.pk006.k5	0.10	0.01	-0.13	-0.10	-0.15	0.00	0.08	0.02	unknown protein; protein id: At5g06240.1 [*At*]	1e-43
1716	WAW	waw1c.pk006.k6	0.03	0.03	0.04	-0.04	-0.09	-0.10	-0.08	0.05	putative transcription factor; protein id: At4g29000.1 [*At*]	2e-58
1717	WAW	waw1c.pk006.k7	-0.10	0.09	-0.05	0.13	0.04	0.06	0.02	-0.02	hypothetical protein XP_173868 [*Hs*]	0.33
1718	WAW	waw1c.pk006.k8	-0.07	0.02	-0.29	-0.20	0.00	-0.11	0.01	0.02	Unknown protein [*At*]	2e-57
1719	WAW	waw1c.pk006.k9	-0.05	0.12	0.00	0.05	0.02	0.00	-0.02	0.06	expressed protein; protein id: At2g40830.1[*At*]	5e-11
1720	WAW	waw1c.pk006.l1	1.41	0.41	0.34	0.41	0.37	-0.01	0.00	-0.17	hypothetical protein~predicted by GeneMark.hmm etc. [*Os*]	0.001
1721	WAW	waw1c.pk006.l10	-0.23	-0.21	-0.10	-0.14	-0.32	-0.01	-0.10	0.02	Eukaryotic translation initiation factor 5 (eIF-5)	2e-67
1722	WAW	waw1c.pk006.l11	0.01	0.00	-0.07	-0.01	0.02	-0.13	0.01	-0.01	putative mitochondrial dicarboxylate carrier protein [*At*]	8e-27
1723	WAW	waw1c.pk006.l12	-2.51	-1.92	-1.16	-1.54	-0.11	0.16	0.27	-0.04	putative dihydroflavonol reductase [*Os*]	4e-71
1724	WAW	waw1c.pk006.l13	1.57	0.76	0.67	0.75	0.68	0.03	-0.02	-0.28	Histone H2B	6e-47
1725	WAW	waw1c.pk006.l14	-0.47	-0.39	-0.13	-0.40	-0.67	-0.08	0.04	-0.25	methionine synthase protein [*Sb*]	1e-75
1726	WAW	waw1c.pk006.l15	-0.07	-0.10	-0.03	-0.08	-0.10	-0.06	0.00	0.00	no sequence information	
1727	WAW	waw1c.pk006.l16	-0.02	-0.04	0.02	-0.10	0.08	0.13	-0.11	0.06	no homologies found	-
1728	WAW	waw1c.pk006.l17	-0.20	0.16	-0.19	-0.03	0.09	0.08	0.15	0.29	beta-expansin 4 [*Zm*]	9e-58
1729	WAW	waw1c.pk006.l18	0.05	-0.12	-0.21	-0.25	-0.11	0.04	0.00	0.00	no homologies found	-
1730	WAW	waw1c.pk006.l19	0.11	0.09	0.21	0.16	0.06	-0.01	0.02	-0.33	Enolase (2-phosphoglycerate dehydratase) (2-phospho-D-glycerate hydro-lyase) (OSE1)	3e-96
1731	WAW	waw1c.pk006.l2	1.46	0.76	0.68	0.68	0.82	0.03	-0.04	-0.29	no homologies found	-
1732	WAW	waw1c.pk006.l20	-0.08	-0.01	0.15	-0.07	-0.13	0.03	0.01	-0.03	ESTs AU069906(E11917), D48439(S14636), D46007 (S10373), AU030823(E60306)	1e-42
1733	WAW	waw1c.pk006.l21	-0.39	-0.23	-0.17	-0.13	-0.02	-0.03	-0.03	0.20	S-adenosylmethionine decarboxylase proenzyme (AdoMetDC)	1e-88
1734	WAW	waw1c.pk006.l22	0.35	0.25	0.05	0.21	-0.01	-0.05	-0.03	0.00	putative ribosomal protein S10 [*Os*]	4e-24
1735	WAW	waw1c.pk006.l23	-0.01	0.13	0.09	0.05	0.00	-0.02	-0.02	0.02	P0712E02.15 [*Os*]	7e-47
1736	WAW	waw1c.pk006.l3	1.44	0.51	0.52	0.51	0.48	0.03	0.00	-0.32	Histone H2B.2	5e-46
1737	WAW	waw1c.pk006.l5	0.00	-0.03	-0.08	-0.03	-0.03	-0.04	0.06	0.05	hypothetical protein [*Np*]	0.21
1738	WAW	waw1c.pk006.l6	-0.04	-0.10	-0.09	-0.15	0.09	0.10	0.05	0.08	no homologies found	-
1739	WAW	waw1c.pk006.l7	0.35	0.38	0.51	0.25	0.15	-0.04	-0.03	0.06	topoisomerase, putative; protein id: At4g24800.1 [*At*]	9e-20
1740	WAW	waw1c.pk006.l8	-0.29	-0.07	0.00	0.01	0.10	0.04	0.05	0.11	betaine-aldehyde dehydrogenase [*Ta*]	1e-51
1741	WAW	waw1c.pk006.l9	-0.17	-0.21	-0.19	-0.08	-0.01	0.00	0.06	0.09	serine/threonine protein phosphatase PP1	2e-58
1742	WAW	waw1c.pk006.m1	0.14	-0.04	0.02	-0.07	-0.04	-0.12	-0.09	-0.08	Tubulin alpha chain	5e-78
1743	WAW	waw1c.pk006.m10	0.22	0.01	0.09	0.04	-0.04	0.09	0.04	0.06	SET domain protein SUVR2 [*At*]	7e-08
1744	WAW	waw1c.pk006.m11	-0.18	-0.11	0.16	-0.06	-0.04	0.03	0.01	-0.03	hexose transporter [*Hv* subsp. vulgare]	2e-66
1745	WAW	waw1c.pk006.m12	0.34	0.19	-0.08	0.11	0.23	0.00	-0.01	0.07	unnamed protein product [*Os*]	0.008
1746	WAW	waw1c.pk006.m13	-0.06	-0.05	0.05	-0.06	0.07	0.05	0.04	0.00	putative dolichyl-phosphate beta-glucosyltransferase; protein id: At2g39630.1	3e-42
1747	WAW	waw1c.pk006.m14	0.02	-0.03	-0.10	-0.02	-0.02	-0.05	-0.01	0.06	putative stripe rust resistance protein Yr10/Mla1 [*Sb*]	1e-27
1748	WAW	waw1c.pk006.m15	0.03	-0.07	-0.12	-0.01	-0.10	-0.02	-0.02	0.04	cellulose synthase-7 [*Zm*]	4e-58
1749	WAW	waw1c.pk006.m16	0.15	0.16	0.35	0.23	0.19	-0.01	-0.03	-0.03	ACTIN 66	1e-105
1750	WAW	waw1c.pk006.m17	0.07	0.04	0.09	-0.03	-0.07	0.00	-0.03	-0.06	putative methyltransferase; protein id: At4g10760.1 [*At*]	6e-07
1751	WAW	waw1c.pk006.m18	-0.05	-0.21	0.06	-0.11	-0.05	-0.06	0.01	-0.01	conserved hypothetical protein [*Xc* pv. campestris str. ATCC 33913]	0.49
1752	WAW	waw1c.pk006.m19	0.03	0.10	0.23	0.17	0.05	0.04	0.07	-0.06	no homologies found	-
1753	WAW	waw1c.pk006.m20	0.02	-0.11	0.01	0.01	-0.07	-0.02	0.04	-0.09	PDR-like ABC transporter [*Os*]	3e-85
1754	WAW	waw1c.pk006.m21	-0.33	-0.38	-0.27	-0.34	-0.23	0.02	0.14	0.12	transmembrane protein [*Hv* subsp. vulgare]	4e-93
1755	WAW	waw1c.pk006.m22	0.04	-0.03	-0.07	-0.06	-0.09	0.00	0.02	0.04	unnamed protein product [*Os*]	1e-103
1756	WAW	waw1c.pk006.m23	-0.06	-0.32	-0.46	-0.30	-0.47	-0.10	0.07	0.00	ubiquitin conjugating enzyme [*Zm*]	1e-25
1757	WAW	waw1c.pk006.m3	0.22	0.14	0.21	0.13	0.06	-0.05	-0.04	0.00	kinesin heavy chain [*Zm*]	2e-74
1758	WAW	waw1c.pk006.m4	0.01	-0.05	0.12	0.16	0.06	-0.09	-0.01	-0.24	no homologies found	-
1759	WAW	waw1c.pk006.m5	-0.06	0.08	0.28	0.09	-0.01	0.02	0.06	-0.03	probable ethylene-response protein - rice	2e-54
1760	WAW	waw1c.pk006.m6	0.06	0.11	0.06	0.14	0.05	-0.03	-0.02	-0.05	unknown protein [*At*]	0.002
1761	WAW	waw1c.pk006.m7	-0.14	0.03	0.00	0.17	0.00	0.03	0.01	0.04	developmental protein, putative; protein id: At1g17730.1 [*At*]	1e-13
1762	WAW	waw1c.pk006.m8	-0.13	-0.09	-0.11	-0.10	-0.03	-0.05	0.12	0.11	H+/Ca2+ exchanger 2 [Ipomoea nil]	4e-37
1763	WAW	waw1c.pk006.m9	-0.55	-0.80	-0.64	-0.81	-0.95	-0.09	-0.08	-0.08	unnamed protein product [*Os*]	1e-67
1764	WAW	waw1c.pk006.n1	0.07	0.00	0.05	0.05	0.02	0.00	-0.04	0.00	no homologies found	-
1765	WAW	waw1c.pk006.n10	0.14	0.79	0.77	0.90	0.69	-0.04	0.08	0.00	no homologies found	-
1766	WAW	waw1c.pk006.n11	-0.15	0.34	0.44	0.28	0.48	0.07	-0.11	0.12	putative protein; protein id: At4g20850.1 [*At*]	6e-83
1767	WAW	waw1c.pk006.n12	0.05	0.03	0.14	-0.01	-0.09	0.07	-0.04	-0.02	chromomethylase [*Zm*]	8e-83
1768	WAW	waw1c.pk006.n14	-0.37	-0.11	-0.28	0.00	-0.14	-0.05	0.06	0.06	no homologies found	-
1769	WAW	waw1c.pk006.n15	1.24	0.83	1.01	0.54	0.59	-0.01	-0.13	0.09	peroxidase family; protein id: At4g16270.1 [*At*]	2e-17
1770	WAW	waw1c.pk006.n16	-0.20	0.13	0.21	0.19	0.10	-0.06	0.04	0.03	unknown protein; protein id: At1g18270.1 [*At*]	9e-87
1771	WAW	waw1c.pk006.n17	0.19	0.04	0.02	-0.14	0.01	0.08	0.00	0.08	no homologies found	-
1772	WAW	waw1c.pk006.n18	0.24	0.11	0.12	0.01	-0.05	-0.01	0.12	-0.06	putative protein; protein id: At5g11240.1 [*At*]	5e-43
1773	WAW	waw1c.pk006.n19	-0.18	-0.15	-0.09	-0.15	-0.14	0.02	0.02	0.00	contains ESTs D25106 (R3184), AU184634 (R3184)~diphosphonucleotide phosphatase-like protein [*Os]*	4e-32
1774	WAW	waw1c.pk006.n2	0.07	-0.04	-0.08	-0.09	-0.03	0.10	0.10	0.05	oj000126_13.8 [*Os*]	2e-66
1775	WAW	waw1c.pk006.n20	0.16	0.12	0.20	0.18	0.04	-0.04	-0.14	0.00	P0506E04.15 [*Os*]	2e-64
1776	WAW	waw1c.pk006.n22	-0.23	-0.21	-0.08	-0.17	-0.16	0.17	0.03	0.11	no homologies found	-
1777	WAW	waw1c.pk006.n23	-0.41	0.12	0.16	0.30	0.36	0.06	0.08	0.04	2-oxoglutarate/malate translocator (clones OMT134 and OMT106), mitochondrial membrane - proso millet	2e-91
1778	WAW	waw1c.pk006.n24	0.41	1.97	1.64	1.69	1.54	0.03	0.01	0.19	no homologies found	-
1779	WAW	waw1c.pk006.n3	0.44	0.25	0.11	0.21	0.08	-0.07	0.09	0.05	no homologies found	-
1780	WAW	waw1c.pk006.n4	-1.19	-1.68	-1.20	-1.65	-1.60	0.11	0.03	0.11	fumarylacetoacetate hydrolase-like protein; protein id: At1g12050.1 [*At]*	4e-66
1781	WAW	waw1c.pk006.n5	-0.06	-0.03	0.25	0.03	0.03	0.00	0.11	-0.03	hypothetical protein; protein id: At2g39950.1 [*At*]	7e-15
1782	WAW	waw1c.pk006.n6	-0.13	0.08	0.30	0.13	-0.04	0.04	0.10	-0.08	putative elicitor response protein [*Os*]	3e-31
1783	WAW	waw1c.pk006.n7	-0.09	-0.02	0.06	-0.03	0.08	0.02	-0.02	0.07	no homologies found	-
1784	WAW	waw1c.pk006.n8	-0.09	-0.06	-0.07	-0.10	-0.04	-0.14	-0.12	-0.05	Tubulin alpha chain	8e-77
1785	WAW	waw1c.pk006.n9	-0.16	-0.15	-0.02	-0.05	0.21	-0.04	-0.10	0.13	HSP70 [*Ta*]	4e-88
1786	WAW	waw1c.pk006.o1	-0.24	-0.29	-0.17	-0.24	-0.06	-0.06	0.01	-0.04	AT4g13930 [*At*]	2e-62
1787	WAW	waw1c.pk006.o10	-0.08	-0.08	-0.18	-0.16	-0.38	0.03	-0.06	-0.02	putative protein; protein id: At4g24610.1 [*At*]	6e-17
1788	WAW	waw1c.pk006.o11	0.11	0.25	0.39	0.25	0.11	-0.15	-0.27	-0.35	chitin-inducible gibberellin-responsive protein [*Os*]	7e-73
1789	WAW	waw1c.pk006.o12	0.05	0.00	-0.15	-0.12	-0.10	-0.03	0.08	-0.12	cytochrome P450 [Anopheles gambiae]	0.82
1790	WAW	waw1c.pk006.o13	0.12	0.21	0.07	0.06	-0.09	-0.03	0.01	0.05	putative glyoxylate reductase [*Os*]	1e-59
1791	WAW	waw1c.pk006.o14	0.11	0.15	0.17	0.08	0.26	0.00	-0.03	0.08	similar to cDNA sequence AB025049 [*Mm*]	0.59
1792	WAW	waw1c.pk006.o15	-0.16	-0.06	-0.01	-0.11	-0.02	0.02	0.03	0.08	OSJNBa0089K24.29 [*Os*]	0.063

#	ID	EST name	Temporal *M*					*Ph* mutant *M*			Top BLASTx hit	e-val
			PM	LP	DA	TT	T	*1b*	*2a*	*2b*		
1793	WAW	waw1c.pk006.o16	0.09	0.05	-0.03	0.03	-0.08	0.06	0.12	0.06	histidine-containing phosphotransfer protein [*Zm*]	4e-46
1794	WAW	waw1c.pk006.o17	0.00	0.07	0.03	0.17	0.07	-0.06	0.05	-0.22	plasma membrane H+ ATPase [*Os*]	7e-12
1795	WAW	waw1c.pk006.o19	-0.38	-0.13	0.03	-0.11	-0.08	-0.04	0.00	0.01	OSJNBb0012E08.11 [*Os*]	3e-79
1796	WAW	waw1c.pk006.o2	0.05	-0.17	-0.47	-0.15	-0.21	-0.02	-0.03	0.06	unknown protein [*At*]	9e-57
1797	WAW	waw1c.pk006.o20	0.04	0.32	0.23	0.29	0.88	-0.10	-0.22	-0.07	putative protein; protein id: At5g40270.1 [*At]*	5e-47
1798	WAW	waw1c.pk006.o21	-0.07	0.08	-0.02	0.08	0.07	0.11	0.07	0.04	Putative C-4 sterol methyl oxidase [*Os*]	2e-46
1799	WAW	waw1c.pk006.o22	-0.11	0.51	0.69	0.59	0.76	0.00	-0.07	-0.08	bHLH protein; protein id: At2g16910.1 [*At*]	0.004
1800	WAW	waw1c.pk006.o23	0.86	0.31	0.25	0.25	0.20	-0.06	-0.05	-0.29	putative cell cycle regulatory protein [*Os*]	1e-59
1801	WAW	waw1c.pk006.o24	0.00	-0.09	-0.02	0.02	-0.04	0.05	-0.03	0.07	Putative RNA-binding protein [*Os*]	2e-57
1802	WAW	waw1c.pk006.o3	0.08	-0.05	-0.43	-0.12	-0.28	-0.07	-0.04	-0.05	Putative MLA6 protein [*Os*]	1e-45
1803	WAW	waw1c.pk006.o4	-0.24	-0.50	-0.56	-0.43	-0.33	-0.09	-0.04	0.09	kinase-like protein [*Os*]	0.31
1804	WAW	waw1c.pk006.o5	0.13	0.20	0.08	0.23	0.08	0.01	0.03	0.03	aminotriazole resistance protein	0.91
1805	WAW	waw1c.pk006.o6	-0.33	0.13	0.15	0.27	0.41	0.03	-0.02	0.06	probable enoyl-[acyl-carrier-protein] reductase (NADH2)- rice	2e-54
1806	WAW	waw1c.pk006.o7	-0.16	0.20	0.27	0.10	0.00	-0.08	0.02	0.03	putative fructose 1-,6-biphosphate aldolase [*Ta*]	1e-98
1807	WAW	waw1c.pk006.o8	-0.24	-0.09	0.01	-0.10	0.01	0.00	0.06	0.01	no homologies found	-
1808	WAW	waw1c.pk006.o9	0.04	0.25	0.29	0.25	0.25	0.05	-0.06	0.11	glyoxalase II [*Os*]	3e-60
1809	WAW	waw1c.pk006.p1	0.03	0.43	-0.07	0.55	0.84	0.07	0.15	0.43	DnaJ protein homolog 2	3e-78
1810	WAW	waw1c.pk006.p10	0.07	0.15	0.17	0.13	0.05	-0.05	-0.14	-0.01	putative protein; protein id: At4g38600.1 [*At*]	4e-74
1811	WAW	waw1c.pk006.p12	0.03	-0.07	-0.13	-0.09	-0.06	0.05	-0.07	-0.02	calmodulin-binding protein; protein id: At2g18750.1 [*At*]	2e-39
1812	WAW	waw1c.pk006.p13	0.22	0.13	0.10	0.14	-0.01	0.00	0.02	0.07	RNA-binding protein, putative; protein id: At1g51510.1	0.021
1813	WAW	waw1c.pk006.p14	-0.24	-0.14	-0.24	-0.09	-0.03	-0.05	-0.03	0.00	unknown protein [*At*]	1e-36
1814	WAW	waw1c.pk006.p15	-0.02	-0.07	0.10	-0.03	-0.13	-0.06	-0.09	-0.01	cytoplasmic aconitate hydratase [*At*]	7e-96
1815	WAW	waw1c.pk006.p16	-0.57	-0.84	-0.71	-0.72	-0.69	-0.02	-0.07	-0.15	putative CER1 [*Os*]	3e-71
1816	WAW	waw1c.pk006.p17	0.32	0.08	0.07	-0.12	0.00	0.06	0.01	0.07	histone deacetylase [*Zm*]	1e-107
1817	WAW	waw1c.pk006.p18	-0.01	-0.10	-0.31	-0.07	-0.07	0.07	0.08	0.11	no homologies found	-
1818	WAW	waw1c.pk006.p19	-0.05	-0.09	-0.16	-0.13	-0.11	-0.03	0.00	0.09	expressed protein; protein id: At2g03890.1 [*At*]	2e-19
1819	WAW	waw1c.pk006.p2	0.19	0.11	-0.01	0.06	0.01	-0.09	-0.04	0.05	transportin [*At*]	4e-78
1820	WAW	waw1c.pk006.p20	-0.10	-0.03	-0.07	-0.05	-0.19	-0.04	0.03	-0.02	peroxisomal multifunctional protein [*Os*]	3e-36
1821	WAW	waw1c.pk006.p21	0.07	-0.08	-0.05	-0.08	-0.03	-0.01	0.01	-0.01	Deoxyuridine 5'-triphosphate nucleotidohydrolase (dUTPase) (dUTP pyrophosphatase) (P18)	1e-05
1822	WAW	waw1c.pk006.p22	-0.23	-0.26	-0.08	-0.12	0.14	-0.07	0.04	-0.03	putative glutathione S-transferase [*Os*]	1e-69
1823	WAW	waw1c.pk006.p23	-0.07	-0.06	-0.01	-0.07	0.05	0.02	-0.05	0.05	no homologies found	-
1824	WAW	waw1c.pk006.p24	0.27	0.00	0.05	0.04	-0.10	0.09	0.07	-0.03	Ribosomal protein S7 [*Hv* subsp. vulgare]	1e-95
1825	WAW	waw1c.pk006.p3	-0.01	-0.10	-0.33	-0.25	-0.33	-0.01	0.11	-0.14	glycine-rich RNA-binding protein GRP1 - wheat	4e-18
1826	WAW	waw1c.pk006.p4	-0.04	0.00	-0.09	-0.07	-0.02	0.10	0.10	-0.03	pyridoxal kinase -like protein; protein id: At5g37850.1	1e-29
1827	WAW	waw1c.pk006.p6	-0.99	-0.78	-0.60	-0.74	-0.60	0.16	0.27	-0.03	no homologies found	-
1828	WAW	waw1c.pk006.p7	0.07	0.13	0.25	0.18	0.05	0.04	0.03	-0.28	Enolase 2 (2-phosphoglycerate dehydratase 2) (2-phospho-D-glycerate hydro-lyase 2)	3e-34
1829	WAW	waw1c.pk006.p8	-0.18	-0.07	0.07	-0.03	0.02	0.05	0.04	-0.12	no homologies found	-
1830	WAW	waw1c.pk006.p9	-0.01	-0.21	-0.22	-0.17	-0.07	0.10	0.07	-0.03	no homologies found	-

BIBLIOGRAPHY

Adams, M.D., Kelley, J.M., Gocayne, J.D., Dubnick, M., Polymeropoulos, M.H., Xiao, H., Merril, C.R., Wu, A., Olde, B., Moreno, R.F., *et al*. 1991. Complementary DNA sequencing: expressed sequence tags and human genome project. *Science*. **252:** 1651-1656.

Ahn, S., Anderson, J.A., Sorrells, M.E. and Tanksley, S.D. 1993. Homoeologous relationships of rice, wheat and maize chromosomes. *Mol. Gen. Genet.* **241:** 483-490.

Ajimura, M., Leem, S.H. and Ogawa, H. 1993. Identification of new genes required for meiotic recombination in *Saccharomyces cerevisiae*. *Genetics*. **133:** 51-66.

Alani, E., Padmore, R. and Kleckner, N. 1990. Analysis of wild-type and *Rad50* mutants of yeast suggests an intimate relationship between meiotic chromosome synapsis and recombination. *Cell*. **61:** 419-436.

Albini, S.M. and Jones, G.H. 1987. Synaptonemal complex spreading in *Allium cepa* and *Allium fistulosum*. I. The initiation and sequence of pairing. *Chromosoma*. **95:** 324-338.

Albini, S.M. and Jones, G.H. 1988. Synaptonemal complex spreading in *Allium cepa* and *Allium fistulosum*: II. Pachytene observations: The SC karyotype and the correspondence of late recombination nodules and chiasmata. *Genome*. **30:** 399-410.

Alekseev, S.B., Ebralidze, L.K., Stepanova, L.G. and Boikov, P. 1986. Glucose metabolism and template synthesis in the mitotic cycle of human diploid fibroblasts. *Biokhimiia*. **51:** 140-145.

Allen, J.W., Dix, D.J., Collins, B.W., Merrick, B.A., He, C., Selkirk, J.K., Poorman-Allen, P., Dresser, M.E. and Edd, E.M. 1996. HSP70-2 is part of the synaptonemal complex in mouse and hamster spermatocytes. *Chromosoma*. **104:** 414-421.

Altschul, S.F., Madden, T.L., Schaffer, A.A., Zhang, J.H., Zhang, Z., Miller, W. and Lipman, D.J. 1997. Gapped blast and psi-blast - a new generation of protein database search programs. *Nucleic Acids Res.* **25:** 3389-3402.

Alwine, J.C., Kemp, D.J. and Stark, G.R. 1977. Method for detection of specific RNAs in agarose gels by transfer to diazobenzyloxymethyl-paper and hybridization with DNA probes. *Proc Natl Acad Sci U S A*. **74:** 5350-5354.

Anderson, L.K., Hooker, K.D. and Stack, S.M. 2001. The distribution of early recombination nodules on zygotene bivalents from plants. *Genetics*. **159:** 1259-1269.

Anderson, L.K., Offenberg, H.H., Verkuijlen, W.M.H.C. and Heyting, C. 1997. RecA-like proteins are components of early meiotic nodules in lily. *Proc. Natl. Acad. Sci. USA*. **94:** 6868-6873.

Anderson, L.K., Stack, S.M., Todd, R.J. and Ellis, R.P. 1994. A monoclonal antibody to lateral element proteins in synaptonemal complexes of *Lilium longiflorum*. *Chromosoma*. **103:** 357-367.

Ansley, H.R. 1958. Histones of mitosis and meiosis in *Loxa flavicolis* (hemipteran). *Journal of Biophysical & Biochemical Cytology*. **4:** 59-62.

Appeldoorn, N.J., Sergeeva, L., Vreugdenhil, D., Van Der Plas, L.H. and Visser, R.G. 2002. *In situ* analysis of enzymes involved in sucrose to hexose-phosphate conversion during stolon-to-tuber transition of potato. *Physiol Plant*. **115:** 303-310.

Aragon-Alcaide, L., Reader, S., Beven, A., Shaw, P., Miller, T. and Moore, G. 1997b. Association of homologous chromosomes during floral development. *Curr. Biol.* **7:** 905-908.

Aragon-Alcaide, L., Reader, S., Miller, T. and Moore, G. 1997a. Centromeric behaviour in wheat with high and low homeologous chromosomal pairing. *Chromosoma*. **106:** 327-333.

Aravind, L. and Koonin, E.V. 1998. The HORMA domain: a common structural denominator in mitotic checkpoints, chromosome synapsis and DNA repair. *Trends Biochem. Sci.* **23:** 284-286.

Armstrong, S.J., Caryl, A.P., Jones, G.H. and Franklin, F.C. 2002. Asy1, a protein required for meiotic chromosome synapsis, localizes to axis-associated chromatin in *Arabidopsis* and *Brassica*. *J Cell Sci*. **115:** 3645-3655.

Arumuganathan, K. and Earle, E.D. 1991. Nuclear DNA content of some important plant species. *Plant Mol. Biol. Rep.* **9:** 208-219.

Avivi, L. and Feldman, M. 1973. The mechanism of somatic association in common wheat, *Triticum aestivum* L. IV. Further evidence for modification of spindle tubulin through the somatic association genes as measured by vinblastine binding. *Genetics*. **73:** 379-385.

Avivi, L. and Feldman, M. 1980. Arrangement of chromosomes in the interphase nucleus of plants. *Human Genetics*. **55:** 281-295.

Avivi, L., Feldman, M. and Brown, M. 1982. An ordered arrangement of chromosomes in the somatic nucleus of common wheat, *Triticum aestivum* L. II. Spatial relationships between chromosomes of different genomes. *Chromosoma*. **86:** 17.

Avivi, L., Feldman, M. and Bushuk, W. 1970. The mechanism of somatic association in common wheat, *Triticum aestivum* L. II. Differential affinity for colchicine of spindle microtubules of plants having different doses of the somatic association suppressor. *Genetics*. **65:** 585-592.

Babiychuk, E., Kushnir, S., Belles-Boix, E., Van Montagu, M. and Inze, D. 1995. *Arabidopsis thaliana* NADPH oxidoreductase homologs confer tolerance of yeasts toward the thiol-oxidizing drug diamide. *J Biol Chem*. **270:** 26224-26231.

Bass, H.W., Marshall, W.F., Sedat, J.W., Agard, D.A. and Cande, W.Z. 1997. Telomeres cluster de novo before the initiation of synapsis: a three dimensional spatial analysis of telomere positions before and during meiotic prophase. *Journal of Cell Biology*. **137:** 5-18.

Baudat, F. and Nicolas, A. 1997. Clustering of meiotic double strand breaks on yeast chromosome III. *Proc. Natl. Acad. Sci. USA*. **94:** 5213-5218.

Baxevanis, A.D. and Landsman, D. 1995. The HMG-1 box protein family: classification and functional relationships. *Nucleic Acids Res.* **23:** 1604-1613.

Benavente, E., Orellana, J. and Fernandezcalvin, B. 1998. Comparative analysis of the meiotic effects of wheat *ph1b* and *ph2b* mutations in wheat X rye hybrids. *Theor. Appl. Genet.* **96:** 1200-1204.

Bennett, M.D. 1971. The duration of meiosis. *Proceedings of the Royal Society of London. Series B. Biological Sciences*. **178:** 277-299.

Bennett, M.D., Dover, G.A. and Riley, R. 1974. Meiotic duration in wheat genotypes with and without homoeologous chromosome pairing. *Proceedings of the Royal Society of London. Series B. Biological Sciences*. **187:** 191-207.

Bennett, M.D., Finch, R.A., Smith, J.B. and Rao, M.K. 1973. The time and duration of female meiosis in wheat, rye and barley. *Proceedings of the Royal Society of London. Series B. Biological Sciences*. **183:** 301-319.

Bennett, M.D. and Kaltsikes, P.J. 1973. The duration of meiosis in diploid rye, a tetraploid wheat and the hexaploid triticale derived from them. *Can. J. Genet. Cytol.* **15:** 671.

Bennett, M.D. and Smith, J.B. 1972. The effects of polyploidy on meiotic duration and pollen development in cereal anthers. *Proceedings of the Royal Society of London. Series B. Biological Sciences*. **181:** 81-107.

Bennett, M.D. and Smith, J.B. 1979. The effect of colchicine on fibrillar material in wheat meiocytes. *Journal of Cell Science*. **38:** 33-47.

Bennett, M.D., Smith, J.B., Simpson, S. and Wells, B. 1979. Intranuclear fibrillar material in cereal pollen mother cells. *Chromosoma*. **71:** 289-332.

Berk, A.J. and Sharp, P.A. 1977. Sizing and mapping of early adenovirus mRNAs by gel electrophoresis of S1 endonuclease-digested hybrids. *Cell*. **12:** 721-732.

Bielig, L.M. and Driscoll, C.J. 1970. Substitution of rye chromosome 5RL for chromosome 5B of wheat and its effect on chromosome pairing. *Genetics*. **65:** 241-247.

Bishop, D.K. 1994. RecA homologues Dmc1 and Rad51 interact to form multiple nuclear complexes prior to meiotic chromosome synapsis. *Cell*. **79:** 1081-1092.

Bishop, D.K., Park, D., Xu, L. and Kleckner, L. 1992. DMC1: A meiosis specific yeast homologue of *E. coli* recA required for recombination, synaptonemal complex formation, and cell cycle progression. *Cell*. **69:** 439-456.

Blake, N.K., Lehfeldt, B.R., Hemphill, A., Shan, X. and Talbert, L.E. 1998. DNA sequence analysis suggests a monophyletic origin of the wheat B genome. *Proceedings of the 9th International Wheat Genetics Symposium*. University of Saskatchewan, Saskatoon, Saskatchewan, Canada. 14-16.

Boehm, M. and Bonifacino, J.S. 2001. Adaptins: the final recount. *Mol Biol Cell*. **12:** 2907-2920.

Bohmert, K., Camus, I., Bellini, C., Bouchex, D., Caboche, M. and Benning, C. 1998. *AGO1* defines a novel locus of *Arabidopsis* controlling leaf development. *Embo J*. **17:** 170-180.

Bruhn, S.L., Pil, P.M., Essigmann, J.M., Housman, D.E. and Lippard, S.J. 1992. Isolation and characterization of human cDNA clones encoding a high mobility group box protein that recognizes structural distortions to DNA caused by binding of the anticancer agent cisplatin. *Proc. Natl. Acad. Sci. USA*. **89:** 2307-2311.

Buckley, M.J. 2000 Spot user's guide. In. Sydney, Australia: CSIRO Mathematical and Information Sciences.

Bullard, S.A., Kim, S., Galbraith, A.M. and Malone, R.E. 1996. Double-strand breaks at the HIS2 recombination hot spot in *Saccharomyces cerevisiae*. *Proc. Natl. Acad. Sci. USA*. **93:** 13054-13059.

Burger, C., Wick, M., Brusselbach, S. and Muller, R. 1994. Differential induction of 'metabolic genes' after mitogen stimulation and during normal cell cycle progression. *J Cell Sci*. **107:** 241-252.

Bustin, M. 1999. Regulation of DNA-dependent activities by the functional motifs of the high-mobility-group chromosomal proteins. *Mol. Cell. Biol.* **19:** 5237-5246.

Bustin, M., Lehn, D.A. and Landsman, D. 1990. Structural features of the HMG chromosomal proteins and their genes. *Biochim Biophys Acta*. **1049:** 231-243.

Cao, L., Alani, E. and Kleckner, N. 1990. A pathway for generation and processing of double strand breaks during meiotic recombination in *S. cerevisiae*. *Cell*. **61:** 1089-1101.

Carpenter, A.C.T. 1975. Electron microscopy of of meiosis in *Drosophila melanogaster* females. II. The recombination nodule-a recombination -associated structure at pachytene? *Proc. Natl. Acad. Sci. USA*. **72:** 3186-3189.

Carpenter, A.C.T. 1979a. Recombination nodules and aynaptonemal complex in recombination-defective females of *Drosophila melanogaster*. *Genetics*. **75:** 259-292.

Carpenter, A.C.T. 1979b. Synaptonemal complex and recombination nodules in wild-type *Drosophila melanogaster* females. *Genetics*. **92:** 511-541.

Carpenter, A.C.T. 1987. Gene conversion, recombination nodules, and initiation of meiotic synapsis. *BioEssays*. **6:** 232-236.

Carpenter, A.C.T. 1988. Thoughts on recombination nodules, meiotic recombination, and chiasmata. In *Genetic Recombination*. Kucherlapati, R., and Smith, G.R. (eds.) Washington, DC: American Society of Microbiology, pp. 529-548.

Cayrol, C., Cougoule, C. and Wright, M. 2002. The beta2-adaptin clathrin adaptor interacts with the mitotic checkpoint kinase BubR1. *Biochem Biophys Res Commun*. **298:** 720-730.

Ceoloni, C., Avivi, L. and Feldman, M. 1984. Spindle sensitivity to colchicine of the *Ph1* mutant in common wheat. *Can. J. Genet. Cytol.* **26:** 111-118.

Chaudhury, A.M., Lavithis, M., Taylor, P.E., Craig, S., Singh, M.B., Signer, E.R., Knox, R.B. and Dennis, E.S. 1994. Genetic control of male fertility in *Arabidopsis thaliana*: Structural analysis of premeiotic developmental mutants. *Sex. Plant Reprod*. **7:** 17-28.

Cho, R.J., Campbell, M.J., Winzeler, E.A., Steinmetz, L., Conway, A., Wodicka, L., Wolfsberg, T.G., Gabrielian, A.E., Landsman, D., Lockhart, D.J. and Davis, R.W. 1998. A genome-wide transcriptional analysis of the mitotic cell cycle. *Mol Cell*. **2:** 65-73.

Chu, S., DeRisi, J., Eisen, M., Mulholland, J., Botstein, D., Brown, P.O. and Herskowitz, I. 1998. The transcriptional program of sporulation in budding yeast. *Science*. **282:** 699-705.

Cleveland, W.S. 1979. Robust locally weighted regression and smoothing scatterplots. *J. Amer. Stat. Assoc.* **74:** 829-836.

Comings, D.E. and Riggs, A.D. 1971. Molecular mechanisms of chromosome pairing, folding and function. *Nature (London)*. **233:** 48-50.

Crothers, D.M. 1993. Architectural elements in nucleoprotein complexes. *Curr. Biol.* **3:** 675-676.

Dawe, R.K. 1998. Meiotic chromosome organization and segregation in plants. *Annual Review of Plant Physiology & Plant Molecular Biology*. **49:** 371-395.

Dawson, J., Wilson, Z.A., Aarts, M.G.M., Braithwaite, A.F., Briarty, L.G. and Mulligan, B.J. 1993. Microspore and pollen development in six male-sterile mutants of *Arabidopsis thaliana*. *Candian Journal of Botany*. **71:** 629-638.

Dernburg, A.F., Sedat, J.W., Cande, W.Z. and Bass, H.W. 1995. Cytology of telomeres. In *Telomeres*. Blackburn, E.H., and Greider, C.W. (eds.) Cold Spring Harbour, NY: Cold Spring Harbour Laboratories Press, pp. 295-338.

Dickinson, H.G. 1987. The physiology and biochemistry of meiosis in the anther. *Int. Rev. Cytol*. **107:** 79-109.

Dobson, M.J., Pearlman, R.E., Karaiskakis, A., Spyropoulos, B. and Moens, B.P. 1994. Synaptonemal complex proteins: occurance, epitope mapping and chromosome disjunction. *Journal of Cell Science*. **107:** 2749-2760.

Dong, C., Whitford, R. and Langridge, P. 2002. A DNA mismatch repair gene links to the *Ph2* locus in wheat. *Genome*. **45:** 116-124.

Doutriaux, M.P., Couteau, F., Bergounioux, C. and White, C. 1998. Isolation and characterisation of RAD51 and DMC1 homologues from *Arabidopsis thaliana*. *Molecular and General Genetics*. **257:** 283-291.

Downs, S.M., Humpherson, P.G., Martin, K.L. and Leese, H.J. 1996. Glucose utilization during gonadotropin-induced meiotic maturation in cumulus cell-enclosed mouse oocytes. *Mol Reprod Dev*. **44:** 121-131.

Driscoll, C.J. 1972. Genetic suppression of homoeologous chromosome pairing in hexaploid wheat. *Can. J. Genet. Cytol.* **14:** 39-42.

Driscoll, C.J. 1973. Minor genes affecting homoeologous pairing in hybrids between wheat and related genera. *Genetics*. **74s:** 566.

Dubcovsky, J., Luo, M.C. and Dvorak, J. 1995. Differentiation between homoeologous chromosomes 1a of wheat and 1A(M) of *Triticum monococcum* and its recognition by the wheat *Ph1* locus. *Proc. Natl. Acad. Sci. USA*. **92:** 6645-6649.

Dudoit, S., Yang, Y.H. and Bolstad, B. 2002a. Using R for the analysis of DNA microarray data. *R News*. **2:** 24-32.

Dudoit, S., Yang, Y.H., Callow, M.J. and Speed, T.P. 2002b. Statistical methods for identifying differentially expressed genes in replicated cDNA microarray experiments. *Statistica Sinica*. **12:** 111-139.

Dunford, R.P., Kurata, N., Laurie, D.A., Money, T.A., Minobe, Y. and Moore, G. 1995. Conservation of fine-scale DNA marker order in the genomes of rice and the Triticeae. *Nucleic Acids Res.* **23:** 2724-2728.

Eberwine, J., Yeh, H., Miyashiro, K., Cao, Y., Nair, S., Finnell, R., Zettel, M. and Coleman, P. 1992. Analysis of gene expression in single live neurons. *Proc Natl Acad Sci U S A*. **89:** 3010-3014.

Eisen, M.B., Spellman, P.T., Brown, P.O. and Botstein, D. 1998. Cluster analysis and display of genome-wide expression patterns. *Proc Natl Acad Sci U S A*. **95:** 14863-14868.

Evrard, J.L., Nguyen, I., Bergdoll, M., Mutterer, J., Steinmetz, A. and Lambert, A.M. 2002. A novel pollen-specific alpha-tubulin in sunflower: structure and characterization. *Plant Mol Biol*. **49:** 611-620.

Fawcett, D.W. 1956. The fine structure of chromosomes in the meiotic prophase of vertebrate spermatocytes. *J. Biophys. Biochem. Cytol.* **2:** 403-406.

Feinberg, A.P. and Vogelstein, B. 1983. A technique for radiolabeling DNA restriction endonuclease fragments to high specific activity. *Analytical Biochemistry*. **132:** 6-13.

Feldman, M. 1966. The effect of chromosomes 5B, 5D and 5A on chromosomal pairing in *Triticum aestivum*. *Proc. Natl. Acad. Sci. USA*. **55:** 1447-1453.

Feldman, M. 1968. Regulation of somatic association and meiotic pairing in common wheat. *Proceedings of the Third International Wheat Genetics Symposium*. Canberra. 31-40.

Feldman, M. 1993. Cytogenetic activity and mode of action of the pairing homoeologous (*Ph1*) gene of wheat. *Crop Sci.* **33:** 894-897.

Feldman, M. and Avivi, L. 1984. Ordered arrangement of chromosomes in wheat. In *Chromosomes Today*. Bennett, M.D., Gropp, A., and Wolf, U. (eds.) London: Allen and Unwin, pp. 181.

Feldman, M. and Mello-Sampayo, T. 1967. Suppression of homoeologous chromosome pairing in hybrids of polyploid wheats X *Triticum speltoides*. *Can. J. Genet. Cytol.* **9:** 303-317.

Franckowiak, J. 1997. Revised linkage maps for morphological markers in barley, *Hordeum vulgare*. *Barley Genetics Newsletter*. **26:** 9-21.

Gale, M.D. and Devos, K.M. 1998. Comparative genetics in the grasses. *Proc. Natl. Acad. Sci. USA*. **95:** 1971-1974.

Gale, M.D. and Miller, T.E. 1987. The introduction of alien genetic variation into wheat. In *Wheat Breeding: Its Scientific Basis*. Lupton, F.G.H. (ed.) London: Chapman and Hall Ltd., pp. 173-210.

Garcia, V., Bruchet, H., Camescasse, D., Granier, F., Bouchez, D. and Tissier, A. 2003. AtATM is essential for meiosis and the somatic response to DNA damage in plants. *Plant Cell*. **15:** 119-132.

Garcia, V., Salanoubat, M., Choisne, N. and Tissier, A. 2000. An ATM homologue from *Arabidopsis thaliana*: complete genomic organisation and expression analysis. *Nucleic Acids Res*. **28:** 1692-1699.

Gibson, S.I., Surosky, R.T. and Tye, B.K. 1990. The phenotype of the minichromosome maintenance mutant mcm3 is characteristic of mutants defective in DNA replication. *Mol. Cell. Biol.* **10:** 5707-5720.

Gill, K.S., Gill, B.S., Endo, T.R. and Boyko, E.V. 1996. Identification and high density mapping of gene-rich regions in chromosome group 5 in wheat. *Genetics*. **143:** 1001-1012.

Gill, K.S., Gill, B.S., Endo, T.R. and Mukai, Y. 1993. Fine physical mapping of *Ph1*, a chromosome pairing regulator gene in polyploid wheat. *Genetics*. **134:** 1231-1236.

Gillies, C.B. 1972. Reconstruction of the *Neurospora crassa* pachytene karyotype from serial sections of synaptonemal complexes. *Chromosoma*. **36:** 119-130.

Glover, J., Grelon, M., Craig, S., Chaudhury, A. and Dennis, E. 1998. Cloning and characterization of ms5 from *Arabidopsis* - a gene critical in male meiosis. *Plant J.* **15:** 345-356.

Goldway, M., Sherman, A., Zenvirth, D., Arbel, T. and Simchen, G. 1993. A short chromosomal region with major roles in yeast chromosome III meiotic disjunction, recombination and double strand breaks. *Genetics*. **133:** 159-169.

Golubovskaya, I., Grebennikova, Z.K., Avalkina, N.A. and Sheridan, W.F. 1993. The role of the ameiotic1 gene in the initiation of meiosis and in subsequent meiotic events in maize. *Genetics*. **135:** 1151-1166.

Golubovskaya, I.N., Grebennikova, Z.K., Auger, D.L. and Sheridan, W.F. 1997. The maize desynaptic1 mutation disrupts meiotic chromosome synapsis. *Dev. Genet.* **21:** 146-159.

Grasser, K.D. 1998. HMG1 and HU proteins: architectural elements in plant chromatin. *Trends Plant Sci.* **3:** 260-265.

Grosschedl, R. 1995. Higher-order nucleoprotein complexes in transcription: analogies with site-specific recombination. *Curr. Opin. Cell Biol.* **7:** 362-370.

Grosschedl, R., Giese, K. and Pagel, J. 1994. HMG domain proteins: architectural elements in the assembly of nucleoprotein structures. *Trends Genet*. **10:** 94-100.

Guidet, F., Rogowsky, P., Taylor, C., Song, W. and Langridge, P. 1991. Cloning and characterisation of a new rye-specific repeated sequence. *Genome*. **34:** 81-87.

He, C.P., Tirlapur, U., Cresti, M., Peja, M., Crone, D.E. and Mascarenhas, J.P. 1996. An *Arabidopsis* mutant showing aberrations in male meiosis. *Sexual Plant Reproduction*. **9:** 54-57.

Hennessy, K.M., Clark, C.D. and Botstein, D. 1990. Subcellular localization of yeast CDC46 varies with the cell cycle. *Genes Dev*. **4:** 2252-2263.

Heyting, C., Dietrich, A.J.J., Redeker, E.J.W. and Vink, A.C. 1985. Structure and composition of synaptonemal complexes, isolated from rat spermatocytes. *Eur. J. Cell Biol.* **36:** 307-314.

Hihara, Y., Hara, C. and Uchimiya, H. 1996. Isolation and characterization of two cDNA clones for mRNAs that are abundantly expressed in immature anthers of rice (*Oryza sativa* L.). *Plant Mol Biol*. **30:** 1181-1193.

Hiraoka, Y., Dernburg, A.F., Parmelee, S.J., Rykowski, M.C. and Agard, D.A. 1993. The onset of homologous chromosome pairing during *Drosophila melanogaster* embryogenesis. *J. Cell Biol.* **120:** 591-600.

Hodgkin, J., Horvitz, H.R. and Brenner, S. 1979. Nondisjunction mutants of the nematode *C. elegans*. *Genetics*. **91:** 67-94.

Holboth, P. 1981. Chromosome pairing in allohexaploid wheat var. Chinese Spring. Transformation of multivalents into bivalents, a mechanism for exclusive bivalent formation. *Carlsberg Res. Commun.* **46:** 129-173.

Holliday, R. 1964. A mechanism for gene conversion in fungi. *Genetic Research Cambridge*. **5:** 282-304.

Holliday, R. 1968. Genetic recombination in fungi. In *Replication and Recombination of Genetic Material*. Peacock, W.J., and Brooks, R.D. (eds.) Canberra: Australian Academy of Science, pp. 157-174.

Hollingsworth, N.M. and Byers, B. 1989. HOP1: a yeast meiotic pairing gene. *Genetics*. **121:** 445-462.

Hollingsworth, N.M., Goetsch, L. and Byers, B. 1990. The *HOP1* gene encodes a meiosis-specific component of yeast chromosomes. *Cell*. **61:** 73-84.

Holm, P.B. 1988a. Chromosome pairing and synaptonemal complex formation in allohexaploid wheat, monosomic for chromosome 5B. *Carlsberg Research Communication*. **53:** 57-89.

Holm, P.B. 1988b. Chromosome pairing and synaptonemal complex formation in allohexaploid wheat, nullisomic for chromosome 5B. *Carlsberg Research Communication*. **53:** 91-110.

Holm, P.B. and Wang, X. 1988. The effect of chromosome 5B on synapsis and chiasma formation in wheat *Triticum aestivum* cv. Chinese Spring. *Carlsberg Research Communication*. **53:** 191-208.

Hotta, Y. and Stern, H. 1971. Analysis of DNA synthesis during meiotic prophase in *Lilium*. *Journal of Molecular Biology*. **55:** 337-355.

Inoue, H., Nojima, H. and Okayama, H. 1990. High efficiency transformation of *Escherichia coli* with plasmids. *Gene*. **96:** 23-28.

Ivanov, E.L., Korolev, V.G. and Fabre, F. 1992. XRS2, DNA repair gene of *Saccharomyces cerevisiae*, is needed for meiotic recombination. *Genetics*. **132:** 651-664.

Ivanov, E.L., Sugawara, N., White, C.I., Fabre, F. and Haber, J.F. 1994. Mutations in XRS2 and RAD50 delay but do not prevent mating-type switching in *Saccharomyces cerevisiae*. *Mol. Cell. Biol.* **14:** 3414-3425.

Ji, L.H. 1992. A study of meiosis in allohexaploid wheat: The molecular aspects. Doctor of Philosophy. Department of Plant Science, The University of Adelaide. Adelaide, Australia.

Ji, L.H. and Langridge, P. 1994. An early meiosis cDNA clone from wheat. *Mol. Gen. Genet.* **243:** 17-23.

Johnson, R.E., Kovvali, G.K., Prakash, L. and Prakash, S. 1996. Requirement of the yeast MSH3 and MSH6 genes for MSH2-dependent genomic stability. *J Biol Chem*. **271:** 7285-7288.

Keeney, S., Giroux, C.N. and Kleckner, N. 1997. Meiosis-specific DNA double-strand breaks are catalyzed by *Spo11*, a member of a widely conserved protein family. *Cell*. **88:** 375-384.

Kitada, K. and Omura, T. 1983. Genetic control of meiosis in rice, *Oryza sativa* L. II. Cytogenetical analyses of desynaptic mutants. *Jpn. J. Genet.* **58:** 567-577.

Kitada, K. and Omura, T. 1984. Genetic control of meiosis in rice, *Oryza sativa* L. IV. Cytogenetical analyses of asynaptic mutants. *Can. J. Genet. Cytol.* **26:** 264-271.

Klapholz, S., Waddell, C.S. and Esposito, R.E. 1985. The role of the SPO11 gene in meiotic recombination in yeast. *Genetics*. **110:** 187-216.

Klein, F., Laroche, T., Cardenas, M.E., Hoffmann, J., F., Schweizer, D. and Gadder, S.M. 1992. Localisation of RAP1 and topoisomerase II in nuclei and meiotic chromosomes of yeast. *J. Cell. Biol.* **117:** 935-948.

Klein, F., Mahr, P., Galova, M., Buonoma, S.B.D. and Michaelis, C. 1999. A central role for cohesins in sister chromatid cohesion: formation of axial elements and recombination during yeast meiosis. *Cell*. **98:** 91-103.

Klein, S., Zenvirth, D., Dror, V., Barton, A.B., Kaback, D.B. and Simchen, G. 1996. Patterns of meiotic double strand breakage on native and artificial yeast chromosomes. *Chromosoma*. **105:** 276-284.

Klimyuk, V.I. and Jones, J.D. 1997. AtDMC1, the *Arabidopsis* homologue of the yeast DMC1 gene: characterization, transposon-induced allelic variation and meiosis-associated expression. *Plant J*. **11:** 1-14.

Kobayashi, T., Kobayashi, E., Sato, S., Hotta, Y., Miyajima, N., Tanaka, A. and Tabata, S. 1994. Characterization of cDNAs induced in meiotic prophase in lily microsporocytes. *DNA Res*. **1:** 15-26.

Koebner, R.M.D. and Shepherd, K.W. 1985. Induction of recombination between rye chromosome 1RL and wheat chromosomes. *Theor. Appl. Genet.* **71:** 208-215.

Kolodoner, R. 1996. Biochemistry and genetics of eukaryotic mismatch repair. *Genes and Dev.* **10:** 1433-1442.

Kolodoner, R. and Marsischky, G.T. 1999. Eukaryotic DNA mismatch repair. *Current Opin. Genet. Dev.* **9:** 89-96.

Lammers, J.H.M., Offenberg, H.H., van Aalderen, M., Vink, A.C.J., Dietrich, A.J.J. and Heyting, C. 1994. The gene encoding a major component of the lateral elements of synaptonemal complexes of the rat is related to X-linked lymphocyte regulated genes. *Mol. Cell. Biol.* **14:** 1137-1146.

Langridge, P., Karakousis, A., Collins, N., Kretschmer, J. and Manning, S. 1995. A consensus linkage map of barley. *Mol. Breeding*. **1:** 389-395.

Lazo, G.R. 2003. Charting contig-component relationships within the Triticeae. *23rd Stadler Genetics Symposium, Genome Exploitation*: *Data Mining*. Columbia, MO. USA.

Letarte, J. 1996. Identification and characterisation of early meiotic genes in wheat. Doctor of Philosophy. Department of Plant Science, The University of Adelaide. Adelaide, Australia.

Liang, P. and Pardee, A.B. 1992. Differential display of eukaryotic messenger RNA by means of the polymerase chain reaction. *Science*. **257:** 967-971.

Lipshutz, R.J., Morris, D., Chee, M., Hubbell, E., Kozal, M.J., Shah, N., Shen, N., Yang, R. and Fodor, S.P. 1995. Using oligonucleotide probe arrays to access genetic diversity. *Biotechniques*. **19:** 442-447.

Liu, J.G., Yuan, L., Brundell, E., Bjorkroth, B., Daneholt, B. and Hoog, C. 1996. Localisation of the N terminus of SCP1 to the central element of the synaptonemal complex and evidence for direct interactions between the N termini of SCP1 molecules organised head to head. *Exp. Cell Res.* **226:** 11-19.

Loidl, J. 1990. The initiation of meiotic chromosome pairing: The cytological view. *Genome*. **33:** 759-778.

Loidl, J., Klein, F. and Scherthan, H. 1994. Homologous pairing is reduced but not abolished in asynaptic mutants of yeast. *Journal of Cell Biology*. **125:** 1191-1200.

Lonnstedt, I. and Speed, T.P. 2002. Replicated Microarray Data. *Statistical Sinica*. **12:** 31-46.

Luo, M.C., Dubcovsky, J. and Dvorak, J. 1996. Recognition of homeology by the wheat *Ph1* locus. *Genetics*. **144:** 1195-1203.

Maguire, M., Paredes, A.M. and Riess, R.W. 1991. The desynaptic mutant of maize as a combined defect of synaptonemal complex and chiasma maintenance. *Genome*. **34:** 879-887.

Maguire, M.P. 1977. Homologous chromosome pairing. *Philosophical Transactions of the Royal Society of London. Series B: Biological Sciences*. **277:** 245-258.

Maguire, M.P. 1983. Chromosome behaviour at premeiotic mitosis in maize. *The Journal of Heredity*. **74:** 93-96.

Maguire, M.P., Riess, R.W. and Paredes, A.M. 1993. Evidence from a maize desynaptic mutant points to a probable role of synaptonemal complex central region components in provision for subsequent chiasma maintenance. *Genome*. **36:** 797-807.

Marsischky, G.T., Filosi, N., Kane, M.F. and Kolodner, R. 1996. Redundancy of Saccharomyces cerevisiae MSH3 and MSH6 in MSH2-dependent mismatch repair. *Genes Dev*. **10:** 407-420.

Martin, W., Gierl, A. and Saedler, H. 1989. Molecular evidence for pre-Cretaceous angiosperm origins. *Nature*. **339:** 46-48.

Martinez, M., Cunado, N., Carcelen, N. and Romero, C. 2001. The *Ph1* and *Ph2* loci play different roles in synaptic behaviour of hexaploid wheat *Triticum aestivum*. *Theor. Appl. Genet.* **103:** 398-405.

Martinez-Perez, E., Shaw, P., Reader, S., Aragon-Alcaide, L., Miller, T. and Moore, G. 1999. Homologous chromosome pairing in wheat. *Journal of Cell Science*. **112:** 1761-1769.

Mata, J., Lyne, R., Burns, G. and Bahler, J. 2002. The transcriptional program of meiosis and sporulation in fission yeast. *Nat Genet*. **32:** 143-147.

McClintock, B. 1941. The association of mutants with homozygous deficiencies in *Zea mays*. *Genetics*. **25:** 542-571.

McClintock, B. 1951. Chromosome organisation and genic expression. *Cold Spring Harbour Symp. Quant. Biol.* **16:** 13-47.

McLeish, J. and Snoad, B. 1958 *Looking at Chromosomes*: St Martin's, Macmillon.

Mellema, S., Eichenberger, W., Rawyler, A., Suter, M., Tadege, M. and Kuhlemeier, C. 2002. The ethanolic fermentation pathway supports respiration and lipid biosynthesis in tobacco pollen. *Plant J*. **30:** 329-336.

Mello-Sampayo, T. 1971. Genetic regulation of meiotic chromosome pairing by chromosome 3D of *Triticum aestivum*. *Nature New Biol.* **230:** 23-24.

Mello-Sampayo, T. 1972. Compensated monosomic 5B-trisomic 5A plants in tetraploid wheat. *Can. J. Genet. Cytol.* **14:** 463-475.

Mello-Sampayo, T. and Canas, P. 1973. Suppressors of meiotic chromosome pairing in common wheat. *Proceedings of the Fourth International Wheat Genetics Symposium*. Columbia, Missouri. 709-713.

Mello-Sampayo, T. and Lorente, R. 1968. The role of chromosome 3D in the regulation of meiotic pairing in hexaploid wheat. *EWAC Newsletter*. **2:** 16-24.

Menees, T.M., Ross Mac Donald, P.B. and Roeder, G.S. 1992. ME14, a meiosis specific yeast gene required for chromosome synapsis. *Mol. Cell. Biol.* **12:** 1340-1351.

Menu, T., Rothan, C., Dai, N., Petreikov, M., Etienne, C., Destrac-Irvine, A., Schaffer, A., Granot, D. and Ricard, B. 2001. Cloning and characterization of a cDNA encoding hexokinase from tomato. *Plant Sci*. **160:** 209-218.

Mercier, R., Grelon, M., Vezon, D., Horlow, C. and Pelletier, G. 2001. How to characterize meiotic functions in plants? *Biochimie*. **83:** 1023-1028.

Meselson, M.S. and Radding, C.M. 1975. A general model for genetic recombination. *Proc. Natl. Acad. Sci. USA*. **72:** 358-361.

Meuwissen, R.L., Offenberg, H.H., Dietrich, A.J., Riesewijk, A., van Iersel, M. and Heyting, C. 1992. A coiled-coil related protein specific for synapsed regions of meiotic prophase chromosomes. *EMBO Journal*. **11:** 5091-5100.

Mikhailova, E.I., Naranjo, T., Shepherd, K., Eden, J.W., Heyting, C. and de Jong, J.H. 1998. The effect of the wheat *Ph1* locus on chromatin organisation and meiotic chromosome pairing analysed by genome painting. *Chromosoma*. **107:** 339-350.

Miller, T.E. and Riley, R. 1972. Meiotic chromosome pairing in wheat rye combinations. *Genet. Iber.* **24:** 241-250.

Modrich, P. and Lahue, R. 1996. Mismatch repair in replication fidelity, genetic recombination, and cancer biology. *Annu Rev Biochem*. **65:** 101-133.

Moens, P.B. 1969. Genetic and cytological effects of three desynaptic genes in the tomato. *Can. J. Genet. Cytol.* **11:** 857-869.

Moens, P.B., Chen, D.J., Shen, Z., Kolas, N., Tarsounas, M., Heng, H.H. and Spyropoulos, B. 1997. Rad51 immunocytology in rat and mouse spermatocytes and oocytes. *Chromosoma*. **106:** 207-215.

Moens, P.B. and Earnshaw, W.C. 1989. Anti-topoisomeraseII recognises meiotic specific cores. *Chromosoma*. **98:** 317-322.

Moens, P.B. and Spyropoulos, B. 1995. Immunocytology of chiasmata and chromosomal disjunction at mouse meiosis. *Chromosoma*. **104:** 175-182.

Moore, G. 2002. Meiosis in allopolyploids-the importance of 'Teflon' chromosomes. *Trends Genet.* **18:** 456.

Moore, G., Devos, K.M., Wang, Z. and Gale, M.D. 1995. Cereal genome evolution - Grasses, line up and form a circle. *Curr. Biol.* **5:** 737-739.

Mori, C., Welch, J.E., Fulcher, K.D., O'Brien, D.A. and Eddy, E.M. 1993. Unique hexokinase messenger ribonucleic acids lacking the porin-binding domain are developmentally expressed in mouse spermatogenic cells. *Biol Reprod*. **49:** 191-203.

Moses, M.J. 1956. Chromosome structure in crayfish spermatocytes. *J. Biophys. Biochem. Cytol.* **2:** 215-218.

Moses, M.J. 1968. Synaptonemal complex. *Ann. Rev. Genet*. **2:** 363-412.

Muller, R., Mumberg, D. and Lucibello, F.C. 1993. Signals and genes in the control of cell-cycle progression. *Biochim Biophys Acta*. **1155:** 151-179.

Nag, D.K., Scherthan, H., Rockmill, B., Bhargava, J. and Roeder, G.S. 1995. Heteroduplex DNA formation and homolog pairing in yeast meiotic mutants. *Genetics*. **141:** 75-86.

Netzker, R., Hermfisse, U., Wein, K.H. and Brand, K. 1994. Expression of glycolytic isozymes in rat thymocytes during cell cycle progression. *Biochim Biophys Acta*. **1224:** 371-376.

Offenberg, H.H., Schalk, J.A., Meuwissen, R.L., van Aaldereren, M. and Kester, H.A. 1998. SCP2: a major protein component of the axial elements of synaptonemal complexes of the rat. *Nucleic Acids Res.* **26:** 2572-2579.

Ohyama, T., Iwaikawa, Y., Kobayashi, T., Hotta, Y. and Tabata, S. 1992. Isolation of synaptonemal complexes from lily microsporocytes. *Journal of Plant Science*. **86:** 115-124.

Okubo, K., Hori, N., Matoba, R., Niiyama, T., Fukushima, A., Kojima, Y. and Matsubara, K. 1992. Large scale cDNA sequencing for analysis of quantitative and qualitative aspects of gene expression. *Nat Genet*. **2:** 173-179.

op den Camp, R.G. and Kuhlemeier, C. 1997. Aldehyde dehydrogenase in tobacco pollen. *Plant Mol Biol*. **35:** 355-365.

Orr-Weaver, T.L. 1995. Meiosis in *Drosophila*: Seeing is believing. *Proc. Natl. Acad. Sci. USA*. **92:** 10443-10449.

Ozkan, H. and Feldman, M. 2001. Genotypic variation in tetraploid wheat affecting homoeologous pairing in hybrids with *Aegilops peregrina*. *Genome*. **44:** 1000-1006.

Pallotta, M.A., Graham, R.D., Langridge, P., Sparrow, D.H.B. and Barker, S.J. 2000. RFLP mapping of manganese efficiency in barley. *Theor. Appl. Genet.* **101:** 1100-1108.

Peirson, B.N., Owen, H.A., Feldmann, K.A. and Makaroff, C.A. 1996. Characterization of three male-sterile mutants of *Arabidopsis thaliana* exhibiting alterations in meiosis. *Sexual Plant Reproduction*. **9:** 1-16.

Powell, L.M., Wallis, S.C., Pease, R.J., Edwards, Y.H., Knott, T.J. and Scott, J. 1987. A novel form of tissue-specific RNA processing produces apolipoprotein-B48 in intestine. *Cell*. **50:** 831-840.

Primig, M., Williams, R.M., Winzeler, E.A., Tevzadze, G.G., Conway, A.R., Hwang, S.Y., Davis, R.W. and Esposito, R.E. 2000. The core meiotic transcriptome in budding yeasts. *Nat Genet*. **26:** 415-423.

Prolla, T.A., Pang, Q., Alani, E., Kolodoner, R.D. and Liskay, R.M. 1994. MLH1, PMS1 and MSH2 interactions during the initiation of DNA mismatch repair in yeast. *Science*. **265:** 1091-1093.

Riley, R. 1968. The basic and applied genetics of chromosome pairing. *Proceedings of the Third International Wheat Genetics Symposium*. 185-195.

Riley, R. and Chapman, V. 1958. Genetic control of the cytologically diploid behavior of hexaploid wheat. *Nature*. **182:** 713-715.

Riley, R., Chapman, V. and Kimber, G. 1960. Position of the gene determining the diploid-like meiotic behaviour of wheat. *Nature*. **186:** 259-260.

Riley, R., Chapman, V., Young, R.M. and Belfield, A.M. 1966. Control of meiotic chromosome pairing by the chromosomes of homoeologous group 5 of *Triticum aestivum*. *Nature*. **212:** 1475-1477.

Roberts, J.W., Roberts, C.W. and Craig, N.L. 1978. *Escherichia coli* recA gene product inactivates phage l suppressor. *Proc. Natl. Acad. Sci. USA*. **75:** 4714-4718.

Roberts, M.A., Reader, S.M., Dalgliesh, C., Miller, T.E., Foote, T.N., Fish, L.J., Snape, J.W. and Moore, G. 1999. Induction and characterization of *Ph1* wheat mutants. *Genetics*. **153:** 1909-1918.

Rockmill, B., Engebrecht, J., Scherthan, H., Loidl, J. and Roeder, G.S. 1995. The yeast MER2 gene is required for meiotic recombination and chromosome synapsis. *Genetics*. **141:** 49-59.

Rockmill, B. and Roeder, G.S. 1991. A meiosis specific protein kinase homologue required for chromosome synapis and recombination. *Genes and Dev.* **5:** 2392-2404.

Roeder, G.S. 1995. Sex and the single cell: meiosis in yeast. *Proc. Natl. Acad. Sci. USA*. **92:** 10450-10456.

Roeder, G.S. 1997. Meiotic chromosomes: It takes two to tango. *Genes Dev.* **11:** 2600-2611.

Rogers, H.J., Greenland, A.J. and Hussey, P.J. 1993. Four members of the maize beta-tubulin gene family are expressed in the male gametophyte. *Plant J*. **4:** 875-882.

Ross, K.J., Fransz, P., Armstrong, S.J., Vizir, I., Mulligan, B., Franklin, F.C.H. and Jones, G.H. 1997. Cytological characterization of four meiotic mutants of *Arabidopsis* isolated from t-dna-transformed lines. *Chromosome Research*. **5:** 551-559.

Ross-Macdonald, P. and Roeder, G.S. 1994. Mutation of a meiosis-specific MutS homolog decreases crossing over but not mismatch correction. *Cell*. **79:** 1069-1080.

Roth, T.F. and Ito, M. 1967. DNA-dependent formation of the synaptonemal complex at meiotic prophase. *Journal of Cell Biology*. **35:** 247-255.

Rottgers, K., Krohn, N.M., Lichota, J., Stemmer, C., Merkle, T. and Grasser, K.D. 2000. DNA-interactions and nuclear localisation of the chromosomal HMG domain protein SSRP1 from maize. *Plant J*. **23:** 395-405.

Sabelli, P.A., Burgess, S.R., Kush, A.K., Young, M.R. and Shewry, P.R. 1996. cDNA cloning and characterisation of a maize homologue of the MCM proteins required for the initiation of DNA replication. *Mol Gen Genet*. **252:** 125-136.

Sabelli, P.A., Parker, J.S. and Barlow, P.W. 1999. cDNA and promoter sequences for MCM3 homologues from maize, and protein localization in cycling cells. *J. Exp. Bot.* **50:** 1315-1322.

Salunga, R.C., Guo, H., Lou, L., Bittner, A., Joy, K.C., Chambers, J.R., Wan, J.S., Jackson, M.R. and Erlander, M.G. 1999. Gene expression analysis via cDNA microarrays of laser capture microdissected cells from fixed tissue. In *DNA Microarrays*. Schena, M. (ed.) New York: Oxford University Press Inc., pp. 121-137.

Sambrook, F., Fritsch, E.F. and Maniatis, F. 1989 *Molecular cloning: A laboratory manual*. New York: Cold Spring Harbour Laboratory.

Sargent, T.D. and Dawid, I.B. 1983. Differential gene expression in the gastrula of *Xenopus laevis*. *Science*. **222:** 135-139.

Sasaki, T., Matsumoto, T., Yamamoto, K., Sakata, K., Baba, T., Katayose, Y., Wu, J., Niimura, Y., Cheng, Z., Nagamura, Y., Antonio, B.A., Kanamori, H., Hosokawa, S.,

Masukawa, M., Arikawa, K.*, et al.* 2002. The genome sequence and structure of rice chromosome 1. *Nature*. **420:** 312-316.

Sato, S., Hotta, Y. and Tabata, S. 1995. Structural analysis of a recA-like gene in the genome of *Arabidopsis thaliana*. *DNA Res*. **2:** 89-93.

Schena, M., Shalon, D., Davis, R.W. and Brown, P.O. 1995. Quantitative monitoring of gene expression patterns with a complementary DNA microarray. *Science*. **270:** 467-470.

Scherthan, H., Bahler, J. and Kohli, J. 1994. Dynamics of chromosome organisation and pairing during meiotic prophase in fission yeast. *Journal of Cell Biology*. **127:** 273-285.

Scherthan, H., Weich, S., Schwegler, H., Heyting, C., Harle, M. and Cremer, T. 1996. Centromere and telomere movements during early meiotic prophase of mouse and man are associated with the onset of chromosome pairing. *J. Cell Biol.* **134:** 1109-1125.

Schmekel, K. and Daneholt, B. 1995. The central region of the synaptonemal complex revealed in three dimensions. *Trends Cell Biol.* **5:** 239-242.

Schmekel, K., Meuwissen, R.L., Dietrich, A.J., Vink, A.C., van Marle, J., van Veen, H. and Heyting, C. 1996. Organisation of SCP1 protein molecules within synaptonemal complexes of the rat. *Exp. Cell Res.* **226:** 20-30.

Schwacha, A. and Kleckner, N. 1994. Identification of joint molecules that form frequently between homologs but rarely between sister chromatids during yeast meiosis. *Cell*. **76:** 51-63.

Schwacha, A. and Kleckner, N. 1997. Interhomolog bias during meiotic recombination: Meiotic functions promote a highly differentiated interhomolog-only pathway. *Cell*. **90:** 1123-1135.

Schwartz, D. 1953. The behaviour of an X-ray-induced ring chromosome in maize. *Am. Nat.* **87:** 19-28.

Schwarzacher, T. 1997. Three stages of meiotic homologous chromosome pairing in wheat - Cognition, alignment and synapsis. *Sexual Plant Reproduction*. **10:** 324-331.

Schwarzacher, T. 2003. Meiosis, recombination and chromosomes: a review of gene isolation and fluorescent *in situ* hybridization data in plants. *Journal of Experimental Botany*. **54:** 11-23.

Sears, E.R. 1941. Chromosome pairing and fertility in hybrids and amphidiploids in the Triticeae. *Research Bulletin of the Missouri Experimental station*. **33:** 20.

Sears, E.R. 1952. Homoeologous chromosomes in *Triticum aestivum*. *Genetics*. **37:** 624.

Sears, E.R. 1976. Genetic control of chromosome pairing in wheat. *Annu. Rev. Genet.* **10:** 31-51.

Sears, E.R. 1977. An induced mutant with homoeologous pairing in common wheat. *Can. J. Genet. Cytol.* **19:** 585-593.

Sears, E.R. 1982. A wheat mutant conditioning an intermediate level of homoeologous chromosome pairing. *Can. J. Genet. Cytol.* **24:** 715-719.

Sears, E.R. and Okamoto, M. 1958. Intergenomic chromosome relationships in hexaploid wheat. *Proceedings of the Tenth International Congress of Genetics*. 258-259.

Shaw, P. and Moore, G. 1998. Meiosis: *vive la* difference! *Curr. Opin. Plant Biol.* **1:** 458-462.

Sherman, J.D. and Stack, S.M. 1995. Two dimensional spreads of synaptonemal complexes from solanaceous plants. VI. High-resolution recombination nodule map for tomato. *Genetics*. **141:** 683-708.

Shiloh, Y. 1997. Ataxia-telangiectasia and the Nijmegen breakage syndrome: related disorders but genes apart. *Annu Rev Genet*. **31:** 635-662.

Shinohara, A., Ogawa, H. and Ogawa, T. 1992. Rad51 protein involved in repair and recombination in *S. cerevisiae* is a RecA-like protein. *Cell*. **69:** 457-470.

Smilde, W.D., Haluskova, J., Sasaki, T. and Graner, A. 2001. New evidence for the synteny of rice chromosome 1 and barley chromosome 3H from rice expressed sequence tags. *Genome*. **44:** 361-367.

Smith, A.V. and Roeder, G.S. 1997. The yeast Red1 protein localises to the cores of meiotic chromosomes. *J. Cell Biol.* **136:** 957-967.

Smithies, O. and Powers, P.A. 1986. Gene conversions and their relation to homologous chromosome pairing. *Transactions of the Royal Society of London*. **312:** 291-302.

Smyth, G.K., Yang, Y.H. and Speed, T. 2002. Statistical Issues in cDNA Microarray Data Analysis. In *Functional Genomics: methods and protocols*. Brownstein, M.J., and Khodursky, A.B. (eds.) Totowa, NJ: Humana Press.

Southern, E.M. 1975. Detection of specific DNA sequences among DNA fragments seperated by gel electrophoresis. *Journal of Molecular Biology*. **98:** 503-517.

Spellman, P.T., Sherlock, G., Zhang, M.Q., Iyer, V.R., Anders, K., Eisen, M.B., Brown, P.O., Botstein, D. and Futcher, B. 1998. Comprehensive identification of cell cycle-regulated genes of the yeast *Saccharomyces cerevisiae* by microarray hybridization. *Mol Biol Cell*. **9:** 3273-3297.

Spielman, M., Preuss, D., Li, F.L., Browne, W.E., Scott, R.J. and Dickinson, H.G. 1997. TETRASPORE is required for male meiotic cytokinesis in *Arabidopsis thaliana*. *Development*. **124:** 2645-2657.

Stack, S.M. and Anderson, L.K. 1986a. Two dimensional spreads of synaptonemal complexes from Solanaceous plants II. Synapsis in *Lycopersicum esculentum*. *Am. J. Bot.* **73:** 264-281.

Stack, S.M. and Anderson, L.K. 1986b. Two dimensional spreads of synaptonemal complexes from Solanaceous plants III. Recombination and crossing over in *Lycopersicum esculentum* (tomato). *Chromosoma*. **94:** 253-258.

Stack, S.M., Anderson, L.K. and Sherman, J.D. 1989. Chiasmata and recombination nodules in *Lilium Longiflorum*. *Genome*. **32:** 486-498.

Stack, S.M., Sherman, J.D., Anderson, L.K. and Herickhoff, L.S. 1993. Meiotic nodules in vascular plants. *Chromosomes Today*. **11:** 301-311.

Stadler, D.R. and Towe, A.M. 1971. Evidence for meiotic recombination in Ascobolus involving only one member of a tetrad. *Genetics*. **68:** 401-413.

Staiger, C.J. and Cande, W.Z. 1993. Cytoskeletal analysis of maize meiotic mutants. In *Molecular and Cell Biology of the Plant Cell Cycle*. Ormrod, J.C., and Francis, D. (eds.) Dordrecht. The Netherlands: Kluwer Academic Publishers, pp. 37-41.

Stassen, N.Y., Logsdon, J.M., Vora, G.J., Offenberg, H.H., Palmer, J.D. and Zolan, M.E. 1997. Isolation and characterisation of rad51 orthologs from *Coprinus cinereus* and *Lycopersicon esculentum*, and phylogenetic analysis of eukaryotic recA homologues. *Curr. Genet.* **31:** 144-157.

Stern, H. and Hotta, Y. 1985. Molecular biology of meiosis: synapsis-associated phenomena. In *Aneuploidy: Etiology and Consequences*. Dellarco, V.L., Voytek, P.E., and Hollaender, A. (eds.) New York: Plenum Press, pp. 305-316.

Stern, H. and Hotta, Y. 1987. The biochemistry of meiosis. In *Meiosis*. P. B. Moens (ed.) Orlando, Florida: Academic Press, pp. 303-331.

Sun, H., Treco, D., Schultes, N.P. and Szostak, J.W. 1989. Double strand breaks at an initiation site for meiotic gene conversion. *Nature*. **338:** 87-90.

Sym, M., Engebrecht, J.A. and Roeder, G.S. 1993. *Zip1* is a synaptonemal complex protein required for meiotic chromosome synapsis. *Cell*. **72:** 365-378.

Sym, M. and Roeder, G.S. 1995. Zip-1 induced changes in synaptonemal complex structure and polycomplex assembly. *J. Cell Biol.* **128:** 455-466.

Szostak, J.W., Orr-Weaver, T.L., Rothstein, R.J. and Stahl, F.W. 1983. The double-strand break model for recombination. *Cell*. **33:** 25-35.

Tarsounas, M., Morita, T., Pearlman, R.E. and Moens, P.B. 1999. RAD51 and DMC1 form mixed complexes associated with mouse meiotic chromosome cores and synaptonemal complexes. *J Cell Biol*. **147:** 207-220.

Thomas, J.O. and Travers, A.A. 2001. HMG1 and 2, and related 'architectural' DNA-binding proteins. *Trends Biochem. Sci.* **26:** 167-174.

Thomas, S.W. 1997. Molecular studies of homologous chromosome pairing in *Triticum aestivum*. Doctor of Philosophy. Department of Plant Science, The University of Adelaide. Adelaide, Australia.

Tsuchiya, T., Toriyama, K., Ejiri, S. and Hinata, K. 1994. Molecular characterization of rice genes specifically expressed in the anther tapetum. *Plant Mol Biol*. **26:** 1737-1746.

Tsuji, H., Tsutsumi, N., Sasaki, T., Hirai, A. and Nakazono, M. 2003. Organ-specific expressions and chromosomal locations of two mitochondrial aldehyde dehydrogenase genes from rice (*Oryza sativa* L.), ALDH2a and ALDH2b. *Gene*. **305:** 195-204.

Uphadya, M.D. and Swaminathan, M.S. 1967. Mechanisms regulating chromosome pairing in *Triticum*. *Biologisches Zentralblatt*. **87s:** 239-255.

Van Gelder, R.N., von Zastrow, M.E., Yool, A., Dement, W.C., Barchas, J.D. and Eberwine, J.H. 1990. Amplified RNA synthesized from limited quantities of heterogeneous cDNA. *Proc Natl Acad Sci U S A*. **87:** 1663-1667.

Vandeynze, A.E., Nelson, J.C., Odonoughue, L.S., Ahn, S.N., Siripoonwiwat, W., Harrington, S.E., Yglesias, E.S., Braga, D.P., McCouch, S.R. and Sorrells, M.E. 1995. Comparative mapping in grasses - Oat relationships. *Mol. Gen. Genet.* **249:** 349-356.

Vega, J.M. and Feldman, M. 1998. Effect of the pairing gene *Ph1* on centromere misdivision in common wheat. *Genetics*. **148:** 1285-1294.

Velculescu, V.E., Zhang, L., Vogelstein, B. and Kinzler, K.W. 1995. Serial analysis of gene expression. *Science*. **270:** 484-487.

Vierling, E. 1991. The Roles Of Heat Shock Proteins In Plants. *Annu. Rev. Plant Physiol. Plant Mol. Biol*. **42:** 579-620.

Villemur, R., Haas, N.A., Joyce, C.M., Snustad, D.P. and Silflow, C.D. 1994. Characterization of four new beta-tubulin genes and their expression during male flower development in maize (Zea mays L.). *Plant Mol Biol*. **24:** 295-315.

von Wettstein, D., Rasmussen, S.W. and Holm, P.B. 1984. The synaptonemal complex in genetic segregation. *Annu. Rev. Genet.* **18:** 331-413.

Wall, A.M., Riley, R. and Chapman, V. 1971. Wheat mutants permitting homoeologous meiotic chromosomes pairing. *Genet. Res.* **18:** 311-328.

Wang, S., Nakashima, S., Numata, O., Fujiu, K. and Nozawa, Y. 1999a. Molecular cloning and cell-cycle-dependent expression of the acetyl-CoA synthetase gene in Tetrahymena cells. *Biochem J*. **343:** 479-485.

Wang, T.F., Kleckner, N. and Hunter, N. 1999b. Functional specificity of MutL homologs in yeast: Evidence for three Mlh1-based heterocomplexes with distinct roles during meiosis in recombination and mismatch correction. *Proc. Natl. Acad. Sci. USA*. **96:** 13914-13919.

Weiner, B.M. and Kleckner, N. 1994. Chromosome pairing via multiple interstitial interactions before and during meiosis in yeast. *Cell*. **77:** 977-991.

Whitford, R. 2002. From intimate chromosome associations to wild sex in wheat (*Triticum aestivum*). Doctor of Philosophy. Department of Plant Science, The University of Adelaide. Adelaide, Australia.

Wicker, T., Matthews, D.E. and Keller, B. 2002. TREP: a database for Triticeae repetitive elements. *Trends Plant Sci*. **7:** 561-562.

Wicker, T., Stein, N., Albar, L., Feuillet, C., Schlagenhauf, E. and Keller, B. 2001. Analysis of a contiguous 211 Kb sequence in diploid wheat (*Triticum monococcum* L.) reveals multiple mechanisms of genome evolution. *Plant J*. **26:** 307-316.

Wolfe, K.H., Gouy, M., Yang, Y.W., Sharp, P.M. and Li, W.H. 1989. Date of the monocot-dicot divergence estimated from chloroplast DNA sequence data. *Proc. Natl. Acad. Sci. USA*. **86:** 6201-6205.

Wu, T.C. and Lichten, M. 1994. Meiosis-induced double-strand break sites determined by yeast chromatin structure. *Science*. **263:** 515-518.

Xiang, C.C., Kozhich, O.A., Chen, M., Inman, J.M., Phan, Q.N., Chen, Y. and Brownstein, M.J. 2002. Amine-modified random primers to label probes for DNA microarrays. *Nat Biotechnol*. **20:** 738-742.

Yacobi, Y.Z., Levanony, H. and Feldman, M. 1985a. An ordered arrangement of bivalents at first meiotic metaphase of wheat. I. Hexaploid wheat. *Chromosoma*. **91:** 347.

Yacobi, Y.Z., Levanony, H. and Feldman, M. 1985b. An ordered arrangement of bivalents at first meiotic metaphase of wheat. II. Tetraploid wheat. *Chromosoma*. **91:** 355.

Yang, I.V., Chen, E., Hasseman, J.P., Liang, W., Frank, B.C., Wang, S., Sharov, V., Saeed, A.I., White, J., Li, J., Lee, N.H., Yeatman, T.J. and Quackenbush, J. 2002a. Within the fold: assessing differential expression measures and reproducibility in microarray assays. *Genome Biol*. **3:** research0062.

Yang, Y.H., Dudoit, S., Luu, P., Lin, D.M., Peng, V., Ngai, J. and Speed, T.P. 2002b. Normalization for cDNA microarray data: a robust composite method addressing single and multiple slide systematic variation. *Nucleic Acids Res*. **30:** e15.

Zetka, M. and Rose, A. 1995. The genetics of meiosis in *Caenorhabditis elegans*. *Trends Genet.* **11:** 27-31.

Zetka, M.C., Kawasaki, I., Strome, S. and Mueller, F. 1999. Synapsis and chiasma formation in *C. elegans* require HIM-3, a meiotic chromosome core component that functions in chromosome segregation. *Genes Dev.* **13:** 2258-2270.

Zhao, H., Hastie, T., Whitfield, M.L., Borresen-Dale, A.L. and Jeffrey, S.S. 2002. Optimization and evaluation of T7 based RNA linear amplification protocols for cDNA microarray analysis. *BMC Genomics*. **3:** 31.

Zickler, D. and Kleckner, N. 1999. Meiotic chromosomes: Integrating structure and function. *Annu. Rev. Genet.* **33:** 603-754.